

# Abstract

Title of dissertation: Rh(II) Catalyzed Reactions Of C-H Insertion  
And Oxonium Ylide Generation

Deana M. Jaber, Doctor of Philosophy, 2011

Dissertation directed by: Dr. Michael P. Doyle  
Professor and chair  
Department of Chemistry and Biochemistry

Catalysis of metal carbene transformations with selected dirhodium(II) catalysts is a useful technology for constructing complex polycycles via intramolecular cyclopropanation, C-H insertion, and ylide derived reactions of diazoacetates and diazoacetoacetates. In this thesis, novel methodologies based upon intramolecular C-H insertion and the oxonium ylides rearrangements are investigated, and a new understanding of oxonium ylide formation and rearrangements is presented.

In chapter 1, in work done under the supervision of Dr. Herman O. Sintim, a novel methodology for the synthesis of enantiopure tertiary alcohols is described. The key step in the methodology is an intramolecular C-H insertion reaction whereby a new connector between a carbene center and the C-H target, the N-O tether, is introduced. The resulting C-H insertion products were converted to tertiary-amino alcohols *via* cleavage of the N-O tether. This approach allows the regioselective insertion of metal carbenes into the C-H bond alpha to a heteroatom and leads to the formation of tertiary stereocenters. Key concepts are outlined that aim at achieving selectivity in C-H insertion using a new tether that facilitates the construction of five membered rings, thus enabling remote functionalization of complex molecules.

In chapter 2, a detailed analysis of the mechanism of oxonium ylide generation and rearrangement, which has not been previously reported, was performed to gain insight into the mechanistic pathway by which oxonium ylides rearrange. The mechanism was studied via the synthesis of oxabicyclo[4.2.1]nonane compounds. Catalytic ylide formation and subsequent [1,2]-Stevens rearrangement unexpectedly resulted in a 70:30 molar ratio of two diastereoisomers formed in high yield. There was negligible dependence of the ratio of the two diastereoisomers on either para substituents on the aromatic ring or on the catalyst employed. However, the use of a large aryl substituent (e.g., anthranyl, mesityl, and 2,6-dimethyl-4-nitrophenyl) resulted in the formation of a single diastereoisomer. The importance of the size of the aryl group, coupled with the absence of a substituent effect on the ratio of the [1,2]-Stevens rearrangement diastereoisomers suggest that conformational influences are responsible for the apparent isomerization. Each diazoacetoacetate conformer forms a different oxonium ylide and subsequent rearrangement of each of these oxonium ylides leads to the formation of a distinct diastereoisomeric product.

In chapter 3, the mechanism of oxonium ylides rearranging *via* the [2,3]-sigmatropic rearrangement pathway was also investigated. Rh(II) catalyzed oxonium ylide generation of *trans*-3-styryltetrahydropyranone-5-diazoacetoacetates and its subsequent rearrangement forms two diastereoisomers in both the [1,2]-Stevens and [2,3]-sigmatropic processes. The two diastereoisomers of the [2,3]-sigmatropic processes, (78:22) molar ratio, are formed in high yield, but with negligible dependence on either para substituents on the aromatic ring or on the catalyst employed. The formation of a second diastereoisomer for the symmetry-allowed concerted [2,3]-sigmatropic rearrangement process is supportive of a concerted

mechanism leading to the two diastereoisomers of the [2,3]-sigmatropic processes *via* the presence of two conformational isomers of *trans*-3-styryltetrahydropyranone-5-diazoacetates.

RH(II) CATALYZED C-H INSERTION REACTIONS AND OXONIUM YLIDE  
GENERATION

By

Deana Majdi Jaber

Dissertation submitted to the faculty of the Graduate School of the University of  
Maryland at College Park in partial fulfillment of the requirements for the degree of  
Doctor of Philosophy  
2011

Advisory Committee:

Professor  
Professor  
Professor  
Professor  
Professor

Jeffery Davis  
Michael P. Doyle, Chairman/Advisor  
Daniel Falvey  
Andrei Vedernikov  
Liangli Yu

DEDICATION

To my parents and grandparents

To my loving husband  
**Yousef Munayyer**

## Acknowledgements

From Palestine to Massachusetts to Singapore to Maryland there are a number of individuals who are greatly responsible for helping me reach this point today. Foremost among them is my thesis advisor, Professor Michael P. Doyle. Dr. Doyle has consistently provided support, encouragement and guidance as I pursued research under his direction as part of his research group. More importantly, Dr. Doyle welcomed me into his research group and believed in my abilities and ambition at a difficult moment in my graduate career. His guidance in both the laboratory and classroom settings played a vital role in my development as a graduate student. Dr. Doyle would often ask “Where is the rest of the starting material?” he then would request to see the  $^1\text{H}$ NMR of the reaction crude and we would discuss the reaction outcome. It is those practices that made me a better scientist today. Dr. Doyle’s constant demands for improvement and thoughtful criticisms helped me tremendously in reaching the potential he was able to see in me and in making this thesis into a much improved product over several drafts.

I also want to thank Dr. Herman Sintim who welcomed me into his research group when I was in the early stages of the graduate program. In the Sintim group I learned a great deal and I am indebted to Dr. JingXing Wang, with whom I collaborated on research projects and learned from in the process. I was also fortunate to overlap in the Sintim group with a visiting Post-Doc Dr. Bogdan Stefane who, even in a short period of time, taught me a great deal. I also had the pleasure of working with two

undergraduate students Chris Vickery and Mohamad Diop during my time in the Sintim group as well as a number of other lab mates and colleagues.

I greatly appreciate Dr. Herman Ammon and Dr. Jeffery Davis under whom I worked as a teaching assistant at different periods during my time in the program. The guidance and experience provided by these two outstanding instructors has given me resources which I have already employed in the classroom today as a professor and will surely continue to use well into the future.

My thanks also go to Dr. Yiu-Fai Lam, whose help with NMR experiments was instrumental, Dr. Peter Zavalij who provided assistance with x-ray crystallography, and Dr. Eugene P. Mazzola who made himself available often for NMR questions regarding my research.

I am also grateful for Dr. John Fourkas who provided very important support as Director of Graduate Programs at a critical juncture in my time in the program.

Dr. Daniel Falvey and Dr. Andre Vadernikov also welcomed questions and provided help and guidance in various moments throughout my graduate research. Their accessibility and willingness to help students outside their research groups are unique and admirable qualities.

From the Doyle Research group I want to thank Dr. Ryan Burgin who I encountered toward the end of my time in the program. Dr. Burgin partnered with me on research projects and provided important support in the laboratory as well as guidance for an aspiring yet often worn out graduate student. I'm indebted also to other lab mates from the Doyle group including Maxim Ratnikov, Dmitry Shabashov, Yu Liu, Xiaochen Wang, and Phong Truong who were always helpful and frequently went out of their way to be supportive. I also wish to thank my lab mates from the Doyle

research group for warmly welcoming this female graduate student into what was previously an all-boys club. I will sincerely miss the warm and friendly working environment among them and the valuable and often entertaining discussions we had. Prior to coming to the University of Maryland a number of individuals and institutions played a role in helping me reach this point. I thank Dr. Sejal Patel, Dr. Thomas Keller and Dr. Paul Herling at the Novartis Institute of Tropical Diseases in Singapore whose encouragement, support and guidance propelled me into a graduate career in chemistry.

I'd also like to thank Professors Darren Hamilton and Maria Gomez who taught and guided me in my undergraduate work at Mount Holyoke College in South Hadley, Massachusetts. Their help and support continued after graduation and I am very much grateful for that.

A special thanks goes to my high school chemistry teacher Ms. Nadia. Her passion for chemistry was evidence by the scars on her face from a past laboratory accident which still didn't prevent her from teaching chemistry in the lackluster conditions of a high school in Nablus, Palestine. Without the equipment that is standard in laboratories in advanced nations due to limited resources, Ms. Nadia compensated for this through creativity and dedication to her pupils. This early experience continues to serve as an inspiration for me today, both in the laboratory and in the classroom.

Finally, I would like to thank my family. I owe much to my parents, who have endured not seeing their daughter as much as they would have liked. It's been ten years since I left home and I hope being away from home was worth it. My Grandfather who has since passed away would have been very proud to witness this moment as he supported my travel abroad to seek an education. I would not be writing

an acknowledgment for my Ph.D. thesis if it wasn't for one very important factor; my beloved husband Yousef Munayyer. It is his continuous and endless support that got me through the difficult times of being a graduate student. It was him that continuously told me that I can do it at times when I was ready to give up. I have been very lucky to have such a wonderful supportive loving husband and I am very much grateful to him.

To those I have listed and to those I unintentionally neglected to include, thank you for everything.

# Table of contents

<b>Dedication.....</b>	<b>ii</b>
<b>Acknowledgement.....</b>	<b>iii</b>
<b>Table of contents.....</b>	<b>vii</b>
<b>List of Tables.....</b>	<b>x</b>
<b>List of Figures.....</b>	<b>xii</b>
<b>List of Schemes.....</b>	<b>xiii</b>
<b>List of Abbreviations.....</b>	<b>xv</b>

## **Chapter 1:** Towards the Development of New Tethers for Intramolecular C-H Insertion Reactions

I. Introduction.....	1
1.1 Carbenes and metal carbenes	
1.2 C-H functionalization by metal carbene insertion	
1.3 Factors affecting reactivity and selectivity of C-H insertion reactions	
1.4 Reaction mechanism	
1.5 Tethered intramolecular C-H insertion	
II. Research Discussion.....	17
2.1 Synthesis of model substrate for N-O tethered C-H insertion	
2.2 Different methods for the synthesis of <i>N</i> -alkoxydiazoamides substrates	
2.2a Method A (using diketene or diketene acetone adduct)	
2.2b Method B (using methyl malonyl chloride)	
2.2c Method C (using phthalylglycyl chloride)	
2.3 C-H insertion reaction, screening and optimization	
2.4 Substrate scope of the intramolecular C-H insertion reaction	
III. Conclusion.....	30
IV. Experimental.....	31

**Chapter 2:** Control of selectivity in the generation and reactions of oxonium ylides via [1,2]-Stevens rearrangement

I. Introduction.....	104
1.1 Ylides	
1.2 Oxonium ylides	
1.3 Oxonium ylide rearrangements	
1.3a [1,2]-Stevens rearrangement of oxonium ylides	
1.3a(i) Examples of [1,2]-Stevens rearrangement of oxonium ylides.	
1.3a(ii) Mechanism of the [1,2]-Stevens rearrangement of oxonium ylides.	
1.3b [2,3]-sigmatropic rearrangement of allylic oxonium ylides	
1.3c Other reactions of oxonium ylides	
II. Research Discussion.....	124
2.1 Strategy for the synthesis of oxabicyclo[4.2.1]nonane framework	
2.2 Synthesis of the Mukaiyama-Michael addition products	
2.3 Catalytic dinitrogen extrusion reactions	
2.4 Mechanism of the [1,2]-Stevens rearrangement	
2.5 Conformation controls product formation	
2.5a Synthesis of the Mukaiyama-Michael addition products	
2.5b Catalytic dinitrogen extrusion reactions	
III. Conclusion.....	148
IV. Experimental.....	150

**Chapter 3:** Competition between [1,2]-Stevens and [2,3]-sigmatropic rearrangements

I. Introduction.....	221
1.1 Mechanistic background	
1.1a The Woodward-Hoffmann description of the [1,2] vs. [2,3] rearrangements	
1.1b The HOMO-LUMO interaction	
1.1c Aromatic/antiaromatic transition state theory	
1.2 Competition between [2,3]-sigmatropic and [1,2]-Stevens rearrangement	
1.2a The [2,3]-sigmatropic dominates over the [1,2]-Stevens rearrangement	
1.2b The [1,2]-Stevens dominates over the [2,3]-sigmatropic rearrangement	
II. Results and Discussion.....	234
2.1 Model substrate for investigating the competition between [1,2]-Stevens and [2,3]-sigmatropic rearrangements	
2.2 Synthesis of the Mukaiyama-Michael addition products	
2.3 Catalytic dinitrogen extrusion reactions	
2.4 Mechanism of the [2,3]-sigmatropic rearrangement	
2.5 Control of regioselectivity	
2.5a Synthesis of vinyl diazoacetoacetate tetrahydropyranone <b>195</b>	
2.5b Nitrogen extrusion reactions of vinyl diazoacetoacetate tetrahydropyranone <b>195a</b> and <b>195b</b>	
III. Conclusion.....	249
IV. Experimental.....	250

## List of Tables

- Table 1** The effect of ligand variation on regioselectivity in C-H insertion reactions
- Table 2** The effect of bulky ligand variation on regioselectivity in C-H insertion reactions
- Table 3** Dirodium(II) ligand effect on metal carbene reactions
- Table 4** Synthesis of *N*-alkoxyamine **48**
- Table 5** Solvent screening
- Table 6** Catalyst optimization
- Table 7** Temperature optimization
- Table 8** Catalyst loading optimization
- Table 9** Substrate scope of the C-H insertion reaction
- Table 10** 1,5 vs. 1,7-C-H insertion
- Table 11** Intramolecular generation and rearrangement of oxonium ylides by Roskamp & Johnson
- Table 12** Catalyst and ring size effects on the selectivity of oxonium ylide rearrangements
- Table 13** Preference for five-membered oxonium ylide formation of diazoketone **81**
- Table 14** Isolation of homodimers in the decomposition reaction of diazoketone **86**
- Table 15** Lack of isolation of homodimers in the decomposition reaction of diazoketone **90**
- Table 16** Intermolecular generation of allylic oxonium ylides and their stereoselective [2,3]-sigmatropic rearrangement
- Table 17** Synthesis of *trans*-3-aryltetrahydropyranone-5-diazoacetoacetates **134**
- Table 18** Rh(II) catalyzed decomposition of *trans*-3-aryltetrahydropyranone-5-diazoacetoacetates **134**
- Table 19** Catalyst screening for the decomposition of *trans*-3-aryltetrahydropyranone-5-diazoacetoacetates **134a**
- Table 20** Rhodium-catalyzed reaction of 2-aryl-2-diazoacetate **143** with enantiopure (R,R)-**142** leads to different diastereoisomeric ratios of the [1,2]-Stevens product
- Table 21** Synthesis of *trans*-3-aryltetrahydropyranone -5-diazoacetoacetates **134**
- Table 22** Enantioselective cyclic allylic oxonium ylide formation and rearrangement of aromatic substrates catalyzed by Rh<sub>2</sub>(*S*-PTTL)<sub>4</sub>
- Table 23** Enantioselective cyclic allylic oxonium ylide formation and rearrangement of aliphatic substrates catalyzed by Rh<sub>2</sub>(*S*-PTTL)<sub>4</sub>
- Table 24** The [2,3]-sigmatropic rearrangement dominates over the [1,2]-Stevens rearrangement using diazoketone **162**
- Table 25** Catalyst influence on oxonium ylide generation and its rearrangement pathways
- Table 26** Ring-size influence on oxonium ylide generation and its rearrangement pathways
- Table 27** The [1,2]-Stevens rearrangement dominates over the [2,3]-sigmatropic rearrangement using diazoketone **174**
- Table 28** Synthesis of *trans*-3-styryltetrahydropyranone-5-diazoacetoacetates **177**
- Table 29** Rh(II) catalyzed decomposition of *trans*-3-styryltetrahydropyranone-5-diazoacetoacetates **177**
- Table 30** Catalyst screening for the decomposition of *trans*-3-styryltetrahydropyranone-5-diazoacetoacetates **177**
- Table 31** Cyclization reaction of diazoketone **187** leads to isomeric mixtures of both [2,3] and [1,2] rearrangement processes

**Table 32** Catalyst effects the diastereoselective synthesis of tetrahydrofuranones  
**Table 33** Synthesis of vinyl diazoacetoacetate tetrahydropyranone **195**

## List of Figures

- Figure 1** Metal carbene C-H insertion
- Figure 2** Reactive conformers based on conformational preferences
- Figure 3** Transition state structures for the intermolecular generation of allylic oxonium ylides
- Figure 4** Representative examples of bridged oxa-[*n*.2.1] skeletons
- Figure 5** <sup>1</sup>H NOE correlation of *trans*-3-phenyltetrahydropyranone-5-diazoacetate **134a**
- Figure 6** <sup>1</sup>H NMR reaction mixture of rhodium(II) catalyzed decomposition of *trans*-3-phenyltetrahydropyranone-5-diazoacetates **134a**
- Figure 7** COSY of [1,2]-Stevens rearrangement **136a**
- Figure 8** HMBC of [1,2]-Stevens rearrangement **136a**
- Figure 9** The crystal structure of *syn*-**136a** and *anti*-**136a**
- Figure 10** <sup>1</sup>H NOE correlation of elimination product *cis*-**140** and *trans*-**140**
- Figure 11** Depiction of the frontier orbitals for the [2,3] and [1,2] rearrangement processes
- Figure 12** <sup>1</sup>H NMR of rhodium(II) catalyzed decomposition reaction mixture of *trans*-3-styryltetrahydropyranone-5-diazoacetates **177a**
- Figure 13** Crystal structure for the [1,2]-Stevens rearrangement product-major isomer and the [2,3]-sigmatropic rearrangement product-minor isomer

## List of Schemes

- Scheme 1** Formation of carbenes *via* the decomposition of diazocarbonyl compounds
- Scheme 2** Electrophilic and nucleophilic metal carbenes
- Scheme 3** Preparation of highly functionalized cyclopentane derivatives by intramolecular C-H insertion
- Scheme 4** Ring-size effects predominate over the order of reactivity of the C-H bond
- Scheme 5** General scheme of C-H insertion and the groups around the diazo functionality (X= O, N, CH<sub>2</sub>) (Z= H, COR, CO<sub>2</sub>Et, PO(OR)<sub>2</sub>, SO<sub>2</sub>Ar)
- Scheme 6** Electronic effects on the regioselectivity of C-H insertion
- Scheme 7**  $\beta$ -lactam formation due to conformational influence
- Scheme 8** Mechanism of the C-H insertion according to Doyle
- Scheme 9** Mechanism of the C-H insertion according to Nakamura
- Scheme 10** The use of tethering groups
- Scheme 11** Silicon tethered intramolecular C-H insertion reactions
- Scheme 12** Sulfonate tethered intramolecular C-H insertion reactions
- Scheme 13** The use of labile N-O tether in intramolecular C-H insertion reactions
- Scheme 14** Seebach and Weber's asymmetric approach towards the synthesis of tertiary alcohols
- Scheme 15** Sharpless asymmetric dihydroxylation
- Scheme 16** Three-pot synthesis of *N*-alkoxydiazoalkoxyamide **49**
- Scheme 17** Synthesis of *N*-alkoxydiazoamide **49**, method A
- Scheme 18** Synthesis of *N*-alkoxydiazoamide **49**, method B
- Scheme 19** Synthesis of *N*-alkoxydiazoamide **49**, method C
- Scheme 20** Towards the synthesis of *N*-alkoxydiazoamide **49**, (R = *p*-nitrobenzyl)
- Scheme 21** Intramolecular C-H insertion
- Scheme 22** Intramolecular C-H insertion on an enantiomerically enriched substrate
- Scheme 23** N-O cleavage to afford the 1,3-hydroxy amino functionality
- Scheme 24** C-H insertion versus cyclopropanation
- Scheme 25** Ylides
- Scheme 26** Generation of ylides from metal carbenes
- Scheme 27** Generation of oxonium ylides via transition metal catalyzed decomposition of diazo compounds
- Scheme 28** Reactions and rearrangements of oxonium ylides
- Scheme 29** First example of intermolecular [1,2]-oxonium ylide rearrangement reported by Nozaki in 1966
- Scheme 30** Elimination product formation
- Scheme 31** Concerted mechanism for the decomposition of diazoketone **90**, as proposed by West
- Scheme 32** The [2,3]-sigmatropic reaction
- Scheme 33** Intramolecular [2,3]-sigmatropic rearrangement affords five-, six-, and eight-membered oxygen heterocycles
- Scheme 34** Intramolecular [2,3]-sigmatropic rearrangement also possible with propargylic ethers
- Scheme 35** Ring expansion of cyclic acetal systems
- Scheme 36** Mechanism of the ring expansion of cyclic acetal systems

- Scheme 37** Synthesis of the Tigliane-Daphnane skeleton via an oxonium ylide intermediate followed by [1,2]-Stevens rearrangement
- Scheme 38** Synthetic strategy
- Scheme 39** Rational for the exclusive formation of *trans*-3-aryltetrahydropyranone-5-diazoacetates **134**
- Scheme 40** [1,2]-Stevens rearrangement possible pathways
- Scheme 41** Formation of two diastereoisomers for the [1,2]-Stevens rearrangement of *trans*-3-phenyltetrahydropyranone-5-diazoacetates **134a**
- Scheme 42** Possible intermediates with a stepwise mechanism for the [1,2]-Stevens rearrangement of oxonium ylides
- Scheme 43** Possible mechanistic pathways for the [1,2]-Stevens rearrangement of oxonium ylide **135a**
- Scheme 44** Stepwise mechanism for the decomposition of *trans*-3-phenyl tetrahydropyranone-5-diazoacetates **134a** via homolytic or heterolytic cleavage
- Scheme 45** Concerted mechanism for the decomposition of *trans*-3-aryltetrahydropyranone-5-diazoacetates **134** via conformational isomers
- Scheme 46** Dirhodium pivalate and dirhodium triphenylacetate have a minor effect on the ratio of the [1,2]-Stevens rearrangement products
- Scheme 47** Formation of a single diastereoisomer of the [1,2]-Stevens rearrangement product when the aryl group is a large substituent
- Scheme 48** Concerted mechanism for the decomposition of *trans*-3-aryltetrahydropyranone-5-diazoacetates **134** when Ar = large substituent (e.g., anthranyl, mesityl, and 2,6-dimethyl-4-nitro phenyl)
- Scheme 49** Five-membered ring transition state of the [2,3]-sigmatropic rearrangement showing the orbital overlap as the new bond is formed
- Scheme 50** Three-membered ring transition state of the [1,2]-Stevens rearrangement showing the orbital overlap as the new bond is formed
- Scheme 51** Copper(II) catalyzed decomposition of diazoacetate **165** affords solely the [1,2]-Stevens rearrangement product
- Scheme 52** Investigating the competition between [2,3] and [1,2] rearrangement processes
- Scheme 53** Rhodium(II) catalyzed decomposition reaction of *trans*-3-styryl tetrahydropyranone-5-diazoacetates **177a**
- Scheme 54** Conformational isomers explain the formation of two diastereoisomers for the [2,3]-sigmatropic rearrangement process
- Scheme 55** Mechanism of the [2,3]-sigmatropic rearrangement via a metal-bound ylide
- Scheme 56** Investigating the possibility of controlling the regioselectivity between [2,3] and [1,2] processes using diazoacetate tetrahydropyranones **195a** and **195b** as model substrate
- Scheme 57** Rh(II) catalyzed decomposition of vinyl diazoacetate tetrahydropyranone **195a** and **195b**
- Scheme 58** Nitrogen extrusion reactions of diazoacetate **203**
- Scheme 59** Possible mechanism of the formation of methyl chromone **204**

## List of Abbreviations

acac	acetylacetonate
acam	acetamide
Ar	aromatic
Bn	benzyl
<sup>t</sup> Bu	<i>tert</i> -butyl
cap	caprolactam
DCM	dichloromethane
DCE	1,2- dichloroethane
DEAD	diethyl azodicarboxylate
DIAD	diisopropyl azodicarboxylate
DOSP	( <i>N</i> -dodecylbenzenesulfonyl)prolinate
d.r.	diastereomeric ratio
EDA	ethyldiazoacetate
ee	enantiomeric excess
Et <sub>3</sub> N	triethylamine
EtOAc	ethyl acetate
Equiv	equivalent
h	hour
hfacac	hexafluoroacetylacetonate
Me	methyl
MEOX	oxazolidine-4-carboxylic acid methyl ester
MEPY	pyrrolidine-4-carboxylic acid methyl ester

ML <sub>n</sub>	transition metal with ligands
MsN <sub>3</sub>	methanesulfonyl azide
MS	molecular sieves
NMR	nuclear magnetic resonance
OAc	acetate
oct	octanoate
piv	pivalate
pfb	perfluorobutyrate
PTTL	phtaloyl-tert-leucinate
Ph	phenyl
<sup>i</sup> Pr	<i>iso</i> -propyl
Red-Al	sodium bis(2-methoxyethoxy)aluminium hydride
rt	room temperature
TBAF	tetra- <i>n</i> -butylammonium fluoride
TBS	<i>tertiary</i> -Butyldimethylsilyl
tfa	trifluoroacetate
THF	tetrahydrofuran
TMS	trimethylsilyl
Tol	<i>p</i> -methylphenyl
Ts	<i>p</i> -toluenesulfonyl (tosyl)
TPA	triphenylacetate

*Chapter 1:*

**Towards the Development of New Tethers for Intramolecular C-H Insertion Reactions**

Research in chapter 1 was performed under Dr. Herman O. Sintim's supervision

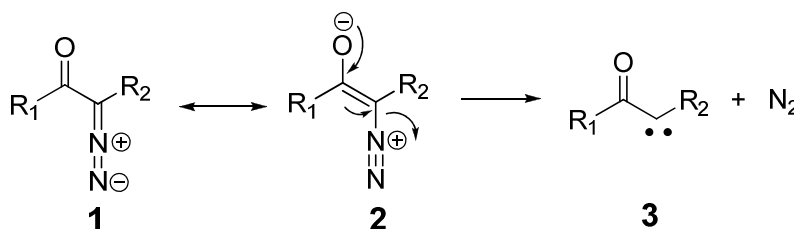
---

# I. Introduction

---

## 1.1 Carbenes and metal carbenes

Carbenes are highly reactive neutral species containing a carbon atom with six valence electrons. One method to generate carbenes is the decomposition of diazocarbonyl compounds (Scheme 1).<sup>1</sup> Diazocarbonyl compounds are used as carbene precursors because they are easily prepared and possess an electron-withdrawing carbonyl group that stabilizes the negative charge of the diazocarbonyl compound. The formation of gaseous nitrogen is the driving force for this reaction (Scheme 1).<sup>1</sup>



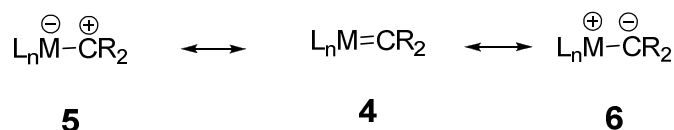
**Scheme 1.** Formation of carbenes *via* the decomposition of diazocarbonyl compounds.

The utility of diazocarbonyl compounds as carbene precursors became more attractive once transition metals were used.<sup>1</sup> Metal-complexed carbenes are known as metal carbenes; these metal carbenes can either be nucleophilic or electrophilic depending on the metal itself and the ligands associated with it (Scheme 2).<sup>1</sup> Metal carbenes are less reactive than free carbenes and hence can undergo the same types of

---

<sup>1</sup> (a) M. P. Doyle in: *Comprehensive Organometallic Chemistry II*; Hegedus, L. S. E.; Pergamon Press: New York, **1995**; Vol 12., Chapter 5.2, pp. 421-468. (b) Doyle, M. *Synthetic carbene and nitrene chemistry*; John Wiley & Sons, Inc. : NJ, 2004, 561-592. (c) Doyle, M. P.; Duffy, R.; Ratnikov, M.; Zhou, L. *Chem. Rev.*, **2010**, *110*, 704-724.

reactions with higher selectivity and greater yield than the corresponding reactions of free carbenes. The reactivity and stability of metal carbenes is influenced by the metal itself, the ligands attached to the metal, and the degree of  $\pi$ -back donation from the metal to the carbene.<sup>1</sup>



**Scheme 2.** Electrophilic and nucleophilic metal carbenes.

Metal carbenes undergo insertion reactions with O-H, N-H, Si-H, S-H, and C-H bonds as well as react with heteroatoms to form ylides. This chapter will focus on C-H insertion reactions whereas the next two chapters will discuss oxonium ylide formation and rearrangement.

## **1.2 C-H functionalization by metal carbene insertion:**

Introduction of new functionalities in C-H bonds, directly through transforming them, opens up new avenues in organic synthesis. Although significant progress has been made towards C-H functionalization,<sup>2</sup> this field still presents unsolved problems in synthetic chemistry. A promising C-H functionalization method involves the insertion of metal carbenes into C-H bonds.<sup>2</sup> This methodology has experienced a considerable amount of interest<sup>3</sup> due to its broad applicability to the synthesis of complex natural products and potential pharmaceutical agents.

Functionalization of the C-H bond via the metal carbene has shown great promise for transforming unactivated C-H bonds.<sup>2</sup> The metal carbene is formed from its diazocarbonyl precursor and the metal atom does not interact directly with the

<sup>2</sup> (a) Davies, H. M. L.; Manning, J. R. *Nature*, **2008**, *451*, 417-424. (b) Doyle, M. P.; Duffy, R.; Ratnikov, M.; Zhou, L. *Chem. Rev.*, **2010**, *110*, 704-724.

<sup>3</sup> Davies, H. M. L.; Du Bois, J.; Yu, J.-Q. *Chem. Soc. Rev.*, **2011**, *40*, 1855-1856.

alkane C-H bond. The highly reactive metal carbene inserts into the C-H bond to form the C-H insertion product and regenerates the metal for another catalytic cycle (Figure 1).<sup>4</sup>

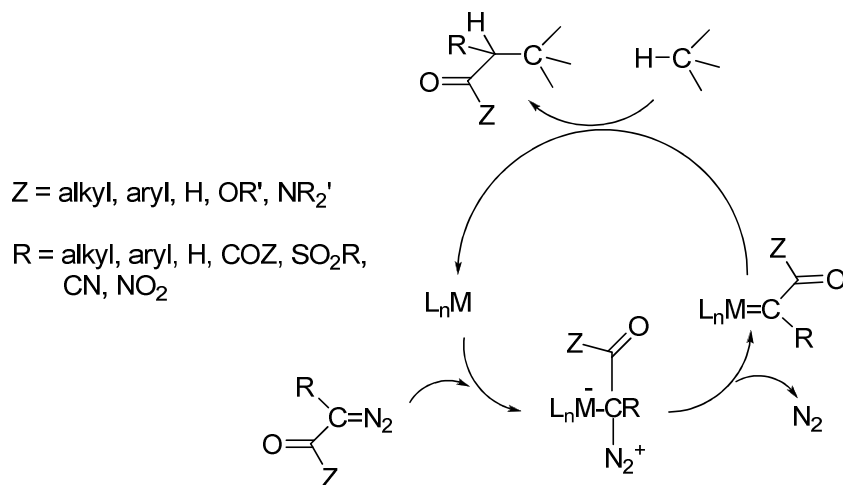


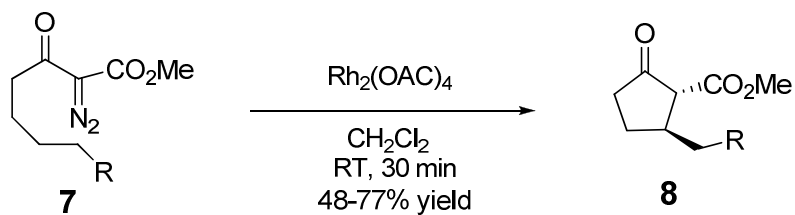
**Figure 1.** Metal carbene C-H insertion.

Intramolecular C-H insertion reactions have proven to be useful technologies for constructing complex polycycles.<sup>5</sup> One of the first systems to be investigated was  $\alpha$ -diazo- $\beta$ -ketoester **7**.<sup>7</sup> Taber showed that C-H insertion can be efficient, even in acyclic and freely rotating systems, such as compound **7**, to afford 2-carbalkoxy cyclopentanones **8** in up to 77% yield (Scheme 3).<sup>6</sup>

<sup>4</sup> (a) Doyle, M. P.; McKervey, M. A.; Ye, T. *Modern Catalytic Methods for Organic Synthesis with Diazo Compounds*, Wiley, New York, **1998**. (b) Doyle, M. P.; Duffy, R.; Ratnikov, M.; Zhou, L. *Chem. Rev.*, **2010**, *110*, 704-724.

<sup>5</sup> (a) Taber, D. F. In *Comprehensive organic synthesis: selectivity, strategy, and efficiency in modern organic chemistry*; Trost, B. M.; Fleming, I. Eds.; Pergamon Press: New York, 1991. (b) Taber, D. F.; Petty, E. H. *J. Org. Chem.*, **1982**, *47*, 4808-4809. (c) Doyle, M. P.; Westrum, L. J.; Wolthuis, W. N. E.; See, M. M.; Boone, W. P.; Bagheri, V.; Pearson, M. M. *J. Am. Chem. Soc.*, **1993**, *115*, 958-964.

<sup>6</sup> Taber, D. F.; Petty, E. H. *J. Org. Chem.*, **1982**, *47*, 4808-4809.



**Scheme 3.** Preparation of highly functionalized cyclopentane derivatives by intramolecular C-H insertion.

### **1.3 Factors affecting reactivity and selectivity of C-H insertion reactions:**

Intramolecular C-H insertion reactions typically occur with high levels of regioselectivity.<sup>2-5</sup> A hallmark of such processes is the strong bias towards five-membered-ring formation *via* a 1,5-C-H insertion. However, steric and electronic factors may override this preference for five-membered ring formation. Notable exceptions have been reported, especially in the reactions of diazoacetamides<sup>7</sup> and sterically constrained systems<sup>8</sup> which undergo a 1,4-intramolecular C-H insertion to form  $\beta$ -lactams. Furthermore, 1,3,<sup>9</sup> 1,6,<sup>10</sup> and even 1,7<sup>11</sup> C-H insertion reactions have all been observed when the C-H bond is activated by a neighboring heteroatom or if the system is structurally rigid.

The reactivity of the C-H site increases with an increasing number of alkyl substituents; the general order of reactivity is methine > methylene >> methyl. Taber has shown that the ring-size effects predominate over this order.<sup>7</sup> For example, treatment of diazoacetate **9** with rhodium acetate afforded cyclopentanone **10** in 55% yield (Scheme 4).

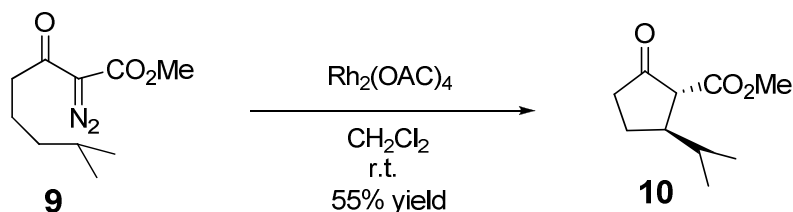
<sup>7</sup> Doyle, M. P.; Pieters, R. J.; Taunton, J.; Pho, H. Q.; Padwa, A.; Hertzog, D. L.; Precedo, L. *J. Org. Chem.*, **1991**, *56*, 820-829.

<sup>8</sup> Doyle, M. P.; Taunton, J.; Pho, H. Q. *Tetrahedron Lett.*, **1989**, *30*, 5397-5400.

<sup>9</sup> Shi, W.; Zhang, B.; Zhang, J.; Liu, B.; Zhang, S.; Wang, J. *Org. Lett.*, **2005**, *7*, 3103-3106.

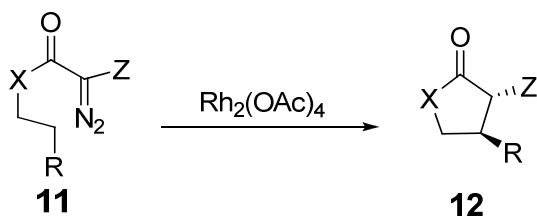
<sup>10</sup> (a) John, J. P.; Novikov, A. V. *Organic Lett.*, **2007**, *9*, 61-63. (b) Hinman, A.; Du Bois, J. *J. Am. Chem. Soc.*, **2003**, *125*, 11510-11511. (c) Cane, D. E.; Thomas, P. J. *J. Am. Chem. Soc.*, **1984**, *106*, 5295-303.

<sup>11</sup> Lee, E.; Choi, I.; Song, S. Y. *J. Chem. Soc., Chem. Commun.*, **1995**, 321-322.



**Scheme 4.** Ring-size effects predominate over the order of reactivity of the C-H bond.

There are a number of factors that should be taken into account when employing C-H insertion reactions to construct complex molecules. Substituents on the diazocarbonyl functional group (**Z**, in Scheme 5) have a significant effect on the reactivity of diazocarbonyl compounds.<sup>12</sup> For example, diazocarbonyl compounds where **Z** = hydrogen or an alkyl substituent are substantially more reactive than those with an electron-withdrawing substituent (**Z** = COR, CO<sub>2</sub>Et, PO(OR)<sub>2</sub>, SO<sub>2</sub>Ar) that further stabilize the negative charge of the diazocarbonyl compound.<sup>12</sup>



**Scheme 5.** General scheme of C-H insertion and the groups around the diazo functionality (**X** = O, N, CH<sub>2</sub>) (**Z** = H, COR, CO<sub>2</sub>Et, PO(OR)<sub>2</sub>, SO<sub>2</sub>Ar).

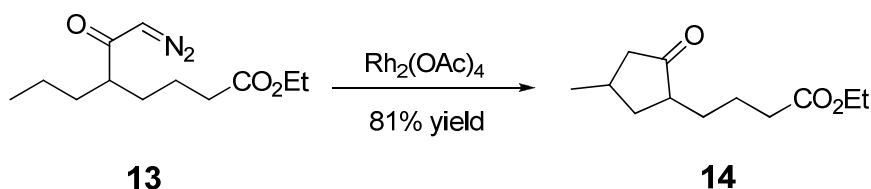
Electronic factors have a tremendous effect on directing C-H insertion reactions.<sup>8</sup> Electron-donating substituents activate adjacent C-H bonds whereas electron withdrawing substituents deactivate C-H bonds in metal carbene insertion reactions.<sup>12,13</sup> This can be explained by hyperconjugative effects where the lone pair

<sup>12</sup> Doyle, M. P.; Forbes, D. C. *Chem. Rev.*, **1998**, *98*, 911-935.

<sup>13</sup> Doyle, M. P.; Pieters, R. J.; Taunton, J.; Pho, H. Q.; Padwa, A.; Hertzog, D. L.; Precedo, L. *J. Org. Chem.*, **1991**, *56*, 820-829.

of a heteroatom donates into the  $\sigma^*$  of the C-H adjacent to it, raising the HOMO level and making it more reactive.<sup>13</sup>

Stork and Nakatani<sup>14</sup> have reported the influence of electronic effects on the regioselectivity of the C-H insertion reaction. They reported that electron-withdrawing groups such as carboxyl groups can deactivate the methylene group adjacent to it ( $\beta$  or  $\gamma$  position). Treatment of diazoketone **13** with rhodium acetate formed cyclopentanone **14** in 81% yield. No C-H insertion into the methylene group adjacent to the ester functionality was observed.



**Scheme 6.** Electronic effects on the regioselectivity of C-H insertion.

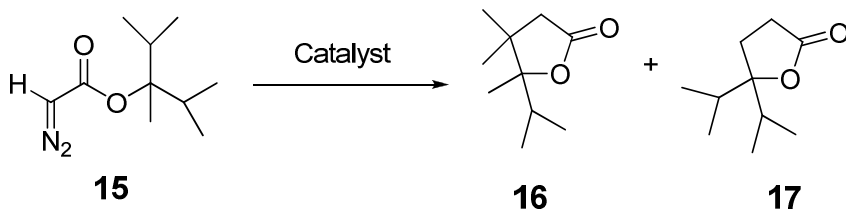
Rhodium(II) carboxylates are the catalysts of choice for C-H insertion reactions.<sup>1-3</sup> The ligands on the dirhodium catalysts play an important role in determining the regioselectivity of the C-H insertion product.<sup>15</sup> Doyle has shown that treatment of diazoacetate **15** with  $\text{Rh}_2(\text{OAc})_4$  resulted in the formation of nearly equal amounts of the  $\gamma$ -lactones **16** and **17** (Table 1).<sup>16</sup> Interestingly, the use of  $\text{Rh}_2(\text{pfb})_4$  afforded more of  $\gamma$ -lactone **17**, molar ratio of **16**:**17** equals 32:68, while the use of catalyst  $\text{Rh}_2(\text{acam})_4$  led to the exclusive formation of lactone **16**.<sup>16</sup> As enumerated in Table 1, the regioselectivity for C-H insertion varied depending on which rhodium(II) catalyst was used.

<sup>14</sup> Stork, G.; Nakatani, K. *Tetrahedron Lett.*, **1988**, 29, 2283-2286.

<sup>15</sup> Padwa, A.; Austin, D. J. *Angew. Chem. Int. Ed. Engl.*, **1994**, 33, 1797-1815.

<sup>16</sup> Doyle, M. P.; Bagheri, V.; Pearson, M. M.; Edwards, J. D. *Tetrahedron Lett.*, **1989**, 30, 7001-7004.

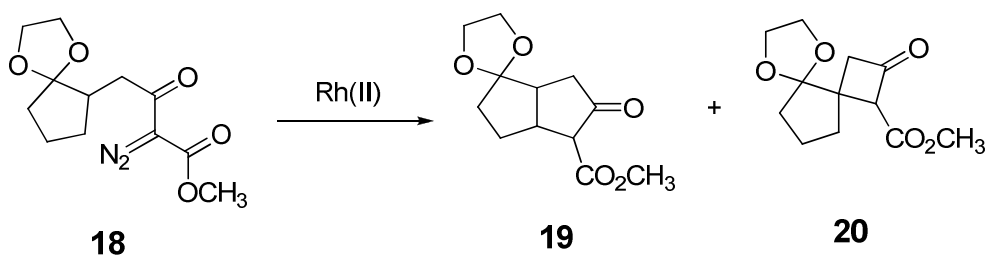
**Table 1.** The effect of ligand variation on regioselectivity in C-H insertion reactions.



Entry	Catalyst	Ratio (16:17)	Yield (%) (16+17)
1	Rh <sub>2</sub> (OAc) <sub>4</sub>	53:47	81
2	Rh <sub>2</sub> (pfb) <sub>4</sub>	32:68	56
3	Rh <sub>2</sub> (acam) <sub>4</sub>	99:1	96

Furthermore, variation of the steric bulk of the ligand also influences selectivity. Ikegami<sup>17</sup> demonstrated that the bulky rhodium(II) triphenylacetate, Rh<sub>2</sub>(TPA)<sub>4</sub>, favours insertion into a methylene C-H bond rather than a methine C-H bond (Table 2).

**Table 2.** The effect of bulky ligand variation on regioselectivity in C-H insertion reactions.



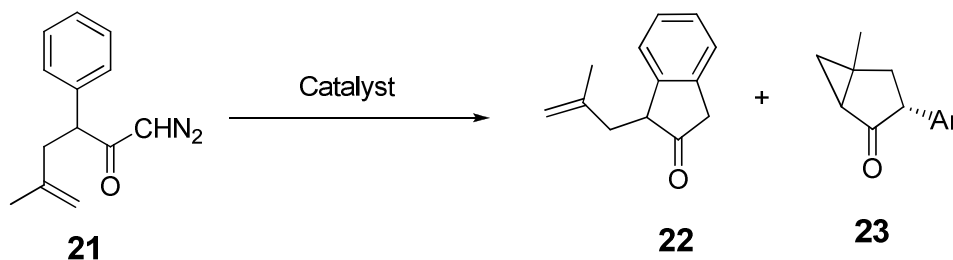
Entry	Catalyst	Ratio (19:20)	Yield (%) (19+20)
1	Rh <sub>2</sub> (OAc) <sub>4</sub>	37:63	64

<sup>17</sup> Hashimoto, S.; Watanabe, N.; Ikegami, S. *Tetrahedron Lett.*, **1992**, *33*, 2709-2712.

2	Rh <sub>2</sub> (TPA) <sub>4</sub>	96:4	75
---	------------------------------------	------	----

Varying the ligands on the dirhodium catalysts can provide exceptional chemoselectivity in catalytic metal carbene reactions.<sup>18</sup> For example, Doyle and Padwa have reported that by changing the dirhodium(II) ligand from perfluorobutyrate to caprolactam, the metal carbene reaction can be transformed from aromatic substitution, product **22**, to cyclopropanation, product **23** (Table 3).<sup>18</sup> In these two transformations chemoselectivity varies based on the electronic demand of the ligands from the dirhodium(II) carbene intermediate; with the perfluorobutyrate ligands being more electron withdrawing than those of caprolactam. The perfluorobutyrate ligands result in exclusive formation of the aromatic substitution product, while the caprolactam ligands afford only the cyclopropanation product.

**Table 3.** Dirhodium(II) ligand effect on metal carbene reactions.



Entry	Catalyst	Ratio (22:23)	Yield (%) 22	Yield (%) 23
1	Rh <sub>2</sub> (OAc) <sub>4</sub>	52:48	48	44
2	Rh <sub>2</sub> (pfb) <sub>4</sub>	100:0	86	0
3	Rh <sub>2</sub> (cap) <sub>4</sub>	0:100	0	75

<sup>18</sup> Padwa, A.; Austin, D. J.; Hornbuckle, S. F.; Semones, M. A.; Doyle, M. P.; Protopopova, M. N. *J. Am. Chem. Soc.*, **1992**, *114*, 1874-1876.

Conformational preferences can also affect the selectivity of the C-H insertion reaction.<sup>19</sup> Doyle argues that conformational preferences of the rhodium metal carbene intermediate in diazoacetoacetamides can influence the site selectivity of the intramolecular rhodium metal carbene mediated C-H insertion reaction.<sup>19d</sup> He further postulates that the nonbonding nitrogen electrons overlap with the LUMO of the carbonyl group thus fixing the amide conformation and resulting in the preferred reactive conformer. This conformer is represented by **A** in Figure 2, where the larger *N*-substituent is placed *syn* to the sterically less demanding amide carbonyl group. Consequently, the smaller *N*-substituent is placed in close proximity to the reactive rhodium metal carbene center for facile C-H insertion.

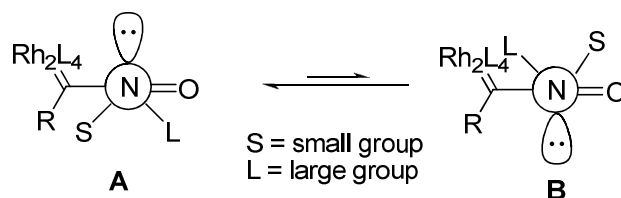


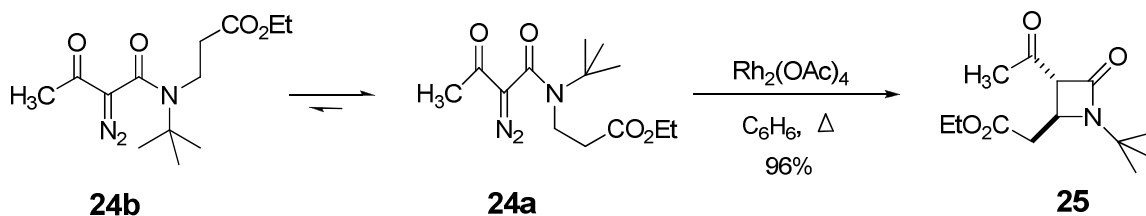
**Figure 2.** Reactive conformers based on conformational preferences.

When such a conformational bias is present, site selectivity for C-H insertion is retained. This can clearly be seen in the results from intramolecular metal carbene reactions of diazoacetoacetamides (Scheme 7).<sup>20</sup> Neither C-H insertion into the C-H bond of the *tert*-butyl group nor C-H insertion into the position  $\alpha$  to the ester functional group occurred, even though both would have produced an ordinarily favored five-membered ring. However, the methylene group adjacent to the ester functionality is deactivated due to the presence of an electron-withdrawing group.

<sup>19</sup> (a) Taber, D. F.; Ruckle, R. E., Jr. *J. Am. Chem. Soc.*, **1986**, *108*, 7686-7693. (b) Wee, A. G. H.; Liu, B.; Zhang, L. *J. Org. Chem.*, **1992**, *57*, 4404-4414. (c) Doyle, M. P.; Taunton, J.; Pho, H. Q. *Tetrahedron Lett.*, **1989**, *30*, 5397-5400. (d) Doyle, M. P.; Pieters, R. J.; Taunton, J.; Pho, H. Q.; Padwa, A.; Hertzog, D. L.; Precedo, L. *J. Org. Chem.*, **1991**, *56*, 820-829.

<sup>20</sup> Doyle, M. P.; Pieters, R. J.; Taunton, J.; Pho, H. Q.; Padwa, A.; Hertzog, D. L.; Precedo, L. *J. Org. Chem.*, **1991**, *56*, 820-829.

The large *N-tert*-butyl substituent fixes the amide conformation and results in the preferred reactive conformer **A** (Figure 2), allowing C-H insertion only into the smaller *N*-substituent.

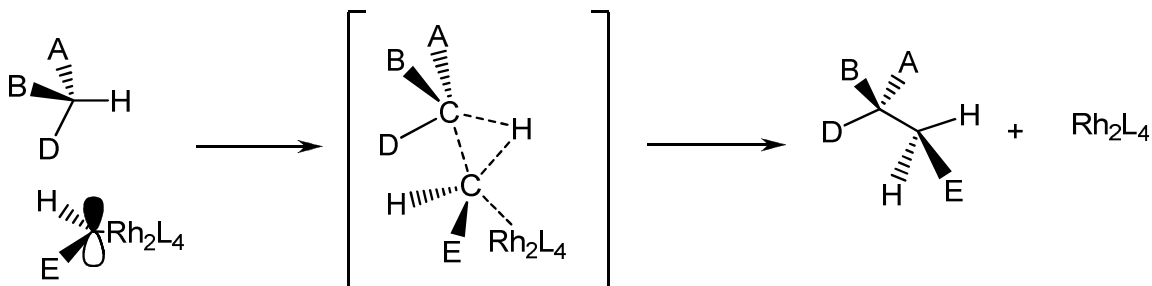


**Scheme 7.**  $\beta$ -lactam formation due to conformational influence.

The examples presented in this section illustrate that the controlling features of C-H insertion reactions include both electronic and steric interactions that define the preferred conformation of the reactive rhodium(II) metal carbene.

#### 1.4 Reaction mechanism:

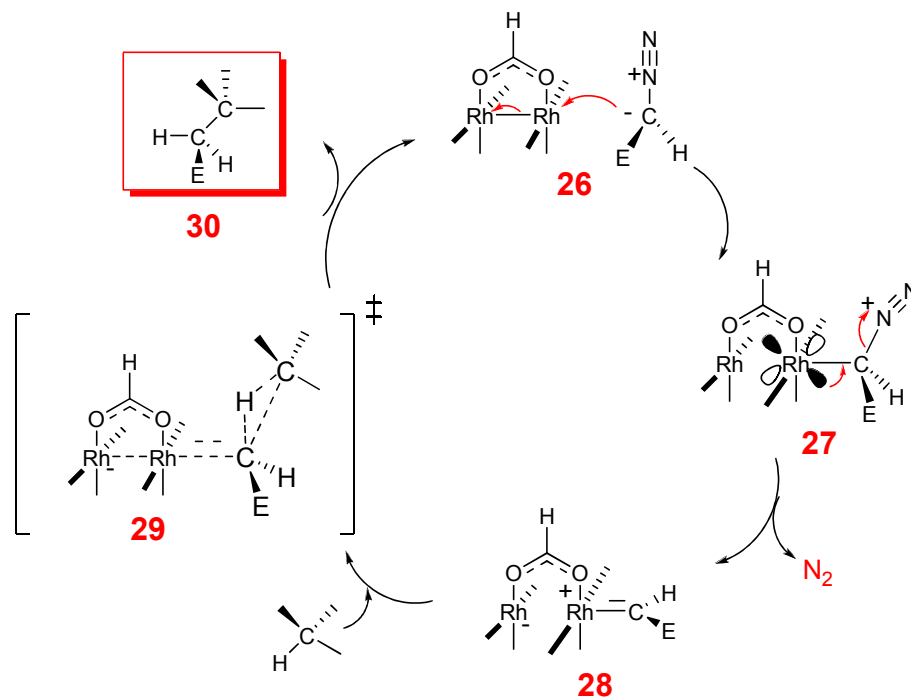
Doyle describes a three-centered concerted transition state of the C-H insertion mechanism (Scheme 8).<sup>21</sup> Doyle suggests that there is overlap of the metal carbene's p-orbital with the  $\sigma$ -orbital of the reacting C-H bond. This initiates the formation of the C-C and C-H bond concurrently with dissociation of the metal as shown in the three-centered concerted transition state.<sup>21</sup>



**Scheme 8.** Mechanism of the C-H insertion according to Doyle.

<sup>21</sup> Doyle, M. P.; Westrum, L. J.; Wolthuis, W. N. E.; See, M. M.; Boone, W. P.; Bagheri, V.; Pearson, M. *M. J. Am. Chem. Soc.*, **1993**, *115*, 958-964.

Nakamura *et al*<sup>22</sup> used B3LYP density functional theory to perform studies on the dirhodium tetracarboxylate-catalyzed C-H insertion reaction of methyl diazoacetate/diazomethane with methane or propane. These studies revealed the energetics, the electronic nature, and the geometry of important intermediates and transition states in the catalytic cycle.<sup>23</sup> The first step involves nucleophilic addition of methyl diazoacetate to the metal complex and breakage of the Rh-Rh bond, followed by loss of dinitrogen to generate the metal carbene. The two most crucial C-H insertion steps in Nakamura's model involve transfer of hydrogen from the alkane to the carbene carbon, and the other is regeneration of the Rh-Rh bond and formation of a new C-C bond, as depicted in transition state **29** (Scheme 9).<sup>23</sup> Nakamura's theoretical calculations confirmed the mechanistic proposal originally advanced by Doyle.<sup>23</sup>



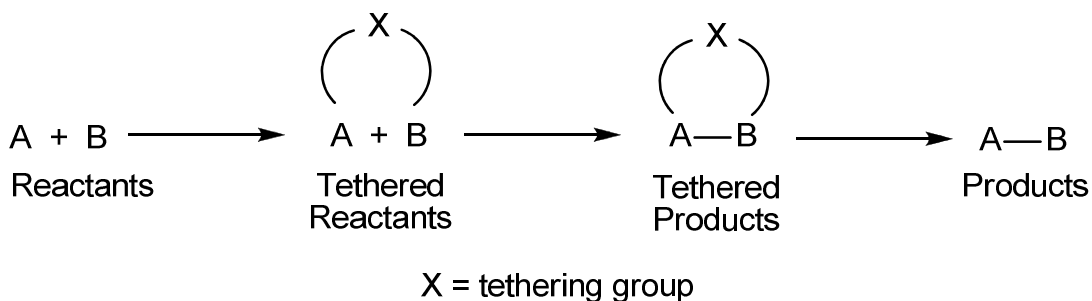
<sup>22</sup> Nakamura, E.; Yoshikai, N.; Yamanaka, M. *J. Am. Chem. Soc.*, **2002**, *124*, 7181-7192.

<sup>23</sup> Doyle, M. P.; Duffy, R.; Ratnikov, M.; Zhou, L. *Chem. Rev.*, **2010**, *110*, 704-724.

**Scheme 9.** Mechanism of the C-H insertion reaction according to Nakamura.

### **1.5 Tethered Intramolecular C-H insertion:**

Intramolecular C-H insertion reactions often display a high degree of both regio- and stereoselectivity which is important in the synthesis of complex molecules. Tethering groups have been used as protecting groups in intramolecular reactions and have also been transformed into other functionalities.<sup>24</sup> This strategy, for example, can involve tethering the reactants, carrying out the intramolecular reaction, and finally removing the tether (Scheme 10).<sup>24</sup> The nature of the tether is critical; if the tether is not desired in the final product; mild reagents should remove the tether chemoselectively. Even more desirable is using a tether that can be utilized in subsequent reactions.



**Scheme 10.** The use of tethering groups.

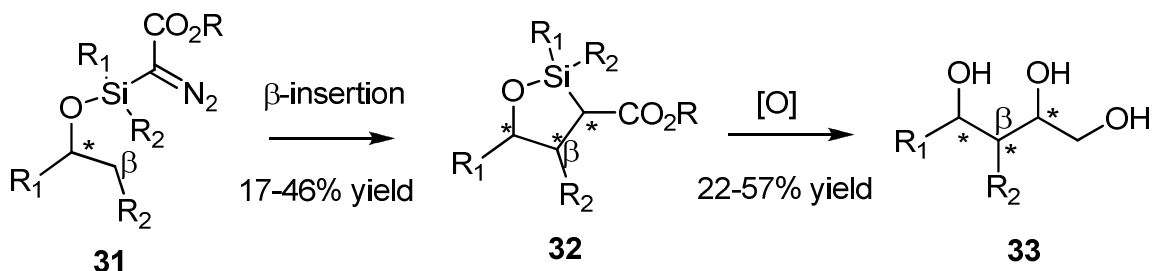
Both the silyl and the sulfonate groups have emerged as tethers for C-H functionalization.<sup>25</sup> Marsden reported the synthesis of stereocontrolled polyol **33** via C-H insertion reactions of silicon tethered diazoacetates **31** (Scheme 11).<sup>25a</sup> The versatility of the silyl group, such as being able to be transformed into hydroxyl functionalities *via* the Tamao-Fleming oxidation,<sup>26</sup> has allowed the synthesis of

<sup>24</sup> Bols, M.; Skrydstrup, T. *Chem. Rev.*, **1995**, *95*, 1253-1277.

<sup>25</sup> (a) Kablean, S. N.; Marsden, S. P.; Craig, A. M. *Tetrahedron Lett.*, **1998**, *39*, 5109-5112. (b) John, J. P.; Novikov, A. V. *Organic Lett.*, **2007**, *9*, 61-63. (c) Wolckenhauer, S. A.; Devlin, A. S.; Du Bois, J. *Organic Lett.*, **2007**, *9*, 4363-4366.

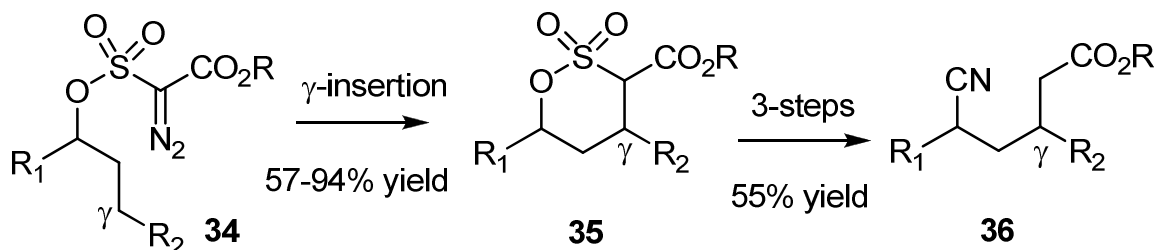
<sup>26</sup> Fleming, I.; Henning, R.; Plaut, H. *J. Chem. Soc., Chem. Commun.*, **1984**, 29-31.

polyols in a stereo- and regio-controlled manner. However, the C-H insertion reactions of silicon tethered diazoacetates **31** were relatively low yielding for most substrates tested.<sup>27</sup>



**Scheme 11.** Silicon tethered intramolecular C-H insertion reactions.

Another tether reported for intramolecular C-H insertion is the sulfonate tether. Novikov<sup>25b</sup> and Du Bois<sup>25c</sup> devised sulfonate ester derivatives, exemplified by **34**, that are strongly biased towards 1,6-C-H insertion and thus offer a general method for assembling  $\delta$ -sulfones **35**. The value of these heterocycles is demonstrated in both reductive and oxidative reactions that make possible the excision of the sulfonate group (Scheme 12). Nonetheless, the removal of the sulfonate group requires the use of sodium cyanide and oxalyl chloride, which makes the sulfonate tether less attractive as a synthetic intermediate en route to complex molecules.

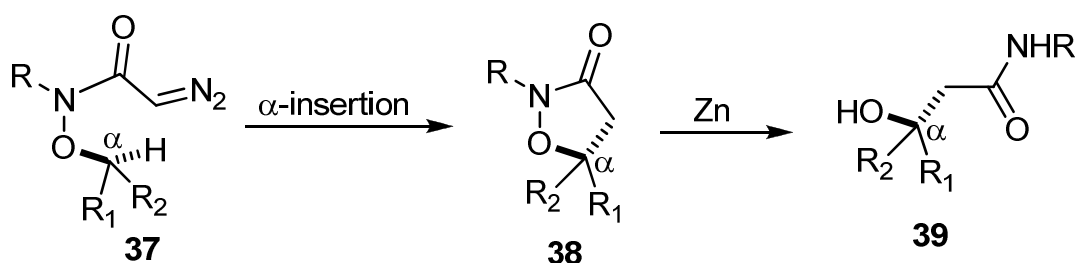


**Scheme 12.** Sulfonate tethered intramolecular C-H insertion reactions.

The developments by Marsden, Novikov, and Dubois are examples of the metal carbene inserting into the C-H bond that is *beta* and *gamma* to the heteroatom bearing the silicon tethered diazoacetates and the diazosulfonate moiety, respectively.

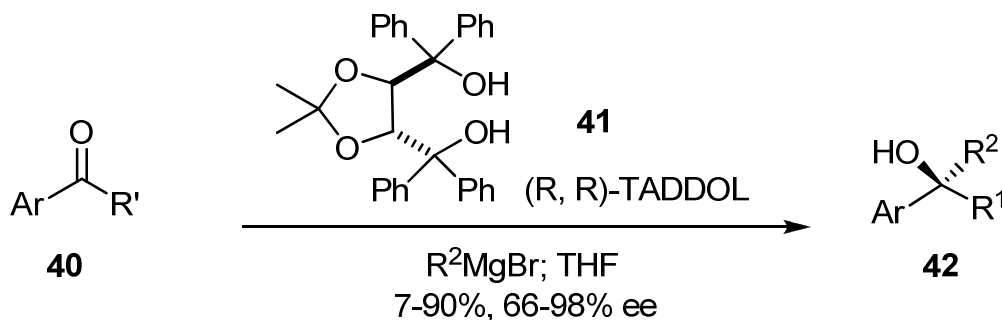
<sup>27</sup> Taber, D. F.; Petty, E. H. *J. Org. Chem.*, **1982**, *47*, 4808-4809.

To further expand on the versatility of tethered intramolecular C-H insertion reactions, we aimed to use a new tether, the N-O tether, where insertion of the metal carbene into the C-H bond that is *alpha* to the heteroatom bearing the diazo functionality is favored. Once the 1,5-C-H insertion into the hydrogen *alpha* to the heteroatom has occurred, cleavage of the N-O bond provides facile synthesis of enantiopure tertiary alcohols (Scheme 13). This methodology serves to address a void in methods to making tertiary alcohols in optically active form.



**Scheme 13.** The use of labile N-O tether in intramolecular C-H insertion reactions.

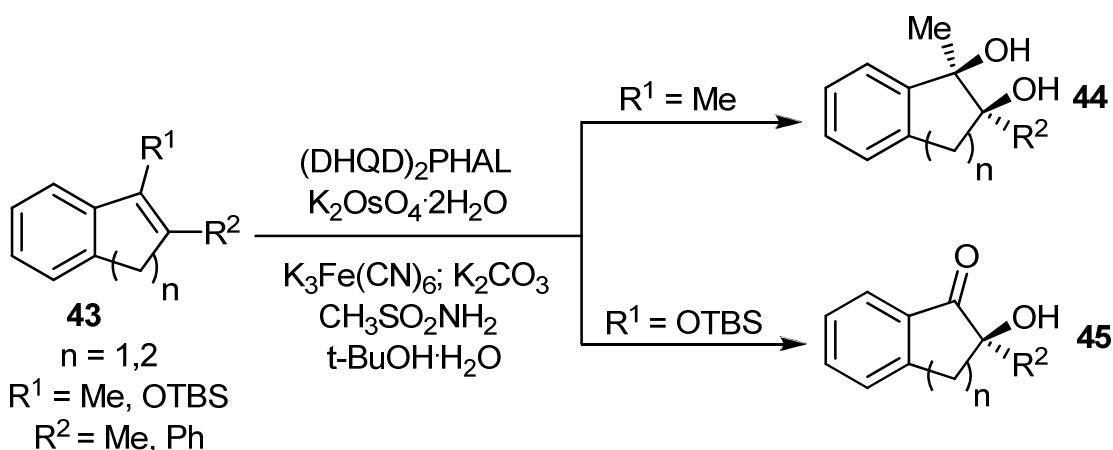
One approach to making tertiary alcohols is the enantioselective addition of organolithium, or Grignard reagents, to ketones.<sup>28</sup> Seebach and Weber developed an effective asymmetric addition of alkyl Grignard reagents to ketones **40**, however, they used stoichiometric amounts of (R,R)-TADDOL **41** (Scheme 14).<sup>28</sup>



**Scheme 14.** Seebach and Weber's asymmetric approach towards the synthesis of tertiary alcohols.

<sup>28</sup> (a) Weber, B.; Seebach, D. *Angew. Chem. Int. Ed.*, **1992**, *31*, 84-86. (b) Weber, B.; Seebach, D. *Tetrahedron*, **1994**, *50*, 6117-6128.

The synthesis of tertiary alcohols has also been reported in Sharpless's asymmetric dihydroxylation (Scheme 15).<sup>29</sup> Tertiary alcohols **45**, (*S*)-2-hydroxy-2,3-dihydro-1*H*-inden-1-one and (*S*)-2-hydroxy-3,4-dihydronaphthalen-1(2*H*)-one, are obtained with high enantioselectivity by asymmetric dihydroxylation of 1,1-disubstituted, trisubstituted, and tetrasubstituted olefins.<sup>29</sup> However, the synthesis of tertiary diols **44**, (1*R*,2*S*)-dihydroindene-1,2-diol and (1*R*,2*S*)-tetrahydronaphthalene-1,2-diol, using asymmetric dihydroxylation introduces an additional hydroxyl functionality that might not be required in the desired product.



**Scheme 15.** Sharpless asymmetric dihydroxylation.

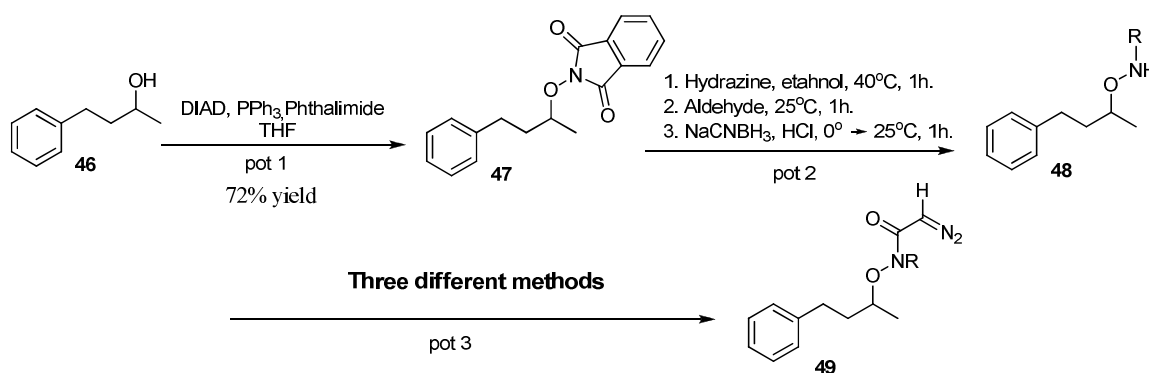
There remains a lack of an efficient methodology to access optically-pure tertiary alcohols despite the progress achieved towards their synthesis. Therefore, there is still a need to further explore an efficient, wide scope, and a facile way of making tertiary alcohols. The labile N-O tether methodology has the potential to produce the “difficult-to-make” tertiary alcohols in optically active form.

<sup>29</sup> Morikawa, K.; Park, J.; Andersson, P. G.; Hashiyama, T.; Sharpless, K. B. *J. Am. Chem. Soc.*, **1993**, *115*, 8463-8464.

## 2. Research Discussion

### 2.1 Synthesis of model substrate for N-O tethered C-H insertion:

The preparation of the starting material, *N*-alkoxydiazooamides **49**, was accomplished via a three-pot synthesis, starting from secondary alcohol **46** (Scheme 16). Gram quantities of the diazo compound **49** were first synthesized by isolating each intermediate in seven separate steps. In order to make our methodology more efficient, we explored combining several steps in the same pot without isolation/purification. The Scheme below outlines the three-pot synthesis of the *N*-alkoxydiazooamide **49**.



**Scheme 16.** Three-pot synthesis of *N*-alkoxydiazooamide **49**.

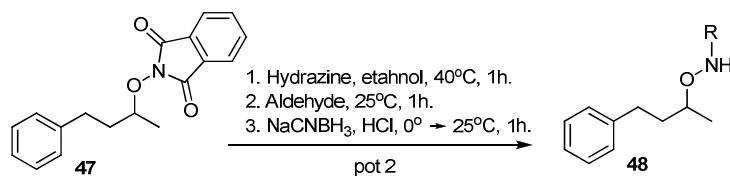
We first tried to perform the Mitsunobu reaction<sup>30</sup> with the subsequent oxime formation in one pot. However, combining these two reactions was not successful. We conjectured that the byproduct from the Mitsunobu reaction, diisopropyl hydrazine-1,2-dicarboxylate, might have inhibited oxime formation by reacting with the aldehyde. Therefore, phthalimide **47** was purified after the Mitsunobu reaction to remove the diisopropyl hydrazine-1,2-dicarboxylate. The Mitsunobu reaction was sensitive to the ester alkyl group of the azocarboxylate used. For example, the use of

<sup>30</sup> Grochowski, E.; Jurczak, J. *Synthesis*, **1976**, 682-684.

diethylazocarboxylate resulted in a complex product mixture whereas both isopropyl and *tert*-butyl azocarboxylates gave phthalimide **47** in 72% yield.

Next, we explored whether hydrazine hydrolysis of phthalimide **47** followed by tandem imine formation and sodium cyanoborohydride reduction could afford *N*-alkoxyamine **48** in one pot (Scheme 16, pot 2). While performing the hydrazine hydrolysis, I noticed that the oxime was forming from adventitious acetone which prompted me to believe that hydrazine hydrolysis and oxime formation could be performed in the same pot. The one-pot synthesis of *N*-alkoxyamine **48** via hydrazine hydrolysis, oxime formation, and sodium cyanoborohydride reduction proceeded smoothly to afford *N*-alkoxyamine **48** in 80-92% yield (Table 4).

**Table 4.** Synthesis of *N*-alkoxyamine **48**.

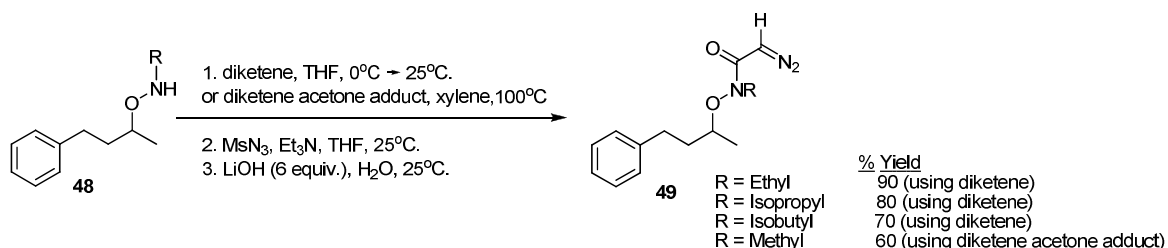


Entry	R	Yield (%)
1	Methyl	90
2	Ethyl	92
3	Isopropyl	79
4	Isobutyl	80
5	Mesityl	83
6	Benzyl	87
7	<i>p</i> -methoxy benzyl	81
8	<i>p</i> -nitro benzyl	91

## 2.2 Different methods for the synthesis of *N*-alkoxydiazamide substrates

With gram quantities of *N*-alkoxyamine **48** in hand, we proceeded to synthesize the *N*-alkoxydiazamides **49** needed for the C-H insertion studies. We investigated three different methods for this synthesis; and the yields ranged from 50-90%, depending on the R group and the method used. The following subsections provide a breakdown of the three methods that were used for the synthesis of *N*-alkoxydiazamides **49** and the challenges faced with each one.

### 2.2a Method A (using diketene or diketene acetone adduct)



**Scheme 17.** Synthesis of *N*-alkoxydiazamide **49**, method A.

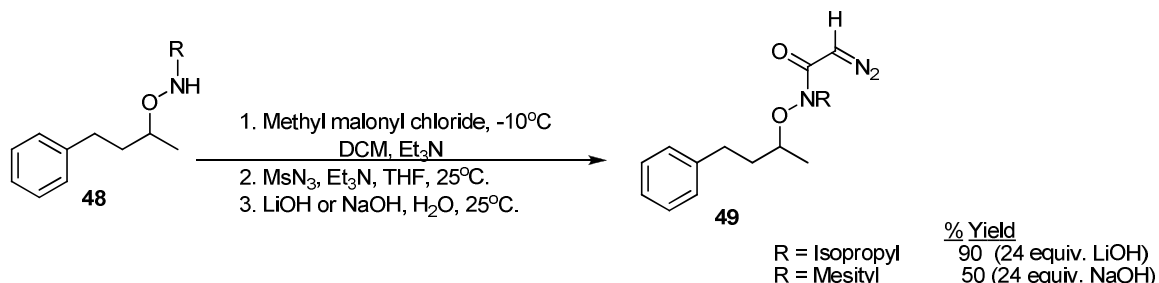
A one-pot conversion<sup>31</sup> of **48** into *N*-alkoxydiazamide **49** was accomplished by treating compound **48** with freshly distilled diketene<sup>32</sup> in THF overnight. Mesityl azide and triethylamine were then added, and the reaction mixture was stirred overnight. Lastly, six equivalents of LiOH in water was added, and the diazo compound **49** was finally obtained in an average yield of 80% ± 5. Despite the good yields obtained using the diketene reagent, looking into an alternative method for the synthesis of *N*-alkoxydiazamides **49** was unavoidable due to commercial shortage of the diketene reagent. A different chemical, 2,2,6-trimethyl-4*H*-1,3-dioxin-4-one, also known as the diketene acetone adduct, was used to react with *N*-

<sup>31</sup> Chen, Z.; Chen, Z.; Jiang, Y.; Hu, W. *Tetrahedron*, **2005**, *61*, 1579-1586.

<sup>32</sup> Doyle, M. P.; Winchester, W. R.; Protopopova, M. N.; Kazala, A. P.; Westrum, L. J. *Org. Synth.*, **1996**, *73*, 13-24.

alkoxyamine **48** in xylene at 100°C.<sup>33</sup> The diketene acetone adduct method resulted in moderate yields (60% yield, R = methyl) but we continued to consider other alternative methods to synthesize *N*-alkoxydiazamides **49** to achieve better yields (70-90 % yield).

### **2.2b Method B (using methyl malonyl chloride)**



**Scheme 18.** Synthesis of *N*-alkoxydiazamide **49**, method B.

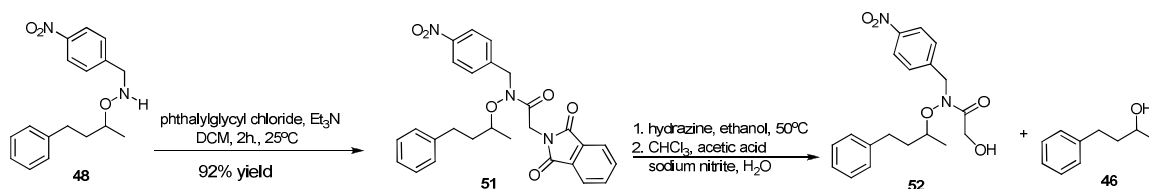
A one-pot conversion<sup>34</sup> of *N*-alkoxyamine **48** into *N*-alkoxydiazacetamide **49** was accomplished by treating compound **48** with methyl malonyl chloride in DCM at -10°C for 2 hours. Mesyl azide and triethylamine were then added, and the reaction mixture was stirred overnight. The problem that was faced with this method was the deacylation step. The deacylation step would slowly take place but only after treating the diazo compound with at least 24 equivalents of sodium hydroxide overnight. The amount of either LiOH or NaOH that was required makes this method inefficient and hence our efforts to find a better method to synthesize *N*-alkoxydiazamides **49** continued.

### **2.2c Method C (using phthalylglycyl chloride)**

<sup>33</sup> Clemens, R. J.; Hyatt, J. A. *J. Org. Chem.*, **1985**, *50*, 2431-2435.

<sup>34</sup> Tietze, L. F.; Schuenke, C. *Eur. J. Org. Chem.*, **1998**, 2089-2099.

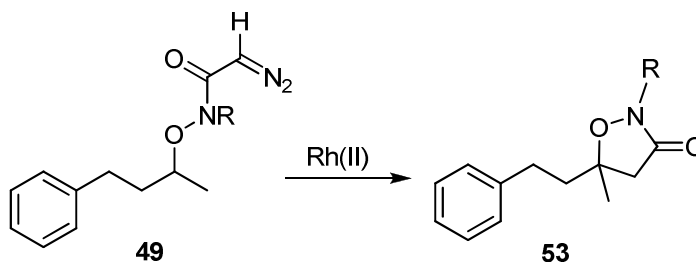




**Scheme 20.** Towards the synthesis of *N*-alkoxydiazamide **49**, (R = *p*-nitrobenzyl).

### **2.3 C-H insertion reaction, screening and optimization:**

Next, Jingxin Wang investigated the intramolecular C-H insertion reaction *alpha* to the oxygen atom bearing the diazocarbonyl moiety (Scheme 21).



**Scheme 21.** Intramolecular C-H insertion.

Jingxin initially explored the intramolecular C-H insertion reaction using different solvents to observe whether there is any solvent effect on the yield of the C-H insertion reaction (Table 5). We concluded that the polarity of the solvent does not affect the efficiency of the C-H insertion step; similar yields for the C-H insertion products were obtained in non-polar solvents such as hexane (entry 6, Table 5) and in more polar solvents such as DCM and DCE (entries 1 and 2, Table 5). Also, the product yield obtained in  $\alpha,\alpha,\alpha$ -trifluorotoluene is similar to that obtained using

toluene as the solvent, albeit in lower yields, possibly due to the rhodium acetate being less soluble in these solvents (entry 3 and 4, Table 5).

**Table 5.** Solvent screening.

Entry	Solvent	Yield (%) <b>53</b> <sup>a</sup>
1	DCM	50 <sup>b</sup>
2	DCE	50 <sup>b</sup>
3	Trifluorotoluene	33 <sup>b</sup>
4	Toluene	20 <sup>b</sup>
5	THF	48 <sup>c</sup>
6	Hexane	60 <sup>c</sup>

<sup>a</sup> Isolated yield of **53**, trace amount of 1,7-C-H insertion product was observed, average ratio 95:5. <sup>b</sup> 2 mol% of rhodium acetate, 20h, and at 25°C.

<sup>c</sup> 2 mol% of rhodium acetate, 1.5h, and at 40°C. Yield reported by Jingxin Wang.<sup>36</sup>

After exploring the effects of solvents on the yield of the C-H insertion reaction, Jingxin examined the effect of the dirhodium catalysts on product yield (Table 6). A number of different rhodium catalysts was screened, and the yield of the 1,5-C-H insertion product **53** was significant with Rh<sub>2</sub>(tfa)<sub>4</sub> (80% yield) and moderate with Rh<sub>2</sub>(pfb)<sub>4</sub> (50% yield), Rh<sub>2</sub>(OAc)<sub>4</sub> (50% yield), Rh<sub>2</sub>(oct)<sub>4</sub> (44% yield), and

---

<sup>36</sup> Wang, J.; Stefane, B.; Jaber, D.; Smith, J. A. I.; Vickery, C.; Diop, M.; Sintim, H. O. *Angew. Chem., Int. Ed.*, **2010**, *49*, 3964-3968.

Rh<sub>2</sub>(esp)<sub>2</sub> (53% yield). While the expected 1,5-C-H insertion product was the major product with all dirhodium catalysts, a C-H insertion byproduct resulting from the 1,7-C-H insertion was observed with all dirhodium catalysts (average ratio 95:5) except for those with the trifluoroacetate and perfluorobutyrate ligands. However, when using the electron withdrawing ligands, trifluoroacetate and perfluorobutyrate, the formation of the 1,7-C-H insertion byproduct was increased (ratio 62:38). We decided to choose rhodium acetate as our catalyst of choice because it was available in abundance.

**Table 6.** Catalyst optimization.

Entry <sup>[a]</sup>	Catalyst	Yield <sup>a</sup> (%) 53
1	Rh <sub>2</sub> (OAc) <sub>4</sub>	50 <sup>b</sup>
2	Rh <sub>2</sub> (esp) <sub>2</sub>	53 <sup>c</sup>
3	Rh <sub>2</sub> (tfa) <sub>4</sub>	79 <sup>d</sup>
4	Rh <sub>2</sub> (pfb) <sub>4</sub>	48 <sup>e</sup>
5	Rh <sub>2</sub> (oct) <sub>4</sub>	44 <sup>b</sup>
8	Rh <sub>2</sub> (cap) <sub>4</sub>	22 <sup>f</sup>

<sup>a</sup> All reactions are based on a 0.5 mmole scale. <sup>b</sup> 2 mol% catalyst, 20h, and at 25°C, in DCM. <sup>c</sup> 0.5 mol % catalyst, DCM, 1h, 40°C. <sup>d</sup> 2 mol% catalyst, DCM, 40°C, 1.5h. Yield reported by Jingxin Wang.<sup>44</sup> <sup>e</sup> 2 mol% catalyst, DCM, 40°C, 1.5h, using a different substrate. Yield reported by Jingxin Wang. <sup>f</sup> 0.5 mol % catalyst, DCE, 1h, 70°C.

Next, Jingxin and I investigated the effect that the reaction temperature plays in product yield (Table 7). Most C-H insertion reactions in the literature have been performed in DCM, at 40°C reflux. A few others were done at room temperature, and very few at 0°C. We obtained better yields (60%) when the C-H insertion reaction was performed at 40°C (compare entries 1,2,3 in Table 7). Since the boiling point of

dichloromethane is 40°C, 1,2-dichloroethane was used for the higher temperatures (84°C) (entry 5, Table 7). In addition, the duration of the reaction did not affect the product yield at 40°C. The same conditions were used to perform the C-H insertion reactions (entry 3, 4, Table 7) that were left to stir for 20 hours and for one hour at 40°C. These reactions afforded the 1,5-C-H insertion product **53** in 60% yield.

**Table 7<sup>a</sup>.** Temperature optimization.

<b>Entry<sup>[a]</sup></b>	<b>Temp./°C</b>	<b>Time/h</b>	<b>Yield (%) <b>53</b></b>
1	20	20	50
2	0	20	40
3	40	20	61
4	40	1	60

<sup>a</sup> All reactions were performed using 2 mol% of rhodium acetate in DCM. Trace amount of the 1,7-C-H insertion product was observed, average ratio 92:8.

Finally, Jingxin and I explored the catalyst loading effects on the yield of the intramolecular C-H insertion of *N*-alkoxydiazoacetamide. Lowering the catalyst loading from 2 mol% to 0.5 mol% did not drastically change the yield of the reaction (compare entries 1-3, Table 8). The 1,5-C-H insertion product **53** can be obtained by using a catalyst loading as low as 0.5 mol%. After exploring different conditions for the intramolecular C-H insertion reaction, the C-H insertion reactions were performed using rhodium acetate in reflux dichloromethane.

**Table 8<sup>a</sup>.** Catalyst loading optimization.

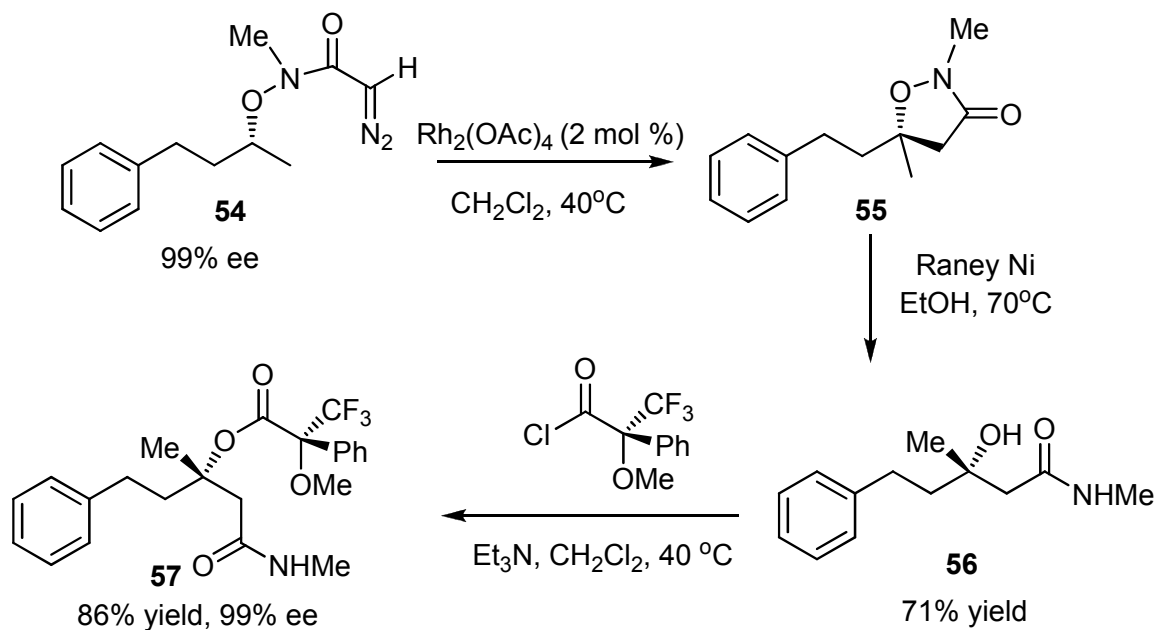
Entry <sup>a</sup>	Solvent	Catalyst Load (mol %)	Temp./°C	Yield (%) <b>53</b>
1	DCM	2	40	60
2	DCM	1	40	71
3	DCM	0.5	40	71
4	DCE	0.5	70	74

<sup>a</sup> All reactions were performed using rhodium acetate, 1h on a 1.0 mmole reaction scale. Trace amount of the 1,7-C-H insertion product was observed average ratio 95:5.

Next, Jingxin investigated the decomposition reaction of enantiomerically enriched *N*-alkoxydiazoacetamide **54** (99% ee) (Scheme 22).<sup>37</sup> The C-H insertion reaction is stereospecific,<sup>38</sup> it occurs with retention of stereochemistry in line with literature precedent.<sup>38</sup> Accordingly, subjecting enantiopure *N*-alkoxydiazoacetamide compound **54** to dirhodium catalysis resulted in enantiomerically enriched compound **55** (99% ee). Then treating the enantiopure 1,5-C-H insertion product **55** with raney nickel afforded enantiopure tertiary alcohol **56** in 99% ee; conforming that racemization does not occur in N-O tethered C-H insertion reactions.

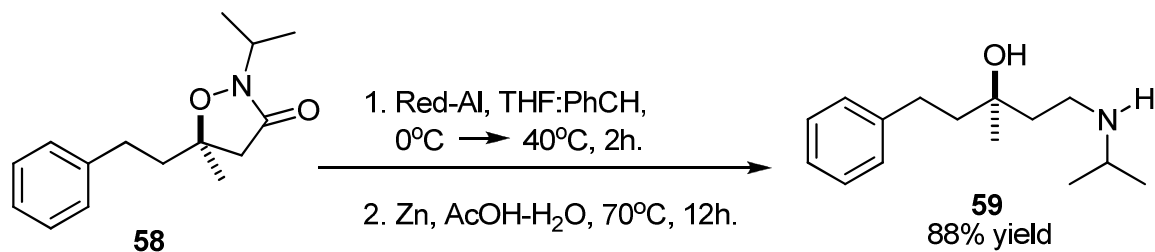
<sup>37</sup> Wang, J.; Stefane, B.; Jaber, D.; Smith, J. A. I.; Vickery, C.; Diop, M.; Sintim, H. O. *Angew. Chem., Int. Ed.*, **2010**, *49*, 3964-3968. The reactions in this scheme were performed by Jingxin Wang.

<sup>38</sup> Taber, D. F.; Petty, E. H.; Raman, K. *J. Am. Chem. Soc.*, **1985**, *107*, 196-199.



**Scheme 22.** Intramolecular C-H insertion on an enantiomerically enriched substrate.

In addition to cleaving the N-O linkage using Raney Ni, I examined the feasibility of the cleavage of the N-O moiety in **58** after reducing the carbonyl group to afford 1,3- hydroxy amino compound **59** (Scheme 23). The reduction of the carbonyl group and the N-O moiety can be conveniently achieved by treatment of **58** with Red-Al in anhydrous THF and toluene, followed by a subsequent treatment with zinc dust to afford the desired tertiary alcohol **59** in 88% yield.

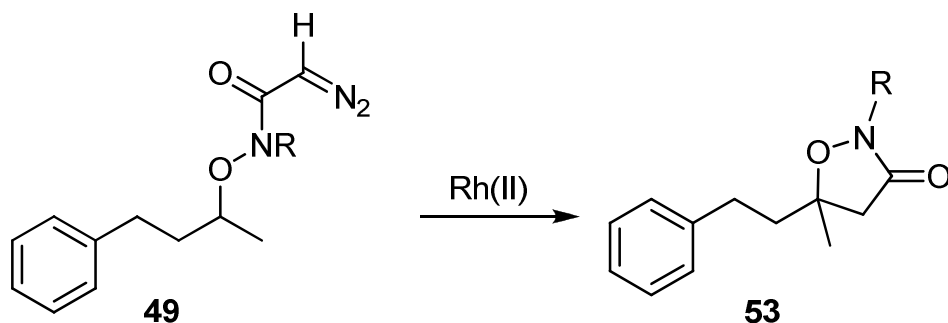


**Scheme 23.** N-O cleavage to afford the 1,3 hydroxy amino functionality.

#### 2.4 Substrate scope of the intramolecular C-H insertion reaction:

To evaluate the scope and the generality of the N-O tethered intramolecular C-H insertion method Jingxin investigated the effect of the *N*-substituent on the outcome of the C-H insertion step. The following table (Table 9) contains the substrates that were investigated by varying the substituent on nitrogen. The major product for all substrates was the 1,5-C-H insertion product **53** regardless of whether the R group was an alkyl or an aromatic substituent. Some byproducts were also observed such as the 1,7-C-H insertion, 1,6-C-H insertion and the ketone byproduct. There was no C-H insertion to the substituent on nitrogen that was observed.

**Table 9.** Substrate scope of the C-H insertion reaction.



Entry	R	Yield (%) <sup>[a]</sup>
1	Methyl	41
2	Ethyl	61
3	Isopropyl	69
4	Isobutyl	51
5	Mesityl	58
6	Benzyl	59
7	<i>p</i> -methoxy benzyl	62

<sup>a</sup> In all cases the 1,5-C-H insertion is the major product. Byproducts such as the 1,7-C-H insertion product and a ketone product and in some cases the 1,6-C-H insertion product were also observed. Yield for most reactions reported by Jingxin Wang.<sup>39</sup>

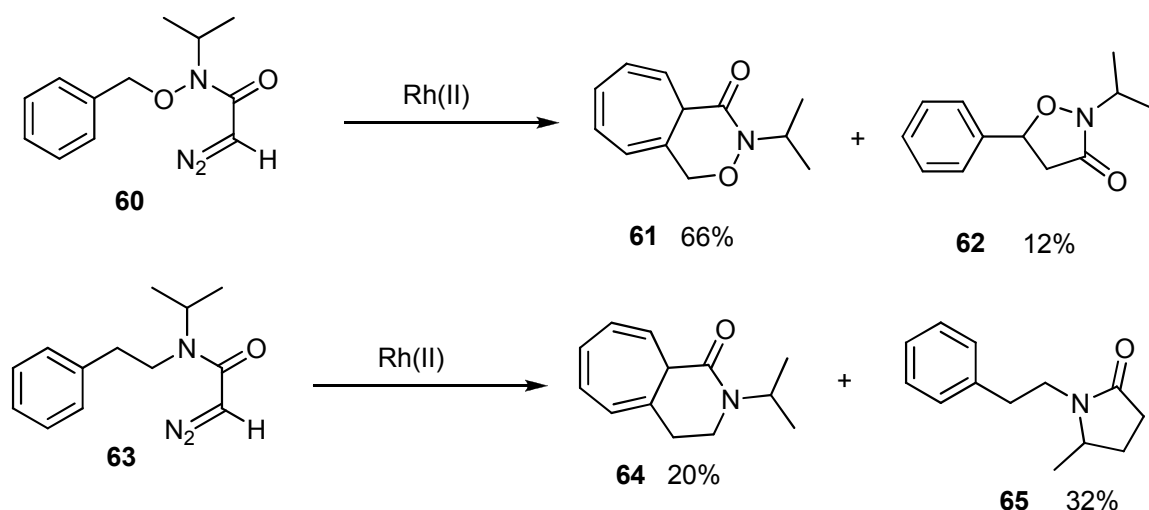
To further expand our knowledge and understanding of the effect the N-O linkage has on product selectivity, I synthesized two similar *N*-alkoxydiazoacetamide compounds where **60** contains the N-O linkage, and **63** does not (Scheme 24).<sup>40</sup> Preliminary results performed by Jingxin Wang show that the major product of the diazo decomposition of compound **63** (without the N-O linkage) is the C-H insertion product whereas the major product for the diazo decomposition of compound **60** (with the N-O linkage) is the aromatic cycloaddition product (Scheme 24).<sup>41</sup> Furthermore, the C-H insertion product of the two *N*-alkoxydiazoacetamide decomposition reactions are different. In the presence of the N-O linkage (compound **60**) the carbene inserts next to the oxygen heteroatom whereas in the absence of the N-O linkage (compound **63**) insertion occurs into the methyl group of the isopropyl nitrogen substituent. This result further supports our hypothesis that electronics of

<sup>39</sup> Wang, J.; Stefane, B.; Jaber, D.; Smith, J. A. I.; Vickery, C.; Diop, M.; Sintim, H. O. *Angew. Chem., Int. Ed.*, **2010**, *49*, 3964-3968.

<sup>40</sup> C-H insertion reactions performed by Jingxin Wang.

<sup>41</sup> The diazo compounds were synthesized by myself and the decomposition reactions were performed by Jingxin Wang.

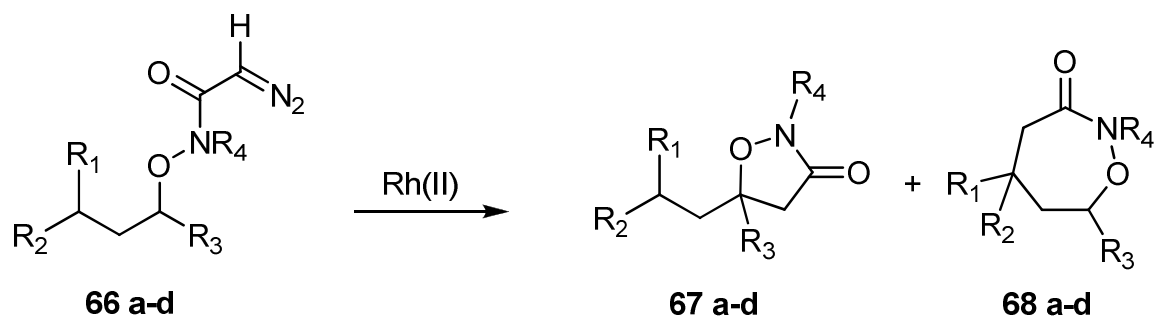
the *N*-alkoxydiazooacetamide play a role in determining the *N*-alkoxydiazooacetamide substrate conformation.



**Scheme 24.** C-H insertion versus cyclopropanation.

We have shown that the desired 1,5-C-H insertion product is a significant result of the C-H insertion reaction. We can, however, manipulate the substrate to deactivate the 1,5-C-H bond and promote the 1,7-C-H insertion product to take place. This was nicely illustrated using *N*-alkoxydiazooacetamide compounds **66a-b**, when the carbon  $\alpha$  to the oxygen heteroatom is a methylene group ( $R_3 = \text{H}$ ) the amount of the 1,7-C-H insertion product increased (Table 10, entry 1-2). Furthermore, with *N*-alkoxydiazooacetamide compounds **66c-d** deactivating the C-H bond adjacent to the oxygen heteroatom was achieved by positioning an electron withdrawing group next to that C-H bond, and thus the 1,7-C-H insertion product was predominately formed (Table 10, entry 3-4).

**Table 10<sup>a</sup>.** 1,5 vs. 1,7-C-H insertion.



Entry	Substrate	R1	R2	R3	R4	Yield <sup>b</sup> (%) (67+68)	Ratio <sup>c</sup> 67:68
1	66a	Ph	H	H	<i>p</i> -methoxy benzyl	65	40:25
2	66b	Ph	Me	H	<i>p</i> -methoxy benzyl	65	36:29
3	66c	Me	H	CO <sub>2</sub> Et	Bn	53	5:48
4	66d	Ph	H	CO <sub>2</sub> Et	Bn	54	0:54

<sup>a</sup> C-H insertion reactions performed by Jingxin Wang.<sup>49</sup> <sup>b</sup>Yield of isolated product. <sup>c</sup>Ratio based on the yields of pure isolated products.

### 3. Conclusion

In conclusion, we have devised a novel labile tether, the N-O tether, for intramolecular C-H insertion reactions that has the potential to be used for the synthesis of tertiary alcohols in optically active form. The present work represents the first example of intramolecular C-H insertion reaction of *N*-alkoxydiazoacetamide. The resulting C-H insertion products were converted to tertiary-amino alcohols *via* cleavage of the N-O tether. This approach allows the regioselective insertion of metal carbenes into the C-H bond alpha to a heteroatom and leads to the formation of tertiary stereocenters.

### 4. Experimental

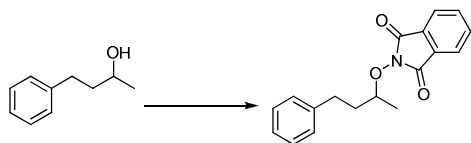
**General:** All reagents were obtained commercially unless otherwise noted. Reactions were performed using oven-dried glassware under an atmosphere of argon. Air- and moisture-sensitive liquids and solutions were transferred via syringe or stainless steel cannula. Thin-layer chromatography (TLC) was performed on Merck Kieselgel 60 F<sub>254</sub> plates. Visualization of the developed chromatogram was accomplished by ultraviolet light or by staining with iodine, butanolic ninhydrin, *p*-anisaldehyde, or phosphomolybdic acid (PMA) solution. Chromatographic purification of products was accomplished using forced-flow chromatography on silica gel (230x400 mesh). Compounds purified by chromatography on silica gel were typically applied to the absorbent bed using the indicated solvent conditions with a minimum amount of added dichloromethane as needed for solubility. Unless otherwise described, reactions were carried out at ambient temperature. Combined organic extracts were dried over anhydrous MgSO<sub>4</sub>. Solvents were removed from the reaction mixture or combined organic extracts by concentration under reduced pressure using a rotary evaporator with bath at 30-35°C.

NMR spectra were obtained on Bruker AV-400, Bruker DRX-400 (<sup>1</sup>H at 400 MHz, <sup>13</sup>C at 100 MHz), Bruker DRX-500 (<sup>1</sup>H at 500 MHz, <sup>13</sup>C at 125 MHz), or Bruker AVIII-600 (<sup>1</sup>H at 600 MHz, <sup>13</sup>C at 150 MHz). Absorptions and their splitting from <sup>1</sup>H NMR spectra are recorded as follows relative to residual solvent peaks: (s = singlet, d = doublet, t = triplet, q = quartet, dd = doublet of doublets, td = triplet of doublets, dq = doublet of quartets, ddd = doublet of doublet of doublets, tdd triplet of doublet of doublets, dddd = doublet of doublet of doublet of doublets, m = multiplet, comp = composite), coupling constant (Hz), and integration. Chemical shifts (δ, ppm) for <sup>13</sup>C NMR spectra are reported relative to the residual solvent peak. All spectra are

recorded in  $\text{CDCl}_3$  as solvent, unless otherwise described. High resolution mass spectra (HRMS) were recorded on a JEOL AccuTOF-CS system (ESI positive, needle voltage 1800-2400eV, flow rate 50uL/min). IR spectra were recorded on a JASCO FT-IR-4100 instrument. Optical rotations for chiral compounds were measured using a digital polarimeter (DIP-1000). The rhodium catalysts were obtained commercially from Sigma-Aldrich.

### General Experimental Procedures

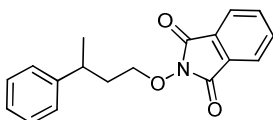
#### Procedure for the Mitsunobu Reaction of 2-(4-phenylbutan-2-yloxy)isoindoline-1,3-dione



4-Phenyl-2-butanol (5.0g, 0.033 moles), *N*-hydroxyphthalimide (5.4g, 0.033 mmoles), and triphenylphosphine (8.7g, 0.033 moles) were dissolved in THF (166 mL) and treated with diisopropyl azodicarboxylate (7.1 ml, 0.036 moles). The reaction mixture became dark-red and the color disappeared after a few minutes. The reaction is exothermic as heat was produced on mixing of the reagents. The solution was left to stir at room temperature for 24 hours. The solvent was dried over anhydrous  $\text{MgSO}_4$  and then evaporated under reduced pressure. The residue was purified by chromatography on silica gel (gradient elution: hexane/ethyl acetate (98% to 90% hexane); 72% yield, based on a 0.033 mole scale of 4-phenol-2-butanol.  $^1\text{H}$  NMR (400 MHz,  $\text{CDCl}_3$ )  $\delta$  ppm 7.92-7.82 (comp, 2H), 7.82-7.72 (comp, 2H), 7.34-7.28 (comp, 4H), 7.24-7.19 (m, 1H), 4.46 (sext.,  $J = 6.4$  Hz, 1H), 2.92 (t,  $J = 8.0$  Hz, 2H), 2.23-2.11 (m, 1H), 1.99-1.90 (m, 1H), 1.41 (d,  $J = 6.4$  Hz, 3H).  $^{13}\text{C}$  NMR (100

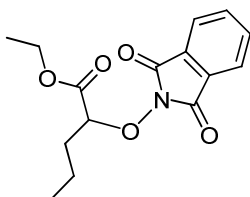
MHz, CDCl<sub>3</sub>)  $\delta$  ppm 164.4, 141.7, 134.4, 128.9, 128.4, 128.3, 125.8, 123.4, 83.7, 36.7, 31.4, 18.9. HRMS (ESI<sup>+</sup>): expected mass 296.1287, found 296.1297.

### 2-(3-phenylbutoxy)isoindoline-1,3-dione



The Mitsunobu reaction procedure of 2-(4-phenylbutan-2-yloxy)isoindoline-1,3-dione was repeated with 3-phenyl-1-butanol. The residue from the reaction was purified by chromatography on silica gel (gradient elution: hexane/ethyl acetate (100% to 98% hexane) 99% yield, based on a 5.3 mmole scale of 3-phenyl-1-butanol. <sup>1</sup>H NMR (400 MHz, CDCl<sub>3</sub>)  $\delta$  ppm 7.89-7.79 (comp, 2H), 7.80-7.70 (comp, 2H), 7.34-7.27 (comp, 4H), 7.23-7.18 (m, 1H), 4.16-4.07 (m, 2H), 3.1 (sext.,  $J = 7.6$  Hz, 1H), 2.15-2.00 (m, 2H), 1.36 (d,  $J = 7.6$  Hz, 3H). <sup>13</sup>C NMR (100 MHz, CDCl<sub>3</sub>)  $\delta$  ppm 163.6, 146.1, 134.4, 128.9, 128.4, 127.0, 126.2, 123.4, 76.7, 36.5, 36.1, 22.1. HRMS (ESI<sup>+</sup>): expected mass 296.1287, found 296.1290.

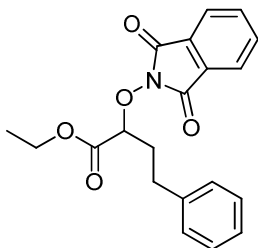
### Ethyl 2-(1,3-dioxoisindolin-2-yloxy)pentanoate



The Mitsunobu reaction procedure of 2-(4-phenylbutan-2-yloxy)isoindoline-1,3-dione was repeated with ethyl 2-hydroxyvalerate. The residue from the reaction was purified by chromatography on silica gel (gradient elution: hexane/ethyl acetate (98% to 95% hexane) 97% yield, based on a 10 mmole scale of ethyl-2-hydroxy valerate.

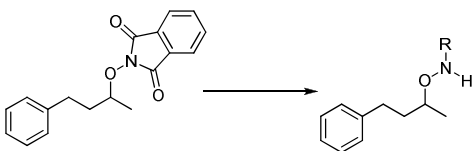
$^1\text{H}$  NMR (400 MHz,  $\text{CDCl}_3$ )  $\delta$  ppm 7.70-7.63 (comp, 4H), 4.6 (t,  $J = 6.4$  Hz, 1H), 4.16-4.04 (m, 2H), 1.93-1.83 (m, 1H), 1.80-1.71 (m, 1H), 1.53-1.44 (comp, 2H), 1.15 (t,  $J = 7.0$  Hz, 3H), 0.88 (t,  $J = 7.5$  Hz, 3H).  $^{13}\text{C}$  NMR (100 MHz,  $\text{CDCl}_3$ )  $\delta$  ppm 169.2, 162.8, 134.3, 128.4, 123.2, 84.9, 77.0, 61.1, 32.4, 17.8, 13.6, 13.3. HRMS (ESI<sup>+</sup>): expected mass 292.1179, found 292.1181.

### Ethyl 2-(1,3-dioxoisindolin-2-yloxy)-4-phenylbutanoate



The Mitsunobu reaction procedure of 2-(4-phenylbutan-2-yloxy)isindoline-1,3-dione was repeated with ethyl 2-hydroxy-4-phenylbutyrate. The residue from the reaction was purified by chromatography on silica gel (gradient elution: hexane/ethyl acetate (100% to 97% hexane) 97% yield, based on a 5.3 mmole scale of (*R*)-ethyl 2-hydroxy-4-phenylbutanoate.  $^1\text{H}$  NMR (500 MHz,  $\text{CDCl}_3$ )  $\delta$  ppm 7.88-7.84 (comp, 2H), 7.79-7.76 (comp, 2H), 7.34-7.29 (comp, 4H), 7.24-7.21 (m, 1H), 4.80 (dd,  $J = 7.8, 5.0$  Hz, 1H), 4.30-4.20 (comp, 2H), 2.98 (t,  $J = 8.0$  Hz, 2H), 2.43-2.22 (comp, 2H), 1.31 (t,  $J = 7.0$  Hz, 3H).  $^{13}\text{C}$  NMR (100 MHz,  $\text{CDCl}_3$ )  $\delta$  ppm 169.2, 163.2, 140.6, 134.6, 128.8, 128.5, 128.4, 126.1, 123.6, 84.72, 61.6, 32.6, 30.9, 14.0. HRMS (ESI<sup>+</sup>): expected mass 354.1336, found 354.1342.

### Procedure for the Preparation of Hydroxylamine Substrates

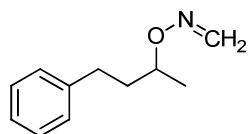


### ***N*-isopropyl-*O*-(4-phenylbutan-2-yl) hydroxylamine**

2-(4-phenylbutan-2-yloxy)isoindoline-1,3-dione (7.1 g, 0.024 moles) was dissolved in ethanol (240 mL) and to that mixture was added hydrazine (2.3 g, 0.072 moles). An immediate change of color was observed when hydrazine was added; the solution was a bright red/orange color then soon afterwards it became less red before immediately becoming an insoluble milky white suspension. The reaction was left to stir for one hour at 40°C. Once the reaction was complete, as judged by TLC analysis, excess dry acetone (4.2 g, 0.072 moles) was added; and the reaction was left to stir at room temperature for one hour. After TLC analysis showed complete consumption of starting material, NaCNBH<sub>3</sub> (8.8 g, 0.14 moles) was added at 0°C, and the pH was adjusted to three by adding drops of hydrochloric acid (35% in H<sub>2</sub>O). The reaction was left to stir for one hour in open air and warmed to room temperature. The ethanol was evaporated under reduced pressure, and the solution was neutralized to pH eight by adding solid NaOH. The aqueous layer was extracted with CH<sub>2</sub>Cl<sub>2</sub> three times. The organic layer was dried over MgSO<sub>4</sub>, filtered, and the solvent was evaporated under reduced pressure.

### **Characterization Data for hydroxylamine substrates**

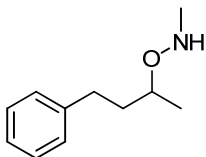
#### **Formaldehyde *O*-4-phenylbutan-2-yl oxime**



Purified by chromatography on silica gel (gradient elution: hexane/ethyl acetate (100% to 98% hexane)); 86% yield, based on a 4.2 mmole scale of 2-(4-phenylbutan-2-yloxy)isoindoline-1,3-dione. <sup>1</sup>H NMR (400 MHz, CDCl<sub>3</sub>) δ ppm 7.36-7.32 (comp,

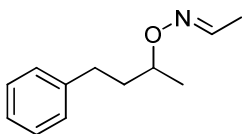
2H), 7.27-7.22 (comp, 3H), 7.09 (d,  $J = 8.8$  Hz, 1H), 6.47 (d,  $J = 8.8$  Hz, 1H), 4.33 (sext.,  $J = 6.4$  Hz, 1H), 2.84-2.69 (comp, 2H), 2.06 (m, 1H), 1.90-1.81 (m, 1H), 1.34 (d,  $J = 6.4$  Hz, 3H).  $^{13}\text{C}$  NMR (101 MHz,  $\text{CDCl}_3$ )  $\delta$  ppm 142.0, 136.4, 128.3, 128.3, 125.7, 78.5, 37.3, 31.6, 19.7. HRMS (ESI+): expected mass 177.12, found 178.13.

#### ***N*-methyl-*O*-(4-phenylbutan-2-yl) hydroxylamine**



Purified by chromatography on silica gel (gradient elution: hexane/ethyl acetate (100% to 95% hexane)); 94 % yield, based on a 3.3 mmole scale of formaldehyde *O*-4-phenylbutan-2-yl oxime.  $^1\text{H}$  NMR (400 MHz,  $\text{CDCl}_3$ )  $\delta$  ppm 7.32-7.27 (comp, 2H), 7.23-7.18 (comp, 3H), 4.92 (s, br, 1H), 3.75 (sext.,  $J = 6.0$  Hz, 1H), 2.78-2.62 (comp, 2H), 2.73(s, 3H), 1.95-1.86 (m, 1H), 1.74-1.65 (m, 1H), 1.21 (d,  $J = 6.0$  Hz, 3H).  $^{13}\text{C}$  NMR (100 MHz,  $\text{CDCl}_3$ )  $\delta$  ppm 142.3, 128.3, 128.3, 125.6, 77.6, 39.7, 37.0, 31.9, 19.3. HRMS (ESI+): expected mass 179.13, found 180.14.

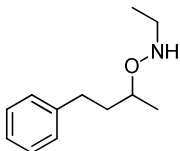
#### **Acetaldehyde *O*-4-phenylbutan-2-yl oxime**



Purified by chromatography on silica gel (gradient elution: hexane/ethyl acetate (100% to 98% hexane)); 98% yield, based on a 29 mmole scale of 2-(4-phenylbutan-2-yloxy)isoindoline-1,3-dione.  $^1\text{H}$  NMR (400 MHz,  $\text{CDCl}_3$ )  $\delta$  ppm 7.47 (q,  $J = 6.0$  Hz, 1H), 7.33 (t,  $J = 7.5$  Hz, 2H), 7.24 (dd,  $J = 14.3, 7.2$  Hz, 3H), 4.25 (sext.,  $J = 6.4$  Hz, 1H), 2.84-2.69 (comp, 2H), 2.08-1.99 (m, 1H), 1.90 (d,  $J = 6.0$  Hz, 3H), 1.85-1.79 (m, 1H), 1.32 (d,  $J = 6.4$  Hz, 3H).  $^{13}\text{C}$  NMR (101 MHz,  $\text{CDCl}_3$ )  $\delta$  ppm 145.8, 142.2,

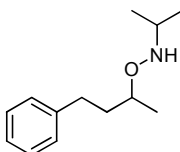
128.3, 128.2, 125.6, 77.7, 37.3, 31.7, 19.7, 15.3. HRMS (ESI+): expected mass 192.1388, found 192.1380.

***N*-ethyl-*O*-(4-phenylbutan-2-yl) hydroxylamine**



Purified by chromatography on silica gel (gradient elution: hexane/ethyl acetate (100% to 98% hexane); 86% yield, based on a 29 mmole scale of acetaldehyde *O*-4-phenylbutan-2-yl oxime. <sup>1</sup>H NMR (400 MHz, CDCl<sub>3</sub>) δ ppm 7.31-7.27 (comp, 2H), 7.22-7.17 (comp, 3H), 5.24 (s, br, 1H), 3.74 (sext., *J* = 6.0 Hz, 1H), 2.98 (q, *J* = 7.0 Hz, 2H), 2.78-2.62 (comp, 2H), 1.95-1.86 (m, 1H), 1.75-1.66 (m, 1H), 1.21 (d, *J* = 6.0 Hz, 3H), 1.11 (t, *J* = 7.0 Hz, 3H). <sup>13</sup>C NMR (100 MHz, CDCl<sub>3</sub>) δ ppm 142.4, 128.3, 128.3, 125.6, 78.0, 46.8, 37.1, 31.9, 19.3, 12.5. HRMS (ESI+): expected mass 194.1545, found 194.1541.

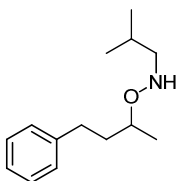
***N*-isopropyl-*O*-(4-phenylbutan-2-yl) hydroxylamine**



Purified by chromatography on silica gel (gradient elution: hexane/ethyl acetate (98% to 95% hexane); 79% yield, based on a 20 mmole scale of 2-(4-phenylbutan-2-yloxy)isoindoline-1,3-dione. <sup>1</sup>H NMR (400 MHz, CDCl<sub>3</sub>) δ ppm 7.31-7.27 (comp, 2H), 7.23-7.17 (comp, 3H), 5.07 (s, br, 1H), 3.75 (sext., *J* = 6.4 Hz, 1H), 3.16 (hept., *J* = 6.3 Hz, 1H), 2.73-2.77 (m, 1H), 2.62-2.67 (m, 1H), 1.96-1.87 (m, 1H), 1.69-1.73

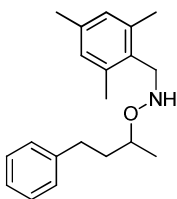
(m, 1H), 1.21 (d,  $J = 6.4$  Hz, 3H), 1.08 (dd,  $J = 6.3, 0.8$  Hz, 6H).  $^{13}\text{C}$  NMR (100 MHz,  $\text{CDCl}_3$ )  $\delta$  ppm 142.2, 128.1, 128.0, 125.4, 78.0, 51.3, 37.1, 31.8, 20.0, 19.1. HRMS (ESI+): expected mass 208.1701, found 208.1691.

### ***N*-isobutyl-*O*-(4-phenylbutan-2-yl) hydroxylamine**



Purified by chromatography on silica gel (gradient elution: hexane/ethyl acetate (100% to 98% hexane)); 80% yield, based on a 3.2 mmole scale of Phenol butoxyphthalimide.  $^1\text{H}$  NMR (400 MHz,  $\text{CDCl}_3$ )  $\delta$  ppm 7.33-7.29 (comp, 2H), 7.25-7.19 (comp, 3H), 3.76 (sext.,  $J = 6.4$  Hz, 1H), 2.76 (d,  $J = 6.8$  Hz, 2H), 2.79-2.63 (comp, 2H), 1.97-1.84 (comp, 2H), 1.77-1.68 (m, 1H), 1.22 (d,  $J = 6.4$  Hz, 3H), 0.96 (d,  $J = 6.5$  Hz, 6H).  $^{13}\text{C}$  NMR (100 MHz,  $\text{CDCl}_3$ )  $\delta$  ppm 142.4, 128.3, 128.2, 125.6, 77.8, 60.3, 37.0, 31.9, 25.9, 20.6, 20.6, 19.3. HRMS (ESI+): expected mass 222.1858, found 222.1864.

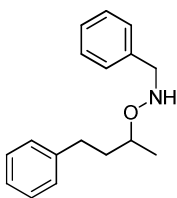
### ***O*-(4-Phenylbutan-2-yl)-*N*-(2,4,6-trimethylbenzyl) hydroxylamine**



Purified by chromatography on silica gel (gradient elution: hexane/ethyl acetate (100% to 98% hexane)); 83% yield, based on a 5.4 mmole scale of 2-(4-phenylbutan-2-yloxy)isoindoline-1,3-dione.  $^1\text{H}$  NMR (400 MHz,  $\text{CDCl}_3$ )  $\delta$  ppm 7.36-7.32 (comp,

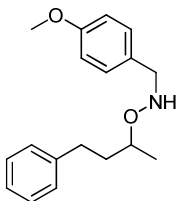
2H), 7.26-7.22 (comp, 3H), 6.92 (s, 2H), 5.19 (s, br, 1H), 4.17 (s, 2H), 3.80 (sext.,  $J = 6.2$  Hz, 1H), 2.81-2.66 (comp, 2H), 2.45 (s, 6H), 2.32 (s, 3H), 2.04-1.94 (m, 1H), 1.80-1.71 (m, 1H), 1.26 (d,  $J = 6.2$ , 3H).  $^{13}\text{C}$  NMR (100 MHz,  $\text{CDCl}_3$ )  $\delta$  ppm 142.3, 137.8, 137.0, 129.6, 128.9, 128.3, 128.2, 125.6, 77.7, 50.4, 36.9, 31.8, 20.9, 19.6, 19.3. HRMS (ESI<sup>+</sup>): expected mass 298.2171, found 298.2179.

### ***N*-Benzyl-*O*-(4-phenylbutan-2-yl) hydroxylamine**



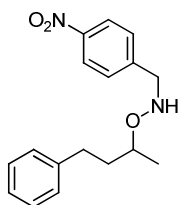
Purified by chromatography on silica gel (gradient elution: hexane/ethyl acetate (100% to 98% hexane)); 87% yield, based on a 3.6 mmole scale of 2-(4-phenylbutan-2-yloxy)isoindoline-1,3-dione.  $^1\text{H}$  NMR (400 MHz,  $\text{CDCl}_3$ )  $\delta$  ppm 7.45-7.40 (comp, 5H), 7.37-7.34 (comp, 2H), 7.26-7.21 (comp, 3H), 5.46 (s, br, 1H), 4.11 (s, 2H), 3.78 (sext.,  $J = 6.4$  Hz, 1H), 2.77-2.70 (m, 1H), 2.67-2.60 (m, 1H), 1.98-1.88 (m, 1H), 1.78-1.69 (m, 1H), 1.24 (d,  $J = 6.4$  Hz, 3H).  $^{13}\text{C}$  NMR (100 MHz,  $\text{CDCl}_3$ )  $\delta$  ppm 142.3, 137.6, 129.0, 128.3, 128.2, 127.3, 125.6, 78.0, 56.9, 36.9, 31.8, 19.3. HRMS (ESI<sup>+</sup>): expected mass 256.1701, found 256.1710.

### ***N*-(4-methoxybenzyl)-*O*-(4-phenylbutan-2-yl) hydroxylamine**



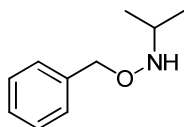
Purified by chromatography on silica gel (gradient elution: hexane/ethyl acetate (100% to 98% hexane)); 81% yield, based on a 4.1 mmole scale of 2-(4-phenylbutan-2-yloxy)isoindoline-1,3-dione.  $^1\text{H}$  NMR (400 MHz,  $\text{CDCl}_3$ )  $\delta$  ppm 7.34-7.28 (comp, 4H), 7.22-7.18 (comp, 3H), 6.91-6.88 (comp, 2H), 5.40 (s, br, 1H), 4.01 (s, 2H), 3.82 (s, 3H), 3.74 (sext.,  $J = 6.0$  Hz, 1H), 2.74-2.67 (m, 1H), 2.64-2.57 (m, 1H), 1.95-1.86 (m, 1H), 1.73-1.65 (m, 1H), 1.20 (d,  $J = 6.0$  Hz, 3H).  $^{13}\text{C}$  NMR (100 MHz,  $\text{CDCl}_3$ )  $\delta$  ppm 158.9, 142.4, 130.3, 129.6, 128.3, 128.2, 125.6, 113.7, 78.0, 56.3, 55.2, 36.9, 31.8, 19.3. HRMS (ESI+): expected mass 286.1807, found 286.1814.

***N*-(4-nitrobenzyl)-*O*-(4-phenylbutan-2-yl) hydroxylamine**



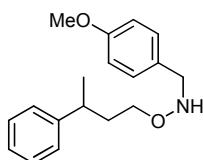
Purified by chromatography on silica gel (gradient elution: hexane/ethyl acetate (100% to 96% hexane)); 91% yield, based on a 3.4 mmole scale of 2-(4-phenylbutan-2-yloxy)isoindoline-1,3-dione.  $^1\text{H}$  NMR (400 MHz,  $\text{CDCl}_3$ )  $\delta$  ppm 8.24-8.18 (comp, 2H), 7.57-7.53 (comp, 2H), 7.30-7.25 (comp, 2H), 7.23-7.18 (m, 1H), 7.15-7.12 (comp, 2H), 5.62 (s, br, 1H), 4.15 (s, 2H), 3.68 (sext.,  $J = 6.0$  Hz, 1H), 2.66-2.50 (comp, 2H), 1.90-1.80 (m, 1H), 1.71-1.62 (m, 1H), 1.16 (d,  $J = 6.0$  Hz, 3H).  $^{13}\text{C}$  NMR (101 MHz,  $\text{CDCl}_3$ )  $\delta$  ppm 147.2, 145.9, 142.1, 129.6, 128.3, 128.2, 125.7, 123.5, 78.3, 55.9, 36.8, 31.7, 19.1. HRMS (ESI+): expected mass 301.1552, found 301.1556.

***O*-benzyl-*N*-isopropyl hydroxylamine**



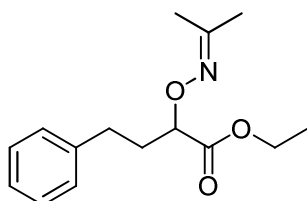
Purified by chromatography on silica gel (gradient elution: hexane/ethyl acetate (100% to 97% hexane); 83% yield, based on a 16 mmole scale of *O*-benzylamine hydrochloride.  $^1\text{H}$  NMR (400 MHz,  $\text{CDCl}_3$ )  $\delta$  ppm 7.39-7.28 (comp, 5H), 5.36 (s, br, 1H), 4.73 (s, 2H), 3.21 (sept.,  $J = 6.3$  Hz, 1H), 1.08 (d,  $J = 6.3$  Hz, 6H).  $^{13}\text{C}$  NMR (101 MHz,  $\text{CDCl}_3$ )  $\delta$  ppm 137.9, 128.3, 128.3, 127.7, 76.7, 51.6, 20.1. HRMS (ESI+): expected mass 166.1232, found 166.1240.

***N*-(4-Methoxybenzyl)-*O*-(3-phenylbutyl) hydroxylamine**



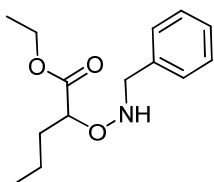
Purified by chromatography on silica gel (gradient elution: hexane/ethyl acetate (100% to 98% hexane); 93% yield, based on a 4.1 mmole scale of 2-(3-phenylbutoxy)isoindoline-1,3-dione.  $^1\text{H}$  NMR (400 MHz,  $\text{CDCl}_3$ )  $\delta$  ppm 7.35-7.26 (comp, 4H), 7.22-7.17 (comp, 3H), 6.90-6.88 (comp, 2H), 5.50 (t,  $J = 6.5$  Hz, 1H), 3.98 (d,  $J = 6.5$  Hz, 2H), 3.82 (s, 3H), 3.59 (dt,  $J = 6.5, 1.5$  Hz, 2H), 2.82 (sext.,  $J = 7.2$  Hz, 1H), 1.91-1.81 (comp, 2H), 1.25 (d,  $J = 7.2$  Hz, 3H).  $^{13}\text{C}$  NMR (100 MHz,  $\text{CDCl}_3$ )  $\delta$  ppm 158.9, 147.0, 130.1, 129.5, 128.3, 126.9, 125.9, 113.7, 72.1, 55.8, 55.2, 36.9, 36.5, 22.3. HRMS (ESI+): expected mass 286.1807, found 286.1810.

**Ethyl 4-phenyl-2-(propan-2-ylideneaminoxy)butanoate**



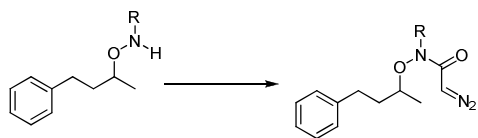
Purified by chromatography on silica gel (gradient elution: hexane/ethyl acetate (94% hexane); 80% yield, based on a 2.0 mmole scale of ethyl 2-(1,3-dioxoisindolin-2-yloxy)-4-phenylbutanoate.  $^1\text{H}$  NMR (400 MHz,  $\text{CDCl}_3$ ) ppm 7.32-7.27 (comp, 2H), 7.22-7.19 (comp, 3H), 4.59-4.56 (m, 1H), 4.25-4.16 (comp, 2H), 2.85-2.72 (comp, 2H), 2.20-2.11 (comp, 2H), 1.96 (s, 3H), 1.89 (s, 3H), 1.28 (t,  $J = 7.1$  Hz, 3H).  $^{13}\text{C}$  NMR (101 MHz,  $\text{CDCl}_3$ ) ppm 172.6, 156.5, 141.2, 128.4, 128.4, 126.0, 79.9, 60.7, 33.0, 31.5, 21.8, 15.8, 14.2. HRMS (ESI+): expected mass 264.1600, found 264.1609.

### Ethyl 2-(benzylaminooxy) pentanoate



Purified by chromatography on silica gel (gradient elution: hexane/ethyl acetate (90% hexane); 70% yield, based on a 3.4 mmole scale of ethyl 2-(1,3-dioxoisindolin-2-yloxy)pentanoate.  $^1\text{H}$  NMR (400 MHz,  $\text{CDCl}_3$ )  $\delta$  ppm 7.35-7.27 (comp, 5H), 6.09 (t,  $J = 6.5$  Hz, 1H), 4.24-4.16 (comp, 2H), 4.13-4.03 (comp, 2H), 1.62-1.56 (comp, 2H), 1.42-1.24 (comp, 2H), 1.28 (t,  $J = 7.0$  Hz, 3H), 0.83 (t,  $J = 7.5$  Hz, 3H).  $^{13}\text{C}$  NMR (100 MHz,  $\text{CDCl}_3$ )  $\delta$  ppm 173.2, 137.3, 128.9, 128.3, 127.3, 81.9, 60.5, 56.2, 33.3, 18.6, 14.2, 13.6. HRMS (ESI+): expected mass 252.1594, found 252.1603.

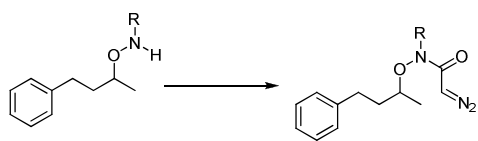
### Procedure for the Preparation of *N*-alkoxy diazoacetamides - Method A



### *N*-Ethyl-*N*-(4-phenylbutan-2-yloxy)-2-diazoacetamide

To a solution of *N*-ethyl-*O*-(4-phenylbutan-2-yl)hydroxylamine (0.55g, 2.8 mmoles) in freshly distilled anhydrous xylene (11 mL) was added 2,2,6-trimethyl-4*H*-1,3-dioxin-4-one (0.59g, 4.3 mmoles). The reaction was heated from room temperature to 100°C in an oil bath. After one hour at 100°C, the cooled reaction mixture was concentrated under reduced pressure. The reaction mixture was dissolved in THF (3.5 mL) and methyl sulfonylazide<sup>42</sup> (1.7g, 5.7 mmoles) was added to that followed by dry triethylamine (1 mL). The reaction was left to stir under argon at room temperature overnight. Once the second reaction was complete judged by TLC analysis, eight equivalents of lithium hydroxide in water (5.6 mL) was added to the reaction mixture and left to stir for eight hours at room temperature. The reaction was neutralized to pH 7, measured using pH paper, by adding drops of hydrochloric acid (35% in H<sub>2</sub>O), then the solvent was extracted with ethyl acetate twice, dried over MgSO<sub>4</sub>, and filtered.

#### Procedure for the Preparation of *N*-alkoxy diazoacetamides - Method B



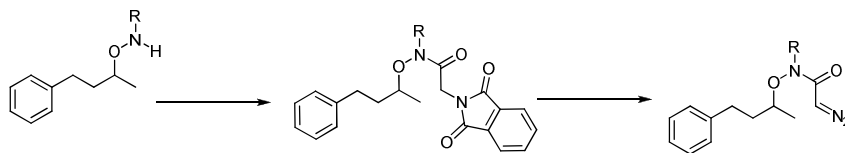
#### *N*-(4-phenylbutan-2-yloxy)-*N*-(2,4,6-trimethylbenzyl)-2-diazoacetamide

A solution of *O*-(4-phenylbutan-2-yl)-*N*-(2,4,6-trimethylbenzyl)hydroxylamine (0.27g, 0.91 mmoles) and triethyl amine (0.58g, 5.5 mmoles) in DCM (1.4 mL) was added dropwise to a solution of methyl malonyl chloride (0.13g, 1.0 mmoles) in DCM (1.3 mL) at -10°C. The reaction was warmed up to 25°C and left to stir. After two hours the reaction was complete as judged by TLC analysis. The reaction was quenched by water, and the organic and aqueous layer were separated. The organic

<sup>42</sup> Danheiser, R. L.; Miller, R. F.; Brisbois, R. G.; Park, S. Z. *J. Org. Chem.*, **1990**, *55*, 1959-1964.

layer was washed with 10% aqueous solution of  $\text{Na}_2\text{CO}_3$ , dried over  $\text{MgSO}_4$ , and evaporated under reduced pressure. The reaction mixture was dissolved in THF (1.2 mL), and methyl sulfonylazide<sup>5</sup> (0.22g, 1.82 mmoles) was added to the solution followed by triethylamine (0.15g, 1.4 mmoles) that was dried with molecular sieves. The reaction was left to stir under argon at room temperature overnight. Once the second reaction was complete judged by TLC analysis, 24 equivalents of sodium hydroxide in water (3.6 mL) was added to the reaction mixture and left to stir overnight at room temperature. The reaction mixture was neutralized to pH 7, measured using pH paper, by adding drops of hydrochloric acid (35% in  $\text{H}_2\text{O}$ ), then extracted with ethyl acetate twice and dried over anhydrous  $\text{MgSO}_4$ .

#### Procedure for the Preparation of *N*-alkoxy diazoacetamides - Method C



#### 2-(1,3-dioxoisindolin-2-yl)-*N*-isobutyl-*N*-(4-phenylbutan-2-yloxy)acetamide

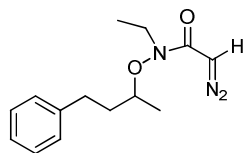
To a mixture of phthalylglycyl chloride (0.39g, 1.7 mmol), alkoxyamine *N*-isobutyl-*O*-(4-phenylbutan-2-yl)hydroxylamine (0.38g, 1.7 mmol) in anhydrous  $\text{CH}_2\text{Cl}_2$  (8.6 mL), dry  $\text{NEt}_3$  (0.36g, 3.4 mmol) was added slowly via a syringe under argon. After stirring the reaction mixture at room temperature for 2 h, the solution was concentrated under reduced pressure and dried over anhydrous  $\text{MgSO}_4$ . The product on TLC could be visualized under UV light, or by staining with PMA solution followed by gentle heating.

#### *N*-Isobutyl-*N*-(4-phenylbutan-2-yloxy)-2-diazoacetamide

To an ethanol solution (8.0 mL) of phthalimide 2-(1,3-dioxoisindolin-2-yl)-*N*-isobutyl-*N*-(4-phenylbutan-2-yloxy)acetamide (0.66g, 1.6 mmol), hydrazine hydrate (0.27g, 8.2 mmol) was added at room temperature and the reaction mixture was heated to 50 °C. After stirring for 1 h, a white suspension was formed, and the reaction mixture was left to stir overnight at 50 °C to reach completion before cooling. The reaction mixture was then filtered, and the white solid was washed thoroughly with CHCl<sub>3</sub> (5 mL x 5). The combined filtrate was concentrated under reduced pressure. The material was dissolved in CHCl<sub>3</sub> (8.0 mL) and acetic acid (0.80 mL) was added at room temperature. After the reaction was allowed to stir, sodium nitrite (0.13g, 2.0 mmol) was added in water (1.8 mL) and the reaction mixture was stirred rapidly for 30 min at 25 °C, resulting with a golden transparent solution. The reaction mixture was then neutralized by 1 M NaHCO<sub>3</sub> immediately and was extracted with CHCl<sub>3</sub> (10 mL x 4). The combined organic layer was dried over anhydrous MgSO<sub>4</sub> and then concentrated under reduced pressure. The product on TLC was visualized under UV light, or by staining with PMA solution followed by gentle heating.

### Characterization Data for *N*-alkoxydiazoacetamide substrates

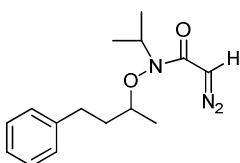
#### *N*-Ethyl-*N*-(4-phenylbutan-2-yloxy)-2-diazoacetamide – Method A



Purified by chromatography on silica gel (gradient elution: hexane/ethyl acetate (100% to 94% hexane); 97% yield, based on a 2.8 mmole scale of *N*-ethyl-*O*-(4-phenylbutan-2-yl) hydroxylamine. <sup>1</sup>H NMR (400 MHz, CDCl<sub>3</sub>) δ ppm 7.32-7.28

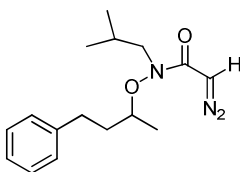
(comp, 2H), 7.23-7.18 (comp, 3H), 5.30 (s, 1H), 3.91 (sext.,  $J = 6.0$  Hz, 1H), 3.74 (qd,  $J = 14.0, 7.0$  Hz, 1H), 3.50 (qd,  $J = 14.0, 7.0$  Hz, 1H), 2.78-2.64 (comp, 2H), 2.02-1.93 (m, 1H), 1.83-1.74 (m, 1H), 1.26 (d,  $J = 6.0$  Hz, 3H), 1.16 (t,  $J = 7.0$  Hz, 3H).  $^{13}\text{C}$  NMR (100 MHz,  $\text{CDCl}_3$ )  $\delta$  ppm 169.9, 141.2, 128.5, 128.2, 126.1, 78.4, 47.2, 42.6, 36.5, 31.7, 18.7, 11.7. HRMS (ESI+): expected mass 262.1556, found 262.1555.

#### ***N*-Isopropyl-*N*-(4-phenylbutan-2-yloxy)-2-diazoacetamide - Method A**



Purified by chromatography on silica gel (gradient elution: hexane/ethyl acetate (100% to 90% hexane)); 76% yield, based on a 7.2 mmole scale of *N*-isopropyl-*O*-(4-phenylbutan-2-yl) hydroxylamine.  $^1\text{H}$  NMR (400 MHz,  $\text{CDCl}_3$ )  $\delta$  ppm 7.32-7.28 (comp, 2H), 7.22-7.18 (comp, 3H), 5.33 (s, 1H), 4.42 (sept.,  $J = 7.0$  Hz, 1H), 3.95 (sext.,  $J = 6.0$  Hz, 1H), 2.77-2.69 (comp, 2H), 2.07-1.98 (m, 1H), 1.81-1.72 (m, 1H), 1.27 (d,  $J = 6.0$  Hz, 3H), 1.21 (dd,  $J = 7.0, 3.5$  Hz, 6H).  $^{13}\text{C}$  NMR (100 MHz,  $\text{CDCl}_3$ )  $\delta$  ppm 172.4, 141.2, 128.4, 128.2, 126.0, 80.7, 52.7, 48.0, 36.8, 31.9, 19.9, 18.6. HRMS (ESI+): expected mass 276.1712, found 276.1725.

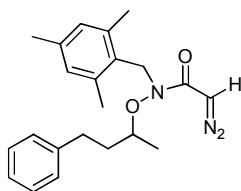
#### ***N*-Isobutyl-*N*-(4-phenylbutan-2-yloxy)-2-diazoacetamide - Method A or Method C**



Purified by chromatography on silica gel (gradient elution: hexane/ethyl acetate (100% to 95% hexane)); 70% yield, based on a 2.3 mmole scale of *N*-isobutyl-*O*-(4-

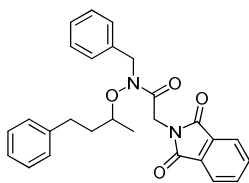
phenylbutan-2-yl) hydroxylamine.  $^1\text{H}$  NMR (400 MHz,  $\text{CDCl}_3$ )  $\delta$  ppm 7.32-7.28 (comp, 2H), 7.23-7.17 (comp, 3H), 5.31 (s, 1H), 3.94 (sext.,  $J = 6.0$  Hz, 1H), 3.51 (dd,  $J = 14.5, 8.0$  Hz, 1H), 3.35 (dd,  $J = 14.5, 7.0$  Hz, 1H), 2.78-2.63 (comp, 2H), 2.13-2.02 (m, 1H), 2.01-1.92 (m, 1H), 1.83-1.74 (m, 1H), 1.25 (d,  $J = 6.0$  Hz, 3H), 0.90 (t,  $J = 6.5$  Hz, 6H).  $^{13}\text{C}$  NMR (100 MHz,  $\text{CDCl}_3$ )  $\delta$  ppm 169.1, 141.1, 128.5, 128.2, 126.1, 78.0, 54.2, 46.7, 36.5, 31.7, 26.6, 20.1, 20.0. HRMS (ESI+): expected mass 290.1869, found 290.1881.

***N*-(4-phenylbutan-2-yloxy)-*N*-(2,4,6-trimethylbenzyl)-2-diazoacetamide - Method B**



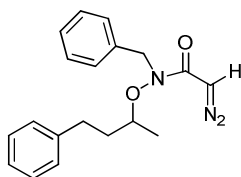
Purified by chromatography on silica gel (gradient elution: hexane/ethyl acetate (100% to 96% hexane); 50% yield, based on 1.0 mmole scale of *O*-(4-phenylbutan-2-yl)-*N*-(2,4,6-trimethylbenzyl)hydroxylamine.  $^1\text{H}$  NMR (400 MHz,  $\text{CDCl}_3$ )  $\delta$  ppm 7.31-7.26 (comp, 2H), 7.24-7.19 (m, 1H), 7.07-7.04 (comp, 2H), 6.84 (s, 2H), 5.40 (s, 1H), 4.93 (d,  $J = 14.0$  Hz, 1H), 4.80 (d,  $J = 14.0$  Hz, 1H), 3.29-3.21 (m, 1H), 2.40-2.35 (comp, 2H), 2.38 (s, 6H), 2.29 (s, 3H), 1.82-1.71 (m, 1H), 1.53-1.45 (m, 1H), 1.02 (d,  $J = 6.4$  Hz, 3H).  $^{13}\text{C}$  NMR (100 MHz,  $\text{CDCl}_3$ )  $\delta$  ppm 172.1, 141.3, 138.1, 137.3, 129.1, 128.9, 128.4, 128.1, 125.9, 80.5, 47.8, 47.6, 36.4, 31.7, 20.9, 19.8, 18.2 (2C). HRMS (ESI+): expected mass 366.2176, found 366.2191.

***N*-benzyl-2-(1,3-dioxoisindolin-2-yl)-*N*-(4-phenylbutan-2-yloxy) acetamide— Method C**



Purified by chromatography on silica gel (gradient elution: hexane/ethyl acetate (100% to 85% hexane); 99% yield, based on 1.0 mmole scale of *N*-(benzyl)-*O*-(4-phenylbutan-2-yl)-hydroxylamine.  $^1\text{H}$  NMR (400 MHz,  $\text{CDCl}_3$ )  $\delta$  ppm 7.92 (dd,  $J = 5.5, 3.0$  Hz, 2H), 7.76 (dd,  $J = 5.5, 3.0$  Hz, 2H), 7.40-7.22 (comp, 8H), 7.15 (d,  $J = 7.0$  Hz, 2H), 4.90 (d,  $J = 15.5$  Hz, 1H), 4.86 (d,  $J = 15.5$  Hz, 1H), 4.70 (s, 2H), 4.10 (sext.,  $J = 6.0$  Hz, 1H), 2.71-2.59 (comp, 2H), 2.06-1.97 (m, 1H), 1.90-1.81 (m, 1H), 1.38 (d,  $J = 6.0$  Hz, 3H).  $^{13}\text{C}$  NMR (100 MHz,  $\text{CDCl}_3$ )  $\delta$  ppm 168.8, 167.9, 141.0, 135.8, 133.9, 132.2, 128.5, 128.4, 128.2, 128.1, 127.6, 126.0, 123.4, 78.4, 51.1, 39.5, 36.2, 31.5, 18.4. HRMS (ESI+): expected mass 443.1971, found 443.1959.

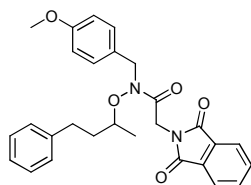
#### ***N*-benzyl-*N*-(4-phenylbutan-2-yloxy)-2-diazoacetamide – Method C**



Purified by chromatography on silica gel (gradient elution: hexane/ethyl acetate (100% to 90% hexane); 60% yield, based on a 1.3 mmole scale of *N*-benzyl-2-(1,3-dioxoisindolin-2-yl)-*N*-(4-phenylbutan-2-yloxy)acetamide.  $^1\text{H}$  NMR (400 MHz,  $\text{CDCl}_3$ )  $\delta$  ppm 7.34-7.27 (comp, 5H), 7.22-7.18 (comp, 2H), 7.13-7.11 (comp, 2H), 5.36 (s, 1H), 4.80 (d,  $J = 15.5$  Hz, 1H), 4.73 (d,  $J = 15.5$  Hz, 1H), 3.91 (sext.,  $J = 6.0$  Hz, 1H), 2.58 (t,  $J = 8.0$  Hz, 2H), 1.97-1.88 (m, 1H), 1.81-1.68 (m, 1H), 1.23 (d,  $J = 6.0$  Hz, 3H).  $^{13}\text{C}$  NMR (100 MHz,  $\text{CDCl}_3$ )  $\delta$  ppm 170.0, 141.1, 136.5, 128.4, 128.4,

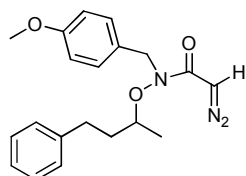
128.4, 128.2, 127.5, 126.0, 78.7, 51.7, 47.2, 36.4, 31.6, 18.6. HRMS (ESI+): expected mass 324.1712, found 324.1722.

**2-(1,3-dioxisoindolin-2-yl)-N-(4-methoxybenzyl)-N-(4-phenylbutan-2-yloxy)acetamide – Method C**



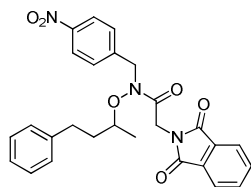
Purified by chromatography on silica gel (gradient elution: hexane/ethyl acetate (100% to 90% hexane); 99% yield, based on 2.2 mmole scale of *N*-(4-methoxybenzyl)-*O*-(4-phenylbutan-2-yl)-hydroxylamine.  $^1\text{H}$  NMR (400 MHz,  $\text{CDCl}_3$ )  $\delta$  ppm 7.87 (dd,  $J = 5.5, 3.0$  Hz, 2H), 7.72 (dd,  $J = 5.5, 3.0$  Hz, 2H), 7.31-7.28 (comp, 2H), 7.23-7.13 (comp, 5H), 6.87-6.83 (comp, 2H), 4.76 (d,  $J = 15.5$  Hz, 1H), 4.67 (d,  $J = 15.5$  Hz, 1H), 4.64 (s, 2H), 4.07 (sext.,  $J = 6.0$  Hz, 1H), 3.79 (s, 3H), 2.71-2.59 (comp, 2H), 2.04-1.95 (m, 1H), 1.88-1.79 (m, 1H), 1.35 (d,  $J = 6.0$  Hz, 3H).  $^{13}\text{C}$  NMR (100 MHz,  $\text{CDCl}_3$ )  $\delta$  ppm 168.7, 167.9, 159.0, 141.0, 133.9, 132.2, 129.5, 128.4, 128.2, 127.9, 126.0, 123.4, 113.9, 78.3, 55.1, 50.4, 39.5, 36.2, 31.5, 18.4. HRMS (ESI+): expected mass 473.2071, found 473.2089.

***N*-(4-methoxybenzyl)-*N*-(4-phenylbutan-2-yloxy)-2-diazoacetamide – Method C**



Purified by chromatography on silica gel (gradient elution: hexane/ethyl acetate (100% to 90% hexane); 60% yield, based on a 2.0 mmole scale of 2-(1,3-dioxoisindolin-2-yl)-*N*-(4-methoxybenzyl)-*N*-(4-phenylbutan-2-yloxy)acetamide.  $^1\text{H}$  NMR (400 MHz,  $\text{CDCl}_3$ )  $\delta$  ppm 7.31-7.27 (comp, 2H), 7.25-7.18 (comp, 3H), 7.14-7.12 (comp, 2H), 6.86-6.82 (comp, 2H), 5.32 (s, 1H), 4.71 (d,  $J = 15.5$  Hz, 1H), 4.66 (d,  $J = 15.5$  Hz, 1H), 3.90 (sext.,  $J = 6.0$  Hz, 1H), 3.79 (s, 3H), 2.63-2.59 (comp, 2H), 1.97-1.88 (m, 1H), 1.77-1.68 (m, 1H), 1.22 (d,  $J = 6.0$  Hz, 3H).  $^{13}\text{C}$  NMR (100 MHz,  $\text{CDCl}_3$ )  $\delta$  ppm 170.1, 159.0, 141.1, 129.8, 128.7, 128.4, 128.2, 126.0, 113.7, 78.7, 55.2, 51.2, 47.3, 36.4, 31.7, 18.6. HRMS (ESI+): expected mass 354.1818, found 354.1796.

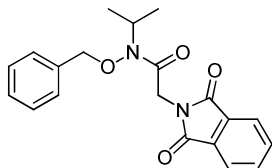
**2-(1,3-dioxoisindolin-2-yl)-*N*-(4-nitrobenzyl)-*N*-(4-phenylbutan-2-yloxy)acetamide – Method C**



Purified by chromatography on silica gel (gradient elution: hexane/ethyl acetate (100% to 80% hexane); 92% yield, based on a 2.8 mmole scale of *N*-(4-nitrobenzyl)-*O*-(4-phenylbutan-2-yl)-hydroxylamine.  $^1\text{H}$  NMR (400 MHz,  $\text{CDCl}_3$ ) ppm 8.18 (d,  $J = 8.7$  Hz, 2H), 7.88 (dd,  $J = 5.5, 3.0$  Hz, 2H), 7.74 (dd,  $J = 5.5, 3.0$  Hz, 2H), 7.38 (d,  $J = 8.7$  Hz, 2H), 7.31-7.29 (comp, 2H), 7.23-7.20 (m, 1H), 7.14-7.10 (comp, 2H), 4.82 (q,  $J = 16.2$  Hz, 2H), 4.67 (d,  $J = 1.6$  Hz, 2H), 4.04 (sext.,  $J = 6.0$  Hz, 1H), 2.66 (t,  $J = 7.8$  Hz, 2H), 2.06-1.97 (m, 1H), 1.91-1.82 (m, 1H), 1.38 (d,  $J = 6.0$  Hz, 3H).  $^{13}\text{C}$  NMR (101 MHz,  $\text{CDCl}_3$ ) ppm 169.4, 167.9, 147.4, 143.2, 140.6, 134.1, 132.1,

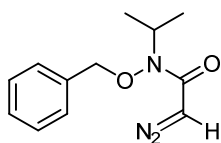
128.7, 128.6, 128.2, 126.3, 123.9, 123.5, 78.9, 50.8, 39.3, 36.1, 31.4, 18.5. HRMS (ESI+): expected mass 488.1822, found 488.1830.

***N*-(benzyloxy)-2-(1,3-dioxoisindolin-2-yl)-*N*-isopropyl acetamide - Method C**



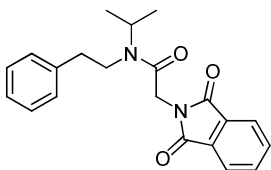
Purified by chromatography on silica gel (gradient elution: hexane/ethyl acetate (100% to 85% hexane)); 95% yield, based on a 4.1 mmole scale of *N*-isopropyl-*O*-benzyl hydroxyamine. <sup>1</sup>H NMR (400 MHz, CDCl<sub>3</sub>) ppm 7.86 (dd, *J* = 5.5, 3.0 Hz, 2H), 7.71 (dd, *J* = 5.5, 3.0 Hz, 2H), 7.46-7.38 (comp, 5H), 5.06 (s, 2H), 4.58 (s, 2H), 4.55-4.49 (m, 1H), 1.34 (d, *J* = 6.8 Hz, 6H). <sup>13</sup>C NMR (101 MHz, CDCl<sub>3</sub>) ppm 169.0, 167.9, 134.3, 134.0, 132.2, 129.0, 128.8, 128.7, 123.4, 79.7, 51.5, 39.6, 19.7 (2C). HRMS (ESI+): expected mass 353.1501, found 353.1478.

***N*-(benzyloxy)-*N*-isopropyl-2-diazoacetamide – Method C**



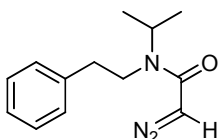
Purified by chromatography on silica gel (gradient elution: hexane/ethyl acetate (100% to 98% hexane)); 60% yield, based on a 3.8 mmole scale of *N*-(benzyloxy)-2-(1,3-dioxoisindolin-2-yl)-*N*-isopropylacetamide. <sup>1</sup>H NMR (400 MHz, CDCl<sub>3</sub>) ppm 7.41-7.37 (comp, 5H), 5.30 (s, 1H), 4.86 (s, 2H), 4.60 (sept., *J* = 6.7 Hz, 1H), 1.27 (d, *J* = 6.7 Hz, 6H). <sup>13</sup>C NMR (101 MHz, CDCl<sub>3</sub>) ppm 170.7, 134.8, 128.8, 128.7, 127.0, 79.6, 51.2, 47.5, 19.5 (2C). HRMS (ESI+): expected mass 234.1243, found 234.1264.

**2-(1,3-dioxoisindolin-2-yl)-*N*-isopropyl-*N*-phenethyl acetamide – Method C**



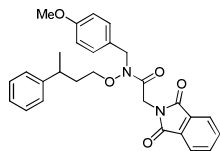
Purified by chromatography on silica gel (gradient elution: hexane/ethyl acetate (100% to 85% hexane)); 50% yield over two steps, based on a 8.0 mmole scale of phenethylamine.  $^1\text{H}$  NMR (400 MHz,  $\text{CDCl}_3$ ) ppm 7.93-7.89 (comp, 2H), 7.77-7.74 (comp, 2H), 7.42-7.20 (comp, 5H), 4.58 (s, 2H), 4.10 (sept.,  $J = 6.7$  Hz, 1H), 3.43-3.38 (comp, 2H), 2.92-2.88 (comp, 2H), 1.31 (d,  $J = 6.7$  Hz, 6H).  $^{13}\text{C}$  NMR (101 MHz,  $\text{CDCl}_3$ ) ppm 168.1, 164.8, 139.4, 134.0, 132.3, 128.8, 128.4, 126.2, 123.5, 47.9, 43.7, 39.5, 35.3, 21.1 (2C). HRMS (ESI+): expected mass 351.1703, found 351.1699.

#### ***N*-Isopropyl-*N*-phenethyl-2-diazoacetamide – Method C**



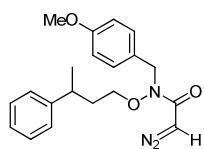
Purified by chromatography on silica gel (gradient elution: hexane/ethyl acetate (100% to 90% hexane)); 60% yield, based on a 1.9 mmole scale of 2-(1,3-dioxoisoindolin-2-yl)-*N*-isopropyl-*N*-phenethylacetamide.  $^1\text{H}$  NMR (400 MHz,  $\text{CDCl}_3$ ) ppm 7.34-7.30 (comp, 2H), 7.25-7.21 (comp, 3H), 4.97 (s, 1H), 3.39-3.19 (comp, 3H), 2.87 (t,  $J = 8.0$  Hz, 2H), 1.19 (d,  $J = 6.8$  Hz, 6H).  $^{13}\text{C}$  NMR (101 MHz,  $\text{CDCl}_3$ ) ppm 165.5, 139.2, 128.9, 128.8, 126.8, 47.2 (2C), 44.4, 37.1, 21.1 (2C). HRMS (ESI+): expected mass 232.1450, found 232.1451.

## 2-(1,3-dioxoisindolin-2-yl)-N-(4-methoxybenzyl)-N-(3-phenylbutoxy)acetamide- Method C



Purified by chromatography on silica gel (gradient elution: hexane/ethyl acetate (100% to 85% hexane); 96% yield, based on a 3.3 mmole scale of *N*-(4-methoxybenzyl)-*O*-(3-phenylbutyl)hydroxylamine.  $^1\text{H}$  NMR (400 MHz,  $\text{CDCl}_3$ )  $\delta$  ppm 7.88 (dd,  $J = 5.5, 3.0$  Hz, 2H), 7.73 (dd,  $J = 5.5, 3.0$  Hz, 2H), 7.32-7.27 (comp, 2H), 7.22-7.19 (m, 1H), 7.17-7.13 (comp, 4H), 6.85-6.83 (comp, 2H), 4.64 (q,  $J = 15.3$  Hz, 2H), 4.55 (s, 2H), 3.80 (s, 3H), 3.79-3.74 (comp, 2H), 2.81 (sext.,  $J = 7.0$  Hz, 1H), 1.96-1.86 (comp, 2H), 1.25 (d,  $J = 7.0$  Hz, 3H).  $^{13}\text{C}$  NMR (100 MHz,  $\text{CDCl}_3$ )  $\delta$  ppm 167.8, 159.2, 145.6, 134.0, 132.2, 129.7, 128.6, 127.8, 126.8, 126.4, 123.4, 123.4, 113.9, 73.3, 55.3, 49.8, 38.9, 36.4, 36.0, 22.8. HRMS (ESI+): expected mass 473.2076, found 473.2078.

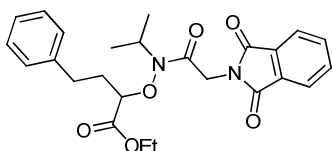
## *N*-(4-methoxybenzyl)-*N*-(3-phenylbutoxy)-2-diazoacetamide- Method C



Purified by chromatography on silica gel (gradient elution: hexane/ethyl acetate (98% to 92% hexane); 50% yield, based on a 2.6 mmole scale of 2-(1,3-dioxoisindolin-2-yl)-*N*-(4-methoxybenzyl)-*N*-(3-phenylbutoxy)acetamide.  $^1\text{H}$  NMR (400 MHz,  $\text{CDCl}_3$ )  $\delta$  ppm 7.32-7.28 (comp, 2H), 7.23-7.19 (comp, 3H), 7.14-7.11 (comp, 2H), 6.85-6.82 (comp, 2H), 5.15 (s, 1H), 4.63 (q,  $J = 15.0$  Hz, 2H), 3.80 (s, 3H), 3.66-3.56 (comp, 2H), 2.76 (sext.,  $J = 7.0$  Hz, 1H), 1.89-1.80 (comp, 2H), 1.22 (d,  $J = 7.0$  Hz, 3H).  $^{13}\text{C}$

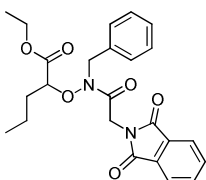
NMR (100 MHz, CDCl<sub>3</sub>)  $\delta$  ppm 168.5, 159.0, 145.8, 129.9, 128.5, 126.8, 126.4, 126.1, 113.8, 73.2, 55.2, 50.3, 46.5, 36.5, 35.9, 22.7. HRMS (ESI<sup>+</sup>): expected mass 354.1818, found 354.1825.

**Ethyl 2-(2-(1,3-dioxoisindolin-2-yl)-*N*-isopropylacetamidooxy)-4-phenylbutanoate – Method C**



Purified by chromatography on silica gel (gradient elution: hexane/ethyl acetate (100% to 87% hexane); 99% yield, based on a 2.2 mmole scale of ethyl 4-phenyl-2-(propan-2-ylideneaminooxy)butanoate. <sup>1</sup>H NMR (400 MHz, CDCl<sub>3</sub>) ppm 7.86 (dd, *J* = 5.4, 3.1 Hz, 2H), 7.70 (dd, *J* = 5.4, 3.1 Hz, 2H), 7.33-7.29 (comp, 2H), 7.24-7.21 (comp, 3H), 5.13 (d, *J* = 17.6 Hz, 1H), 4.62 (dd, *J* = 17.6, 7.2 Hz, 1H), 4.52 (t, *J* = 6.5 Hz, 1H), 4.40-4.28 (comp, 2H), 4.26-4.20 (m, 1H), 2.85-2.71 (comp, 2H), 2.23-2.18 (comp, 2H), 1.34 (t, *J* = 7.2 Hz, 3H), 1.29 (d, *J* = 7.0 Hz, 6H). <sup>13</sup>C NMR (101 MHz, CDCl<sub>3</sub>) ppm 170.4, 168.0, 140.0, 133.9, 132.3, 128.6, 128.3, 126.4, 123.3, 82.8, 61.7, 53.7, 40.4, 32.9, 30.9, 20.1, 19.5, 14.2. HRMS (ESI<sup>+</sup>): expected mass 453.2020, found 453.2030.

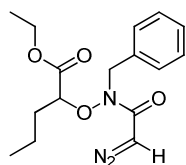
**Ethyl 2-(*N*-benzyl-2-(1,3-dioxoisindolin-2-yl)acetamidooxy)pentanoate – Method C**



Purified by chromatography on silica gel (gradient elution: hexane/ethyl acetate (90% to 85% hexane); 99% yield, based on a 0.76 mmole scale of ethyl 2-

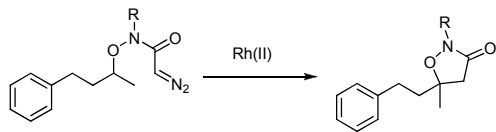
(benzylaminoxy)pentanoate.  $^1\text{H}$  NMR (400 MHz,  $\text{CDCl}_3$ )  $\delta$  ppm 7.88 (dd,  $J = 5.5$ , 3.0 Hz, 2H), 7.72 (dd,  $J = 5.5$ , 3.0 Hz, 2H), 7.36-7.32 (comp, 2H), 7.31-7.27 (comp, 3H), 5.18 (d,  $J = 17.6$  Hz, 1H), 4.97 (d,  $J = 15.8$  Hz, 1H), 4.75 (d,  $J = 15.8$  Hz, 1H), 4.70 (d,  $J = 17.6$  Hz, 1H), 4.47 (t,  $J = 6.5$  Hz, 1H), 4.25 (q,  $J = 7.0$  Hz, 2H), 1.81-1.68 (comp, 2H), 1.40-1.24 (comp, 2H), 1.29 (t,  $J = 7.0$  Hz, 3H), 0.89 (t,  $J = 7.5$  Hz, 3H).  $^{13}\text{C}$  NMR (100 MHz,  $\text{CDCl}_3$ )  $\delta$  ppm 170.6, 167.9, 135.6, 133.9, 132.3, 128.6, 128.0, 127.7, 123.4, 81.6, 61.6, 51.3, 39.8, 33.3, 18.2, 14.1, 13.7. HRMS (ESI+): expected mass 439.1864, found 439.1871.

### Ethyl 2-(*N*-benzyl-2-diazoacetamidoxy)pentanoate- Method C



Purified by chromatography on silica gel (gradient elution: hexane/ethyl acetate (95% to 80% hexane)); 46% yield, based on a 1.2 mmole scale of Ethyl 2-(*N*-benzyl-2-(1,3-dioxisoindolin-2-yl)acetamidoxy)pentanoate.  $^1\text{H}$  NMR (400 MHz,  $\text{CDCl}_3$ )  $\delta$  ppm 7.33-7.27 (comp, 5H), 5.78 (s, 1H), 4.85 (d,  $J = 15.5$  Hz, 1H), 4.75 (d,  $J = 15.5$  Hz, 1H), 4.28 (t,  $J = 6.5$  Hz, 1H), 4.17 (q,  $J = 7.0$  Hz, 2H), 1.73-1.62 (comp, 2H), 1.37-1.23 (comp, 2H), 1.27 (t,  $J = 7.0$  Hz, 3H), 0.88 (t,  $J = 7.5$  Hz, 3H).  $^{13}\text{C}$  NMR (100 MHz,  $\text{CDCl}_3$ )  $\delta$  ppm 171.3, 171.0, 136.3, 128.5, 128.4, 127.6, 82.2, 61.2, 52.6, 48.1, 33.3, 18.2, 14.1, 13.7. HRMS (ESI+): expected mass 320.1605, found 320.1608.

### Procedure for the C-H insertion Reaction

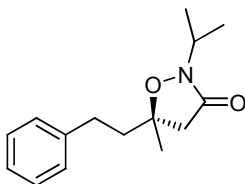


### 2-isopropyl-5-methyl-5-phenethylisoxazolidin-3-one

Thoroughly dried *N*-isopropyl-*N*-(4-phenylbutan-2-yloxy)-2-diazoacetamide (0.15g, 0.53 mmol) was dissolved in DCM (4.0 mL) and was transferred to an additional funnel that was attached to a dried three-neck flask. Rhodium acetate (4.7mg, 2.0 mol %), dissolved in DCM (7.0 mL), was next transferred to the three neck flask. Both the diazo starting material and the catalyst were degassed for 20 minutes. After degassing, *N*-isopropyl-*N*-(4-phenylbutan-2-yloxy)-2-diazoacetamide was added dropwise to the reaction mixture via the additional funnel over an hour. The reaction mixture was left to stir at reflux (40°C) for one hour. The solvent was then evaporated under reduced pressure and dried over anhydrous MgSO<sub>4</sub>.

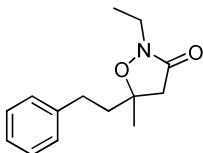
#### Characterization Data for C-H insertion substrates

##### 2-Isopropyl-5-methyl-5-phenethylisoxazolidin-3-one



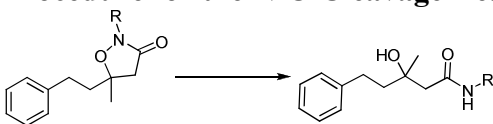
Purified by chromatography on silica gel (gradient elution: hexane/ethyl acetate (95% to 85% hexane)); 71% yield, based on a 0.53 mmol scale of 2-diazo-*N*-isopropyl-*N*-(4-phenylbutan-2-yloxy) acetamide. <sup>1</sup>H NMR (400 MHz, CDCl<sub>3</sub>) δ ppm 7.32-7.28 (comp, 2H), 7.22-7.18 (comp, 3H), 4.44 (sept., *J* = 6.8 Hz, 1H), 2.80-2.64 (comp, 2H), 2.68 (d, *J* = 16.0, 1H), 2.54 (d, *J* = 16.0, 1H), 2.09-2.01 (m, 1H), 1.95-1.88 (m, 1H), 1.44 (s, 3H), 1.26 (d, *J* = 6.8 Hz, 3H), 1.24 (d, *J* = 6.8 Hz, 3H). <sup>13</sup>C NMR (100 MHz, CDCl<sub>3</sub>) δ ppm 166.2, 141.1, 128.4, 128.1, 126.0, 82.1, 45.9, 44.5, 40.4, 30.2, 23.7, 19.3, 19.1. HRMS (ESI<sup>+</sup>): expected mass 248.1651, found 248.1658. [α]<sub>D</sub><sup>21</sup> = -5.48 (c = 1, CHCl<sub>3</sub>).

### 2-ethyl-5-methyl-5-phenethylisoxazolidin-3-one



Purified by chromatography on silica gel (gradient elution: hexane/ethyl acetate (100% to 80% hexane)); 61% yield, based on a 0.79 mmole scale of 2-diazo-*N*-ethyl-*N*-(4-phenylbutan-2-yloxy)acetamide.  $^1\text{H}$  NMR (400 MHz,  $\text{CDCl}_3$ ) ppm 7.32-7.28 (comp, 2H), 7.22-7.17 (comp, 3H), 3.59 (q,  $J = 7.0$  Hz, 2H), 2.77-2.64 (comp, 2H), 2.69 (d,  $J = 16.0$  Hz, 1H), 2.56 (d,  $J = 16.0$  Hz, 1H), 2.08-2.00 (m, 1H), 1.96-1.89 (m, 1H), 1.44 (s, 3H), 1.22 (t,  $J = 7.0$  Hz, 3H).  $^{13}\text{C}$  NMR (101 MHz,  $\text{CDCl}_3$ ) ppm 167.2, 141.2, 128.5, 128.2, 126.1, 82.4, 44.2, 40.7, 39.3, 30.3, 24.0, 12.2. HRMS (ESI+): expected mass 234.1494, found 234.1498.

### Procedure for the N-O Cleavage Reaction



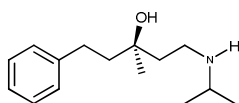
### 1-(isopropylamino)-3-methyl-5-phenylpentan-3-ol

Thoroughly dried 2-isopropyl-5-methyl-5-phenethylisoxazolidin-3-one (0.51g, 2.1 mmoles) was dissolved in THF (0.69 mL) and toluene (1.4 mL). The mixture was cooled to  $0^\circ\text{C}$  while Red-Al (2.0g, 10 mmoles) was added dropwise via an additional funnel. Once the reaction mixture turned to a clear solution it was heated to  $40^\circ\text{C}$  and was left to stir at that temperature for two hours. After the reaction was complete,

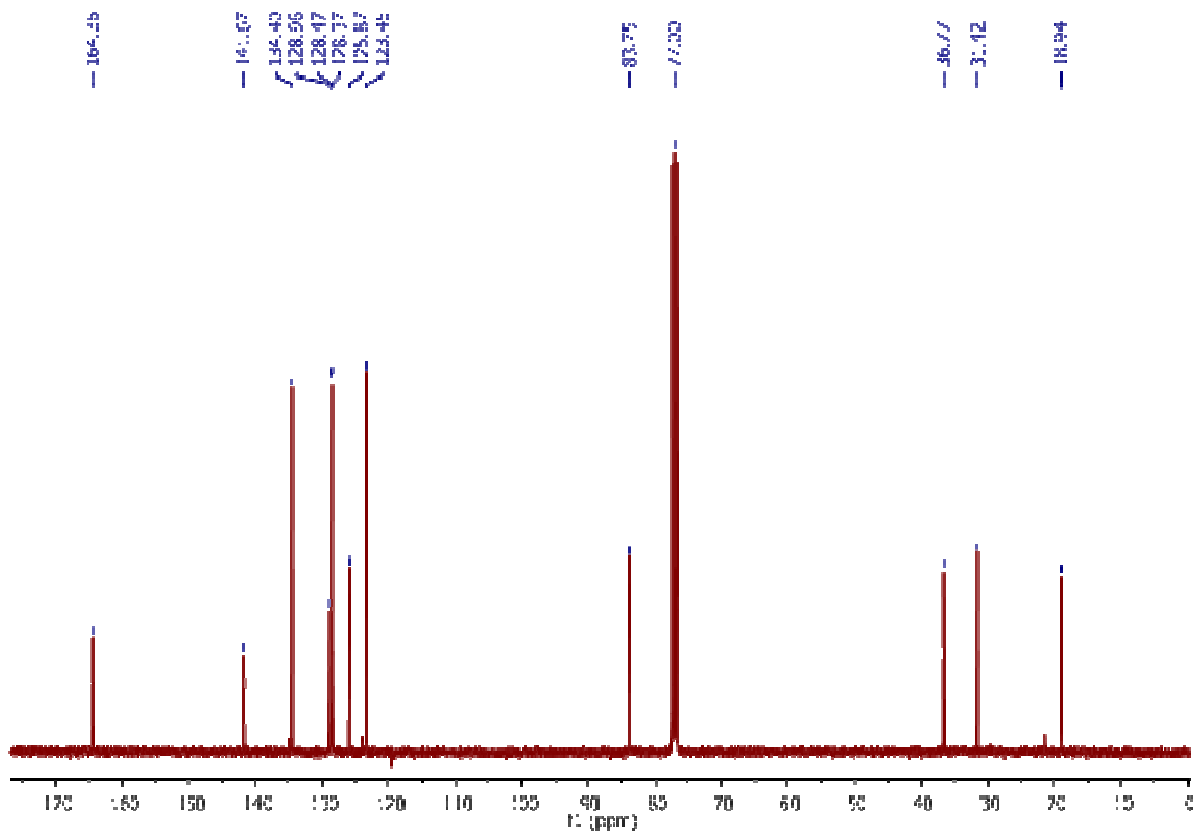
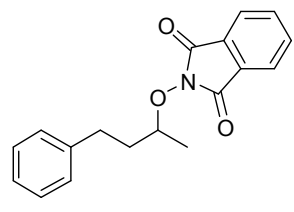
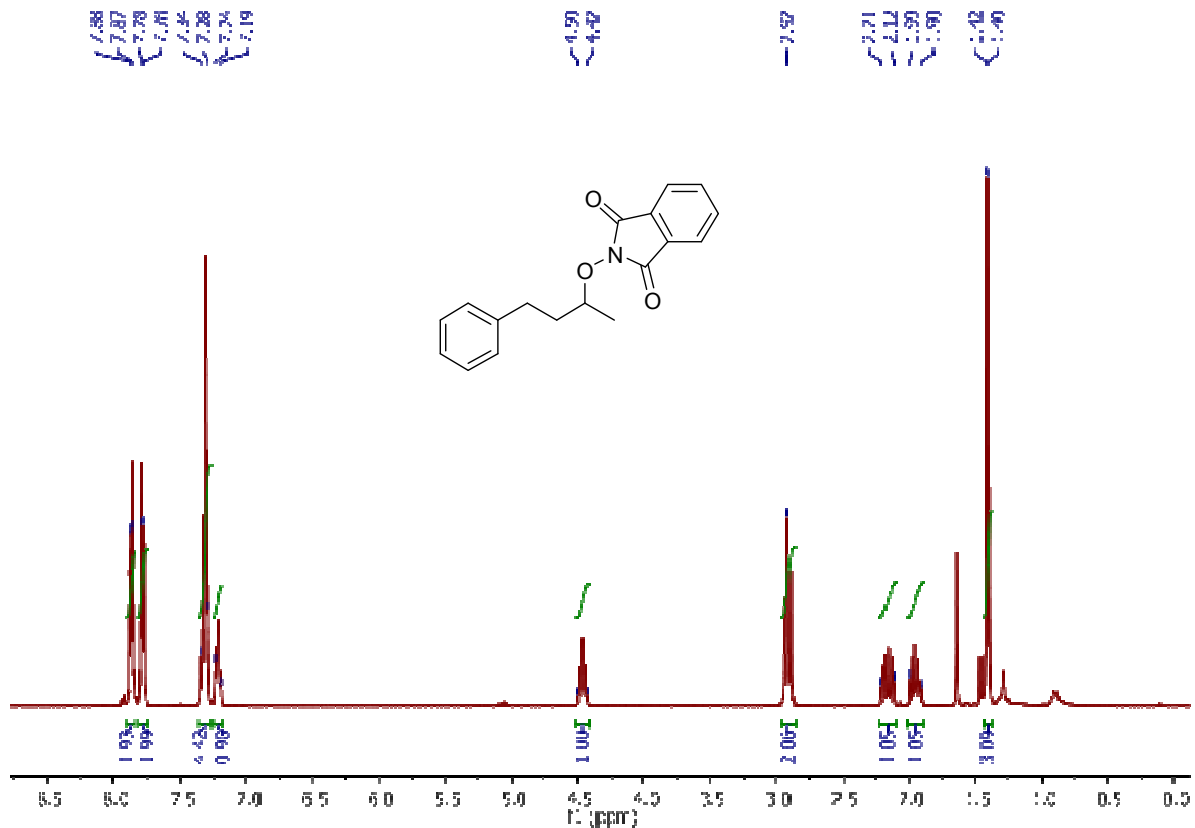
judged by TLC analysis, it was hydrolyzed with NaOH (1M, 38 mL) carefully because unreacted Red-Al reacts vigorously with water. The two layers were then separated and the organic layer was washed with water twice and the solvent was evaporated under reduced pressure. A 1:1 mixture of NaOH:THF (2M, 60 mL) was added to the organic layer and left to stir for one hour then the organic layer was extracted with ethyl acetate (3 X 50mL). Hydrochloric acid (2M, 100 mL) was added to the ethyl acetate layer, left to stir for 10 minutes, then the two layers were separated into a,b. (a) Solid sodium hydroxide was added to the aqueous layer (pH = 9) then the water layer was extracted with DCM, dried over MgSO<sub>4</sub>, and the solvent was evaporated under reduced pressure. (b) Sodium hydroxide (2M, 50mL) was added to the organic layer and left to stir for five minutes. The two layers were separated and the organic layer was dried over MgSO<sub>4</sub> and the solvent was evaporated under reduced pressure. The resulting material (27mg, 0.12 mmoles) was dissolved in AcOH:H<sub>2</sub>O (0.9 mL: 0.2 mL) and degassed for ten minutes. After degassing was complete, Zn dust (0.23g, 3.5 mmoles) was added to the mixture and left to stir overnight at 70°C. After the reaction was complete judging by TLC analysis, the reaction mixture was quenched with sat. NaHCO<sub>3</sub> and solid NaOH (pH = 9). The aqueous layer was extracted with ethyl acetate (3 X 50mL), dried over MgSO<sub>4</sub>, and the solvent was evaporated over reduced pressure.

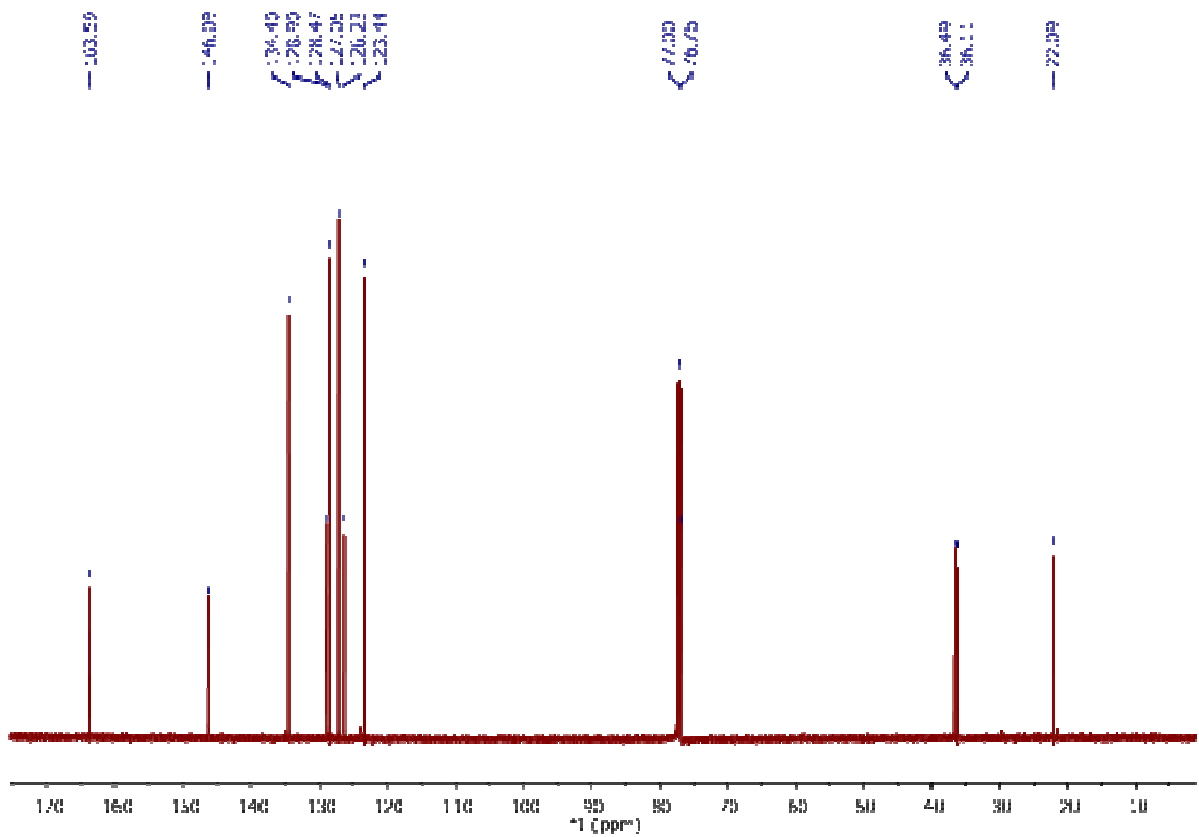
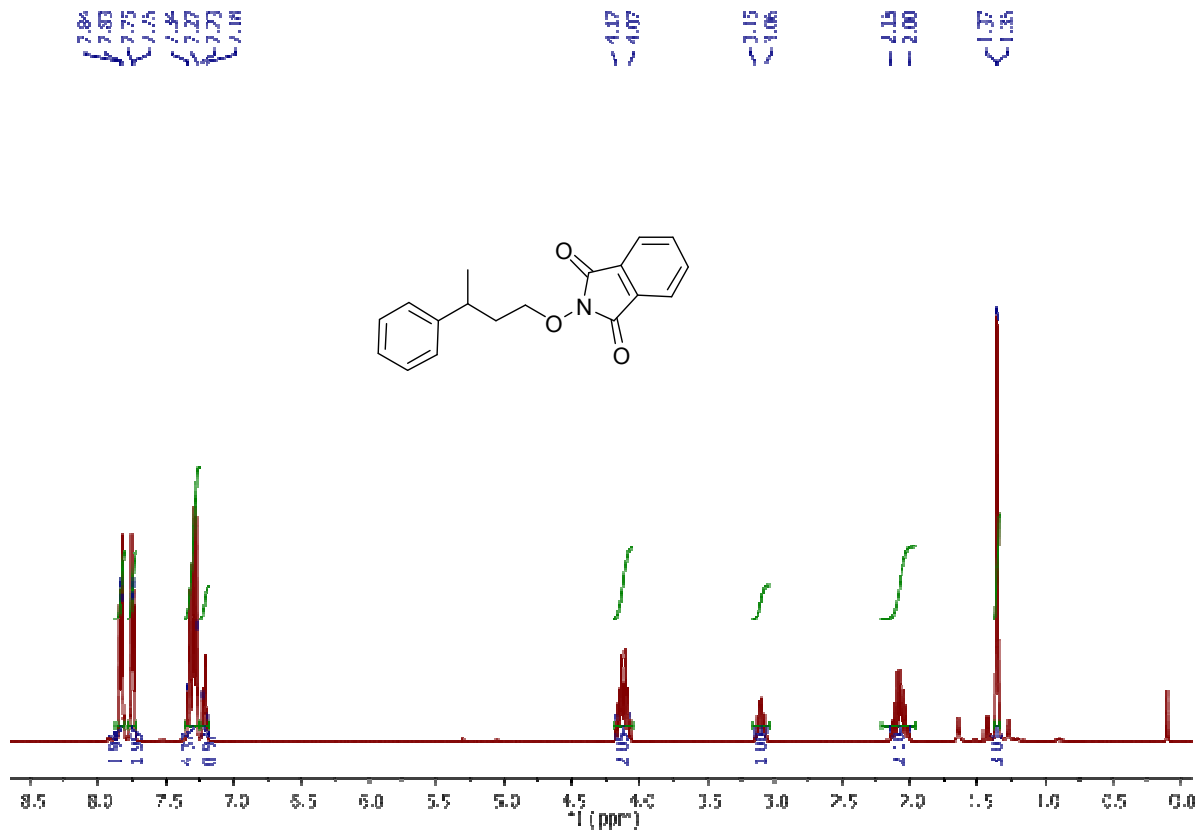
### Characterization Data for N-O cleavage products

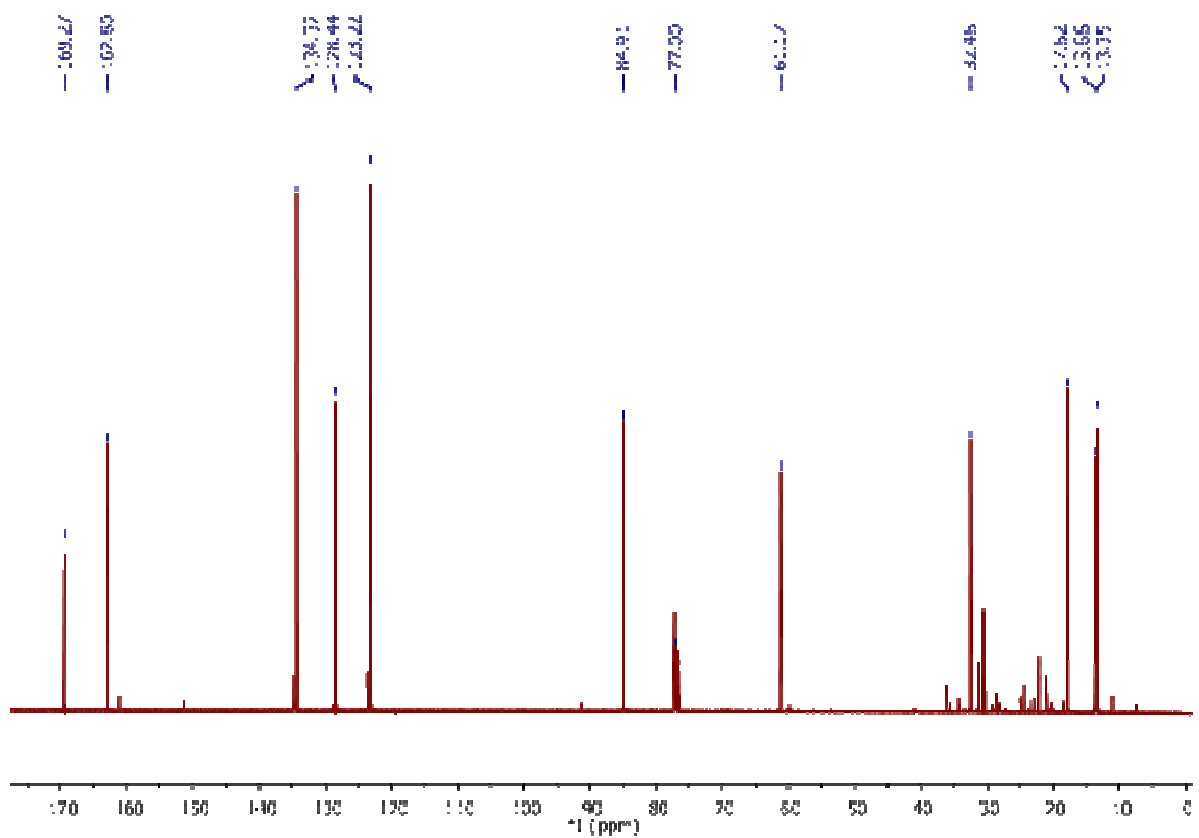
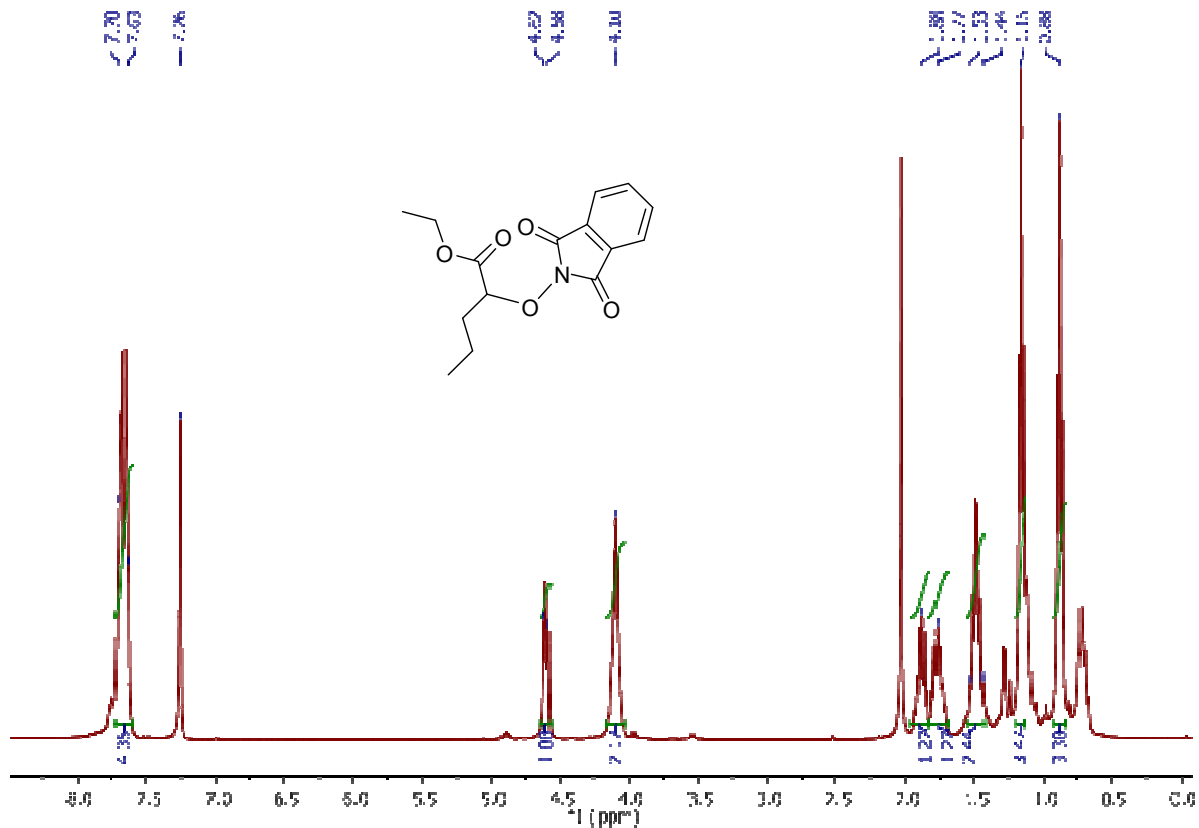
#### 1-(isopropylamino)-3-methyl-5-phenylpentan-3-ol



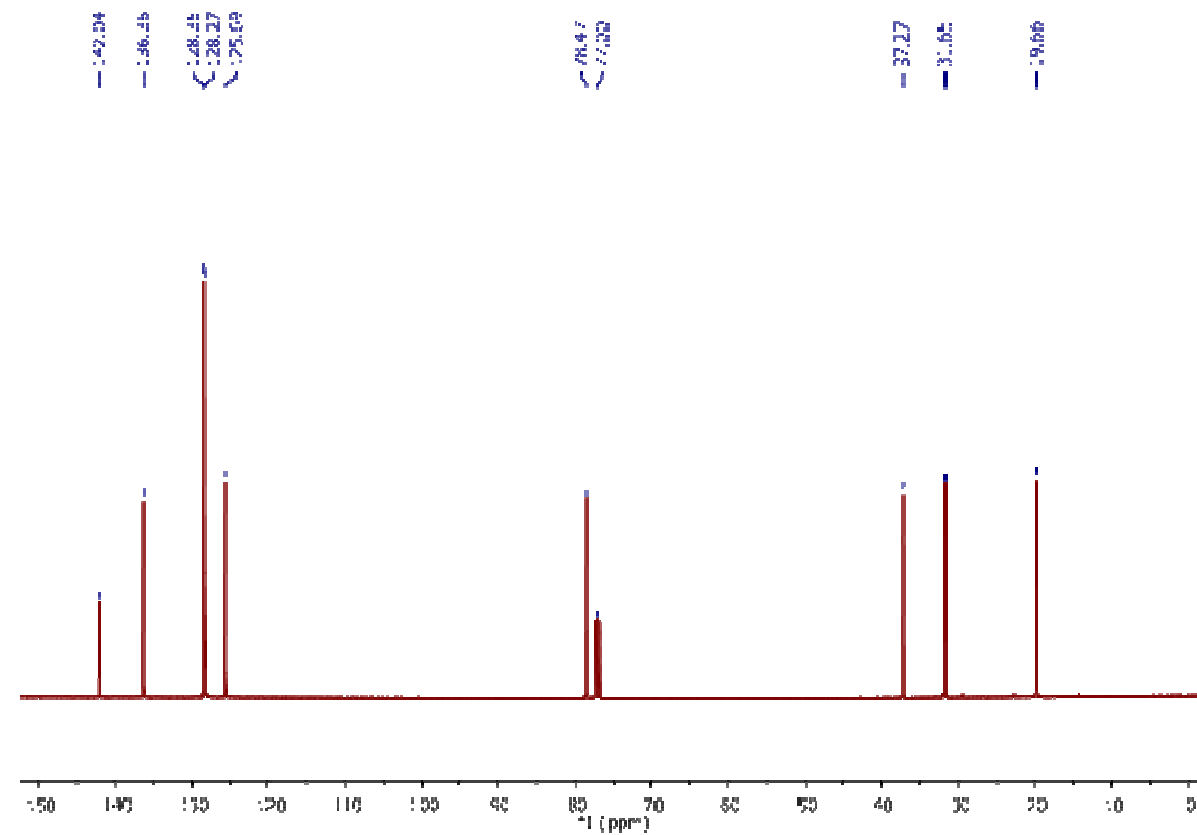
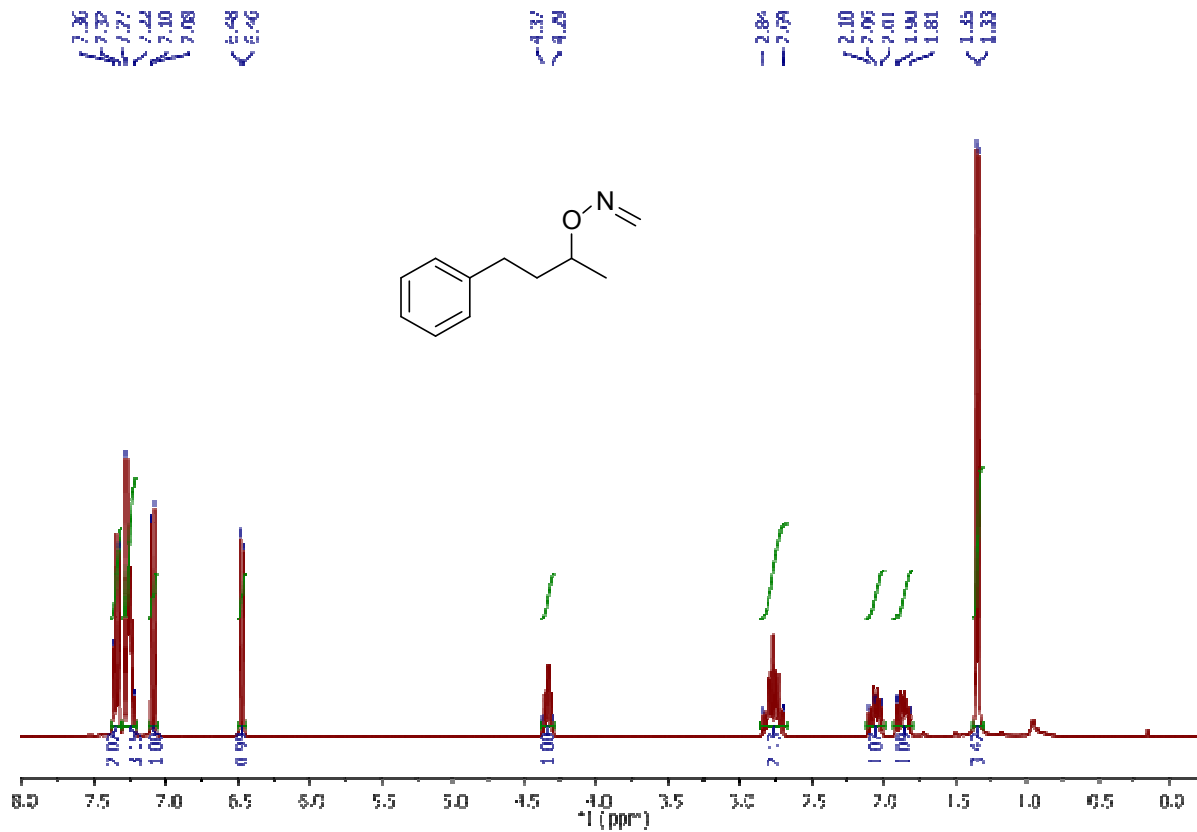
Purified by chromatography on silica gel (gradient elution; chloroform(80%) : methanol (20%); 70% overall yield, based on a 2.1 mmol scale of 2-isopropyl-5-methyl-5-phenethylisoxazolidin-3-one.  $^1\text{H}$  NMR (400 MHz,  $\text{CDCl}_3$ ) ppm 9.28 (s, bs, 1H), 7.28-7.24 (comp, 2H), 7.19-7.15 (comp, 3H), 3.33-3.26 (m, 1H), 3.15-3.07 (comp, 2H), 2.75-2.59 (comp, 2H), 2.21 (s, bs, 1H), 1.89-1.71 (comp, 4H), 1.31 (d,  $J = 5.0$  Hz, 6H), 1.28 (s, 3H).  $^{13}\text{C}$  NMR (101 MHz,  $\text{CDCl}_3$ ) ppm 142.1, 128.3, 128.3, 125.7, 72.5, 50.1, 43.9, 41.5, 36.4, 30.0, 25.3, 19.2, 19.0. HRMS (ESI+): expected mass 236.2014, found 236.2020.  $[\alpha]_{\text{D}}^{23} = -1.41$  (c = .5,  $\text{CHCl}_3$ ).

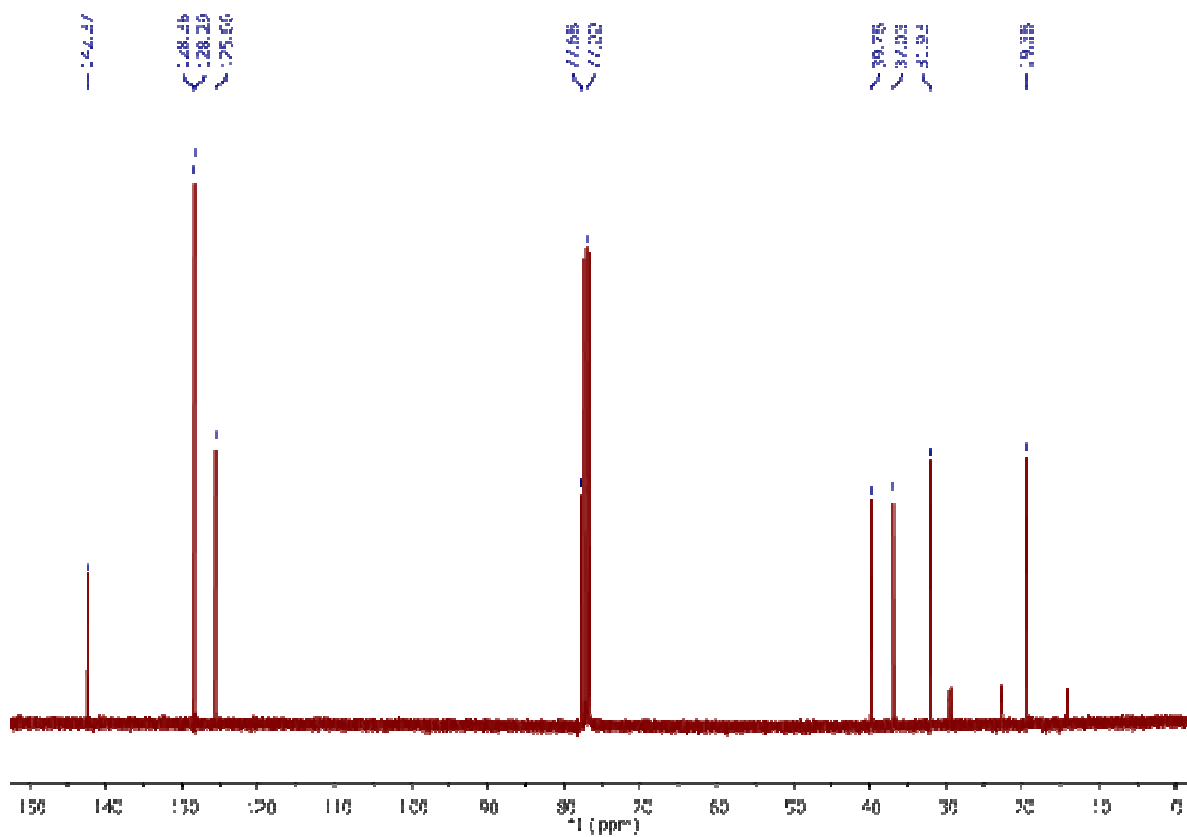
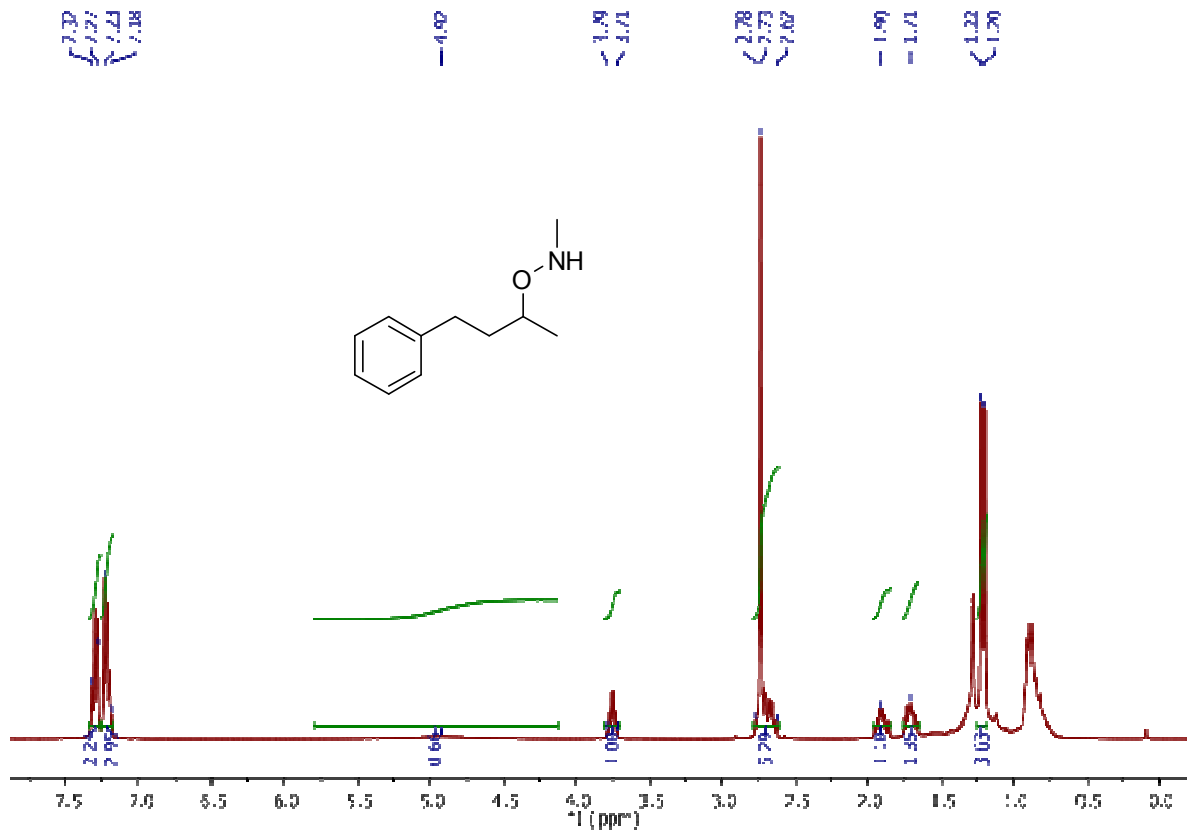


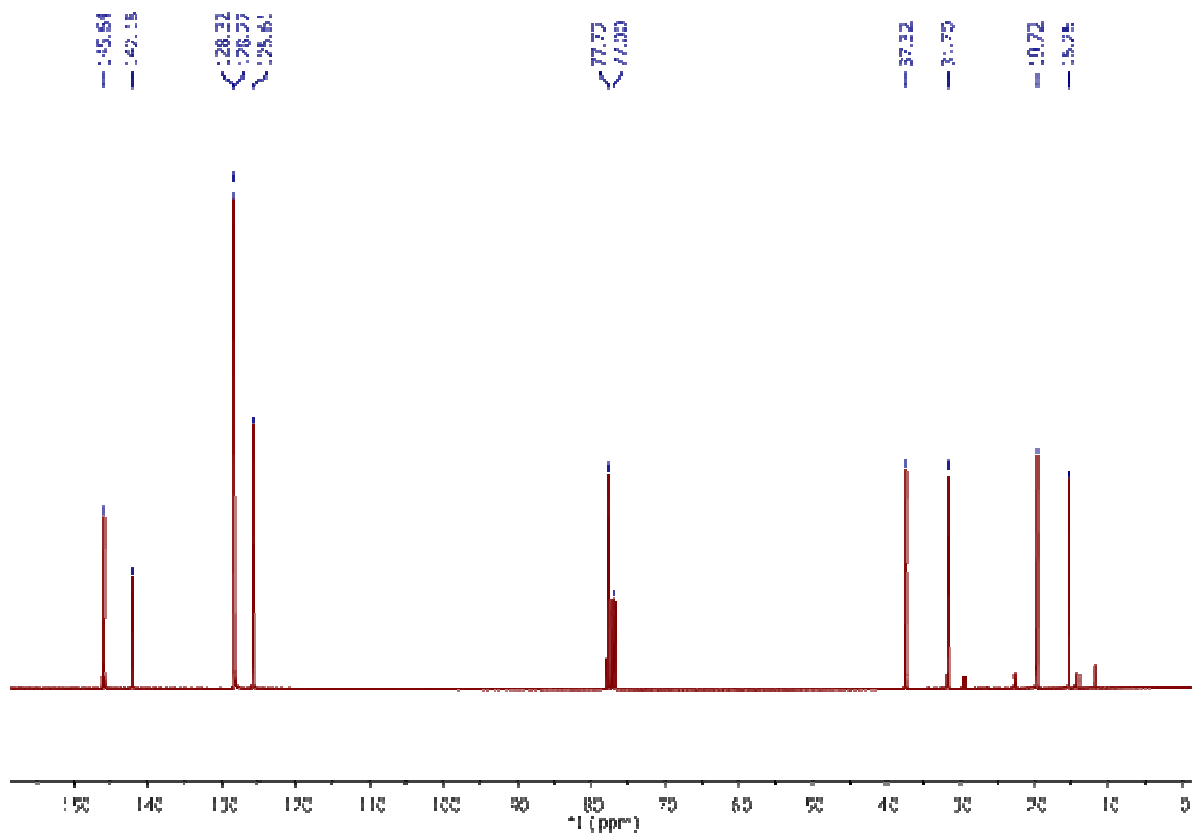
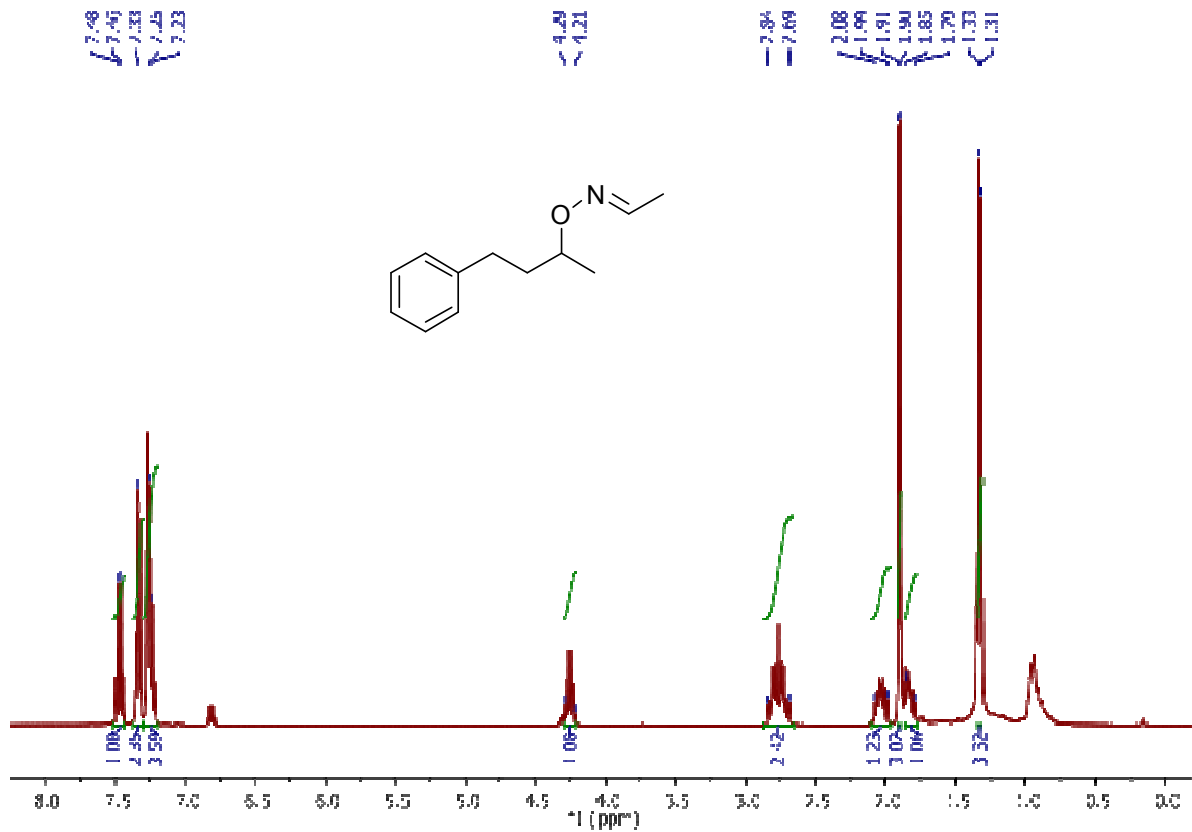


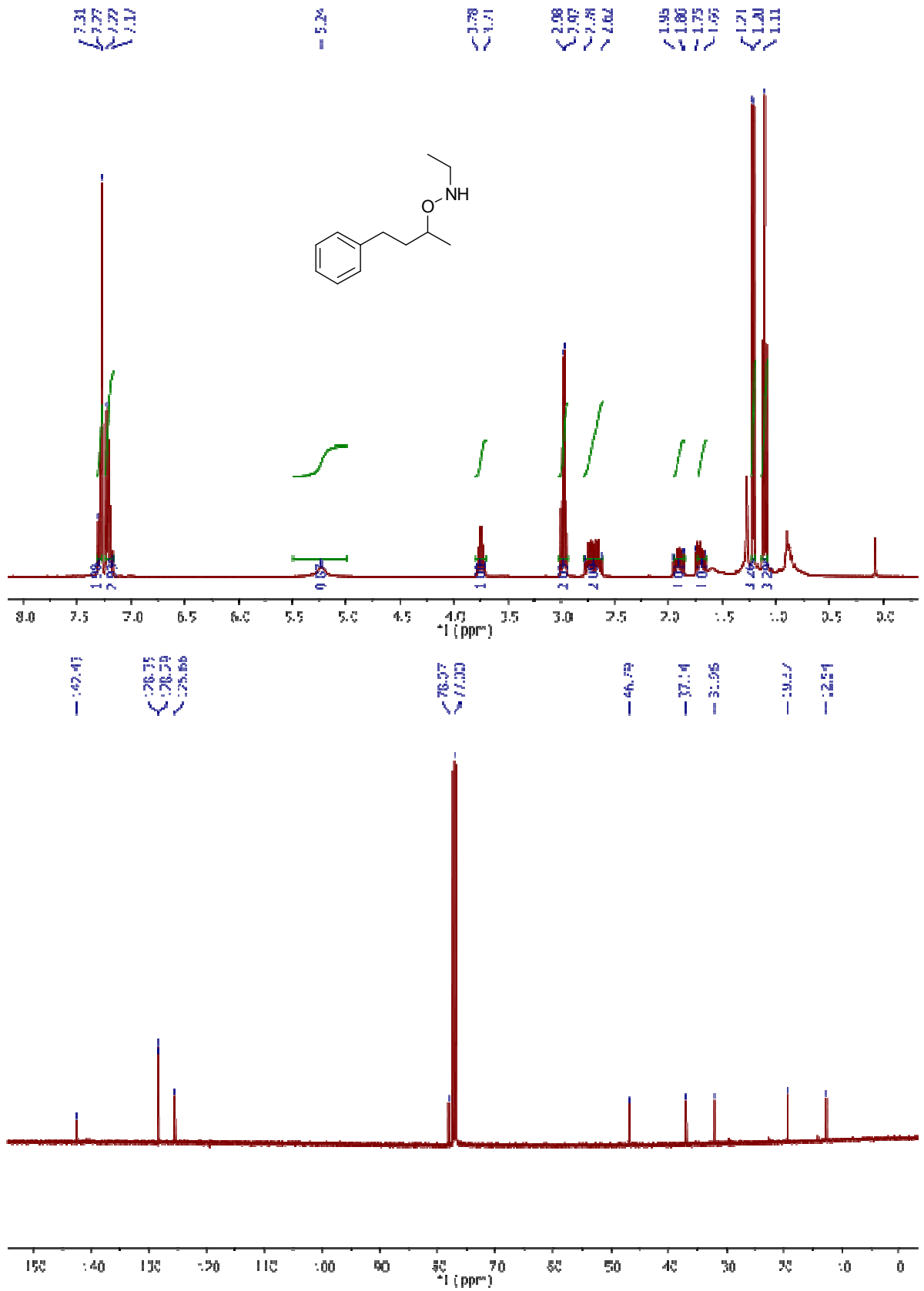


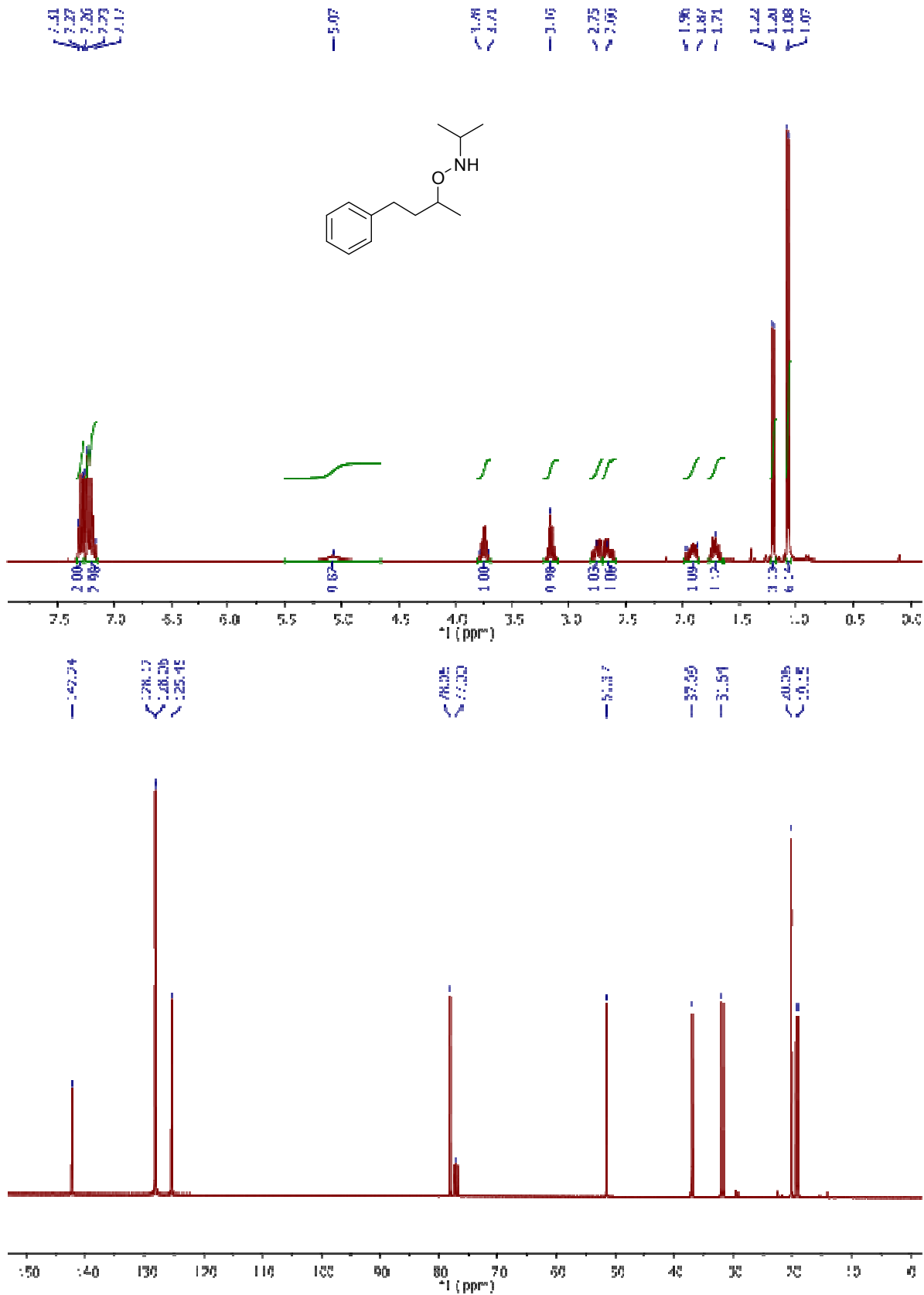


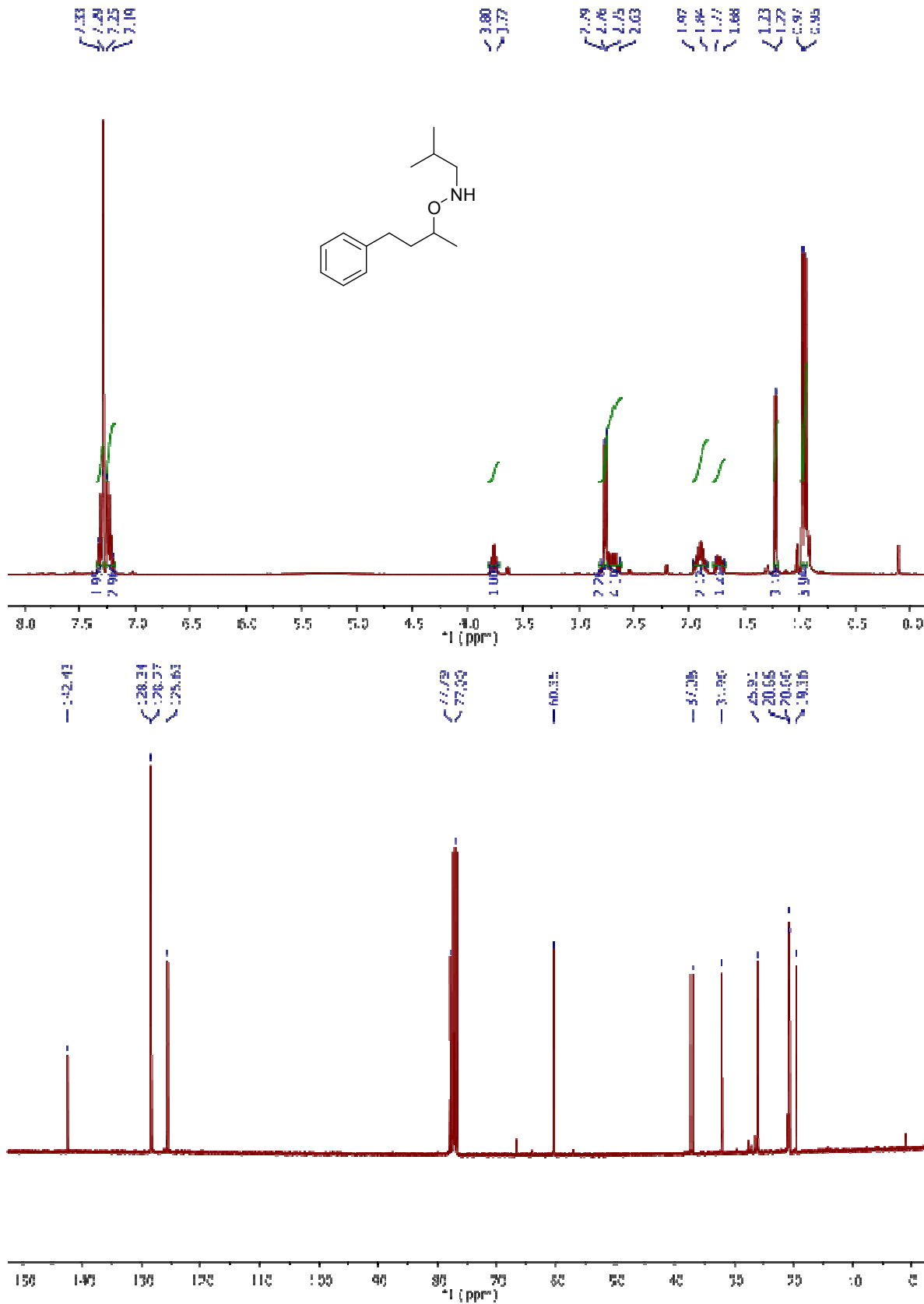


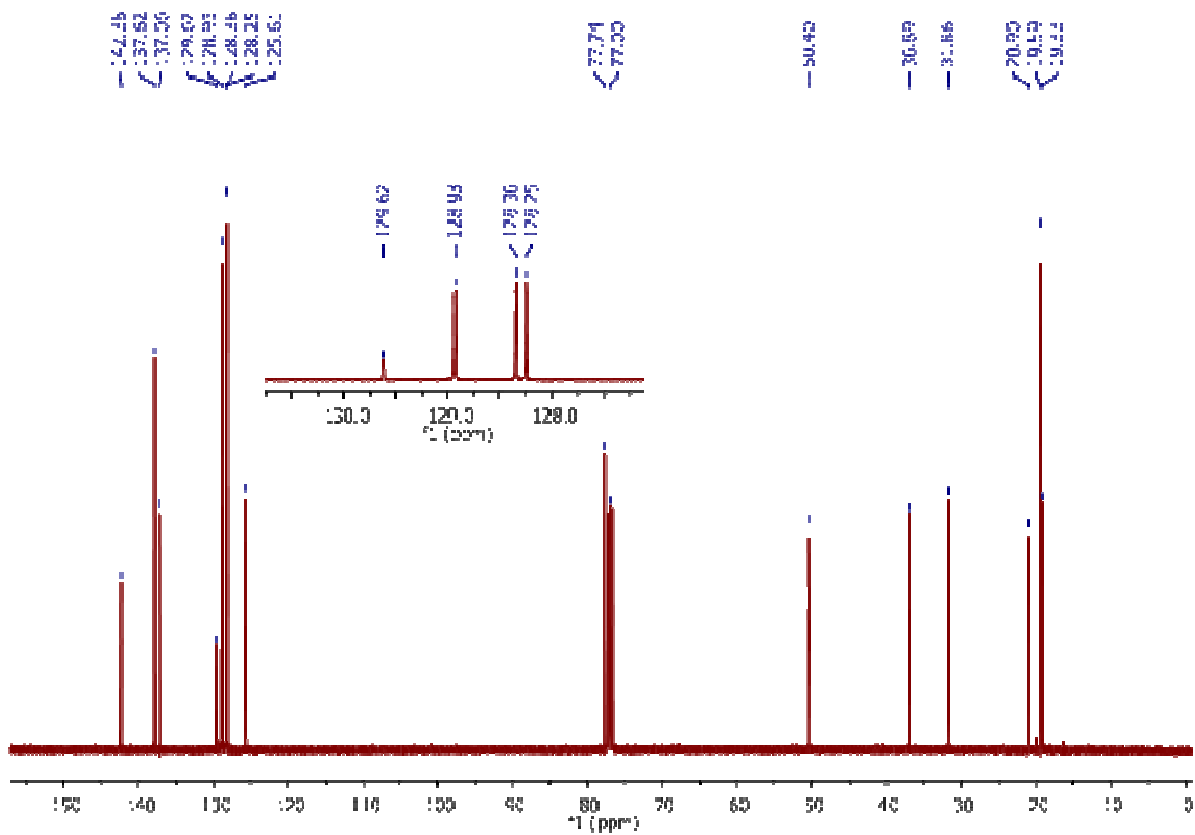
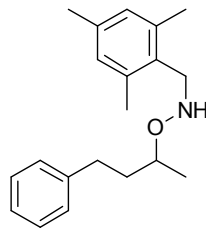
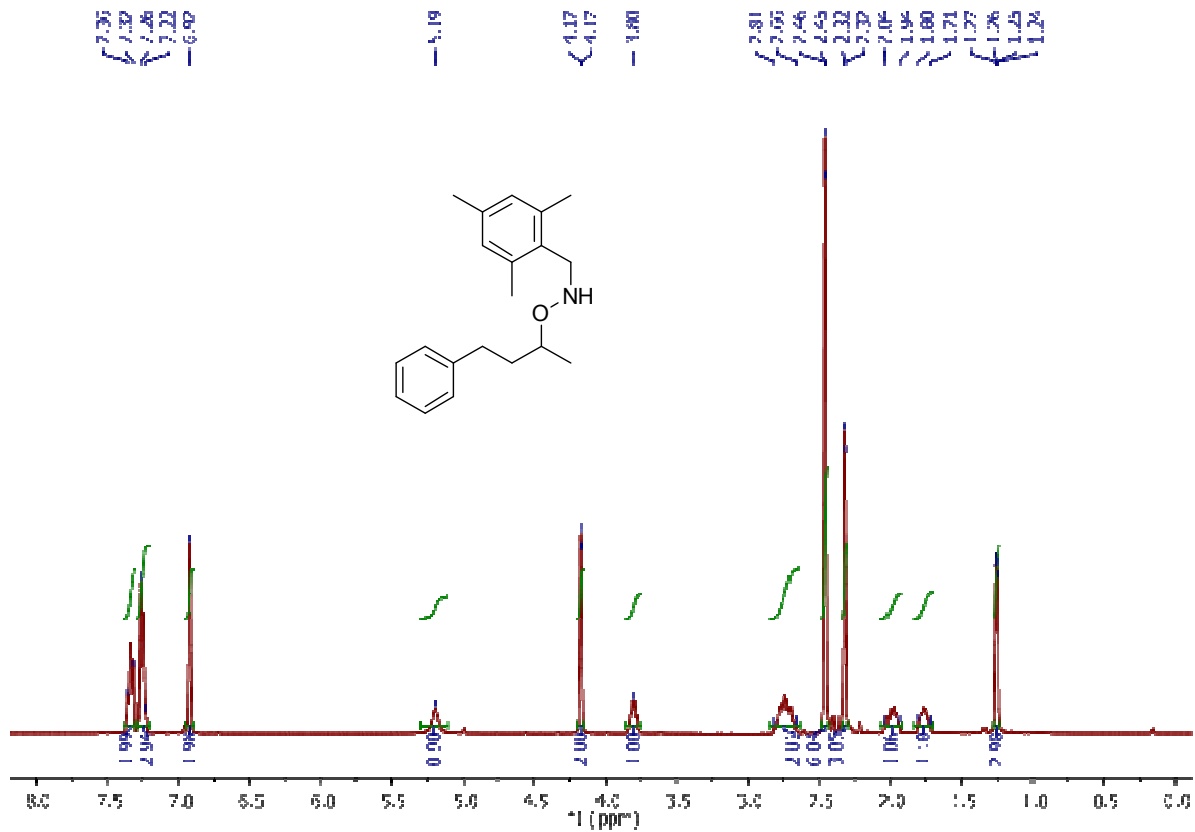


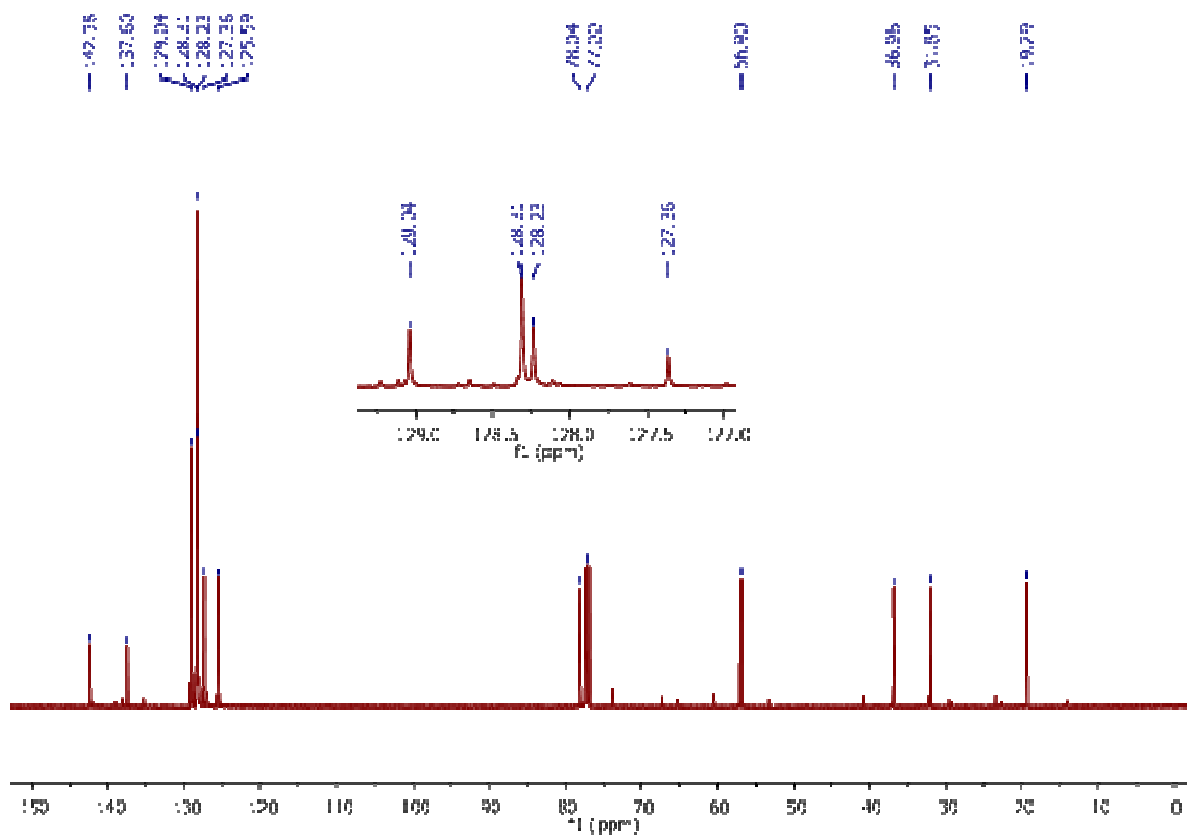
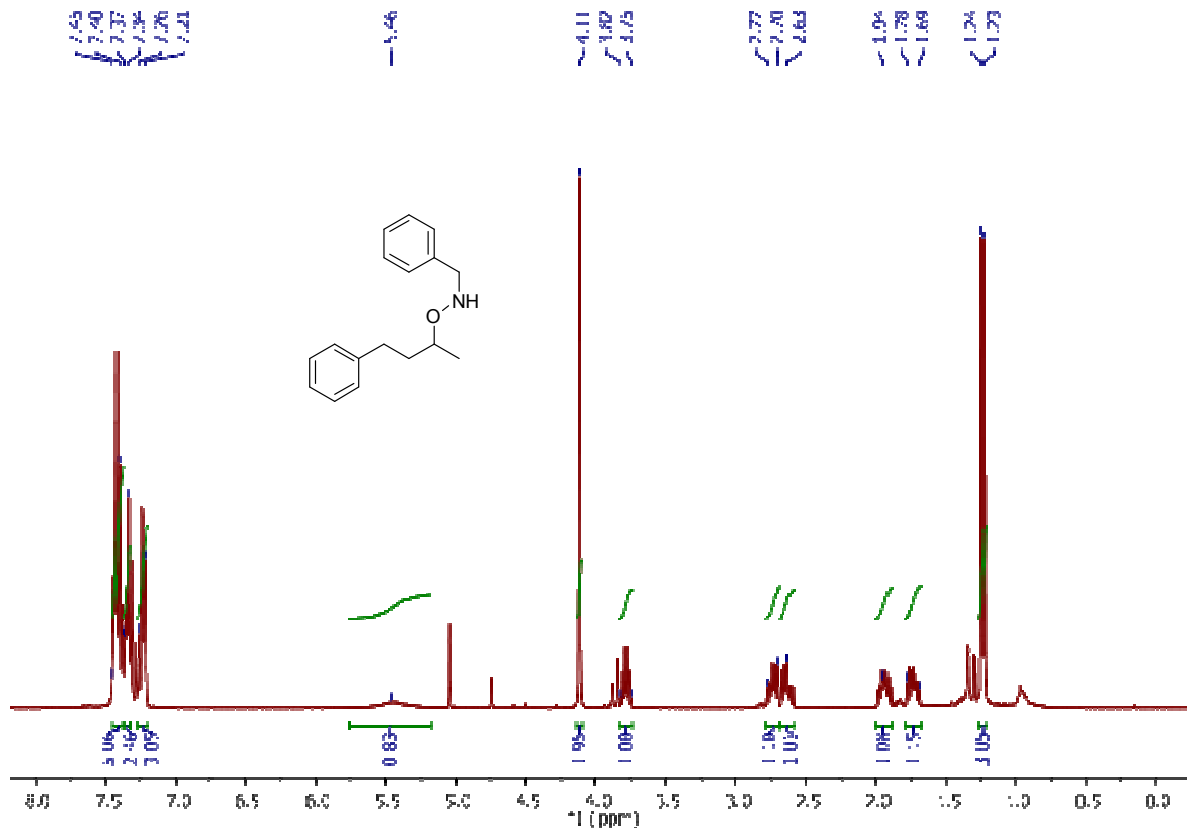


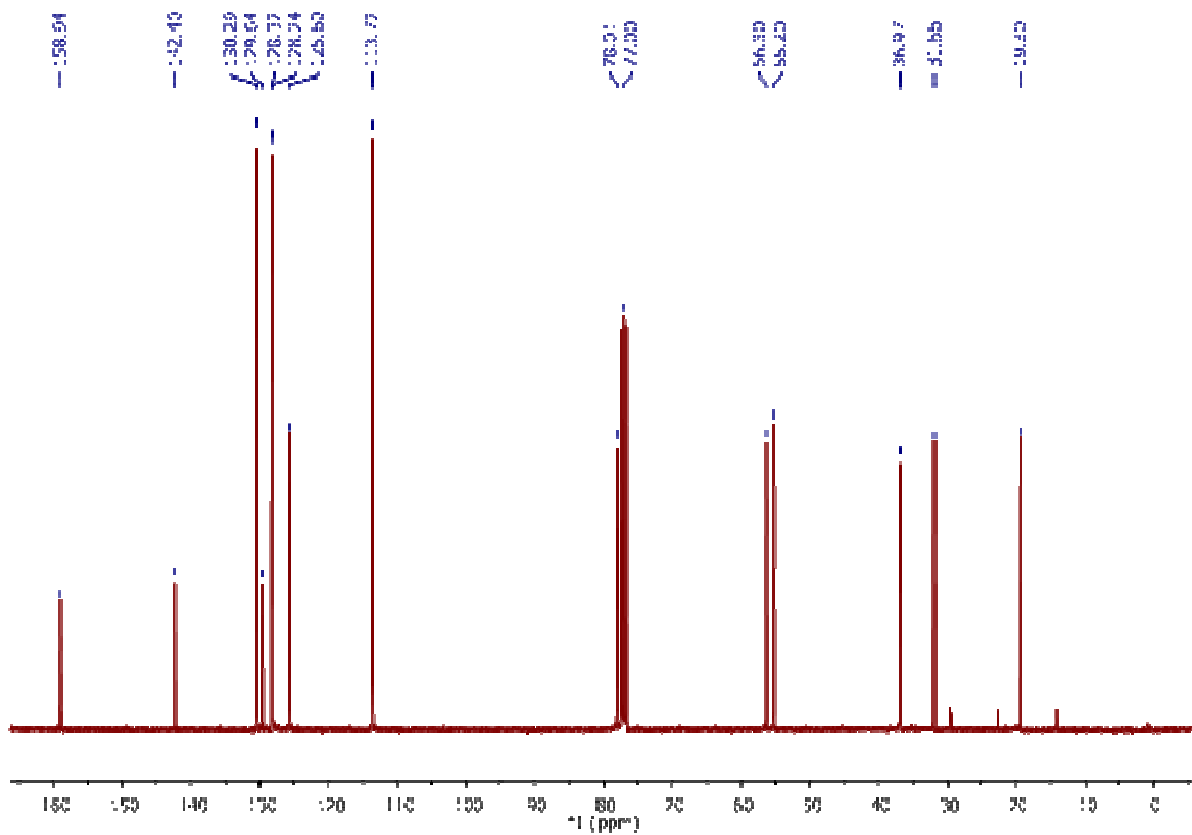
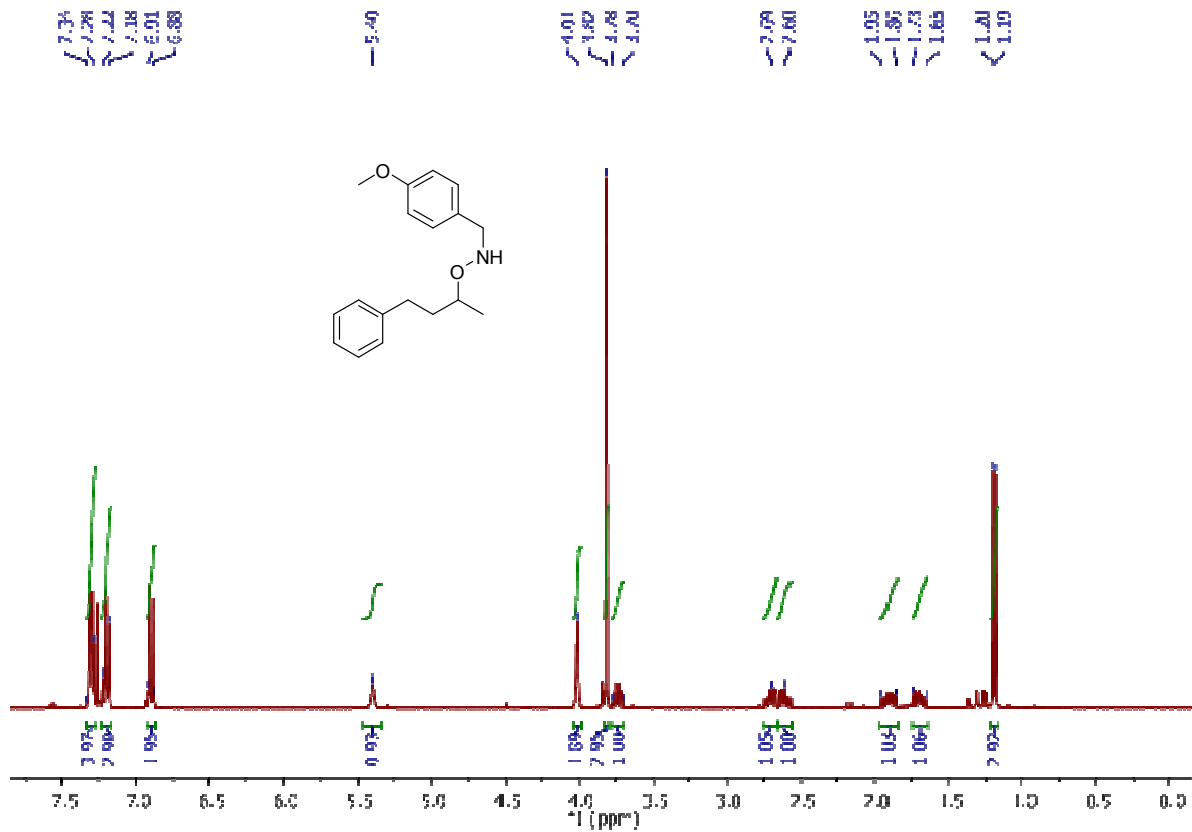


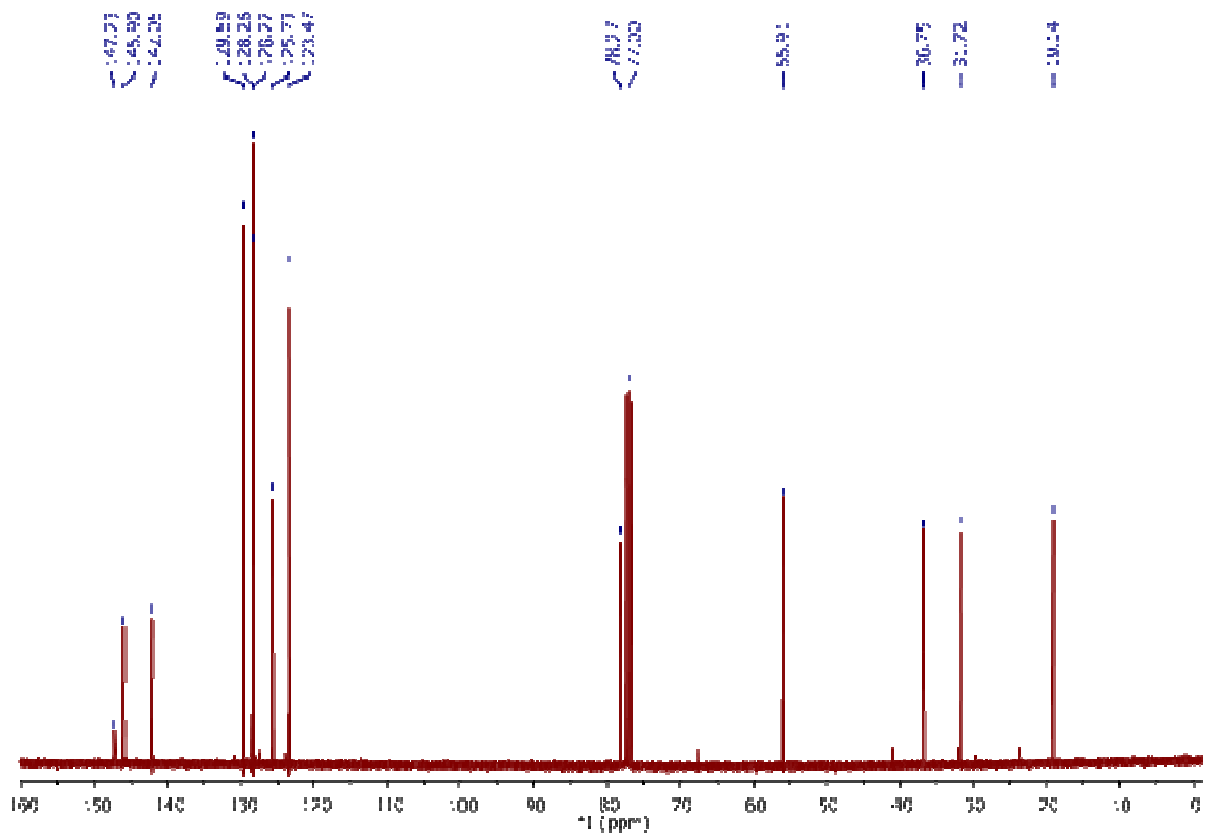
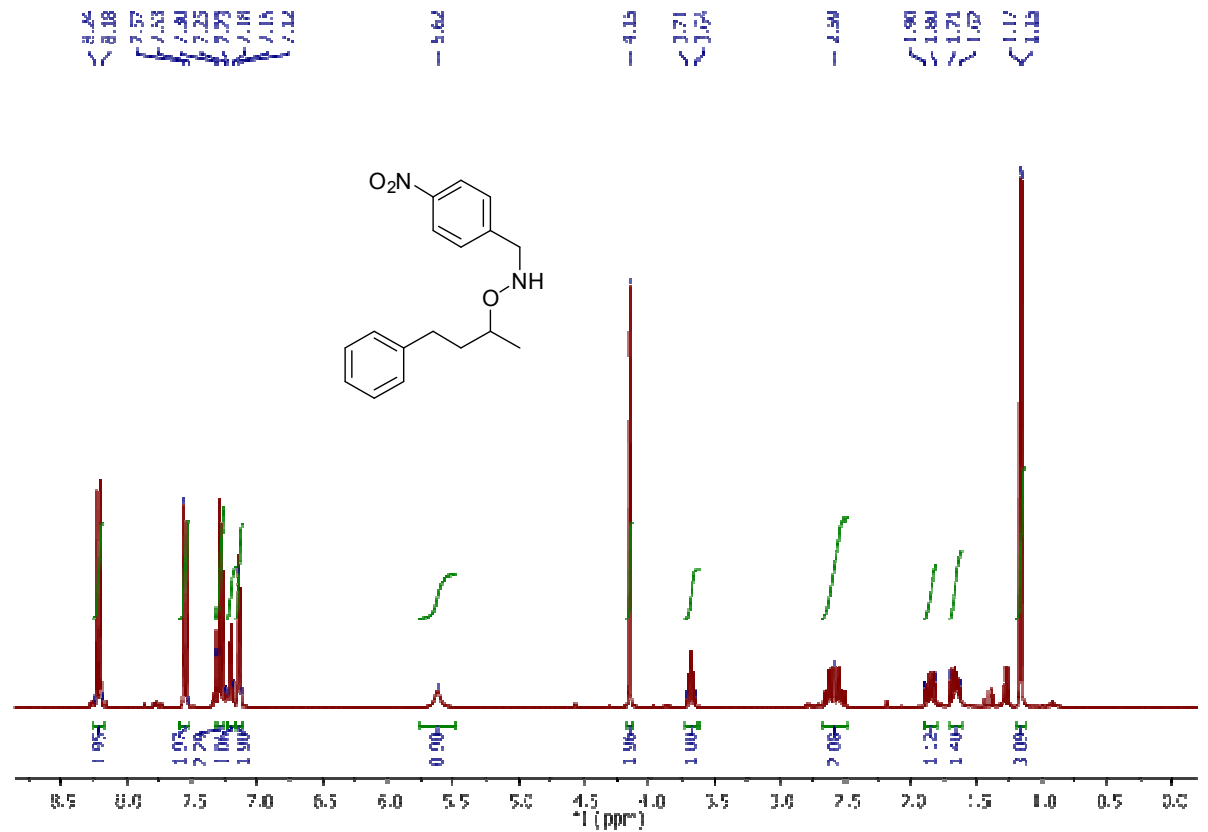


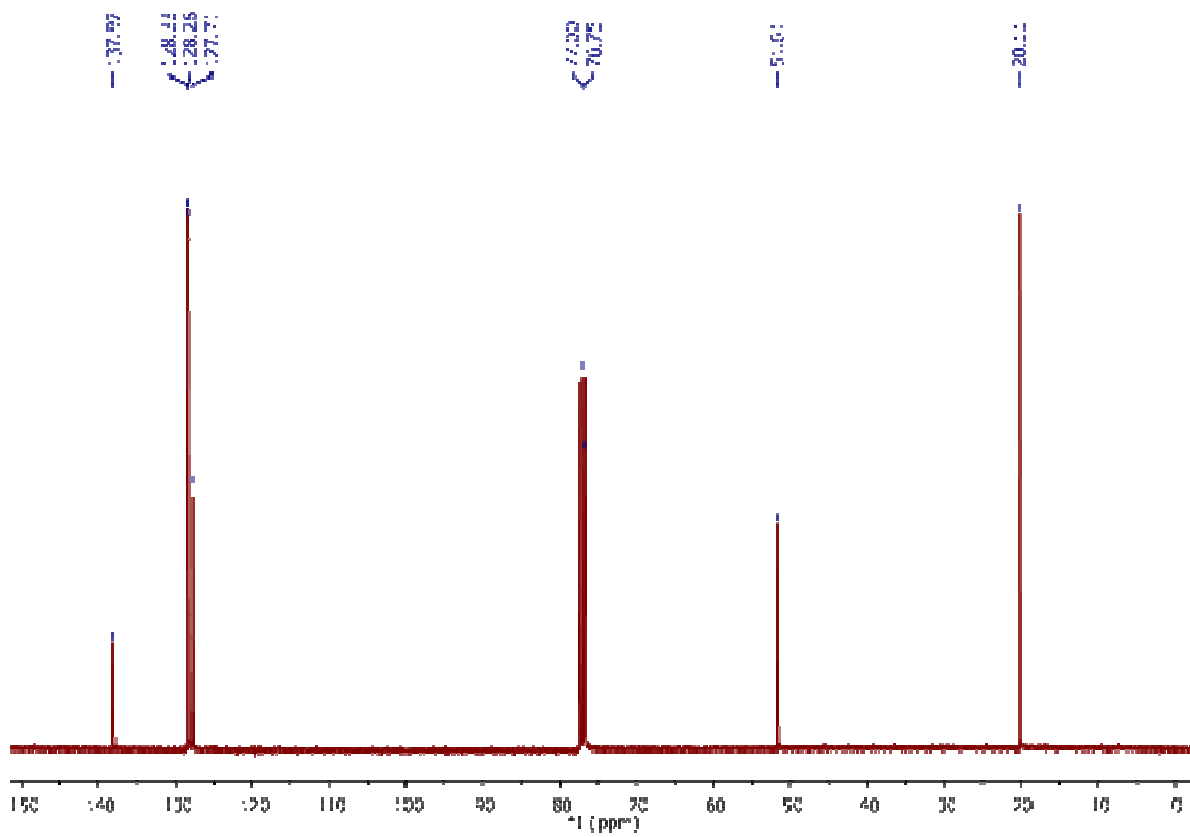
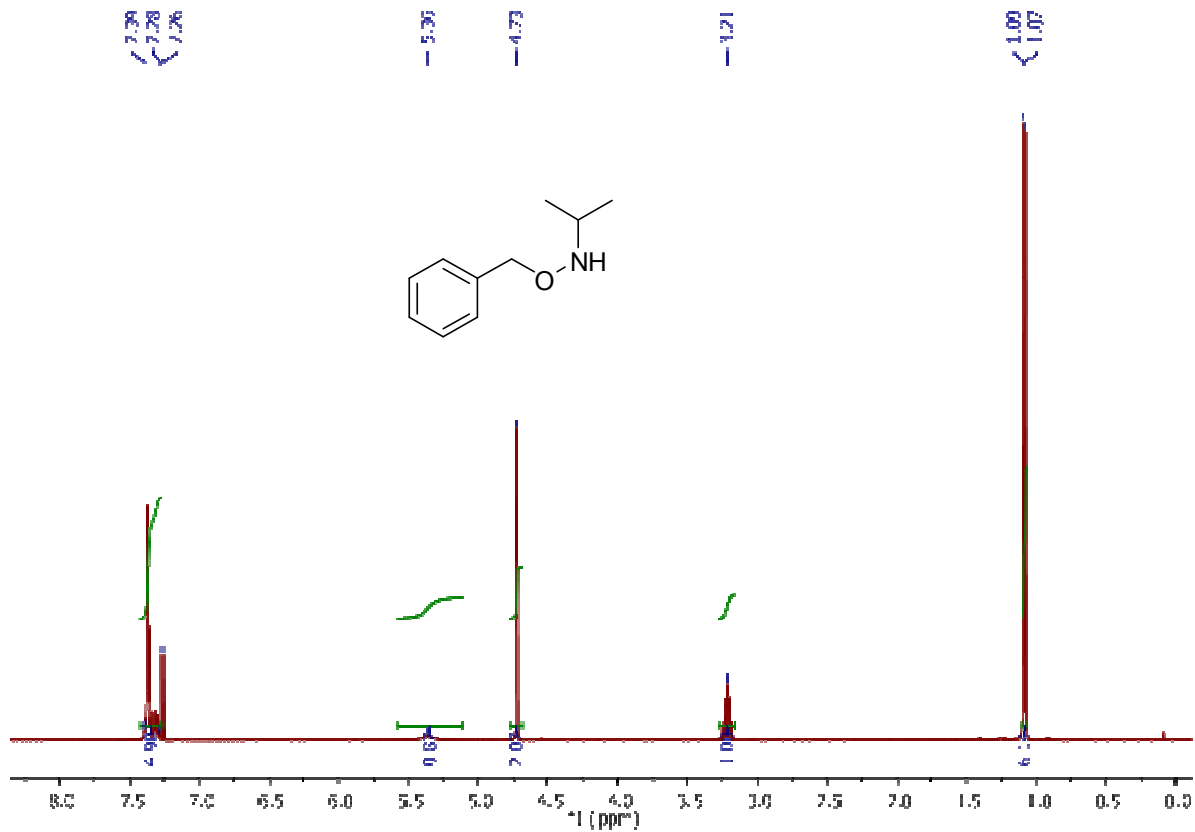


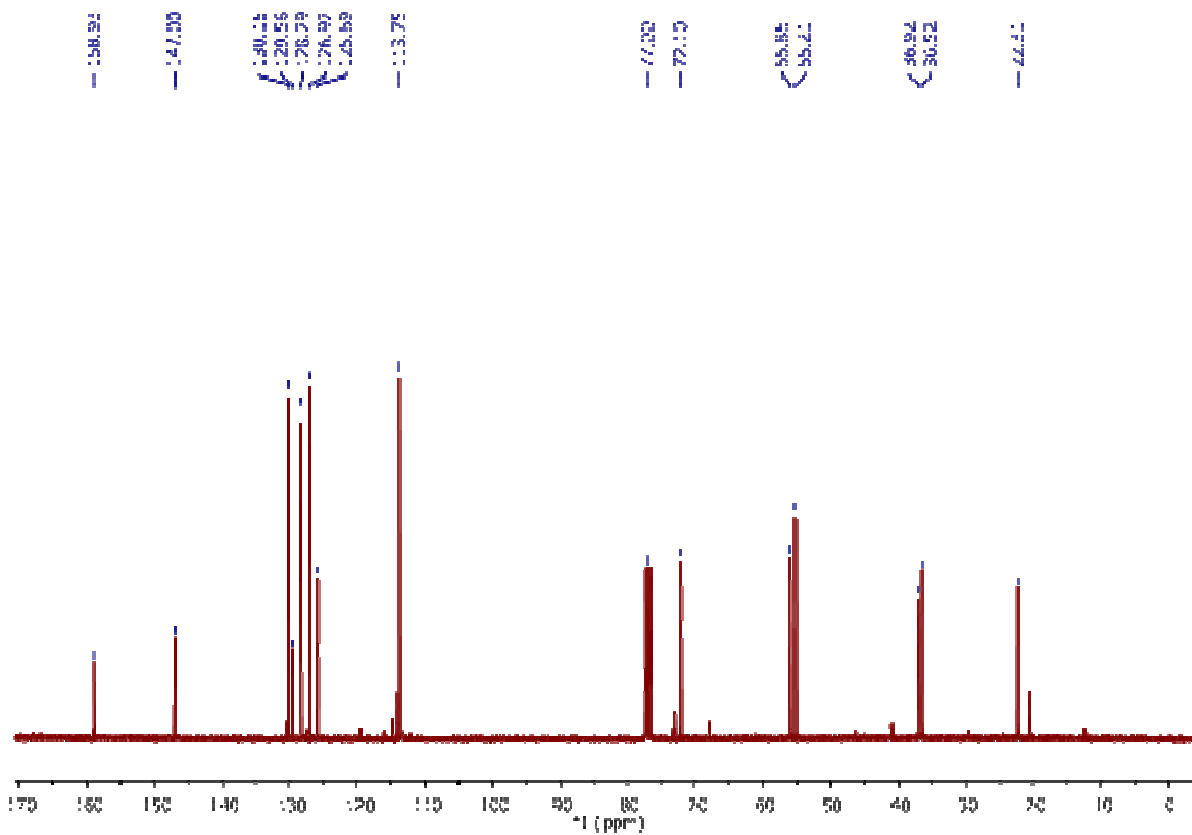
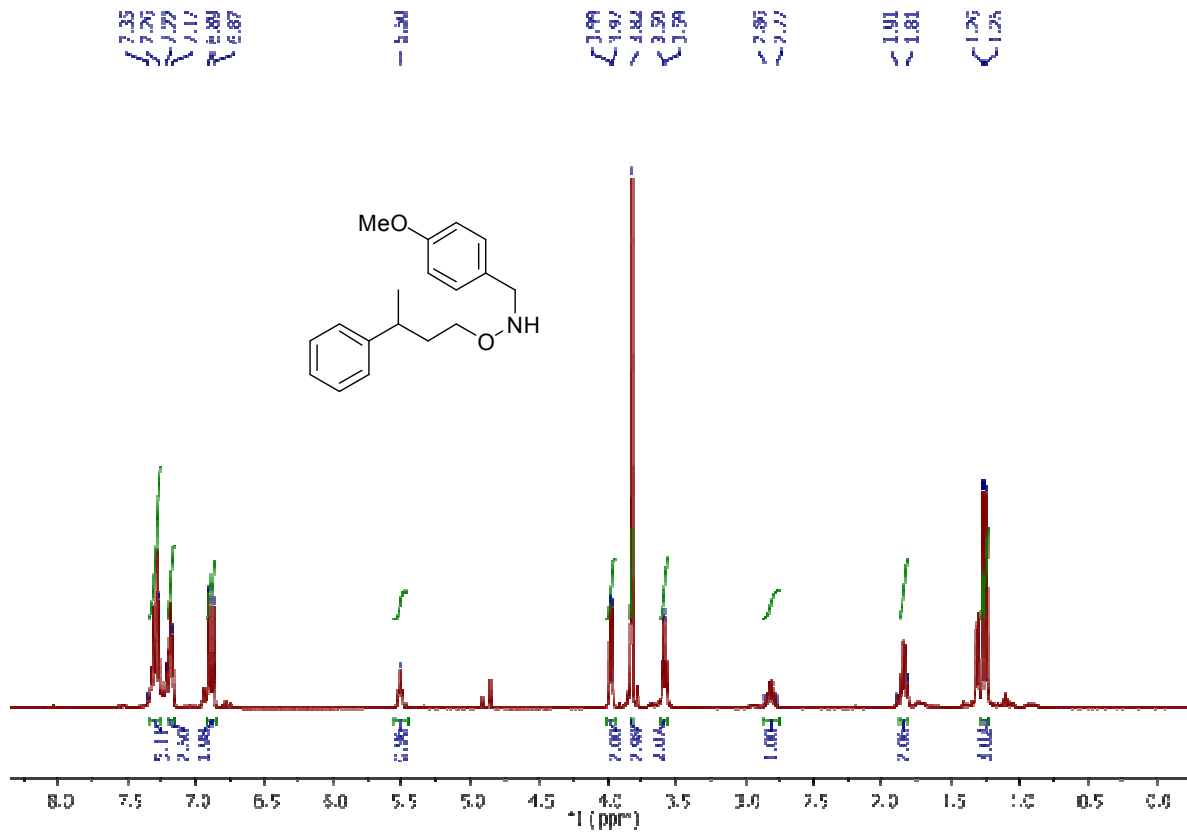


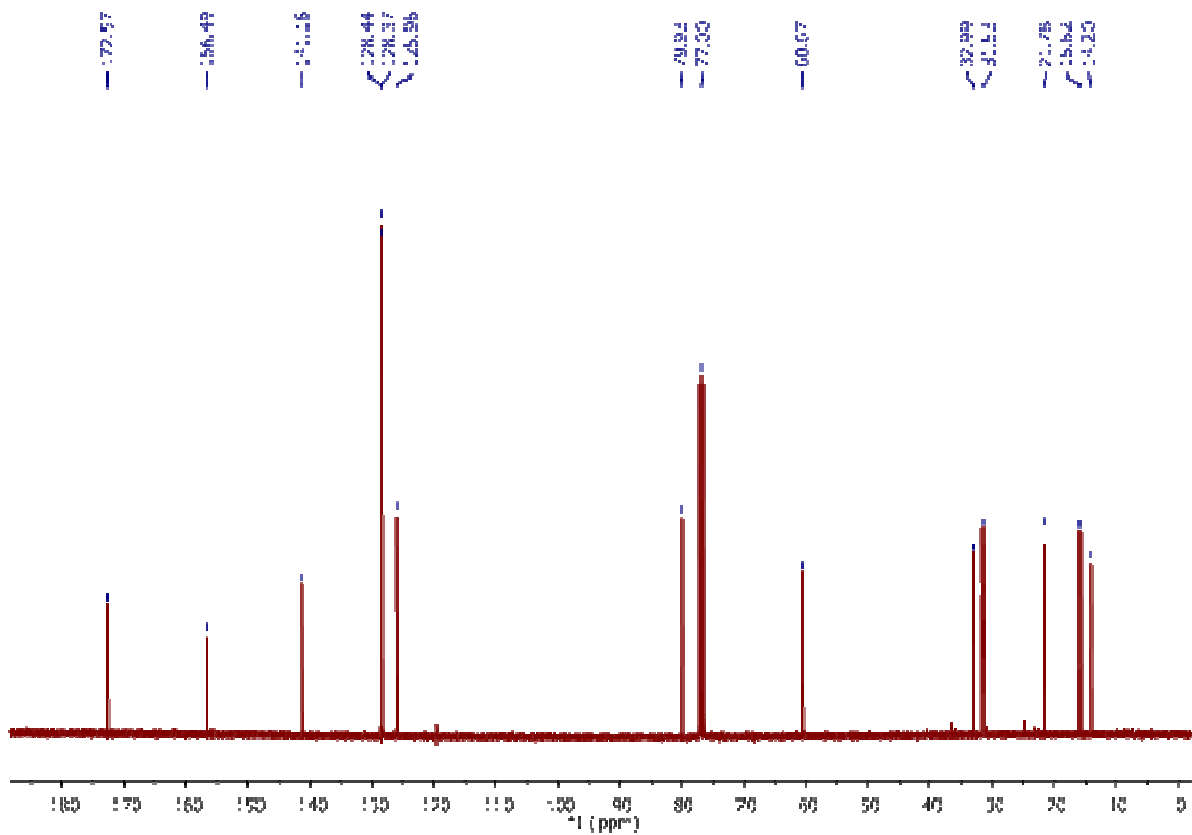
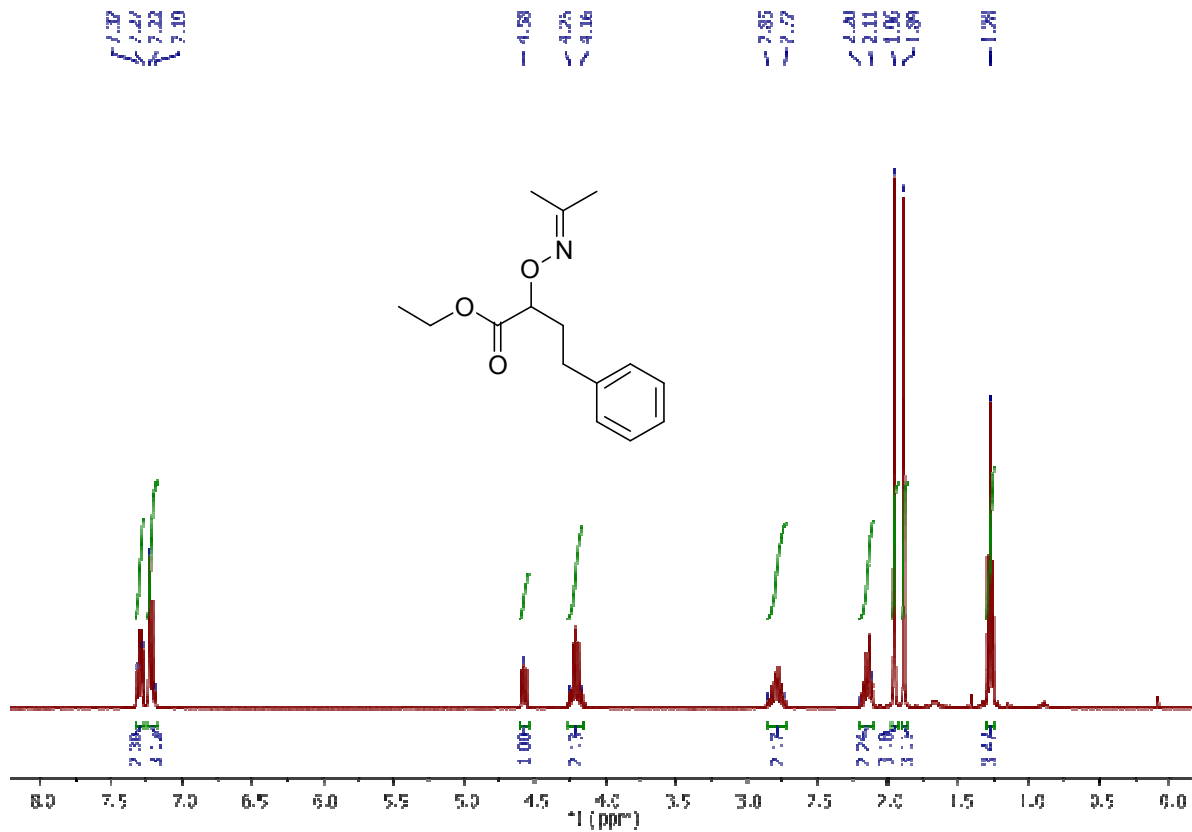


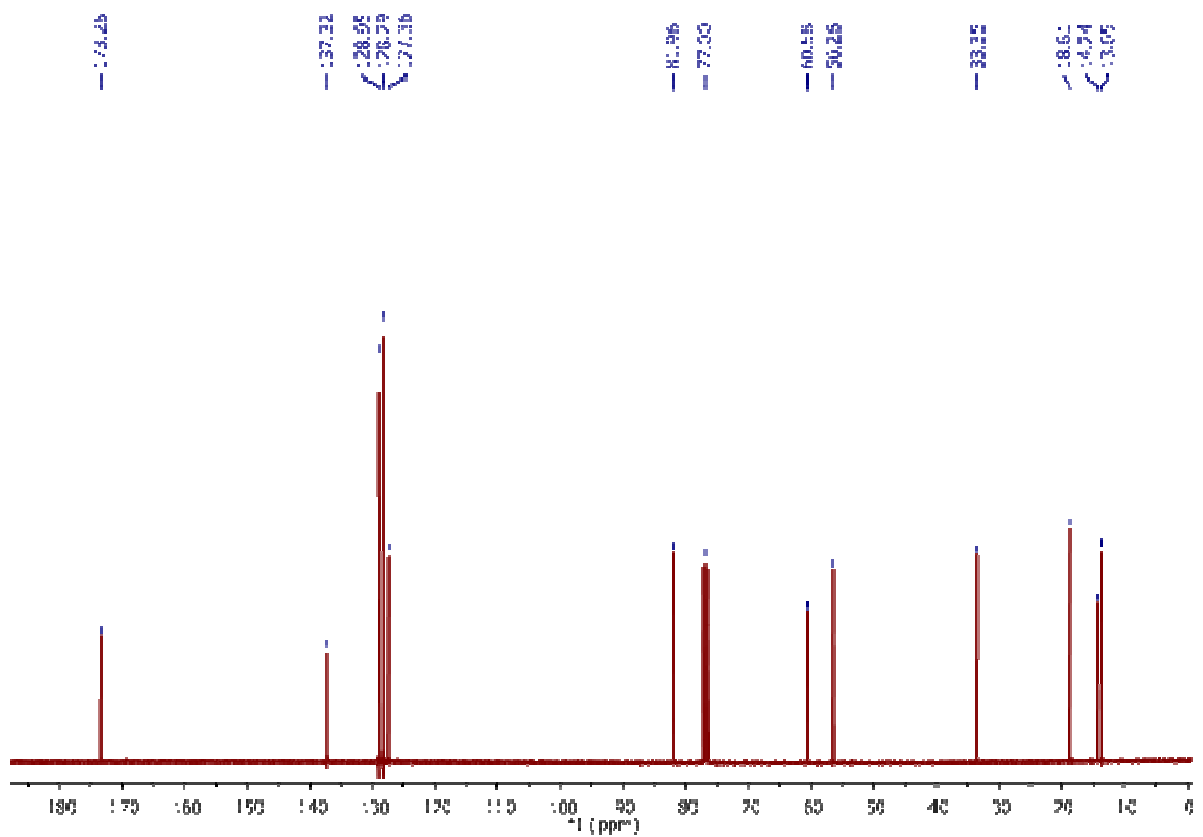
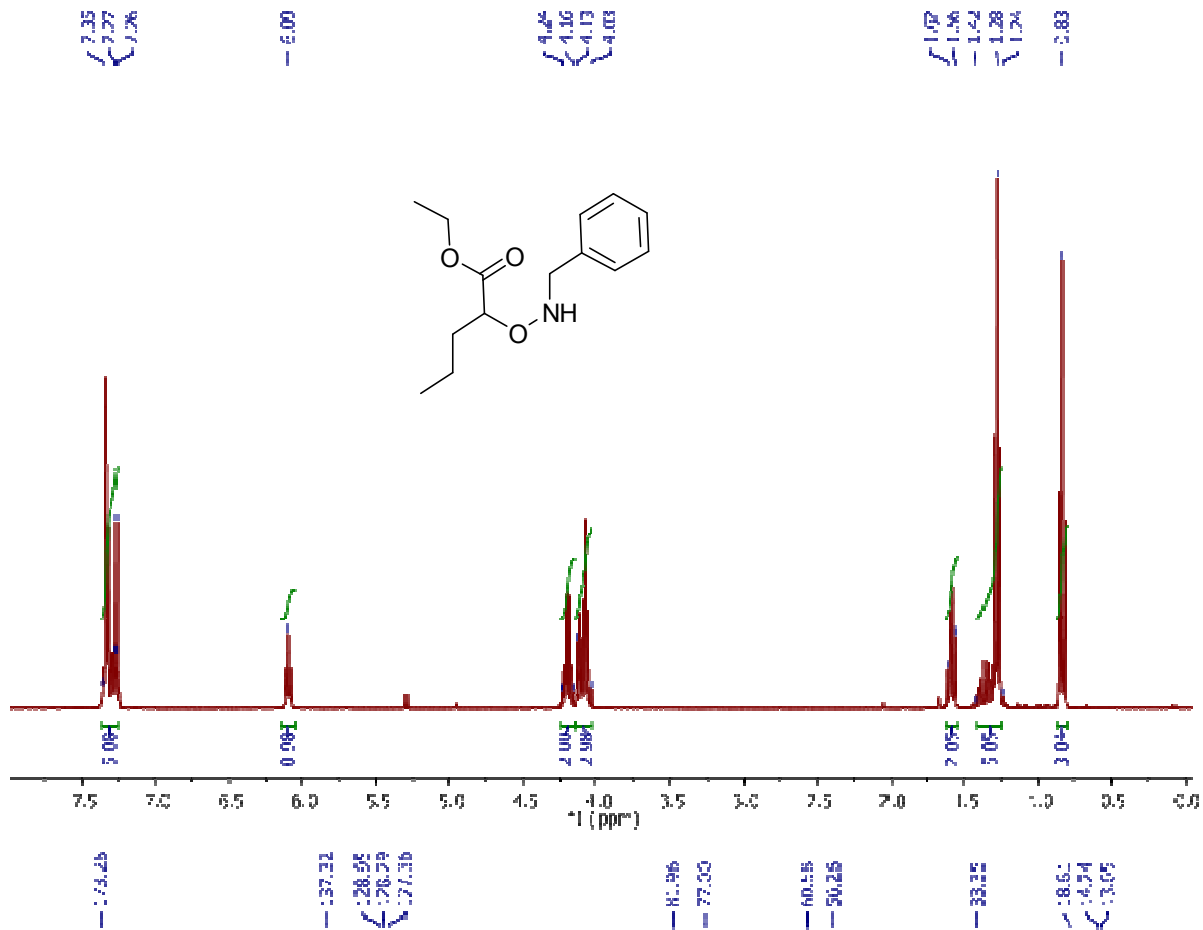


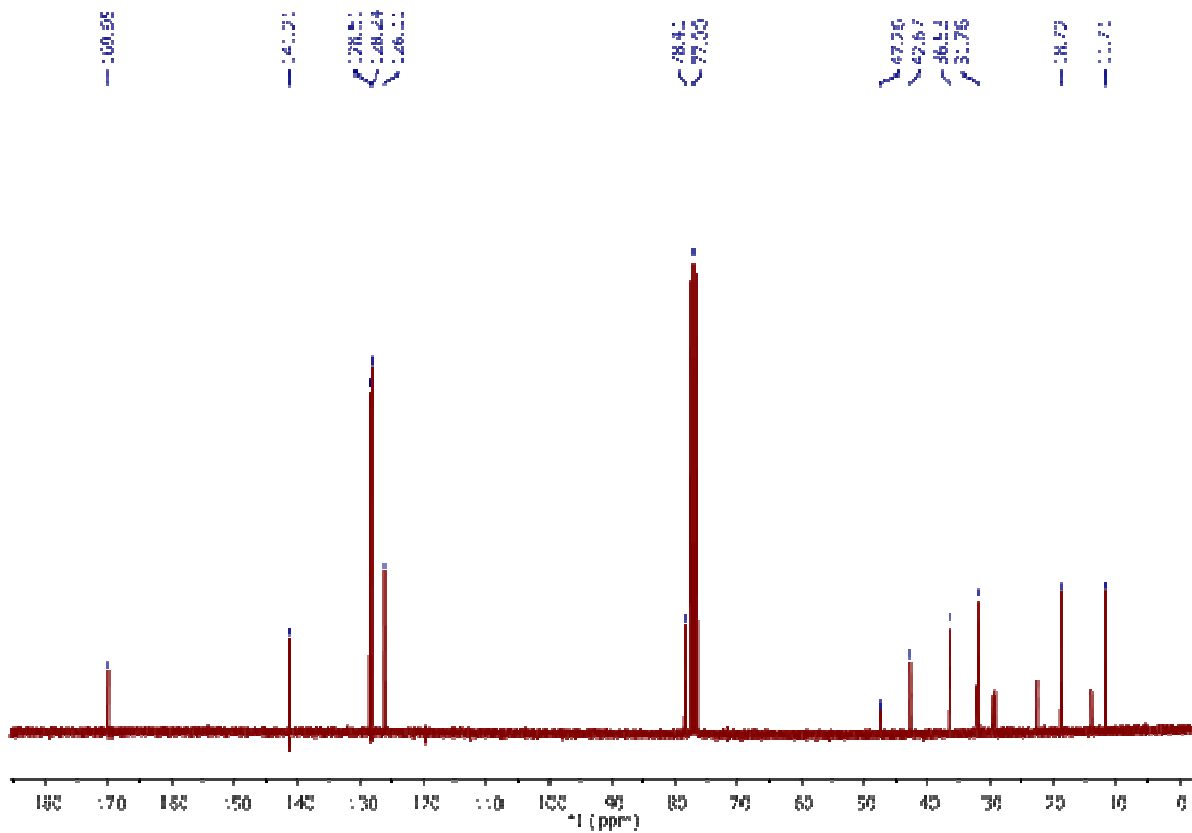
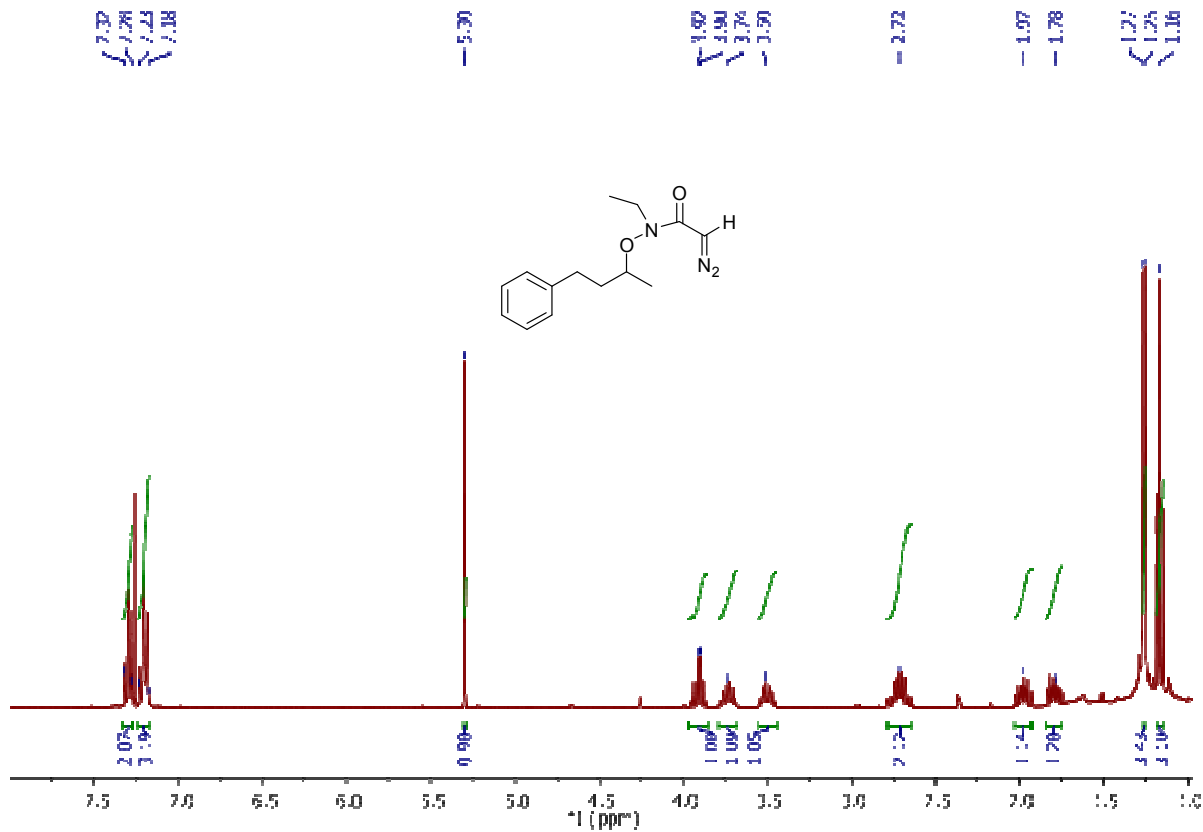


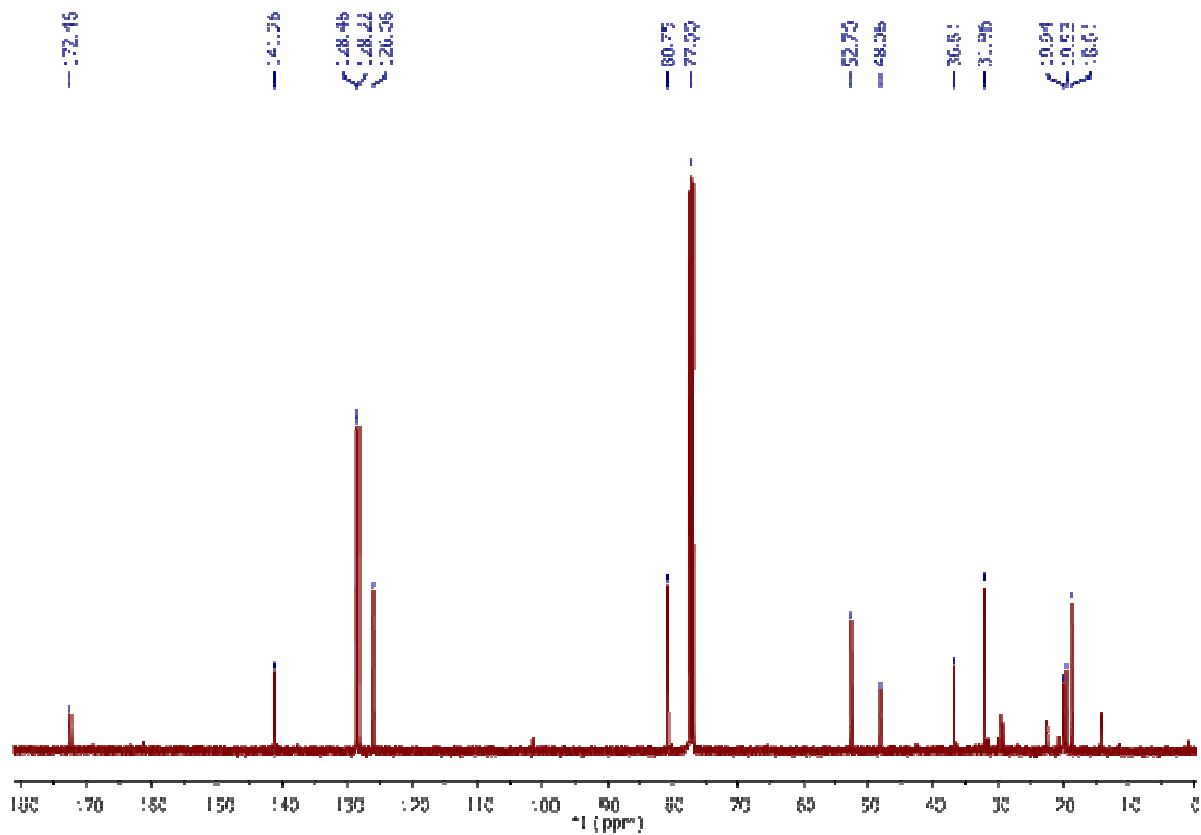
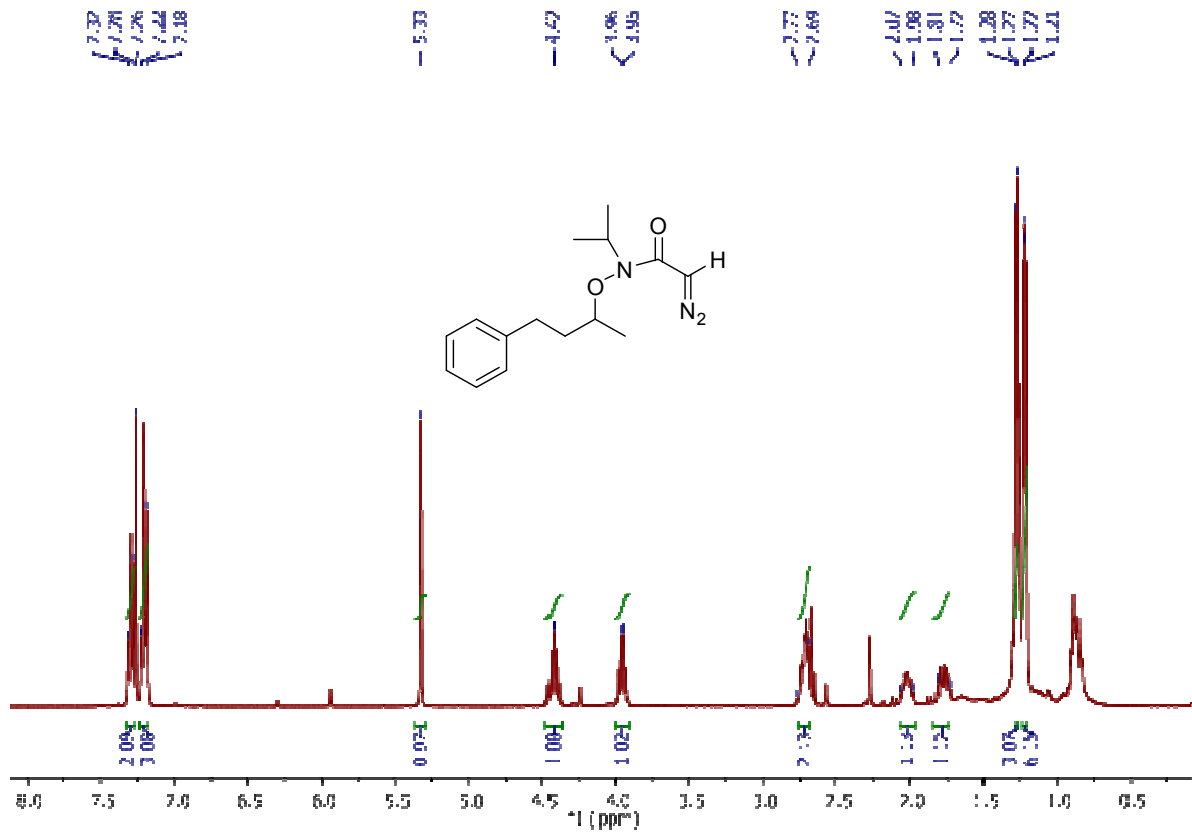


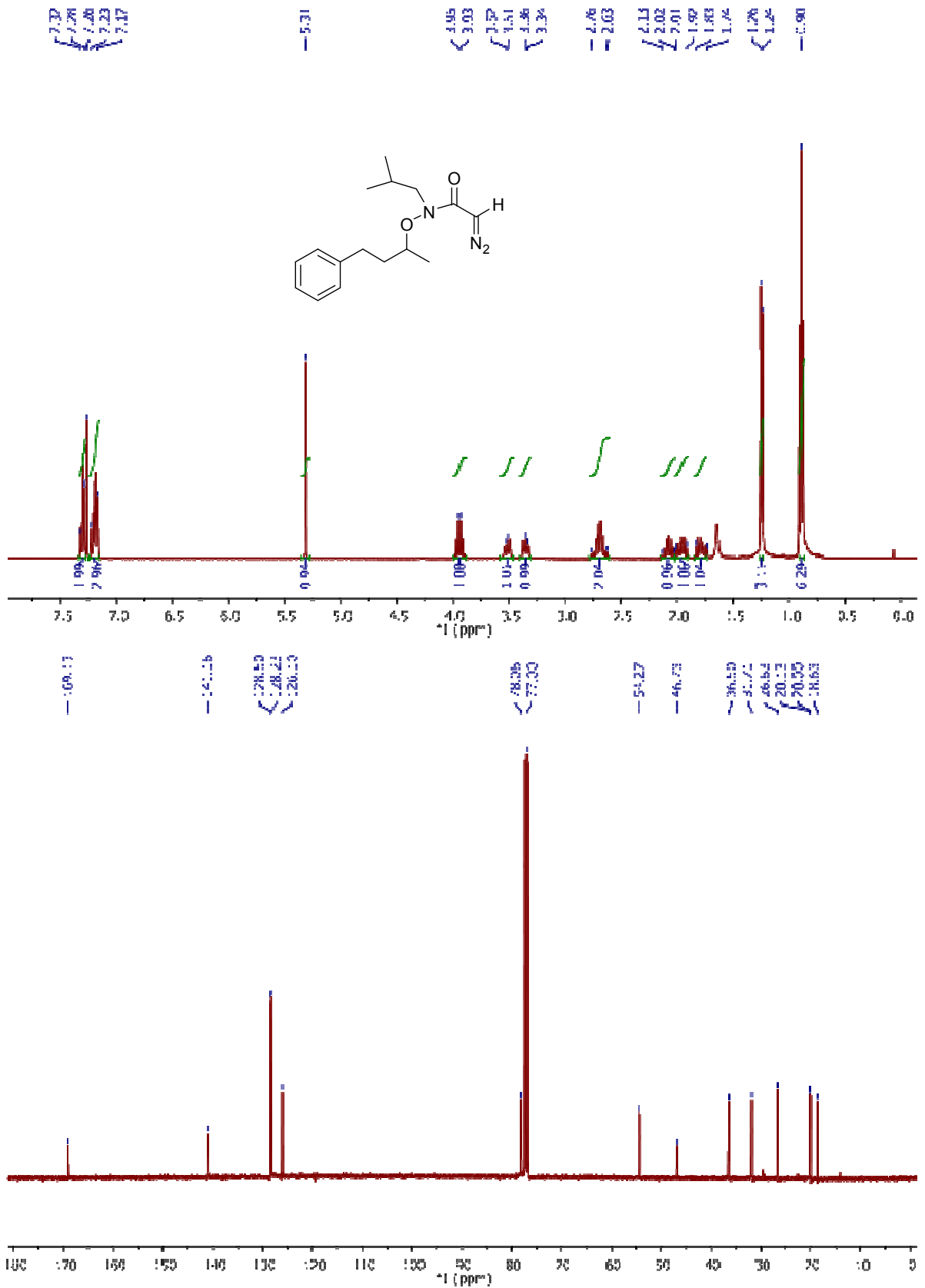


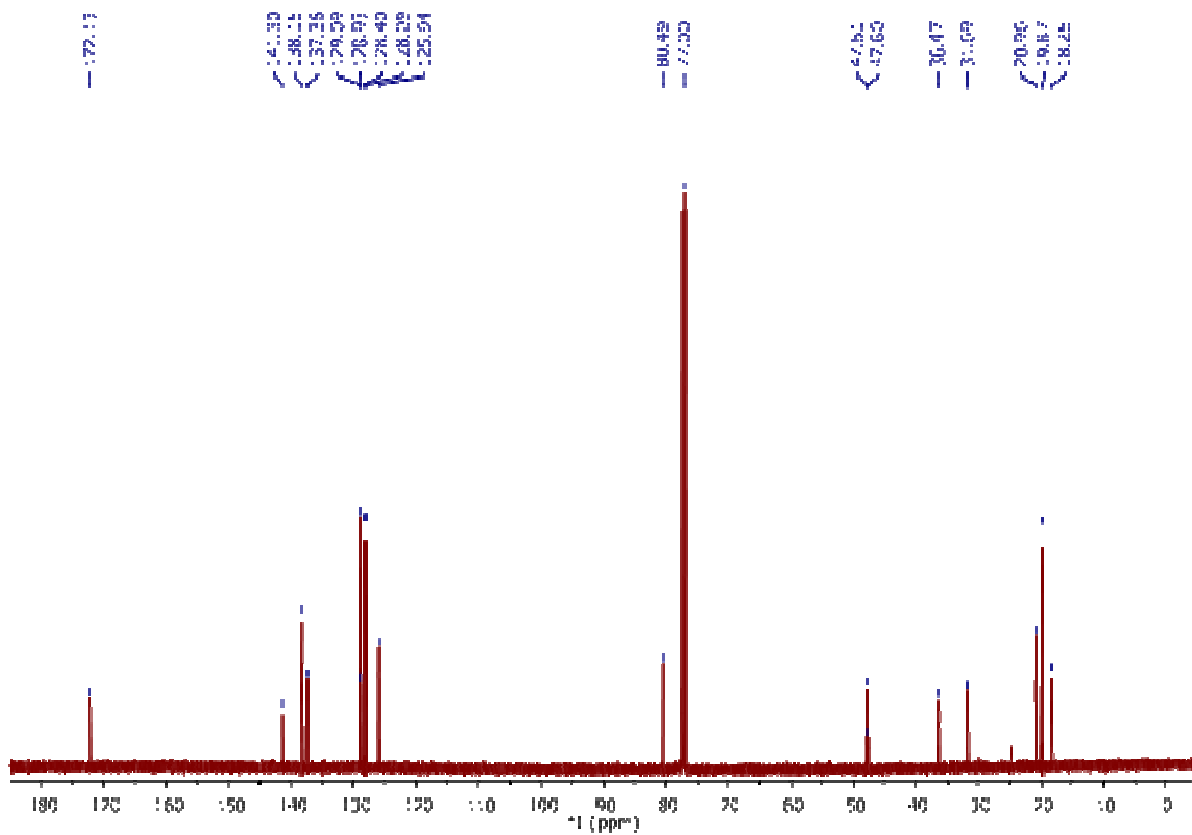
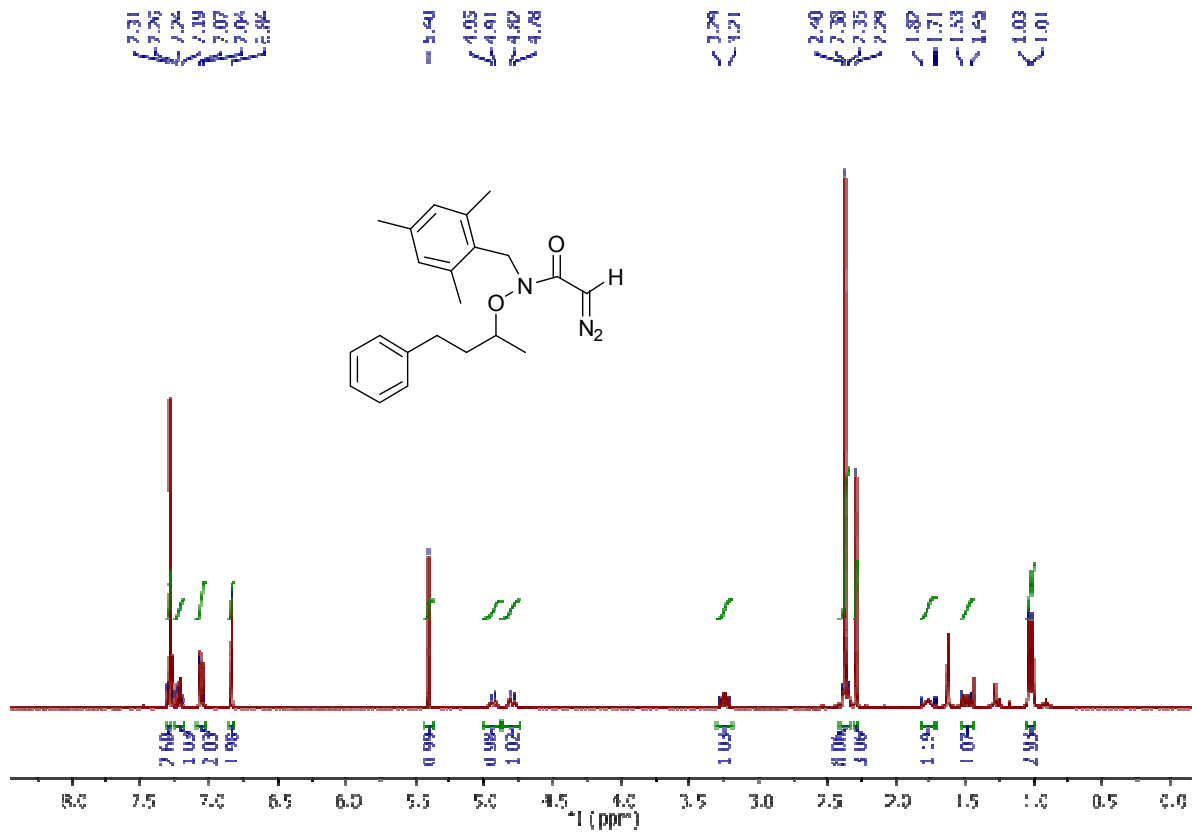


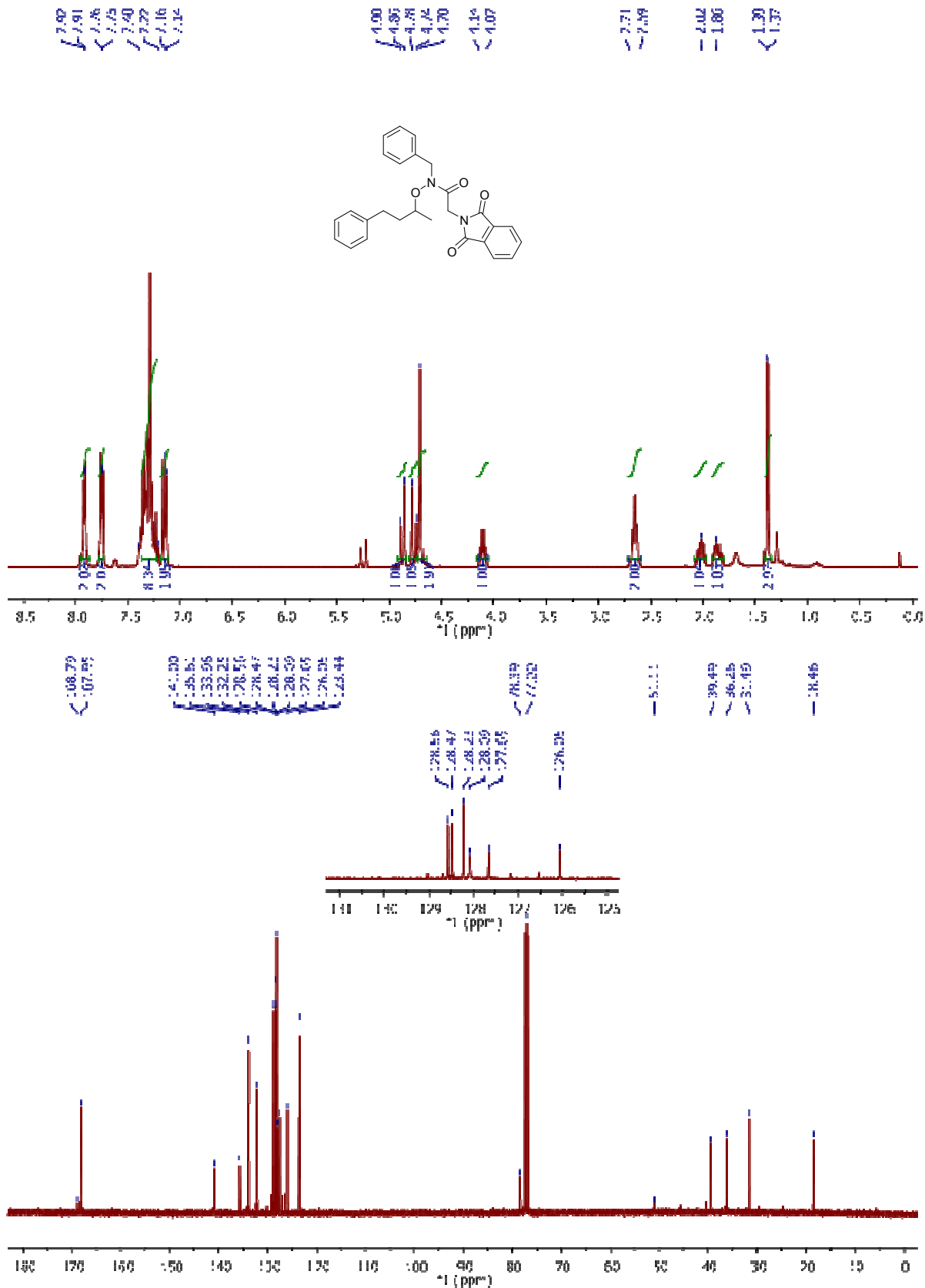


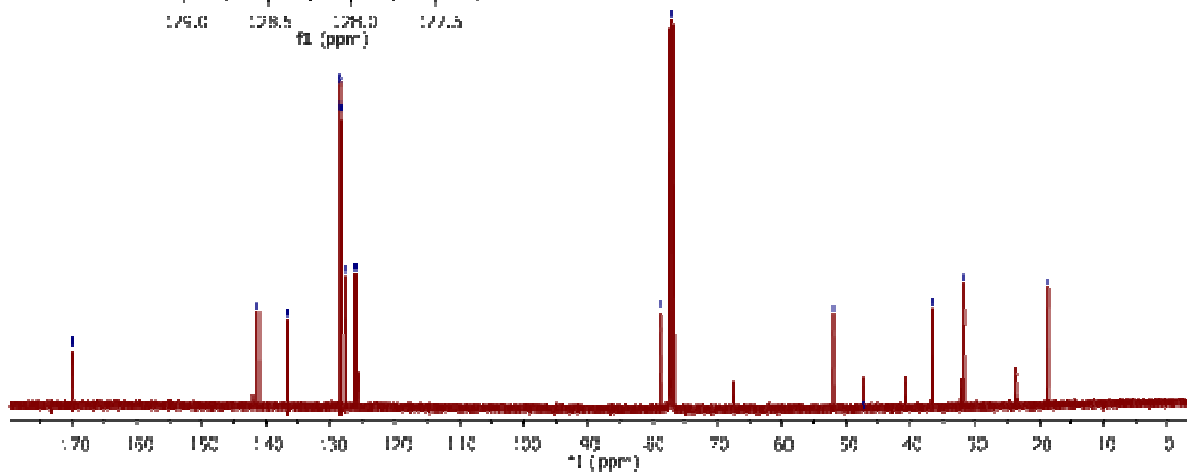
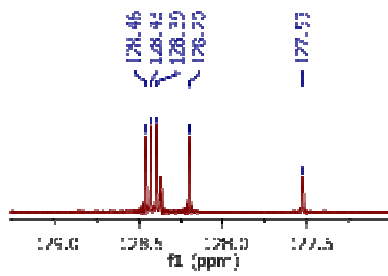
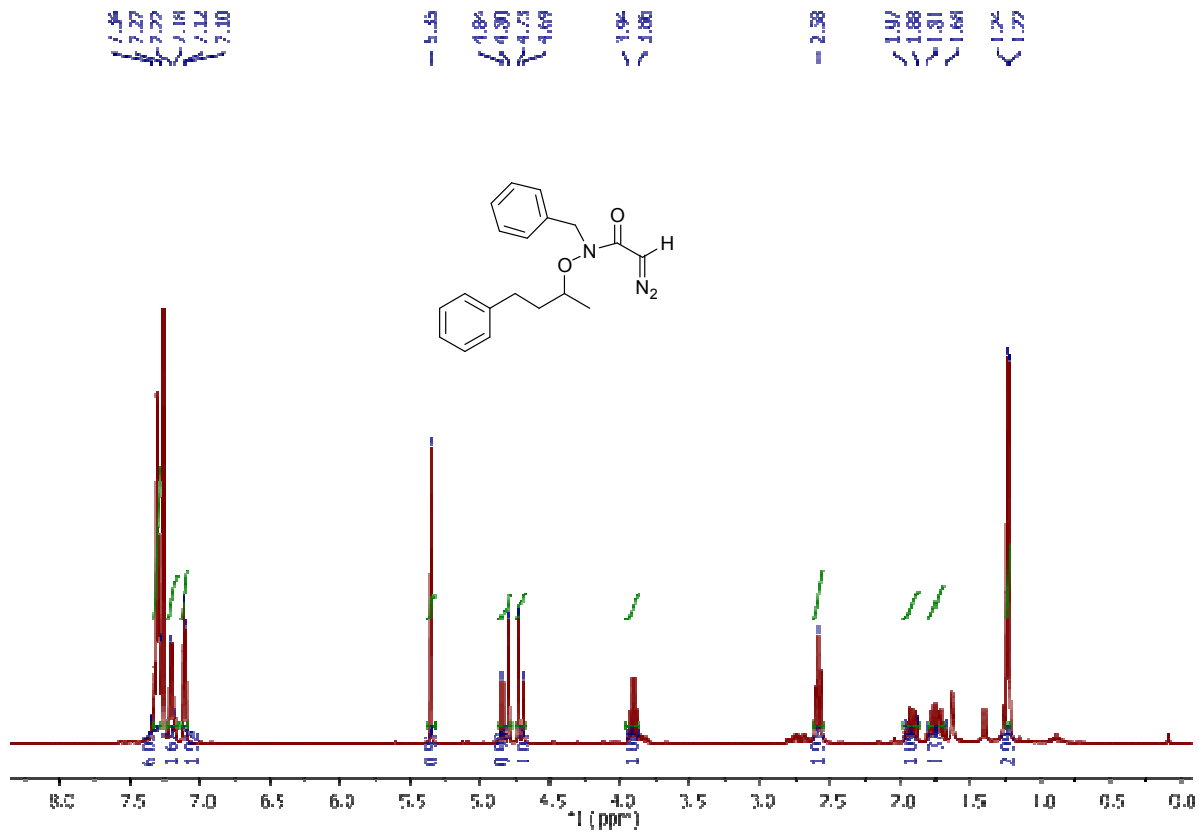


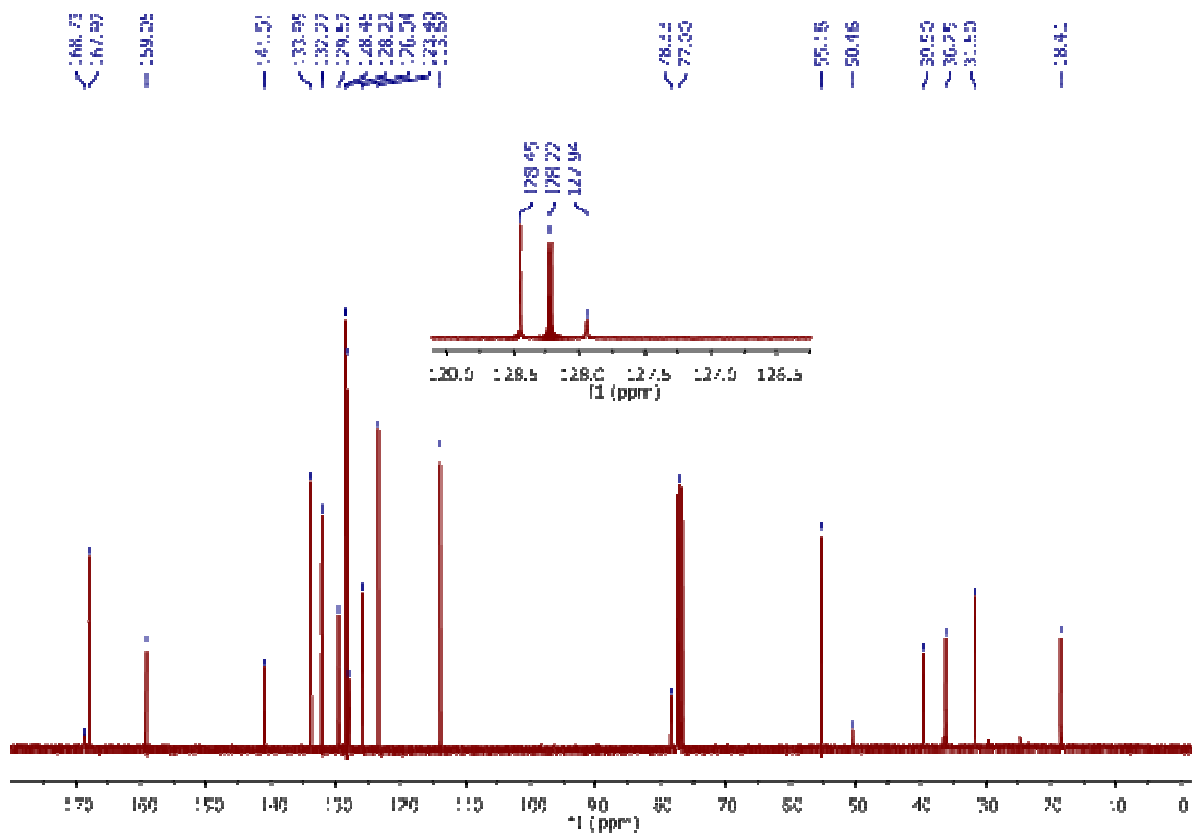
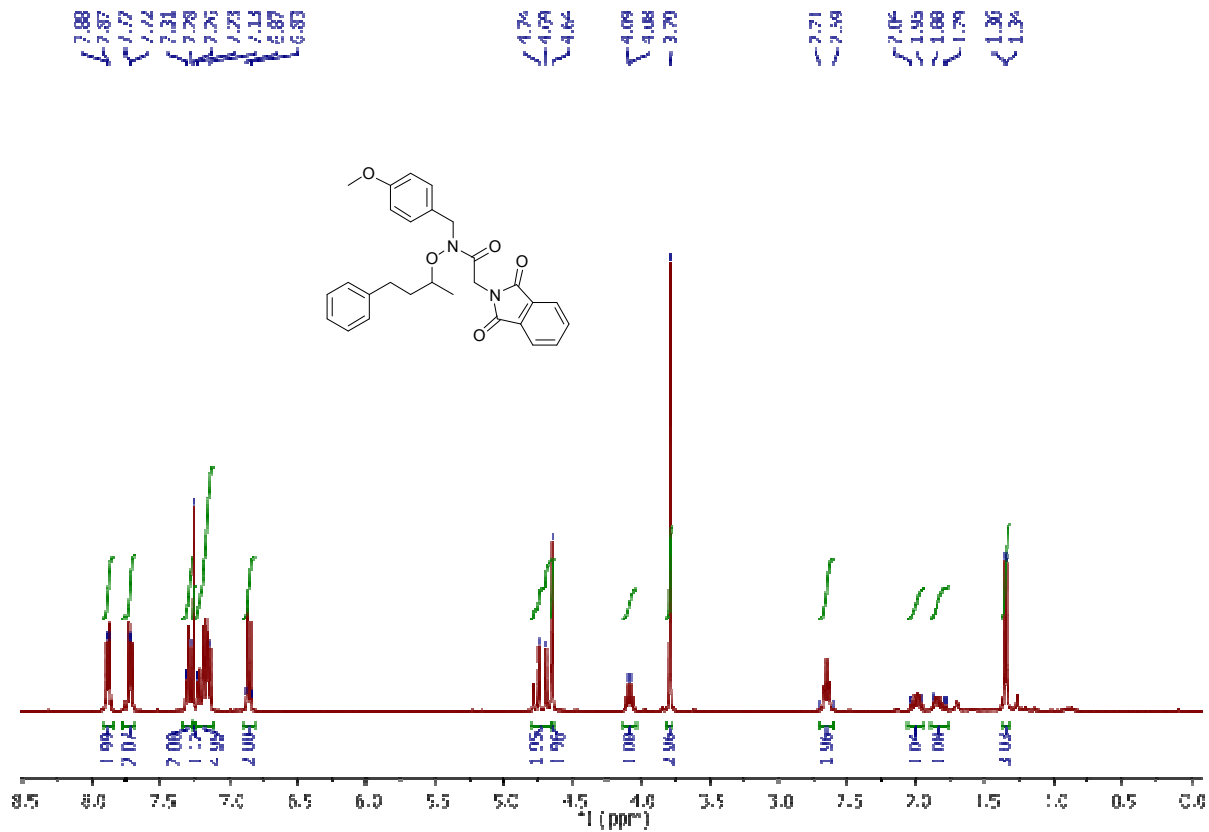


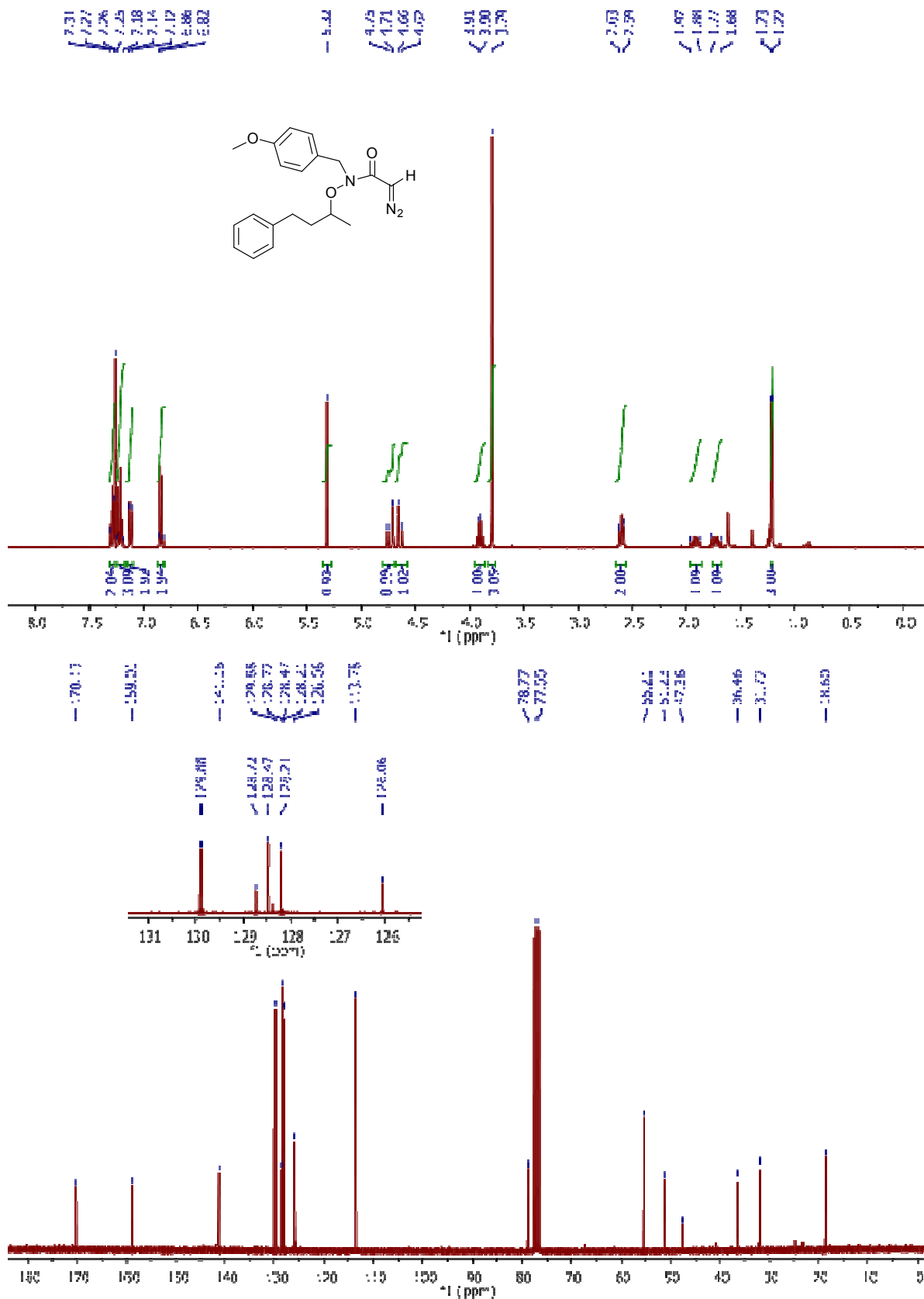


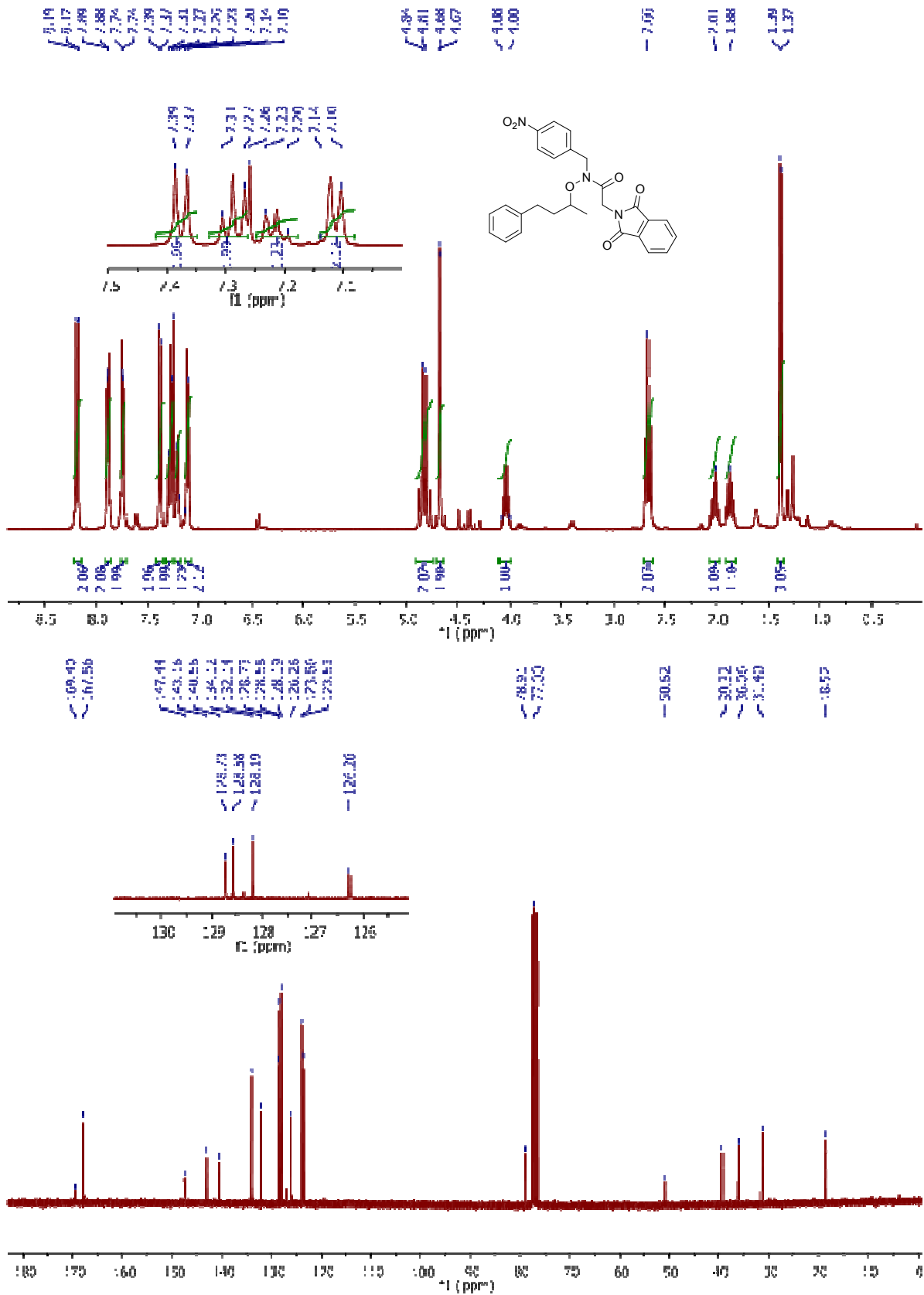


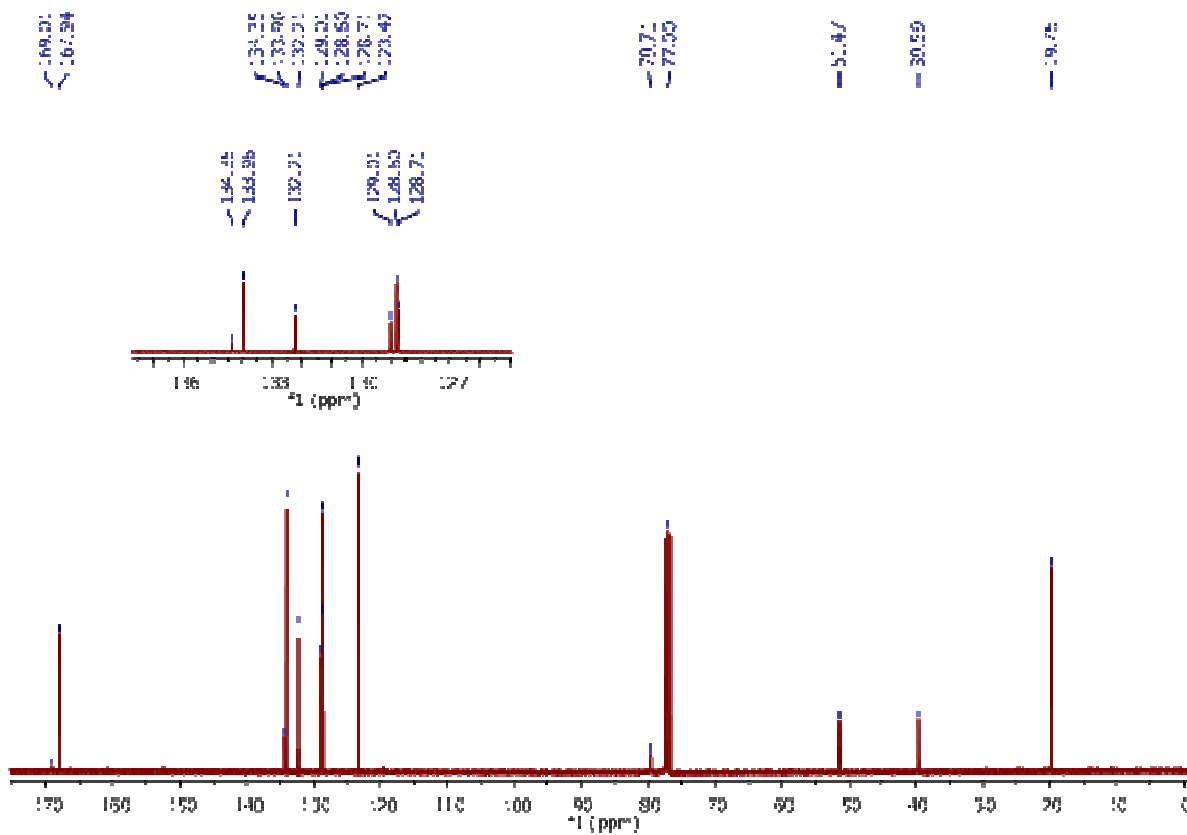
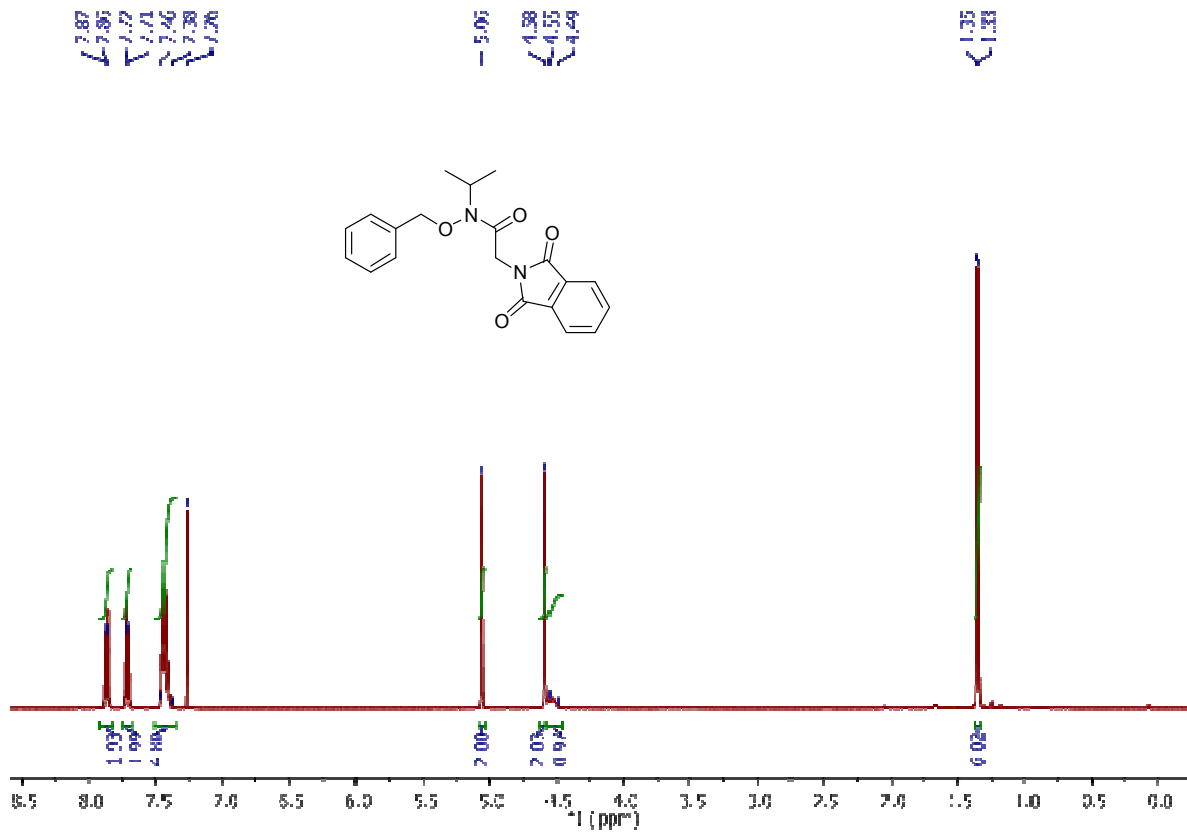


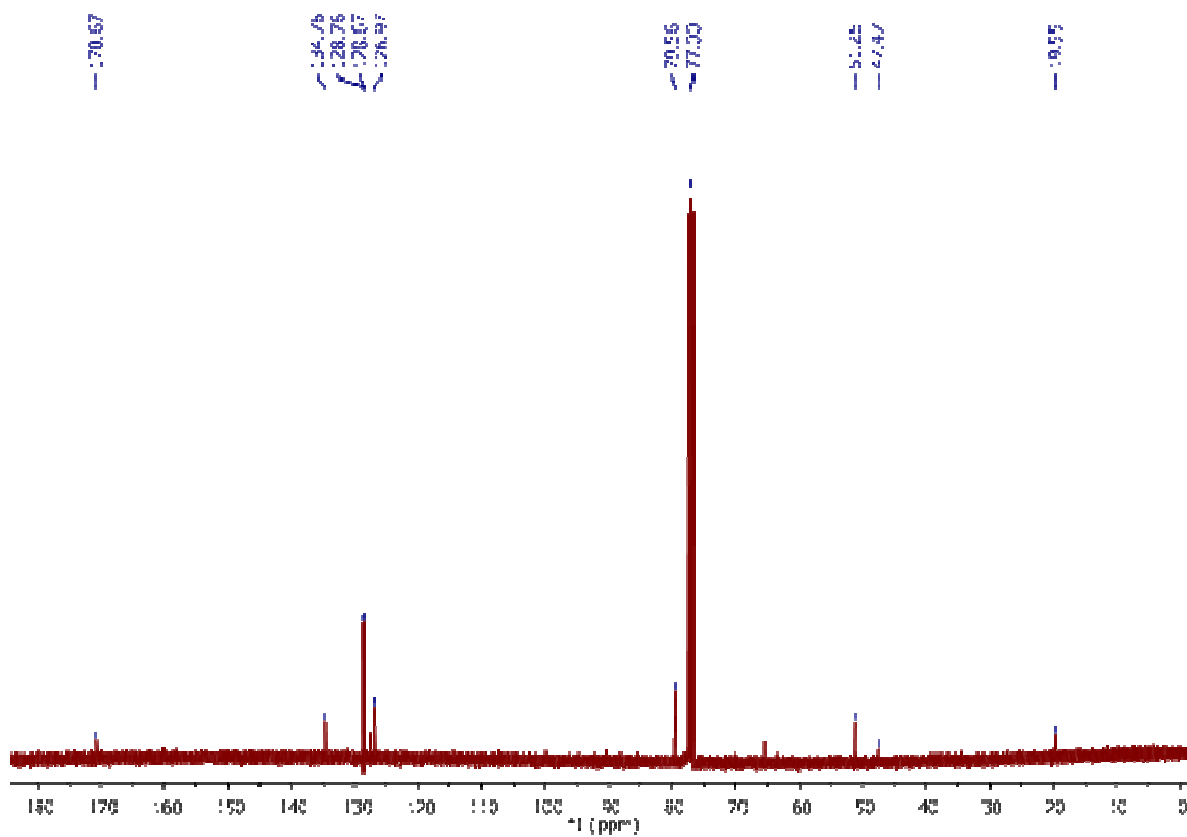
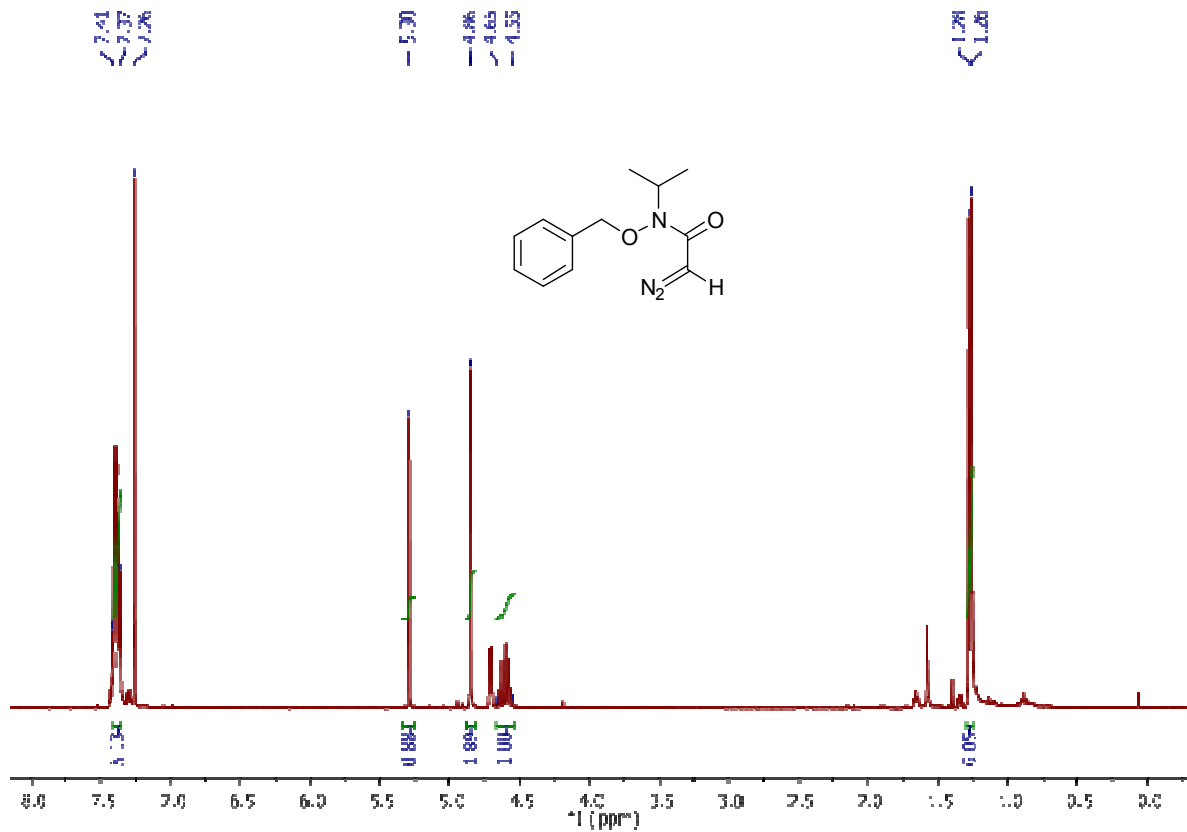


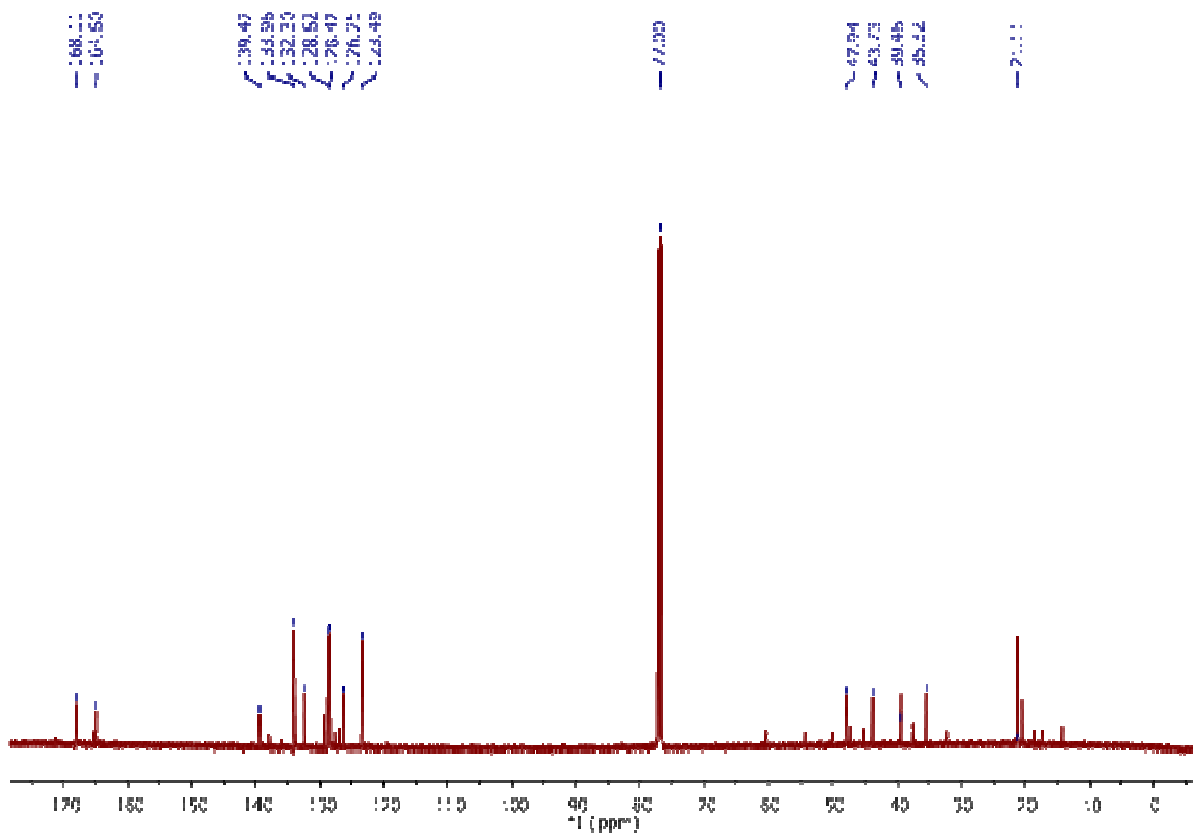
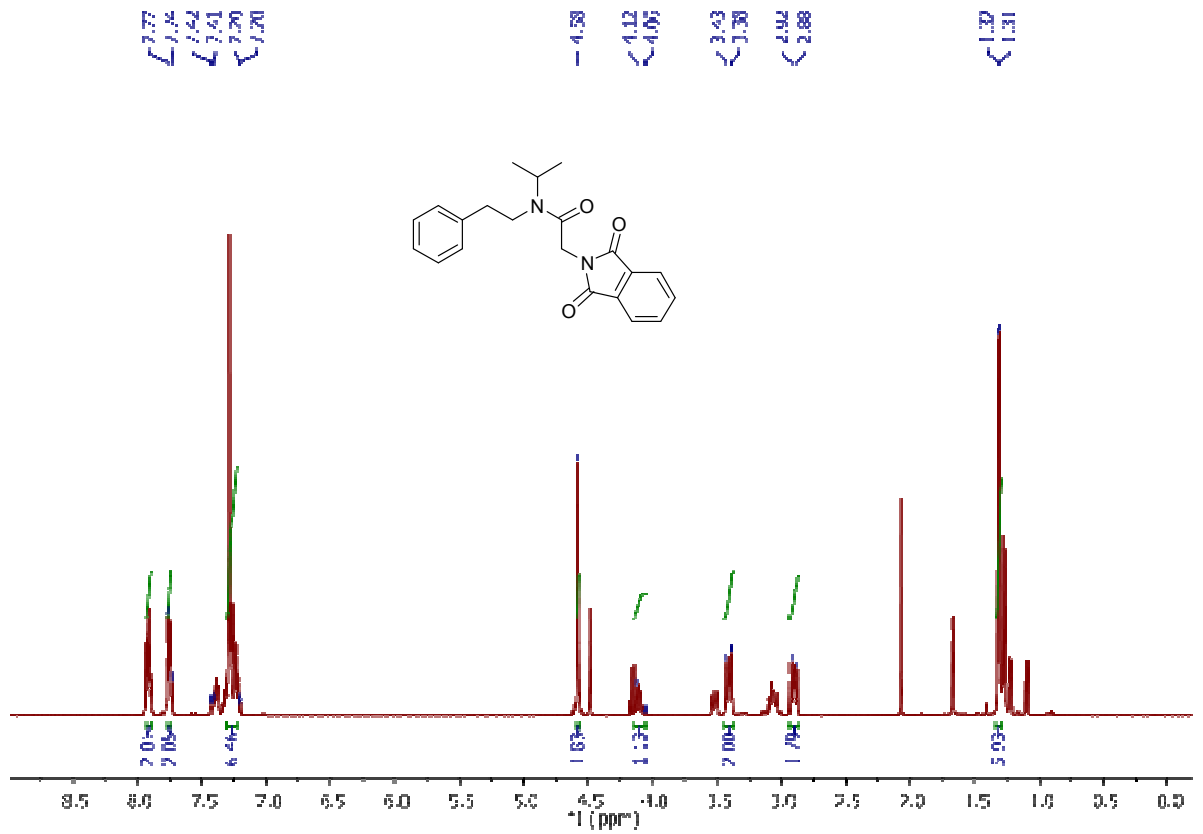


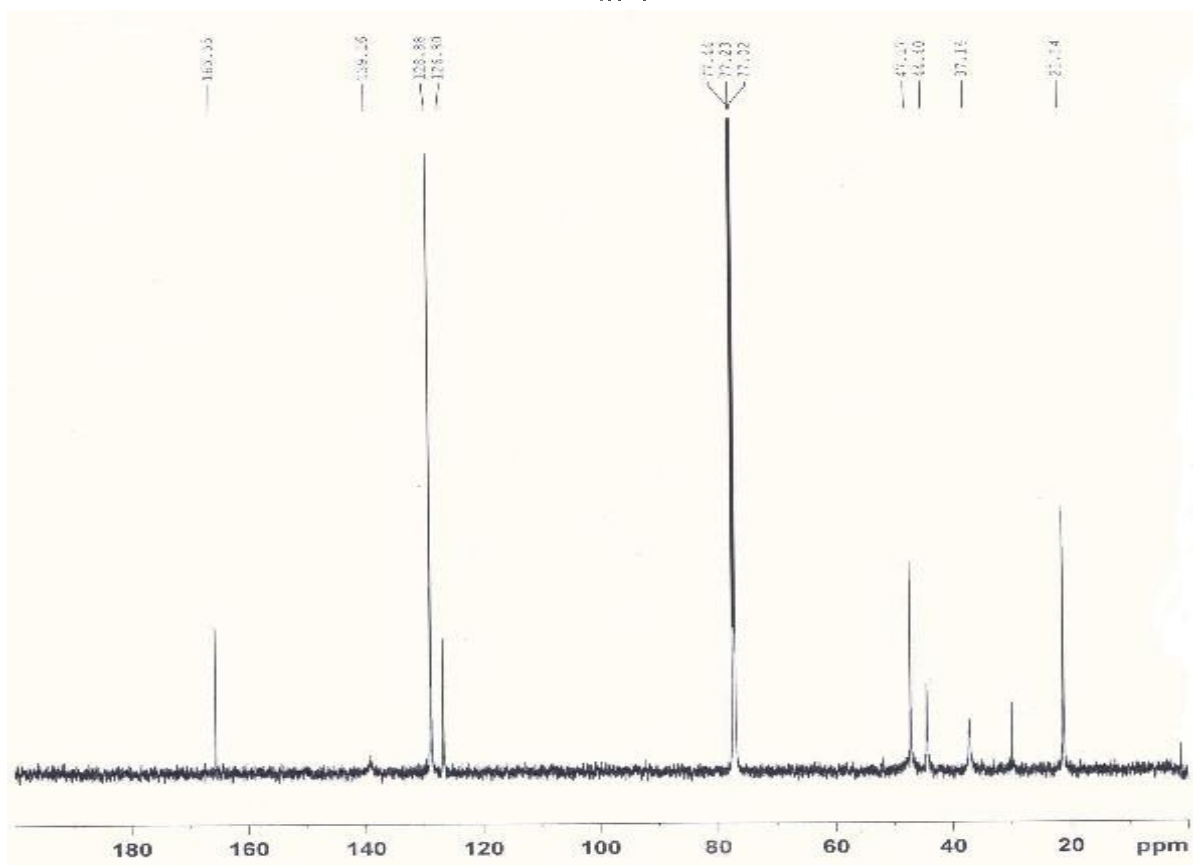
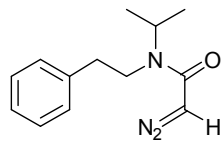
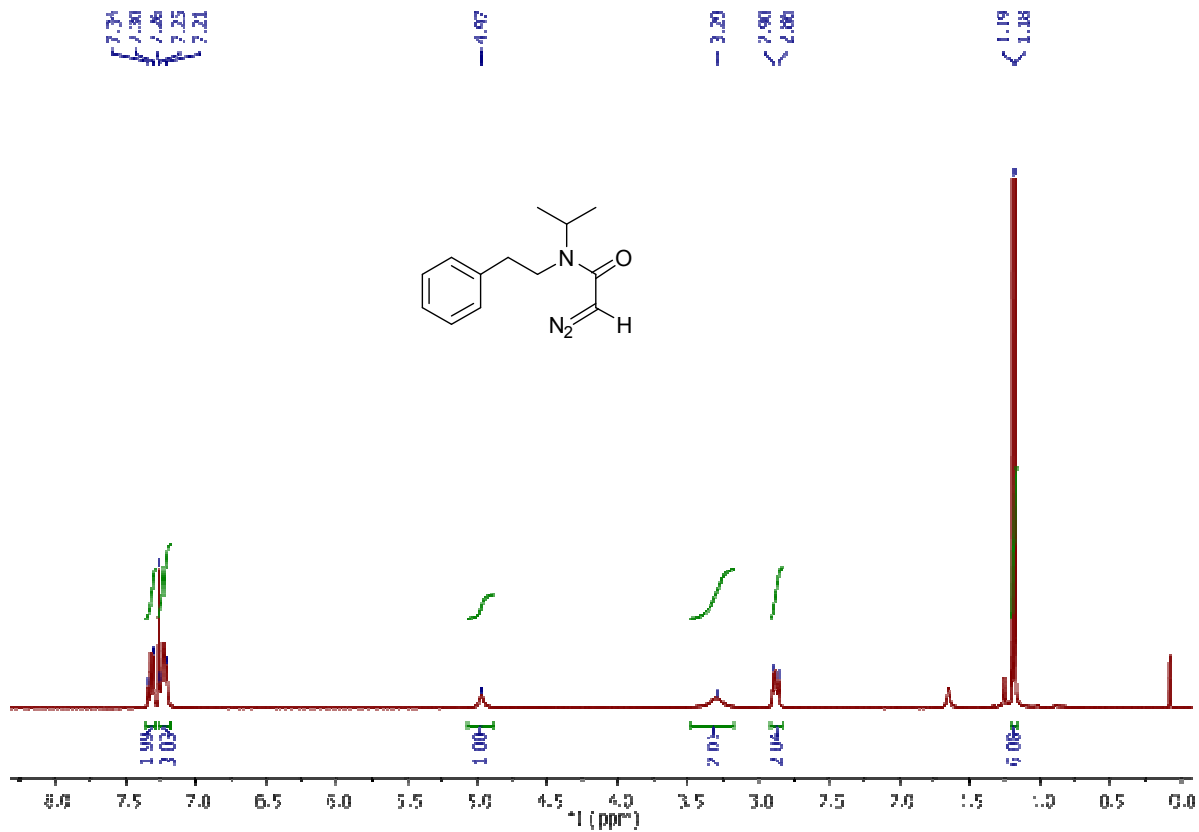


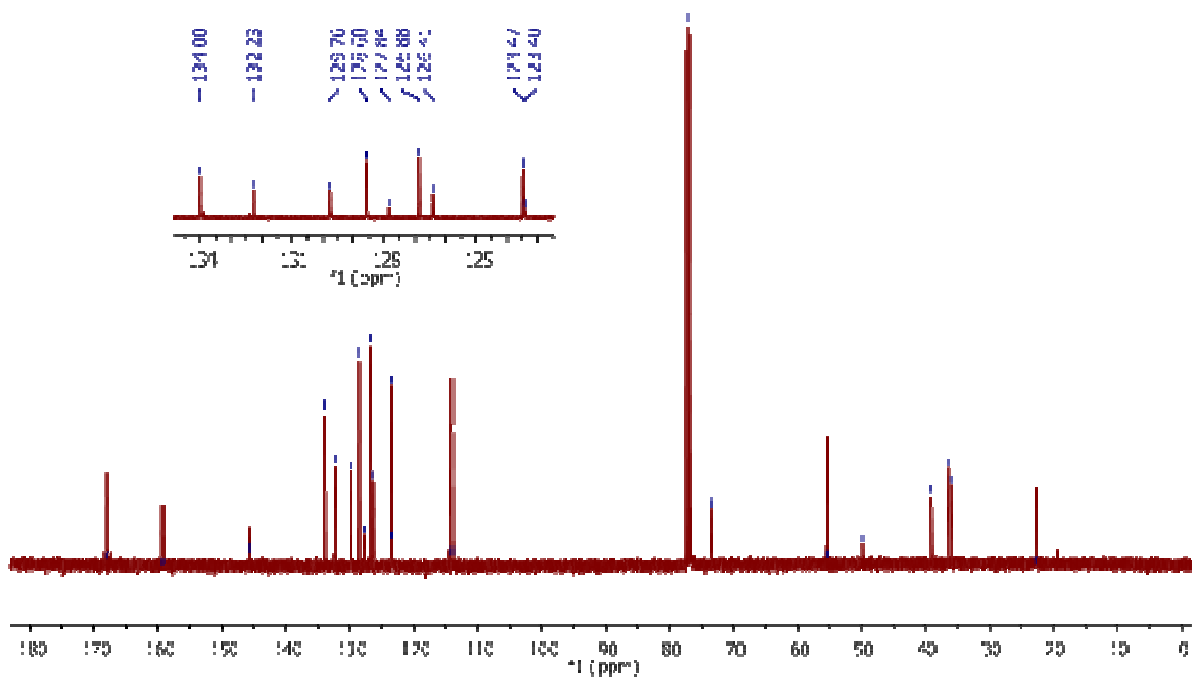
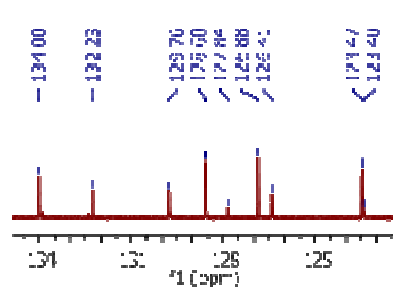
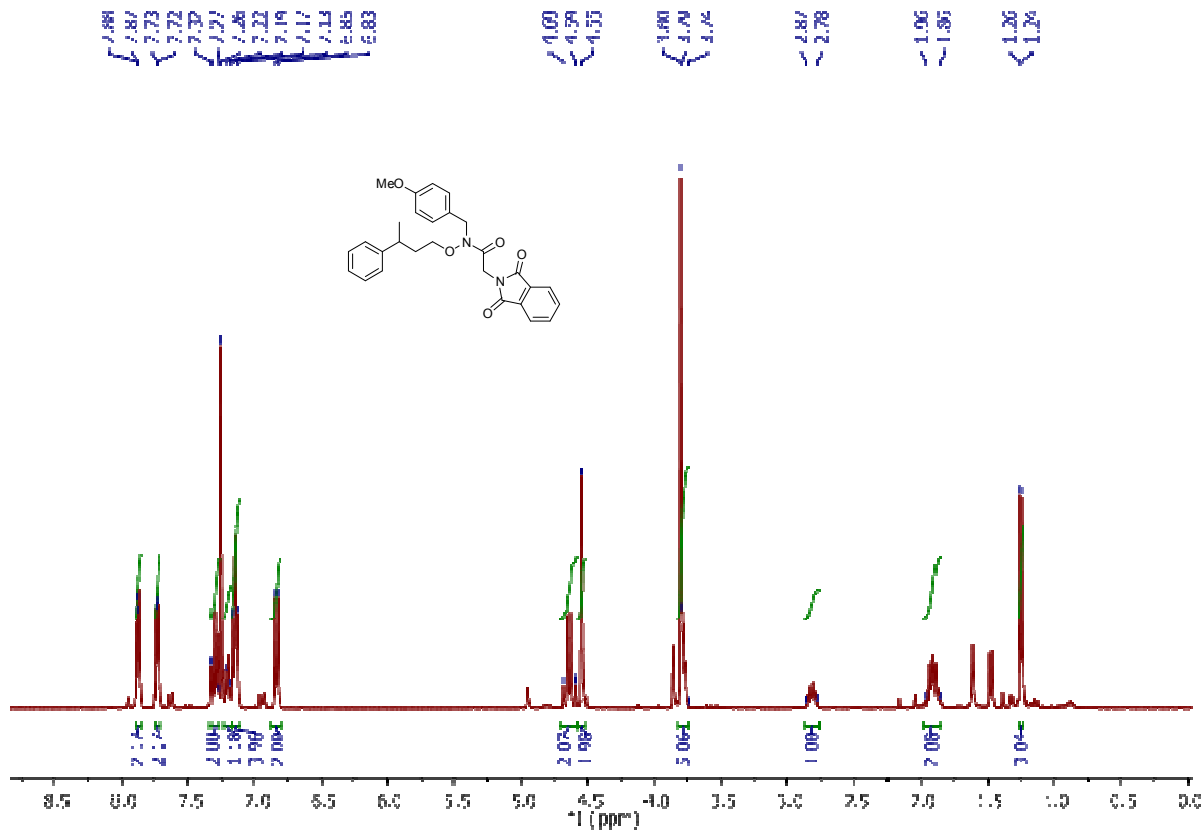


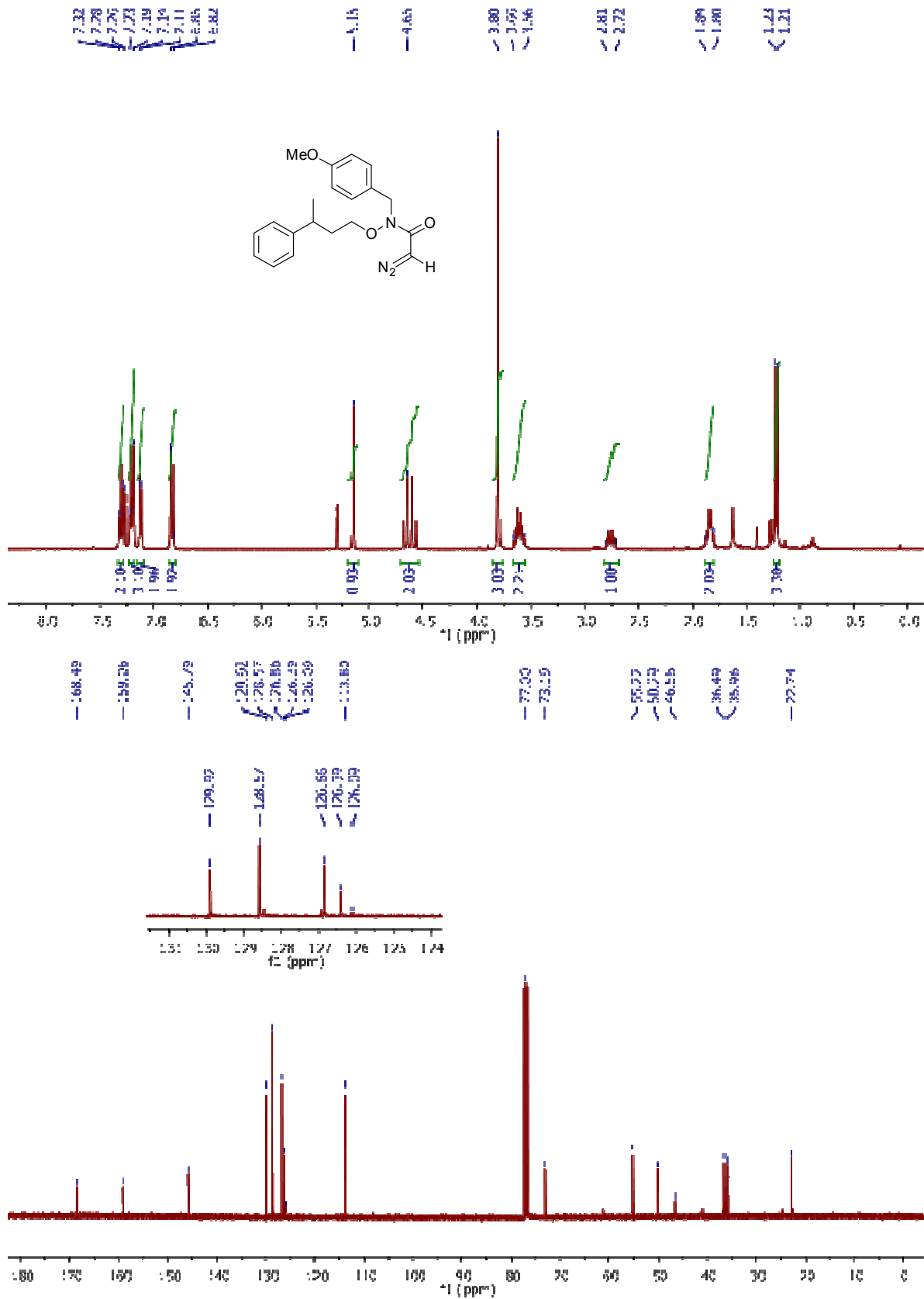


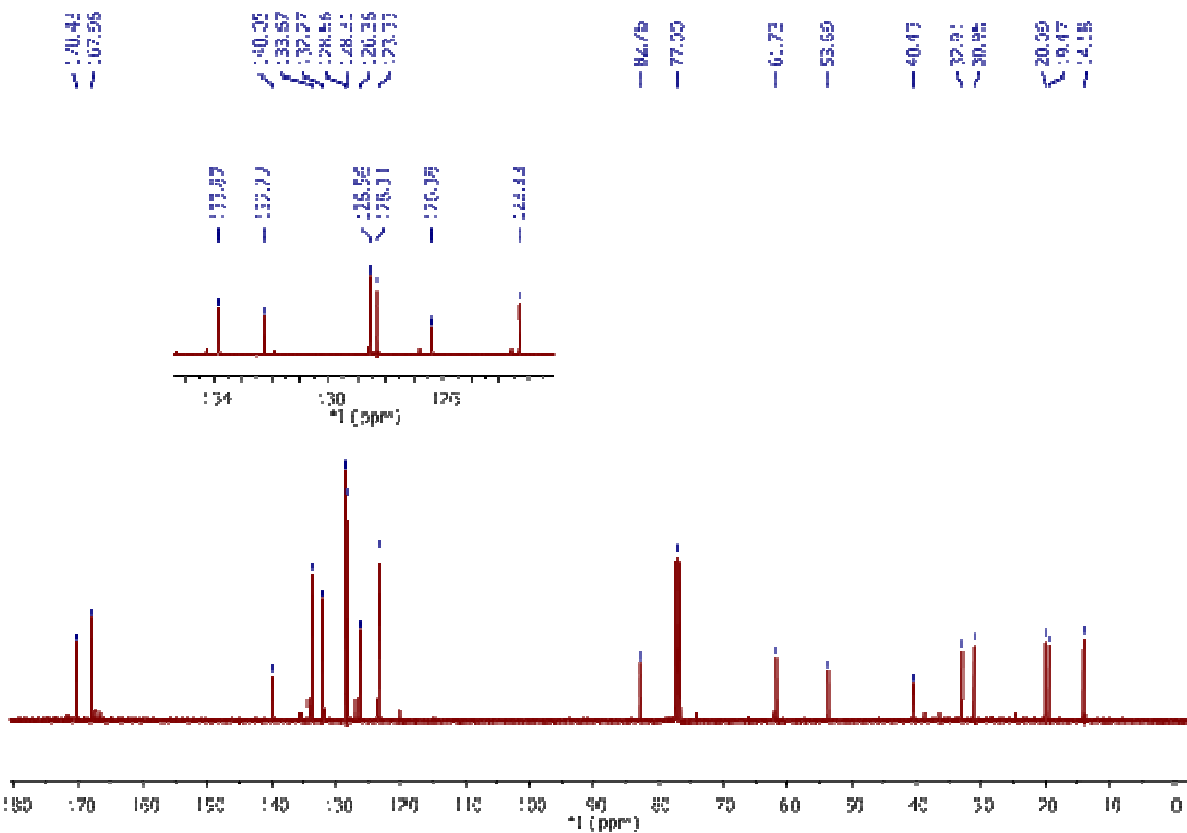
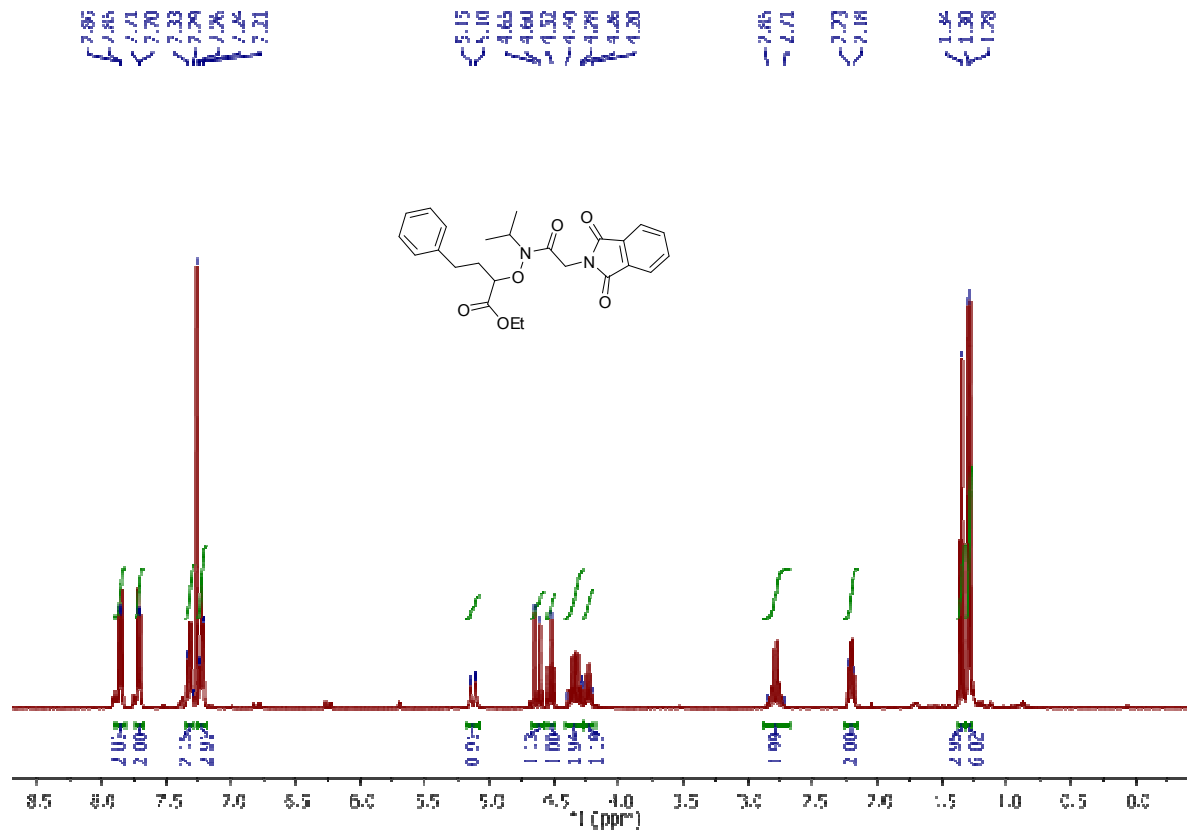




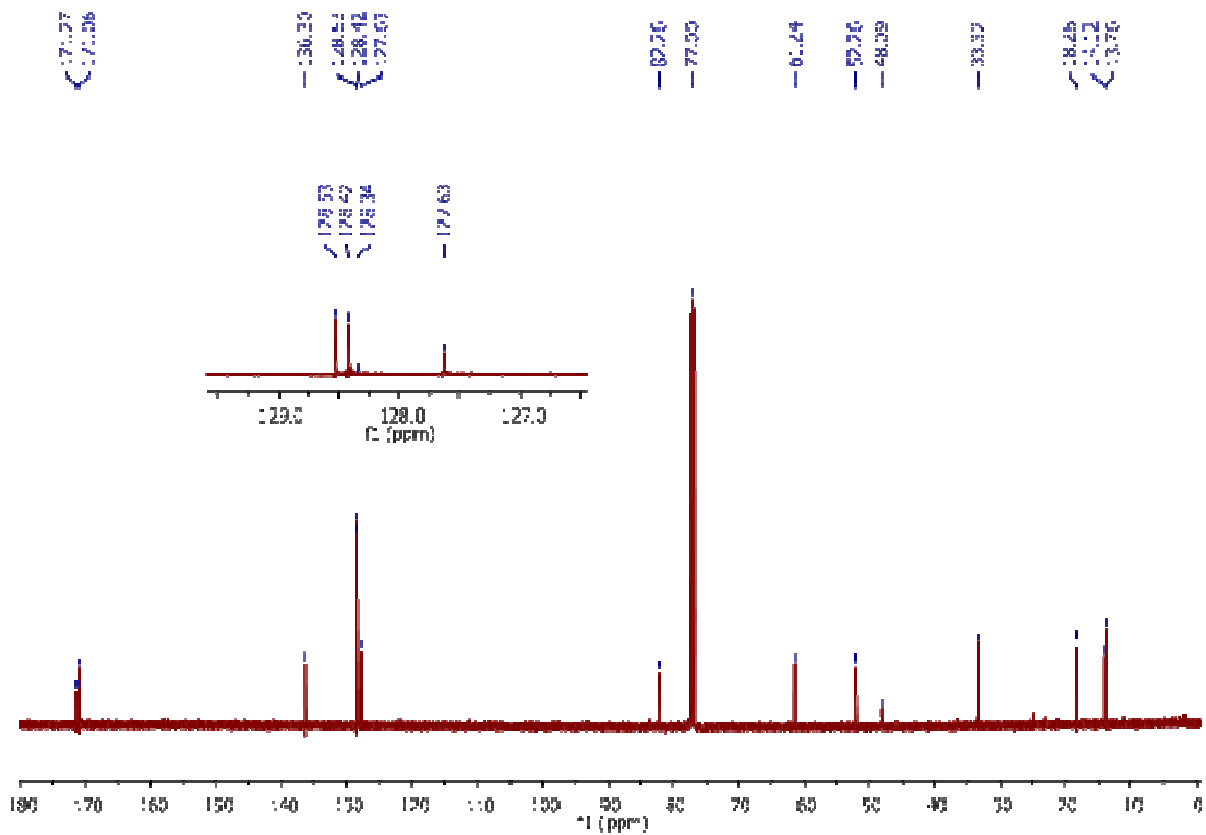
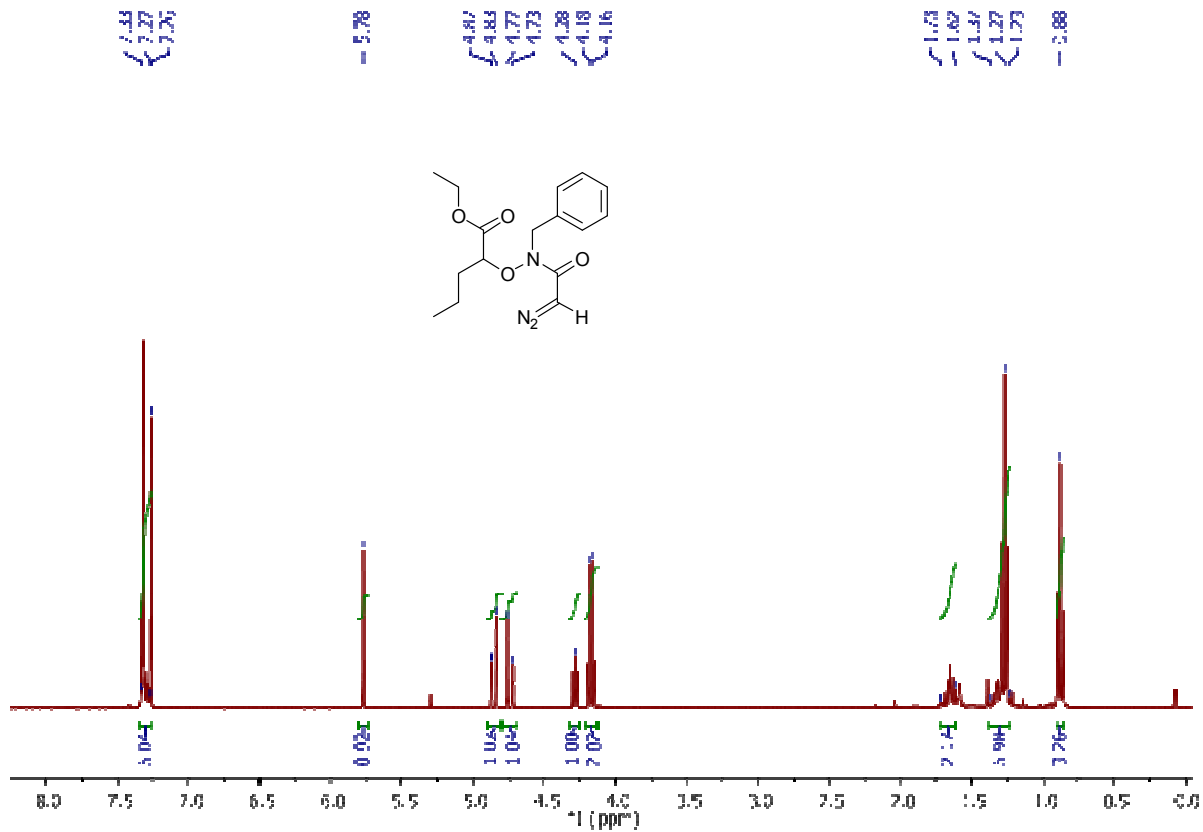


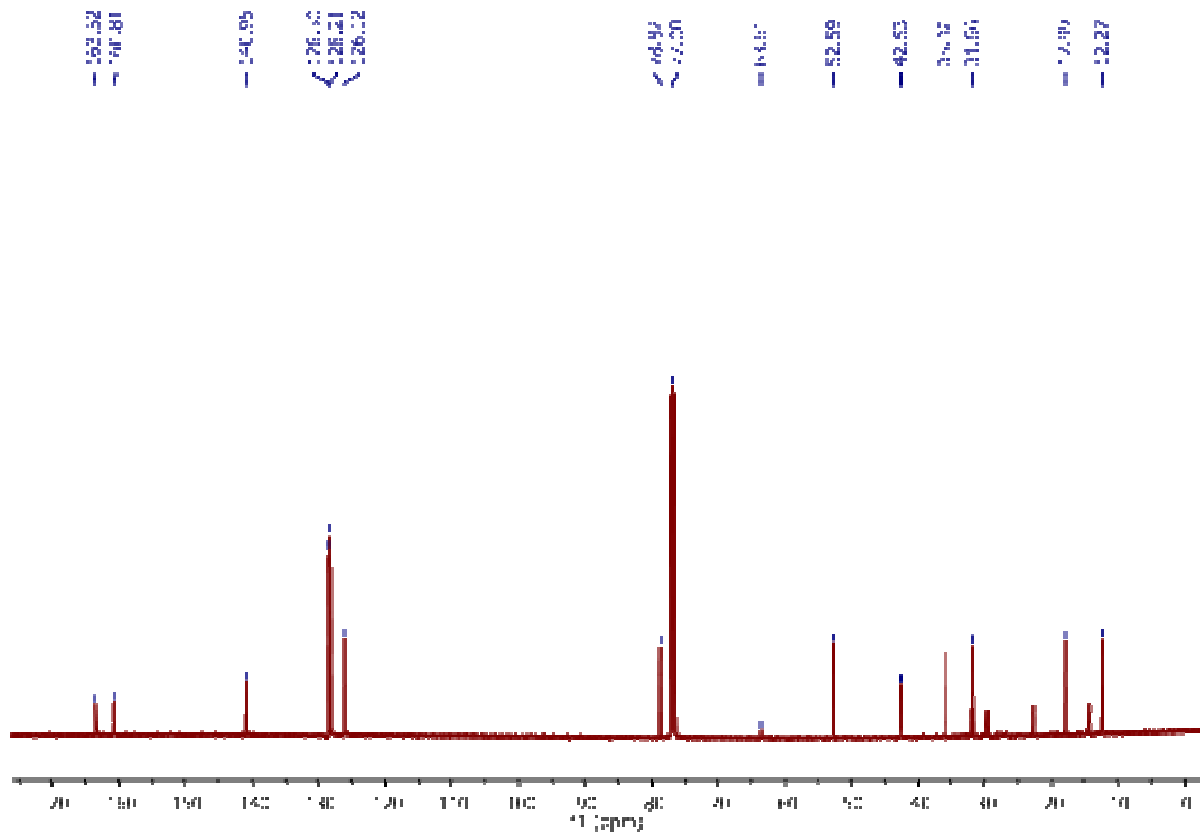
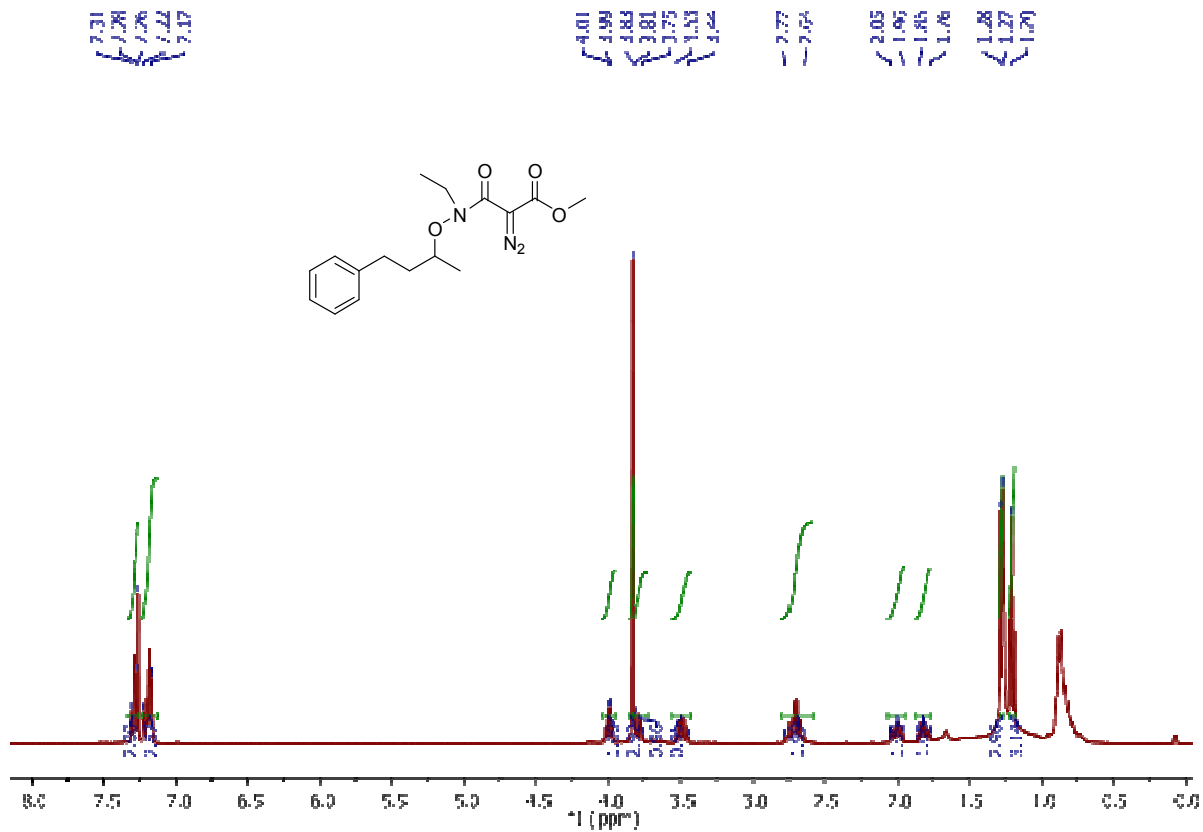


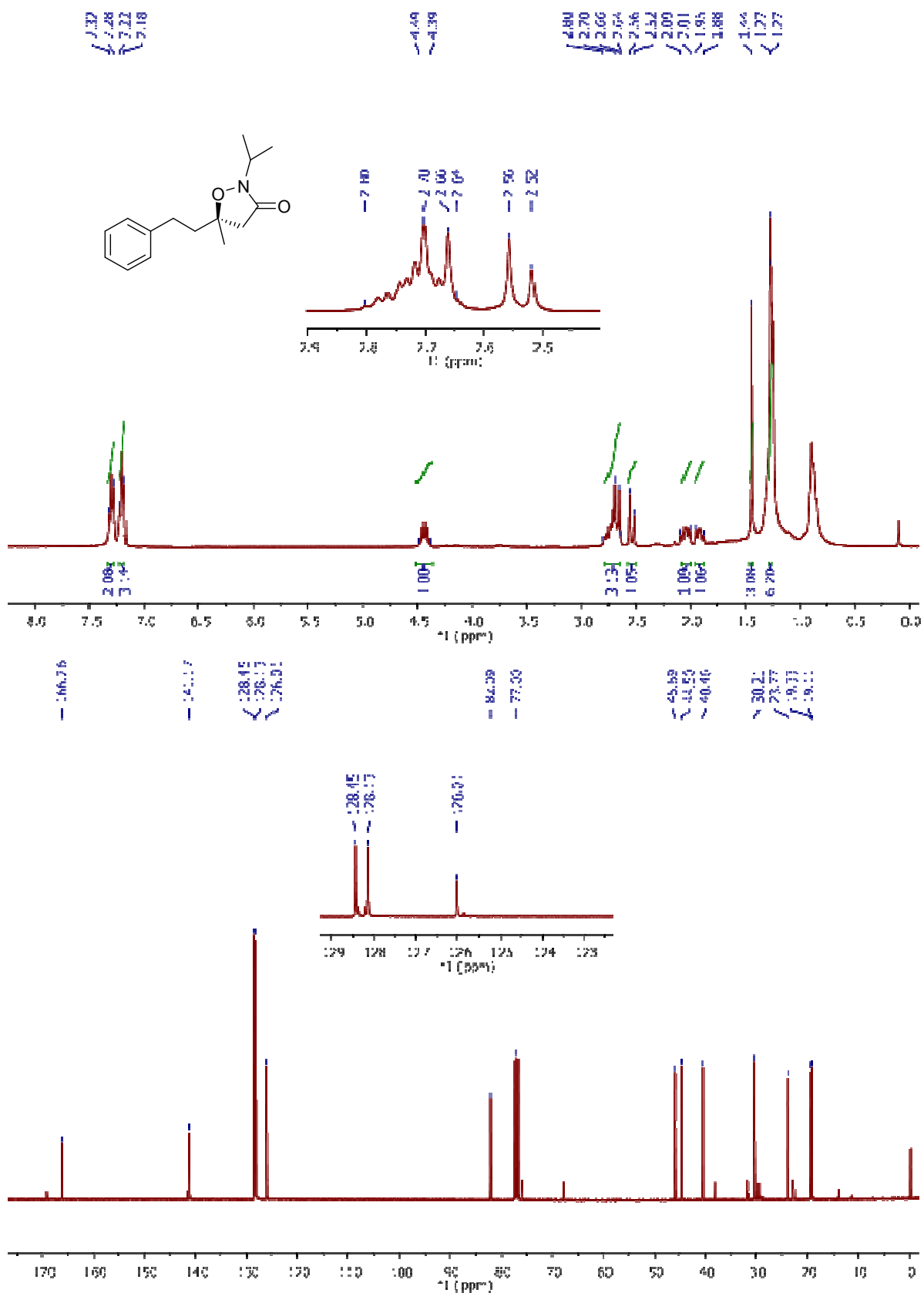


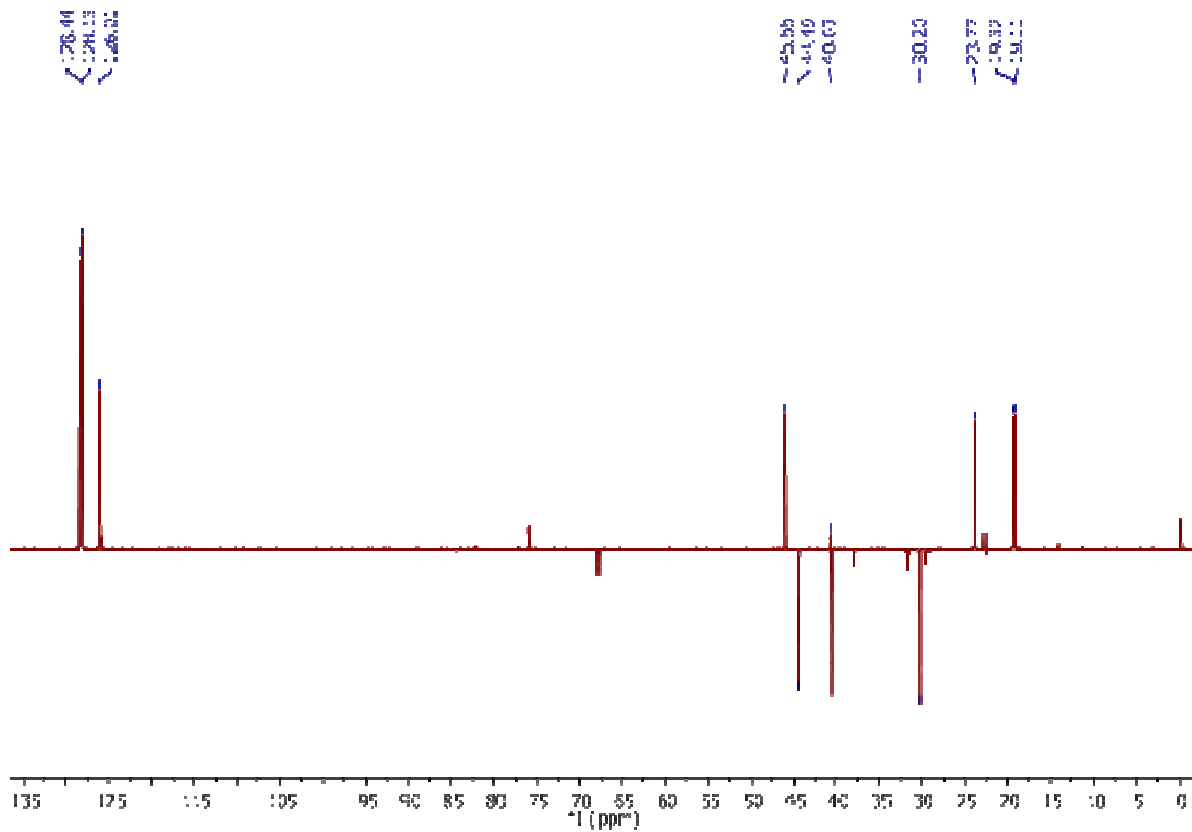




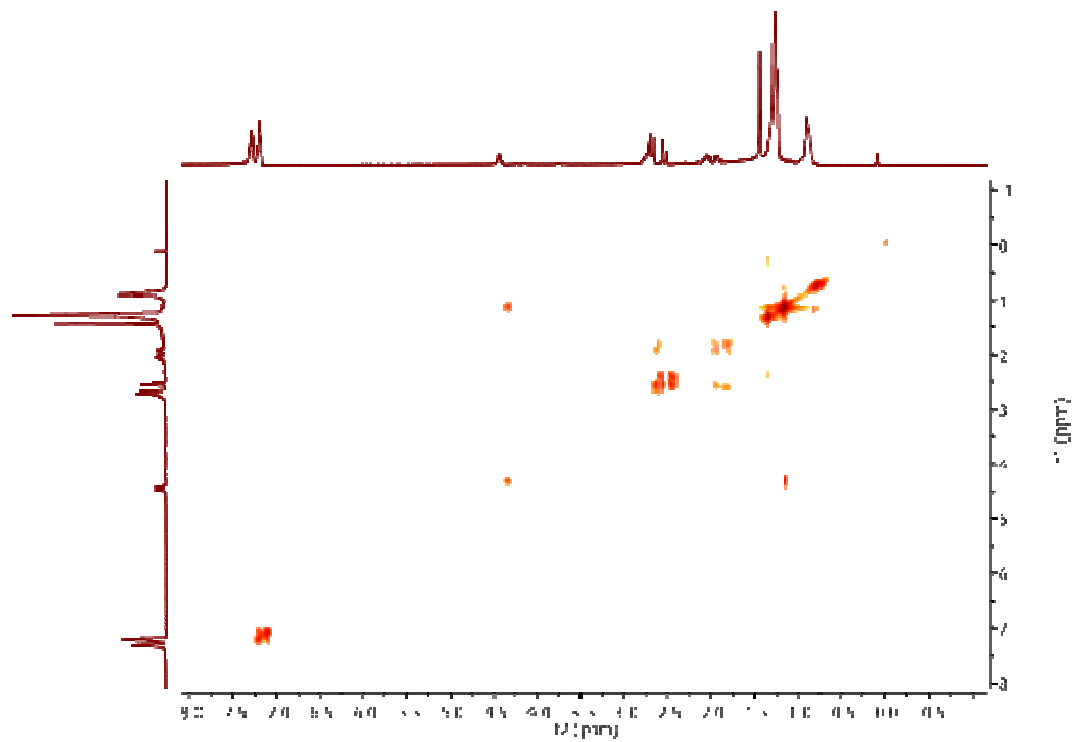


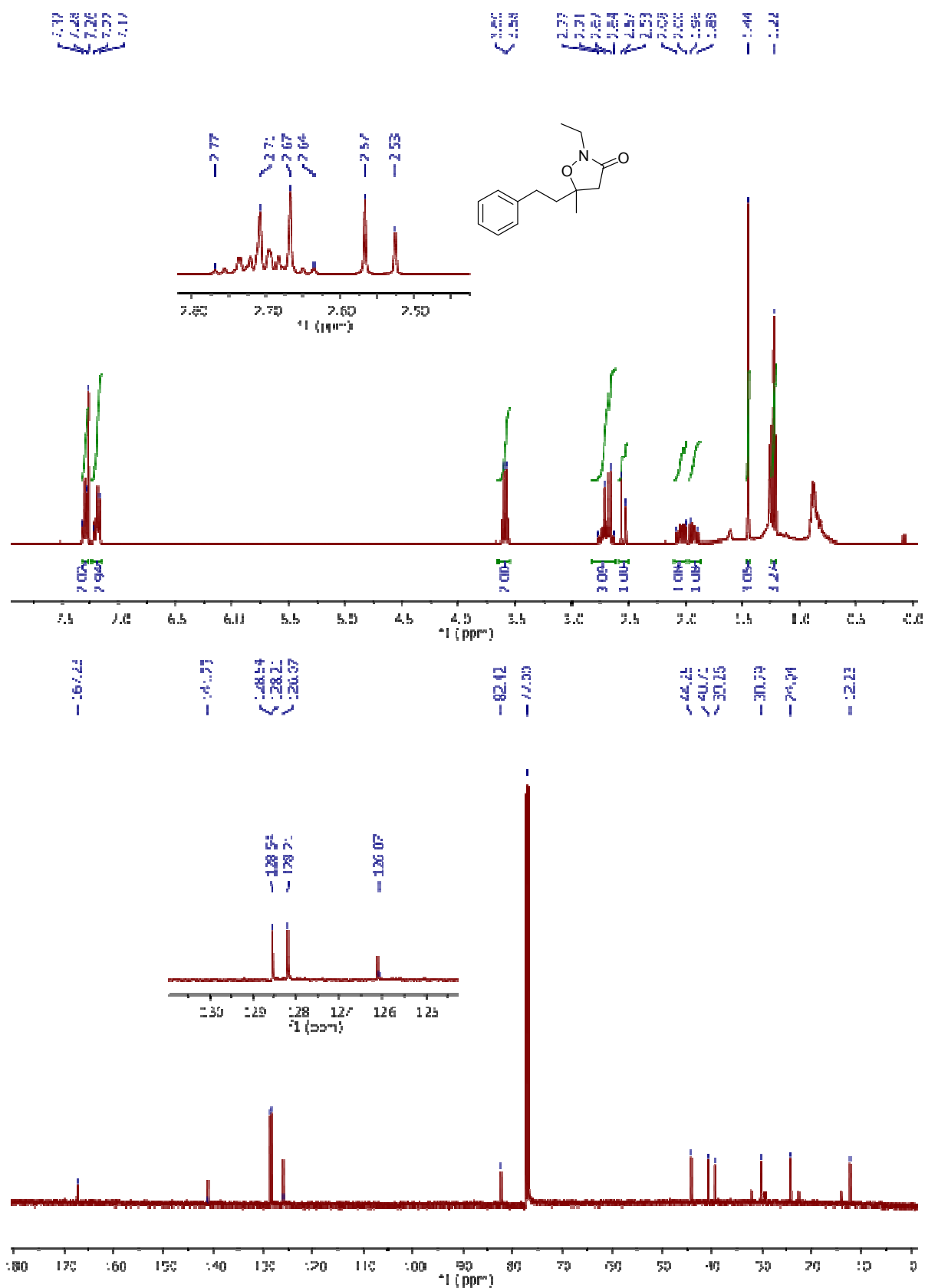


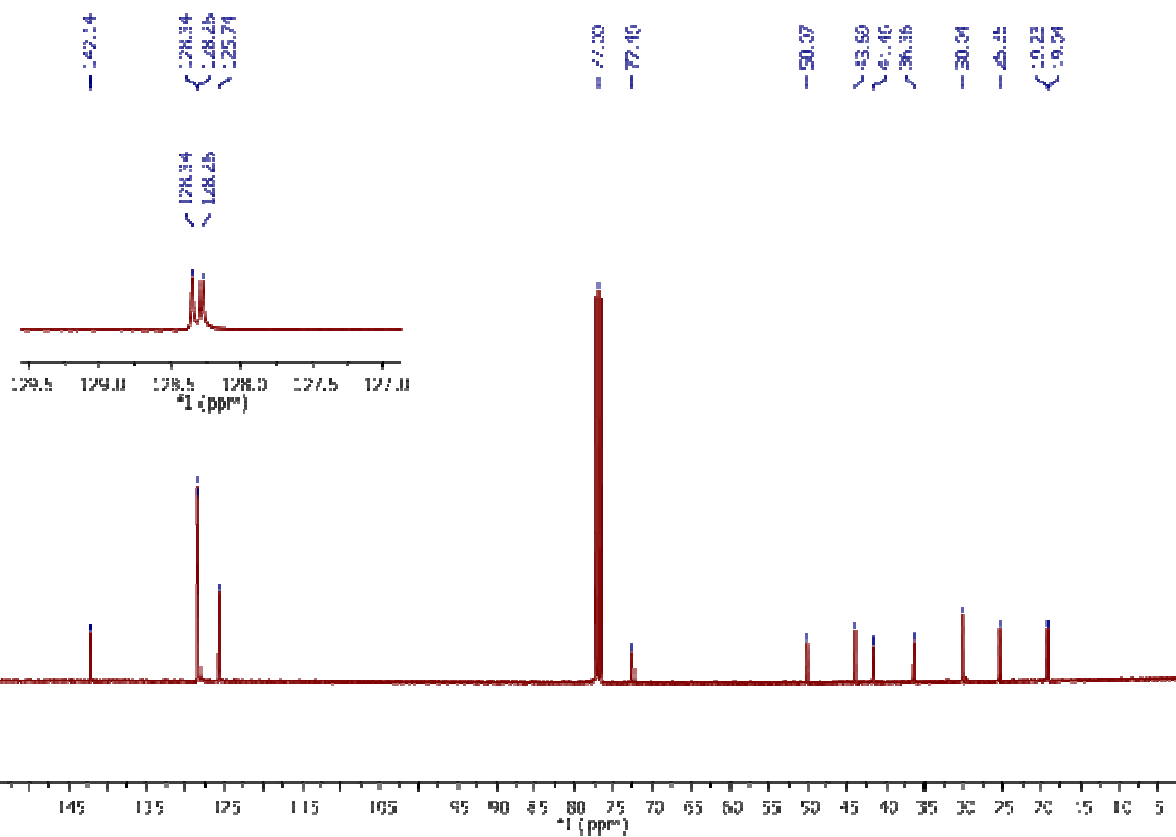
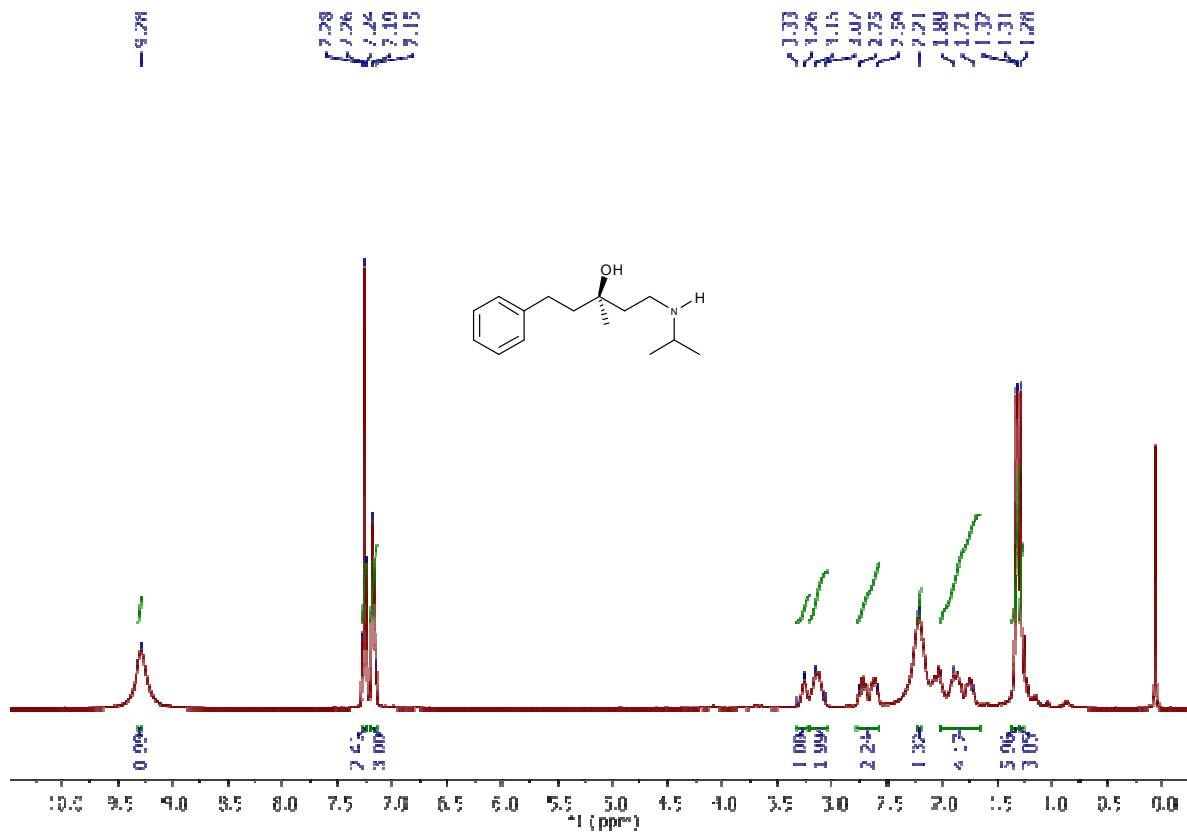




COSY







## **5. Bibliography**

- Bols, M.; Skrydstrup, T. *Chem. Rev.*, **1995**, *95*, 1253-1277.
- Cane, D. E.; Thomas, P. J. *J. Am. Chem. Soc.*, **1984**, *106*, 5295-303.
- Chen, Z.; Chen, Z.; Jiang, Y.; Hu, W. *Tetrahedron*, **2005**, *61*, 1579-1586.
- Clemens, R. J.; Hyatt, J. A. *J. Org. Chem.*, **1985**, *50*, 2431-2435.
- Danheiser, R. L.; Miller, R. F.; Brisbois, R. G.; Park, S. Z. *J. Org. Chem.*, **1990**, *55*, 1959-1964.
- Davies, H. M. L.; Du Bois, J.; Yu, J.-Q. *Chem. Soc. Rev.*, **2011**, *40*, 1855-1856.
- Davies, H. M. L.; Manning, J. R. *Nature*, **2008**, *451*, 417-424.
- Doyle, M. P.; Bagheri, V.; Pearson, M. M.; Edwards, J. D. *Tetrahedron Lett.*, **1989**, *30*, 7001-7004.
- Doyle, M. P.; Duffy, R.; Ratnikov, M.; Zhou, L. *Chem. Rev.*, **2010**, *110*, 704-724.
- Doyle, M. P.; Forbes, D. C. *Chem. Rev.*, **1998**, *98*, 911-935.
- Doyle, M. P.; Pieters, R. J.; Taunton, J.; Pho, H. Q.; Padwa, A.; Hertzog, D. L.; Precedo, L. *J. Org. Chem.*, **1991**, *56*, 820-829.
- Doyle, M. P.; Taunton, J.; Pho, H. Q. *Tetrahedron Lett.*, **1989**, *30*, 5397-5400.
- Doyle, M. P.; Westrum, L. J.; Wolthuis, W. N. E.; See, M. M.; Boone, W. P.; Bagheri, V.; Pearson, M. M. *J. Am. Chem. Soc.*, **1993**, *115*, 958-964.
- Doyle, M. P.; Winchester, W. R.; Protopopova, M. N.; Kazala, A. P.; Westrum, L. J. *Org. Synth.*, **1996**, *73*, 13-24.
- Fleming, I.; Henning, R.; Plaut, H. *J. Chem. Soc., Chem. Commun.*, **1984**, 29-31.

- Grochowski, E.; Jurczak, J. *Synthesis*, **1976**, 682-684.
- Hashimoto, S.; Watanabe, N.; Ikegami, S. *Tetrahedron Lett.*, **1992**, *33*, 2709-2712.
- Hinman, A.; Du Bois, J. *J. Am. Chem. Soc.*, **2003**, *125*, 11510-11511.
- John, J. P.; Novikov, A. V. *Organic Lett.*, **2007**, *9*, 61-63.
- Kablean, S. N.; Marsden, S. P.; Craig, A. M. *Tetrahedron Lett.*, **1998**, *39*, 5109-5112.
- Lee, E.; Choi, I.; Song, S. Y. *J. Chem. Soc., Chem. Commun.*, **1995**, 321-322.
- Morikawa, K.; Park, J.; Andersson, P. G.; Hashiyama, T.; Sharpless, K. B. *J. Am. Chem. Soc.*, **1993**, *115*, 8463-8464.
- Nakamura, E.; Yoshikai, N.; Yamanaka, M. *J. Am. Chem. Soc.*, **2002**, *124*, 7181-7192.
- Padwa, A.; Austin, D. J. *Angew. Chem. Int. Ed. Engl.*, **1994**, *33*, 1797-1815.
- Padwa, A.; Austin, D. J.; Hornbuckle, S. F.; Semones, M. A.; Doyle, M. P.; Protopopova, M. N. *J. Am. Chem. Soc.*, **1992**, *114*, 1874-1876.
- Shi, W.; Zhang, B.; Zhang, J.; Liu, B.; Zhang, S.; Wang, J. *Org. Lett.*, **2005**, *7*, 3103-3106.
- Stork, G.; Nakatani, K. *Tetrahedron Lett.*, **1988**, *29*, 2283-2286.
- Taber, D. F. In *Comprehensive organic synthesis : selectivity, strategy, and efficiency in modern organic chemistry*; Trost, B. M.; Fleming, I. Eds.; Pergamon Press: New York, 1991.
- Taber, D. F.; Petty, E. H. *J. Org. Chem.*, **1982**, *47*, 4808-4809.
- Taber, D. F.; Petty, E. H.; Raman, K. *J. Am. Chem. Soc.*, **1985**, *107*, 196-199.

Taber, D. F.; Ruckle, R. E., Jr. *J. Am. Chem. Soc.*, **1986**, *108*, 7686-7693.

Tietze, L. F.; Schuenke, C. *Eur. J. Org. Chem.*, **1998**, 2089-2099.

Wang, J.; Stefane, B.; Jaber, D.; Smith, J. A. I.; Vickery, C.; Diop, M.; Sintim, H. O. *Angew. Chem., Int. Ed.*, **2010**, *49*, 3964-3968.

Weber, B.; Seebach, D. *Angew. Chem. Int. Ed.*, **1992**, *31*, 84-86.

Weber, B.; Seebach, D. *Tetrahedron*, **1994**, *50*, 6117-6128.

Wee, A. G. H.; Liu, B.; Zhang, L. *J. Org. Chem.*, **1992**, *57*, 4404-4414.

Wolckenhauer, S. A.; Devlin, A. S.; Du Bois, J. *Organic Lett.*, **2007**, *9*, 4363-4366.

Yoon, U. C.; Jin, Y. X.; Oh, S. W.; Park, C. H.; Park, J. H.; Campana, C. F.; Cai, X.; Duesler, E. N.; Mariano, P. S. *J. Am. Chem. Soc.*, **2003**, *125*, 10664-10671.

*Chapter 2:*

**Control of selectivity in the generation and reactions of oxonium ylides via [1,2]-Stevens rearrangement**

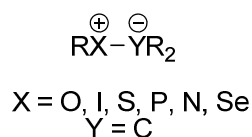
---

# I. Introduction

---

## 1.1 Ylides

Ylides are reactive neutral dipolar intermediates in which a formally positively charged heteroatom is connected to a formally negatively charged atom. The anionic site  $Y^-$  is originally a carbon atom while the  $X^+$  can be a number of heteroatoms (Scheme 25). In this chapter we will discuss a subclass of ylides known as oxonium ylides having the negative charge on carbon, that originated from a metal carbene, and the positive charge on oxygen.

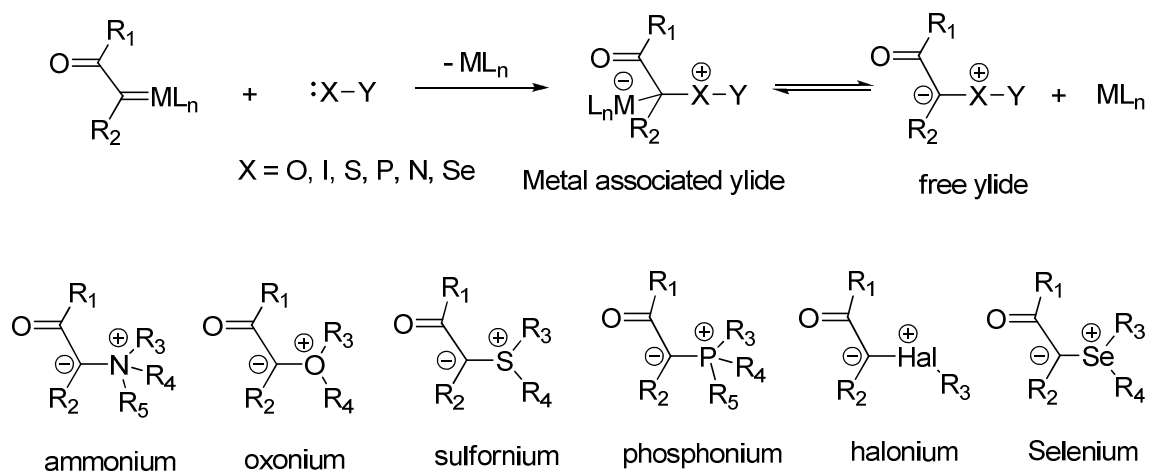


**Scheme 25.** Ylides

Some metal carbenes act as Lewis acids and can accept electrons from a Lewis base. The interaction of the lone pair of a heteroatom (Lewis base) with the electron deficient carbon of the metal carbene intermediate (Lewis acid) generates a metal associated ylide which can dissociate to a free ylide (Scheme 26).<sup>40</sup>

---

<sup>40</sup> Padwa, A.; Hornbuckle, S. F. *Chem. Rev.*, **1991**, *91*, 263-309.



**Scheme 26.** Generation of ylides from metal carbenes.

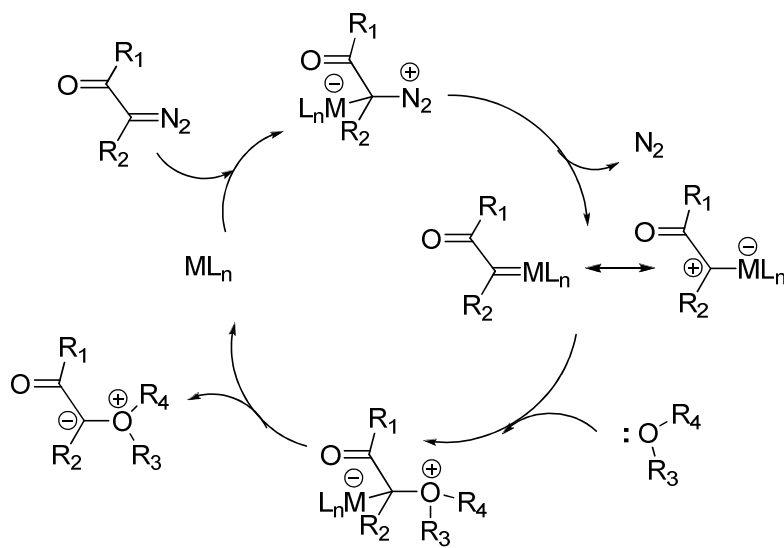
The Lewis bases that are known to trap carbenes in order to generate ylides include frequently investigated ethers, sulfides, and amines. Fewer investigations have been reported for the generation of ylides with heteroatoms such as selenium, phosphorous and halogens (Scheme 26).<sup>40</sup> Ylide intermediates are known to undergo synthetically useful transformations, such as rearrangements ([1,2]-Stevens and [2,3]-sigmatropic rearrangements) and dipolar cycloaddition reactions to form stable products. The chemistry of oxonium ylides have received little attention compared to the chemistry of ammonium and sulfonium ylides. Highlighting the chemistry of oxonium ylides will be the primary focus of discussion within this chapter.<sup>41</sup>

## 1.2 Oxonium ylides

The formation of oxonium ylides is readily achieved by transition metal catalyzed decomposition of diazocarbonyl compounds in the presence of oxygen containing compounds. The metal complex (generally from copper(I) or dirhodium(II)) acts as a

<sup>41</sup> (a) Ye, T.; McKervey, M. A. *Chem. Rev.*, **1994**, *94*, 1091-1160. (b) M. P. Doyle in: *Comprehensive Organometallic Chemistry II*; Hegedus, L. S. E.: Pergamon Press: New York, **1995**; Vol 12, Chapter 5.2, pp.421-468. (c) J. Wang in: *Comprehensive Organometallic Chemistry* Vol. 11 (Eds, R. H. Crabtree, D. M. Mingos) Elsevier **2007**, volume 11, pp. 151-178.

Lewis acid and accepts electrons from the diazo carbon at its vacant coordination site (Scheme 27). Electron back donation from the metal to the carbene carbon results in the concomitant loss of dinitrogen that generates a metal carbene species. The metal carbene intermediate can accept electrons from the oxygen heteroatom of an ether to generate the metal associated ylide which could eventually lose the metal to form a free ylide.<sup>42</sup> Whether you form a metal associated ylide or a free ylide depends on the relative strength of the metal-carbene and carbene-oxygen bonds, since, in principle, these processes are reversible.



**Scheme 27.** Generation of oxonium ylides via transition metal catalyzed decomposition of diazocarbonyl compounds.

### 1.3 Oxonium ylide rearrangements

Unlike ammonium and sulfonium ylides from which stable ylide intermediates have been isolated and characterized,<sup>43</sup> oxonium ylides are known for their instability and

<sup>42</sup> Doyle, M. P.; McKervey, M. A.; Ye, T. *Modern Catalytic Methods for Organic Synthesis with Diazo Compounds*, Wiley, New York, **1998**.

<sup>43</sup> (a) Padwa, A.; Hornbuckle, S. F. *Chem. Rev.*, **1991**, *91*, 263-309. (b) Diekmann, J. *J. Org. Chem.*, **1965**, *30*, 2272-2275. (c) Ando, W.; Yagihara, T.; Tozune, S.; Nakaido, S.; Migita, T. *Tetrahedron Lett.*, **1969**, 1979-1982. (d) Ando, W.; Hagiwara, T.; Migita, T. *Tetrahedron Lett.*, **1974**, 1425-1428. (e) Kappe, C. O.

high reactivity. They have not yet been isolated and characterized.<sup>44</sup> Most of the evidence for the existence of oxonium ylides is based on analysis of the final products after the reaction has occurred. Until the end of 1970's, the carbene complexes which generated ylides were usually carried out in the presence of copper in different oxidation states.<sup>43</sup> However, these transformations were relatively unselective and dirhodium(II) carboxylates<sup>45</sup> emerged as highly efficient catalysts for ylide generation.

Oxonium ylides can find a widespread upsurge of synthetic utility due to their ease of formation by the reactions of dirhodium(II) carboxylates with ethers and alcohols.<sup>46</sup> Once formed, there are multiple reaction pathways that allyl-substituted oxonium ylides may undergo, of which the [2,3]-sigmatropic rearrangement and the [1,2]-Stevens rearrangement are the most common. The oxonium ylides may also undergo competing reactions such as  $\beta$ -hydride elimination,<sup>47</sup> [1,4]-shift reactions,<sup>48</sup> and reactions with nucleophiles<sup>49</sup> after a ring opening of the oxonium ylide has occurred

---

*Tetrahedron Lett.*, **1997**, 38, 3323-3326. (f) Ollis, W. D.; Rey, M.; Sutherland, I. O. *J. Chem. Soc., Perkin Trans. 1*, **1983**, 1009-1027. (g) Padwa, A.; Snyder, J. P.; Curtis, E. A.; Sheehan, S. M.; Worsencroft, K. J.; Kappe, C. O. *J. Am. Chem. Soc.*, **2000**, 122, 8155-8167.

<sup>44</sup> Sweeney, J. B. *Chem. Soc. Rev.*, **2009**, 38, 1027-1038.

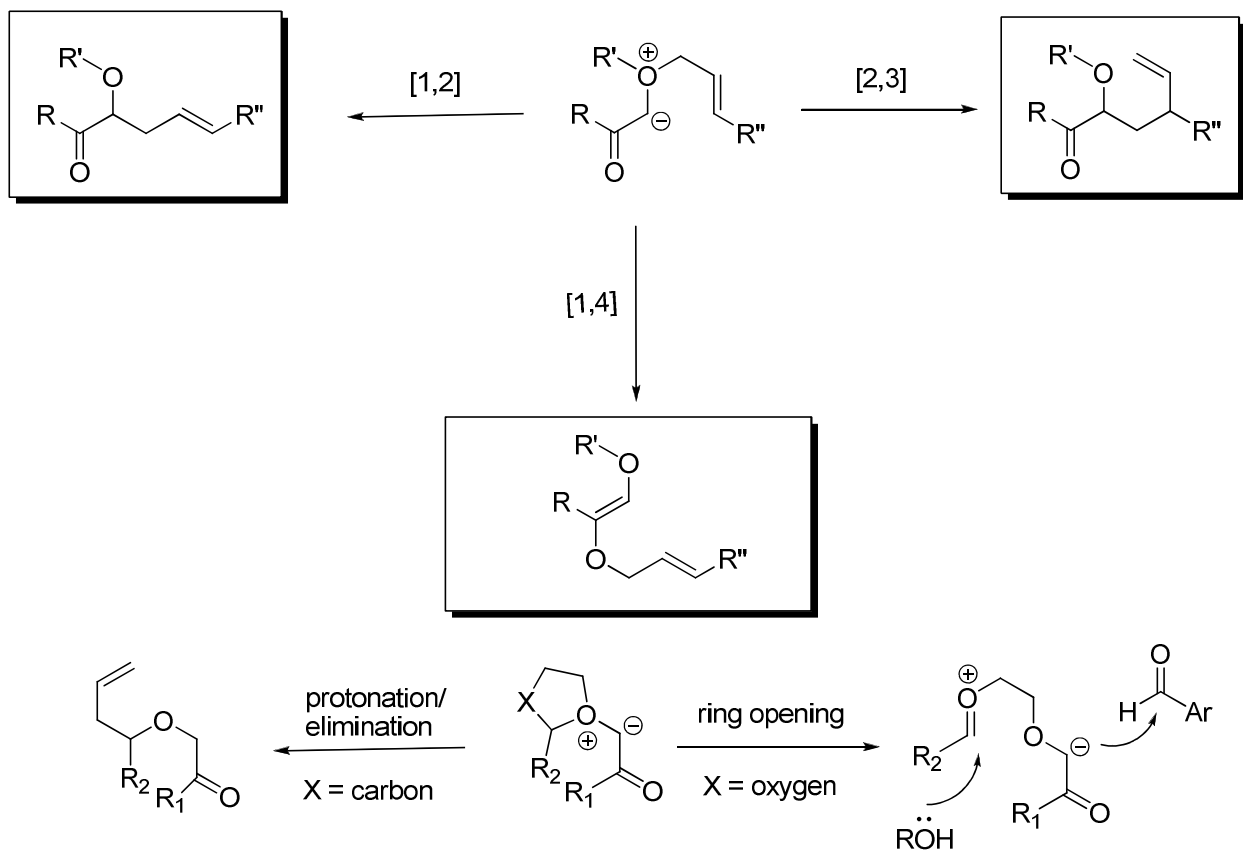
<sup>45</sup> (a) Noels, A. F.; Hubert, A. J.; Teyssie, P. *J. Organomet. Chem.*, **1979**, 166, 79-86. (b) Nazarova, L. A.; Maiorova, A. G. *Zh. Neorg. Khim.*, **1976**, 21, 1070-1074. Noels, A. F.; Hubert, A. J.; Teyssie, P. *J. Organomet. Chem.*, **1979**, 166, 79-86. (c) Anciaux, A. J.; Hubert, A. J.; Noels, A. F.; Petiniot, N.; Teyssie, P. *J. Org. Chem.*, **1980**, 45, 695-702. (d) Doyle, M. P. *Acc. Chem. Res.*, **1986**, 19, 348-356. (e) Doyle, M. P. *Chem. Rev.*, **1986**, 86, 919-940. (f) Maas, G. *Topics in Current Chemistry*; Springer-Verlag: Berlin, West Germany, **1987**.

<sup>46</sup> (a) Doyle, M. P.; Forbes, D. C. *Chem. Rev.*, **1998**, 98, 911-935. (b) Hodgson, D. M.; Pierard, F. Y. T. M.; Stuppel, P. A. *Chem. Soc. Rev.*, **2001**, 30, 50-61.

<sup>47</sup> Roskamp, E. J.; Johnson, C. R. *J. Am. Chem. Soc.*, **1986**, 108, 6062-6063.

<sup>48</sup> Pirrung, M. C.; Brown, W. L.; Rege, S.; Laughton, P. *J. Am. Chem. Soc.*, **1991**, 113, 8561-8562.

(Scheme 28). These transformations can be in competition with each other, and the outcome of the oxonium ylide reaction is governed by the electronic nature of the substrate as well as the catalyst that is being employed.



**Scheme 28.** Reactions and rearrangements of oxonium ylides.

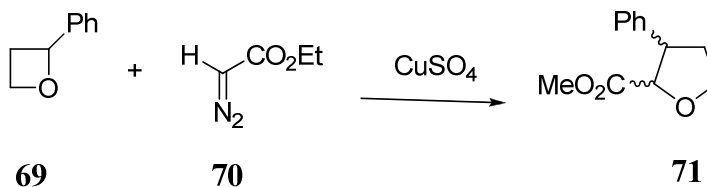
### 1.3a [1,2]-Stevens rearrangement of oxonium ylides

#### 1.3a.(i) Examples of [1,2]-Stevens rearrangement of oxonium ylides

In 1966 Nozaki and co-workers reported the first example of an intermolecular [1,2]-oxonium ylide rearrangement in a catalytic reaction with a diazocarbonyl

<sup>49</sup> (a) Oku, A.; Ohki, S.; Yoshida, T.; Kimura, K. *Chem. Commun.*, **1996**, 1077-1078. (b) Sawada, Y.; Mori, T.; Oku, A. *J. Org. Chem.*, **2003**, *68*, 10040-10045. (c) Muthusamy, S.; Krishnamurthi, J.; Suresh, E. *Chem. Commun.*, **2007**, 861-863. (d) Lu, C.-D.; Liu, H.; Chen, Z.-Y.; Hu, W.-H.; Mi, A.-Q. *Org. Lett.*, **2005**, *7*, 83-86. (e) Hu, W.; Xu, X.; Zhou, J.; Liu, W.-J.; Huang, H.; Hu, J.; Yang, L.; Gong, L.-Z. *J. Am. Chem. Soc.*, **2008**, *130*, 7782-7783.

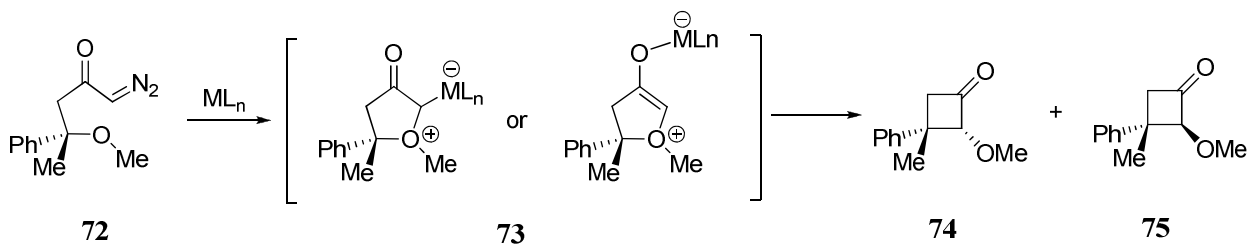
compound.<sup>50</sup> In that report a copper(II) catalyzed reaction of phenyloxetane **69** with ethyl diazoacetate **70** using CuSO<sub>4</sub> afforded diastereoisomeric tetrahydrofurans **71** in 87% yield (Scheme 29).<sup>50</sup>



**Scheme 29.** First example of intermolecular [1,2]-oxonium ylide rearrangement reported by Nozaki in 1966.

Roskamp and Johnson<sup>51</sup> investigated the intramolecular generation and rearrangement of oxonium ylides. They showed that treating (*S*)-1-diazo-4-methoxy-4-phenylpentan-2-one **72** with three distinct catalysts gave different ratios of the diastereomeric cyclobutanones **74** and **75** (Table 11).<sup>51</sup> The authors proposed that a change in the product ratios, as a result of changing the catalyst employed, meant that the rearrangement proceeds *via* metal associated complex intermediates **73** and not a free ylide.

**Table 11.** Intramolecular generation and rearrangement of oxonium ylides by Roskamp and Johnson.



<sup>50</sup> (a) Nozaki, H.; Takaya, H.; Noyori, R. *Tetrahedron*, **1966**, 22, 3393-3401. (b) Nozaki, H.; Takaya, H.; Moriuti, S.; Noyori, R. *Tetrahedron*, **1968**, 24, 3655-3669.

<sup>51</sup> Roskamp, E. J.; Johnson, C. R. *J. Am. Chem. Soc.*, **1986**, 108, 6062-6063.

Entry	Catalyst	Ratio (74:75)	Yield (%) 74 <sup>a</sup>	Yield (%) 75
1	Rh <sub>2</sub> (OAc) <sub>4</sub>	3:1	57	17
2	Cu(acac) <sub>2</sub>	1:6	n/a	n/a
3	RhCl(PPh <sub>3</sub> )	1:10	n/a	n/a

<sup>a</sup>The absolute configuration at the quaternary center in **74** was established by conversion to *S*-dimethyl-3-methyl-3-phenyl-1,4-dibutanoate using [Mo<sub>3</sub>O<sub>2</sub>(CH<sub>3</sub>COO)<sub>6</sub>(H<sub>2</sub>O)<sub>3</sub>]Br<sub>2</sub>·H<sub>2</sub>O.

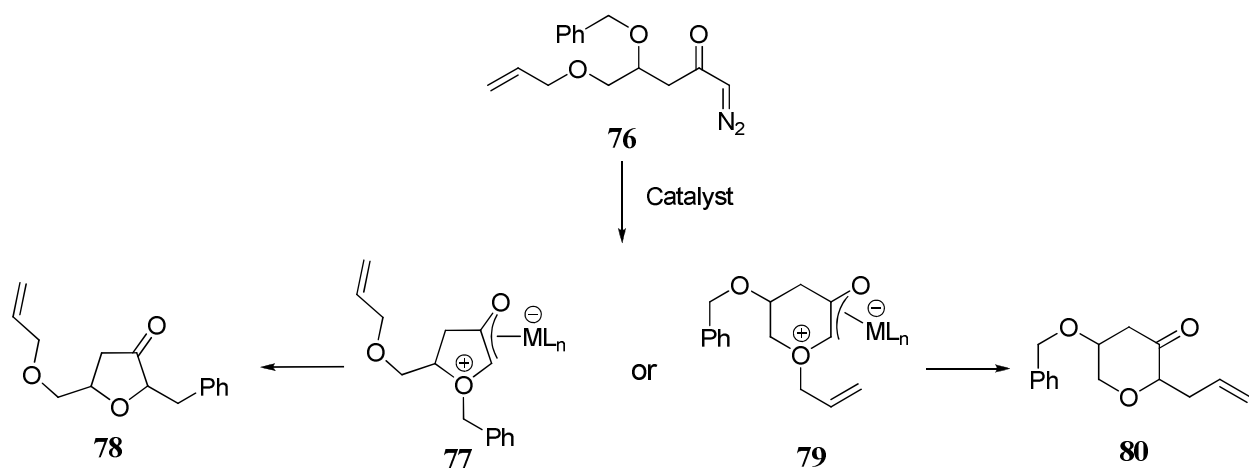
The nature of the catalyst employed not only has an effect on the diastereomeric ratios of the rearrangement products due to the rearrangement proceeding *via* a metal associated complex, as discussed previously, it can also impact ylide reactivity.<sup>52</sup> West reported the competitive formation of two different oxonium ylide intermediates that are formed *via* the same metal carbene (Table 12).<sup>52</sup> These two oxonium ylide intermediates differ in their ring sizes (five *vs.* six) and the type of migrating group they poses (benzylic *vs.* allylic) (Table 12). West and co-workers investigated the decomposition reaction of diazoketone **76** where the metal carbene could undergo reaction at either of the two ether oxygens to form either a five or a six-membered oxonium ylide intermediate **77** and **79** (Table 12).<sup>52</sup> When Rh<sub>2</sub>(OAc)<sub>4</sub> and Rh<sub>2</sub>(tpa)<sub>4</sub> were employed as catalysts, the five-membered [1,2]-Stevens rearrangement product **78** product was formed as the major product (entry 2 and 3, Table 12). However, by using Cu(tfacac)<sub>2</sub> as the catalyst the selectivity was altered; affording predominately the six-membered rearrangement product **80** in 67% yield (entry 1, Table 12). Both rearrangement products **78** and **80** were formed as mixtures of *cis* and *trans* diastereoisomers with varying ratios<sup>53</sup> which indicates that the ylide intermediate that is formed in the reaction is a metal-associated ylide.

<sup>52</sup> Marmsater Fredrik, P.; Vanecko John, A.; West, F. G. *Org. Lett.*, **2004**, *6*, 1657-1660.

<sup>53</sup> Ratios of the *cis* and *trans* rearrangement products were not clearly reported in the paper. Authors claim that the ratios were varied. The ones reported varied between 1:1 to 4:1.

**Table 12.** Catalyst and ring size effects on the selectivity of oxonium ylide

rearrangements.

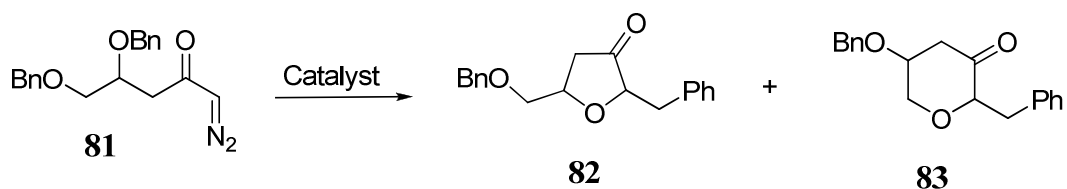


Entry	Catalyst	Temp. (°C)	Ratio 78:80	Yield (%)	
				78	80
1	Cu(tfacac) <sub>2</sub>	40	19:81	16	67
2	Rh <sub>2</sub> (OAc) <sub>4</sub>	25	65:35	50	27
3	Rh <sub>2</sub> (tpa) <sub>4</sub>	25	71:29	54	22

In the same report, West<sup>52</sup> further investigated whether oxonium ylide rearrangements favor proceeding through five-membered or six-membered cyclic

oxonium ylides. Diazoketone **81** was treated with a number of rhodium(II) and copper catalysts to afford predominately the five-membered [1,2]-Stevens rearrangement product **82** product which is formed via a five-membered oxonium ylide (Table 13). West<sup>52</sup> and Pirrung<sup>54</sup> both have shown that oxonium ylide rearrangements proceeding through five-membered cyclic oxonium ylides usually result in significantly greater product yield than their counterparts which involve six-membered ylides.

**Table 13.** Preference for five-membered oxonium ylide formation of diazoketone **81**.



Entry	Catalyst	Temp. (°C)	Ratio 82:83	Yield (%) <b>82<sup>a</sup></b>	Yield (%) <b>83<sup>a</sup></b>
1	Cu(tfacac) <sub>2</sub>	40	80:20	33	8
2	Cu(hfacac) <sub>2</sub>	40	79:21	48	13
3	Rh <sub>2</sub> (OAc) <sub>4</sub>	25	81:19	56	13
4	Rh <sub>2</sub> (tpa) <sub>4</sub>	25	76:24	58	18

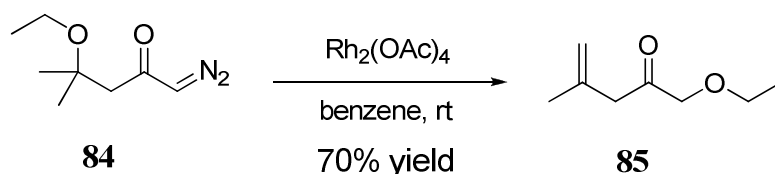
<sup>a</sup> Isolated yields after chromatography. Both diastereomers of **82** and **83** were isolated in some cases with ratios varying from 2:1 to 4:1.

The two oxonium ylide reaction pathways for diazoketone **76** presented a dilemma; while ring size preferences should favor the five-membered ylide **77**, the migrating group preferences (allylic vs. benzylic) should favor the formation of pyranone

<sup>54</sup> Pirrung, M. C.; Werner, J. A. *J. Am. Chem. Soc.*, **1986**, *108*, 6060-6062.

**80** that arises from the facile allylic [2,3]-sigmatropic rearrangement. Interestingly, when diazoketone **76** was treated with  $\text{Cu}(\text{tfacac})_2$ , pyranone **80** was formed in 67% yield and furanone **78** was formed in 16% yield, whereas reactions using Rh(II) catalysts resulted in the formation of mainly furanone **78** (Table 12). These results seem to indicate that the nature of the migrating group (allylic vs. benzylic) in the subsequent rearrangement process can override the inherent selectivity for five-membered ylide intermediates. However, further catalyst screenings, particularly copper catalysts, are needed to confirm these observations.

In addition to the choice of the catalyst directly affecting the outcome of the oxonium ylide reaction, the nature of the migrating group also has an effect on the end result of the reaction. Johnson and Roskamp<sup>55</sup> have shown that vinyl and aryl substituents yield [2,3] and [1,2] rearrangement products, respectively, whereas alkyl substituents do not. Diazoketone **84** did not furnish the [1,2]-Stevens rearrangement product but instead it afforded the elimination product **85** in 70% yield (Scheme 30).



**Scheme 30.** Elimination product formation.

### **1.3a.(ii) Mechanism of the [1,2]-Stevens rearrangement of oxonium ylides**

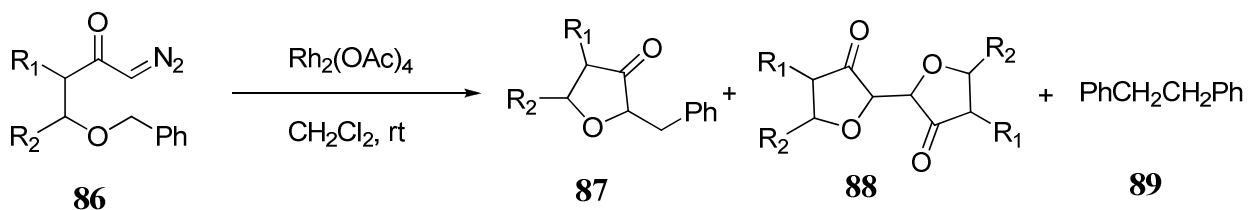
The mechanism of the [1,2]-Stevens rearrangement of oxonium ylides has been a subject of considerable discussion. Three possible mechanisms have been introduced for

<sup>55</sup> Roskamp, E. J.; Johnson, C. R. *J. Am. Chem. Soc.*, **1986**, *108*, 6062-6063.

the [1,2]-rearrangement of oxonium ylides: 1) initial homolysis of the C-O bond<sup>56</sup> to afford a radical pair intermediate that could be held close in a solvent cage, 2) heterolysis of the C-O bond to give a zwitterion pair intermediate, or 3) a concerted mechanism<sup>57</sup> of the oxonium ylide intermediate which directly leads to the [1,2]-Stevens rearrangement product.

West<sup>56</sup> has provided evidence for the existence of the radical-pair mechanism through isolation of homodimers during an investigation into the synthesis of functionalized tetrahydrofuranones **87** from the corresponding diazoketone **86** (Table 14). Isolation of homodimers **88** and **89** suggests the existence of radical-pair intermediates.<sup>56</sup> It is important to note that dimerization products have not been reported elsewhere with oxonium ylides reactions.

**Table 14.** Isolation of homodimers in the decomposition reaction of diazoketone **86**.



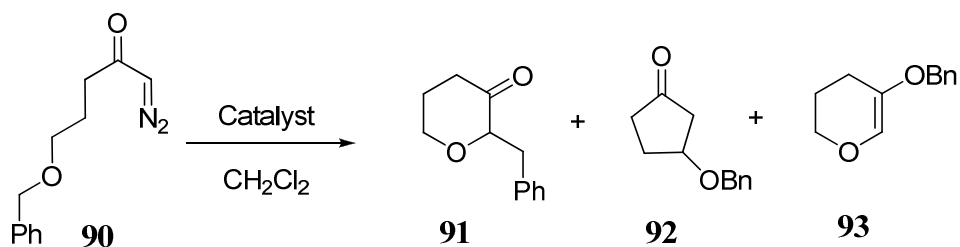
Entry	R <sub>1</sub>	R <sub>2</sub>	Yield (%) <b>87</b>	Yield (%) <b>88</b>	Yield (%) <b>89</b>
1	H	H	64	27	16
2	Me	H	65	17	16
3	H	Me	52	--	11

<sup>56</sup> Eberlein, T. H.; West, F. G.; Tester, R. W. *J. Org. Chem.*, **1992**, *57*, 3479-3482.

<sup>57</sup> Roskamp, E. J.; Johnson, C. R. *J. Am. Chem. Soc.*, **1986**, *108*, 6062-6063.

Interestingly, West<sup>58</sup> also reported that no radical homodimers were observed/isolated when Cu(II) and Rh(II) were used to catalyze the decomposition of diazoketone **90**, which is the next higher homolog of **86** (Table 15). The fact that the same group had reported isolation of homodimers with the decomposition of diazoketone **86** and didn't isolate homodimers with the decomposition of diazoketone **90**, using the same catalyst and solvent, seems contradictory and raises questions about the mechanism of the [1,2]-Stevens rearrangement process with oxonium ylides.

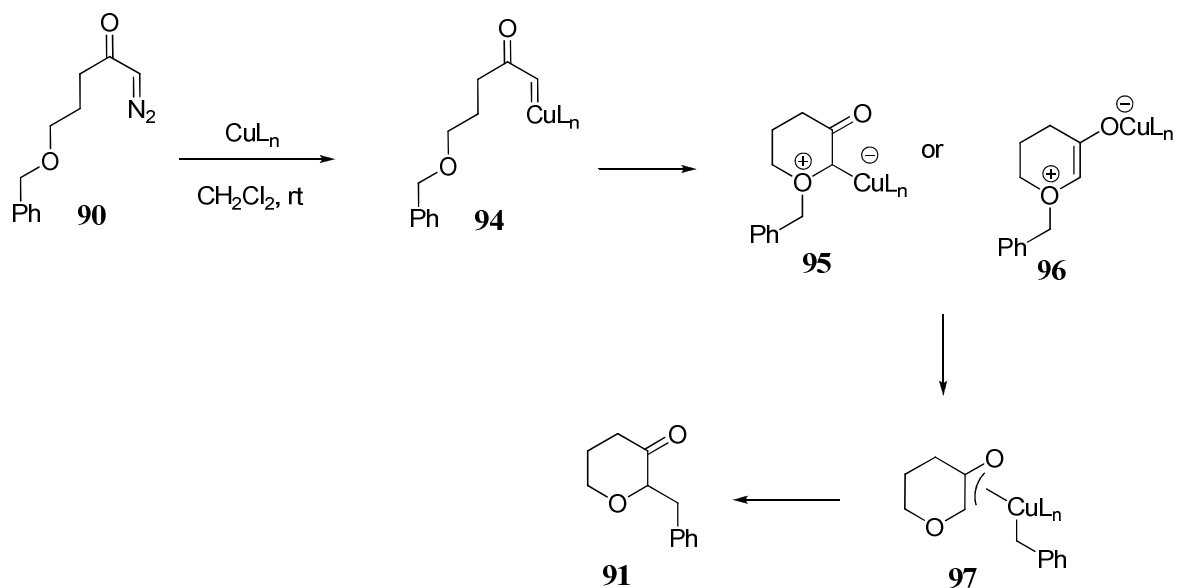
**Table 15.** Lack of isolation of homodimers in the decomposition reaction of diazoketone **90**.



Entry	Catalyst	T[°C]	Yield (%) 91	Yield (%) 92	Yield (%) 93
1	Rh <sub>2</sub> (OAc) <sub>4</sub>	25	16	47	--
2	Cu(hfacac) <sub>2</sub>	40	35	6	24

<sup>58</sup> West, F. G.; Naidu, B. N.; Tester, R. W. *J. Org. Chem.*, **1994**, *59*, 6892-6894.

Due to the absence of homodimers, West proposed a concerted mechanism similar to what was previously proposed by Johnson<sup>59</sup> where metal-associated oxonium ylides **95** or **96** undergo transfer of the migrating group to the metal to give intermediate **97** which then undergoes reductive elimination to afford the [1,2]-Stevens rearrangement product **91** (Scheme 31).



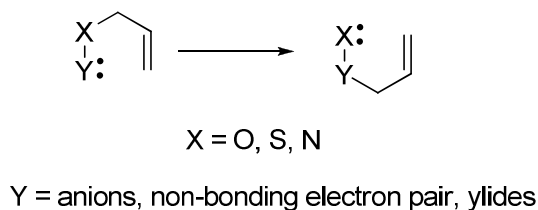
**Scheme 31.** Concerted mechanism for the decomposition of diazoketone **90**, as proposed by West.

<sup>59</sup> Roskamp, E. J.; Johnson, C. R. *J. Am. Chem. Soc.*, **1986**, *108*, 6062-6063.

The two aforementioned examples published by West (Table 14 and 15) indicate that there is uncertainty regarding the mechanism of the oxonium ylide rearrangement process and whether it takes place by a concerted mechanism or by a stepwise mechanism via radical-pair intermediates.

### **1.3b [2,3]-Sigmatropic rearrangement of allylic oxonium ylides**

The [2,3]-sigmatropic rearrangement constitutes an exceptionally versatile class of C-C bond forming processes that is widely used in the construction of complex molecules as well as developing methodologies for organic synthesis.<sup>60</sup> This rearrangement proceeds through a six-electron, five-membered cyclic transition state that occurs in the presence of an allylic group (Scheme 32). Consequently, the presence of an alkene provides the possibility of competing cyclopropanation reactions during ylide formation.<sup>61</sup>



**Scheme 32.** [2,3]-sigmatropic reaction.

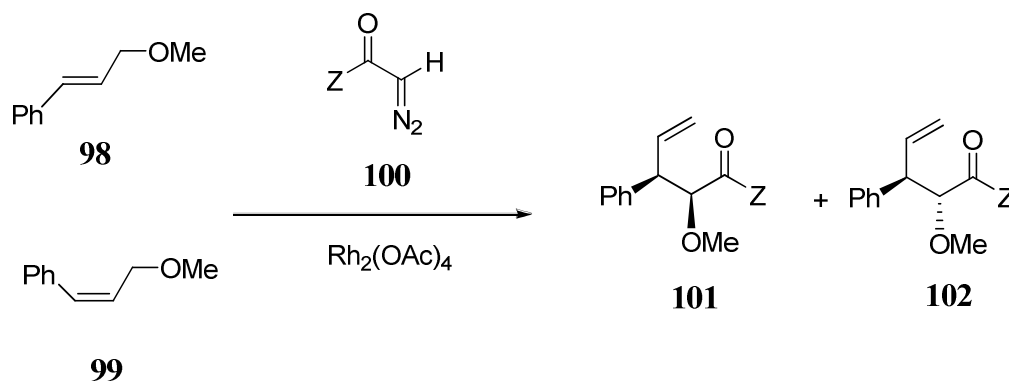
Despite the fact that cyclopropanation reactions are able to compete with [2,3]-sigmatropic rearrangement processes, there are many reports demonstrating that ylide formation and subsequent [2,3]-sigmatropic rearrangement products occur in high yields.

<sup>60</sup> (a) Hoffmann, R. W. *Angew. Chem.*, **1979**, *91*, 625-634. (b) Desimoni, G.; Tacconi, G.; Barco, A.; Pollini, G. P. *Natural Products Synthesis Through Pericyclic Reactions*; American Chemical Society: Washington, DC, **1983**, Chapter 7.

<sup>61</sup> (a) Doyle, M. P.; Tamblyn, W. H.; Bagheri, V. *J. Org. Chem.*, **1981**, *46*, 5094-5102. (b) Doyle, M. P.; Griffin, J. H.; Chinn, M. S.; Van Leusen, D. *J. Org. Chem.*, **1984**, *49*, 1917-1925.

Doyle and co-workers<sup>62</sup> have shown that allylic oxonium ylides, generated by rhodium(II) acetate-catalyzed decomposition of diazocarbonyl compounds in the presence of allyl methyl ethers, undergo almost exclusively the [2,3]-sigmatropic rearrangement with high degree of diastereoselectivity. Treatment of cinnamyl methyl ether **98** with diazoketone/diazoacetate **100** in the presence of rhodium acetate yielded mostly the erythro product **101**, whereas treating *cis*-cinnamyl methyl ether **99** with diazoketone/diazoacetate **100** resulted in mostly threo product **102** (Table 16).

**Table 16.** Intermolecular generation of allylic oxonium ylides and their stereoselective [2,3]-sigmatropic rearrangement.



Entry	Allyl ether	Z	Ratio (101:102)	Yield (%) (101+102)
1	<b>98</b>	Ph	91:9	86
2	<b>99</b>	Ph	19:81	70

<sup>62</sup> Doyle, M. P.; Bagheri, V.; Harn, N. K. *Tetrahedron Lett.*, **1988**, 29, 5119-5122.

3	<b>98</b>	OEt	83:17	73
4	<b>99</b>	OEt	6:94	95

Doyle's results can be explained by steric and/or electronic influences in the transition state structures **103-106** (Figure 3).<sup>62</sup> The alkene geometry plays a major role in dictating the stereochemical outcome of the reaction. The rearrangement of the oxonium ylide is thought to proceed mainly through transition state **103** and **105** due to their lower energies compared to transition state **104** and **106** where eclipsing interactions between the *O*-methyl substituent and the carbonyl group are present. Accordingly, the observed diastereoselectivity in products **101** and **102** is a function of the relative transition state energies for **103** and **105**.<sup>62</sup>

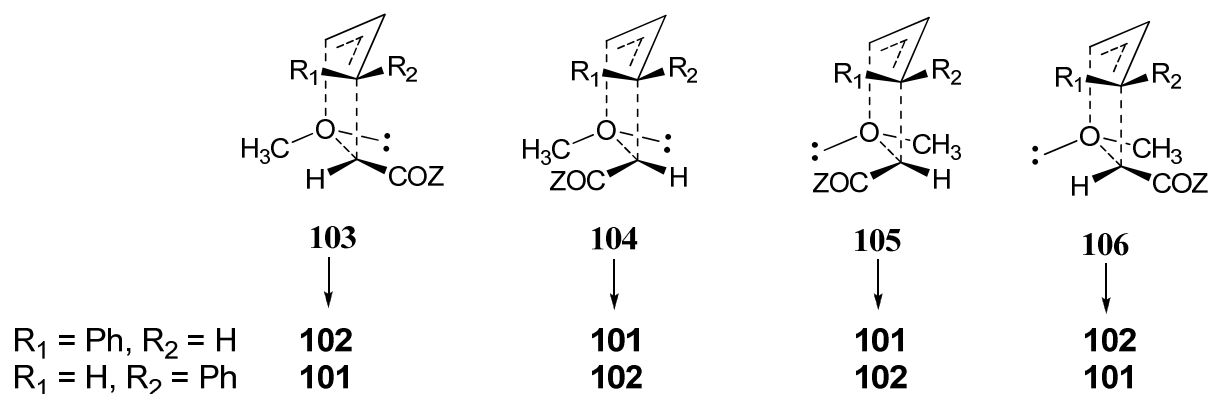
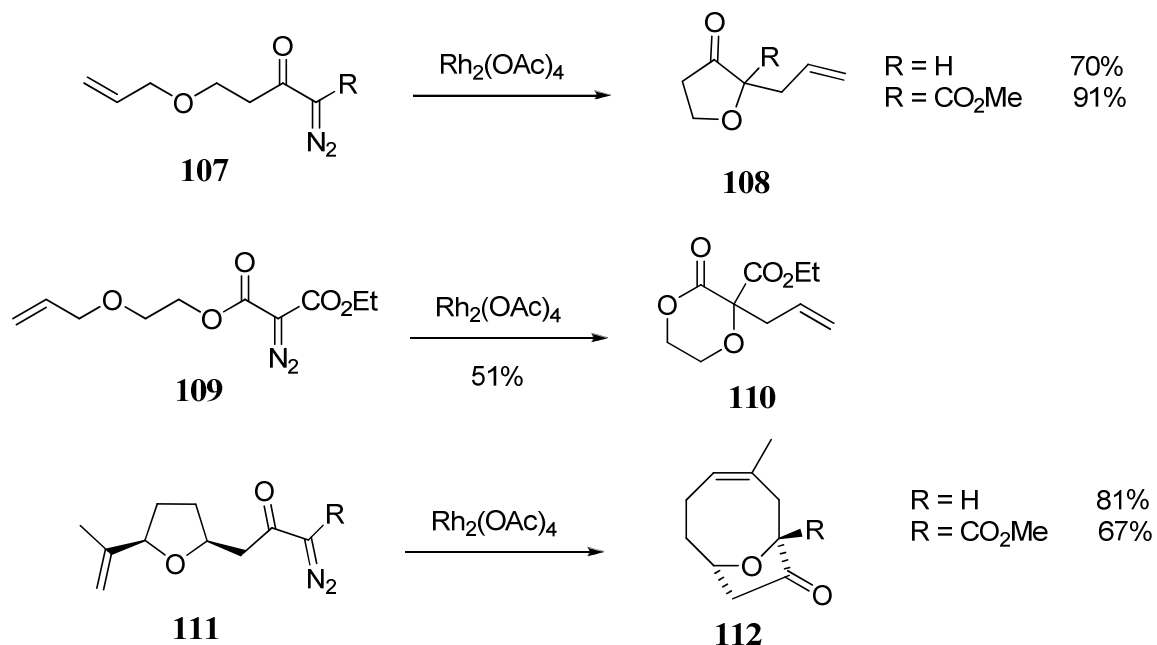


**Figure 3.** Transition state structures for the intermolecular generation of allylic oxonium ylides.

In addition to investigating the intermolecular [2,3]-sigmatropic rearrangement reactions, attention was given to the development of the intramolecular [2,3]-sigmatropic process because the former has limited application in organic synthesis and the latter is a more widely used process in the literature. One of the examples of intramolecular oxonium ylide generation followed by the subsequent [2,3]-sigmatropic rearrangement

was reported by Pirrung and Werner in 1986.<sup>63</sup> Rhodium(II) acetate catalyzed the decomposition of several diazocarbonyl/diazoacetate compounds and yielded five-, six-, and eight-membered oxygen heterocycles (Scheme 33).<sup>63</sup> Transition metal-catalyzed decomposition of **107** and **109** resulted in the formation of furanone **108** and dioxanone **110**, respectively.<sup>63</sup> When **111** was treated with rhodium acetate it afforded the eight-membered oxygen heterocycle **112** via a three-carbon ring expansion.<sup>63</sup> While products **108** and **110** can be achieved *via* either the [1,2]-Stevens or the [2,3]-sigmatropic rearrangements, product **112** can only be achieved via the [2,3]-sigmatropic rearrangement. The latter example clearly illustrates the preference of the oxonium ylide to undergo the [2,3]-sigmatropic rearrangement over the [1,2]-Stevens rearrangement, as also shown by others.<sup>64</sup>

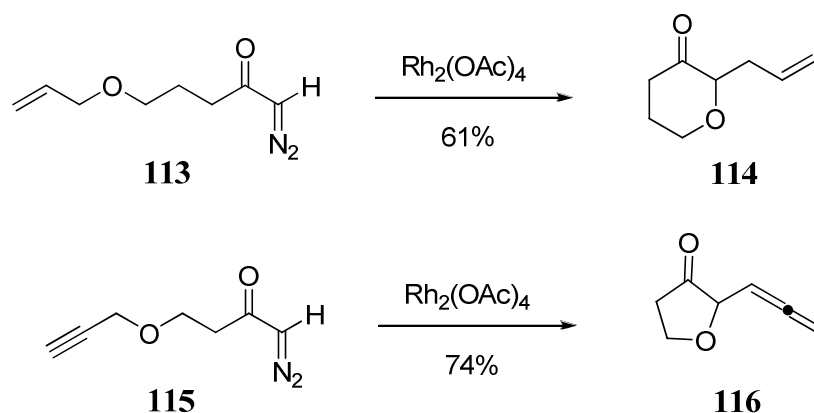


<sup>63</sup> Pirrung, M. C.; Werner, J. A. *J. Am. Chem. Soc.*, **1986**, *108*, 6060-6062.

<sup>64</sup> (a) Doyle, M. P.; Griffin, J. H.; Chinn, M. S.; Van Leusen, D. *J. Org. Chem.*, **1984**, *49*, 1917-1925. (b) Ando, W.; Yagihara, T.; Kondo, S.; Nakayama, K.; Yamato, H.; Nakaido, S.; Migita, T. *J. Org. Chem.*, **1971**, *36*, 1732-1736. (c) Ando, W.; Kondo, S.; Nakayama, K.; Ichibori, K.; Kohoda, H.; Yamato, H.; Imai, I.; Nakaido, S.; Migita, T. *J. Am. Chem. Soc.*, **1972**, *94*, 3870-3876.

**Scheme 33.** Intramolecular [2,3]-sigmatropic rearrangement affords five-, six-, and eight-membered oxygen heterocycles.

Another example of the observation of an intramolecular [2,3]-sigmatropic rearrangement process was reported by Johnson and Roskamp.<sup>65</sup> When diazoketone **113** was treated with rhodium acetate it provided pyran **114** in 61% yield while propargylic ether **115** provided allene **116** in 74% yield (Scheme 34).<sup>65</sup> The latter example once again shows the preference of the ylide to undergo [2,3]-sigmatropic rearrangement over the [1,2]-Stevens rearrangement and also shows that the [2,3]-sigmatropic rearrangement is also possible with propargylic ethers.



**Scheme 34.** Intramolecular [2,3]-sigmatropic rearrangement also possible with propargylic ethers.

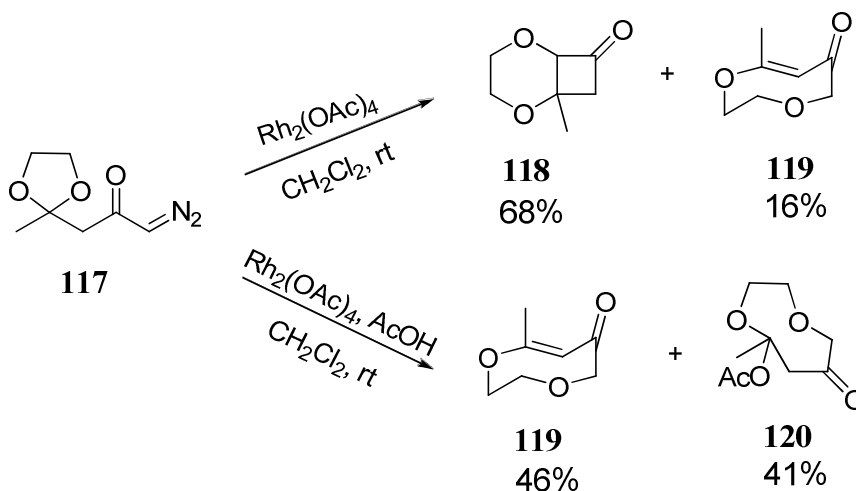
### 1.3c Other reactions of oxonium ylides

Other than the [2,3]-sigmatropic and the [1,2]-Stevens rearrangements, oxonium ylides can also undergo an artifact of the [1,2]-Stevens rearrangement known as the [1,4]-shift rearrangement, fragmentation *via*  $\beta$ -hydride elimination, or react with an external nucleophile after a ring opening of the oxonium ylide has occurred (see Scheme 28 on

<sup>65</sup> Roskamp, E. J.; Johnson, C. R. *J. Am. Chem. Soc.*, **1986**, *108*, 6062-6063.

page 108 for a description of these reactions). The latter reactions would take place when the generated oxonium ylide lacks a competent migrating group (such as a benzyl or an allyl group), as a result, the oxonium ylide can fragment and be trapped *via* other pathways.

In 1997, Oku<sup>66</sup> studied the ring expansion of cyclic acetal systems. The ring expansion process is more difficult to predict due to the competing [1,2]-Stevens rearrangement<sup>67</sup> pathway. Roskamp and Johnson<sup>67</sup> first reported the rhodium-catalyzed decomposition of diazoketone **117** that afforded the [1,2]-Stevens rearrangement product **118** in 68% yield and the elimination product **119** in 16% yield. Oku<sup>66</sup> and co-workers wanted to enhance the formation of the elimination product **119** by protonating the generated oxonium ylide with a bronsted acid (AcOH). Indeed, treating diazoketone **117** with rhodium acetate in the presence of acetic acid yielded the two ring-expansion products **119** and **120** in 87% overall yield.

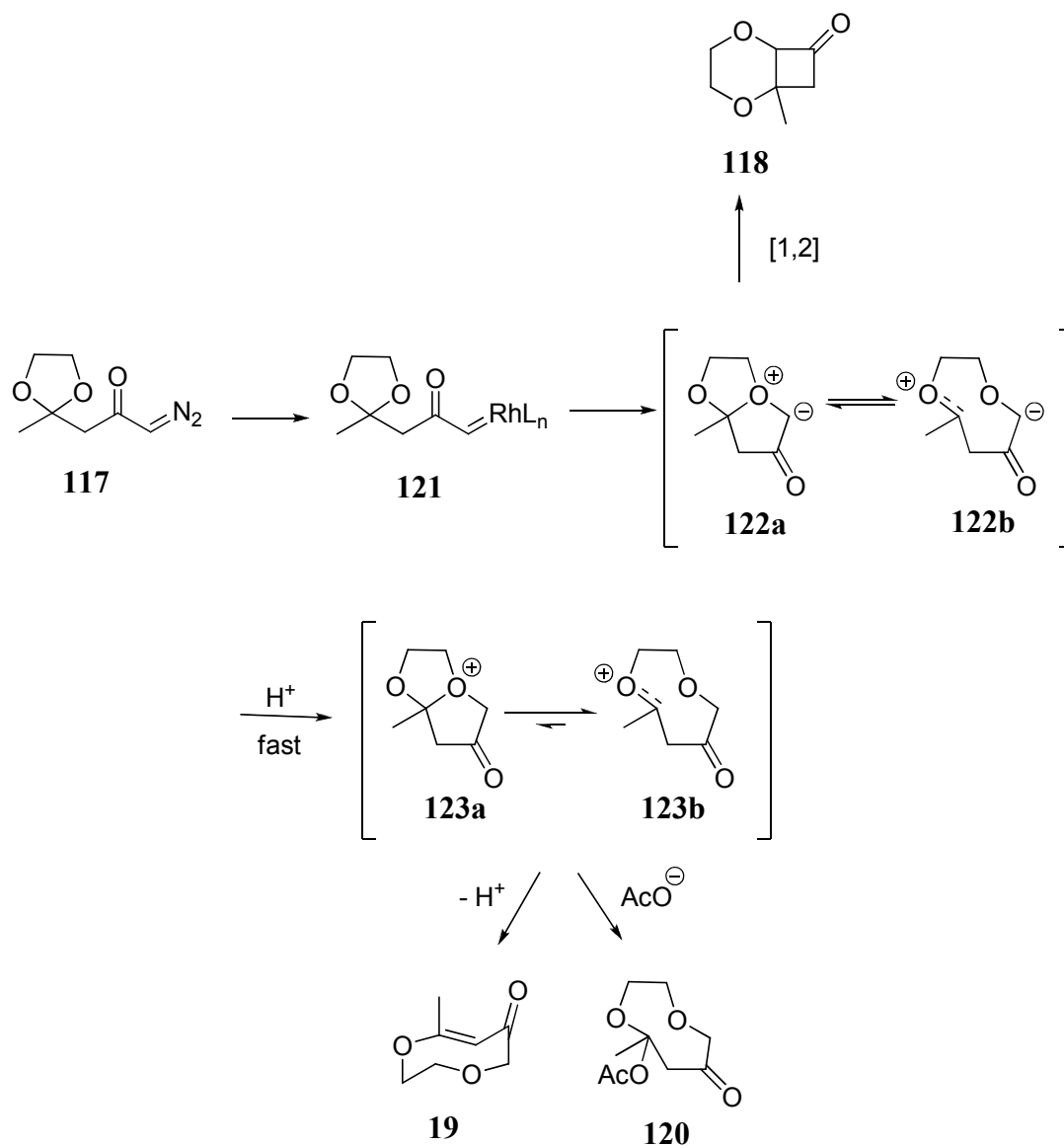


**Scheme 35.** Ring expansion of cyclic acetal systems.

<sup>66</sup> Oku, A.; Murai, N.; Baird, J. J. *Org. Chem.*, **1997**, *62*, 2123-2129.

<sup>67</sup> Roskamp, E. J.; Johnson, C. R. *J. Am. Chem. Soc.*, **1986**, *108*, 6062-6063.

The enhanced formation of the elimination product **119** by protonating the generated oxonium ylide **122** with the bronsted acid (AcOH) led to the suppression of the [1,2]-Stevens product **118**. This can be attributed to the protonation of the oxonium ylide **122** being faster than its [1,2] rearrangement (Scheme 36).<sup>66</sup>



**Scheme 36.** Mechanism of the ring expansion of cyclic acetal systems.

---

# 2. Research Discussion

---

## 2.1 Strategy for the synthesis of the oxabicyclo[4.2.1] nonane framework

The structurally interesting family of bridged oxa-[*n.2.1*] skeletons are well-represented and widely diverse in natural products such as platensimycin,<sup>68</sup> bruguierol,<sup>69</sup> mycoepoxydiene,<sup>70</sup> and sclerophytin B (Figure 4).<sup>71</sup> A number of synthetic approaches have been applied towards accessing these cyclic structures,<sup>81</sup> and the broad ranging biological activity (from anti-inflammatory to antitumor properties) of these complex architectures has increased the interest in developing new synthetic methodologies to access these bridged oxa-bicyclo skeletons.<sup>72</sup>

---

<sup>68</sup> (a) Tiefenbacher, K.; Mulzer, J. *Angew. Chem., Int. Ed.*, **2008**, *47*, 2548-2555. (b) Tiefenbacher, K.; Mulzer, J. *Angew. Chem., Int. Ed.*, **2008**, *47*, 6199-6200.

<sup>69</sup> (a) Ramana, C. V.; Salian, S. R.; Gonnade, R. G. *Eur. J. Org. Chem.*, **2007**, 5483-5486. (b) Solorio, D. M.; Jennings, M. P. *J. Org. Chem.*, **2007**, *72*, 6621-6623. (c) Fananas, F. J.; Fernandez, A.; Cevic, D.; Rodriguez, F. *J. Org. Chem.*, **2009**, *74*, 932-934.

<sup>70</sup> (a) Cai, P.; McPhail, A. T.; Krainer, E.; Katz, B.; Pearce, C.; Boros, C.; Caceres, B.; Smith, D.; Houck, D. R. *Tetrahedron Lett.*, **1999**, *40*, 1479-1482. (b) Takao, K.-i.; Watanabe, G.; Yasui, H.; Tadano, K.-i. *Org. Lett.*, **2002**, *4*, 2941-2943. (c) Ahmed, A. F.; Su, J.-H.; Kuo, Y.-H.; Sheu, J.-H. *J. Nat. Prod.*, **2004**, *67*, 2079-2082. (d) Xiao, W.-L.; Gong, Y.-Q.; Wang, R.-R.; Weng, Z.-Y.; Luo, X.; Li, X.-N.; Yang, G.-Y.; He, F.; Pu, J.-X.; Yang, L.-M.; Zheng, Y.-T.; Lu, Y.; Sun, H.-D. *J. Nat. Prod.*, **2009**, *72*, 1678-1681.

<sup>71</sup> Montana, A. M.; Ponzano, S.; Kociok-Koehn, G.; Font-Bardia, M.; Solans, X. *Eur. J. Org. Chem.*, **2007**, 4383-4401.

<sup>72</sup> (a) Cope, A. C.; McKervy, M. A.; Weinshenker, N. M. *J. Org. Chem.*, **1969**, *34*, 2229-2231. (b) Lipshutz, B. H. *Chem. Rev.*, **1986**, *86*, 795-820. (c) Molander, G. A.; Shubert, D. C. *J. Am. Chem. Soc.*, **1987**, *109*, 6877-6878. (d) Katritzky, A. R.; Dennis, N. *Chem. Rev.*, **1989**, *89*, 827-861. (e) West, F. G.;

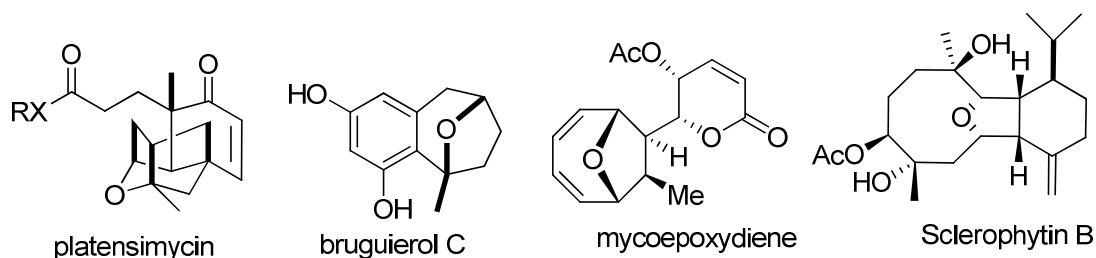


**Figure 4.** Representative examples of bridged oxa-[*n.2.1*] skeletons.

The synthesis and controlled reactions of oxonium ylides formed through catalytic reactions of diazocarbonyl compounds with ethers<sup>73</sup> have high potential for the construction of diverse natural products.<sup>74</sup> West recently reported an expedient synthesis to the fused tricyclic carbon skeleton (found in classes of diterpene natural products) via an oxonium ylide intermediate followed by the [1,2]-Stevens rearrangement.<sup>75</sup> Treatment

---

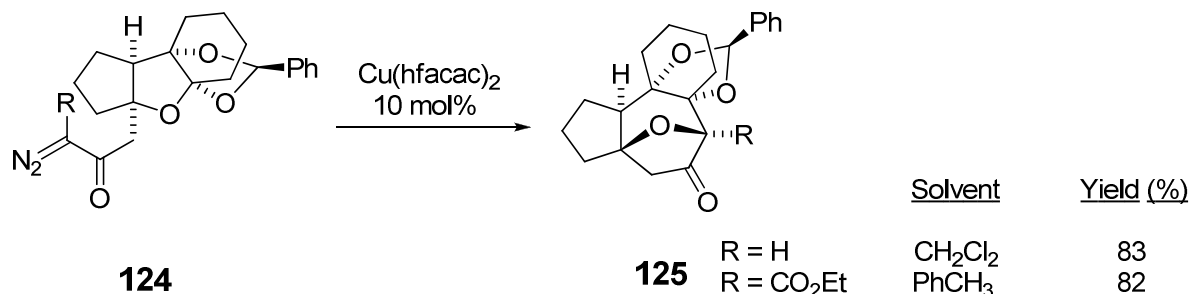
Eberlein, T. H.; Tester, R. W. *J. Chem. Soc., Perkin Trans.*, **1993**, 2857-2859. (f) West, F. G.; Naidu, B. N.; Tester, R. W. *J. Org. Chem.*, **1994**, *59*, 6892-6894. (g) Padwa, A.; Weingarten, M. D. *Chem. Rev.*, **1996**, *96*, 223-269. (h) Clark, J. S.; Whitlock, G.; Jiang, S.; Onyia, N. *Chem. Commun.*, **2003**, 2578-2579. (i) Roberts, E.; Sancon, J. P.; Sweeney, J. B. *Org. Lett.*, **2005**, *7*, 2075-2078. (j) Zhao, W. *Chem. Rev.*, **2010**, *110*, 1706-1745.

<sup>73</sup> (a) Li, A.-H.; Dai, L.-X.; Aggarwal, V. K. *Chem. Rev.*, **1997**, *97*, 2341-2372. (b) Doyle, M. P.; McKerver, M. A.; Ye, T. *Modern Catalytic Methods for Organic Synthesis with Diazo Compounds*; Wiley: New York, **1998**. (c) Yet, L. *Chem. Rev.*, **2000**, *100*, 2963-3007. (d) Clark, J. S. *Nitrogen, Oxygen, and Sulfur Ylide Chemistry. A practical Approach in Chemistry*; ed.: Oxford University Press: Oxford, **2002**. (e) West, F. G. in *Modern Rhodium-Catalyzed Organic Reactions* Evans, P. A., ed.; Wiley-VCH: New York, **2005**, ch. 18. (f) Desimoni, G.; Faita, G.; Jorgensen, K. A. *Chem. Rev.*, **2006**, *106*, 3561-3651. (g) Wee, A. G. H. *Curr. Org. Synth.*, **2006**, *3*, 499-555. (h) Sweeney, J. B. *Chem. Soc. Rev.*, **2009**, *38*, 1027-1038.

<sup>74</sup> (a) Marmsaeter, F. P.; West, F. G. *J. Am. Chem. Soc.*, **2001**, *123*, 5144-5145. (b) Clark, J. S.; Fessard, T. C.; Wilson, C. *Org. Lett.*, **2004**, *6*, 1773-1776. (c) Clark, J. S.; Baxter, C. A.; Castro, J. L. *Synthesis*, **2005**, 3398-3404. (d) Clark, J. S.; Fessard, T. C.; Whitlock, G. A. *Tetrahedron*, **2005**, *62*, 73-78. (e) Yakura, T.; Muramatsu, W.; Uenishi, J. i. *Chem. Pharm. Bull.*, **2005**, *53*, 989-994. (f) Clark, J. S.; Hayes, S. T.; Wilson, C.; Gobbi, L. *Angew. Chem., Int. Ed.*, **2007**, *46*, 437-440. (g) Clark, J. S.; Baxter, C. A.; Dossetter, A. G.; Poigny, S.; Castro, J. L.; Whittingham, W. G. *J. Org. Chem.*, **2008**, *73*, 1040-1055. (h) Hodgson, D. M.; Angrish, D.; Erickson, S. P.; Kloesges, J.; Lee, C. H. *Org. Lett.*, **2008**, *10*, 5553-5556.

<sup>75</sup> Stewart, C.; McDonald, R.; West, F. G. *Org. Lett.*, **2011**, *13*, 720-723.

of diazoketone/diazoacetoacetate **124** with  $\text{Cu}(\text{hfacac})_2$  afforded the single [1,2]-rearrangement product **125** in 80% yield (Scheme 37).



**Scheme 37.** Synthesis of the Tigliane-Daphnane skeleton via an oxonium ylide intermediate followed by [1,2]-Stevens rearrangement.

In our search for viable substrates that could take advantage of oxonium ylide chemistry, we considered the tetrahydro-4-pyranone framework **128** which is accessible in a two step synthetic process from synthetically available reactants (Scheme 38). The first step is the hetero-Diels-Alder reaction which has numerous variations,<sup>76</sup> including those that are highly enantioselective.<sup>77</sup> The subsequent step is the Mukaiyama-Michael

<sup>76</sup> (a) Nicolaou, K. C., Sorensen, E. J. in *Classics in Total Synthesis: Targets, Strategies, Methods* Waldmann, H., ed; VCH: New York, **1996**. (b) Boger, D. L., Weinreb, S. H. in *Hetero-Diels-Alder Methodology in Organic Synthesis*, Wasserman, H. H., ed.; Academic Press: San Diego, **1996**. (c) Tietze, L. F., Ketschau, G. in *Stereoselective Heterocyclic Synthesis*, Metz, I. P., ed.; Springer-Verlag: Berlin, **1997**. (d) Maruoka, K. in *Catalytic Asymmetric Synthesis*, Ojima, I., ed.; VCH: New York, **2000**. (e) Jorgensen, K. A. *Angew. Chem., Int. Ed.*, **2000**, *39*, 3558-3588. (f) Reymond, S.; Cossy, J. *Chem. Rev.*, **2008**, *108*, 5359-5406.

<sup>77</sup> (a) Dossetter, A. G.; Jamison, T. F.; Jacobsen, E. N. *Angew. Chem., Int. Ed.*, **1999**, *38*, 2398-2400. (b) Doyle, M. P.; Phillips, I. M.; Hu, W. *J. Am. Chem. Soc.*, **2001**, *123*, 5366-5367. (c) Long, J.; Hu, J.; Shen, X.; Ji, B.; Ding, K. *J. Am. Chem. Soc.*, **2002**, *124*, 10-11. (d) Doyle, M. P.; Valenzuela, M.; Huang, P. *PNAS*, **2004**, *101*, 5391-5395. (e) Anada, M.; Washio, T.; Shimada, N.; Kitagaki, S.; Nakajima, M.; Shiro, M.; Hashimoto, S. *Angew. Chem., Int. Ed.*, **2004**, *43*, 2665-2668. (f) Unni, A. K.; Takenaka, N.;

reaction which has recently been reported to occur in high yield.<sup>78</sup> Exceptional diastereocontrol is well known in Lewis acid catalyzed reactions of the type **126** with silyl enol ethers.<sup>79</sup> We anticipated that transition metal catalyzed reactions of **128** would form oxonium ylide **129** and the resultant [1,2]-rearrangement product **130** would be obtained with high selectivity<sup>80</sup> (Scheme 38).

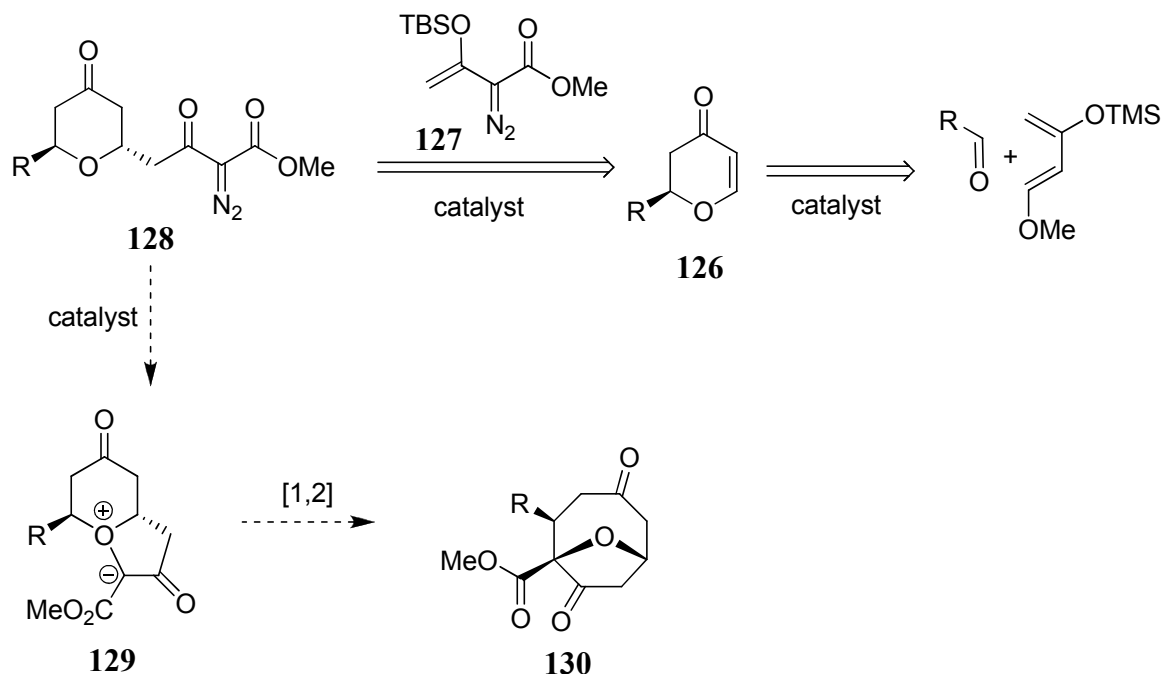
---

Yamamoto, H.; Rawal, V. H. *J. Am. Chem. Soc.*, **2005**, *127*, 1336-1337. (g) Chavez, D. E.; Jacobsen, E. N. *Org. Synth.*, **2005**, *82*, 34-42. (h) Du, H.; Zhang, X.; Wang, Z.; Bao, H.; You, T.; Ding, K. *Eur. J. Org. Chem.*, **2008**, 2248-2254. (i) Li, X.; Meng, X.; Su, H.; Wu, X.; Xu, D. *Synlett*, **2008**, 857-860. (j) Watanabe, Y.; Washio, T.; Shimada, N.; Anada, M.; Hashimoto, S. *Chem. Commun.*, **2009**, 7294-7296. (k) Pellissier, H. *Tetrahedron*, **2009**, *65*, 2839-2877.

<sup>78</sup> Liu, Y.; Zhang, Y.; Jee, N.; Doyle, M. P. *Org. Lett.*, **2008**, *10*, 1605-1608.

<sup>79</sup> (a) Yamashita, Y.; Saito, S.; Ishitani, H.; Kobayashi, S. *J. Am. Chem. Soc.*, **2003**, *125*, 3793-3798. (b) Smith, A. B., III; Razler, T. M.; Ciavarri, J. P.; Hirose, T.; Ishikawa, T. *Org. Lett.*, **2005**, *7*, 4399-4402. (c) Jewett, J. C.; Rawal, V. H. *Angew. Chem., Int. Ed.*, **2007**, *46*, 6502-6504. (d) Anada, M.; Washio, T.; Watanabe, Y.; Takeda, K.; Hashimoto, S. *Eur. J. Org. Chem.*, **2010**, 6850-6854.

<sup>80</sup> Representative examples for [1,2]-rearrangements of oxonium ylides: (a) Doyle, M. P.; Ene, D. G.; Forbes, D. C.; Tedrow, J. S. *Tetrahedron Lett.*, **1997**, *38*, 4367-4370. (b) Oku, A.; Numata, M. *J. Org. Chem.*, **2000**, *65*, 1899-1906. (c) Karche, N. P.; Jachak, S. M.; Dhavale, D. D. *J. Org. Chem.*, **2001**, *66*, 6323-6332. (d) Sawada, Y.; Mori, T.; Oku, A. *J. Org. Chem.*, **2003**, *68*, 10040-10045. (e) Marmaseter, F. P.; Murphy, G. K.; West, F. G. *J. Am. Chem. Soc.*, **2003**, *125*, 14724-14725. (f) Doyle, M. P.; Kundu, K.; Russell, A. E. *Org. Lett.*, **2005**, *7*, 5171-5174. (g) Clark, J. S.; Walls, S. B.; Wilson, C.; East, S. P.; Drysdale, M. J. *Eur. J. Org. Chem.*, **2006**, 323-327.



**Scheme 38.** Synthetic strategy.

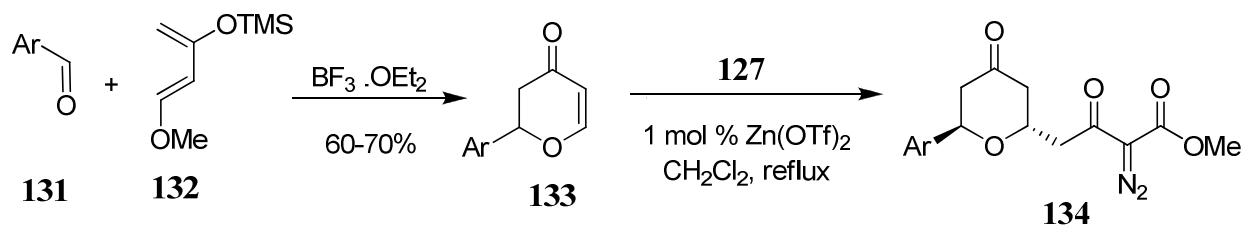
## **2.2 Synthesis of the Mukaiyama-Michael addition products**

2-phenyl-2H-pyran-4(3H)-one **133a** was prepared in 65% isolated yield by a  $\text{BF}_3 \cdot \text{Et}_2\text{O}$ -mediated hetero-Diels-Alder reaction between benzaldehyde and Danishefsky's diene.<sup>81</sup> This process was followed by the Mukaiyama-Michael reaction of **133** with methyl 3-(*tert*-butyldimethylsilyloxy)-2-diazo-3-butenoate **127** that, after optimization<sup>82</sup>, occurred with full conversion using  $\text{Zn}(\text{OTf})_2$  (1 mol%) in refluxing dichloromethane. After hydrolysis and purification **134**, was isolated in 99% yield (Table 17).

**Table 17.** Synthesis of *trans*-3-aryltetrahydropyranone-5-diazoacetates **134**.

<sup>81</sup> (a) Danishefsky, S.; Kerwin, J. F., Jr.; Kobayashi, S. *J. Am. Chem. Soc.*, **1982**, *104*, 358-360. (b) Danishefsky, S.; Larson, E.; Askin, D.; Kato, N. *J. Am. Chem. Soc.*, **1985**, *107*, 1246-1255.

<sup>82</sup> The Mukaiyama-Michael reaction was optimized using different lewis acids:  $\text{Zn}(\text{OTf})_2$ ,  $\text{Sc}(\text{OTf})_2$ ,  $\text{Sn}(\text{OTf})_2$ , and  $\text{La}(\text{OTf})_2$ . When the reaction was performed at 25°C the starting material did not fully convert and therefore to obtain full conversion, the reaction was heated to reflux  $\text{CH}_2\text{Cl}_2$ .



Entry	131	Ar	% yield <sup>a</sup> 133	% yield <sup>a</sup> 134
1	131a	$\text{C}_6\text{H}_5$	65	99
2	131b	<i>p</i> - $\text{NO}_2\text{C}_6\text{H}_4$	70	80
3	131c	<i>p</i> - $\text{CF}_3\text{C}_6\text{H}_4$	60	77
4	131d	<i>p</i> - $\text{CH}_3\text{C}_6\text{H}_4$	65	97
5	131e	<i>p</i> - $\text{MeOC}_6\text{H}_4$	63	92
6	131f	Mesityl	65	99
7	131g	Anthryl	53	90
8	131h	2,6-dimethyl-4-nitro phenyl	50	95

<sup>a</sup> Isolated yield after column chromatography.

The *trans*-stereoselectivity of 3-phenyltetrahydropyranone-5-diazoacetates **134a** was established by an observed  $^1\text{H}$  NOE correlation between  $\text{H}_2$  and  $\text{H}_7$  (1.0% NOE) as well as  $^1\text{H}$  NOE correlation between one of the  $\text{H}_6$  hydrogens and  $\text{H}_7$  (3.0% NOE). There was no  $^1\text{H}$  NOE correlation observed between  $\text{H}_7$  and  $\text{H}_3$  (Figure 5). These NOE results confirmed to us that indeed 3-aryltetrahydropyranone-5-diazoacetates **134** was synthesized as solely the *trans*-isomer.

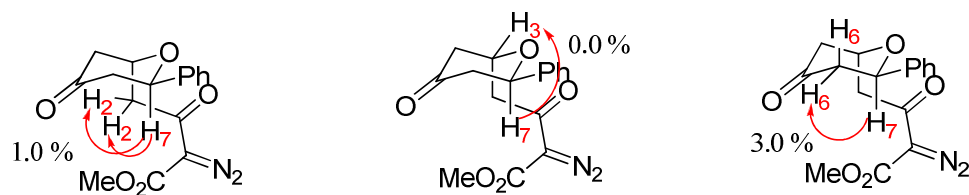
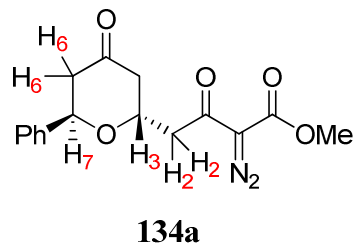
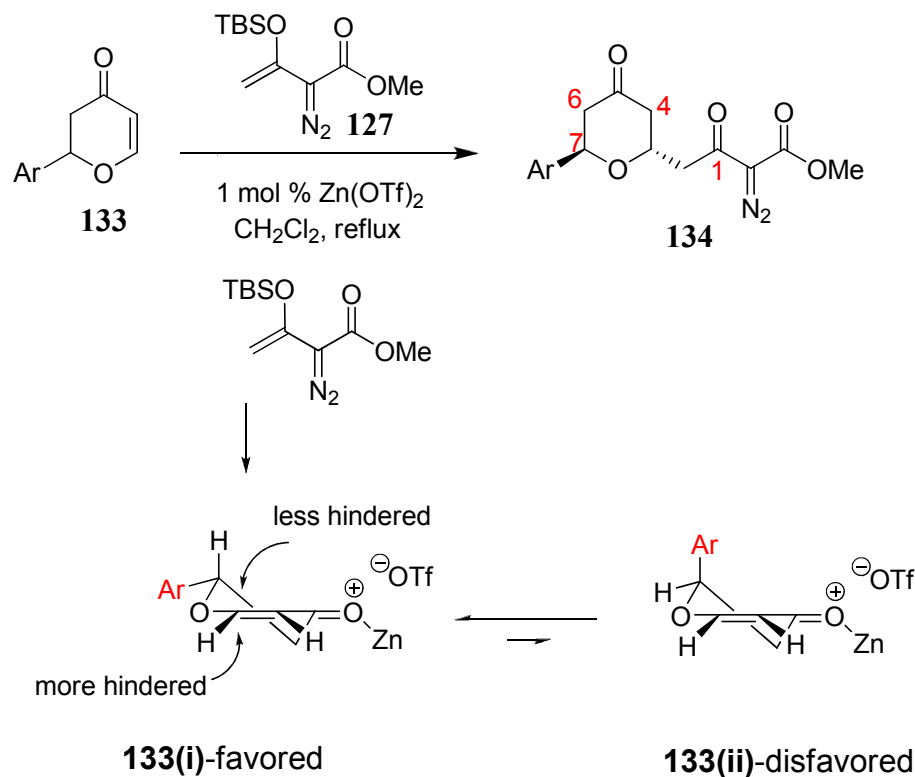


**Figure 5.**  $^1\text{H}$  NOE correlation of *trans*-3-phenyltetrahydropyranone-5-diazoacetates **134a**.  $^1\text{H}$  NMR (400 MHz,  $\text{CDCl}_3$ )  $\delta$  ( $\text{H}_7$ ) 5.29 ppm, ( $\text{H}_3$ ) 4.55 ppm, 2( $\text{H}_2$ ) 3.31 ppm and 3.05 ppm,  $\text{H}_6$  2.87 ppm.

Exceptional diastereocontrol is well known in Lewis acid catalyzed reactions of aryl dihydropyranone **133** with silyl enol ethers; in these reactions the *trans* tetrahydropyranone product is formed as the sole product.<sup>83</sup> The exclusive formation of *trans*-3-aryltetrahydropyranone-5-diazoacetates **134** can be rationalized by the methyl 3-(*tert*-butyldimethylsilyloxy)-2-diazo-3-butenate **127** approaching from the top face of the half-chair conformer **133(i)** in which the C7 aryl substituent is oriented in the pseudoequatorial position, thus blocking the bottom face of the half-chair conformer (Scheme 39). The substrate scope of the Mukaiyama-Michael addition reaction was extended to other aryl groups as shown in Table 17. In theory, there exists two possible conformers **133(i)** and **133(ii)** where the substituent is either in a pseudoequatorial **133(i)** or pseudoaxial **133(ii)** position (Scheme 39). However, when the C7 substituent is an aryl

<sup>83</sup> (a) Anada, M.; Washio, T.; Watanabe, Y.; Takeda, K.; Hashimoto, S. *Eur. J. Org. Chem.*, **2010**, 6850-6854. (b) Jewett, J. C.; Rawal, V. H. *Angew. Chem., Int. Ed.*, **2007**, 46, 6502-6504. (c) Yamashita, Y.; Saito, S.; Ishitani, H.; Kobayashi, S. *J. Am. Chem. Soc.*, **2003**, 125, 3793-3798.

group, only one half-chair conformer is favored, **133(i)**, where the aryl substituent is in the pseudoequatorial position which leads to the methyl 3-(*tert*-butyldimethylsilyloxy)-2-diazo-3-butenoate **127** adding from only one face, the one opposite to the aryl substituent, and hence leads to solely the *trans* isomer.



**Scheme 39.** Rational for the exclusive formation of *trans*-3-aryltetrahydropyranone-5-diazoacetoacetates **134**.

### 2.3 Catalytic dinitrogen extrusion reactions

After obtaining *trans*-3-phenyltetrahydropyranone-5-diazoacetoacetates **134a**, we proceeded to investigate catalytic dinitrogen extrusion. Rhodium(II) catalyzed decomposition of **134a**, using 1.0 mol% of dirhodium perfluorobutyrate [Rh<sub>2</sub>(pfb)<sub>4</sub>] in refluxing dichloromethane, afforded two products in a 71:29 molar ratio, determined by <sup>1</sup>H NMR spectroscopic analysis of the reaction mixture (Figure 6). These two products were spectrally distinguishable by both <sup>1</sup>H NMR and <sup>13</sup>C NMR (see Experimental

Section). The  $^1\text{H}$  NMR spectrum of the reaction mixture showed two sets of singlets around 3.5 and 3.3 ppm and two sets of multiplets around 5.0 and 5.2 ppm. All other remaining  $^1\text{H}$  NMR spectral peaks were also observed in sets of two. Figure six shows the  $^1\text{H}$  NMR of the reaction mixture.

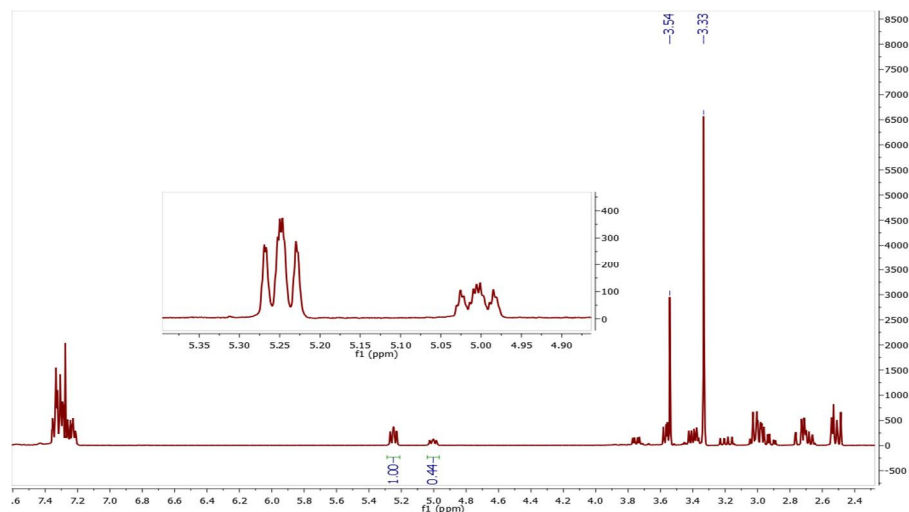
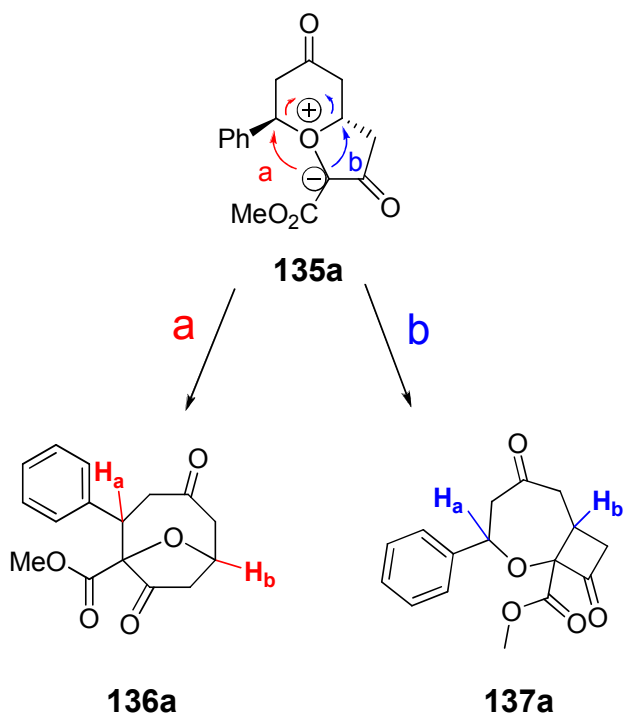


**Figure 6.**  $^1\text{H}$  NMR reaction mixture of rhodium(II) catalyzed decomposition of *trans*-3-phenyltetrahydropyranone-5-diazoacetates **134a**.

The two products were also chromatographically distinguishable and were isolated *via* column chromatography. This was done by using a gradient elution of hexane and ethyl acetate by changing the solvent gradient gradually in 5% increments starting with a 90:10 (Hx:EtOAc) mixture and ending with a 65:35 (Hx:EtOAc) mixture. Each product was isolated as a white solid with a combined yield of 77%.

Our intuition was that these two products were diastereoisomers of the [1,2]-Stevens rearrangement product **136a** that arose from the rearrangement of the oxonium ylide intermediate **135a** (Scheme 40, pathway a). Another possible [1,2]-Stevens rearrangement product was **137a** that would also have been formed via rearrangement of the oxonium ylide intermediate **135a** but through pathway b (Scheme 40). The [1,2]-

Stevens rearrangement product **137a** is less likely to occur because the migrating group for pathway b in the oxonium ylide intermediate **135a** is less favored compared to the benzylic migrating group in pathway a. The  $^1\text{H}$  NMR of the reaction mixture was consistent with the two products being diastereomers of the [1,2]-Stevens rearrangement **136a** where the two sets of multiplets around 5.0 and 5.2 ppm corresponded to  $\text{H}_a$  and  $\text{H}_b$  in **136a** and these chemical shifts don't correspond to  $\text{H}_a$  and  $\text{H}_b$  in **137a** (Scheme 40). Also, the IR of each product was consistent with the absence of a cyclobutanone that has an observed carbonyl stretch frequency of  $\sim 1780\text{ cm}^{-1}$  which was not observed with the two isolated compounds ( $1772\text{ cm}^{-1}$  and  $1769\text{ cm}^{-1}$ ).



**Scheme 40.** [1,2]-Stevens rearrangement possible pathways.

To test the validity of this notion, two-dimensional NMR experiments were performed on each product to confirm their structure and that they have the same connectivity. Two-dimensional COSY experiments for the two products revealed that the

$H_b$  proton is coupled to both  $H_e$  and  $H_d$  protons whereas the  $H_a$  proton is coupled to the two  $H_c$  protons (Figure 7). Two-dimensional HMBC experiments revealed that the non-aromatic quaternary carbon **q** is not coupled to the  $H_d$  protons but couples to the  $H_c$  protons, consistent with the structure of the [1,2]-Stevens rearrangement **136a**. If the product formed was that of **137a**, coupling is expected to occur between the non-aromatic quaternary carbon **q** and the  $H_d$  protons, and no coupling should occur with  $H_c$  protons, which is not what we observed. Two-dimensional HMBC experiments confirmed to us that the two compounds are not the [1,2]-Stevens rearrangement product **137a** but, indeed, they are the [1,2]-Stevens rearrangement **136a**.

**Figure 7.** COSY of [1,2]-Stevens rearrangement **136a**.

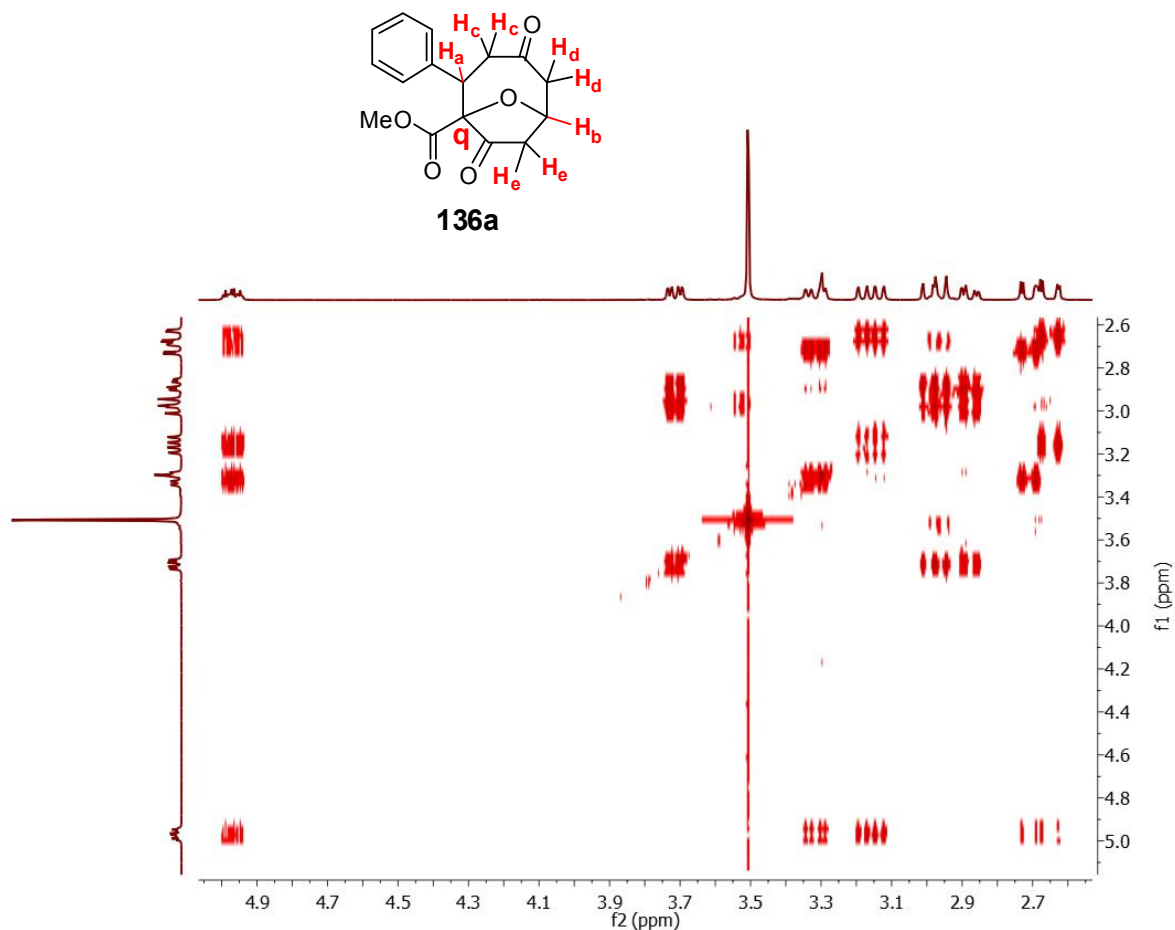
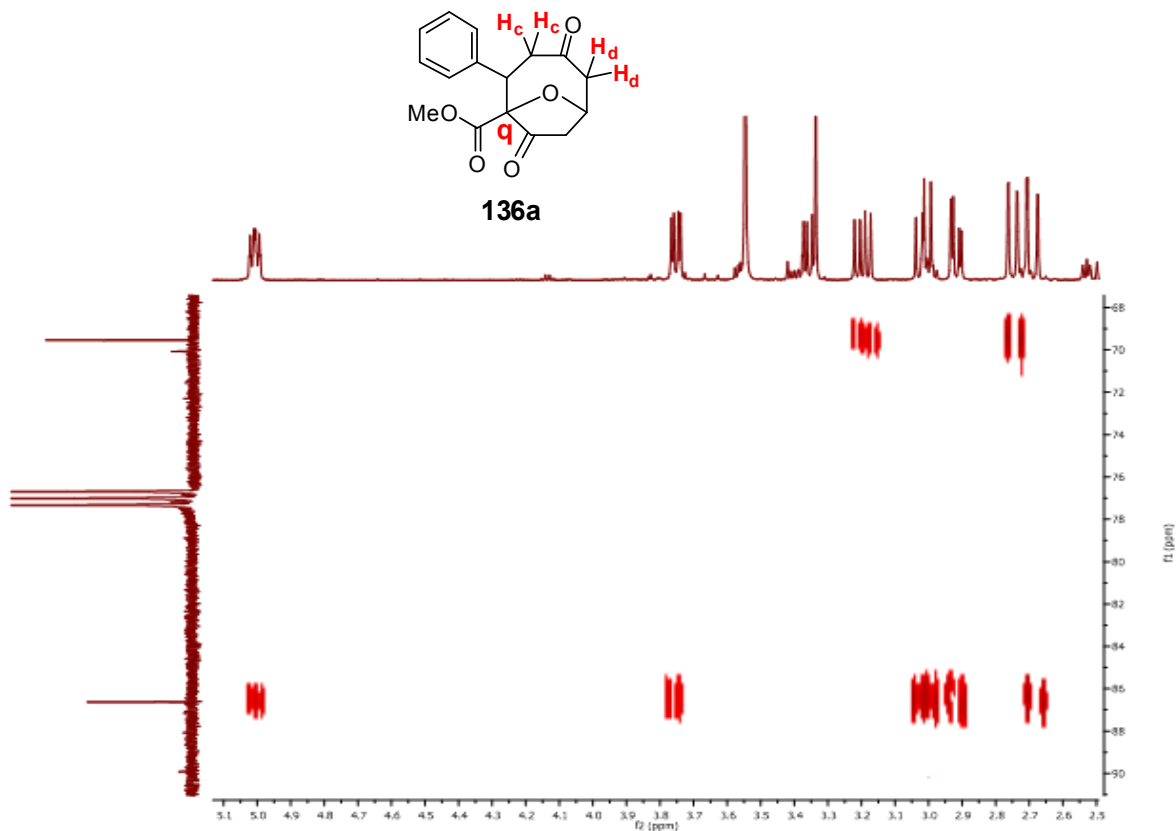
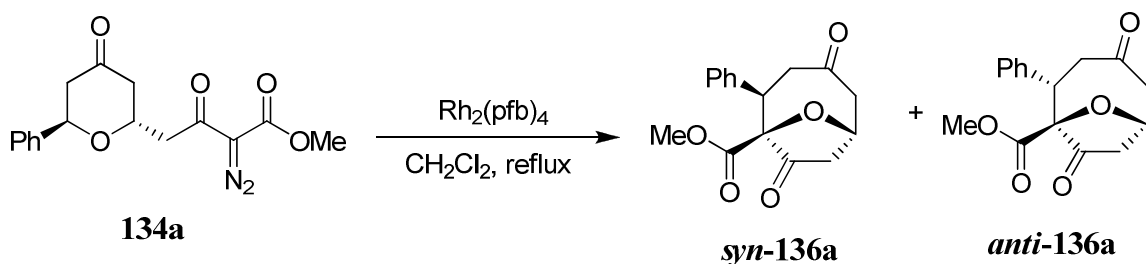


**Figure 8.** HMBC of [1,2]-Stevens rearrangement **136a**.



After establishing that both of the [1,2]-Stevens rearrangement products were constitutionally identical and had the same connectivity, we needed to determine the stereochemistry of the two diastereomers. The crystal structures of both [1,2]-Stevens rearrangement products were obtained (Figure 9), and they provided their identification as the *syn* and *anti* stereoisomers of 1-carbomethoxy-2-phenyl-9-oxabicyclo[4.2.1]nonan-4,8-dione **136a**, with *syn-136a* being the major product and *anti-136a* being the minor one (Scheme 41). Note that the original *trans*-stereochemistry of the reactant **134a** is formally inverted in forming *anti-136a*; this is suggested in the crystal structures of the

products by the positioning of the phenyl substituent relative to the oxygen bridge and the ester substituent which are both pseudo-*trans* in *anti*-**136a**, but pseudo-*cis* in *syn*-**136a**.



**Scheme 41.** Formation of two diastereomers for the [1,2]-Stevens rearrangement of *trans*-3-phenyltetrahydropyranone-5-diazoacetates **134a**.

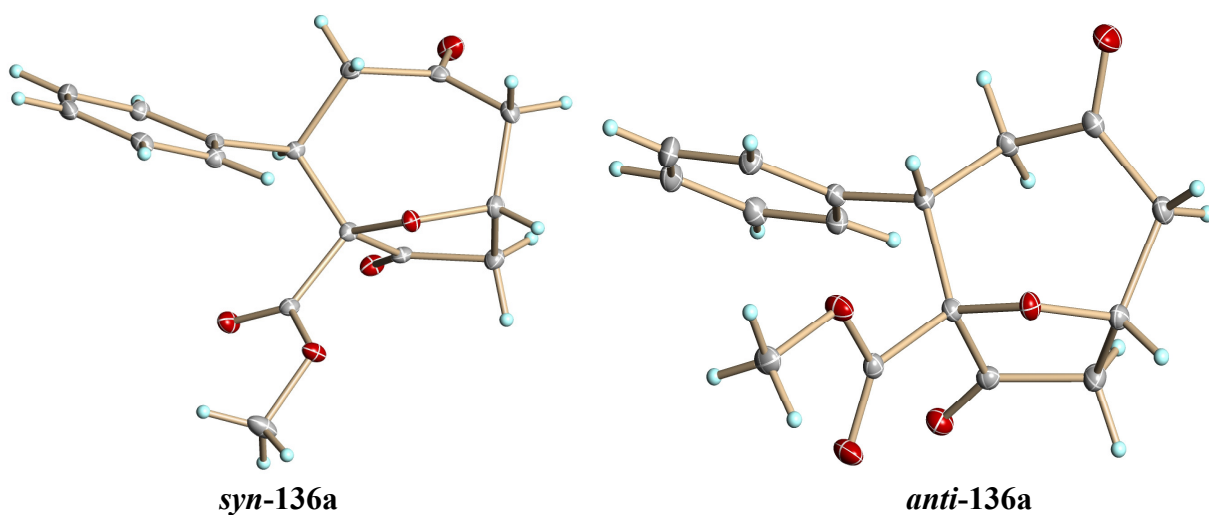
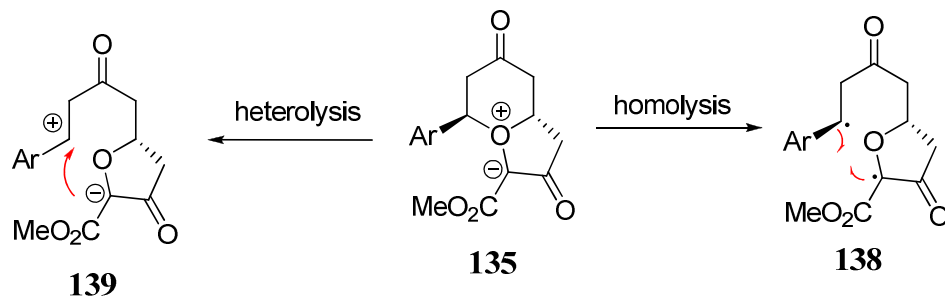


**Figure 9.** The crystal structure of *syn*-**136a** and *anti*-**136a**.

We also investigated the influence of substituents at the *para*-position on the phenyl ring in **134** on the ratio of *syn*-**136** to *anti*-**136**. Doing so would shed insight on the mechanism of the [1,2]-Stevens rearrangement of oxonium ylides. The presence of a substituent effect could suggest that the [1,2]-Stevens rearrangement of oxonium ylides takes place *via* a stepwise mechanism (Scheme 42) whereas the absence of a substituent effect could be more aligned with a concerted mechanism. If the mechanism of [1,2]-Stevens rearrangement of oxonium ylides is stepwise, then the ratio of *syn*-**136** to *anti*-

**136** should vary depending on the electronics of the substituent at the para-position on the phenyl ring. Electron-donating substituents should stabilize the diradical intermediate **138** or the zwitterion intermediate **139** (Scheme 42). These intermediates should have a longer life-time, compared to those with electron-withdrawing substituents, and hence have the opportunity to racemize.



**Scheme 42.** Possible intermediates with a stepwise mechanism for the [1,2]-Stevens rearrangement of oxonium ylides.

The results from the investigation of the influence of substituents at the para-position of the phenyl ring in **134** on the ratio of *syn*-**136** to *anti*-**136** are reported in Table 18. Identifying the products of the catalytic dinitrogen extrusion of **134a** and establishing the structure of both the [1,2]-Stevens rearrangement products provided assistance in analyzing the dinitrogen extrusion reaction for the rest of the substrates presented in Table 18. The dinitrogen extrusion reaction of all **134** substrates afforded two diastereomers of the [1,2]-Stevens rearrangement products; as evidenced by comparison with the  $^1\text{H}$  NMR spectra of *syn*-**136a** and *anti*-**136a**.



competition with [1,2]-rearrangement products *anti*-136 and *syn*-136. The ratios of *syn*-136(d or e) to *anti*-136(d or e) from 134d or 134e were the same, within experimental error, as those from 134a with the same catalyst. Also, the *trans*-140(d and e) to *cis*-140(d and e) ratios were remarkably similar to those of the corresponding ratios of *syn*-136 to *anti*-136, suggesting that the diastereoselection established in the formation of 136 and 140 could have originated in the ylide formation step. The *cis*-stereochemistry of *cis*-140 was established by an observed <sup>1</sup>H NOE correlation (1% NOE) between H<sub>a</sub> and H<sub>b</sub> while *trans*-140 showed no NOE effect between those two same protons.

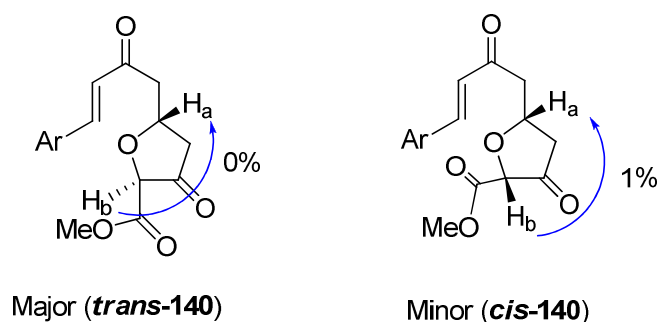


**Figure 10.** <sup>1</sup>H NOE correlation of elimination product *cis*-139 and *trans*-139.

Next, the effect of dirhodium catalysts on the product ratio (*syn*-136: *anti*-136) was investigated to address if the oxonium ylide intermediate was metal-associated or a free ylide. If the *syn*-136:*anti*-136 product ratio is dependent on the catalyst employed, the isomerization process must involve a metal-bound ylide. Results obtained from reactions with a wide spectrum of catalysts under different reaction conditions are reported in Table 19 and show a minor, but reproducible, dependence on catalyst. Product yields were high with dirhodium catalysts, but not with copper catalysts. The reactions with copper catalysts were slow and the starting material 134a did not fully

convert to the [1,2]-Stevens rearrangement products. Solvent and temperature influences were also minor.

Except for reactions catalyzed by dirhodium pivalate (piv) and dirhodium triphenylacetate (TPA), the [1,2]-Stevens rearrangement product ratio **syn-136:anti-136** ratio was invariant with common ligands on dirhodium (pfb = perfluorobutyrate, tfa = trifluoroacetate, OAc, cap = caprolactamate) that cover a broad range of electronic influences. The minor difference in ratio of the [1,2]-Stevens rearrangement products with Rh<sub>2</sub>(TPA)<sub>4</sub> and Rh<sub>2</sub>(piv)<sub>4</sub> can be attributed to the fact that both of these catalysts have ligands with significant steric bulk compared to the standard Rh<sub>2</sub>(OAc)<sub>4</sub>. The catalyst independence of diastereoselectivity support the rationale that the oxonium ylide intermediate **135** is a free ylide and not associated to the metal employed.

**Table 19<sup>a</sup>.** Catalyst screening for the decomposition of *trans*-3-phenyltetrahydropyranone-5-diazoacetoacetates **134a**.

Entry	Catalyst	Solvent	T[°C]	<i>syn</i> -136: <i>anti</i> -136 <sup>b</sup>	% yield <sup>c</sup>
1	Rh <sub>2</sub> (tfa) <sub>4</sub>	CH <sub>2</sub> Cl <sub>2</sub>	40	71:29	70
2	Rh <sub>2</sub> (OAc) <sub>4</sub>	CH <sub>2</sub> Cl <sub>2</sub>	40	71:29	70
3	Rh <sub>2</sub> (pfb) <sub>4</sub>	CH <sub>2</sub> Cl <sub>2</sub>	40	71:29	77
4	Rh <sub>2</sub> (cap) <sub>4</sub>	CH <sub>2</sub> Cl <sub>2</sub>	40	71:29	72
5	Rh <sub>2</sub> (piv) <sub>4</sub>	CH <sub>2</sub> Cl <sub>2</sub>	40	63:37	80
6	Rh <sub>2</sub> (TPA) <sub>4</sub>	CH <sub>2</sub> Cl <sub>2</sub>	40	63:37	81
7	Rh <sub>2</sub> ( <i>S</i> -DOSP) <sub>4</sub>	CH <sub>2</sub> Cl <sub>2</sub>	40	74:26	80
8	Rh <sub>2</sub> (pfb) <sub>4</sub>	PhCH <sub>3</sub>	40	64:36	80
9	Rh <sub>2</sub> (pfb) <sub>4</sub>	ClCH <sub>2</sub> CH <sub>2</sub> Cl	70	70:30	72
10	[Cu(CH <sub>3</sub> CN) <sub>4</sub> ]PF <sub>6</sub>	ClCH <sub>2</sub> CH <sub>2</sub> Cl	70	74:26	15% conv.
11	Cu(acac) <sub>2</sub> <sup>d</sup>	ClCH <sub>2</sub> CH <sub>2</sub> Cl	70	68:32	30% conv.

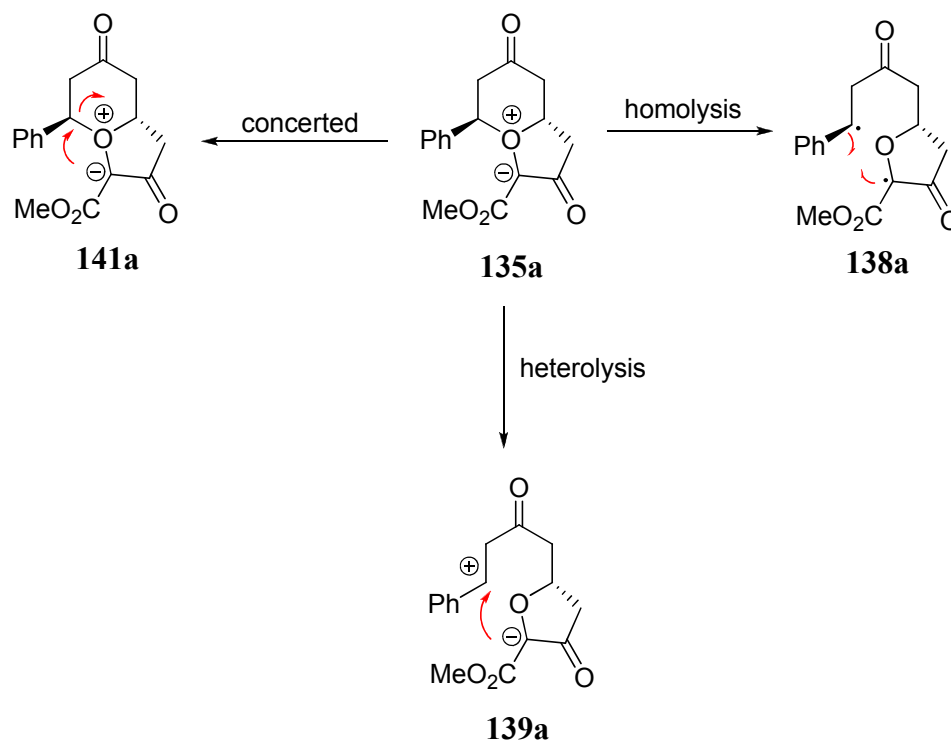
<sup>a</sup>Reactions were performed in refluxing solvent for 2 h using 1.0 mol % of catalyst, unless otherwise noted. Results reported are averages of two or more reactions ±4%. <sup>b</sup> Product ratio determined by <sup>1</sup>H NMR

analysis with variance of  $\pm 4\%$ . <sup>c</sup> Weight yield of isolated *syn*-**136** and *anti*-**136** products following chromatographic separation. <sup>d</sup> 5 mol% of catalyst was used.

Catalytic ylide formation and rearrangement results in a mixture of two diastereoisomers formed in high yield, but with negligible dependence on either para substituents on the aromatic ring or on the catalyst that is employed. With that in mind the mechanism by which oxonium ylide **135** rearranges to afford the two diastereoisomers of the [1,2]-Stevens rearrangement product **136** was further investigated.

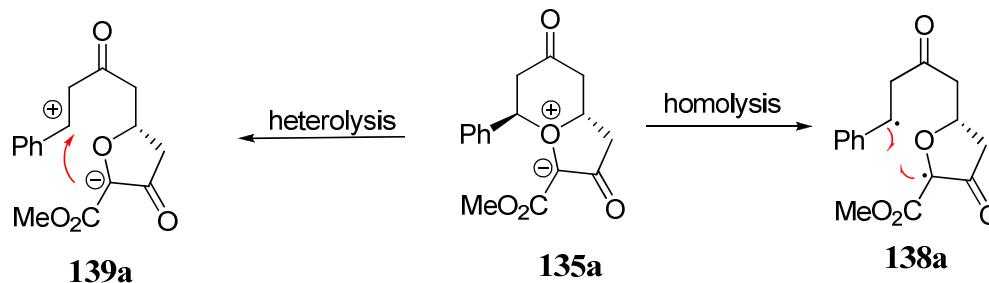
## **2.4 Mechanism of the Stevens rearrangement**

The [1,2]-Stevens rearrangement of oxonium ylide **135a** could proceed through three possible pathways to generate the *anti* and *syn* stereoisomers of 1-carbomethoxy-2-phenyl-9-oxabicyclo[4.2.1]nonan-4,8-dione **136**: initial homolysis of the benzylic C-O bond<sup>56</sup> to afford the radical pair intermediate **138** that could be held close in a solvent cage, heterolysis of the C-O bond to give zwitterion pair intermediate **139**, or a concerted mechanism<sup>57</sup> of the oxonium ylide intermediate **141** which directly leads to the [1,2]-Stevens rearrangement product (Scheme 43).



**Scheme 43.** Possible mechanistic pathways for the [1,2]-Stevens rearrangement of oxonium ylide **135a**.

In our attempts to investigate the mechanism of the Stevens rearrangement using model substrate *trans*-3-phenyltetrahydropyranone-5-diazoacetoacetates **134a**, we rationalized that a stepwise mechanism would involve ylide formation followed by homolytic or heterolytic cleavage of the benzyl-oxygen bond to afford ylide intermediates **138a** and **139a** (Scheme 44), respectively, both of which are subject to substituent effects. Bond rotation at the benzylic carbon and ring closure should lead to the formation of the observed *syn*-**136** and *anti*-**136** rearrangement products.



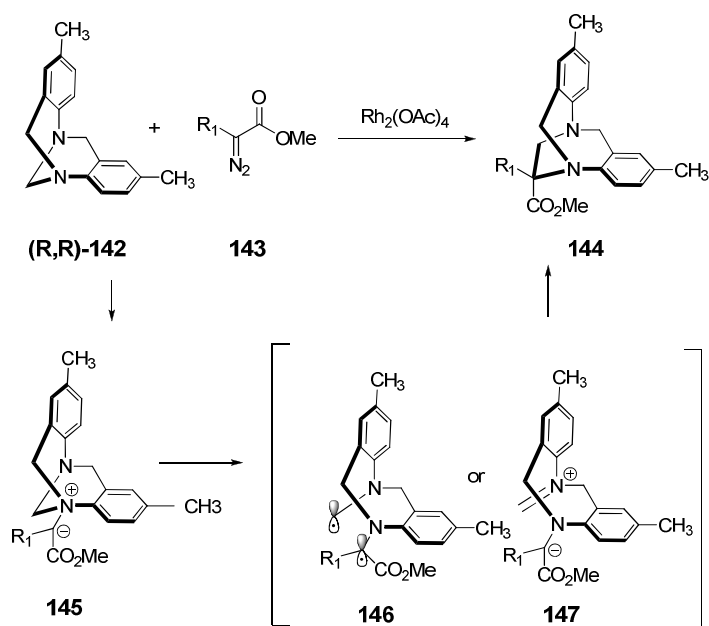
**Scheme 44.** Stepwise mechanism for the decomposition of *trans*-3-phenyltetrahydropyranone-5-diazoacetates **134a** via homolytic or heterolytic cleavage.

As discussed previously (section 2.3), we have investigated the influence of para-substituents on the benzene ring in *trans*-3-aryltetrahydropyranone-5-diazoacetates **134** on the ratio of *syn*-**136** to *anti*-**136**, and the results from this investigation showed no substituent effect on the ratio of the two diastereomers. Ammonium ylides that are known to undergo a stepwise mechanism have been reported to have a substituent effect on the ratio of the [1,2]-Stevens rearrangement products.<sup>84</sup> Rhodium-catalyzed reaction of 2-aryl-2-diazoacetate **143** with enantiopure (*R,R*)-**142** furnished the [1,2]-Stevens rearrangement product **144** in good yields (Table 20).<sup>84</sup> The reaction is believed to go through ammonium ylide intermediate **145** which then generates radical pair **146** and/or zwitterionic species **147** that upon ring-closure form the [1,2]-Stevens product **144**. Interestingly, with stronger stabilization of intermediates **146** and **147** by the electron-withdrawing substituents, ( $R_1 = p\text{-NO}_2\text{C}_6\text{H}_4$ ), that surround the reactive carbon center loss of enantiomeric purity was observed and the diastereomeric ratio of the [1,2]-Stevens product varied from the diastereomeric ratio with electron donating substituents ( $R_1 = p\text{-MeOC}_6\text{H}_4$ ) (Table 20). The observation of different diastereomeric ratios of the [1,2]-Stevens product and the observation of decreased enantiomeric purity with electron-withdrawing substituents can be explained by the fact that radical pair **146** or zwitterionic species **147** have a longer life-time when stabilized by an electron-withdrawing substituent and thus have the opportunity to racemize through planarization.<sup>84</sup>

**Table 20.** Rhodium-catalyzed reaction of aryl diazoacetate **143** with enantiopure (*R,R*)-**142** leads to different diastereomeric ratios of the [1,2]-Stevens product.

---

<sup>84</sup> Sharma, A.; Guenee, L.; Naubron, J.-V.; Lacour, J. *Angew. Chem., Int. Ed.*, **2011**, *50*, 3677-3680.



Entry	R <sub>1</sub>	Yield (%) <b>144</b>	d.r. <b>144</b>	ee (%) <b>144</b>
1	Ph	71	10:1	99
2	<i>p</i> -MeOC <sub>6</sub> H <sub>4</sub>	83	10:1	98
3	<i>p</i> -CF <sub>3</sub> C <sub>6</sub> H <sub>4</sub>	70	12:1	97
4	<i>p</i> -NO <sub>2</sub> C <sub>6</sub> H <sub>4</sub>	82	20:1	64

The presence of a substituent effect in an ammonium ylide that is known to undergo a stepwise mechanism,<sup>84</sup> and the absence of a substituent effect in our oxonium ylide system suggests that radical or cationic intermediates may not be involved in the oxonium ylide rearrangement process. Hence, there needs to be an alternative explanation to that of homolytic/heterolytic cleavage for the formation of the duality of products in our system.

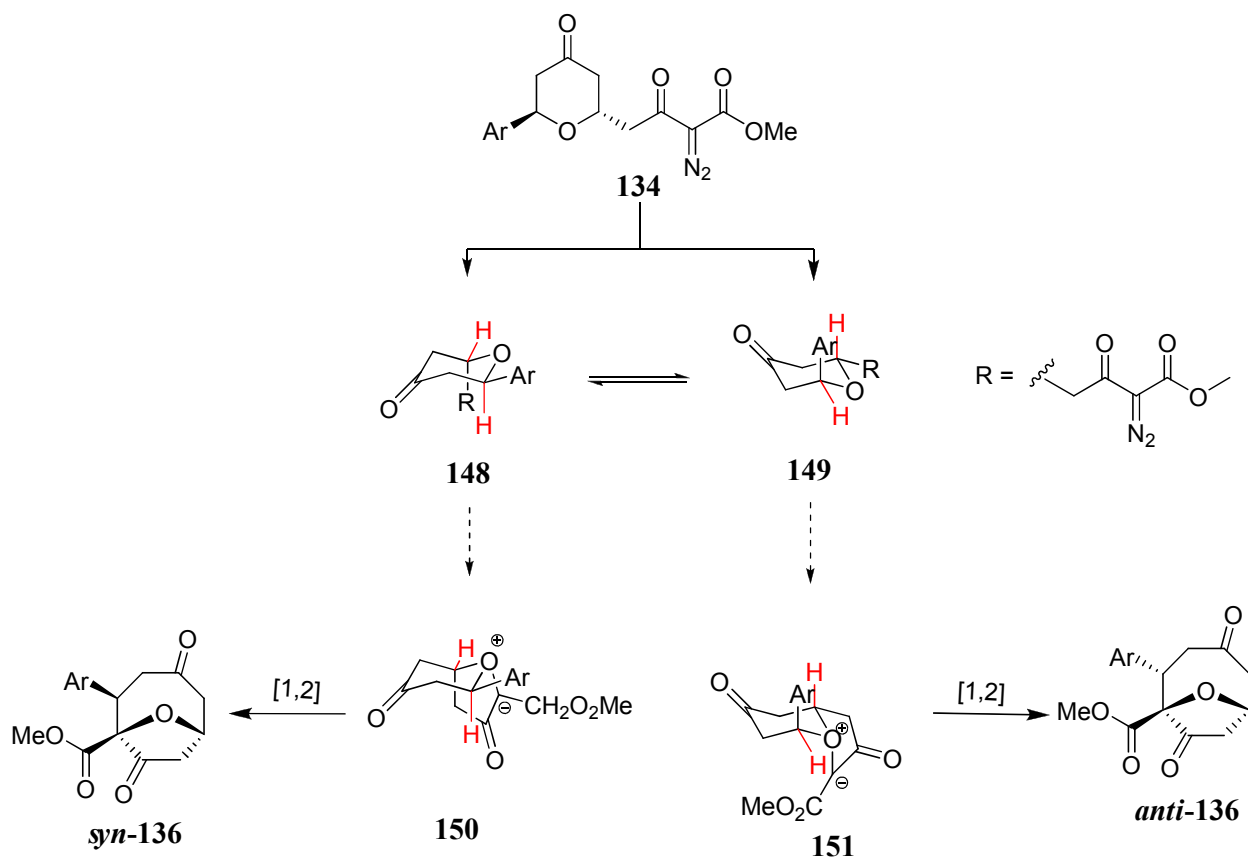
An alternate mechanism is that the apparent isomerization arises from two ylide intermediates **150** and **151** formed from two conformational isomers **148** and **149** of the

metal carbene generated from diazoacetoacetate **134** (Scheme 45). The two conformational isomers **148** and **149** are in equilibrium, where in conformer **148** the aryl group is in the equatorial position and the diazoacetoacetate group is in the axial position whereas the aryl group in conformational isomers **149** is in the axial position and the diazoacetoacetate group is in the equatorial position. Density Functional Theory calculations<sup>85</sup> (PBEPBE/BLANL2-DZ basis set) provided a free energy difference of only 0.16 kcal/mol between the two diazoacetoacetate conformers.<sup>86</sup> Metal-catalyzed decomposition of each conformational isomer **148** and **149** affords the corresponding ylide intermediate **150** and **151**. In this mechanism, product stereochemistry is determined by the stereochemistry of the two ylide intermediates **150** and **151** after they undergo rearrangement to give the corresponding [1,2]-Stevens rearrangement products *syn*-**136** and *anti*-**136**, respectively.

---

<sup>85</sup> Frisch, M. J.; Trucks, G. W.; Schlegel, H. B.; Scuseria, G. E.; Robb, M.A.; Cheeseman, J. R.; J. A. Montgomery, J.; Vreven, T.; Kudin, K. N.; Burant, J. C.; Millam, J. M.; Iyengar, S. S.; Tomasi, J.; Barone, V.; Mennucci, B.; Cossi, M.; Scalmani, G.; Rega, N.; Petersson, G. A.; Nakatsuji, H.; Hada, M.; Ehara, M.; Toyota, K.; Fukuda, R.; Hasegawa, J.; Ishida, M.; Nakajima, T.; Honda, Y.; Kitao, O.; Nakai, H.; Klene, M.; Li, X.; Knox, J. E.; Hratchian, H. P.; Cross, J. B.; Adamo, C.; Jaramillo, J.; Gomperts, R.; Stratmann, R. E.; Yazyev, O.; Austin, A. J.; Cammi, R.; Pomelli, C.; Ochterski, J. W.; Ayala, P. Y.; Morokuma, K.; Voth, G. A.; Salvador, P.; Dannenberg, J. J.; Zakrzewski, V. G.; Dapprich, S.; Daniels, A. D.; Strain, M. C.; Farkas, O.; Malick, D. K.; Rabuck, A. D.; Raghavachari, K.; Foresman, J. B.; Ortiz, J. V.; Cui, Q.; Baboul, A. G.; Clifford, S.; Cioslowski, J.; Stefanov, B. B.; Liu, G.; Liashenko, A.; Piskorz, P.; Komaromi, I.; Martin, R. L.; Fox, D. J.; Keith, T.; Al-Laham, M. A.; Peng, C. Y.; Nanayakkara, A.; Challacombe, M.; Gill, P. M. W.; Johnson, B.; Chen, W.; Wong, M. W.; Gonzalez, C.; J. A. Pople; Gaussian, Inc.: Pittsburgh PA, **2003**.

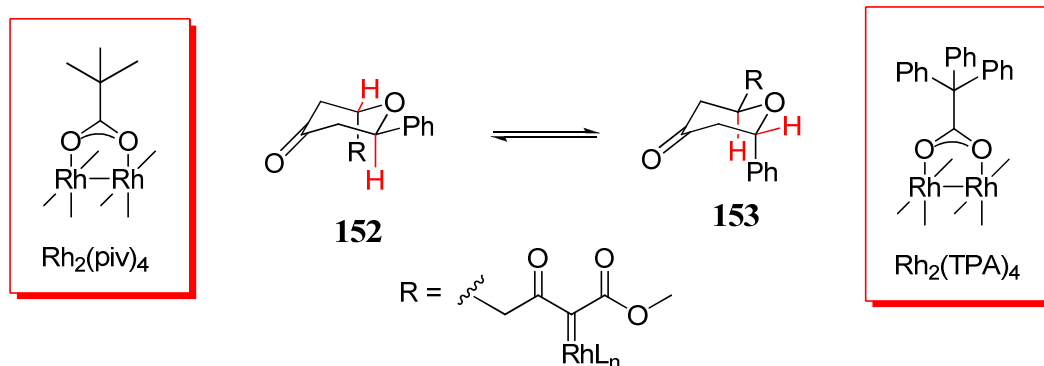
<sup>86</sup> Attempts to observe the two diazoacetoacetate conformers using low temperature NMR experiments in chloroform-d<sub>6</sub> (-55 °C), acetone-d<sub>6</sub> (-87 °C), and THF-d<sub>8</sub> (-96 °C) were not successful.



**Scheme 45.** Concerted mechanism for the decomposition of *trans*-3-aryltetrahydropyranone-5-diazoacetoacetates **134** via conformational isomers.

This concerted mechanism explains why there is a minor difference in the ratio of the [1,2]-Stevens rearrangement products (*syn*-**136a**:*anti*-**136a**) when the dinitrogen extrusion of *trans*-3-phenyltetrahydropyranone-5-diazoacetoacetates **134a** was catalyzed by dirhodium pivalate (piv) and dirhodium triphenylacetate (TPA). Both of these catalysts have ligands with significant steric bulk compared to the standard  $\text{Rh}_2(\text{OAc})_4$ . The minor difference in the ratio of the [1,2]-Stevens rearrangement products can be attributed to the fact that there exists two metal carbene conformational isomers **152** and **153** (Scheme 46) generated from diazoacetoacetate **134a**. The equilibrium between the two metal carbenes **152** and **153** slightly shifts towards metal carbene **153** when larger

ligands are used such as pivalate (piv) and triphenylacetate (TPA) and as a result of that there is a slight difference in the ratio of the [1,2]-Stevens rearrangement products compared to that ratio obtained with the standard catalyst  $\text{Rh}_2(\text{OAc})_4$ .



**Scheme 46.** Dirhodium pivalate and dirhodium triphenylacetate have a minor effect on the ratio of the [1,2]-Stevens rearrangement products.

To test this hypothesis we decided to increase the steric size of the aryl substituent, thereby increasing the equatorial-axial to axial-equatorial conformer ratio and directing the ylide forming process to only one [1,2]-rearrangement product. The rationale is that if the mechanism of the [1,2]-Stevens rearrangement process proceeds *via* a concerted mechanism and is influenced by the conformational isomers **148** and **149** (Scheme 45), then using a large aryl group will shift the equilibrium between these two conformational isomers to only form conformational isomer **148** where the large aryl group is positioned in the equatorial position and thus lead to the formation of a single diastereomer of the [1,2]-Stevens rearrangement, *syn*-**136**.

## 2.5 Conformation controls product formation

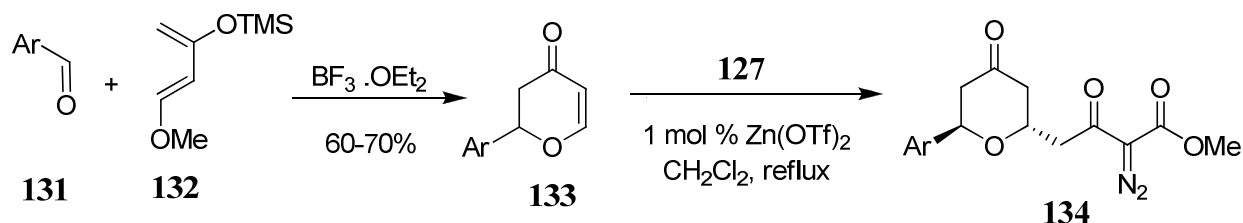
Following the two step synthesis of diazoacetoacetates discussed earlier in section 2.2, the hetero-Diels-Alder reaction followed by the Mukaiyama-Michael addition reaction, several diazoacetoacetate compounds were synthesized where the aryl group is a

large substituent (e.g., anthranyl, mesityl, and 2,6-dimethyl-4-nitro phenyl), and these compounds were screened for their suitability in ylide formation and subsequent [1,2]-Stevens rearrangement.

### **2.5a Synthesis of the Mukaiyama-Michael addition products**

2-aryl-2H-pyran-4(3H)-one **133(f-h)** were prepared in up to 65% isolated yield by a  $\text{BF}_3 \cdot \text{Et}_2\text{O}$ -mediated hetero-Diels-Alder reaction between aldehydes **131f-h** and Danishefsky's diene.<sup>87</sup> This process was followed by the Mukaiyama-Michael reaction of **133** with methyl 3-(*tert*-butyldimethylsilyloxy)-2-diazo-3-butenolate **127** using  $\text{Zn}(\text{OTf})_2$  (1 mol%) in refluxing dichloromethane. After hydrolysis and purification **134** was isolated in up to 99% yield (Table 21) and was determined to be solely the *trans* isomer as observed previously.

**Table 21.** Synthesis of *trans*-3-aryltetrahydropyranone-5-diazoacetoacetates **134**.



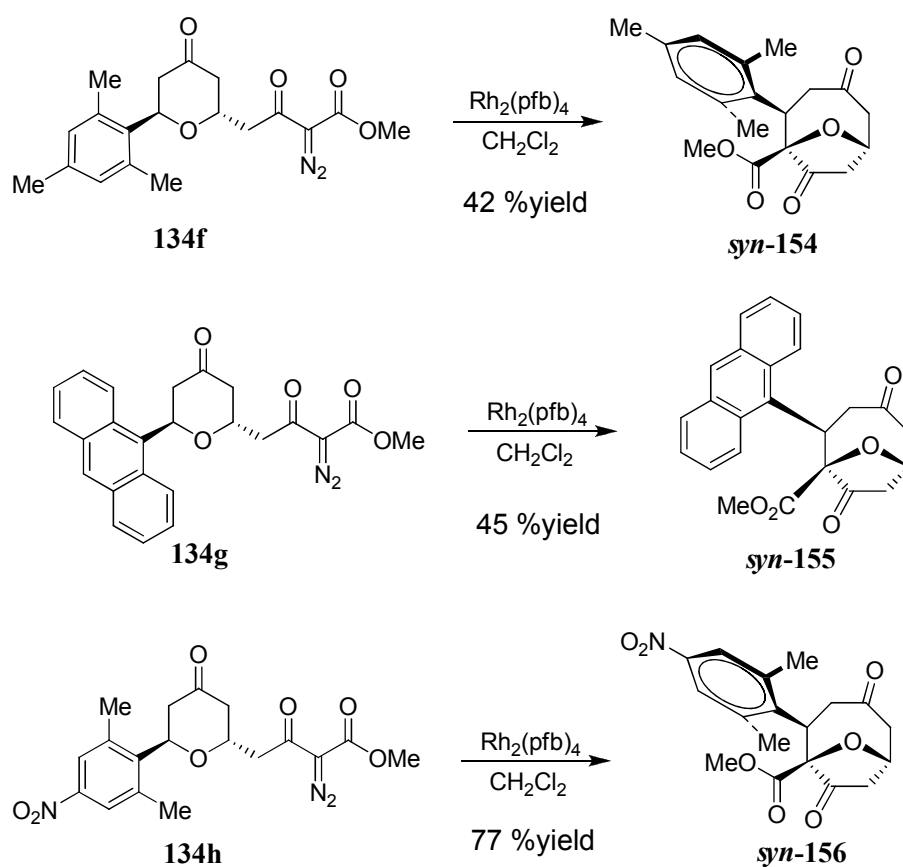
Aldehyde	Ar	% yield <sup>a</sup> <b>133</b>	% yield <sup>a</sup> <b>134</b>
131f	Mesityl	65	99
131g	Anthranyl	53	90
131h	2,6-dimethyl-4-nitro phenyl	50	95

<sup>a</sup> Isolated yield after column chromatography.

### **2.5b Catalytic dinitrogen extrusion reactions**

<sup>87</sup> (a) Danishefsky, S.; Kerwin, J. F., Jr.; Kobayashi, S. *J. Am. Chem. Soc.*, **1982**, *104*, 358-360. (b) Danishefsky, S.; Larson, E.; Askin, D.; Kato, N. *J. Am. Chem. Soc.*, **1985**, *107*, 1246-1255.

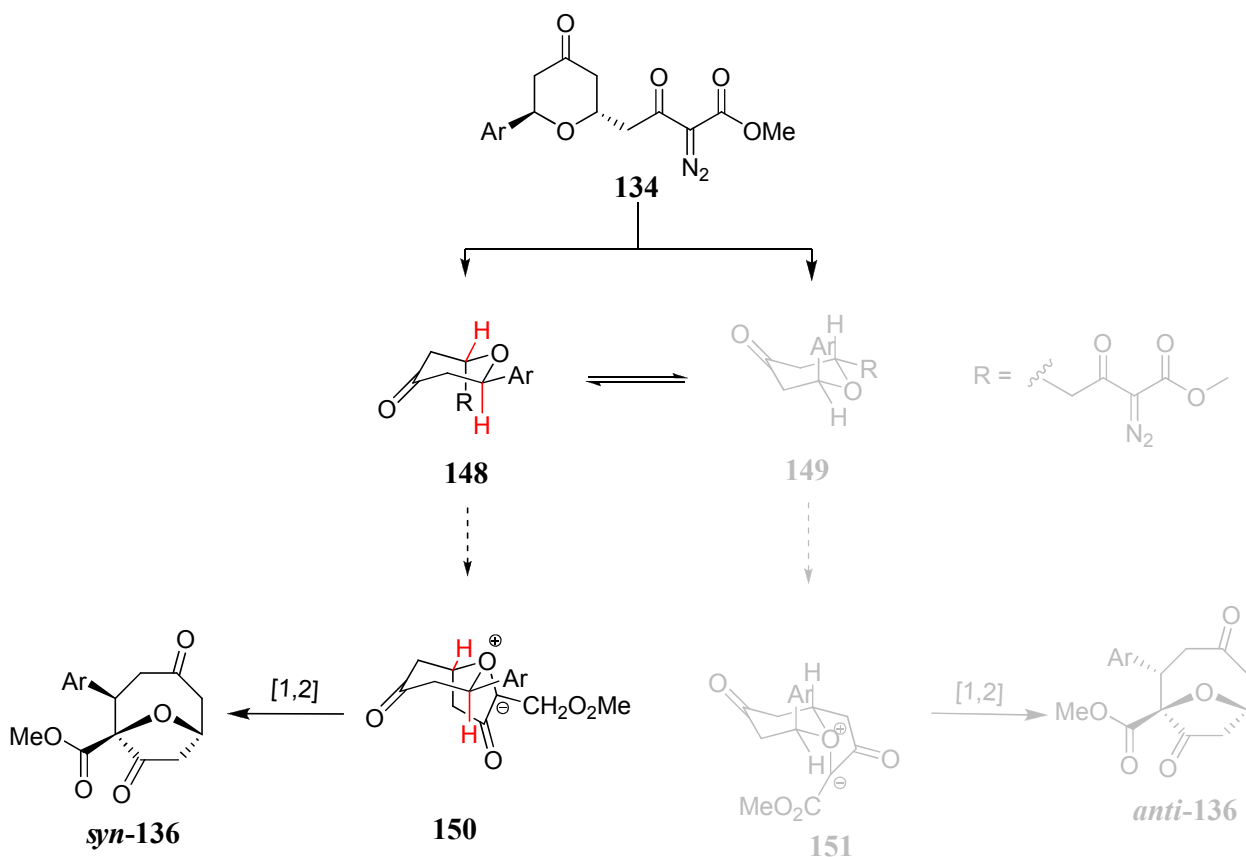
As expected, the dirhodium-catalyzed decomposition of diazoacetoacetates **134f** and **134g** afforded a single isomer of the [1,2]-Stevens rearrangement products **syn-154** and **syn-155**, albeit in less than 50% yield due to the formation of elimination byproducts. However, the *trans*-3-(2,6-dimethyl-4-nitrophenyl)tetrahydropyranone-5-diazoacetoacetates **134h** formed **syn-156** in 77% isolated yield without a measurable contribution, by <sup>1</sup>H NMR analysis, from the potential *anti*-**156** diastereomer (Scheme 47).



**Scheme 47.** Formation of a single diastereomer of the [1,2]-Stevens rearrangement product when the aryl group is a large substituent.

By increasing the size of the aryl group, the equilibrium completely shifted between the two diazoacetoacetate conformational isomers to only form conformational isomer **148** where the large aryl group is positioned in the equatorial position, thus

leading to the formation of the exclusive product *syn*-**136** (Scheme 48). We believe that all three examples provided, where the aryl group of diazoacetoacetate **134** is a large substituent (e.g., anthranyl, mesityl, and 2,6-dimethyl-4-nitro phenyl), that lead to the formation of a single isomer of the [1,2]-Stevens rearrangement products proceed through the concerted mechanism outlined in Scheme 48.



**Scheme 48.** Concerted mechanism for the decomposition of *trans*-3-aryltetrahydropyranone-5-diazoacetoacetates **134** when Ar = large substituent (e.g., anthranyl, mesityl, and 2,6-dimethyl-4-nitro phenyl).

## 2.6 Conclusions

In conclusion, Rh(II) catalyzed oxonium ylide generation with aryl-substituted tetrahydropyranone diazoacetoacetates and their subsequent [1,2]-Stevens rearrangement

forms two oxabicyclo[4.2.1]nonane diastereoisomers. Substituents on the aromatic ring were expected to influence the stability of intermediates for this reaction if formed *via* homolytic or heterolytic cleavage of the benzylic C-O bond, but the ratio of these two diastereoisomers was independent of the electronic nature of the substituent at the *para*-position of the phenyl ring (e.g., electron donating and electron withdrawing groups). However, the use of a large aryl group substituent (e.g., anthranyl, mesityl, and 2,6-dimethyl-4-nitro phenyl) resulted in the formation of a single diastereoisomer. The importance of the size of the aryl group, coupled with the absence of a substituent effect on the ratio of the [1,2]-Stevens rearrangement diastereomers suggest that conformational influences are responsible for the apparent isomerization. Each diazo conformer forms a different oxonium ylide and subsequent rearrangement of each of these oxonium ylides leads to the formation of a distinct diastereoisomeric product.

## **2.7 Experimental**

### **2.7(a) General procedures and methods of analysis**

**General information.** Reagents were obtained commercially unless otherwise noted. Reactions were performed using oven-dried or flame-dried glassware under an atmosphere of nitrogen. Air and moisture sensitive liquids and solutions were transferred via syringe or stainless steel cannula. Dichloromethane (DCM) was passed through a solvent column<sup>88</sup> prior to use. Toluene and 1,2-dichloroethane (DCE) were distilled over CaH<sub>2</sub> and used immediately. Thin-layer chromatography (TLC) was performed on EM Science silica gel 60 F254 plates, and visualization of the developed plates was accomplished by ultraviolet light (254 nm) and/or by staining with iodine, butanolic ninhydrin, *p*-anisaldehyde, or phosphomolybdic acid (PMA) solution. Chromatographic purification of products was performed using air pressure to force the solvent through the column on silica gel (230 x 400 mesh). Compounds purified by chromatography on silica gel were typically applied to the absorbent bed using the indicated solvent conditions with a minimum amount of added dichloromethane as needed for solubility. Unless

---

<sup>88</sup> Pangborn, A. B.; Giardello, M. A.; Grubbs, R. H.; Rosen, R. K.; Timmers, F. J. *Organometallics*, **1996**, *15*, 1518-1520.

otherwise described, reactions were carried out at room temperature. Elevated temperatures were obtained using thermostat-controlled silicone oil baths. Low temperatures were obtained in an ice-water bath or by mixing dry-ice with organic solvents. Anhydrous zinc triflate, boron trifluoride-diethyl ether (BF<sub>3</sub>.OEt<sub>2</sub>), and copper catalysts were purchased from Aldrich and used as received. Rhodium acetate was obtained commercially from Pressure Chemical Company while the rest of the rhodium catalysts (Rh<sub>2</sub>(tfa)<sub>4</sub>,<sup>89</sup> Rh<sub>2</sub>(pfb)<sub>4</sub>,<sup>90</sup> Rh<sub>2</sub>(piv)<sub>4</sub>,<sup>91</sup> Rh<sub>2</sub>(TPA)<sub>4</sub>,<sup>92</sup> and Rh<sub>2</sub>(cap)<sub>4</sub>)<sup>93</sup> were synthesized following literature procedures by Dr. Ryan Burgin. Methyl 3-(*tert*-butyldimethylsilyloxy)-2-diazo-3-butenolate was prepared by the method described by Davies.<sup>94</sup>

NMR spectra were obtained on Bruker AV-400, Bruker DRX-400 (<sup>1</sup>H at 400 MHz, <sup>13</sup>C at 100 MHz), Bruker DRX-500 (<sup>1</sup>H at 500 MHz, <sup>13</sup>C at 125 MHz), or Bruker AVIII-600 (<sup>1</sup>H at 600 MHz, <sup>13</sup>C at 150 MHz). Absorptions and their splitting from <sup>1</sup>H NMR spectra are recorded as follows relative to residual solvent peaks: (s = singlet, d = doublet, t = triplet, q = quartet, dd = doublet of doublets, td = triplet of doublets, dq = doublet of quartets, ddd = doublet of doublet of doublets, tdd triplet of doublet of doublets, dddd = doublet of doublet of doublet of doublets, m = multiplet, comp =

---

<sup>89</sup> Johnson, S. A.; Hunt, H. R.; Neumann, H. M. *Inorg. Chem.*, **1963**, 2, 960-962.

<sup>90</sup> Doyle, M. P.; McKervey, M. A.; Ye, T. *Modern Catalytic Methods for Organic Synthesis with Diazo Compounds*, Wiley, New York, **1998**.

<sup>91</sup> Cotton, F. A.; Felthouse, T. R. *Inorg. Chem.*, **1980**, 19, 323-328.

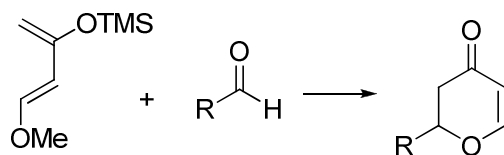
<sup>92</sup> Hashimoto, S.; Watanabe, N.; Ikegami, S. *Tetrahedron Lett.*, **1992**, 33, 2709-2712.

<sup>93</sup> Doyle, M. P.; Westrum, L. J.; Wolthuis, W. N. E.; See, M. M.; Boone, W. P.; Bagheri, V.; Pearson, M. *J. Am. Chem. Soc.*, **1993**, 115, 958-964.

<sup>94</sup> Davies, H. M. L.; Ahmed, G.; Churchill, M. R. *J. Am. Chem. Soc.*, **1996**, 118, 10774-10782.

composite), coupling constant (Hz), and integration. Chemical shifts ( $\delta$ , ppm) for  $^{13}\text{C}$  NMR spectra are reported relative to the residual solvent peak. All spectra are recorded in  $\text{CDCl}_3$  as solvent, unless otherwise described. High resolution mass spectra (HRMS) were recorded on a JEOL AccuTOF-CS system (ESI positive, needle voltage 1800-2400eV, flow rate 50uL/min). IR spectra were recorded on a JASCO FT-IR-4100 instrument. Melting points were determined with a MEL-TEMP digital melting point apparatus.

#### General procedures for the hetero-Diels-Alder (HDA) reaction



All hetero-Diels-Alder products were synthesized using  $\text{BF}_3 \cdot \text{Et}_2\text{O}$  (method A) except for 2-(4-nitrophenyl)-2H-pyran-4(3H)-one and 2-(4-(trifluoromethyl)phenyl)-2H-pyran-4(3H)-one that were synthesized using catalytic amounts of  $\text{Rh}_2(\text{OAc})_4$  (method B) due to higher yields obtained using  $\text{Rh}_2(\text{OAc})_4$  in comparison to using  $\text{BF}_3 \cdot \text{Et}_2\text{O}$  as the Lewis acid.

**HDA reaction using  $\text{BF}_3 \cdot \text{Et}_2\text{O}$ -Method A.** A solution of benzaldehyde (0.20g, 1.9 mmol) and Danishefsky's diene (0.36 g, 2.3 mmol) in dry DCM (19 mL) was cooled to  $-78^\circ\text{C}$ . To that solution was added  $\text{BF}_3 \cdot \text{Et}_2\text{O}$  (0.27g, 1.9 mmol) dropwise, which produced an instant color change from colorless to yellow to dark brown. After 8 hrs at  $-78^\circ\text{C}$ , the reaction was quenched with  $\text{NaHCO}_3$  (10 mL)

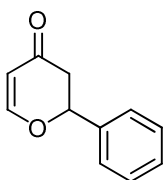
followed by brine (10 mL), then extracted with CH<sub>2</sub>Cl<sub>2</sub> (3 × 15 mL). The combined organic layer was dried over anhydrous MgSO<sub>4</sub>, filtered, and the solvent was evaporated under reduced pressure.

**HDA reaction using Rh<sub>2</sub>(OAc)<sub>4</sub>-Method B.** Rhodium(II) acetate (5.8 mg, 0.013 mmoles, 1mole %) and 4-nitrobenzaldehyde (0.20g, 1.3 mmoles) were dissolved in 5 mL of DCM. The suspension was stirred for 20 minutes at room temperature before adding the Danishefsky diene (0.44g, 2.7 mmoles). The solution was stirred at room temperature for 24 hrs. After the reaction was complete, judging by TLC analysis, TFA (1.0 mL) was added slowly, and the solution was stirred for a further 30 minutes. The material was later washed with saturated NaHCO<sub>3</sub> (10 mL) and brine (10 mL) then extracted into DCM (3 × 15 mL). The organic extracts were combined, dried over anhydrous MgSO<sub>4</sub>, filtered, and the solvent was evaporated.

### Characterization of compounds

#### Characterization for HDA products.

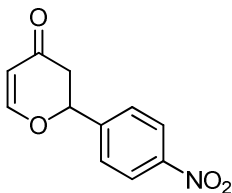
##### Phenyl pyranone



Prepared using BF<sub>3</sub>.Et<sub>2</sub>O - method A. Purified by chromatography on silica gel (gradient elution: hexane/ethyl acetate (90% to 80% hexane)); yellow oil (65% yield), based on a 5.0 mmole scale of benzaldehyde. <sup>1</sup>H NMR (400 MHz, CDCl<sub>3</sub>) δ 7.48 (dd, *J* = 6.0, 0.7 Hz, 1H), 7.43-7.36 (m, 5H), 5.52 (dd, *J* = 6.0, 1.3 Hz, 1H), 5.42 (dd, *J* = 14.4, 3.5 Hz, 1H), 2.90 (dd, *J* = 16.9, 14.5 Hz, 1H), 2.66 (ddd, *J* = 16.9, 3.5, 1.3 Hz, 1H). <sup>13</sup>C NMR

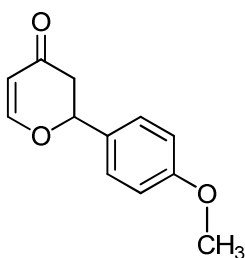
(101 MHz, CDCl<sub>3</sub>)  $\delta$  192.15, 163.06, 137.66, 128.86, 128.78, 126.03, 107.30, 81.01, 43.07. HRMS (ESI<sup>+</sup>): expected mass 175.0754, found 175.0748.

#### 4-Nitro-phenyl pyranone



Prepared using catalytic amounts of Rh<sub>2</sub>(OAc)<sub>4</sub>-method B. Purified by chromatography on silica gel (gradient elution: hexane/ethyl acetate (90% to 60% hexane); yellow solid (65% yield), based on a 3.3 mmole scale of 4-nitrobenzaldehyde. <sup>1</sup>H NMR (400 MHz, CDCl<sub>3</sub>)  $\delta$  8.4-8.37 (comp, 2H), 7.64-7.60 (comp, 2H), 7.54 (dd, *J* = 6.6, 0.6 Hz, 1H), 5.46-5.37 (comp, 2H), 2.47 (dd, *J* = 18.2, 15.2 Hz, 1H), 2.33 (ddd, *J* = 18.2, 4.1, 1.3 Hz, 1H). <sup>13</sup>C NMR (101 MHz, CDCl<sub>3</sub>)  $\delta$  190.66, 162.54, 148.04, 144.83, 126.69, 124.14, 107.90, 79.69, 43.37. HRMS (ESI<sup>+</sup>): expected mass 220.0604, found 220.0610. M.p. 101-102 °C.

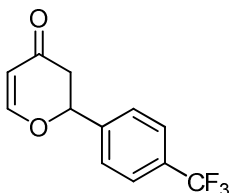
#### 4-Methoxy-phenyl pyranone



Prepared using BF<sub>3</sub>.Et<sub>2</sub>O-method A. Purified by chromatography on silica gel (gradient elution: hexane/ethyl acetate (90% to 70% hexane); yellow oil (65% yield), based on a 3.7 mmole scale of 4-methoxybenzaldehyde. <sup>1</sup>H NMR (400 MHz, CDCl<sub>3</sub>)  $\delta$  7.46 (dd, *J* = 6.0, 0.7 Hz, 1H), 7.35-7.32 (comp, 2H), 6.96-6.93 (comp, 2H), 5.51 (dd, *J* = 6.0, 1.3 Hz, 1H), 5.37 (dd, *J* = 14.5, 3.4 Hz, 1H), 3.83 (s, 3H), 2.93 (dd, *J* = 16.9, 14.5 Hz, 1H), 2.63

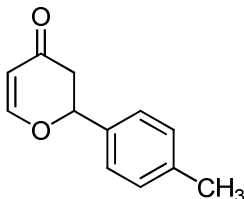
(ddd,  $J = 16.9, 3.4, 1.3$  Hz, 1H).  $^{13}\text{C}$  NMR (101 MHz,  $\text{CDCl}_3$ )  $\delta$  192.45, 163.31, 160.07, 129.79, 127.74, 114.17, 107.24, 80.90, 55.34, 43.15. HRMS (ESI+): expected mass 205.0859, found 205.0857. HRMS (ESI+): expected mass 205.0859, found 205.0857.

#### 4-trifluoromethyl phenyl pyranone



Prepared using  $\text{Rh}_2(\text{OAc})_4$ -method B. Purified by chromatography on silica gel (gradient elution: hexane/ethyl acetate (80% to 60% hexane); yellow solid (60% yield), based on a 3.0 mmole scale of 4-(trifluoromethyl)benzaldehyde.  $^1\text{H}$  NMR (400 MHz,  $\text{CDCl}_3$ )  $\delta$  7.64 (d,  $J = 8.2$  Hz, 2H), 7.50 (d,  $J = 8.2$  Hz, 2H), 7.46 (d,  $J = 6.0$  Hz, 1H), 5.51 (dd,  $J = 6.0, 1.0$  Hz, 1H), 5.46 (dd,  $J = 14.2, 3.6$  Hz, 1H), 2.81 (dd,  $J = 16.9, 14.2$  Hz, 1H), 2.65 (ddd,  $J = 16.9, 3.6, 1.1$  Hz, 1H).  $^{13}\text{C}$  NMR (101 MHz,  $\text{CDCl}_3$ )  $\delta$  191.18, 162.75, 141.81, 130.99 (q,  $J = 32.6$  Hz), 125.82 (q,  $J = 3.8$  Hz), 123.90 (q,  $J = 270.5$  Hz), 107.64, 80.12, 43.36. HRMS (ESI+): expected mass 243.0627, found 243.0629. M.p. 48-49 °C.

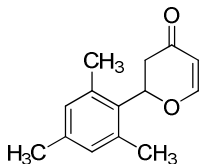
#### 2-*p*-tolyl-2*H*-pyran-4(3*H*)-one



Prepared using  $\text{BF}_3 \cdot \text{Et}_2\text{O}$ -method A. Purified by chromatography on silica gel (gradient elution: hexane/ethyl acetate (90% to 80% hexane); orange solid (65% yield), based on a 4.0 mmole scale of 4-methylbenzaldehyde.  $^1\text{H}$  NMR (400 MHz,  $\text{CDCl}_3$ )  $\delta$  7.46 (dd,  $J = 6.0, 0.6$  Hz, 1H), 7.29-7.27 (comp, 2H), 7.23-7.21 (comp, 2H), 5.51 (dd,  $J = 6.0, 1.3$  Hz,

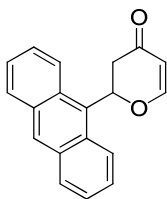
1H), 5.38 (dd,  $J = 14.4, 3.4$  Hz, 1H), 2.90 (dd,  $J = 16.9, 14.4$  Hz, 1H), 2.63 (ddd,  $J = 16.9, 3.4, 1.3$  Hz, 1H), 2.37 (s, 3H).  $^{13}\text{C}$  NMR (101 MHz,  $\text{CDCl}_3$ )  $\delta$  192.24, 163.20, 138.77, 134.75, 129.38, 126.06, 107.15, 80.93, 43.17, 21.09. HRMS (ESI+): expected mass 189.0910, found 189.0910. M.p. 80-81 °C.

### 2-Mesityl-2H-pyran-4(3H)-one (191f)



Prepared using  $\text{BF}_3 \cdot \text{Et}_2\text{O}$ -method A. Purified by chromatography on silica gel (gradient elution: hexane/ethyl acetate (100% to 95% hexane): yellow solid (65% yield), based on 3.4 mmol scale of mesitaldehyde.  $^1\text{H}$  NMR (400 MHz,  $\text{CDCl}_3$ )  $\delta$  7.50 (dd,  $J = 6.0, 0.6$  Hz, 1H), 6.88 (s, 2H), 5.81 (dd,  $J = 16.0, 3.8$  Hz, 1H), 5.53 (dd,  $J = 6.0, 1.2$  Hz, 1H), 3.16 (dd,  $J = 17.2, 16.0$  Hz, 1H), 2.43 (ddd,  $J = 17.2, 3.8, 1.2$  Hz, 1H), 2.38 (s, 6H), 2.28 (s, 3H).  $^{13}\text{C}$  NMR (126 MHz,  $\text{CDCl}_3$ )  $\delta$  192.4, 163.5, 138.3, 136.1, 130.4, 130.4, 107.1, 78.8, 40.4, 20.8, 20.6. HRMS (ESI+): expected mass 217.1223, found 217.1230. M.p. 72-73 °C.

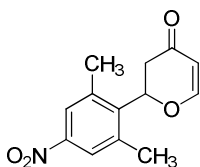
### 2-(Anthracen-9-yl)-2H-pyran-4(3H)-one (191g)



Prepared using  $\text{BF}_3 \cdot \text{Et}_2\text{O}$ -method A. Purified by chromatography on silica gel (gradient elution: hexane/ethyl acetate (100% to 95% hexane): orange solid (53% yield), based on 2.4 mmol of anthracene-9-carbaldehyde.  $^1\text{H}$  NMR (400 MHz,  $\text{CDCl}_3$ )  $\delta$  8.54 (s, 1H), 8.36 (d,  $J = 8.8$  Hz, 2H), 8.07 (dd,  $J = 8.4, 0.8$  Hz, 2H), 7.70 (d,  $J = 6.0$  Hz, 1H), 7.58-

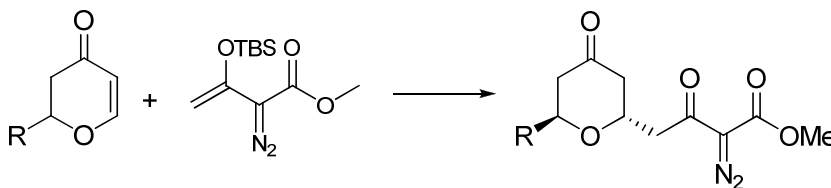
7.49 (comp, 4H), 6.94 (dd,  $J = 16.0, 4.0$  Hz, 1H), 5.74 (dd,  $J = 6.0, 0.8$  Hz, 1H), 3.69 (dd,  $J = 17.8, 16.0$  Hz, 1H), 2.73 (ddd,  $J = 17.8, 4.0, 0.8$  Hz, 1H).  $^{13}\text{C}$  NMR (126 MHz,  $\text{CDCl}_3$ )  $\delta$  192.0, 163.4, 131.4, 129.6, 129.5, 129.0, 127.0, 126.4, 124.8, 123.5, 107.7, 78.1, 41.9. HRMS (ESI+): expected mass 275.1067, found 275.1075. M.p. 160-161 °C.

### 2-(2,6-Dimethyl-4-nitrophenyl)-2H-pyran-4(3H)-one (191h)



Prepared using  $\text{BF}_3 \cdot \text{Et}_2\text{O}$ -method A. Purified by chromatography on silica gel (gradient elution: hexane/ethyl acetate (100% to 85% hexane)); pale yellow solid (50% yield), based on 2.8 mmol scale of 2,6-dimethyl-4-nitro benzaldehyde. The 2,6-dimethyl-4-nitro benzaldehyde was synthesized following literature procedure<sup>95</sup> by Dr. Ryan Burgin.  $^1\text{H}$  NMR (500 MHz,  $\text{CDCl}_3$ )  $\delta$  7.92 (s, 2H), 7.50 (d,  $J = 6.0$  Hz, 1H), 5.87 (dd,  $J = 16.0, 4.0$  Hz, 1H), 5.58 (d,  $J = 6.0$  Hz, 1H), 3.10 (dd,  $J = 17.5, 16.0$  Hz, 1H), 2.52 (s, 6H), 2.45 (ddd,  $J = 17.5, 4.0, 1.0$  Hz, 1H).  $^{13}\text{C}$  NMR (126 MHz,  $\text{CDCl}_3$ )  $\delta$  190.8, 162.7, 147.2, 140.1, 138.1, 124.1, 107.6, 77.9, 39.4, 20.9. HRMS (ESI+): expected mass 248.0917, found 248.0912. M.p. 120-121 °C.

### General Procedure for the Mukaiyama-Michael reaction



<sup>95</sup> Shiina, I.; Miyao, R. *Heterocycles*, **2008**, 76, 1313-1328.

To a flame-dried, 25-mL round bottom flask under nitrogen was added zinc triflate (16 mg, 0.044 mmol), followed by 6-phenylpyranone (0.76g, 4.4 mmol) that was dissolved in dry DCM (8.0 mL). Methyl 3-(*tert*-butyldimethylsilyloxy)-2-diazo-3-butenoate (1.7 g, 6.6 mmol) was then added via syringe all at once. The resulting orange solution was stirred at heated using an oil bath to 40°C for 16 hour and then slowly cooled to room temperature. The Mukaiyama-Michael reactions were worked up using one of two methods, as described below. For the synthesis of Methyl 2-diazo-3-oxo-4-((2*S*\*,6*S*\*)-4-oxo-6-phenyltetrahydro-2*H*-pyran-2-yl)butanoate (**192a**), method C using 4N HCl was followed. However, for diazoacetoacetate substrates where the aryl substituent is electron donating (Methyl 2-diazo-3-oxo-4-((2*S*\*,6*S*\*)-4-oxo-6-*p*-tolyltetrahydro-2*H*-pyran-2-yl)butanoate, Methyl 2-diazo-4-((2*S*\*,6*S*\*)-6-(4-methoxyphenyl)-4-oxotetrahydro-2*H*-pyran-2-yl)-3-oxobutanoate, Methyl 2-diazo-4-((2*S*\*,6*S*\*) 6-mesityl-4-oxotetrahydro-2*H*-pyran-2-yl)-3-oxobutanoate, Methyl 2-diazo-4-((2*S*\*,6*S*\*) 6-(anthracen-9-yl)-4-oxotetrahydro-2*H*-pyran-2-yl)-3-oxobutanoate, and Methyl 2-diazo-4-((2*R*\*,6*R*\*) 6-(2,6-dimethyl-4-nitrophenyl)-4-oxotetrahydro-2*H*-pyran-2-yl)-3-oxobutanoate) TBAF was used for the work up to prevent the formation of elimination byproducts that were observed when the work-up was done with HCl.

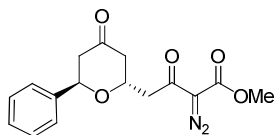
**Mukaiyama-Michael reaction work up using 4N HCl - Method C.** After the reaction was complete, judging by TLC analysis, the reaction mixture was concentrated under reduced pressure then dissolved in 30 mL of tetrahydrofuran (THF). To that was added 10 mL of 4N aqueous HCl solution dropwise. After 4 hrs the reaction was quenched by slow addition of NaHCO<sub>3</sub> (30mL) until the reaction was neutralized. The resulting

solution was extracted with DCM ( $3 \times 30$  mL), and the combined organic layer was dried over anhydrous  $\text{MgSO}_4$ , filtered, and the solvent was evaporated under reduced pressure.

**Mukaiyama-Michael reaction work up using TBAF and AcOH - Method D.** The calculation for the work-up below is based on the substrate 2-(4-methoxyphenyl)pyranone **192 (e)** (0.29g, 1.4 mmoles). After the reaction was complete, judged by TLC analysis, the solvent was evaporated under reduced pressure then dissolved in 14 mL of tetrahydrofuran (THF). To that solution was added AcOH (0.6 mL) and TBAF (1M THF solution, 2mL, 2.1 mmoles). The resulting solution was stirred at  $0^\circ\text{C}$  for 4 hrs. The solution was quenched with  $\text{Et}_3\text{N}$ , then diluted with saturated  $\text{NaHCO}_3$  (15 mL), and the aqueous layer was extracted with DCM (20mL  $\times$  3). The combined organic extracts were washed with brine (15 mL), dried over anhydrous  $\text{MgSO}_4$  and concentrated under reduced pressure after filtration.

#### Data Characterization for Mukaiyama-Michael products

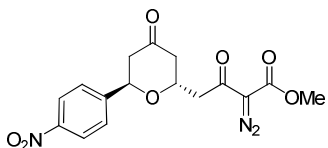
##### Methyl 2-diazo-3-oxo-4-((2*R*\*,6*R*\*)-4-oxo-6-phenyltetrahydro-2*H*-pyran-2-yl)butanoate (**192a**)



Followed method C for the work-up. Purified by chromatography on silica gel (gradient elution: hexane/ethyl acetate (90% to 75% hexane): yellow solid (99% yield), based on a

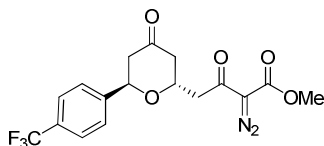
1.2 mmol scale of 2-phenyl-2*H*-pyran-4(3*H*)-one. <sup>1</sup>H NMR (400 MHz, CDCl<sub>3</sub>) δ 7.39-7.28 (comp, 5H), 5.29 (t, *J* = 5.8 Hz, 1H), 4.60-4.53 (m, 1H), 3.79 (s, 3H), 3.31 (dd, *J* = 15.6, 8.0 Hz, 1H), 3.05 (dd, *J* = 15.6, 5.8 Hz, 1H), 2.87 (ddd, *J* = 14.8, 6.4, 1.2 Hz, 1H), 2.79 (ddd, *J* = 14.8, 5.2, 1.2 Hz, 1H), 2.65 (ddd, *J* = 14.8, 4.8, 1.2 Hz, 1H), 2.45 (ddd, *J* = 14.8, 7.2, 1.2 Hz, 1H). <sup>13</sup>C NMR (101 MHz, CDCl<sub>3</sub>) δ 206.2, 188.9, 161.5, 139.6, 128.6, 128.1, 126.8, 74.0, 68.6, 52.3, 46.5, 46.1, 44.5, missing diazo carbon. IR (cm<sup>-1</sup>): 2959, 2925, 2854, 2143 (C=N<sub>2</sub>), 1708, 1664, 1646. HRMS (ESI+): expected mass 317.1132, found 317.1128. M.p. 71-72 °C.

**Methyl 2-diazo-4-((2*R*\*,6*R*\*)-6-(4-nitrophenyl)-4-oxotetrahydro-2*H*-pyran-2-yl)-3-oxobutanoate (192b)**



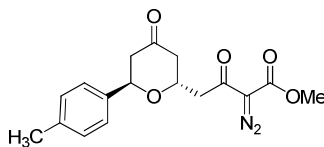
Followed method C for the work-up. Purified by chromatography on silica gel (gradient elution: hexane/ethyl acetate (90% to 60% hexane): yellow solid (80% yield), based on a 2.3 mmol scale of 2-(4-nitrophenyl)-2*H*-pyran-4(3*H*)-one. <sup>1</sup>H NMR (400 MHz, CDCl<sub>3</sub>) δ 8.25-8.22 (comp, 2H), 7.58-7.55 (comp, 2H), 5.35 (dd, *J* = 6.6, 5.4 Hz, 1H), 4.70-4.63 (m, 1H), 3.82 (s, 3H), 3.39 (dd, *J* = 16.0, 8.2 Hz, 1H), 3.04 (dd, *J* = 16.0, 5.2 Hz, 1H), 2.87-2.76 (comp, 2H), 2.69 (ddd, *J* = 14.8, 5.2, 1.2 Hz, 1H), 2.50 (ddd, *J* = 14.8, 6.6, 1.2 Hz, 1H). <sup>13</sup>C NMR (101 MHz, CDCl<sub>3</sub>) δ 204.9, 188.6, 161.5, 147.6, 146.9, 127.5, 123.9, 73.1, 69.3, 52.3, 46.2, 46.1, 44.2, missing diazo carbon. IR (cm<sup>-1</sup>): 2959, 2921, 2849, 2123 (C=N<sub>2</sub>), 1717, 1641, 1598, 1512, 1335, 1302. HRMS (ESI+): expected mass 362.0983, found 362.0984. M.p. 103-104 °C.

**Methyl 2-diazo-3-oxo-4-((2*R*\*,6*R*\*)-4-oxo-6-(4-(trifluoromethyl)phenyl)tetrahydro-2*H*-pyran-2-yl)butanoate (192c)**



Followed method C for the work-up. Purified by chromatography on silica gel (gradient elution: hexane/ethyl acetate (90% to 70% hexane): yellow solid (77% yield), based on a 2.1 mmol scale of 2-(4-(trifluoromethyl)phenyl)-2*H*-pyran-4(3*H*)-one. <sup>1</sup>H NMR (400 MHz, CDCl<sub>3</sub>) δ 7.60 (d, *J* = 8.2 Hz, 2H), 7.48 (d, *J* = 8.2 Hz, 2H), 5.30 (t, *J* = 5.6 Hz, 1H), 4.61-4.54 (m, 1H), 3.77 (s, 3H), 3.32 (dd, *J* = 15.6, 8.1 Hz, 1H), 3.02 (dd, *J* = 15.6, 5.2 Hz, 1H), 2.80 (d, *J* = 5.6 Hz, 2H), 2.64 (dd, *J* = 14.8, 4.6 Hz, 1H), 2.45 (dd, *J* = 14.8, 7.2 Hz, 1H). <sup>13</sup>C NMR (151 MHz, CDCl<sub>3</sub>) δ 205.3, 188.7, 161.5, 143.7, 130.2 (q, *J* = 32.6 Hz), 127.0, 125.5 (q, *J* = 3.7 Hz), 123.90 (q, *J* = 270.5 Hz), 73.4, 69.0, 52.2, 46.2, 46.0, 44.3, missing diazo carbon. HRMS (ESI<sup>+</sup>): expected mass 385.1011, found 385.1005. IR (cm<sup>-1</sup>): 2964, 2921, 2854, 2128 (C=N<sub>2</sub>), 1717, 1641, 1622, 1316. HRMS (ESI<sup>+</sup>): expected mass 385.1011, found 385.1005. M.p. 64-65 °C.

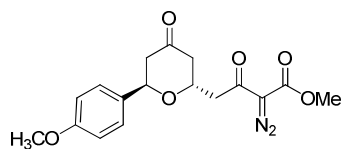
**Methyl 2-diazo-3-oxo-4-((2*R*\*,6*R*\*)-4-oxo-6-*p*-tolyltetrahydro-2*H*-pyran-2-yl)butanoate (192d)**



Followed method D for the work-up. Purified by chromatography on silica gel (gradient elution: hexane/ethyl acetate (90% to 70% hexane): yellow oil (97% yield), based on a 1.2 mmol scale of 2-*p*-tolyl-2*H*-pyran-4(3*H*)-one. <sup>1</sup>H NMR (400 MHz, CDCl<sub>3</sub>) δ 7.24-7.22 (comp, 2H), 7.17-7.15 (comp, 2H), 5.26 (t, *J* = 6.0 Hz, 1H), 4.55-4.48 (m, 1H), 3.79 (s, 3H), 3.29 (dd, *J* = 15.6, 8.0 Hz, 1H), 3.03 (dd, *J* = 15.6, 5.6 Hz, 1H), 2.86 (ddd, *J* = 14.8, 6.0, 1.4 Hz, 1H), 2.77 (ddd, *J* = 14.8, 5.6, 1.2 Hz, 1H), 2.62 (ddd, *J* = 14.8, 4.8, 1.2

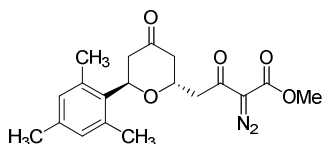
Hz, 1H), 2.43 (ddd,  $J = 14.8, 7.6, 1.2$  Hz, 1H), 2.33 (s, 3H).  $^{13}\text{C}$  NMR (101 MHz,  $\text{CDCl}_3$ )  $\delta$  206.4, 188.9, 161.5, 137.9, 136.5, 129.2, 126.8, 74.0, 68.3, 52.2, 46.5, 45.9, 44.6, 21.1, missing diazo carbon. IR ( $\text{cm}^{-1}$ ): 2906, 2959, 2128 ( $\text{C}=\text{N}_2$ ), 1713, 1646, 1512. HRMS (ESI+): expected mass 331.1288, found 331.1279.

**Methyl 2-diazo-4-((2*R*\*,6*R*\*)-6-(4-methoxyphenyl)-4-oxotetrahydro-2*H*-pyran-2-yl)-3-oxobutanoate (192e)**



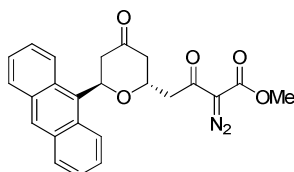
Followed method D for the work-up. Purified by chromatography on silica gel (gradient elution: hexane/ethyl acetate (90% to 75% hexane); yellow oil (92% yield), based on a 1.4 mmol scale of 2-(4-methoxymethylphenyl)-2*H*-pyran-4(3*H*)-one.  $^1\text{H}$  NMR (400 MHz,  $\text{CDCl}_3$ )  $\delta$  7.27-7.24 (comp, 2H), 6.89-6.85 (comp, 2H), 5.25 (t,  $J = 5.6$  Hz, 1H), 4.50-4.44 (m, 1H), 3.78 (s, 6H), 3.27 (dd,  $J = 15.6, 8.0$  Hz, 1H), 3.02 (dd,  $J = 15.6, 5.2$  Hz, 1H), 2.85 (ddd,  $J = 14.8, 6.0, 1.2$  Hz, 1H), 2.76 (ddd,  $J = 14.8, 5.2, 1.2$  Hz, 1H), 2.60 (ddd,  $J = 14.8, 4.4, 1.2$  Hz, 1H), 2.41 (ddd,  $J = 14.8, 8.0, 1.2$  Hz, 1H).  $^{13}\text{C}$  NMR (101 MHz,  $\text{CDCl}_3$ )  $\delta$  206.4, 188.9, 161.5, 159.3, 131.5, 128.3, 113.8, 73.7, 68.1, 55.2, 52.2, 46.5, 45.8, 44.7, missing diazo carbon. IR ( $\text{cm}^{-1}$ ): 3055, 2959, 2835, 2138 ( $\text{C}=\text{N}_2$ ), 1708, 1646, 1607, 1507, 1431. HRMS (ESI+): expected mass 347.1238, found 347.1242.

**Methyl 2-diazo-4-((2*R*\*,6*R*\*)-6-mesityl-4-oxotetrahydro-2*H*-pyran-2-yl)-3-oxobutanoate (192f)**



Followed method D for the work-up. Purified by chromatography on silica gel (gradient elution: hexane/ethyl acetate (90% to 80% hexane): yellow solid (99% yield), based on a 2.0 mmol scale of 2-mesityl-2*H*-pyran-4(3*H*)-one. <sup>1</sup>H NMR (600 MHz, CDCl<sub>3</sub>) δ 6.83 (s, 2H), 5.51 (dd, *J* = 12.0, 3.6 Hz, 1H), 5.11-5.05 (m, 1H), 3.82 (s, 3H), 3.33 (dd, *J* = 15.0, 8.4 Hz, 1H), 3.17 (dd, *J* = 15.0, 6.0 Hz, 1H), 2.97 (dd, *J* = 15.0, 12.0 Hz, 1H), 2.92 (dd, *J* = 15.0, 6.6 Hz, 1H), 2.50 (ddd, *J* = 15.0, 3.0, 2.0 Hz, 1H), 2.46-2.39 (comp, 7H), 2.24 (s, 3H). <sup>13</sup>C NMR (101 MHz, CDCl<sub>3</sub>) δ 206.7, 188.8, 161.5, 137.4, 136.1, 132.7, 130.3, 70.6, 70.3, 52.2, 45.6, 45.5, 42.8, 20.7, 20.5, missing diazo carbon. IR (cm<sup>-1</sup>): 2973, 2359, 2339, 2137 (C=N<sub>2</sub>), 1713, 1652, 1612. HRMS (ESI<sup>+</sup>): expected mass 359.1601, found 359.1609. M.p. 84-85 °C.

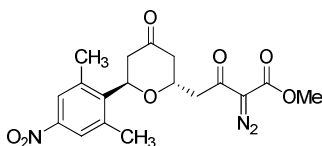
**Methyl 2-diazo-4-((2*R*\*,6*R*\*)-6-(anthracen-9-yl)-4-oxotetrahydro-2*H*-pyran-2-yl)-3-oxobutanoate (192g)**



Followed method D for the work-up. Purified by chromatography on silica gel (gradient elution: hexane/ethyl acetate (90% to 80% hexane): white solid (90% yield), based on a 1.5 mmol scale of 2-(anthracen-9-yl)-2*H*-pyran-4(3*H*)-one. <sup>1</sup>H NMR (400 MHz, CDCl<sub>3</sub>) δ 8.67 (d, *J* = 8.4 Hz, 2H), 8.46 (s, 1H), 8.03-8.01 (comp, 2H), 7.56-7.52 (comp, 2H), 7.49-7.45 (comp, 2H), 6.68 (dd, *J* = 12.0, 3.2 Hz, 1H), 5.40-5.34 (m, 1H), 3.80 (s, 3H), 3.65 (dd, *J* = 15.2, 8.8 Hz, 1H), 3.48 (dd, *J* = 15.2, 12.0 Hz, 1H), 3.30 (dd, *J* = 15.2, 5.6 Hz, 1H), 3.26 (dd, *J* = 15.2, 7.2 Hz, 1H), 2.71-2.67 (comp, 2H). <sup>13</sup>C NMR (101 MHz, CDCl<sub>3</sub>)

$\delta$  206.1, 188.8, 161.6, 131.7, 129.9, 129.5, 129.2, 129.1, 126.2, 124.8, 119.6, 71.7, 70.1, 52.3, 47.5, 46.0, 42.5, missing diazo carbon. IR (cm<sup>-1</sup>): 2361, 2149 (C=N<sub>2</sub>), 1714, 1694, 1633. HRMS (ESI<sup>+</sup>): expected mass 417.1445, found 417.1439. M.p. 157-158 °C.

**Methyl 2-diazo-4-((2*R*\*,6*R*\*)-6-(2,6-dimethyl-4-nitrophenyl)-4-oxotetrahydro-2*H*-pyran-2-yl)-3-oxobutanoate (192h)**



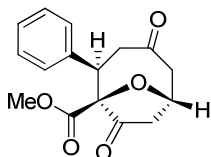
Followed method D for the work-up. Purified by chromatography on silica gel (gradient elution: hexane/ethyl acetate (90% to 80% hexane): yellow solid (95% yield), based on a 1.0 mmol scale of 2-(2,6-dimethyl-4-nitrophenyl)-2*H*-pyran-4(3*H*)-one. <sup>1</sup>H NMR (500 MHz, CDCl<sub>3</sub>)  $\delta$  7.86 (s, 2H), 5.61 (dd, *J* = 12.0, 3.0 Hz, 1H), 5.12-5.08 (m, 1H), 3.82 (s, 3H), 3.31 (dd, *J* = 15.0, 9.0 Hz, 1H), 3.19 (dd, *J* = 15.0, 5.5 Hz, 1H), 2.94 (dd, *J* = 15.0, 6.5 Hz, 1H), 2.90 (dd, *J* = 15.0, 12.0 Hz, 1H), 2.57 (s, 6H), 2.55-2.52 (m, 1H), 2.45-2.41 (m, 1H). <sup>13</sup>C NMR (126 MHz, CDCl<sub>3</sub>)  $\delta$  205.0, 188.6, 161.6, 146.7, 142.5, 138.3, 124.0, 71.0, 70.0, 52.3, 45.5, 44.4, 42.7, 21.0, missing diazo carbon. IR (cm<sup>-1</sup>): 2964, 2144 (C=N<sub>2</sub>), 1711, 1675, 1618, 1421, 1360, 1220. HRMS (ESI<sup>+</sup>): expected mass 390.1296, found 390.1301. M.p. 108-109 °C.

**General Procedure for catalytic dinitrogen extrusion.** The catalyst Rh<sub>2</sub>(pfb)<sub>4</sub> (17 mg, 0.016 mmoles) was transferred to a flame-dried two-neck flask and then dissolved in anhydrous DCM ( 7.0 mL). Methyl 2-diazo-3-oxo-4-(4-oxo-6-phenyltetrahydro-2*H*-pyran-2-yl)butanoate (0.50 g, 1.6 mmoles) was dissolved in anhydrous DCM (3.0 mL) and added dropwise to the reaction mixture via a syringe pump over two hours. Once the addition was complete, the reaction was left to stir at reflux (40 °C) for an additional two

hours. After the reaction reached completion, judging by TLC analysis, it was cooled to room temperature and the solvent was evaporated under reduced pressure.

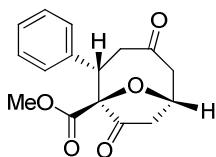
### Data Characterization for Dinitrogen Extrusion Products

#### (1*S*\*,2*R*\*,6*R*\*)-Methyl 4,8-dioxo-2-phenyl-9-oxabicyclo[4.2.1]nonane-1-carboxylate (*syn*-193a)



Purified by chromatography on silica gel (gradient elution: hexane/ethyl acetate (90% to 65% hexane): white solid (77% combined yield). <sup>1</sup>H NMR (400 MHz, CDCl<sub>3</sub>) δ 7.34-7.27 (comp, 4H), 7.24-7.20 (m, 1H), 5.25-5.21 (m, 1H), 3.54 (dd, *J* = 9.6, 6.4 Hz, 1H), 3.38 (dd, *J* = 13.0, 6.4 Hz, 1H), 3.31 (s, 3H), 3.01-2.94 (comp, 2H), 2.69 (ddd, *J* = 11.6, 6.4, 1.6 Hz, 1H), 2.53-2.47 (comp, 2H). <sup>13</sup>C NMR (101 MHz, CDCl<sub>3</sub>) δ 207.0, 206.6, 165.6, 140.1, 128.6, 128.0, 127.4, 89.9, 70.0, 52.6, 52.5, 48.8, 45.5, 40.7. IR (cm<sup>-1</sup>): 1769, 1732, 1693, 1268, 1245, 2925. HRMS (ESI<sup>+</sup>): expected mass 289.1071, found 289.1069. M.p. 165-166 °C.

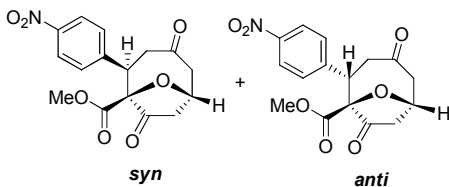
#### (1*S*\*,2*S*\*,6*R*\*)-Methyl 4,8-dioxo-2-phenyl-9-oxabicyclo[4.2.1]nonane-1-carboxylate (*anti*-193a)



Purified by chromatography on silica gel (gradient elution: hexane/ethyl acetate (90% to 65% hexane): white solid (77% combined yield). <sup>1</sup>H NMR (400 MHz, CDCl<sub>3</sub>) δ 7.29-7.27 (comp, 3H), 7.21-7.19 (comp, 2H), 4.99 – 4.95 (m, 1H), 3.72 (dd, *J* = 12.0, 4.0 Hz, 1H), 3.52 (s, 3H), 3.31 (dd, *J* = 16.0, 6.6 Hz, 1H), 3.16 (dd, *J* = 18.8, 10.0 Hz, 1H), 3.03-

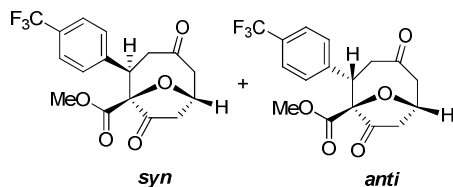
2.96 (m, 1H), 2.87 (dd,  $J = 14.4, 4.0$  Hz, 1H), 2.74-2.65 (comp, 2H).  $^{13}\text{C}$  NMR (101 MHz,  $\text{CDCl}_3$ )  $\delta$  207.2, 206.1, 166.0, 136.6, 128.7, 128.3, 128.0, 86.6, 69.5, 52.7, 51.7, 48.0, 47.5, 44.0. IR ( $\text{cm}^{-1}$ ): 1775, 1727, 1704, 1292, 1235, 2916, 2357, 1064, 1045. HRMS (ESI+): expected mass 289.1071, found 289.1065. M.p. 129-130 °C.

**Methyl 2-(4-nitrophenyl)-4,8-dioxo-9-oxabicyclo[4.2.1]nonane-1-carboxylate (193b)**



Purified by chromatography on silica gel (gradient elution: hexane/ethyl acetate (90% to 60% hexane): yellow solid (94% yield), based on a 0.69 mmol scale of Methyl 2-diazo-4-((2*S*\*,6*S*\*)-6-(4-nitrophenyl)-4-oxotetrahydro-2*H*-pyran-2-yl)-3-oxobutanoate.  $^1\text{H}$  NMR (400 MHz,  $\text{CDCl}_3$ )  $\delta$  8.19-8.13 (comp, 2H), 7.55-7.51 (comp, 2H), 5.30-5.26 (m, 1H), 3.70 (dd,  $J = 9.2, 6.4$  Hz, 1H), 3.42-3.37 (m, 1H), 3.39 (s, 3H), 3.04 (ddd,  $J = 18.0, 9.2, 0.8$  Hz, 1H), 2.99-2.86 (m, 1H), 2.74-2.68 (m, 1H), 2.58-2.52 (comp, 2H).  $^1\text{H}$  NMR (400 MHz,  $\text{CDCl}_3$ )- *anti*-isomer  $\delta$  8.19-8.13 (comp, 2H), 7.49-7.46 (comp, 2H), 5.06 (ddt,  $J = 9.6, 6.8, 1.6$  Hz, 1H), 3.96 (dd,  $J = 9.6, 5.4$  Hz, 1H), 3.62 (s, 3H), 3.24-3.14 (comp, 2H), 2.99-2.86 (comp, 2H), 2.74-2.68 (comp, 2H).  $^{13}\text{C}$  NMR (126 MHz,  $\text{CDCl}_3$ )- *syn*-isomer  $\delta$  206.4, 205.3, 165.3, 147.7, 147.1, 129.0, 123.9, 89.3, 70.3, 53.0, 52.5, 48.2, 45.0, 40.8.  $^{13}\text{C}$  NMR (126 MHz,  $\text{CDCl}_3$ )- *anti*-isomer  $\delta$  207.5, 205.4, 166.1, 147.3, 144.4, 130.1, 123.2, 86.2, 70.4, 53.1, 52.0, 46.6, 45.9, 43.6. IR ( $\text{cm}^{-1}$ ): 2959.23, 2915.84, 2858.95, 1769.37, 1736.58, 1707.66, 1607.38, 1507.10, 1345.11. HRMS (ESI+): expected mass 334.0921, found 334.0918.

**Methyl-4,8-dioxo-2-(4-(trifluoromethyl)phenyl)-9-oxabicyclo[4.2.1]nonane-1-carboxylate (193c)**



Purified by chromatography on silica gel (gradient elution: hexane/ethyl acetate (90% to 60% hexane): yellow solid (92% yield), based on a 0.69 mmol scale of Methyl 2-diazo-3-oxo-4-((2*S*\*,6*S*\*)-4-oxo-6-(4-(trifluoromethyl)phenyl)tetrahydro-2*H*-pyran-2-yl)butanoate.

<sup>1</sup>H NMR (500 MHz, CDCl<sub>3</sub>)- *syn*-isomer δ 7.56-7.53 (comp, 2H), 7.47-7.45 (comp, 2H), 5.26-5.23 (m, 1H), 3.63 (dd, *J* = 9.3, 6.5 Hz, 1H), 3.40-3.34 (m, 1H), 3.35 (s, 3H), 3.01 (dd, *J* = 18.0, 9.3 Hz, 1H), 2.95-2.88 (m, 1H), 2.74-2.65 (m, 1H), 2.56-2.50 (comp, 2H).

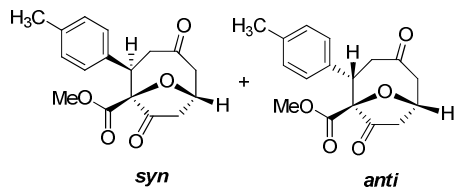
<sup>1</sup>H NMR (500 MHz, CDCl<sub>3</sub>)- *anti*-isomer δ 7.56-7.53 (comp, 2H), 7.38-7.37 (comp, 2H), 5.02 (ddt, *J* = 10.0, 6.5, 1.6 Hz, 1H), 3.84 (dd, *J* = 10.0, 5.7 Hz, 1H), 3.57 (s, 3H), 3.22-3.14 (comp, 2H), 2.95-2.88 (comp, 2H), 2.74-2.65 (comp, 2H).

<sup>13</sup>C NMR (126 MHz, CDCl<sub>3</sub>)- *syn*-isomer δ 206.7, 205.8, 165.5, 144.3, 129.7 (q, *J* = 32.5 Hz), 128.4, 125.6 (q, *J* = 3.7 Hz), 125.3 (q, *J* = 271 Hz), 89.5, 70.2, 52.9, 48.5, 46.8, 45.2, 40.8.

<sup>13</sup>C NMR (126 MHz, CDCl<sub>3</sub>)- *anti*-isomer δ 207.5, 205.5, 166.0, 140.9, 129.7 (q, *J* = 32.5 Hz), 129.4, 125.2 (q, *J* = 3.7 Hz), 125.1 (q, *J* = 271 Hz), 86.3, 70.0, 52.5, 51.9, 47.0, 46.7, 43.9.

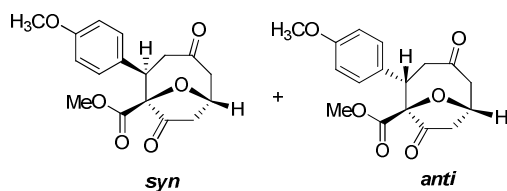
IR (cm<sup>-1</sup>): 2969, 2930, 1769, 1741, 1703, 1331. HRMS (ESI<sup>+</sup>): expected mass 357.0944, found 357.0951.

**Methyl 4,8-dioxo-2-*p*-tolyl-9-oxabicyclo[4.2.1]nonane-1-carboxylate (193d)**



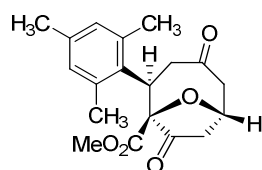
Purified by chromatography on silica gel (gradient elution: hexane/ethyl acetate (90% to 70% hexane): yellow solid (55% yield), based on a 0.79 mmol scale of Methyl 2-diazo-3-oxo-4-((2*S*\*,6*S*\*)-4-oxo-6-*p*-tolyltetrahydro-2*H*-pyran-2-yl)butanoate. <sup>1</sup>H NMR (500 MHz, CDCl<sub>3</sub>)- *syn*-isomer δ 7.22-7.20 (m, 1H), 7.10-7.05 (comp, 3H), 5.24-5.20 (m, 1H), 3.52 (dd, *J* = 9.5, 6.5 Hz, 1H), 3.35 (s, 3H), 3.01-2.94 (comp, 2H), 2.74-2.65 (comp, 2H), 2.52-2.47 (comp, 2H), 2.30 (s, 3H). <sup>1</sup>H NMR (500 MHz, CDCl<sub>3</sub>)- *anti*-isomer δ 7.22-7.20 (m, 1H), 7.10-7.05 (comp, 3H), 5.00-4.96 (m, 1H), 3.70 (dd, *J* = 11.7, 4.5 Hz, 1H), 3.55 (s, 3H), 3.40-3.30 (comp, 3H), 3.18 (dd, *J* = 19.0, 10.0 Hz, 1H), 3.01-2.94 (m, 1H), 2.89-2.86 (m, 1H), 2.31 (s, 3H). <sup>13</sup>C NMR (126 MHz, CDCl<sub>3</sub>)- *syn*-isomer δ 207.1, 206.7, 165.7, 137.1, 136.9, 129.3, 128.0, 90.0, 70.0, 52.7, 52.6, 48.9, 45.3, 40.9, 21.0. <sup>13</sup>C NMR (126 MHz, CDCl<sub>3</sub>)- *anti*-isomer δ 207.2, 206.1, 166.1, 137.7, 133.4, 129.0, 128.5, 86.7, 69.5, 52.7, 51.7, 47.6, 47.6, 44.1, 21.1. IR (cm<sup>-1</sup>): 2959, 2930, 1765, 1746, 1708. HRMS (ESI+): expected mass 303.1227, found 303.1231.

**Methyl 2-(4-methoxyphenyl)-4,8-dioxo-9-oxabicyclo[4.2.1]nonane-1-carboxylate (193e)**



Purified by chromatography on silica gel (gradient elution: hexane/ethyl acetate (90% to 60% hexane): yellow solid (22% yield), based on a 0.69 mmol scale of Methyl 2-diazo-4-((2*S*\*,6*S*\*)-6-(4-methoxyphenyl)-4-oxotetrahydro-2*H*-pyran-2-yl)-3-oxobutanoate. <sup>1</sup>H NMR (500 MHz, CDCl<sub>3</sub>)- *syn*-isomer δ 7.25 -7.21 (comp, 2H), 6.84-6.82 (comp, 2H), 5.23-5.20 (m, 1H), 3.77 (s, 3H), 3.52 (dd, *J* = 9.0, 6.6 Hz, 1H), 3.37 (s, 3H), 3.01-2.93 (comp, 2H), 2.73-2.63 (comp, 2H), 2.52-2.48 (comp, 2H). <sup>1</sup>H NMR (500 MHz, CDCl<sub>3</sub>)- *anti*-isomer δ 7.25 -7.21 (comp, 2H), 7.12-7.11 (m, 1H), 6.84-6.82 (m, 1H), 4.99-4.96 (m, 1H), 3.89-3.79 (m, 1H), 3.78 (s, 3H), 3.71-3.67 (m, 1H), 3.56 (s, 3H), 3.39-3.30 (comp, 2H), 3.18 (dd, *J* = 19.0, 10.0 Hz, 1H), 3.01-2.93 (m, 1H), 2.87 (dd, *J* = 14.5, 4.0 Hz, 1H). <sup>13</sup>C NMR (126 MHz, CDCl<sub>3</sub>)- *syn*-isomer δ 207.2, 206.7, 165.7, 158.8, 129.8, 129.3, 114.0, 90.0, 70.0, 55.2, 52.8, 52.6, 48.9, 45.0, 40.9. <sup>13</sup>C NMR (126 MHz, CDCl<sub>3</sub>)- *anti*-isomer δ 207.4, 206.1, 165.7, 159.2, 131.8, 128.5, 113.7, 86.7, 69.4, 55.1, 52.7, 51.7, 47.7, 47.2, 44.1. IR (cm<sup>-1</sup>): 2954.41, 2920.66, 2834.85, 1769.37, 1741.41, 1707.66, 1607.38, 1507.10, 1254.47. HRMS (ESI<sup>+</sup>): expected mass 319.1176, found 319.1184.

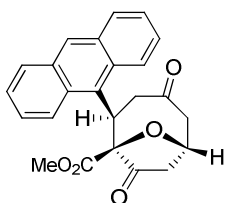
**(1*S*\*,2*R*\*,6*R*\*)-Methyl 2-mesityl-4,8-dioxo-9-oxabicyclo[4.2.1]nonane-1-carboxylate (*syn*-211)**



Purified by chromatography on silica gel (gradient elution: hexane/ethyl acetate (100% to 70% hexane): pale yellow oil (42% yield), based on a 0.59 mmol scale of Methyl 2-

diazo-4-((2*S*\*,6*S*\*)-6-mesityl-4-oxotetrahydro-2*H*-pyran-2-yl)-3-oxobutanoate. <sup>1</sup>H NMR (500 MHz, CDCl<sub>3</sub>) δ 6.81 (d, *J* = 12.0 Hz, 2H), 5.24-5.21 (m, 1H), 3.92 (dd, *J* = 12.0, 6.0 Hz, 1H), 3.41 (dd, *J* = 12.0, 6.0 Hz, 1H), 3.39-3.34 (m, 1H), 3.20 (s, 3H), 2.90 (ddd, *J* = 17.5, 9.0, 0.5 Hz, 1H), 2.53 (s, 3H), 2.44 (s, 3H), 2.34-2.29 (comp, 3H), 2.21 (s, 3H). <sup>13</sup>C NMR (126 MHz, CDCl<sub>3</sub>) δ 207.7, 207.4, 165.7, 138.3, 136.5, 136.3, 133.0, 131.2, 129.2, 89.5, 70.2, 52.6, 52.2, 44.3, 41.7, 39.9, 21.3, 20.6, 20.5. IR (cm<sup>-1</sup>): 2967.96, 2921.85, 1768.57, 1743.99, 1700.67, 1609.83, 1433.53, 1264.48. HRMS (ESI+): expected mass 331.1540, found 331.1549.

**(1*S*\*,2*R*\*,6*R*\*)-Methyl 2-(anthracen-9-yl)-4,8-dioxo-9-oxabicyclo[4.2.1]nonane-1-carboxylate (*syn*-212)**

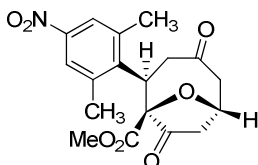


Purified by preparative thin layer chromatography (gradient elution: hexane/ethyl acetate (70% hexane): yellow solid (45% yield), based on a 0.29 mmol scale of Methyl 2-diazo-4-((2*S*\*,6*S*\*)-6-(anthracen-9-yl)-4-oxotetrahydro-2*H*-pyran-2-yl)-3-oxobutanoate. <sup>1</sup>H NMR (500 MHz, CDCl<sub>3</sub>) δ 9.04 (d, *J* = 9.0 Hz, 1H), 8.58 (d, *J* = 9.0 Hz, 1H), 8.39 (s, 1H), 7.99 (t, *J* = 7.2 Hz, 2H), 7.64-7.58 (comp, 2H), 7.50-7.44 (comp, 2H), 5.48 – 5.45 (m, 1H), 5.11 (dd, *J* = 12.0, 5.7 Hz, 1H), 3.80 (t, *J* = 12.0 Hz, 1H), 3.61 (dd, *J* = 12.0, 6.5 Hz, 1H), 3.07 (dd, *J* = 17.5, 9.0 Hz, 1H), 2.70 (s, 3H), 2.60 (comp, 2H), 2.49 (ddd, *J* = 11.0, 5.5, 1.5 Hz, 1H). <sup>13</sup>C NMR (126 MHz, CDCl<sub>3</sub>) δ 207.7, 207.6, 165.3, 131.7, 131.6, 131.4, 131.0, 129.5, 129.2, 129.1, 128.4, 126.9, 125.9, 125.6, 124.9, 124.9, 123.7, 89.4,

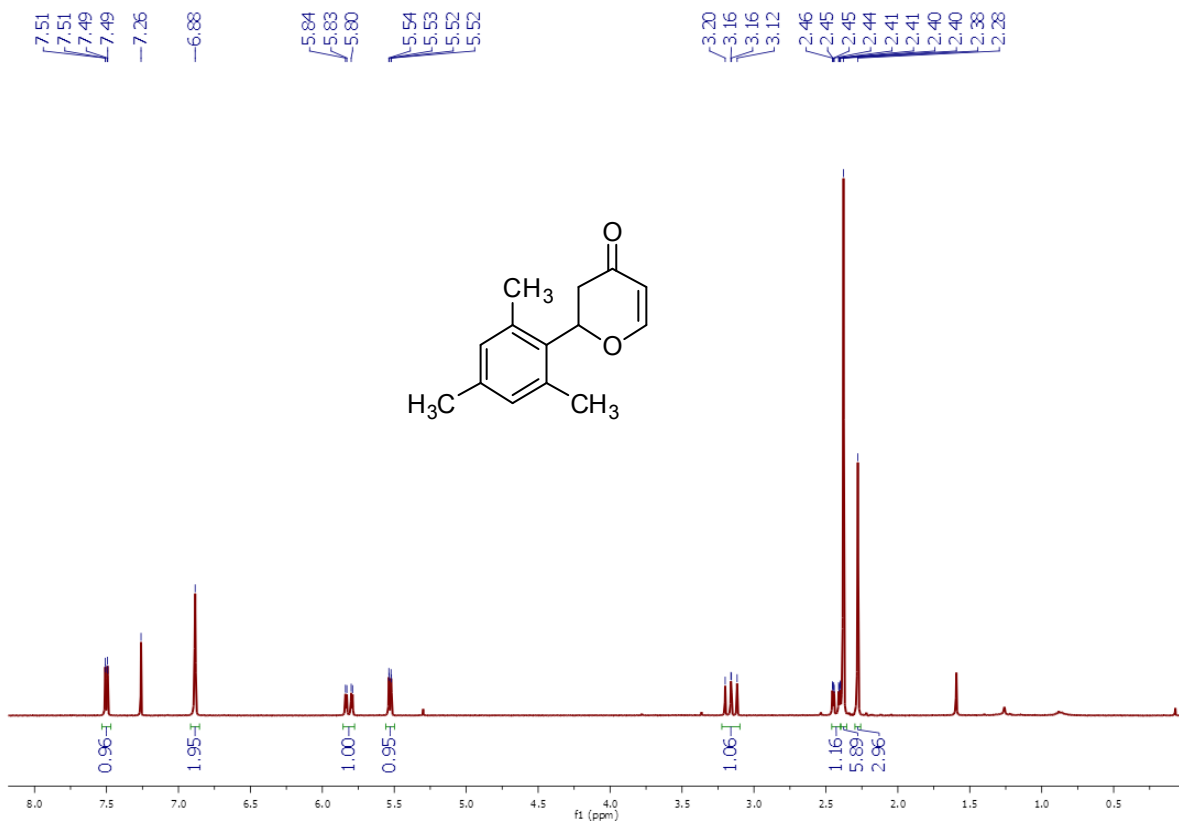
70.7, 52.7, 52.1, 46.2, 41.4, 40.2. IR (cm<sup>-1</sup>): 2953, 2926, 2853, 1772, 1726, 1699, 1597.

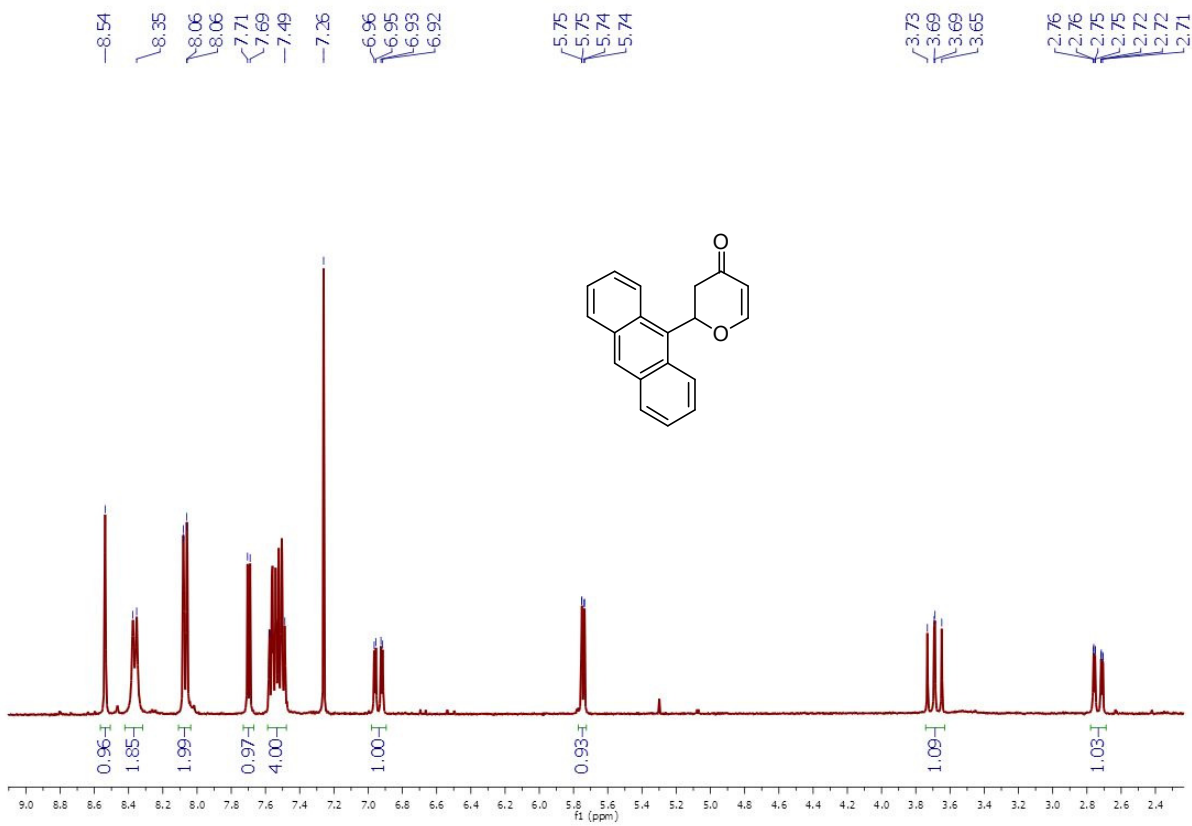
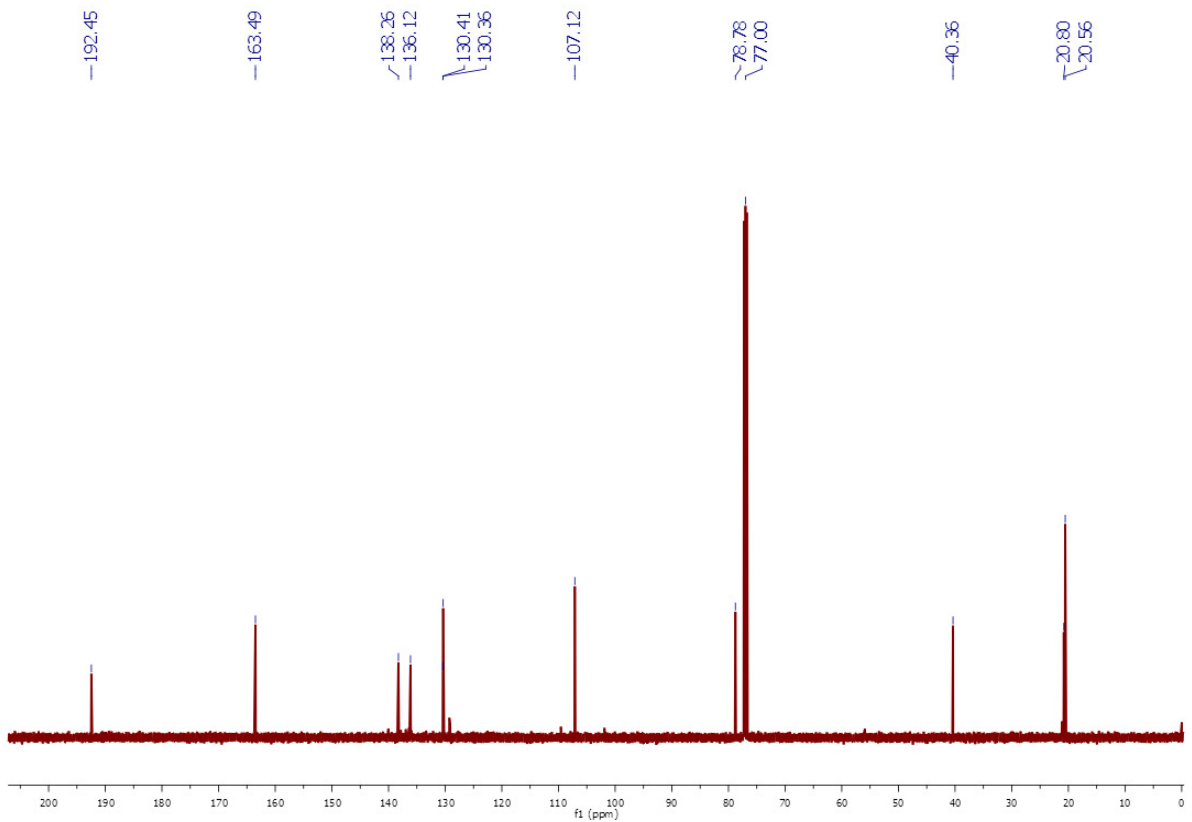
HRMS (ESI<sup>+</sup>): expected mass 389.1384, found 389.1391. M.p. 159-160 °C.

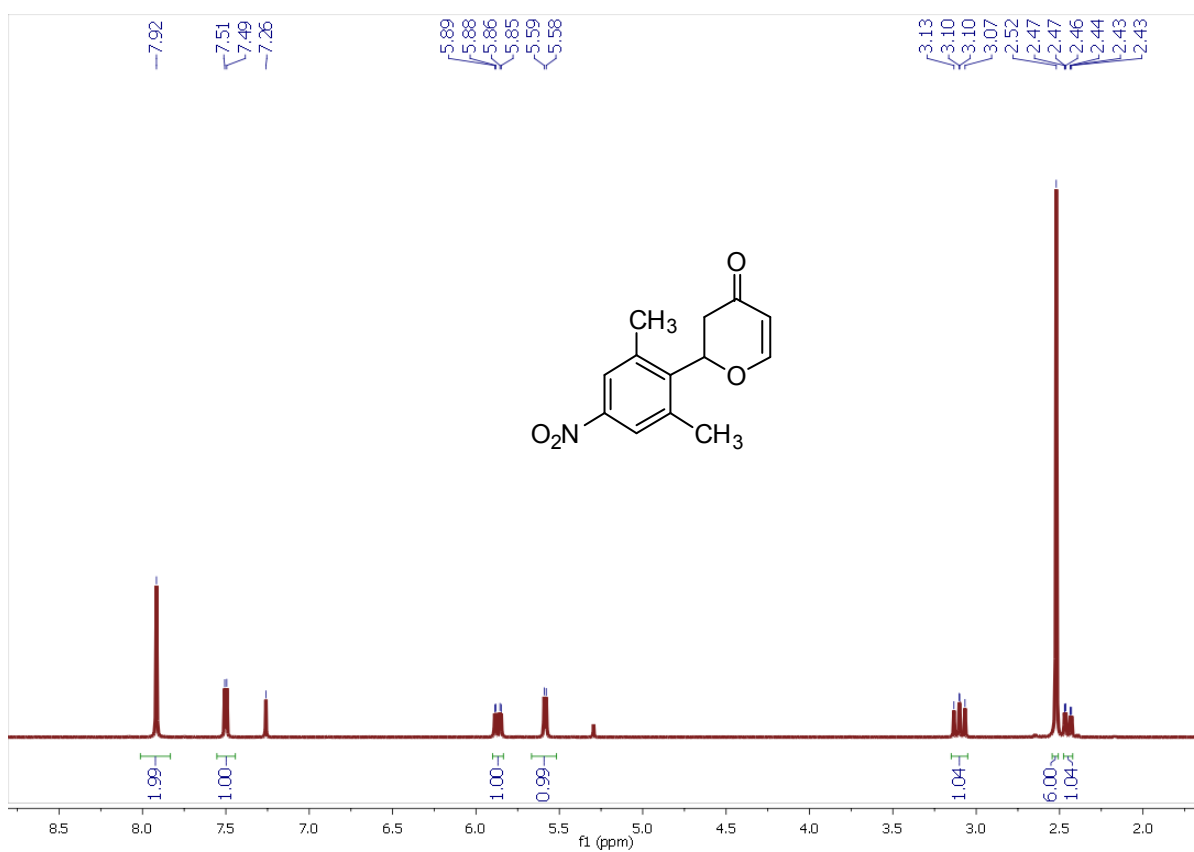
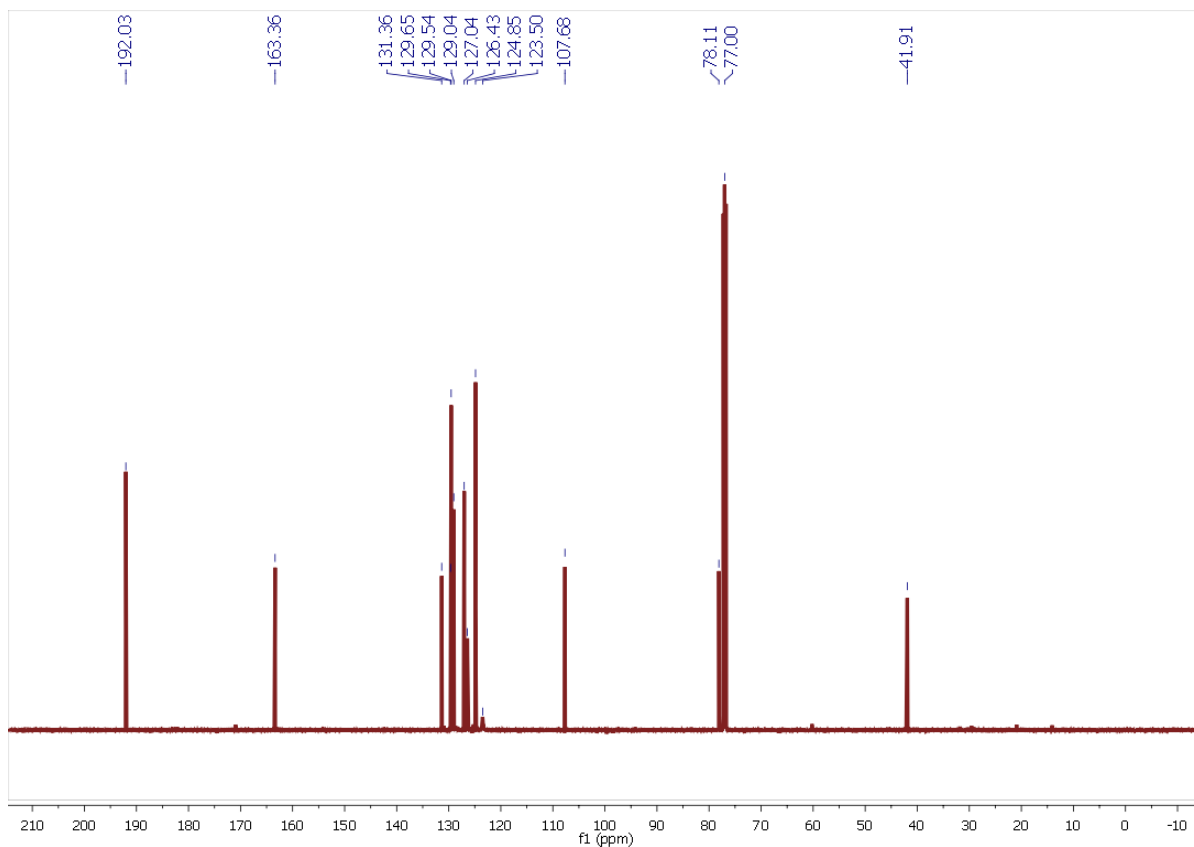
**(1*S*\*,2*R*\*,6*R*\*)-Methyl 2-(2,6-dimethyl-4-nitrophenyl)-4,8-dioxo-9-oxabicyclo[4.2.1]nonane-1-carboxylate (*syn*-213)**

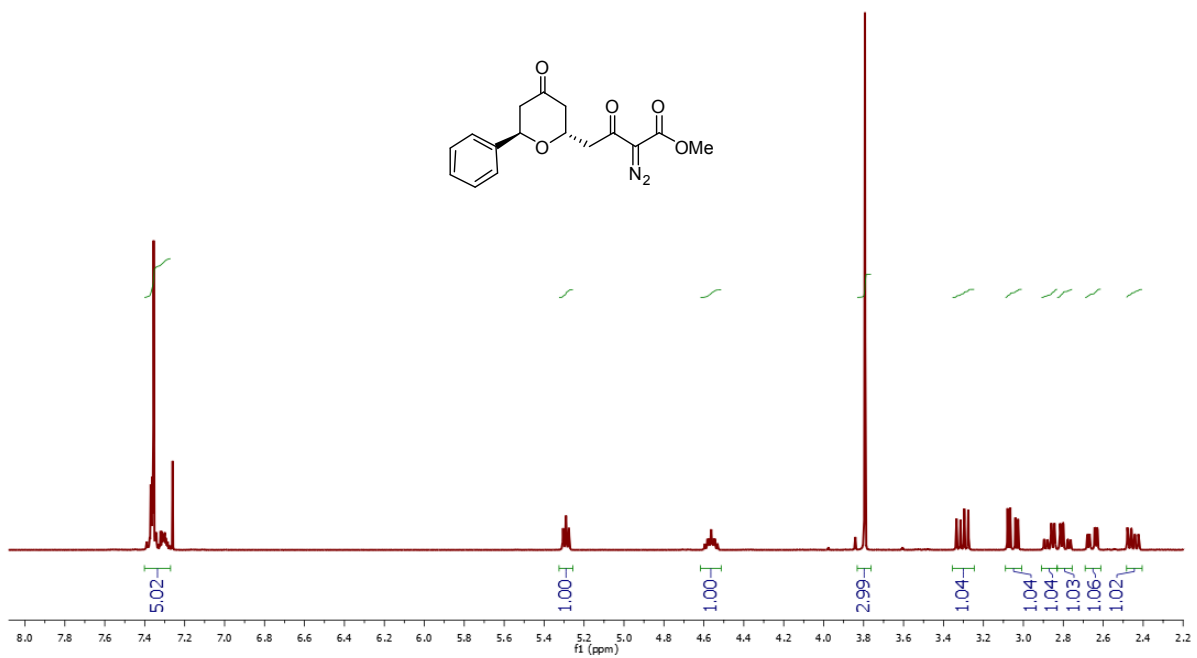
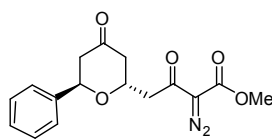
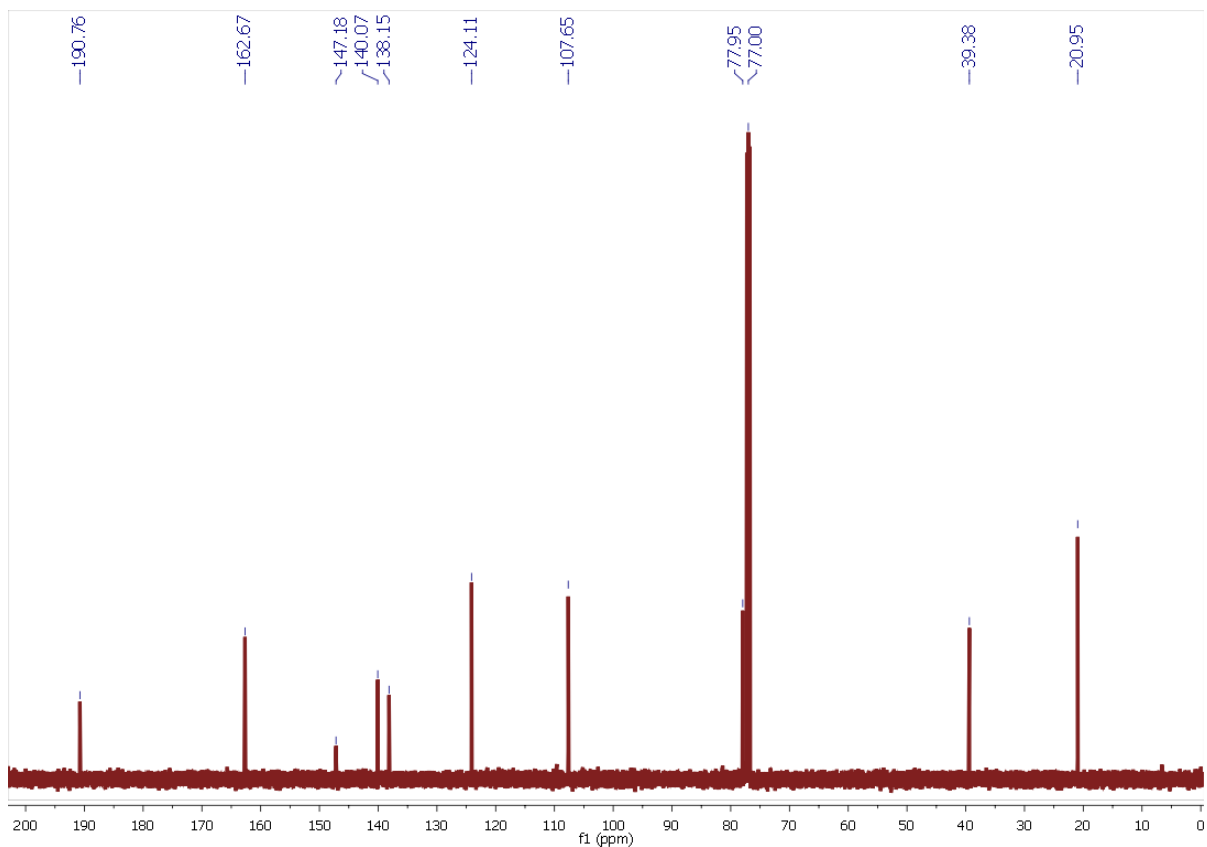


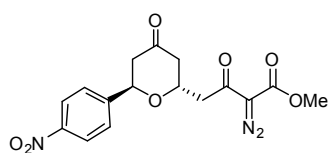
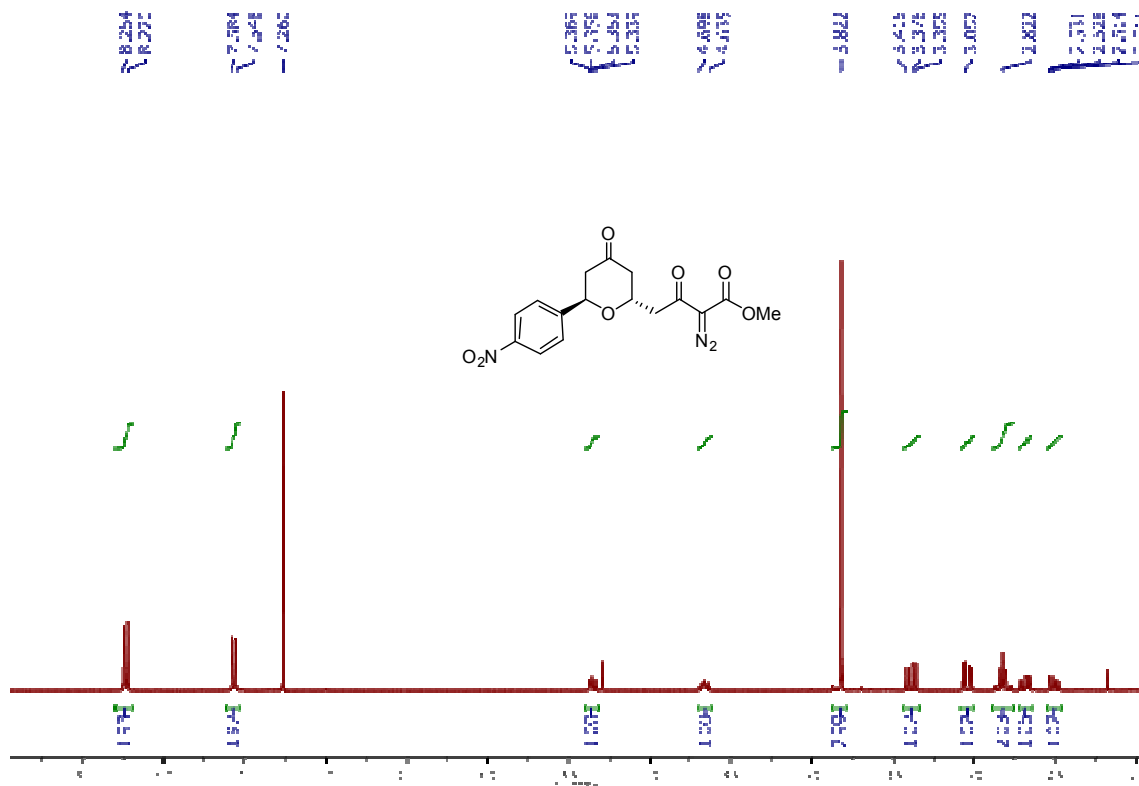
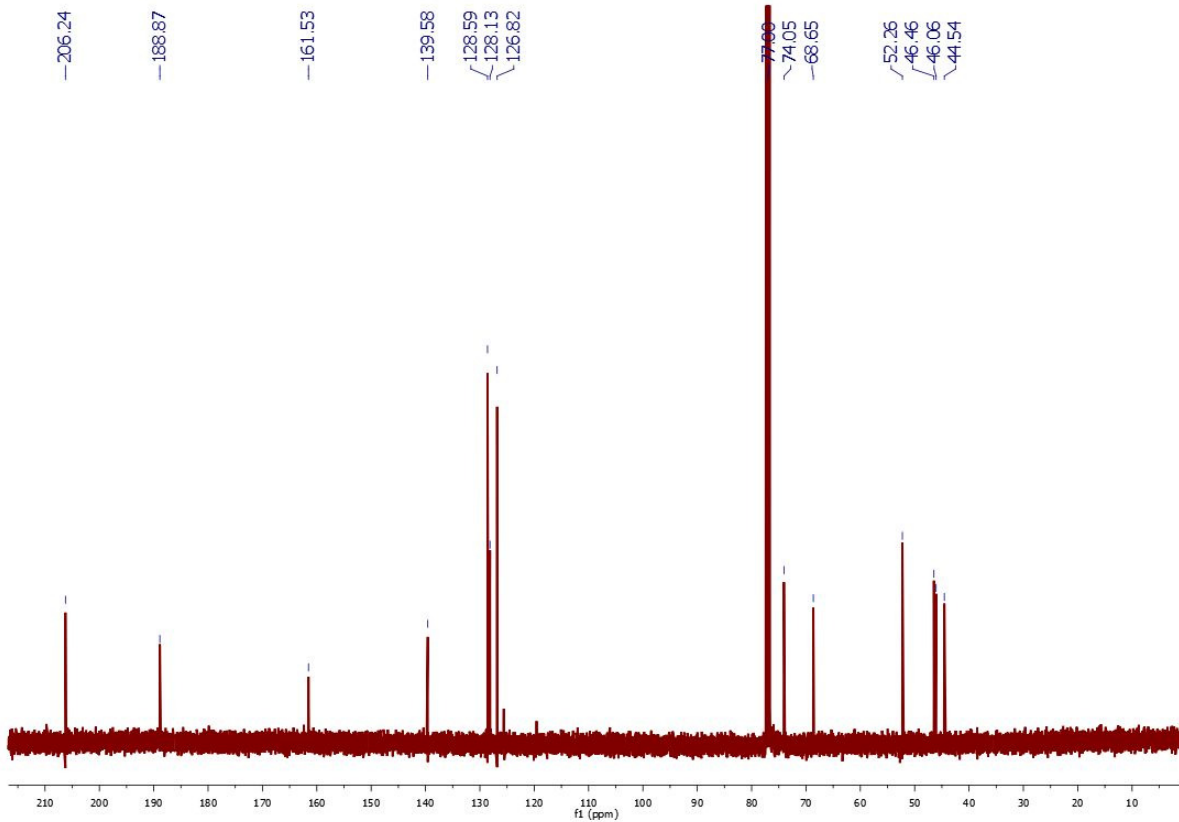
Purified by chromatography on silica gel (gradient elution: hexane/ethyl acetate (90% to 60% hexane): pale yellow solid (77% yield), based on a 0.49 mmol scale of Methyl 2-diazo-4-((2*R*\*,6*R*\*)-6-(2,6-dimethyl-4-nitrophenyl)-4-oxotetrahydro-2*H*-pyran-2-yl)-3-oxobutanoate. <sup>1</sup>H NMR (500 MHz, CDCl<sub>3</sub>) δ 7.86 (dd, *J* = 10.0, 2.5 Hz, 2H), 5.28-5.25 (m, 1H), 4.00 (dd, *J* = 12.0, 5.5 Hz, 1H), 3.42 (dd, *J* = 12.0, 6.5 Hz, 1H), 3.32-3.28 (m, 1H), 3.26 (s, 3H), 2.95 (dd, *J* = 18.0, 9.0 Hz, 1H), 2.66 (s, 3H), 2.59 (s, 3H), 2.51-2.44 (comp, 2H), 2.28 (ddd, *J* = 11.0, 5.5, 1.7 Hz, 1H). <sup>13</sup>C NMR (126 MHz, CDCl<sub>3</sub>) δ 206.8, 206.5, 165.3, 146.2, 144.0, 140.5, 138.3, 125.0, 122.6, 88.8, 70.6, 52.6, 52.6, 43.4, 41.8, 39.7, 21.7, 20.8. IR (cm<sup>-1</sup>): 2923, 2852, 2358, 1747, 1702, 1519, 1346, 1260, 1225. HRMS (ESI<sup>+</sup>): expected mass 362.1234, found 362.1241. M.p. 165-166 °C.

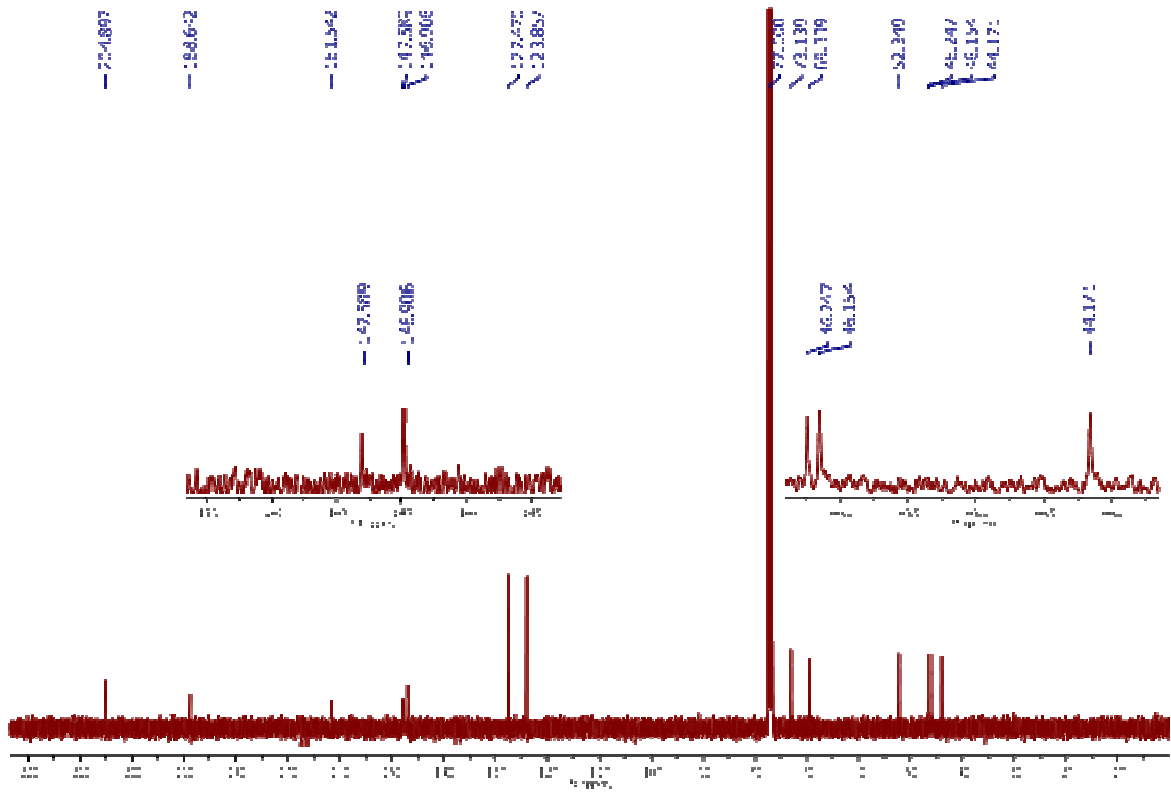


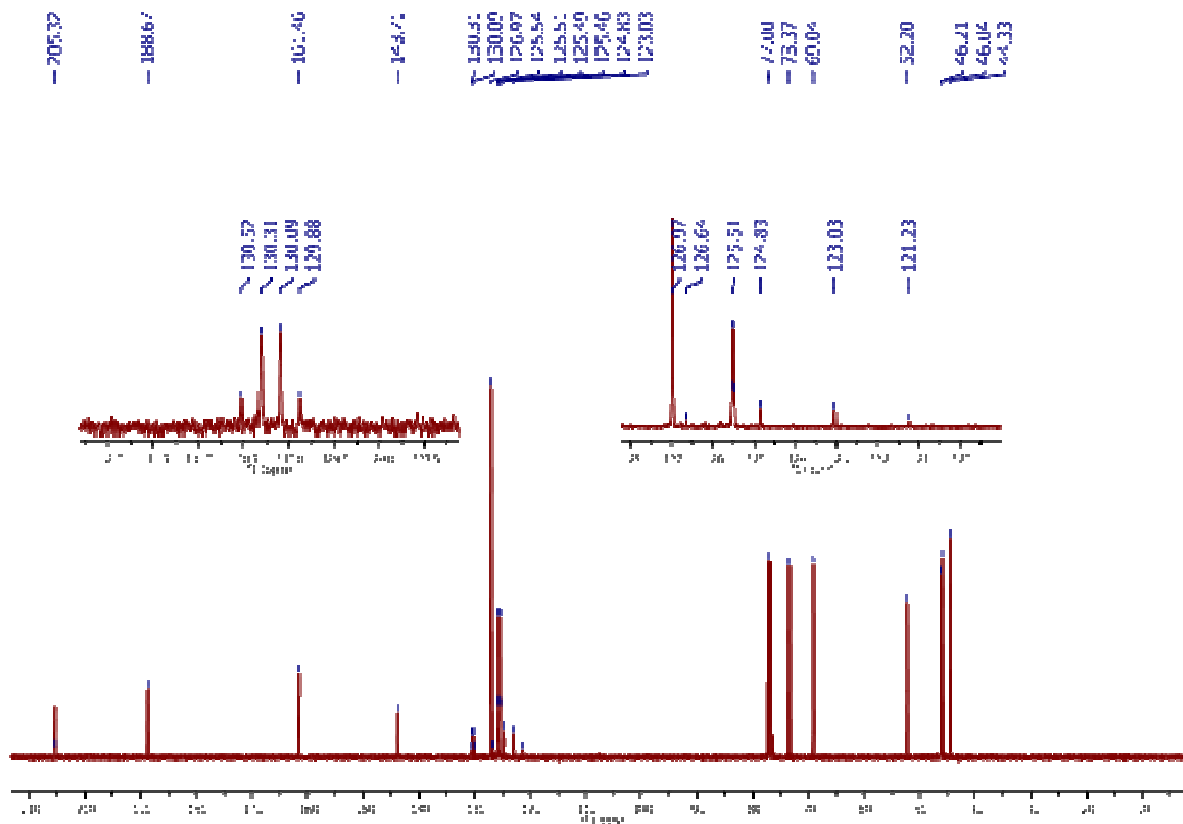
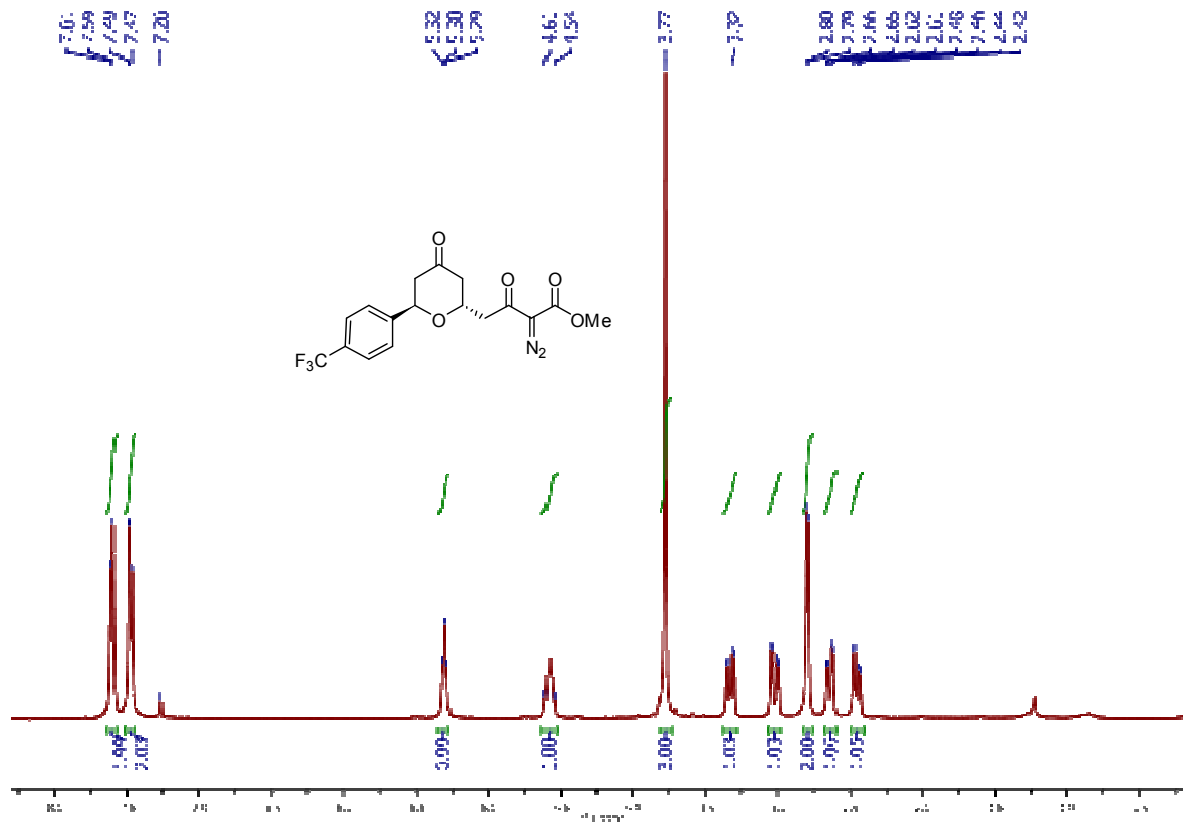


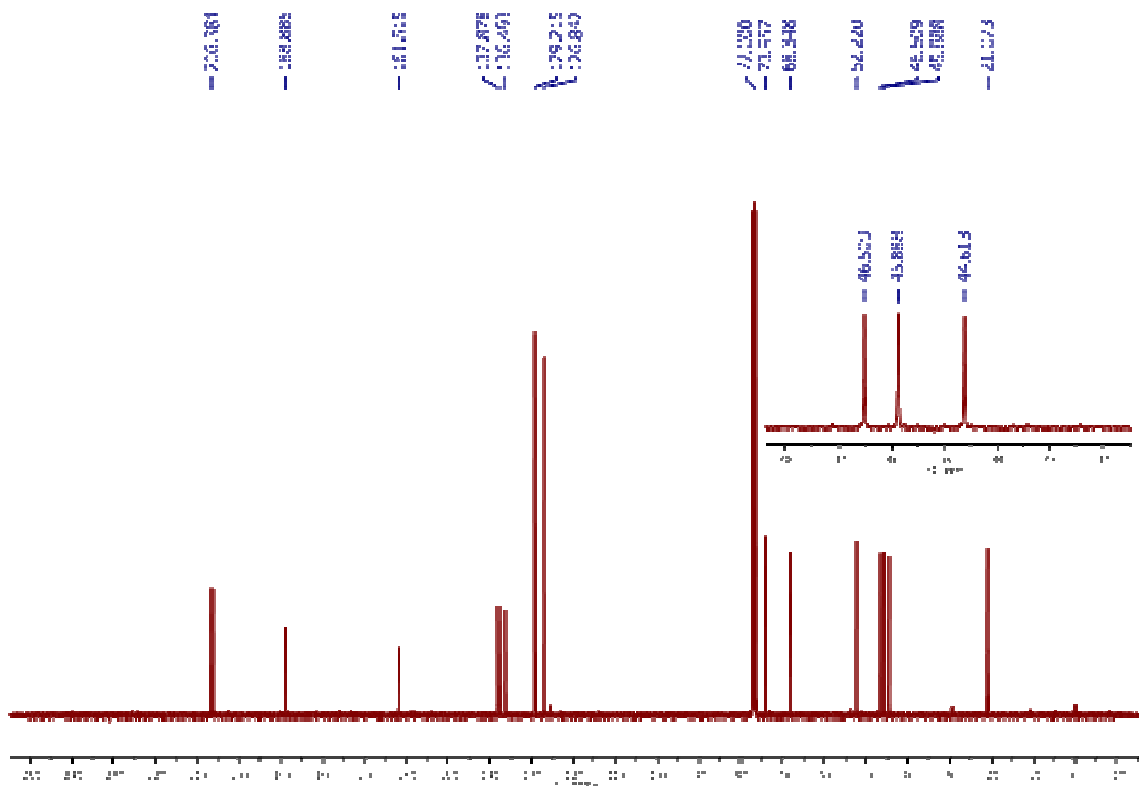
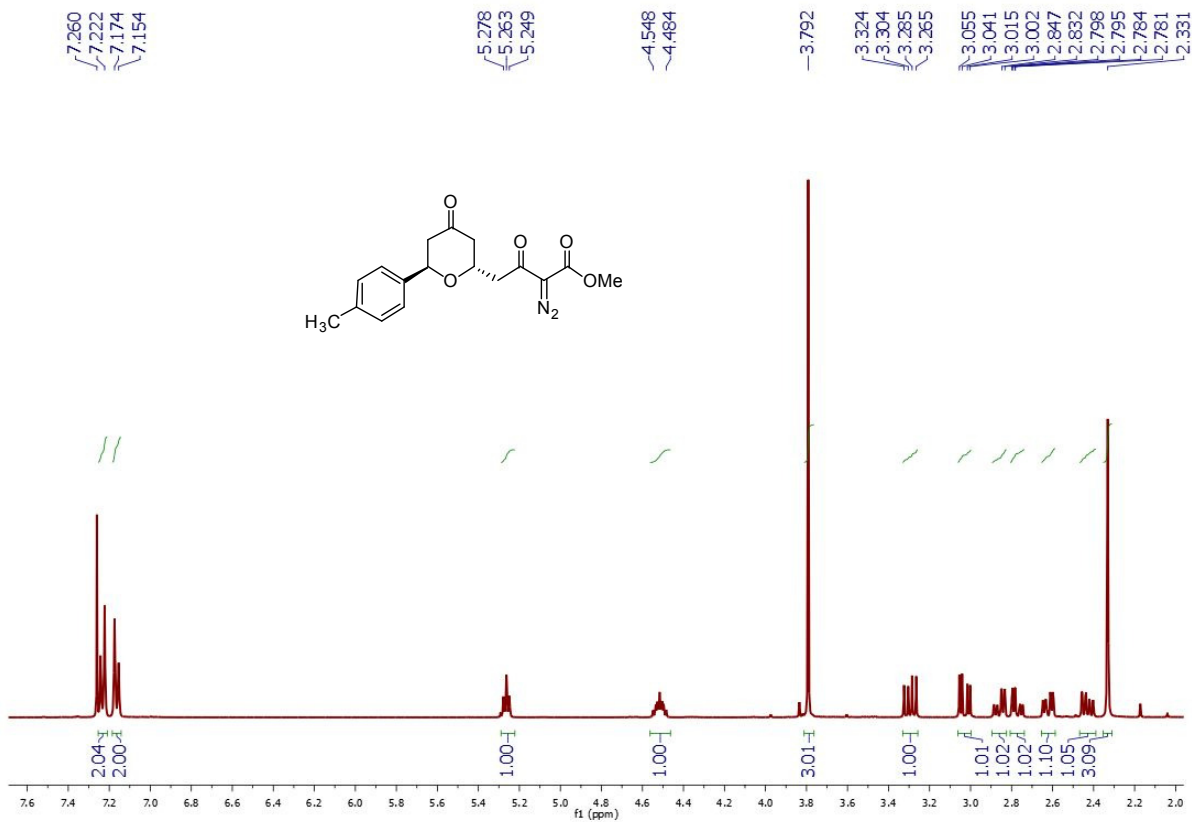


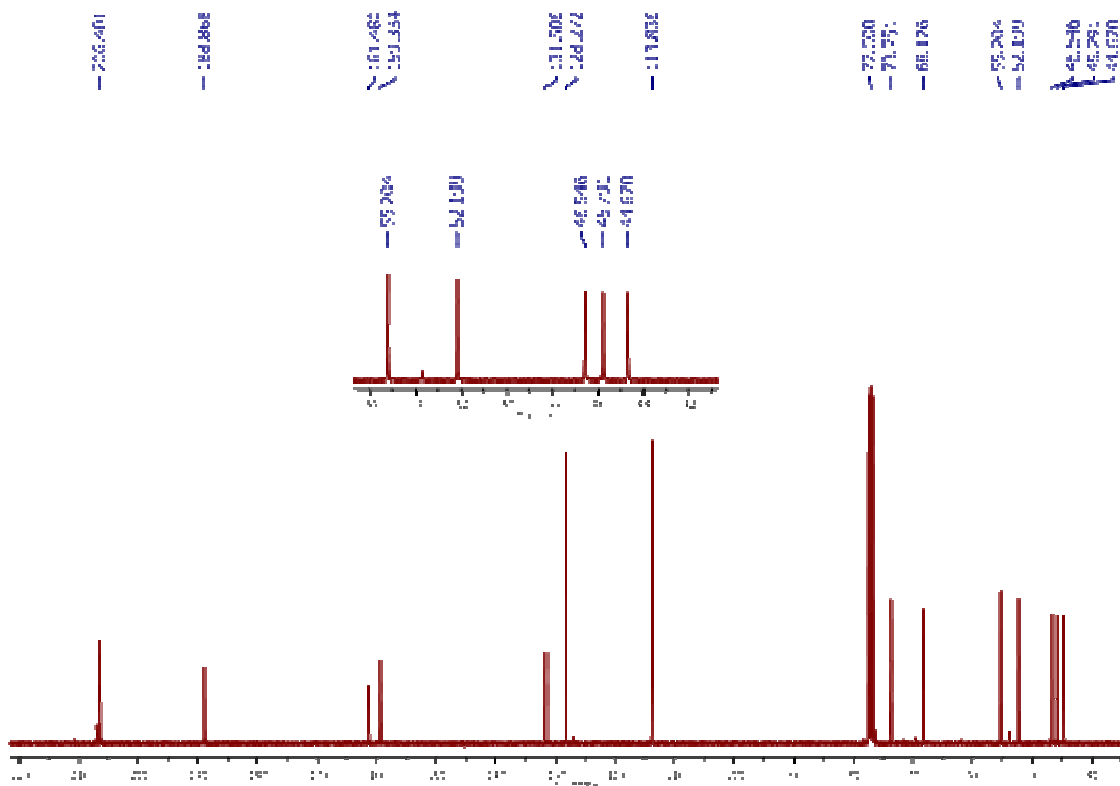
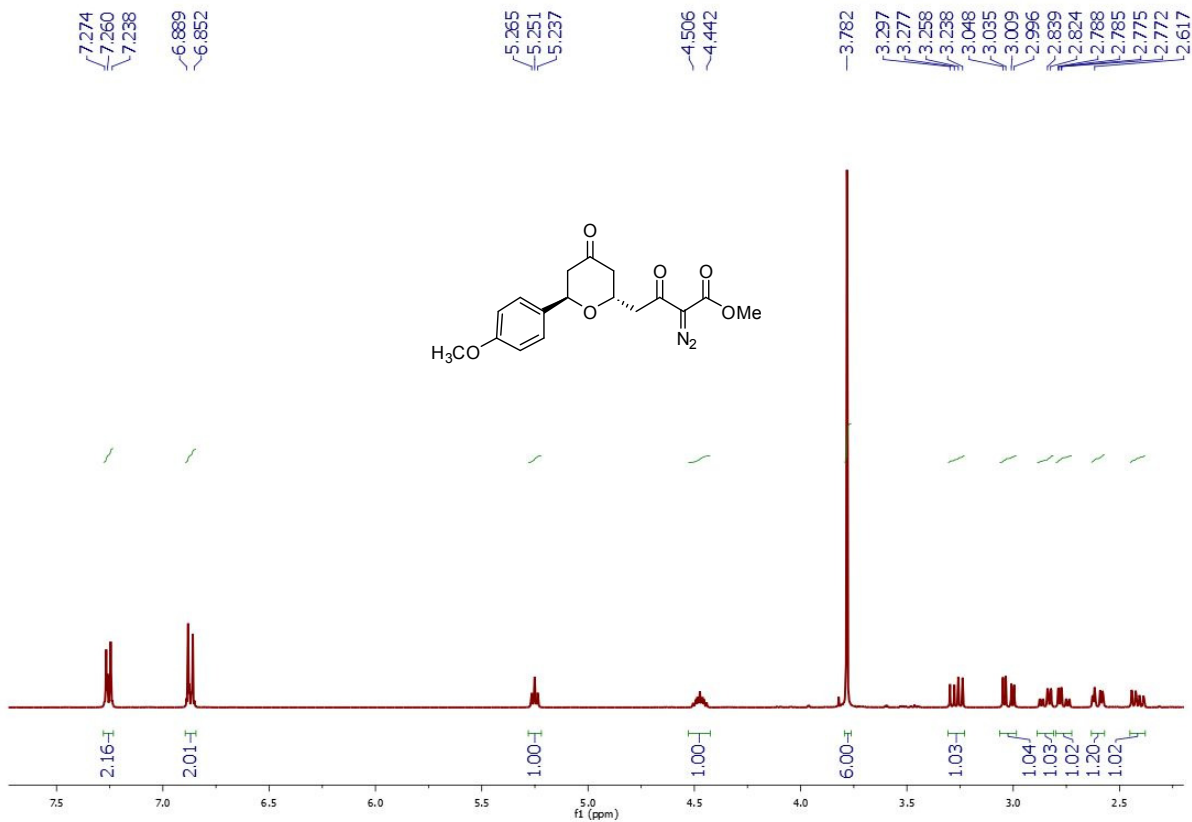


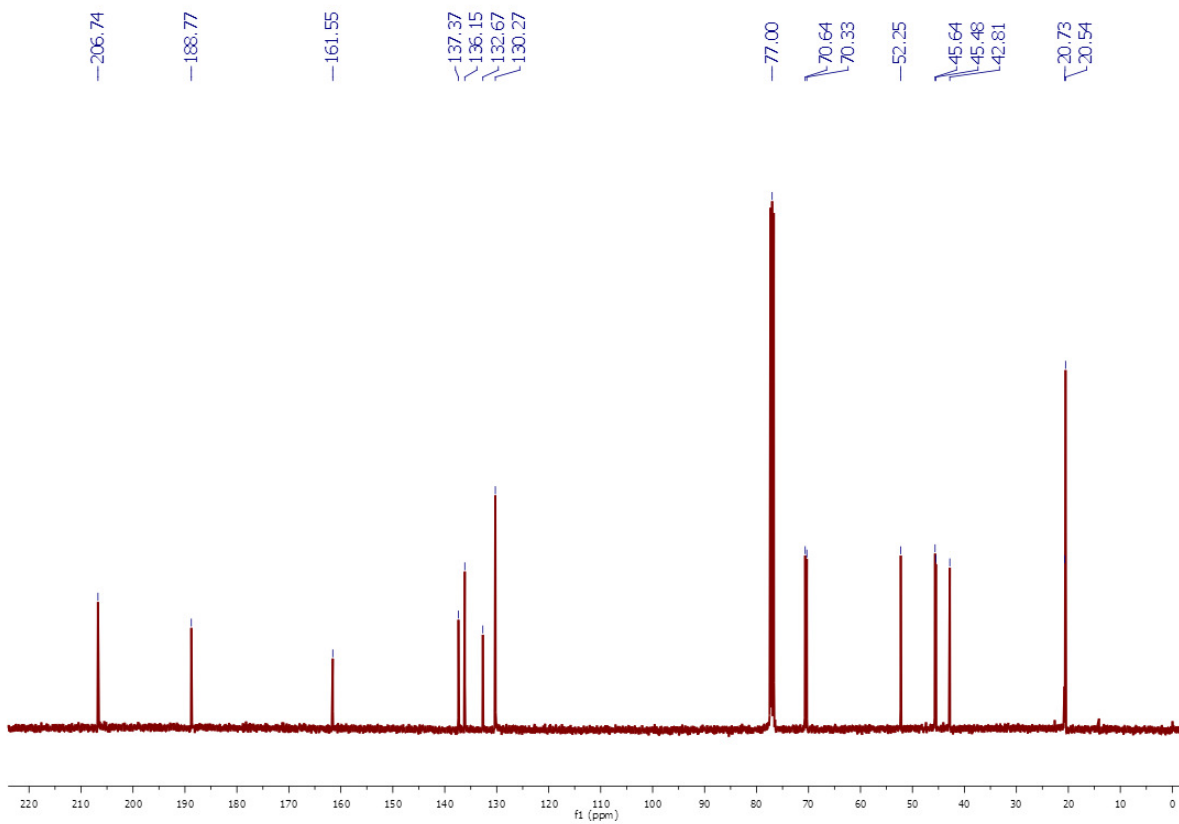
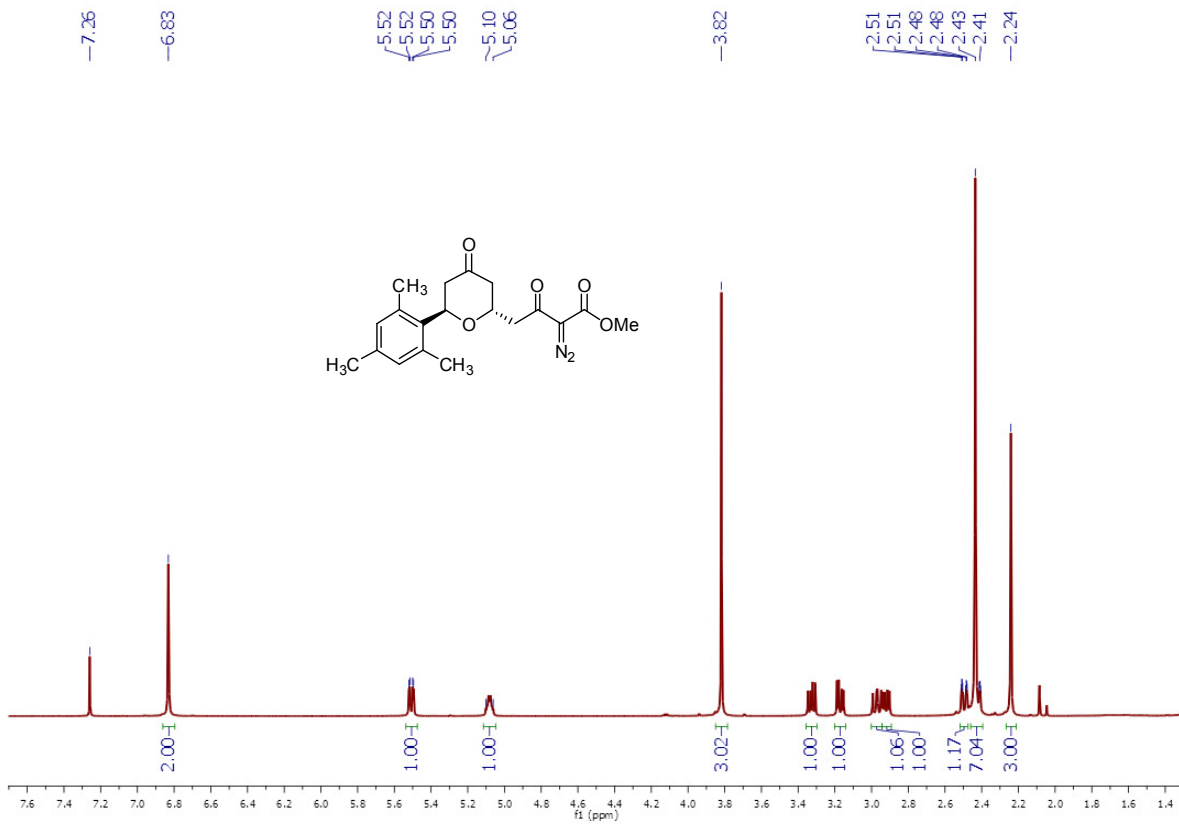


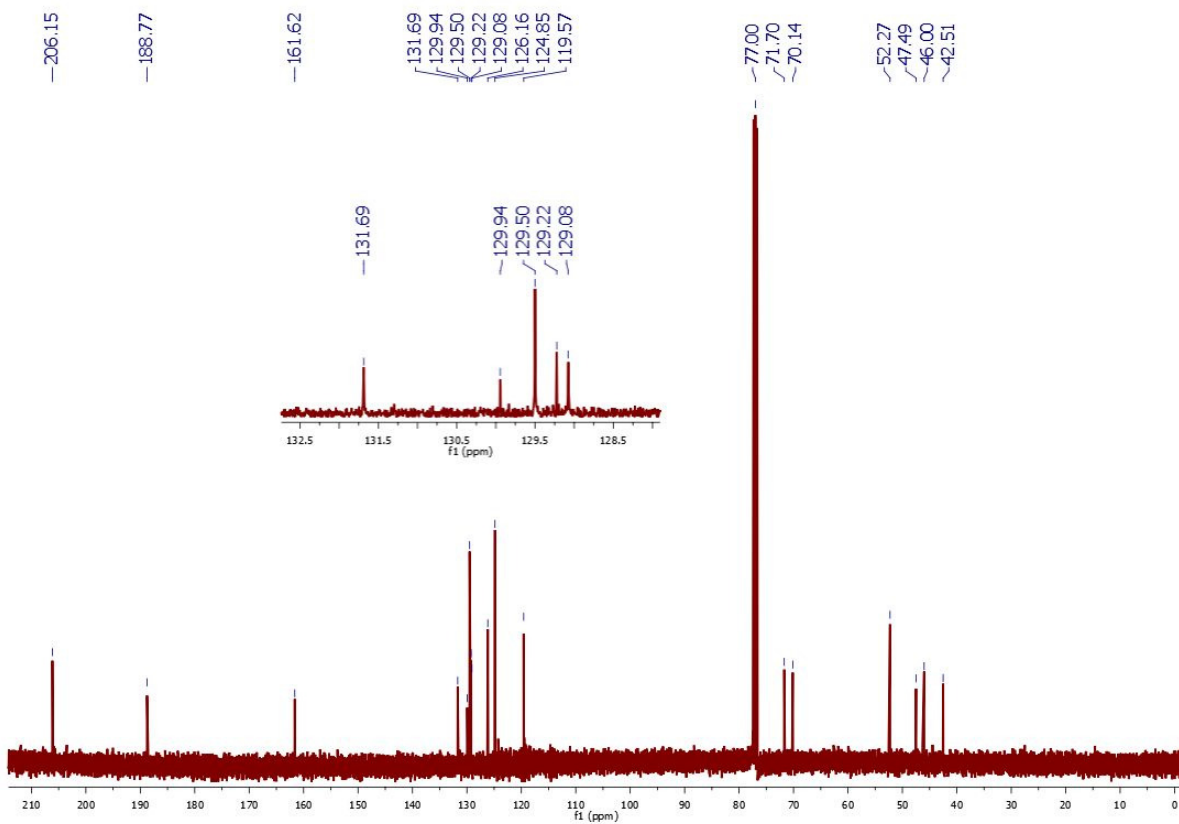
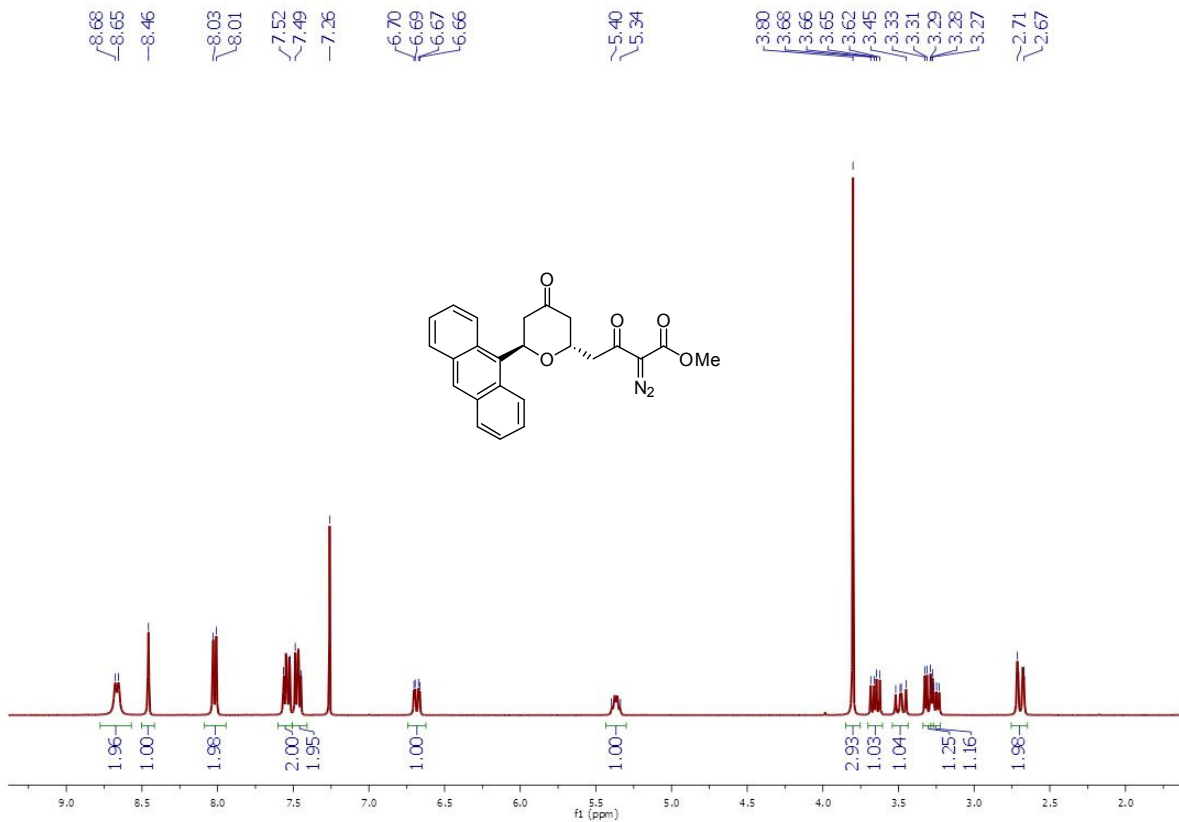


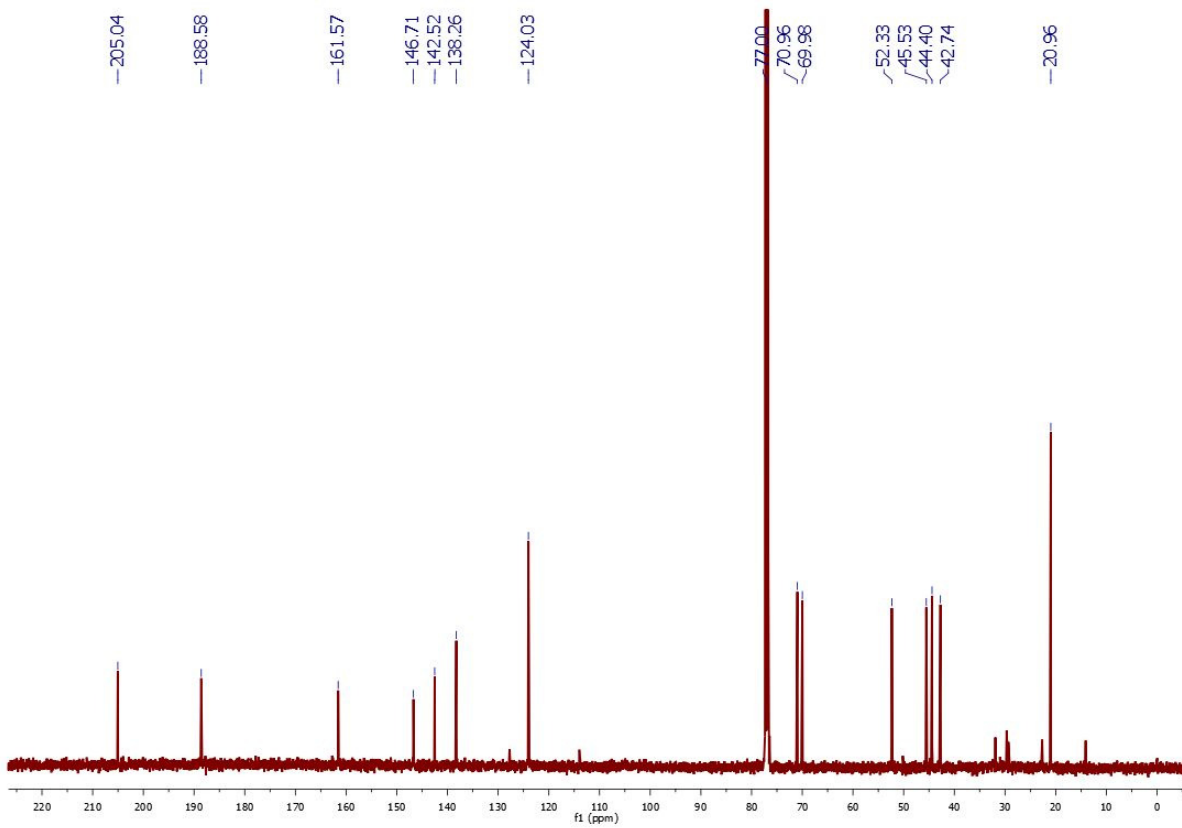
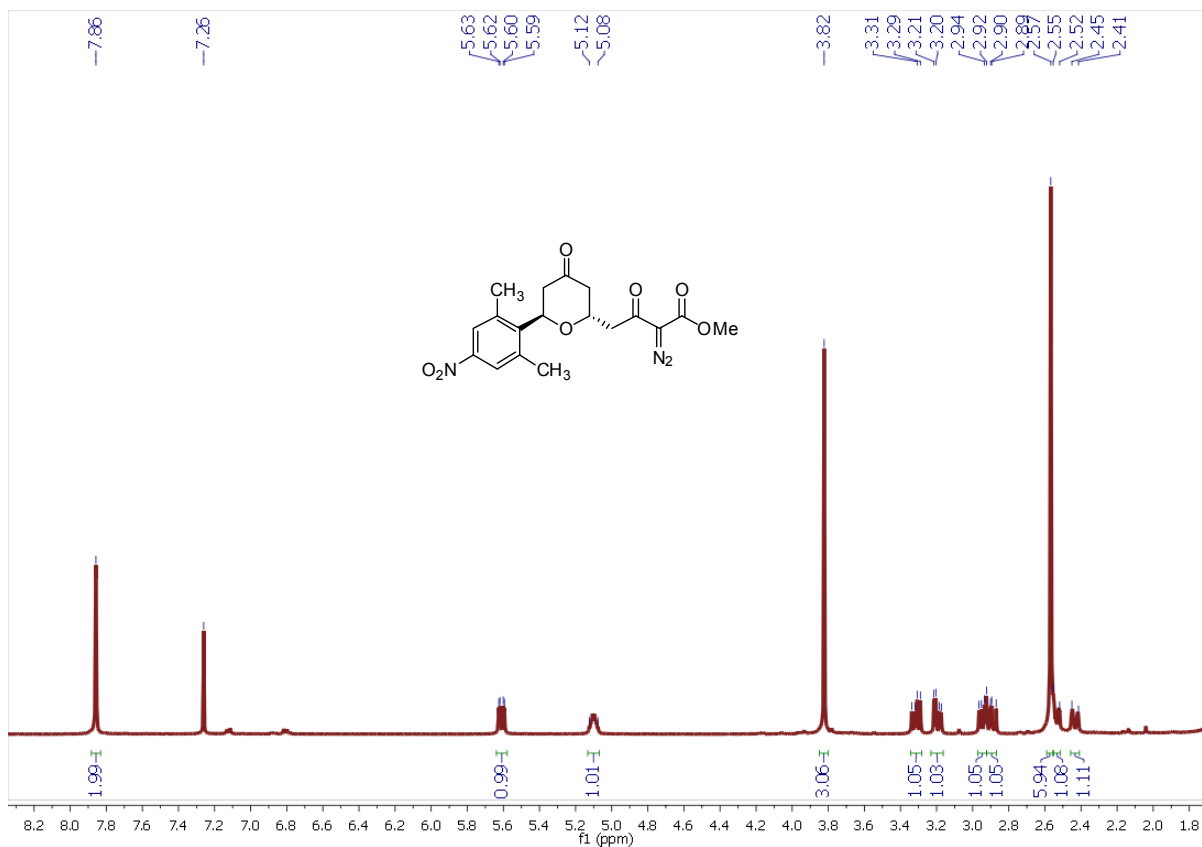


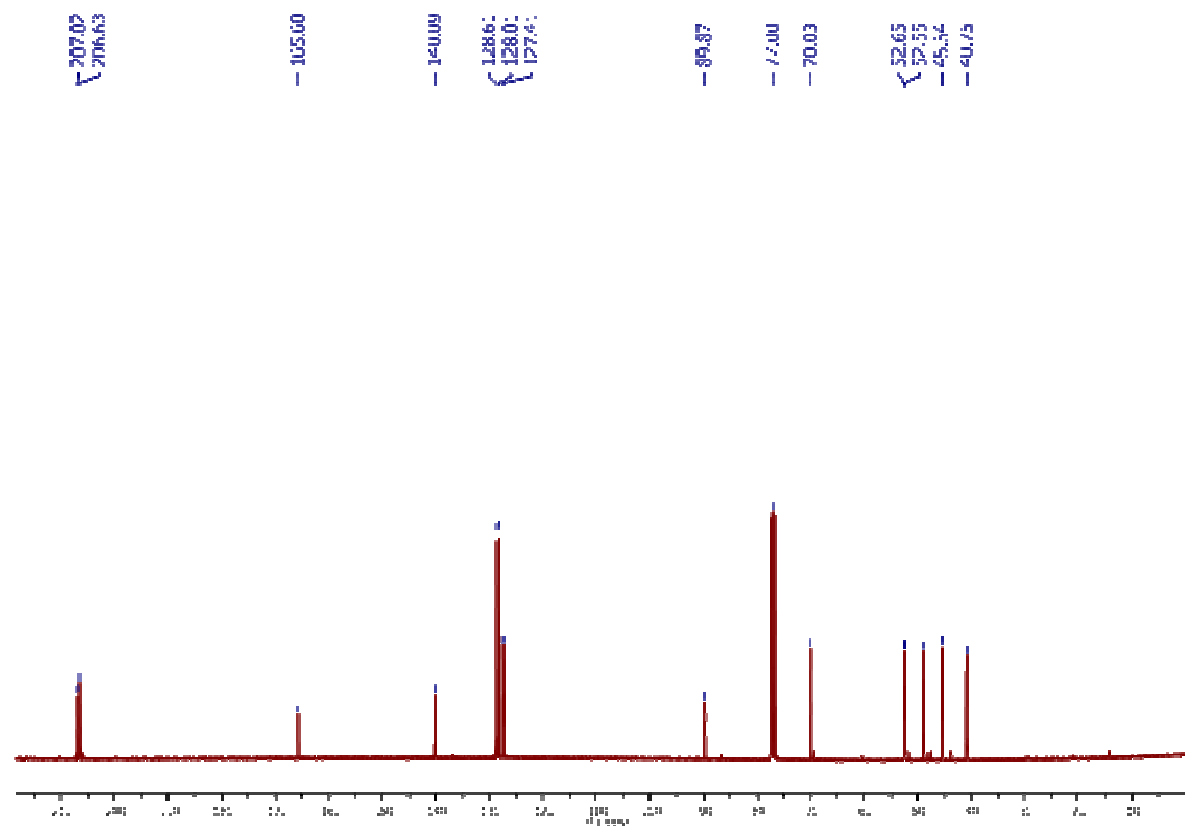
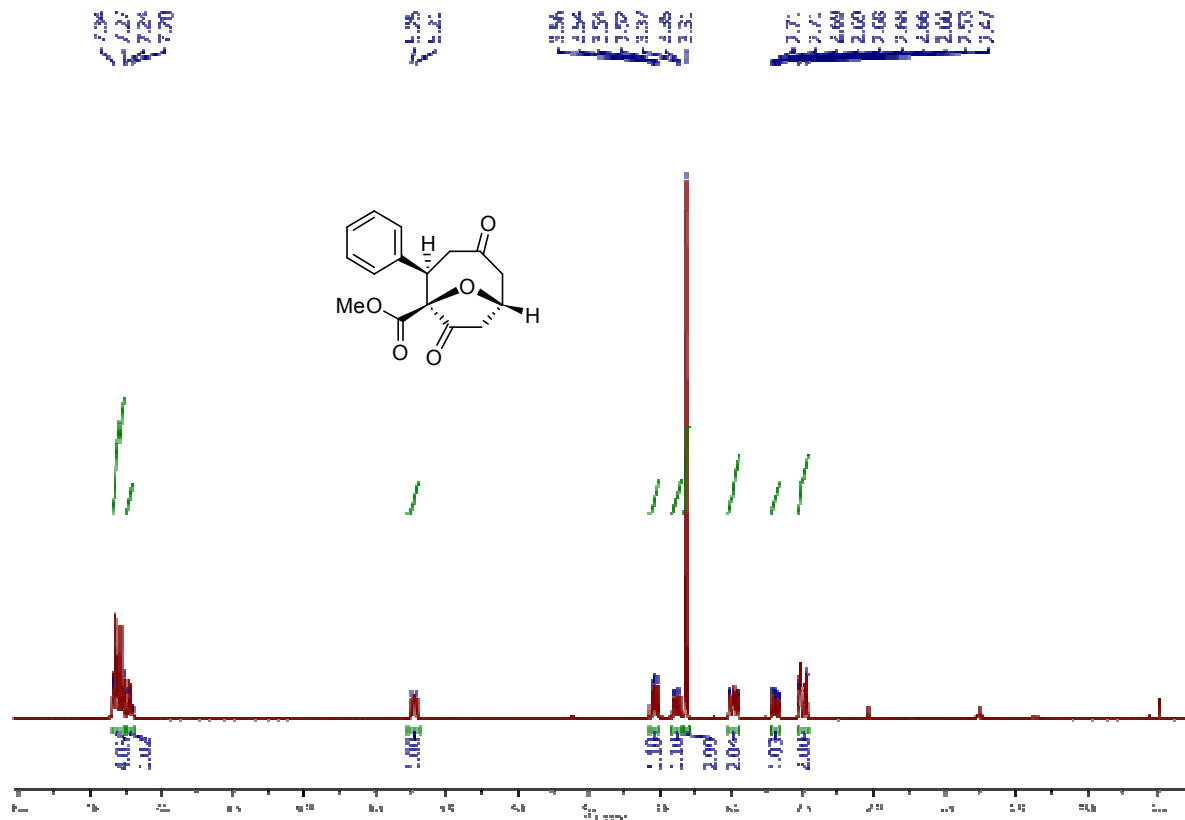


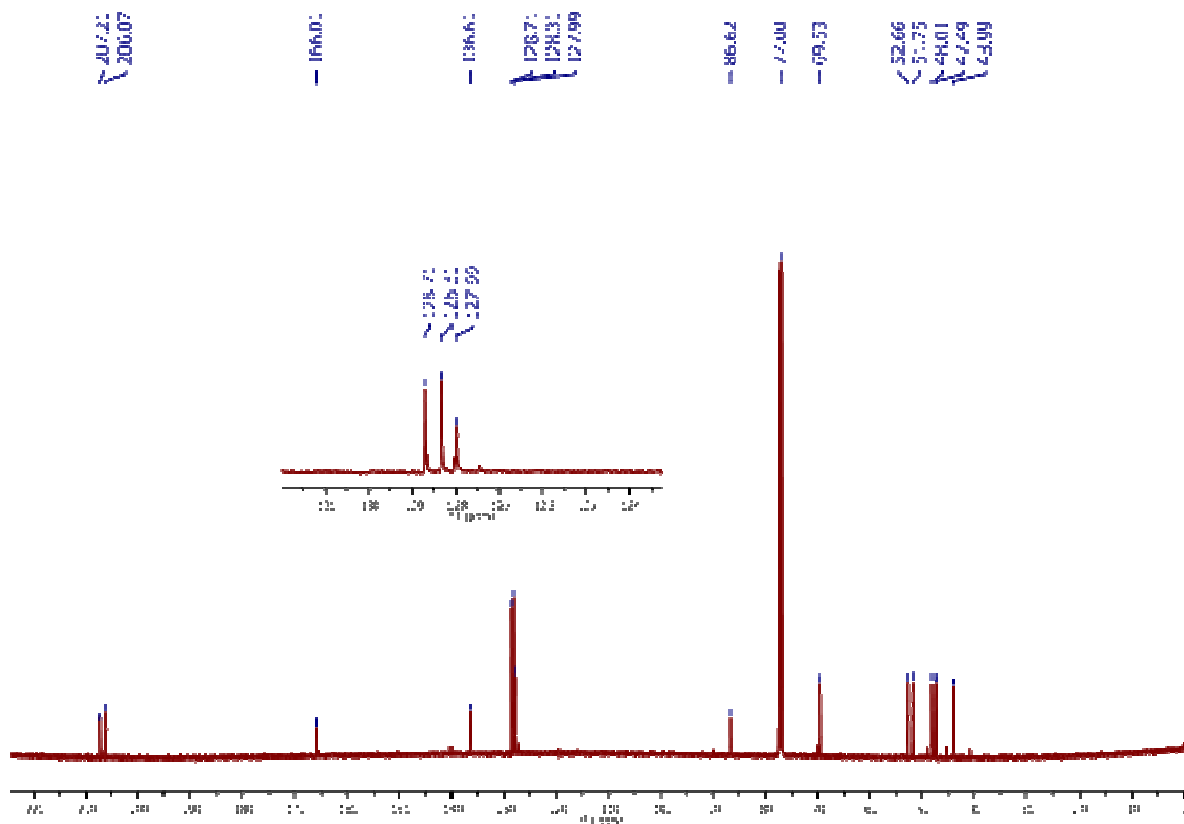
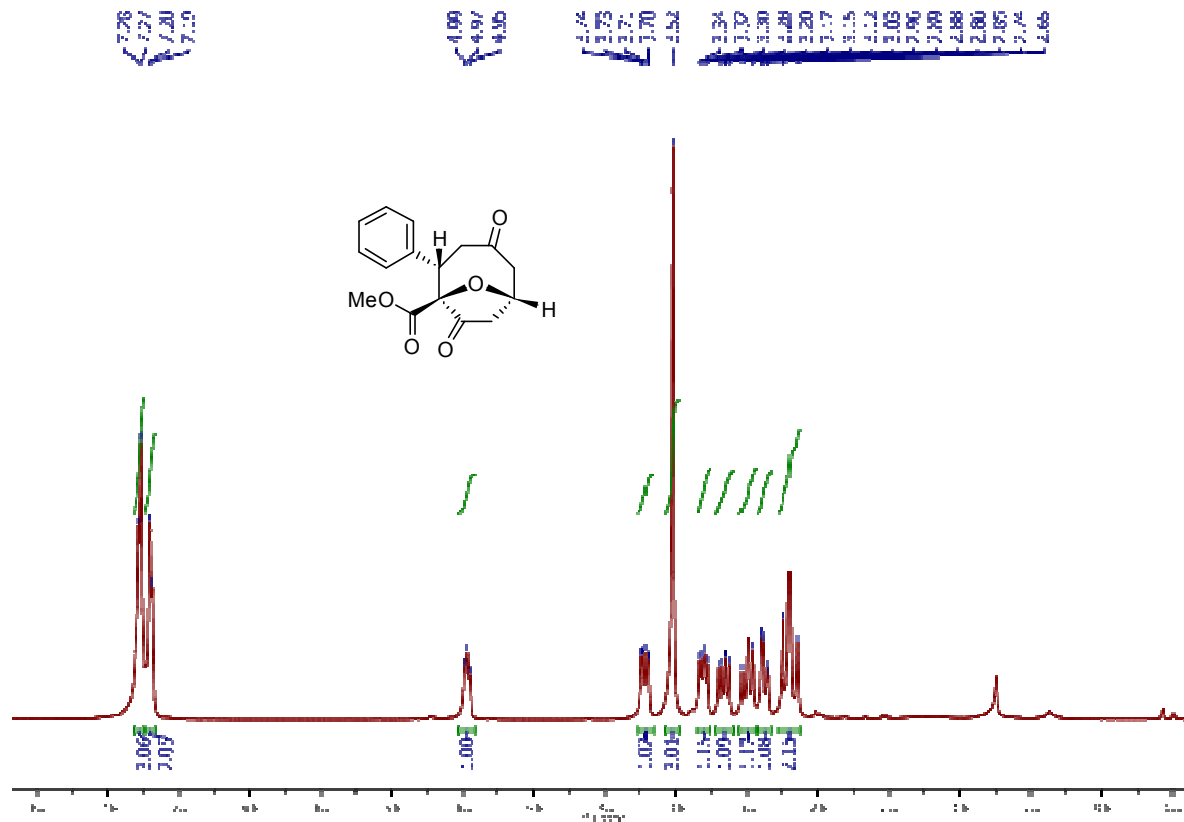


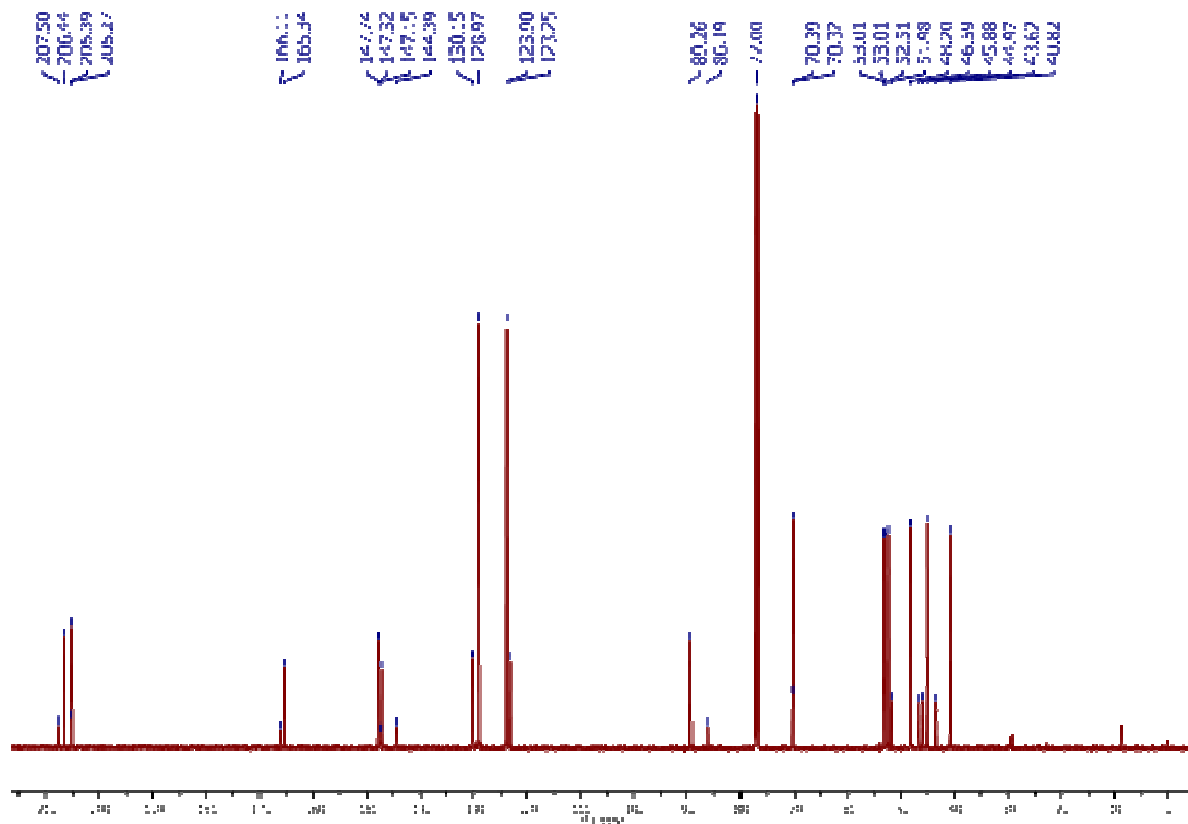
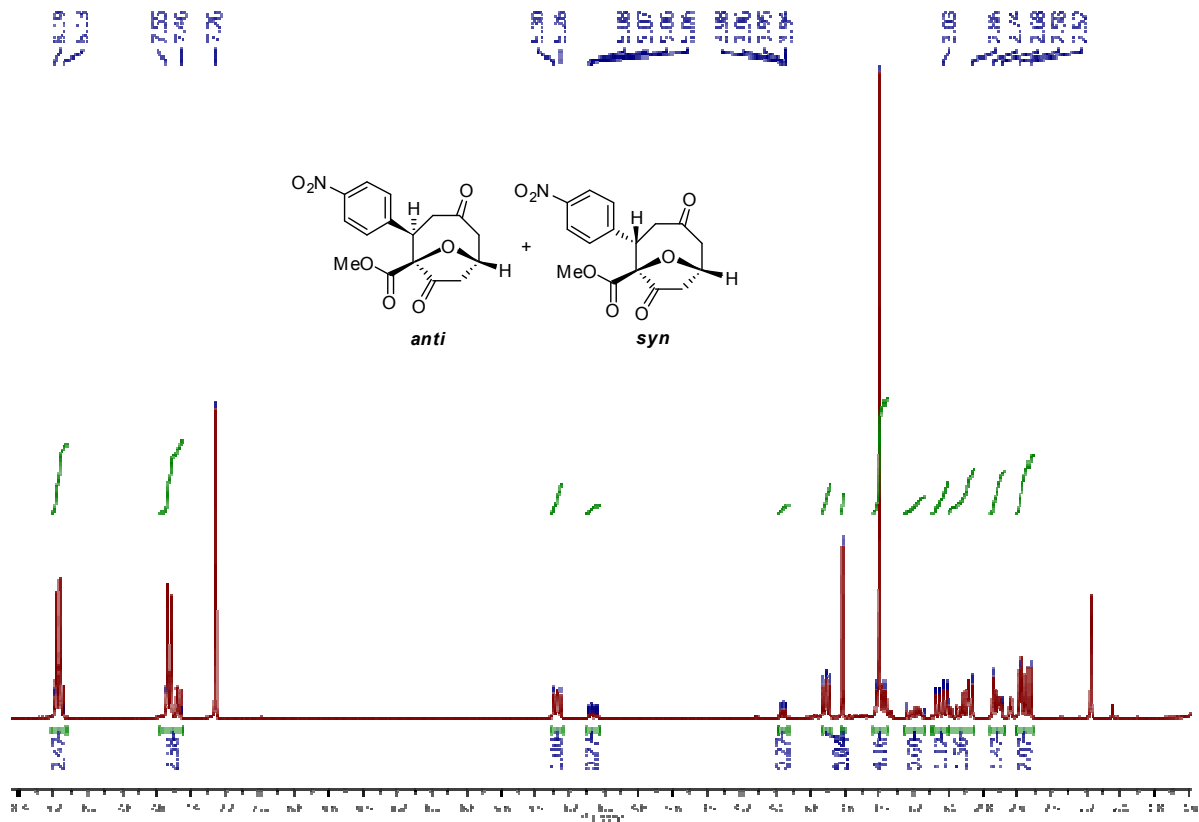


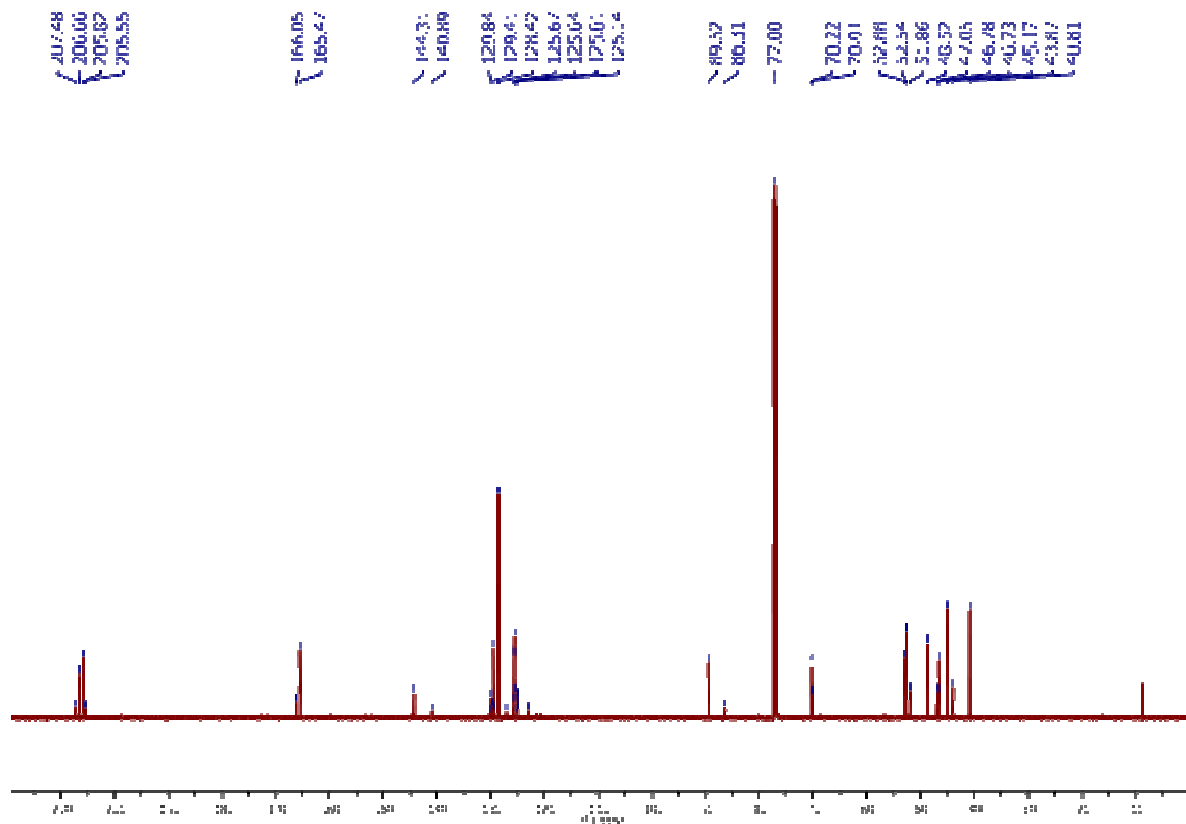
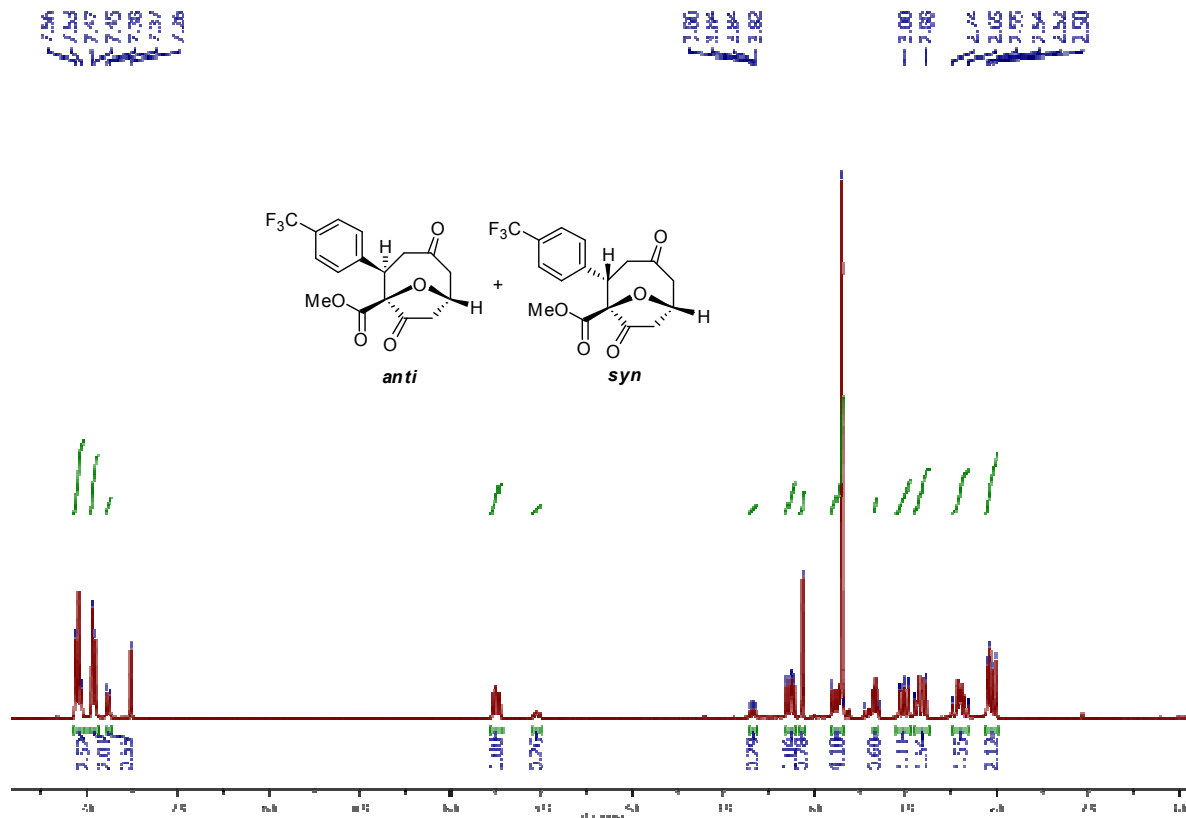


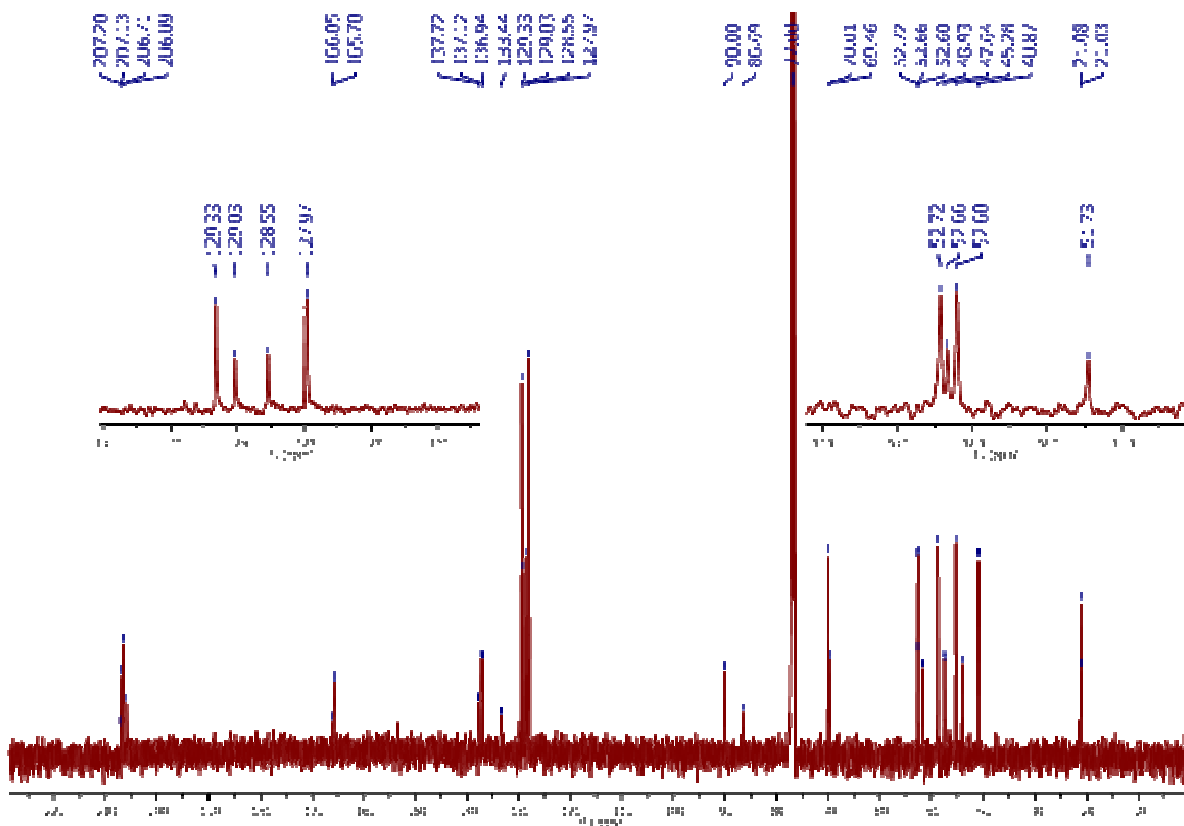
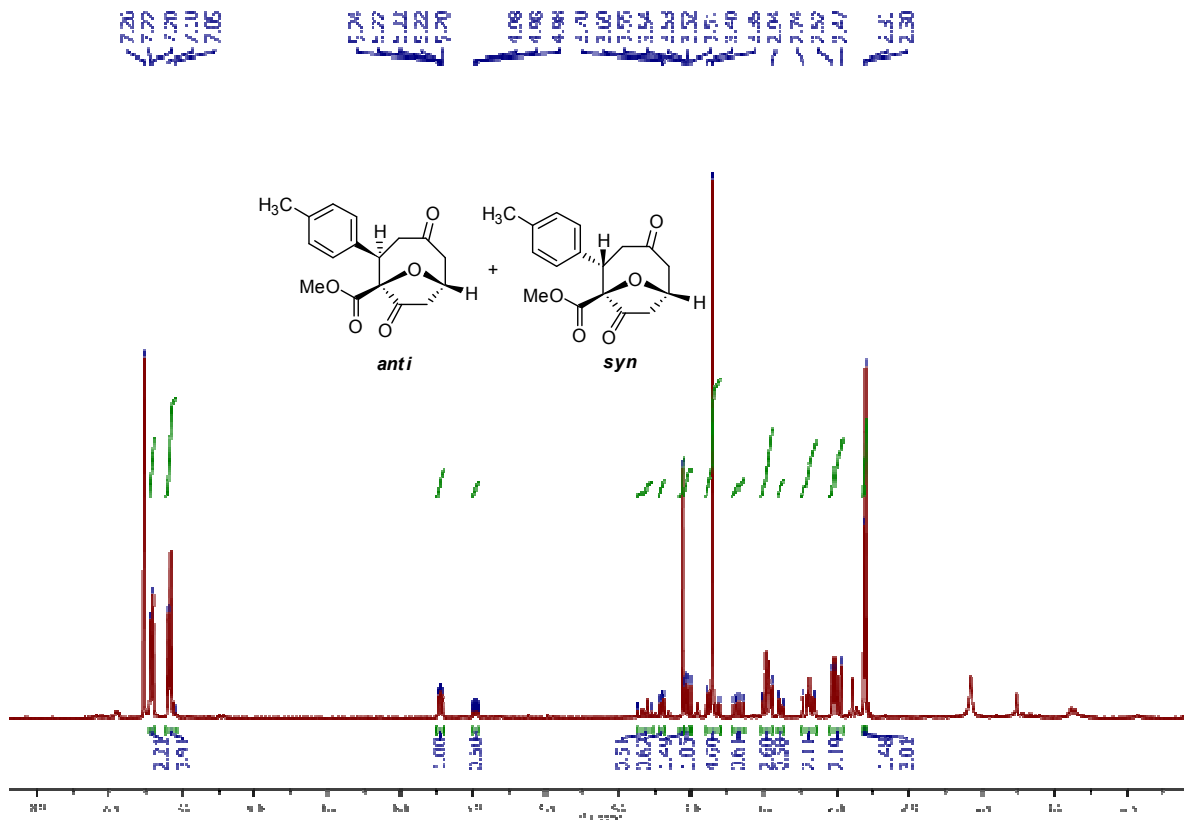


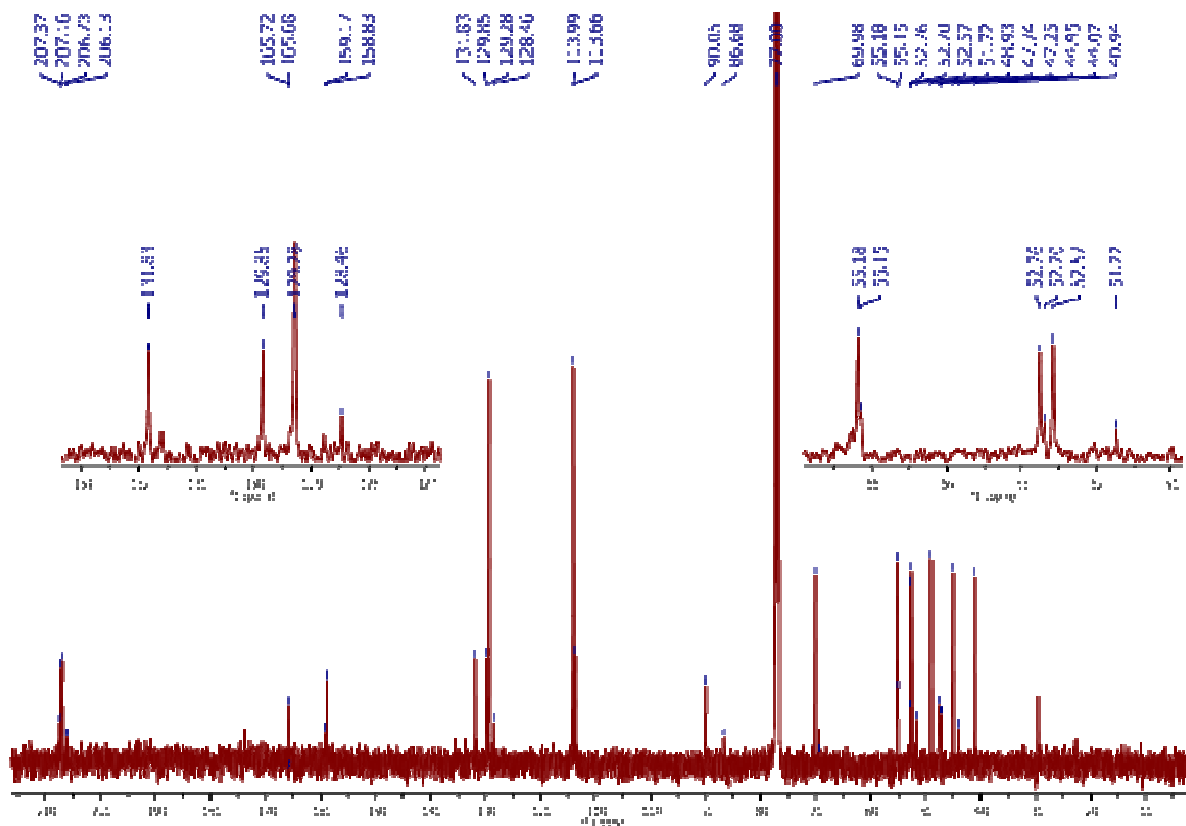
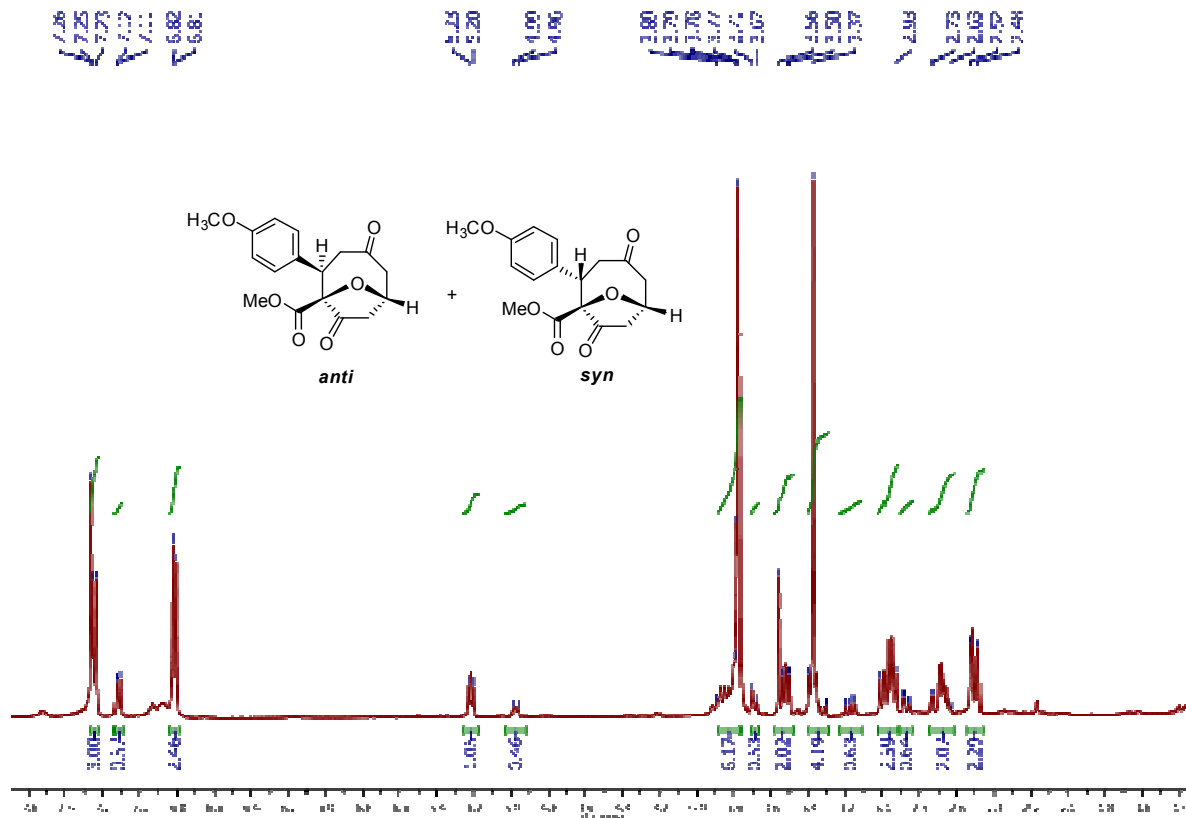


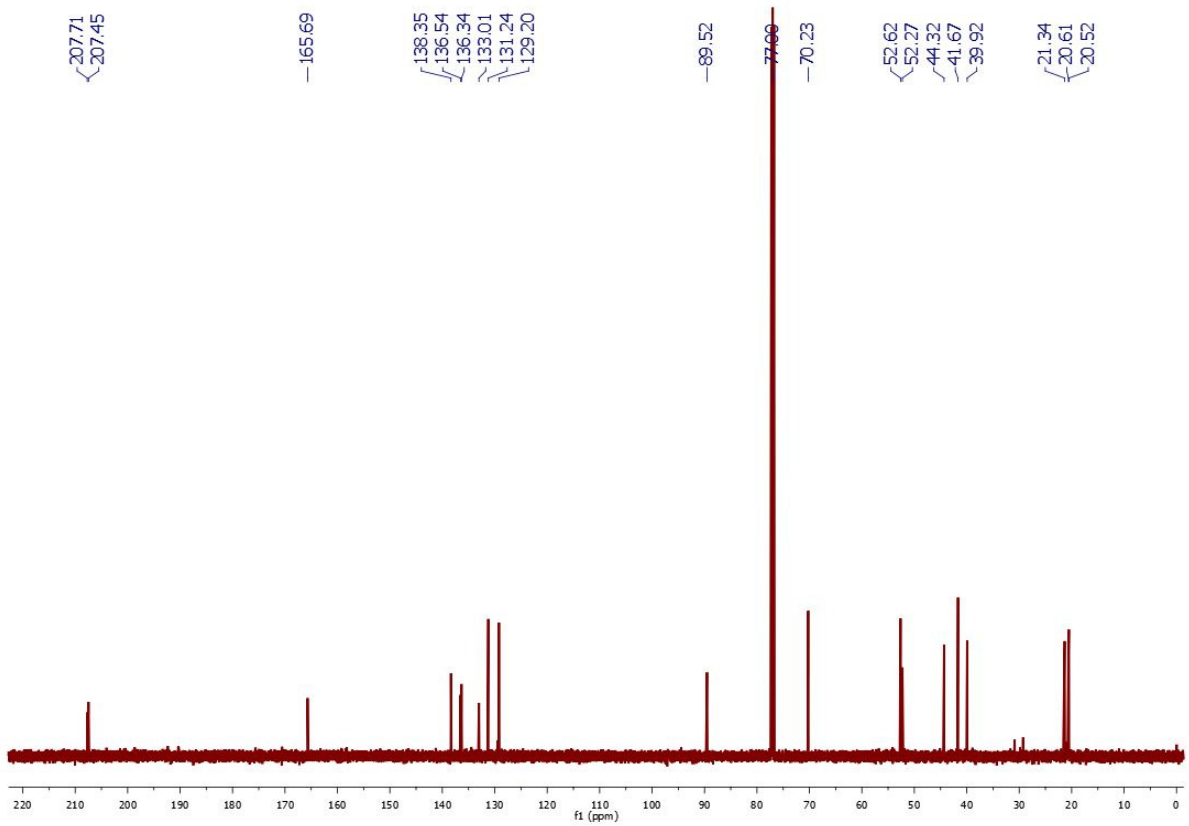
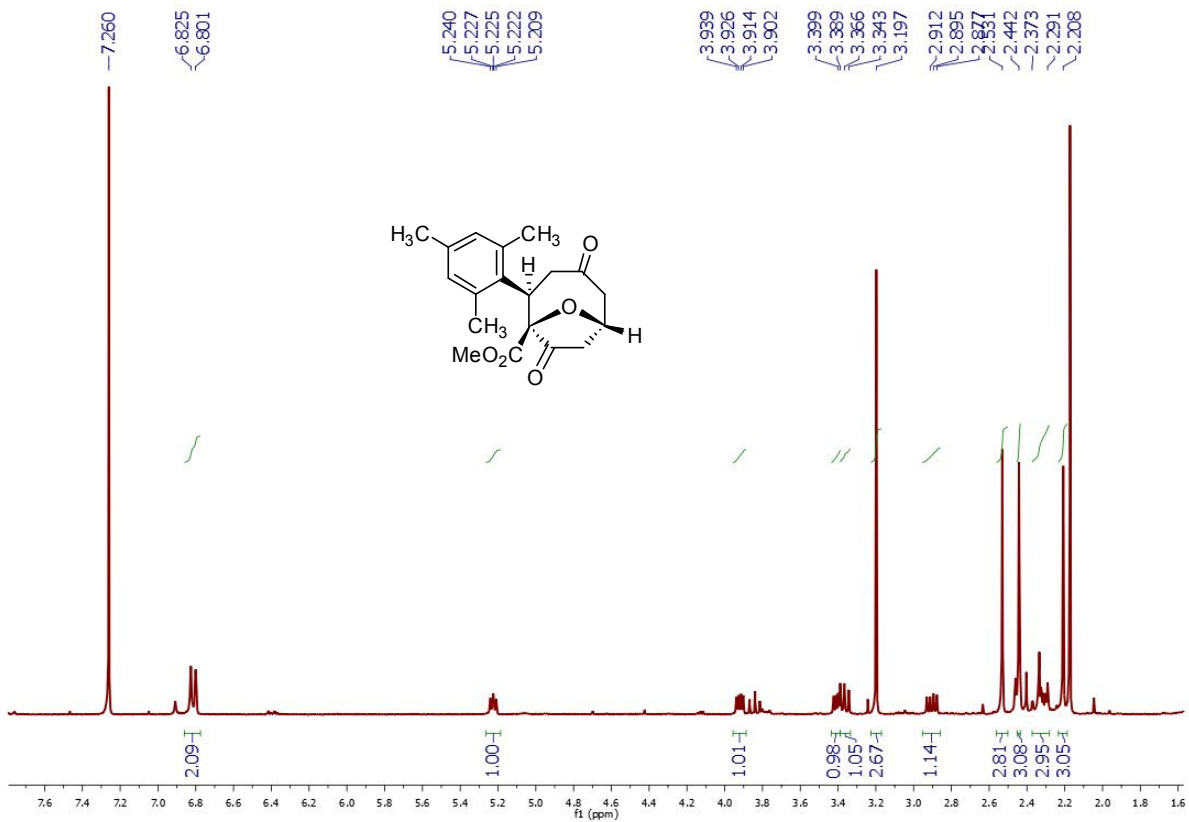


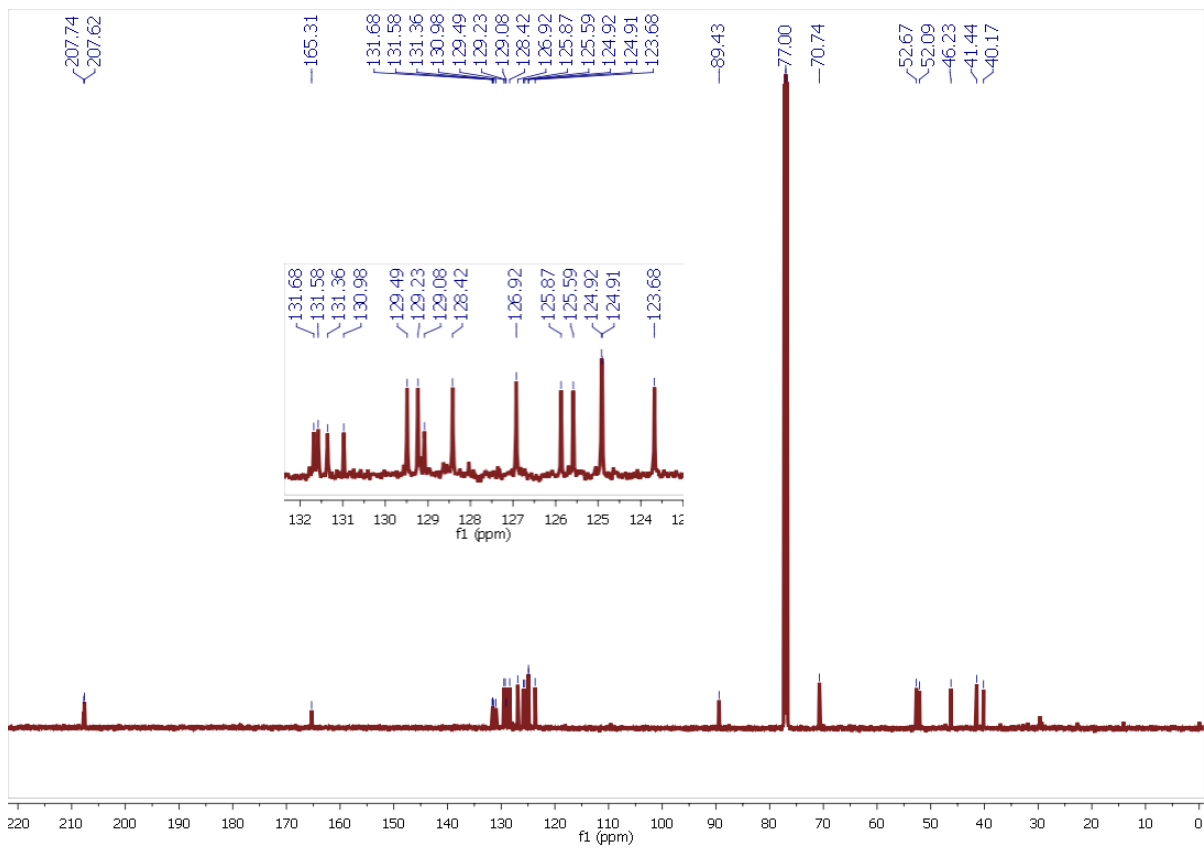
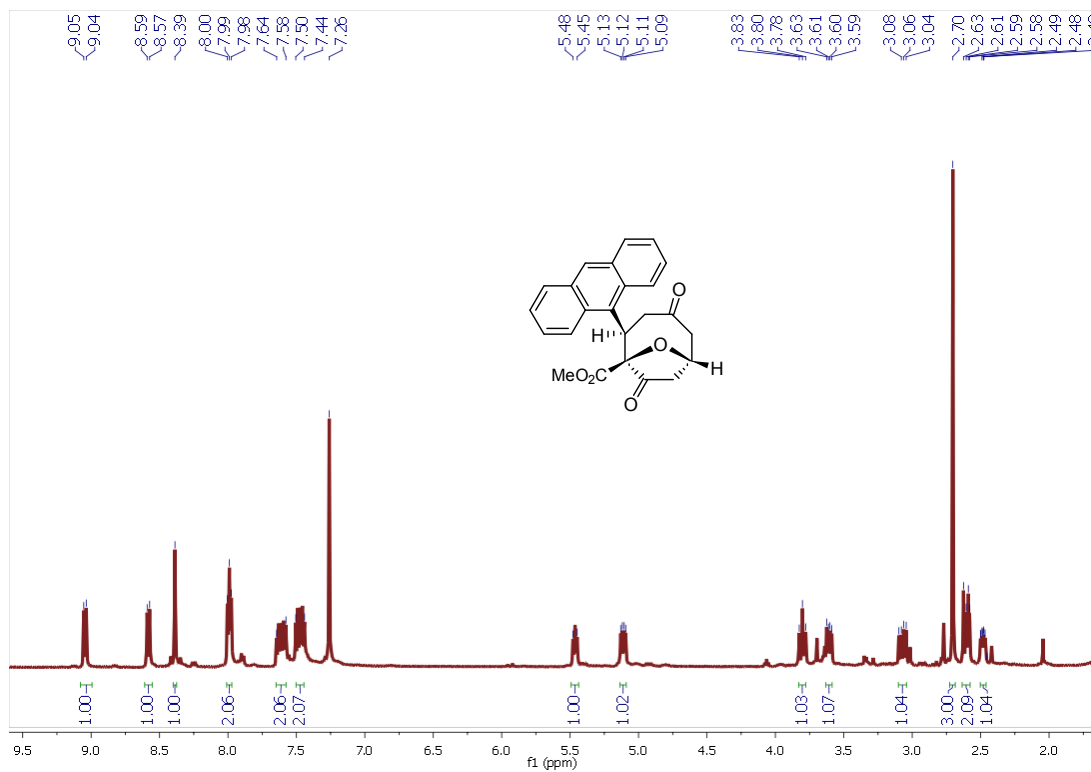


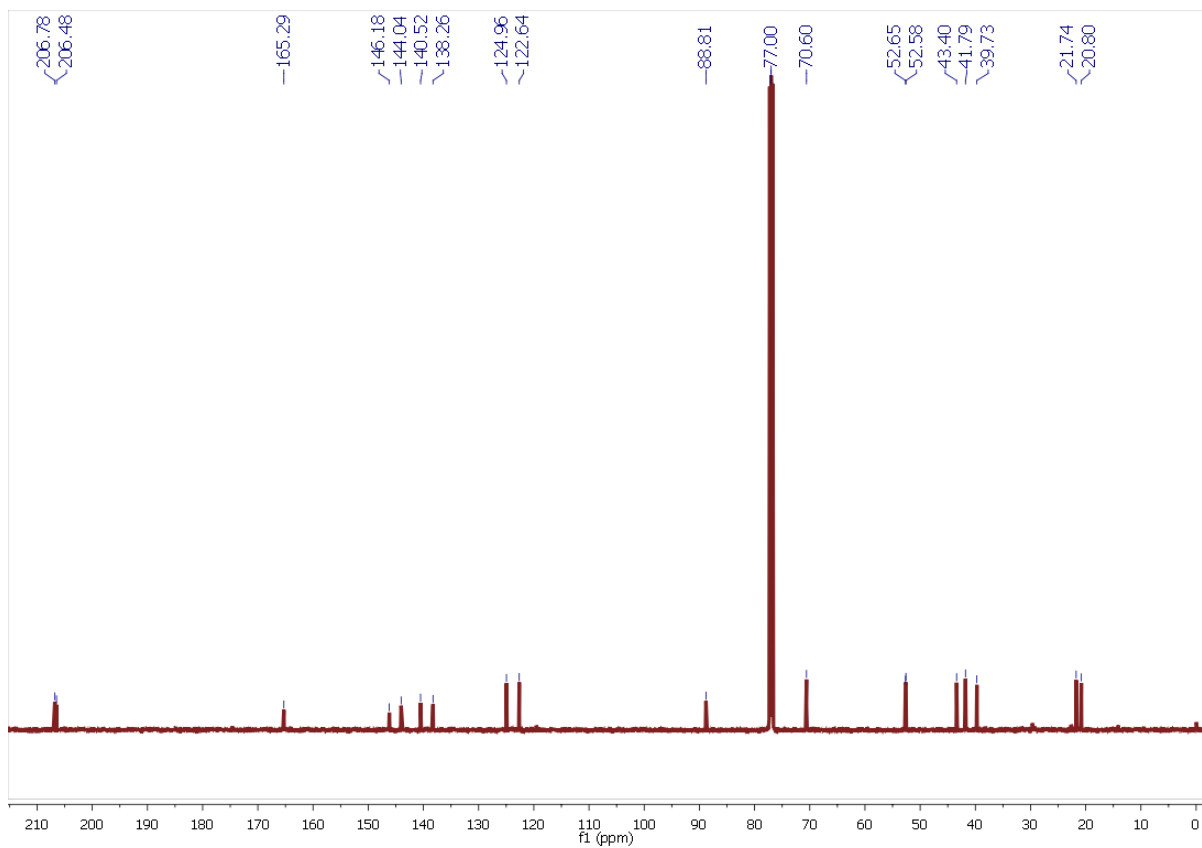
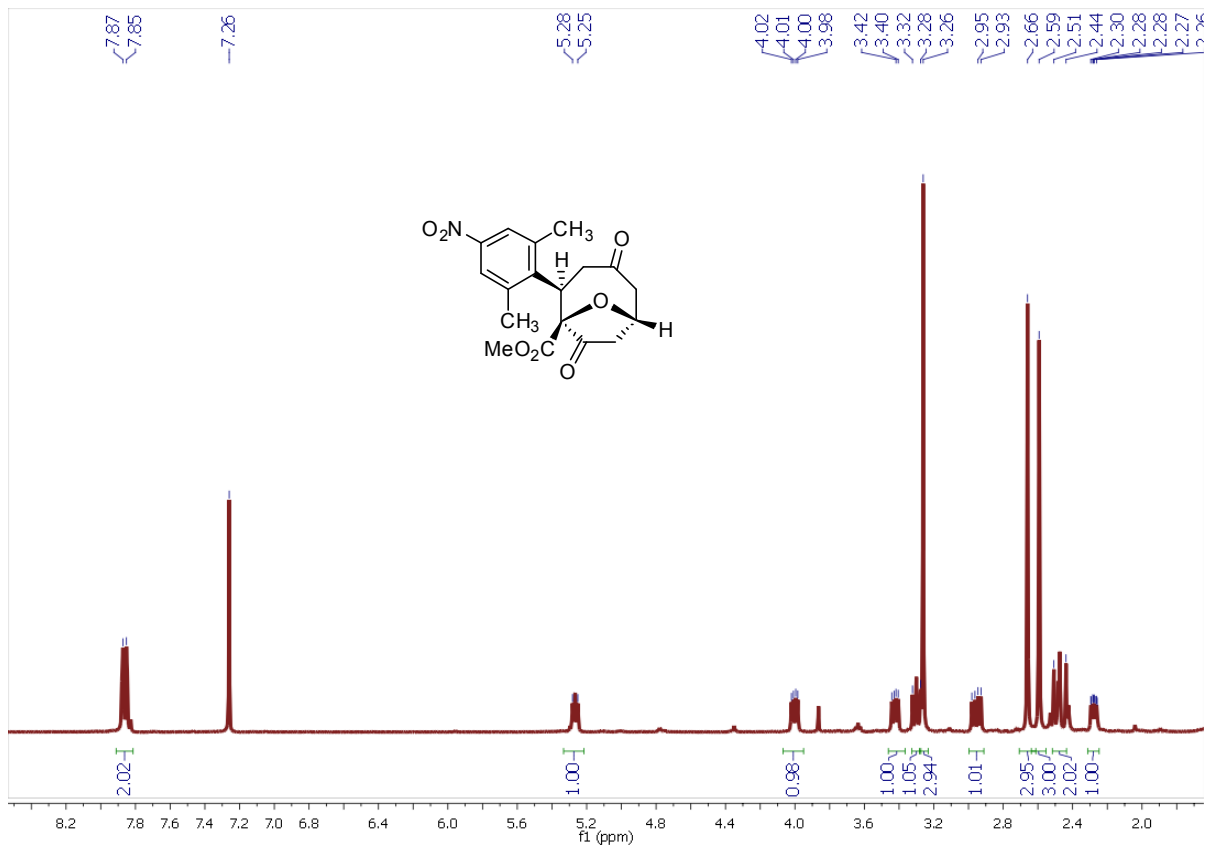








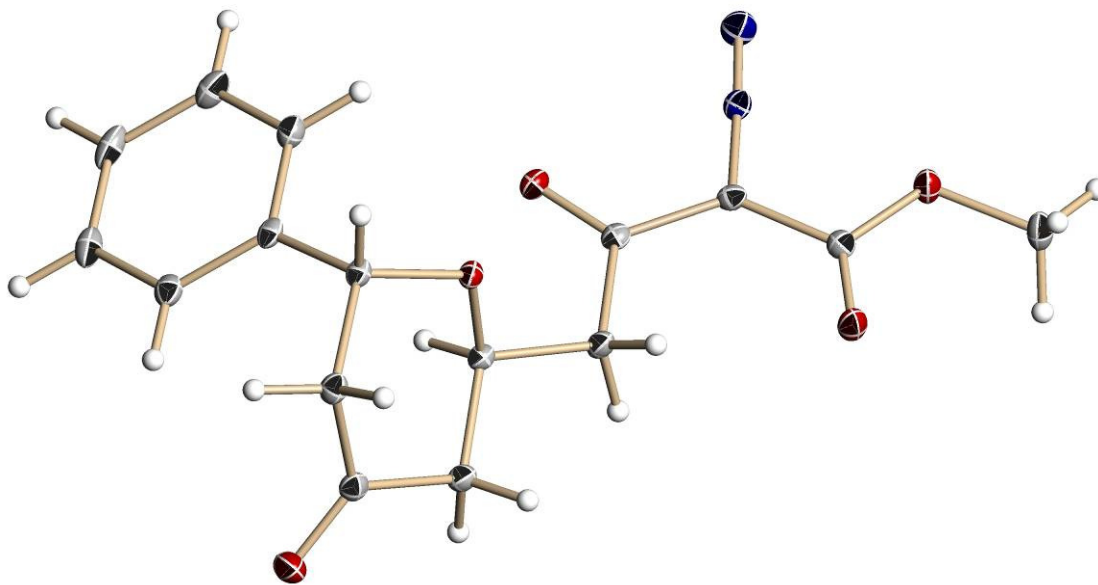




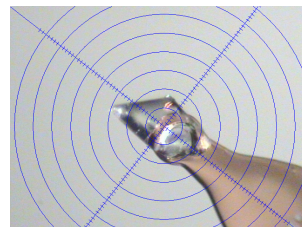
## Crystal Structure Data

Compound name : Methyl 2-diazo-3-oxo-4-((2*S*\*,6*S*\*)-4-oxo-6-phenyltetrahydro-2*H*-pyran-2-yl)butanoate **192(a)**

Chemical formula : C<sub>16</sub>H<sub>16</sub>N<sub>2</sub>O<sub>5</sub>



Crystals were obtained by dissolving 10 mg of yellow solid **192(a)** with minimum amount of hexane:DCM (10:1). A colorless prism-like specimen of C<sub>16</sub>H<sub>16</sub>N<sub>2</sub>O<sub>5</sub>, approximate dimensions 0.17 mm x 0.27 mm x 0.42 mm, was used for the X-ray crystallographic analysis. The X-ray intensity data were measured on a Bruker Smart Apex2 system equipped with a graphite monochromator and a MoK<sub>α</sub> fine-focus sealed tube ( $\lambda = 0.71073 \text{ \AA}$ ).



A total of 1819 frames were collected. The total exposure time was 12.12 hours. The frames were integrated with the Bruker SAINT software package using a narrow-frame algorithm. The integration of the data using a triclinic unit cell yielded a total of 21973 reflections to a maximum  $\theta$  angle of 27.50° (0.77 Å resolution), of which

7204 were independent (average redundancy 3.050, completeness = 99.8%,  $R_{\text{int}} = 1.54\%$ ,  $R_{\text{sig}} = 1.67\%$ ) and 6391 (88.71%) were greater than  $2\sigma(F^2)$ . The final cell constants of  $\underline{a} = 11.0436(6) \text{ \AA}$ ,  $\underline{b} = 11.2585(6) \text{ \AA}$ ,  $\underline{c} = 13.4333(8) \text{ \AA}$ ,  $\alpha = 90.2150(9)^\circ$ ,  $\beta = 107.0708(8)^\circ$ ,  $\gamma = 100.0912(9)^\circ$ , volume =  $1569.23(15) \text{ \AA}^3$ , are based upon the refinement of the XYZ-centroids of 9928 reflections above  $20 \sigma(I)$  with  $4.719^\circ < 2\theta < 62.22^\circ$ . Data were corrected for absorption effects using the multi-scan method (SADABS). The calculated minimum and maximum transmission coefficients (based on crystal size) are 0.9589 and 0.9831.

The structure was solved and refined using the Bruker SHELXTL Software Package, using the space group P -1, with  $Z = 4$  for the formula unit,  $\text{C}_{16}\text{H}_{16}\text{N}_2\text{O}_5$ . The final anisotropic full-matrix least-squares refinement on  $F^2$  with 441 variables converged at  $R1 = 3.36\%$ , for the observed data and  $wR2 = 6.86\%$  for all data. The goodness-of-fit was 0.999. The largest peak in the final difference electron density synthesis was  $0.317 \text{ e}^-/\text{\AA}^3$  and the largest hole was  $-0.176 \text{ e}^-/\text{\AA}^3$  with an RMS deviation of  $0.037 \text{ e}^-/\text{\AA}^3$ . On the basis of the final model, the calculated density was  $1.339 \text{ g/cm}^3$  and  $F(000)$ , 664  $e^-$ .

Table 1. Sample and crystal data for UM2037.

<b>Identification code</b>	UM2037	
<b>Chemical formula</b>	$\text{C}_{16}\text{H}_{16}\text{N}_2\text{O}_5$	
<b>Formula weight</b>	316.31	
<b>Temperature</b>	100(2) K	
<b>Wavelength</b>	0.71073 $\text{\AA}$	
<b>Crystal size</b>	0.17 x 0.27 x 0.42 mm	
<b>Crystal habit</b>	colorless prism	
<b>Crystal system</b>	Triclinic	
<b>Space group</b>	P -1	
<b>Unit cell dimensions</b>	$a = 11.0436(6) \text{ \AA}$	$\alpha = 90.2150(9)^\circ$
	$b = 11.2585(6) \text{ \AA}$	$\beta = 107.0708(8)^\circ$
	$c = 13.4333(8) \text{ \AA}$	$\gamma = 100.0912(9)^\circ$
<b>Volume</b>	$1569.23(15) \text{ \AA}^3$	
<b>Z</b>	4	

Density (calculated)	1.339 Mg/cm <sup>3</sup>
Absorption coefficient	0.101 mm <sup>-1</sup>
F(000)	664

Table 2. Data collection and structure refinement for UM2037.

Diffractometer	Bruker Smart Apex2		
Radiation source	fine-focus sealed tube, MoK <sub>α</sub>		
Theta range for data collection	1.84 to 27.50°		
Index ranges	-14<=h<=14, -14<=k<=14, -17<=l<=17		
Reflections collected	21973		
Independent reflections	7204 [R(int) = 0.0154]		
Coverage of independent reflections	99.8%		
Absorption correction	multi-scan		
Max. and min. transmission	0.9831 and 0.9589		
Structure solution technique	direct methods		
Structure solution program	SHELXS-97 (Sheldrick, 2008)		
Refinement method	Full-matrix least-squares on F <sup>2</sup>		
Refinement program	SHELXL-97 (Sheldrick, 2008)		
Function minimized	Σ w(F <sub>o</sub> <sup>2</sup> - F <sub>c</sub> <sup>2</sup> ) <sup>2</sup>		
Data / restraints / parameters	7204 / 0 / 441		
Goodness-of-fit on F <sup>2</sup>	0.999		
Δ/σ <sub>max</sub>	0.001		
Final R indices	6391 data; I>2σ(I)	R1 = 0.0336,	wR2 = 0.0669
	all data	R1 = 0.0384,	wR2 = 0.0686
Weighting scheme	w=1/[σ <sup>2</sup> (F <sub>o</sub> <sup>2</sup> )+(0.0100P) <sup>2</sup> +0.8850P] where P=(F <sub>o</sub> <sup>2</sup> +2F <sub>c</sub> <sup>2</sup> )/3		
Largest diff. peak and hole	0.317 and -0.176 eÅ <sup>-3</sup>		

Table 3. Atomic coordinates and equivalent isotropic atomic displacement parameters (Å<sup>2</sup>) for UM2037.

U(eq) is defined as one third of the trace of the orthogonalized U<sub>ij</sub> tensor.

	x/a	y/b	z/c	U(eq)
C1A	0.63677(12)	0.91830(10)	0.88520(10)	0.0281(3)
O1A	0.70214(8)	0.02580(7)	0.85019(6)	0.02442(17)
C2A	0.80256(10)	0.09042(10)	0.92376(9)	0.0201(2)
O2A	0.84318(8)	0.06132(7)	0.01196(6)	0.02699(18)
C3A	0.85396(10)	0.20131(10)	0.88219(8)	0.0191(2)
N1A	0.79766(9)	0.21486(8)	0.78055(7)	0.02033(19)
N2A	0.75407(10)	0.22894(10)	0.69674(8)	0.0295(2)
C4A	0.95445(10)	0.30337(10)	0.93352(8)	0.0185(2)
O4A	0.98302(7)	0.38903(7)	0.88349(6)	0.02148(16)

	x/a	y/b	z/c	U(eq)
C5A	0.01742(10)	0.30035(10)	0.04962(8)	0.0213(2)
C6A	0.14488(10)	0.38752(9)	0.08798(8)	0.0180(2)
O6A	0.23501(7)	0.33741(6)	0.04993(6)	0.01818(15)
C7A	0.19043(10)	0.40233(10)	0.20753(8)	0.0206(2)
C8A	0.32838(11)	0.46780(10)	0.24864(8)	0.0214(2)
O8A	0.36400(8)	0.54369(8)	0.32071(7)	0.03083(19)
C9A	0.41851(10)	0.42832(10)	0.19519(9)	0.0214(2)
C10A	0.35990(10)	0.41451(9)	0.07619(8)	0.0186(2)
C11A	0.35336(10)	0.53267(10)	0.02145(9)	0.0193(2)
C12A	0.40644(11)	0.64593(10)	0.07273(10)	0.0234(2)
C13A	0.40139(11)	0.75086(11)	0.01757(11)	0.0290(3)
C14A	0.34182(11)	0.74336(11)	0.91120(11)	0.0310(3)
C15A	0.28762(12)	0.63084(12)	0.85923(10)	0.0302(3)
C16A	0.29382(11)	0.52653(11)	0.91399(9)	0.0246(2)
C1B	0.60971(13)	0.29628(14)	0.44380(12)	0.0427(4)
O1B	0.53563(8)	0.20437(8)	0.48829(7)	0.0305(2)
C2B	0.40972(11)	0.17290(10)	0.43467(9)	0.0224(2)
O2B	0.35850(8)	0.21379(7)	0.35347(6)	0.02729(18)
C3B	0.34546(10)	0.08181(10)	0.48840(8)	0.0206(2)
N1B	0.41943(9)	0.05070(9)	0.57930(7)	0.0232(2)
N2B	0.47720(10)	0.02317(11)	0.65548(8)	0.0341(3)
C4B	0.21054(11)	0.02008(10)	0.46215(8)	0.0201(2)
O4B	0.17907(8)	0.94029(7)	0.51577(6)	0.02546(18)
C5B	0.11542(11)	0.06405(10)	0.37077(9)	0.0228(2)
C6B	0.98577(10)	0.97971(9)	0.33529(8)	0.0192(2)
O6B	0.00583(7)	0.87695(7)	0.28322(6)	0.02043(16)
C7B	0.88369(10)	0.04150(10)	0.26156(9)	0.0212(2)
C8B	0.76370(11)	0.95232(10)	0.20470(8)	0.0215(2)
O8B	0.65590(8)	0.97453(8)	0.18897(7)	0.02835(19)
C9B	0.78819(11)	0.83605(10)	0.16571(9)	0.0233(2)
C10B	0.89216(10)	0.78502(10)	0.24772(9)	0.0208(2)
C11B	0.85209(11)	0.72764(9)	0.33854(9)	0.0208(2)
C12B	0.72517(11)	0.70239(10)	0.34070(9)	0.0245(2)
C13B	0.69297(12)	0.64093(11)	0.42215(10)	0.0291(3)
C14B	0.78782(13)	0.60537(11)	0.50256(10)	0.0311(3)
C15B	0.91541(13)	0.63174(11)	0.50214(10)	0.0326(3)
C16B	0.94718(12)	0.69218(11)	0.42076(10)	0.0283(3)

Table 4. Bond lengths (Å) for UM2037.

C1A-O1A	1.4507(13)	C1A-H1A1	0.98	C1B-O1B	1.4465(14)	C1B-H1B1	0.98
C1A-H1A2	0.98	C1A-H1A3	0.98	C1B-H1B2	0.98	C1B-H1B3	0.98
O1A-C2A	1.3432(13)	C2A-O2A	1.2061(13)	O1B-C2B	1.3473(14)	C2B-O2B	1.2061(14)

C2A-C3A	1.4614(15)	C3A-N1A	1.3455(14)	C2B-C3B	1.4586(15)	C3B-N1B	1.3411(14)
C3A-C4A	1.4579(15)	N1A-N2A	1.1109(13)	C3B-C4B	1.4677(15)	N1B-N2B	1.1130(14)
C4A-O4A	1.2264(13)	C4A-C5A	1.5129(15)	C4B-O4B	1.2202(13)	C4B-C5B	1.5117(15)
C5A-C6A	1.5153(14)	C5A-H5A1	0.99	C5B-C6B	1.5160(15)	C5B-H5B1	0.99
C5A-H5A2	0.99	C6A-O6A	1.4365(12)	C5B-H5B2	0.99	C6B-O6B	1.4323(13)
C6A-C7A	1.5343(15)	C6A-H6A	1.0	C6B-C7B	1.5363(15)	C6B-H6B	1.0
O6A-C10A	1.4397(12)	C7A-C8A	1.5096(15)	O6B-C10B	1.4367(13)	C7B-C8B	1.5104(15)
C7A-H7A1	0.99	C7A-H7A2	0.99	C7B-H7B1	0.99	C7B-H7B2	0.99
C8A-O8A	1.2144(14)	C8A-C9A	1.5087(15)	C8B-O8B	1.2171(14)	C8B-C9B	1.5044(16)
C9A-C10A	1.5343(15)	C9A-H9A1	0.99	C9B-C10B	1.5347(15)	C9B-H9B1	0.99
C9A-H9A2	0.99	C10A-C11A	1.5249(14)	C9B-H9B2	0.99	C10B-C11B	1.5245(15)
C10A-H10A	1.0	C11A-C12A	1.3923(15)	C10B-H10B	1.0	C11B-C12B	1.3894(16)
C11A-C16A	1.3954(16)	C12A-C13A	1.3975(16)	C11B-C16B	1.3969(16)	C12B-C13B	1.3965(16)
C12A-H12A	0.95	C13A-C14A	1.3819(19)	C12B-H12B	0.95	C13B-C14B	1.3822(19)
C13A-H13A	0.95	C14A-C15A	1.3902(19)	C13B-H13B	0.95	C14B-C15B	1.3899(19)
C14A-H14A	0.95	C15A-C16A	1.3893(16)	C14B-H14B	0.95	C15B-C16B	1.3886(17)
C15A-H15A	0.95	C16A-H16A	0.95	C15B-H15B	0.95	C16B-H16B	0.95

Table 5. Bond angles (°) for UM2037.

O1A-C1A-H1A1	109.5	O1A-C1A-H1A2	109.5
H1A1-C1A-H1A2	109.5	O1A-C1A-H1A3	109.5
H1A1-C1A-H1A3	109.5	H1A2-C1A-H1A3	109.5
C2A-O1A-C1A	115.19(9)	O2A-C2A-O1A	124.55(10)
O2A-C2A-C3A	125.03(10)	O1A-C2A-C3A	110.42(9)
N1A-C3A-C4A	113.57(9)	N1A-C3A-C2A	115.72(9)
C4A-C3A-C2A	130.67(10)	N2A-N1A-C3A	177.88(12)
O4A-C4A-C3A	120.20(10)	O4A-C4A-C5A	122.25(10)
C3A-C4A-C5A	117.52(9)	C4A-C5A-C6A	112.65(9)
C4A-C5A-H5A1	109.1	C6A-C5A-H5A1	109.1
C4A-C5A-H5A2	109.1	C6A-C5A-H5A2	109.1
H5A1-C5A-H5A2	107.8	O6A-C6A-C5A	106.42(8)
O6A-C6A-C7A	110.82(8)	C5A-C6A-C7A	110.80(8)
O6A-C6A-H6A	109.6	C5A-C6A-H6A	109.6
C7A-C6A-H6A	109.6	C6A-O6A-C10A	112.58(8)
C8A-C7A-C6A	111.85(9)	C8A-C7A-H7A1	109.2
C6A-C7A-H7A1	109.2	C8A-C7A-H7A2	109.2
C6A-C7A-H7A2	109.2	H7A1-C7A-H7A2	107.9
O8A-C8A-C9A	123.00(10)	O8A-C8A-C7A	122.45(10)

C9A-C8A-C7A	114.52(9)	C8A-C9A-C10A	112.26(9)
C8A-C9A-H9A1	109.2	C10A-C9A-H9A1	109.2
C8A-C9A-H9A2	109.2	C10A-C9A-H9A2	109.2
H9A1-C9A-H9A2	107.9	O6A-C10A-C11A	111.12(8)
O6A-C10A-C9A	109.46(8)	C11A-C10A-C9A	115.25(9)
O6A-C10A-H10A	106.9	C11A-C10A-H10A	106.9
C9A-C10A-H10A	106.9	C12A-C11A-C16A	118.45(10)
C12A-C11A-C10A	123.38(10)	C16A-C11A-C10A	118.15(10)
C11A-C12A-C13A	120.71(11)	C11A-C12A-H12A	119.6
C13A-C12A-H12A	119.6	C14A-C13A-C12A	120.18(11)
C14A-C13A-H13A	119.9	C12A-C13A-H13A	119.9
C13A-C14A-C15A	119.65(11)	C13A-C14A-H14A	120.2
C15A-C14A-H14A	120.2	C16A-C15A-C14A	120.11(12)
C16A-C15A-H15A	119.9	C14A-C15A-H15A	119.9
C15A-C16A-C11A	120.90(11)	C15A-C16A-H16A	119.6
C11A-C16A-H16A	119.6	O1B-C1B-H1B1	109.5
O1B-C1B-H1B2	109.5	H1B1-C1B-H1B2	109.5
O1B-C1B-H1B3	109.5	H1B1-C1B-H1B3	109.5
H1B2-C1B-H1B3	109.5	C2B-O1B-C1B	115.52(9)
O2B-C2B-O1B	124.53(10)	O2B-C2B-C3B	125.25(10)
O1B-C2B-C3B	110.22(9)	N1B-C3B-C2B	115.78(10)
N1B-C3B-C4B	113.19(9)	C2B-C3B-C4B	130.99(10)
N2B-N1B-C3B	177.67(12)	O4B-C4B-C3B	119.83(10)
O4B-C4B-C5B	123.11(10)	C3B-C4B-C5B	117.00(9)
C4B-C5B-C6B	113.18(9)	C4B-C5B-H5B1	108.9
C6B-C5B-H5B1	108.9	C4B-C5B-H5B2	108.9
C6B-C5B-H5B2	108.9	H5B1-C5B-H5B2	107.8
O6B-C6B-C5B	105.87(9)	O6B-C6B-C7B	110.95(9)
C5B-C6B-C7B	111.04(9)	O6B-C6B-H6B	109.6
C5B-C6B-H6B	109.6	C7B-C6B-H6B	109.6
C6B-O6B-C10B	113.09(8)	C8B-C7B-C6B	112.16(9)
C8B-C7B-H7B1	109.2	C6B-C7B-H7B1	109.2
C8B-C7B-H7B2	109.2	C6B-C7B-H7B2	109.2
H7B1-C7B-H7B2	107.9	O8B-C8B-C9B	122.74(10)
O8B-C8B-C7B	122.49(10)	C9B-C8B-C7B	114.73(9)
C8B-C9B-C10B	112.12(9)	C8B-C9B-H9B1	109.2
C10B-C9B-H9B1	109.2	C8B-C9B-H9B2	109.2
C10B-C9B-H9B2	109.2	H9B1-C9B-H9B2	107.9
O6B-C10B-C11B	111.74(9)	O6B-C10B-C9B	109.06(9)
C11B-C10B-C9B	116.11(9)	O6B-C10B-H10B	106.4
C11B-C10B-H10B	106.4	C9B-C10B-H10B	106.4
C12B-C11B-C16B	118.47(11)	C12B-C11B-C10B	123.39(10)
C16B-C11B-C10B	118.02(10)	C11B-C12B-C13B	120.81(11)
C11B-C12B-H12B	119.6	C13B-C12B-H12B	119.6

C14B-C13B-C12B	120.14(11)	C14B-C13B-H13B	119.9
C12B-C13B-H13B	119.9	C13B-C14B-C15B	119.61(11)
C13B-C14B-H14B	120.2	C15B-C14B-H14B	120.2
C16B-C15B-C14B	120.18(12)	C16B-C15B-H15B	119.9
C14B-C15B-H15B	119.9	C15B-C16B-C11B	120.78(12)
C15B-C16B-H16B	119.6	C11B-C16B-H16B	119.6

Table 6. Torsion angles (°) for UM2037.

C1A-O1A-C2A-O2A	3.90(16)	C1A-O1A-C2A-C3A	-175.25(9)
O2A-C2A-C3A-N1A	177.79(11)	O1A-C2A-C3A-N1A	-3.06(13)
O2A-C2A-C3A-C4A	-4.61(19)	O1A-C2A-C3A-C4A	174.54(10)
C4A-C3A-N1A-N2A	12.(3)	C2A-C3A-N1A-N2A	-170.(3)
N1A-C3A-C4A-O4A	-2.11(15)	C2A-C3A-C4A-O4A	-179.75(11)
N1A-C3A-C4A-C5A	176.05(9)	C2A-C3A-C4A-C5A	-1.59(17)
O4A-C4A-C5A-C6A	-19.82(15)	C3A-C4A-C5A-C6A	162.07(9)
C4A-C5A-C6A-O6A	-71.96(11)	C4A-C5A-C6A-C7A	167.48(9)
C5A-C6A-O6A-C10A	177.01(8)	C7A-C6A-O6A-C10A	-62.44(10)
O6A-C6A-C7A-C8A	50.48(12)	C5A-C6A-C7A-C8A	168.39(9)
C6A-C7A-C8A-O8A	139.04(11)	C6A-C7A-C8A-C9A	-42.81(13)
O8A-C8A-C9A-C10A	-137.66(11)	C7A-C8A-C9A-C10A	44.21(12)
C6A-O6A-C10A-C11A	-65.45(11)	C6A-O6A-C10A-C9A	62.98(10)
C8A-C9A-C10A-O6A	-52.47(12)	C8A-C9A-C10A-C11A	73.63(11)
O6A-C10A-C11A-C12A	130.79(10)	C9A-C10A-C11A-C12A	5.55(14)
O6A-C10A-C11A-C16A	-50.84(13)	C9A-C10A-C11A-C16A	-176.09(9)
C16A-C11A-C12A-C13A	-0.69(16)	C10A-C11A-C12A-C13A	177.67(10)
C11A-C12A-C13A-C14A	0.86(17)	C12A-C13A-C14A-C15A	-0.38(18)
C13A-C14A-C15A-C16A	-0.25(18)	C14A-C15A-C16A-C11A	0.42(18)
C12A-C11A-C16A-C15A	0.06(16)	C10A-C11A-C16A-C15A	-178.39(10)
C1B-O1B-C2B-O2B	1.79(18)	C1B-O1B-C2B-C3B	-178.84(11)
O2B-C2B-C3B-N1B	-178.43(11)	O1B-C2B-C3B-N1B	2.21(14)
O2B-C2B-C3B-C4B	-1.0(2)	O1B-C2B-C3B-C4B	179.61(11)
C2B-C3B-N1B-N2B	164.(3)	C4B-C3B-N1B-N2B	-14.(3)
N1B-C3B-C4B-O4B	-7.14(15)	C2B-C3B-C4B-O4B	175.41(11)
N1B-C3B-C4B-C5B	170.20(10)	C2B-C3B-C4B-C5B	-7.25(18)
O4B-C4B-C5B-C6B	-14.82(16)	C3B-C4B-C5B-C6B	167.93(9)
C4B-C5B-C6B-O6B	-73.25(11)	C4B-C5B-C6B-C7B	166.24(9)
C5B-C6B-O6B-C10B	177.78(8)	C7B-C6B-O6B-C10B	-61.66(11)
O6B-C6B-C7B-C8B	48.66(12)	C5B-C6B-C7B-C8B	166.10(9)
C6B-C7B-C8B-O8B	140.45(11)	C6B-C7B-C8B-C9B	-41.71(13)
O8B-C8B-C9B-C10B	-137.81(11)	C7B-C8B-C9B-C10B	44.36(13)
C6B-O6B-C10B-C11B	-66.21(11)	C6B-O6B-C10B-C9B	63.51(11)
C8B-C9B-C10B-O6B	-53.24(12)	C8B-C9B-C10B-C11B	74.05(12)
O6B-C10B-C11B-C12B	136.90(11)	C9B-C10B-C11B-C12B	10.96(15)
O6B-C10B-C11B-C16B	-47.08(13)	C9B-C10B-C11B-C16B	-173.03(10)

C16B-C11B-C12B-C13B	-1.20(17)	C10B-C11B-C12B-C13B	174.80(10)
C11B-C12B-C13B-C14B	0.63(18)	C12B-C13B-C14B-C15B	0.37(18)
C13B-C14B-C15B-C16B	-0.78(19)	C14B-C15B-C16B-C11B	0.19(19)
C12B-C11B-C16B-C15B	0.79(18)	C10B-C11B-C16B-C15B	-175.43(11)

Table 7. Anisotropic atomic displacement parameters ( $\text{\AA}^2$ ) for UM2037.

The anisotropic atomic displacement factor exponent takes the form:  $-2\pi^2 [h^2 a^{*2} U_{11} + \dots + 2 h k a^* b^* U_{12}]$

	$U_{11}$	$U_{22}$	$U_{33}$	$U_{23}$	$U_{13}$	$U_{12}$
C1A	0.0269(6)	0.0205(5)	0.0303(6)	0.0055(5)	0.0025(5)	-0.0024(5)
O1A	0.0233(4)	0.0217(4)	0.0230(4)	0.0042(3)	0.0019(3)	-0.0010(3)
C2A	0.0183(5)	0.0211(5)	0.0211(5)	0.0010(4)	0.0060(4)	0.0042(4)
O2A	0.0294(4)	0.0260(4)	0.0205(4)	0.0057(3)	0.0036(3)	-0.0017(3)
C3A	0.0183(5)	0.0236(5)	0.0156(5)	0.0033(4)	0.0048(4)	0.0050(4)
N1A	0.0169(4)	0.0214(4)	0.0230(5)	0.0033(4)	0.0063(4)	0.0037(4)
N2A	0.0273(5)	0.0344(6)	0.0235(5)	0.0068(4)	0.0026(4)	0.0057(4)
C4A	0.0162(5)	0.0213(5)	0.0205(5)	0.0021(4)	0.0079(4)	0.0059(4)
O4A	0.0217(4)	0.0214(4)	0.0229(4)	0.0055(3)	0.0086(3)	0.0047(3)
C5A	0.0191(5)	0.0251(5)	0.0189(5)	0.0030(4)	0.0068(4)	0.0003(4)
C6A	0.0179(5)	0.0188(5)	0.0186(5)	0.0027(4)	0.0074(4)	0.0036(4)
O6A	0.0177(4)	0.0160(3)	0.0217(4)	0.0011(3)	0.0082(3)	0.0016(3)
C7A	0.0198(5)	0.0235(5)	0.0191(5)	0.0024(4)	0.0073(4)	0.0031(4)
C8A	0.0230(5)	0.0220(5)	0.0184(5)	0.0049(4)	0.0055(4)	0.0032(4)
O8A	0.0301(5)	0.0330(5)	0.0264(4)	-0.0065(4)	0.0086(4)	-0.0019(4)
C9A	0.0182(5)	0.0225(5)	0.0227(5)	0.0038(4)	0.0055(4)	0.0027(4)
C10A	0.0163(5)	0.0181(5)	0.0223(5)	0.0027(4)	0.0077(4)	0.0025(4)
C11A	0.0153(5)	0.0193(5)	0.0261(6)	0.0046(4)	0.0104(4)	0.0032(4)
C12A	0.0208(5)	0.0217(5)	0.0302(6)	0.0014(5)	0.0119(5)	0.0026(4)
C13A	0.0253(6)	0.0182(5)	0.0487(8)	0.0035(5)	0.0195(6)	0.0033(4)
C14A	0.0245(6)	0.0255(6)	0.0502(8)	0.0188(6)	0.0196(6)	0.0089(5)
C15A	0.0237(6)	0.0354(7)	0.0324(7)	0.0149(5)	0.0095(5)	0.0053(5)
C16A	0.0219(5)	0.0241(6)	0.0272(6)	0.0052(5)	0.0084(5)	0.0010(4)
C1B	0.0286(7)	0.0457(8)	0.0394(8)	0.0176(6)	0.0002(6)	-0.0136(6)
O1B	0.0231(4)	0.0322(5)	0.0277(4)	0.0099(4)	0.0005(3)	-0.0052(3)
C2B	0.0220(5)	0.0203(5)	0.0226(6)	0.0011(4)	0.0045(4)	0.0018(4)
O2B	0.0246(4)	0.0273(4)	0.0262(4)	0.0101(3)	0.0036(3)	0.0016(3)
C3B	0.0214(5)	0.0228(5)	0.0169(5)	0.0036(4)	0.0036(4)	0.0057(4)
N1B	0.0202(5)	0.0277(5)	0.0221(5)	0.0036(4)	0.0077(4)	0.0033(4)
N2B	0.0253(5)	0.0512(7)	0.0253(6)	0.0125(5)	0.0064(4)	0.0075(5)
C4B	0.0221(5)	0.0208(5)	0.0186(5)	0.0002(4)	0.0073(4)	0.0049(4)
O4B	0.0253(4)	0.0290(4)	0.0223(4)	0.0075(3)	0.0083(3)	0.0033(3)
C5B	0.0219(5)	0.0217(5)	0.0228(6)	0.0047(4)	0.0043(4)	0.0027(4)
C6B	0.0200(5)	0.0197(5)	0.0184(5)	0.0021(4)	0.0061(4)	0.0039(4)

	$U_{11}$	$U_{22}$	$U_{33}$	$U_{23}$	$U_{13}$	$U_{12}$
O6B	0.0196(4)	0.0206(4)	0.0230(4)	0.0009(3)	0.0095(3)	0.0035(3)
C7B	0.0225(5)	0.0205(5)	0.0203(5)	0.0029(4)	0.0057(4)	0.0046(4)
C8B	0.0236(5)	0.0243(5)	0.0170(5)	0.0066(4)	0.0063(4)	0.0047(4)
O8B	0.0219(4)	0.0305(4)	0.0323(5)	0.0070(4)	0.0067(4)	0.0065(3)
C9B	0.0255(6)	0.0240(5)	0.0187(5)	0.0010(4)	0.0052(4)	0.0023(4)
C10B	0.0221(5)	0.0199(5)	0.0213(5)	0.0003(4)	0.0083(4)	0.0034(4)
C11B	0.0248(5)	0.0163(5)	0.0216(5)	-0.0002(4)	0.0082(4)	0.0026(4)
C12B	0.0237(6)	0.0230(5)	0.0253(6)	-0.0015(4)	0.0073(5)	0.0008(4)
C13B	0.0300(6)	0.0255(6)	0.0318(6)	-0.0046(5)	0.0154(5)	-0.0057(5)
C14B	0.0456(7)	0.0215(6)	0.0255(6)	0.0005(5)	0.0158(6)	-0.0043(5)
C15B	0.0390(7)	0.0284(6)	0.0275(6)	0.0076(5)	0.0063(5)	0.0045(5)
C16B	0.0266(6)	0.0277(6)	0.0313(6)	0.0069(5)	0.0092(5)	0.0054(5)

Table 8. Hydrogen atomic coordinates and isotropic atomic displacement parameters ( $\text{\AA}^2$ ) for UM2037.

	$x/a$	$y/b$	$z/c$	$U(\text{eq})$
H1A1	-0.3054	-0.1403	-0.0963	0.035(2)
H1A2	-0.4407	-0.1174	-0.1709	0.035(2)
H1A3	-0.3877	-0.0600	-0.0536	0.035(2)
H5A1	0.0319	0.2174	0.0661	0.030(3)
H5A2	-0.0417	0.3207	0.0873	0.030(3)
H6A	0.1352	0.4679	0.0584	0.014(3)
H7A1	0.1341	0.4480	0.2313	0.026(2)
H7A2	0.1826	0.3216	0.2365	0.026(2)
H9A1	0.4398	0.3501	0.2213	0.030(4)
H9A2	0.4997	0.4886	0.2131	0.027(3)
H10A	0.4163	0.3714	0.0486	0.017(3)
H12A	0.4465	0.6519	0.1460	0.026(3)
H13A	0.4390	0.8275	0.0533	0.036(4)
H14A	0.3379	0.8147	-0.1262	0.037(4)
H15A	0.2463	0.6253	-0.2139	0.037(4)
H16A	0.2570	0.4500	-0.1222	0.030(4)
H1B1	0.6130	1.2649	0.3767	0.055(3)
H1B2	0.6974	1.3186	0.4914	0.055(3)
H1B3	0.5688	1.3677	0.4331	0.055(3)
H5B1	0.1522	1.0732	0.3117	0.033(3)
H5B2	0.1026	1.1447	0.3905	0.033(3)
H6B	-0.0424	0.9538	0.3974	0.018(3)
H7B1	-0.1397	1.1024	0.3024	0.026(2)
H7B2	-0.0793	1.0843	0.2099	0.026(2)
H9B1	-0.1844	0.8504	0.1023	0.036(4)
H9B2	-0.2929	0.7757	0.1464	0.027(3)
H10B	-0.0842	0.7196	0.2106	0.018(3)

	x/a	y/b	z/c	U(eq)
H12B	-0.3405	0.7272	0.2861	0.028(3)
H13B	-0.3943	0.6235	0.4223	0.035(4)
H14B	-0.2341	0.5631	0.5578	0.039(4)
H15B	-0.0189	0.6084	0.5577	0.042(4)
H16B	0.0346	0.7096	0.4210	0.034(4)

Table 9: Data collection details for UM2037.

Axis	dx/mm	2 $\theta$ / $^{\circ}$	$\omega$ / $^{\circ}$	$\phi$ / $^{\circ}$	$\chi$ / $^{\circ}$	Width/ $^{\circ}$	Frames	Time/s	Wavelength/ $\text{\AA}$
Omega	50.039	-31.50	-31.50	0.00	54.71	0.50	366	24.00	0.71073
Omega	50.039	-31.50	-31.50	120.00	54.71	0.50	366	24.00	0.71073
Omega	50.039	-31.50	-31.50	240.00	54.71	0.50	366	24.00	0.71073
Phi	50.039	-31.50	-211.50	0.00	54.71	0.50	720	24.00	0.71073

Compound name : Major product ***syn-193(a)***  
 Chemical formula : C<sub>16</sub>H<sub>16</sub>O<sub>5</sub>  
 Final R<sub>1</sub> [ $I > 2\sigma(I)$ ] : 3.59 %

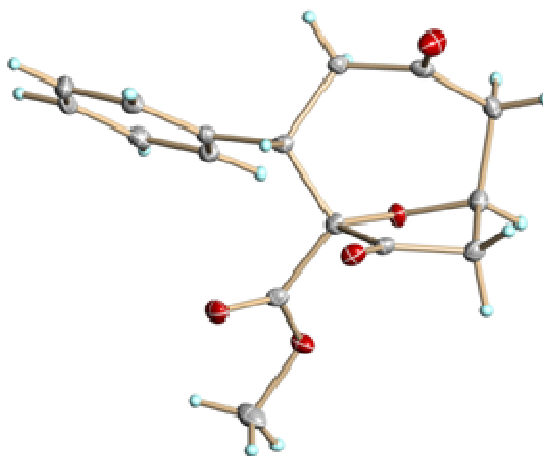


**Figure 1.** A view of UM#1906 showing the anisotropic atomic displacement ellipsoids for the non-hydrogen atoms are shown at the 30% probability level. Hydrogen atoms are displayed with an arbitrarily small radius.

Crystals were obtained by dissolving 10 mg of white solid ***syn-193(a)*** with minimum amount of hexane:ether (10:1). A colorless needle of C<sub>16</sub>H<sub>16</sub>O<sub>5</sub>, approximate dimensions 0.05x0.095x0.53 mm<sup>3</sup>, was used for the X-ray crystallographic analysis. The X-ray intensity data were measured at 120(2) °K on a three-circle diffractometer system equipped with Bruker Smart Apex II CCD area detector using a graphite monochromator

and a MoK  $\alpha$  fine-focus sealed tube ( $\lambda = 0.71073 \text{ \AA}$ ). The detector was placed at a distance of 5.0000 cm from the crystal.

A total of 1830 frames was collected with a scan width of  $-0.3^\circ$  an exposure time of 60 sec/frame using Apex2 (Bruker, 2005). The total data collection time was 33.5 hours. The frames were integrated with Apex2 software package using a narrow-frame integration algorithm. The integration of the data using a Triclinic unit cell yielded a total of 6300 reflections to a maximum  $\theta$  angle of  $27.50^\circ$ , of which 6300 were independent (completeness = 99.7%,  $R_{\text{int}} = 0.00\%$ ,  $R_{\text{sig}} = 2.54\%$ ) and 5367 were greater than  $2\sigma(I)$ . The final cell dimensions of  $a = 10.3115(11) \text{ \AA}$ ,  $b = 11.0094(12) \text{ \AA}$ ,  $c = 13.2743(14) \text{ \AA}$ ,  $\alpha = 89.6028(14)^\circ$ ,  $\beta = 67.7337(13)^\circ$ ,  $\lambda = 80.3302(14)^\circ$ ,  $V = 1372.1(3) \text{ \AA}^3$ , are based upon the refinement of the XYZ-centroids of 8296 reflections with  $2.2 < \theta < 28.3^\circ$  using Apex2 software. Analysis of the data showed 0 % decay during data collection. Data were corrected for absorption effects with the Semi-empirical from equivalents method using SADABS (Sheldrick, 1996). The minimum and maximum transmission coefficients were 0.945 and 0.995.

The structure was solved and refined using the SHELXS-97 (Sheldrick, 1990) and SHELXL-97 (Sheldrick, 1997) software in the space group  $P-1$  with  $Z = 4$  for the formula unit  $\text{C}_{16}\text{H}_{16}\text{O}_5$ . The final anisotropic full-matrix least-squares refinement on  $F^2$  with 498 variables converged at  $R_1 = 3.59\%$  for the observed data and  $wR_2 = 7.79\%$  for all data. The goodness-of-fit was 1.000. The largest peak on the final difference map was  $0.354 \text{ e}/\text{\AA}^3$  and the largest hole was  $-0.227 \text{ e}/\text{\AA}^3$ . On the basis of the final model, the calculated density was  $1.396 \text{ g/cm}^3$  and  $F(000)$ , 608 e.

**Comments:**

- Data quality: very good
- Twinning: non-merohedral twinning in about 1:1 ratio by 180 deg. rotation around 001 axis in real space
- Disorder: none
- H-atoms: all refined
- Residual density: in the middle of the bonds
- Structure quality: very good
- Strong data set, no disorder,  $R_1$  4% maximum. Publishable quality.

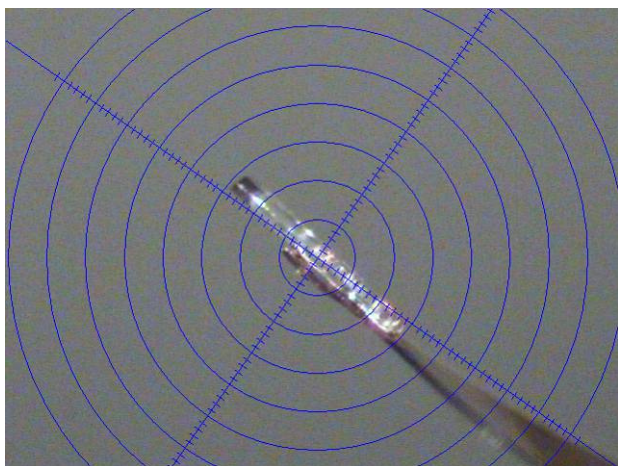
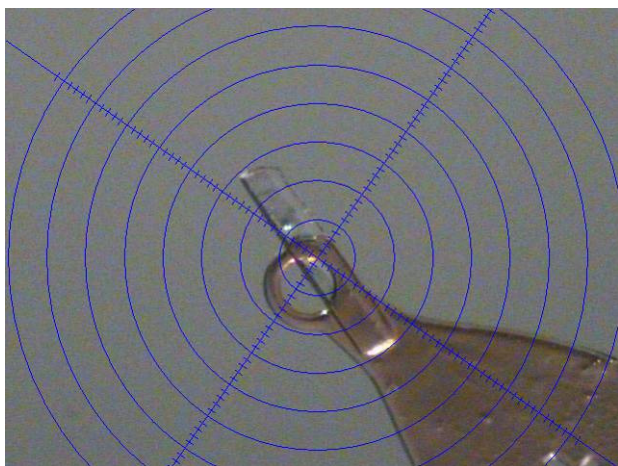


**Table 1.** Crystal data and structure refinement for UM#1906.

X-ray lab book No.	1906
Crystal ID	Doyle/DeanaJaber Diazo Decomp-Major product @
120K	
Empirical formula	C <sub>16</sub> H <sub>16</sub> O <sub>5</sub>
Formula weight	288.29
Temperature	120(2) K
Wavelength	0.71073 Å
Crystal size	0.53×0.095×0.05 mm <sup>3</sup>
Crystal habit	colorless needle
Crystal system	Triclinic

Space group	P-1		
Unit cell dimensions	$a = 10.3115(11) \text{ \AA}$	$\alpha = 89.6028(14)^\circ$	
	$b = 11.0094(12) \text{ \AA}$	$\beta = 67.7337(13)^\circ$	
	$c = 13.2743(14) \text{ \AA}$	$\gamma = 80.3302(14)^\circ$	
Volume	1372.1(3) $\text{ \AA}^3$		
Z	4		
Density, $\rho_{\text{calc}}$	1.396 $\text{ g/cm}^3$		
Absorption coefficient, $\mu$	0.104 $\text{ mm}^{-1}$		
F(000)	608 $\bar{e}$		
Diffractometer	Bruker Smart Apex II CCD area detector		
Radiation source	fine-focus sealed tube, MoK $\alpha$		
Detector distance	5.000 cm		
Data collection method	$\omega$ scans		
Total frames	1830		
Frame size	1024 pixels		
Frame width	-0.3°		
Exposure per frame	60 sec		
Total measurement time	33.5 hours		
$\theta$ range for data collection	1.88 to 27.50°		
Index ranges	$-12 \leq h \leq 13, -14 \leq k \leq 14, 0 \leq l \leq 17$		
Reflections collected	6300		
Independent reflections	6300		
Observed reflection, $I > 2\sigma(I)$	5367		
Coverage of independent reflections	99.7 %		
Variation in check reflections	0 %		
Absorption correction	Semi-empirical from equivalents SADABS (Sheldrick, 1996)		
Max. and min. transmission	0.995 and 0.945		
Structure solution technique	direct		
Structure solution program	SHELXS-97 (Sheldrick, 1990)		
Refinement technique	Full-matrix least-squares on $F^2$		
Refinement program	SHELXL-97 (Sheldrick, 1997)		
Function minimized	$\Sigma w(F_o^2 - F_c^2)^2$		
Data / restraints / parameters	6300 / 0 / 498		
Goodness-of-fit on $F^2$	1.000		
$\Delta/\sigma_{\text{max}}$	0.000		
Final R indices:	$R_1, I > 2\sigma(I)$	0.0359	
	$wR_2, \text{ all data}$	0.0779	
	$R_{\text{int}}$	0.0000	
	$R_{\text{sig}}$	0.0254	
Weighting scheme	$w = 1/[\sigma^2(F_o^2) + (0.02P)^2 + 0.562P], P = [\max(F_o^2, 0) + 2F_o^2]/3$		
Largest diff. peak and hole	0.354	and	-0.227 $\bar{e}/\text{ \AA}^3$

$$R_1 = \Sigma ||F_o| - |F_c|| / \Sigma |F_o|, \quad wR_2 = [\Sigma w(F_o^2 - F_c^2)^2 / \Sigma w(F_o^2)^2]^{1/2}$$

**Table 2.** Atomic coordinates and equivalent\* isotropic atomic displacement parameters ( $\text{ \AA}^2$ ) for UM#1906.

Atom	$x/a$	$y/b$	$z/c$	$U_{\text{eq}}$
C1A	0.22635(16)	0.32619(14)	0.25043(12)	0.0206(3)
C2A	0.10385(16)	0.32845(15)	0.22948(13)	0.0231(3)

C3A	0.05685(16)	0.42586(16)	0.17739(13)	0.0248(3)
C4A	0.13135(17)	0.52299(15)	0.14907(13)	0.0256(3)
C5A	0.25254(16)	0.52239(14)	0.17139(13)	0.0212(3)
C6A	0.30221(15)	0.42319(13)	0.22102(12)	0.0176(3)
C7A	0.44285(15)	0.41846(13)	0.23378(12)	0.0171(3)
C8A	0.55910(16)	0.33459(15)	0.13711(13)	0.0213(3)
C9A	0.70306(16)	0.30808(15)	0.14566(12)	0.0218(3)
O9A	0.79052(12)	0.37467(12)	0.10687(10)	0.0323(3)
C10A	0.73173(17)	0.19566(15)	0.20587(14)	0.0235(3)
C11A	0.63514(16)	0.21148(14)	0.32752(13)	0.0221(3)
O11A	0.48554(10)	0.24223(9)	0.34222(9)	0.0196(2)
C12A	0.65908(17)	0.31795(15)	0.38644(14)	0.0235(3)
C13A	0.55991(16)	0.42593(14)	0.37052(12)	0.0190(3)
O13A	0.56593(12)	0.53390(10)	0.37454(9)	0.0239(2)
C14A	0.44513(15)	0.37263(12)	0.34424(12)	0.0172(3)
C15A	0.30217(15)	0.41986(13)	0.43701(12)	0.0186(3)
O15A	0.24458(12)	0.52596(10)	0.44725(9)	0.0255(2)
O16A	0.25329(12)	0.33268(10)	0.50378(9)	0.0235(2)
C16A	0.1223(2)	0.37689(18)	0.59645(16)	0.0351(4)
C1B	0.75571(16)	0.17931(14)	0.59334(13)	0.0189(3)
C2B	0.87838(16)	0.17725(14)	0.50000(13)	0.0221(3)
C3B	0.92517(16)	0.07956(15)	0.42193(13)	0.0227(3)
C4B	0.84949(17)	-0.01639(15)	0.43792(13)	0.0236(3)
C5B	0.72800(16)	-0.01621(14)	0.53176(12)	0.0200(3)
C6B	0.67989(15)	0.08222(13)	0.61008(12)	0.0169(3)
C7B	0.54159(15)	0.08455(13)	0.70790(12)	0.0165(3)
C8B	0.41969(16)	0.16512(15)	0.68290(13)	0.0209(3)
C9B	0.28052(16)	0.19378(15)	0.78089(13)	0.0221(3)
O9B	0.19379(12)	0.12532(11)	0.80412(10)	0.0312(3)
C10B	0.25798(17)	0.30945(15)	0.85096(14)	0.0236(3)
C11B	0.35803(15)	0.29395(14)	0.91300(13)	0.0203(3)
O11B	0.50630(10)	0.26108(9)	0.83760(9)	0.0186(2)
C12B	0.33458(17)	0.18785(14)	0.98812(13)	0.0213(3)
C13B	0.42953(14)	0.07910(13)	0.91426(11)	0.0163(3)
O13B	0.42212(11)	-0.02891(9)	0.92336(9)	0.0203(2)
C14B	0.54361(14)	0.13076(13)	0.81785(11)	0.0157(3)
C15B	0.68689(14)	0.08060(13)	0.82595(11)	0.0162(3)
O15B	0.74416(11)	-0.02539(9)	0.80080(9)	0.0209(2)
O16B	0.73513(11)	0.16505(9)	0.86709(9)	0.0210(2)
C16B	0.86695(17)	0.11881(17)	0.88156(15)	0.0278(4)

\*  $U_{eq}$  is defined as one third of the trace of the orthogonalized  $U_{ij}$  tensor.

**Table 3.** Anisotropic atomic displacement parameters\* ( $\text{\AA}^2$ ) for UM#1906.

Atom	$U_{11}$	$U_{22}$	$U_{33}$	$U_{23}$	$U_{13}$	$U_{12}$
C1A	0.0239(8)	0.0183(7)	0.0202(7)	-0.0005(6)	-0.0089(6)	-0.0041(6)
C2A	0.0197(7)	0.0237(8)	0.0242(8)	-0.0041(6)	-0.0053(6)	-0.0064(6)
C3A	0.0168(7)	0.0329(9)	0.0227(8)	-0.0054(7)	-0.0075(6)	0.0007(6)
C4A	0.0249(8)	0.0273(8)	0.0234(8)	0.0021(7)	-0.0101(6)	0.0008(6)
C5A	0.0231(7)	0.0189(7)	0.0210(7)	0.0027(6)	-0.0076(6)	-0.0038(6)

C6A	0.0185(7)	0.0184(7)	0.0154(7)	-0.0026(5)	-0.0067(6)	-0.0015(5)
C7A	0.0205(7)	0.0153(7)	0.0173(7)	0.0012(5)	-0.0082(6)	-0.0056(5)
C8A	0.0210(7)	0.0256(8)	0.0187(7)	-0.0018(6)	-0.0088(6)	-0.0046(6)
C9A	0.0207(7)	0.0264(8)	0.0169(7)	-0.0056(6)	-0.0054(6)	-0.0046(6)
O9A	0.0274(6)	0.0427(7)	0.0315(6)	0.0075(5)	-0.0123(5)	-0.0162(5)
C10A	0.0195(7)	0.0223(8)	0.0283(8)	-0.0043(7)	-0.0098(6)	-0.0010(6)
C11A	0.0223(7)	0.0178(7)	0.0276(8)	0.0027(6)	-0.0118(6)	-0.0018(6)
O11A	0.0200(5)	0.0128(5)	0.0254(5)	0.0010(4)	-0.0082(4)	-0.0020(4)
C12A	0.0254(8)	0.0243(8)	0.0245(8)	0.0010(6)	-0.0138(7)	-0.0037(6)
C13A	0.0240(7)	0.0204(7)	0.0142(7)	0.0007(5)	-0.0084(6)	-0.0057(6)
O13A	0.0332(6)	0.0186(5)	0.0244(6)	0.0005(4)	-0.0141(5)	-0.0091(4)
C14A	0.0222(7)	0.0111(6)	0.0195(7)	0.0008(5)	-0.0090(6)	-0.0037(5)
C15A	0.0233(7)	0.0173(7)	0.0168(7)	-0.0006(5)	-0.0091(6)	-0.0047(6)
O15A	0.0306(6)	0.0167(5)	0.0252(6)	-0.0008(4)	-0.0080(5)	-0.0001(4)
O16A	0.0263(6)	0.0178(5)	0.0201(5)	0.0006(4)	-0.0018(4)	-0.0039(4)
C16A	0.0352(10)	0.0267(9)	0.0283(9)	-0.0001(7)	0.0044(8)	-0.0049(8)
C1B	0.0206(7)	0.0159(7)	0.0200(7)	0.0009(6)	-0.0082(6)	-0.0013(5)
C2B	0.0211(7)	0.0200(7)	0.0256(8)	0.0077(6)	-0.0093(6)	-0.0042(6)
C3B	0.0181(7)	0.0249(8)	0.0201(7)	0.0052(6)	-0.0041(6)	0.0016(6)
C4B	0.0269(8)	0.0212(8)	0.0192(7)	-0.0014(6)	-0.0076(6)	0.0021(6)
C5B	0.0234(7)	0.0171(7)	0.0201(7)	0.0017(6)	-0.0096(6)	-0.0026(6)
C6B	0.0186(7)	0.0166(7)	0.0157(7)	0.0025(5)	-0.0075(5)	-0.0017(5)
C7B	0.0176(7)	0.0150(7)	0.0170(7)	0.0017(5)	-0.0063(6)	-0.0043(5)
C8B	0.0220(7)	0.0233(8)	0.0192(7)	0.0023(6)	-0.0105(6)	-0.0030(6)
C9B	0.0185(7)	0.0262(8)	0.0240(8)	0.0033(6)	-0.0120(6)	-0.0011(6)
O9B	0.0229(6)	0.0367(7)	0.0369(7)	0.0015(5)	-0.0125(5)	-0.0104(5)
C10B	0.0191(7)	0.0216(8)	0.0269(8)	0.0021(7)	-0.0070(6)	0.0001(6)
C11B	0.0183(7)	0.0172(7)	0.0224(7)	-0.0030(6)	-0.0052(6)	-0.0016(5)
O11B	0.0166(5)	0.0137(5)	0.0236(5)	-0.0008(4)	-0.0056(4)	-0.0021(4)
C12B	0.0208(7)	0.0222(8)	0.0183(7)	-0.0018(6)	-0.0054(6)	-0.0015(6)
C13B	0.0166(6)	0.0202(7)	0.0148(7)	0.0009(5)	-0.0085(5)	-0.0044(5)
O13B	0.0233(5)	0.0189(5)	0.0204(5)	0.0030(4)	-0.0086(4)	-0.0075(4)
C14B	0.0168(7)	0.0136(6)	0.0167(7)	0.0001(5)	-0.0061(5)	-0.0031(5)
C15B	0.0174(7)	0.0176(7)	0.0127(6)	0.0016(5)	-0.0038(5)	-0.0051(5)
O15B	0.0212(5)	0.0183(5)	0.0212(5)	0.0001(4)	-0.0071(4)	-0.0002(4)
O16B	0.0187(5)	0.0213(5)	0.0253(6)	-0.0009(4)	-0.0102(4)	-0.0053(4)
C16B	0.0197(8)	0.0337(9)	0.0329(9)	-0.0028(8)	-0.0135(7)	-0.0045(7)

\* The anisotropic atomic displacement factor exponent takes the form:  $-2\pi^2 [ h^2a^2U_{11} + \dots + 2hka*b*U_{12} ]$

**Table 4.** Hydrogen atom coordinates and isotropic atomic displacement parameters ( $\text{\AA}^2$ ) for UM#1906.

Atom	$x/a$	$y/b$	$z/c$	$U_{\text{iso}}$
H1A	0.2612(19)	0.2561(17)	0.2840(15)	0.026(5)
H2A	0.0540(19)	0.2605(16)	0.2497(15)	0.027(5)
H3A	-0.027(2)	0.4264(17)	0.1620(15)	0.030(5)
H4A	0.100(2)	0.5921(18)	0.1124(16)	0.032(5)
H5A	0.3014(18)	0.5917(16)	0.1536(14)	0.024(4)
H7A	0.4636(16)	0.5008(15)	0.2304(13)	0.014(4)
H8A	0.5252(18)	0.2558(16)	0.1366(15)	0.025(3)
H8B	0.5689(18)	0.3734(16)	0.0710(15)	0.025(3)

H10A	0.8335(19)	0.1817(16)	0.1959(14)	0.025(3)
H10B	0.7126(18)	0.1247(17)	0.1729(15)	0.025(3)
H11A	0.6451(18)	0.1326(16)	0.3624(15)	0.025(4)
H12A	0.625(2)	0.3082(17)	0.4661(16)	0.032(4)
H12B	0.757(2)	0.3350(17)	0.3586(15)	0.032(4)
H16A	0.136(2)	0.440(2)	0.6374(17)	0.040(3)
H16B	0.099(2)	0.305(2)	0.6394(17)	0.040(3)
H16C	0.048(2)	0.4117(19)	0.5728(17)	0.040(3)
H1B	0.7235(18)	0.2463(16)	0.6444(14)	0.021(4)
H2B	0.9319(19)	0.2444(17)	0.4890(15)	0.029(5)
H3B	1.0141(19)	0.0769(16)	0.3563(15)	0.025(5)
H4B	0.8782(19)	-0.0849(17)	0.3842(15)	0.027(5)
H5B	0.6777(19)	-0.0857(17)	0.5412(15)	0.029(5)
H7B	0.5236(17)	0.0018(15)	0.7187(13)	0.016(4)
H8C	0.4046(19)	0.1212(17)	0.6253(15)	0.028(3)
H8D	0.4496(19)	0.2411(17)	0.6556(15)	0.028(3)
H10C	0.2769(19)	0.3763(17)	0.8047(15)	0.025(3)
H10D	0.1607(19)	0.3261(16)	0.9036(15)	0.025(3)
H11B	0.3524(18)	0.3729(16)	0.9486(14)	0.022(4)
H12C	0.2373(19)	0.1752(16)	1.0226(14)	0.023(3)
H12D	0.3718(18)	0.1969(16)	1.0446(15)	0.023(3)
H16D	0.941(2)	0.0859(18)	0.8126(18)	0.040(3)
H16E	0.892(2)	0.1892(19)	0.9091(17)	0.040(3)
H16F	0.850(2)	0.0550(19)	0.9367(17)	0.040(3)

**Table 5.** Bond lengths (Å) and angles (°) for UM#1906.

C1A-C2A	1.389(2)	C1A-C6A	1.396(2)	C1A-H1A	0.973(18)
C2A-C3A	1.390(2)	C2A-H2A	0.959(18)	C3A-C4A	1.388(2)
C3A-H3A	0.963(19)	C4A-C5A	1.388(2)	C4A-H4A	0.977(19)
C5A-C6A	1.395(2)	C5A-H5A	0.963(17)	C6A-C7A	1.515(2)
C7A-C8A	1.554(2)	C7A-C14A	1.555(2)	C7A-H7A	0.962(16)
C8A-C9A	1.511(2)	C8A-H8A	0.990(18)	C8A-H8B	0.951(18)
C9A-O9A	1.2170(19)	C9A-C10A	1.517(2)	C10A-C11A	1.535(2)
C10A-H10A	0.991(18)	C10A-H10B	0.981(19)	C11A-O11A	1.4593(18)
C11A-C12A	1.517(2)	C11A-H11A	0.990(18)	O11A-C14A	1.4235(16)
C12A-C13A	1.502(2)	C12A-H12A	0.99(2)	C12A-H12B	0.982(19)
C13A-O13A	1.2032(18)	C13A-C14A	1.554(2)	C14A-C15A	1.528(2)
C15A-O15A	1.2015(18)	C15A-O16A	1.3316(17)	O16A-C16A	1.450(2)
C16A-H16A	0.94(2)	C16A-H16B	0.98(2)	C16A-H16C	0.96(2)
C1B-C2B	1.392(2)	C1B-C6B	1.396(2)	C1B-H1B	0.931(18)
C2B-C3B	1.388(2)	C2B-H2B	0.974(18)	C3B-C4B	1.385(2)
C3B-H3B	0.993(18)	C4B-C5B	1.392(2)	C4B-H4B	0.969(19)
C5B-C6B	1.395(2)	C5B-H5B	0.976(18)	C6B-C7B	1.5183(19)
C7B-C8B	1.554(2)	C7B-C14B	1.558(2)	C7B-H7B	0.959(16)
C8B-C9B	1.513(2)	C8B-H8C	0.98(2)	C8B-H8D	0.961(19)
C9B-O9B	1.2155(19)	C9B-C10B	1.515(2)	C10B-C11B	1.534(2)
C10B-H10C	0.953(18)	C10B-H10D	0.968(18)	C11B-O11B	1.4594(17)
C11B-C12B	1.521(2)	C11B-H11B	0.975(18)	O11B-C14B	1.4207(16)
C12B-C13B	1.499(2)	C12B-H12C	0.966(18)	C12B-H12D	0.976(19)
C13B-O13B	1.2067(17)	C13B-C14B	1.5553(19)	C14B-C15B	1.5313(19)
C15B-O15B	1.2026(17)	C15B-O16B	1.3336(17)	O16B-C16B	1.4518(19)
C16B-H16D	0.97(2)	C16B-H16E	0.97(2)	C16B-H16F	1.00(2)
C2A-C1A-C6A	120.16(15)	C2A-C1A-H1A	120.3(11)	C6A-C1A-H1A	119.5(11)

C1A-C2A-C3A	120.55(15)	C1A-C2A-H2A	118.8(11)	C3A-C2A-H2A	120.7(11)
C4A-C3A-C2A	119.35(15)	C4A-C3A-H3A	120.4(11)	C2A-C3A-H3A	120.3(11)
C3A-C4A-C5A	120.41(15)	C3A-C4A-H4A	120.3(11)	C5A-C4A-H4A	119.3(11)
C4A-C5A-C6A	120.39(14)	C4A-C5A-H5A	119.6(10)	C6A-C5A-H5A	120.0(10)
C5A-C6A-C1A	119.10(14)	C5A-C6A-C7A	119.29(13)	C1A-C6A-C7A	121.44(13)
C6A-C7A-C8A	107.42(12)	C6A-C7A-C14A	114.90(12)	C8A-C7A-C14A	110.42(12)
C6A-C7A-H7A	108.6(9)	C8A-C7A-H7A	109.8(10)	C14A-C7A-H7A	105.7(10)
C9A-C8A-C7A	113.75(12)	C9A-C8A-H8A	108.9(10)	C7A-C8A-H8A	106.8(10)
C9A-C8A-H8B	108.7(11)	C7A-C8A-H8B	108.8(11)	H8A-C8A-H8B	109.8(15)
O9A-C9A-C8A	121.31(15)	O9A-C9A-C10A	122.05(15)	C8A-C9A-C10A	116.63(13)
C9A-C10A-C11A	111.75(13)	C9A-C10A-H10A	108.3(10)	C11A-C10A-H10A	110.8(10)
C9A-C10A-H10B	107.6(11)	C11A-C10A-H10B	108.8(11)	H10A-C10A-H10B	109.5(15)
O11A-C11A-C12A	104.56(12)	O11A-C11A-C10A	110.79(13)	C12A-C11A-C10A	112.79(13)
O11A-C11A-H11A	105.8(10)	C12A-C11A-H11A	112.4(11)	C10A-C11A-H11A	110.1(10)
C14A-O11A-C11A	109.51(11)	C13A-C12A-C11A	102.82(12)	C13A-C12A-H12A	106.2(11)
C11A-C12A-H12A	111.2(11)	C13A-C12A-H12B	109.8(11)	C11A-C12A-H12B	115.7(11)
H12A-C12A-H12B	110.5(15)	O13A-C13A-C12A	128.28(14)	O13A-C13A-C14A	124.80(13)
C12A-C13A-C14A	106.90(12)	O11A-C14A-C15A	111.72(11)	O11A-C14A-C13A	104.75(11)
C15A-C14A-C13A	106.84(12)	O11A-C14A-C7A	113.17(12)	C15A-C14A-C7A	110.41(12)
C13A-C14A-C7A	109.60(11)	O15A-C15A-O16A	125.26(14)	O15A-C15A-C14A	121.76(13)
O16A-C15A-C14A	112.96(12)	C15A-O16A-C16A	114.05(12)	O16A-C16A-H16A	109.8(13)
O16A-C16A-H16B	106.2(12)	H16A-C16A-H16B	111.4(18)	O16A-C16A-H16C	110.8(13)
H16A-C16A-H16C	107.5(18)	H16B-C16A-H16C	111.3(17)	C2B-C1B-C6B	120.33(14)
C2B-C1B-H1B	119.8(10)	C6B-C1B-H1B	119.9(10)	C3B-C2B-C1B	120.29(14)
C3B-C2B-H2B	119.5(11)	C1B-C2B-H2B	120.2(11)	C4B-C3B-C2B	119.49(14)
C4B-C3B-H3B	120.1(10)	C2B-C3B-H3B	120.3(10)	C3B-C4B-C5B	120.69(15)
C3B-C4B-H4B	121.4(11)	C5B-C4B-H4B	117.9(11)	C4B-C5B-C6B	120.05(14)
C4B-C5B-H5B	118.8(11)	C6B-C5B-H5B	121.1(11)	C5B-C6B-C1B	119.15(14)
C5B-C6B-C7B	119.03(13)	C1B-C6B-C7B	121.72(13)	C6B-C7B-C8B	108.16(12)
C6B-C7B-C14B	114.57(12)	C8B-C7B-C14B	110.65(12)	C6B-C7B-H7B	108.7(10)
C8B-C7B-H7B	109.6(10)	C14B-C7B-H7B	105.0(10)	C9B-C8B-C7B	113.56(12)
C9B-C8B-H8C	109.0(10)	C7B-C8B-H8C	108.3(11)	C9B-C8B-H8D	109.3(11)
C7B-C8B-H8D	108.5(11)	H8C-C8B-H8D	108.1(15)	O9B-C9B-C8B	121.69(15)
O9B-C9B-C10B	121.85(15)	C8B-C9B-C10B	116.41(13)	C9B-C10B-C11B	111.02(12)
C9B-C10B-H10C	108.4(11)	C11B-C10B-H10C	109.3(11)	C9B-C10B-H10D	109.4(11)
C11B-C10B-H10D	108.5(11)	H10C-C10B-H10D	110.3(15)	O11B-C11B-C12B	104.49(11)
O11B-C11B-C10B	110.75(12)	C12B-C11B-C10B	112.21(13)	O11B-C11B-H11B	104.7(10)
C12B-C11B-H11B	114.6(10)	C10B-C11B-H11B	109.7(10)	C14B-O11B-C11B	109.46(10)
C13B-C12B-C11B	102.67(12)	C13B-C12B-H12C	112.1(11)	C11B-C12B-H12C	115.7(10)
C13B-C12B-H12D	106.3(10)	C11B-C12B-H12D	110.9(10)	H12C-C12B-H12D	108.6(14)
O13B-C13B-C12B	128.67(13)	O13B-C13B-C14B	124.43(13)	C12B-C13B-C14B	106.89(12)
O11B-C14B-C15B	111.85(11)	O11B-C14B-C13B	104.85(11)	C15B-C14B-C13B	105.96(11)
O11B-C14B-C7B	113.47(11)	C15B-C14B-C7B	110.72(11)	C13B-C14B-C7B	109.53(11)
O15B-C15B-O16B	125.27(13)	O15B-C15B-C14B	121.94(13)	O16B-C15B-C14B	112.74(12)
C15B-O16B-C16B	114.22(12)	O16B-C16B-H16D	110.3(12)	O16B-C16B-H16E	105.9(12)
H16D-C16B-H16E	110.2(17)	O16B-C16B-H16F	108.9(12)	H16D-C16B-H16F	111.5(16)
H16E-C16B-H16F	109.8(17)				

**Table 6.** Torsion angles (°) in UM#1906 compared for molecules A and B.

Angle	A	B
C6 - C1 - C2 - C3	1.2(2)	1.0(2)
C1 - C2 - C3 - C4	-1.8(2)	-0.5(2)
C2 - C3 - C4 - C5	0.7(2)	-0.6(2)
C3 - C4 - C5 - C6	1.0(2)	1.1(2)
C4 - C5 - C6 - C1	-1.6(2)	-0.5(2)
C4 - C5 - C6 - C7	173.67(14)	175.83(13)
C2 - C1 - C6 - C5	0.6(2)	-0.5(2)

C2 - C1 - C6 - C7	-174.65(14)	-176.75(14)
C5 - C6 - C7 - C8	-96.87(16)	-95.75(15)
C1 - C6 - C7 - C8	78.33(17)	80.51(17)
C5 - C6 - C7 - C14	139.84(14)	140.34(14)
C1 - C6 - C7 - C14	-44.95(19)	-43.41(19)
C6 - C7 - C8 - C9	-173.00(13)	-169.83(13)
C14 - C7 - C8 - C9	-47.00(17)	-43.59(17)
C7 - C8 - C9 - O9	-90.04(18)	-88.13(18)
C7 - C8 - C9 - C10	89.29(17)	89.41(17)
O9 - C9 - C10 - C11	113.11(17)	107.94(17)
C8 - C9 - C10 - C11	-66.22(18)	-69.60(17)
C9 - C10 - C11 - O11	54.44(17)	56.28(17)
C9 - C10 - C11 - C12	-62.38(17)	-60.05(17)
C12 - C11 - O11 - C14	33.33(15)	33.45(15)
C10 - C11 - O11 - C14	-88.45(14)	-87.57(14)
O11 - C11 - C12 - C13	-32.55(15)	-32.87(15)
C10 - C11 - C12 - C13	87.91(15)	87.17(14)
C11 - C12 - C13 - O13	-157.51(16)	-157.40(15)
C11 - C12 - C13 - C14	21.19(16)	21.58(15)
C11 - O11 - C14 - C15	-134.58(12)	-133.57(12)
C11 - O11 - C14 - C13	-19.29(14)	-19.19(14)
C11 - O11 - C14 - C7	100.05(14)	100.30(13)
O13 - C13 - C14 - O11	176.63(14)	176.56(13)
C12 - C13 - C14 - O11	-2.13(15)	-2.48(14)
O13 - C13 - C14 - C15	-64.72(18)	-65.00(17)
C12 - C13 - C14 - C15	116.52(13)	115.97(12)
O13 - C13 - C14 - C7	54.92(19)	54.46(18)
C12 - C13 - C14 - C7	-123.84(13)	-124.57(12)
C6 - C7 - C14 - O11	89.18(15)	86.99(14)
C8 - C7 - C14 - O11	-32.49(16)	-35.60(15)
C6 - C7 - C14 - C15	-36.88(16)	-39.74(16)
C8 - C7 - C14 - C15	-158.55(12)	-162.32(11)
C6 - C7 - C14 - C13	-154.31(12)	-156.23(12)
C8 - C7 - C14 - C13	84.02(14)	81.18(14)
O11 - C14 - C15 - O15	-174.18(13)	-172.05(12)
C13 - C14 - C15 - O15	71.81(17)	74.25(16)
C7 - C14 - C15 - O15	-47.30(19)	-44.43(18)
O11 - C14 - C15 - O16	7.28(17)	10.44(16)
C13 - C14 - C15 - O16	-106.73(13)	-103.26(13)
C7 - C14 - C15 - O16	134.16(13)	138.06(12)
O15 - C15 - O16 - C16	-2.2(2)	-0.6(2)
C14 - C15 - O16 - C16	176.27(14)	176.77(12)

Compound name : Minor product ***anti*-193(a)**  
 Chemical formula : C<sub>16</sub>H<sub>16</sub>O<sub>5</sub>  
 Final R<sub>1</sub> [*I*>2σ(*I*)] : 2.83 %

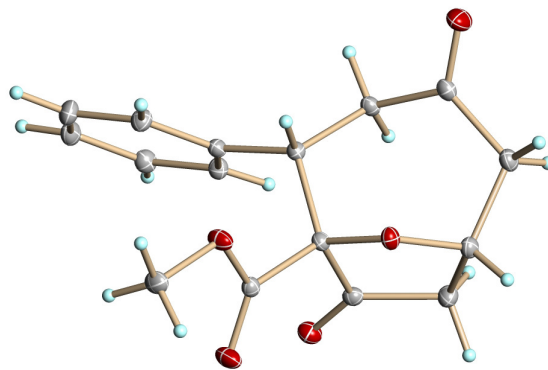


**Figure 1.** A view showing the anisotropic atomic displacement ellipsoids for the non-hydrogen atoms at the 30% probability level. Hydrogen atoms are displayed with an arbitrarily small radius.

Crystals were obtained by dissolving 10 mg of white solid **anti-193(a)** with minimum amount of ether:DCM (10:1). A colorless prism of  $C_{16}H_{16}O_5$ , approximate dimensions  $0.365 \times 0.46 \times 0.51 \text{ mm}^3$ , was used for the X-ray crystallographic analysis. The X-ray intensity data were measured at 150(2) °K on a three-circle diffractometer system equipped with Bruker Smart Apex II CCD area detector using a graphite monochromator and a MoK  $\alpha$  fine-focus sealed tube ( $\lambda = 0.71073 \text{ \AA}$ ). The detector was placed at a distance of 5.000 cm from the crystal.

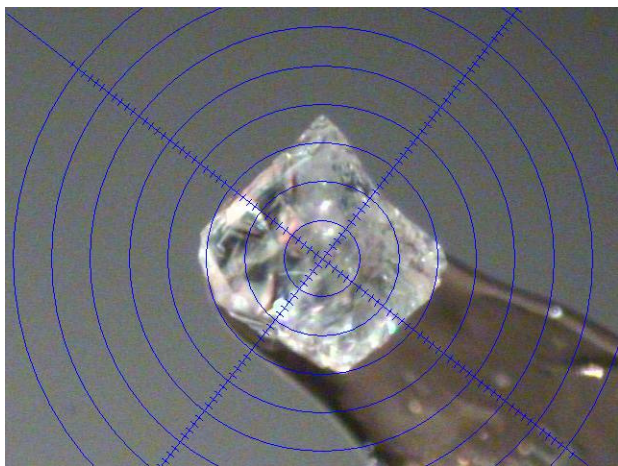
A total of 3030 frames was collected with a scan width of  $-0.30^\circ$  an exposure time of 5 sec/frame using Apex2 (Bruker, 2005). The total data collection time was 9.3 hours. The frames were integrated with Apex2 software package using a narrow-frame integration algorithm. The integration of the data using a Orthorhombic unit cell yielded a total of 17271 reflections to a maximum  $\theta$  angle of  $30.00^\circ$ , of which 4018 were independent (completeness = 100.0%,  $R_{\text{int}} = 1.74\%$ ,  $R_{\text{sig}} = 1.47\%$ ) and 3955 were greater than  $2\sigma(I)$ . The final cell dimensions of  $a = 8.4520(9) \text{ \AA}$ ,  $b = 9.9029(11) \text{ \AA}$ ,  $c = 16.5155(18) \text{ \AA}$ ,  $\alpha = 90^\circ$ ,  $\beta = 90^\circ$ ,  $\lambda = 90^\circ$ ,  $V = 1382.3(3) \text{ \AA}^3$ , are based upon the refinement of the XYZ-centroids of 12995 reflections with  $2.4 < \theta < 32.2^\circ$  using Apex2

software. Analysis of the data showed 0 % decay during data collection. Data were corrected for absorption effects with the Semi-empirical from equivalents method using SADABS (Sheldrick, 1996). The minimum and maximum transmission coefficients were 0.886 and 0.963.

The structure was solved and refined using the SHELXS-97 (Sheldrick, 1990) and SHELXL-97 (Sheldrick, 1997) software in the space group  $P2_12_12_1$  with  $Z = 4$  for the formula unit  $C_{16}H_{16}O_5$ . The final anisotropic full-matrix least-squares refinement on  $F^2$  with 249 variables converged at  $R_1 = 2.83\%$  for the observed data and  $wR_2 = 6.71\%$  for all data. The goodness-of-fit was 1.001. The largest peak on the final difference map was  $0.279 \text{ \AA}^{-3}$  and the largest hole was  $-0.131 \text{ \AA}^{-3}$ . On the basis of the final model, the calculated density was  $1.385 \text{ g/cm}^3$  and  $F(000)$ , 608 e.

**Comments:**

- H-atoms: all refined
- Residual density: in the middle of the
- Absolute configuration: not established



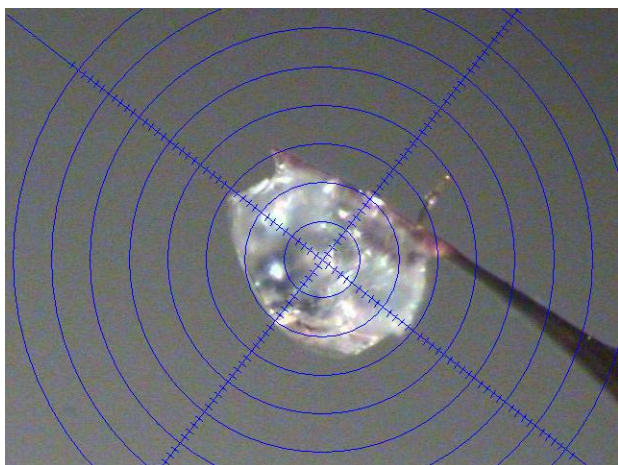


**Table 1.** Crystal data and structure refinement for UM#1972.

X-ray lab book No.	1972
Crystal ID	Doyle/Jaber Phenyl-Mirror product 150K
Empirical formula	$C_{16}H_{16}O_5$
Formula weight	288.29
Temperature	150(2) K
Wavelength	0.71073 Å
Crystal size	0.51×0.46×0.365 mm <sup>3</sup>
Crystal habit	colorless prism
Crystal system	Orthorhombic
Space group	$P2_12_12_1$
Unit cell dimensions	$a = 8.4520(9)$ Å $\alpha = 90^\circ$ $b = 9.9029(11)$ Å $\beta = 90^\circ$ $c = 16.5155(18)$ Å $\gamma = 90^\circ$
Volume	1382.3(3) Å <sup>3</sup>
Z	4
Density, $\rho_{\text{calc}}$	1.385 g/cm <sup>3</sup>
Absorption coefficient, $\mu$	0.103 mm <sup>-1</sup>
F(000)	608 e <sup>-</sup>
Diffractometer	Bruker Smart Apex II CCD area detector
Radiation source	fine-focus sealed tube, MoK $\alpha$
Detector distance	5.000 cm
Data collection method	$\omega$ and $\phi$ scans
Total frames	3030
Frame size	512 pixels
Frame width	-0.30°
Exposure per frame	5 sec
Total measurement time	9.3 hours
$\theta$ range for data collection	2.40 to 30.00°
Index ranges	$-11 \leq h \leq 11, -13 \leq k \leq 13, -23 \leq l \leq 23$
Reflections collected	17271
Independent reflections	4018
Observed reflection, $I > 2\sigma(I)$	3955
Coverage of independent reflections	100.0 %
Variation in check reflections	0 %
Absorption correction	Semi-empirical from equivalents SADABS (Sheldrick, 1996)
Max. and min. transmission	0.963 and 0.886
Structure solution technique	direct

Structure solution program	SHELXS-97 (Sheldrick, 1990)		
Refinement technique	Full-matrix least-squares on $F^2$		
Refinement program	SHELXL-97 (Sheldrick, 1997)		
Function minimized	$\Sigma w(F_o^2 - F_c^2)^2$		
Data / restraints / parameters	4018 / 0 / 249		
Goodness-of-fit on $F^2$	1.001		
$\Delta/\sigma_{\max}$	0.001		
Final R indices:	$R_1, I > 2\sigma(I)$	0.0283	
	$wR_2, \text{ all data}$	0.0671	
	$R_{\text{int}}$	0.0174	
	$R_{\text{sig}}$	0.0147	
Weighting scheme	$w = 1/[\sigma^2(F_o^2) + (0.03P)^2 + 0.3615P], P = [\max(F_o^2, 0) + 2F_o^2]/3$		
Absolute structure parameter	-0.1(5)		
Largest diff. peak and hole	0.279	and	-0.131 $\bar{e}/\text{\AA}^3$

$$R_1 = \Sigma ||F_o| - |F_c|| / \Sigma |F_o|, \quad wR_2 = [\Sigma w(F_o^2 - F_c^2)^2 / \Sigma w(F_o^2)^2]^{1/2}$$

**Table 2.** Atomic coordinates and equivalent\* isotropic atomic displacement parameters ( $\text{\AA}^2$ ) for UM#1972.

Atom	$x/a$	$y/b$	$z/c$	$U_{\text{eq}}$
C1	0.63633(13)	0.34498(11)	0.12104(6)	0.02255(19)
C2	0.50744(13)	0.40226(11)	0.16110(7)	0.0265(2)
C3	0.47345(13)	0.36522(11)	0.24027(7)	0.0253(2)
C4	0.56858(12)	0.27075(11)	0.27916(7)	0.02292(19)
C5	0.69707(12)	0.21306(10)	0.23912(6)	0.01947(18)
C6	0.73282(11)	0.24987(10)	0.15942(6)	0.01721(16)
C7	0.86764(11)	0.18466(9)	0.11182(6)	0.01645(16)
C8	0.86164(11)	0.02867(9)	0.12065(6)	0.01841(17)
C9	0.96906(12)	-0.04768(9)	0.06277(6)	0.01963(17)
O9	0.91467(10)	-0.10121(9)	0.00272(5)	0.03078(18)
C10	1.14397(12)	-0.06139(10)	0.08107(6)	0.02168(18)
C11	1.22046(11)	0.06390(10)	0.11875(6)	0.01985(17)
O11	1.15204(8)	0.18456(7)	0.08136(4)	0.01903(14)
C12	1.19917(13)	0.08142(11)	0.20999(6)	0.02264(19)
C13	1.08724(11)	0.19942(10)	0.21929(6)	0.01819(17)
O13	1.04734(9)	0.25237(8)	0.28150(4)	0.02343(15)
C14	1.03392(11)	0.24102(9)	0.13351(5)	0.01601(16)
C15	1.04838(11)	0.39433(9)	0.12199(6)	0.01749(17)
O15	1.10301(11)	0.46903(8)	0.17182(5)	0.02799(17)
O16	0.99901(9)	0.43324(7)	0.04917(4)	0.02421(15)
C16	1.01805(13)	0.57755(11)	0.03409(7)	0.0249(2)

\*  $U_{\text{eq}}$  is defined as one third of the trace of the orthogonalized  $U_{ij}$  tensor.

**Table 3.** Hydrogen atom coordinates and isotropic atomic displacement parameters ( $\text{\AA}^2$ ) for UM#1972.

Atom	$x/a$	$y/b$	$z/c$	$U_{\text{iso}}$
------	-------	-------	-------	------------------

H1	0.6588(18)	0.3682(15)	0.0667(9)	0.027(4)
H2	0.4400(18)	0.4682(15)	0.1337(9)	0.031(4)
H3	0.3851(18)	0.4029(15)	0.2652(9)	0.029(3)
H4	0.5471(17)	0.2455(15)	0.3343(9)	0.030(4)
H5	0.7570(17)	0.1476(14)	0.2639(8)	0.021(3)
H7	0.8560(15)	0.2051(13)	0.0562(7)	0.015(3)
H8A	0.8851(16)	0.0003(14)	0.1741(8)	0.021(2)
H8B	0.7556(17)	0.0034(14)	0.1080(8)	0.021(2)
H10A	1.1910(18)	-0.0848(16)	0.0318(9)	0.034(3)
H10B	1.1598(19)	-0.1351(16)	0.1159(10)	0.034(3)
H11	1.3320(17)	0.0626(15)	0.1039(8)	0.022(3)
H12A	1.1550(19)	0.0071(16)	0.2369(9)	0.034(3)
H12B	1.3027(18)	0.1031(16)	0.2358(9)	0.034(3)
H16A	0.9537(18)	0.6268(15)	0.0727(9)	0.030(2)
H16B	0.9819(18)	0.5928(15)	-0.0202(9)	0.030(2)
H16C	1.1252(19)	0.5994(16)	0.0386(9)	0.030(2)

**Table 4.** Anisotropic atomic displacement parameters\* ( $\text{\AA}^2$ ) for UM#1972.

Atom	$U_{11}$	$U_{22}$	$U_{33}$	$U_{23}$	$U_{13}$	$U_{12}$
C1	0.0231(5)	0.0239(4)	0.0206(4)	0.0011(4)	-0.0017(4)	0.0030(4)
C2	0.0226(5)	0.0254(5)	0.0316(5)	0.0006(4)	-0.0027(4)	0.0071(4)
C3	0.0190(5)	0.0251(5)	0.0317(5)	-0.0046(4)	0.0038(4)	0.0032(4)
C4	0.0216(5)	0.0232(5)	0.0239(5)	-0.0008(4)	0.0049(4)	-0.0008(4)
C5	0.0193(4)	0.0183(4)	0.0208(4)	0.0015(3)	0.0013(3)	0.0010(3)
C6	0.0166(4)	0.0158(4)	0.0192(4)	-0.0021(3)	-0.0001(3)	-0.0006(3)
C7	0.0170(4)	0.0156(4)	0.0168(4)	-0.0004(3)	0.0002(3)	0.0000(3)
C8	0.0182(4)	0.0153(4)	0.0217(4)	-0.0017(3)	0.0019(3)	-0.0019(3)
C9	0.0230(4)	0.0143(4)	0.0216(4)	-0.0001(3)	0.0025(3)	-0.0011(3)
O9	0.0309(4)	0.0323(4)	0.0291(4)	-0.0116(3)	-0.0025(3)	0.0008(3)
C10	0.0217(4)	0.0185(4)	0.0249(4)	-0.0035(4)	0.0021(4)	0.0022(4)
C11	0.0173(4)	0.0188(4)	0.0235(4)	-0.0017(4)	0.0014(3)	0.0021(3)
O11	0.0194(3)	0.0179(3)	0.0198(3)	0.0000(3)	0.0045(3)	0.0018(3)
C12	0.0231(5)	0.0225(5)	0.0223(4)	-0.0005(4)	-0.0037(4)	0.0040(4)
C13	0.0176(4)	0.0177(4)	0.0193(4)	0.0005(3)	-0.0009(3)	-0.0026(3)
O13	0.0277(4)	0.0237(3)	0.0188(3)	-0.0020(3)	0.0013(3)	-0.0021(3)
C14	0.0174(4)	0.0149(4)	0.0157(4)	-0.0014(3)	0.0012(3)	0.0002(3)
C15	0.0155(4)	0.0167(4)	0.0203(4)	-0.0004(3)	0.0020(3)	0.0007(3)
O15	0.0392(4)	0.0189(3)	0.0259(4)	-0.0018(3)	-0.0074(3)	-0.0045(3)
O16	0.0335(4)	0.0175(3)	0.0217(3)	0.0023(3)	-0.0050(3)	-0.0054(3)
C16	0.0279(5)	0.0174(4)	0.0294(5)	0.0046(4)	-0.0034(4)	-0.0037(4)

\* The anisotropic atomic displacement factor exponent takes the form:  $-2\pi^2 [ h^2a^2U_{11} + \dots + 2hka*b*U_{12} ]$

**Table 5.** Bond lengths ( $\text{\AA}$ ), valence and torsion angles ( $^\circ$ ) for UM#1972.

C1-C2	1.3951(15)	C1-C6	1.3979(14)	C1-H1	0.945(14)	C2-C3
-------	------------	-------	------------	-------	-----------	-------

H7	0.946(12)	C8-C9	1.5198(13)	C8-H8A	0.948(14)	C8-H8B
C13	1.5114(14)	C12-H12A	0.937(16)	C12-H12B	0.997(16)	C13-O13
C2-C1-C6	120.96(10)	C2-C1-H1	120.5(9)	C6-C1-H1	118.5(9)	C3-C2-C1
C6	120.52(9)	C4-C5-H5	120.5(9)	C6-C5-H5	118.9(9)	C1-C6-C5
H8A	108.3(8)	C7-C8-H8A	112.1(8)	C9-C8-H8B	107.1(8)	C7-C8-H8
H10B	108.7(10)	H10A-C10-H10B	106.3(14)	O11-C11-C12	106.07(8)	O11-C11-
H12B	110.0(9)	H12A-C12-H12B	108.5(13)	O13-C13-C12	126.86(9)	O13-C13-
C15-C14	111.94(8)	C15-O16-C16	113.79(8)	O16-C16-H16A	108.6(9)	O16-C16-
C6-C1-C2-C3	0.09(17)	C1-C2-C3-C4	-0.05(17)	C2-C3-C4-C5	-0.18(16)	
79.24(11)	C6-C7-C8-C9	168.33(8)	C14-C7-C8-C9	-64.18(10)	C7-C8-C9-O9	
C13	11.76(10)	C10-C11-C12-C13	-109.41(10)	C11-C12-C13-O13	-174.76(10)	
80.56(12)	C12-C13-C14-C7	99.94(9)	C6-C7-C14-O11	-174.56(7)	C8-C7-C14-O11	
C15-O16	-178.30(8)	C7-C14-C15-O16	-50.85(10)	O15-C15-O16-C16	0.41(14)	

---

## **2.8 Bibliography**

- Ahmed, A. F.; Su, J.-H.; Kuo, Y.-H.; Sheu, J.-H. *J. Nat. Prod.*, **2004**, *67*, 2079-2082.
- Anada, M.; Washio, T.; Shimada, N.; Kitagaki, S.; Nakajima, M.; Shiro, M.; Hashimoto, S. *Angew. Chem., Int. Ed.*, **2004**, *43*, 2665-2668.
- Anada, M.; Washio, T.; Watanabe, Y.; Takeda, K.; Hashimoto, S. *Eur. J. Org. Chem.*, **2010**, 6850-6854.
- Anciaux, A. J.; Hubert, A. J.; Noels, A. F.; Petiniot, N.; Teyssie, P. *J. Org. Chem.*, **1980**, *45*, 695-702.
- Ando, W.; Hagiwara, T.; Migita, T. *Tetrahedron Lett.*, **1974**, 1425-1428.
- Ando, W.; Kondo, S.; Nakayama, K.; Ichibori, K.; Kohoda, H.; Yamato, H.; Imai, I.; Nakaido, S.; Migita, T. *J. Am. Chem. Soc.*, **1972**, *94*, 3870-3876.
- Ando, W.; Yagihara, T.; Kondo, S.; Nakayama, K.; Yamato, H.; Nakaido, S.; Migita, T. *J. Org. Chem.*, **1971**, *36*, 1732-1736.
- Ando, W.; Yagihara, T.; Tozune, S.; Nakaido, S.; Migita, T. *Tetrahedron Lett.*, **1969**, 1979-1982.
- Cai, P.; McPhail, A. T.; Krainer, E.; Katz, B.; Pearce, C.; Boros, C.; Caceres, B.; Smith, D.; Houck, D. R. *Tetrahedron Lett.*, **1999**, *40*, 1479-1482.
- Chavez, D. E.; Jacobsen, E. N. *Org. Synth.*, **2005**, *82*, 34-42.
- Clark, J. S.; Baxter, C. A.; Castro, J. L. *Synthesis*, **2005**, 3398-3404.
- Clark, J. S.; Baxter, C. A.; Dossetter, A. G.; Poigny, S.; Castro, J. L.; Whittingham, W. G. *J. Org. Chem.*, **2008**, *73*, 1040-1055.
- Clark, J. S.; Fessard, T. C.; Whitlock, G. A. *Tetrahedron*, **2005**, *62*, 73-78.
- Clark, J. S.; Fessard, T. C.; Wilson, C. *Org. Lett.*, **2004**, *6*, 1773-1776.
- Clark, J. S.; Hayes, S. T.; Wilson, C.; Gobbi, L. *Angew. Chem., Int. Ed.*, **2007**, *46*, 437-440.

Clark, J. S.; Walls, S. B.; Wilson, C.; East, S. P.; Drysdale, M. J. *Eur. J. Org. Chem.*, **2006**, 323-327.

Clark, J. S.; Whitlock, G.; Jiang, S.; Onyia, N. *Chem. Commun.*, **2003**, 2578-2579.

Cope, A. C.; McKervey, M. A.; Weinshenker, N. M. *J. Org. Chem.*, **1969**, *34*, 2229-2231.

Cotton, F. A.; Felthouse, T. R. *Inorg. Chem.*, **1980**, *19*, 323-328.

Danishefsky, S.; Kerwin, J. F., Jr.; Kobayashi, S. *J. Am. Chem. Soc.*, **1982**, *104*, 358-360.

Danishefsky, S.; Larson, E.; Askin, D.; Kato, N. *J. Am. Chem. Soc.*, **1985**, *107*, 1246-1255.

Davies, H. M. L.; Ahmed, G.; Churchill, M. R. *J. Am. Chem. Soc.*, **1996**, *118*, 10774-10782.

Desimoni, G.; Faita, G.; Jorgensen, K. A. *Chem. Rev.*, **2006**, *106*, 3561-3651.

Diekmann, J. *J. Org. Chem.*, **1965**, *30*, 2272-2275.

Dossetter, A. G.; Jamison, T. F.; Jacobsen, E. N. *Angew. Chem., Int. Ed.*, **1999**, *38*, 2398-2400.

Doyle, M. P. *Chem. Rev.*, **1986**, *86*, 919-940.

Doyle, M. P. *Acc. Chem. Res.*, **1986**, *19*, 348-356.

Doyle, M. P.; Bagheri, V.; Harn, N. K. *Tetrahedron Lett.*, **1988**, *29*, 5119-5122.

Doyle, M. P.; Ene, D. G.; Forbes, D. C.; Tedrow, J. S. *Tetrahedron Lett.*, **1997**, *38*, 4367-4370.

Doyle, M. P.; Forbes, D. C. *Chem. Rev.*, **1998**, *98*, 911-935.

Doyle, M. P.; Griffin, J. H.; Chinn, M. S.; Van Leusen, D. *J. Org. Chem.*, **1984**, *49*, 1917-1925.

Doyle, M. P.; Kundu, K.; Russell, A. E. *Org. Lett.*, **2005**, *7*, 5171-5174.

- Doyle, M. P.; Phillips, I. M.; Hu, W. *J. Am. Chem. Soc.*, **2001**, *123*, 5366-5367.
- Doyle, M. P.; Tamblyn, W. H.; Bagheri, V. *J. Org. Chem.*, **1981**, *46*, 5094-5102.
- Doyle, M. P.; Valenzuela, M.; Huang, P. *PNAS*, **2004**, *101*, 5391-5395.
- Doyle, M. P.; Westrum, L. J.; Wolthuis, W. N. E.; See, M. M.; Boone, W. P.; Bagheri, V.; Pearson, M. M. *J. Am. Chem. Soc.*, **1993**, *115*, 958-964.
- Du, H.; Zhang, X.; Wang, Z.; Bao, H.; You, T.; Ding, K. *Eur. J. Org. Chem.*, **2008**, 2248-2254.
- Eberlein, T. H.; West, F. G.; Tester, R. W. *J. Org. Chem.*, **1992**, *57*, 3479-3482.
- Fananas, F. J.; Fernandez, A.; Cevic, D.; Rodriguez, F. *J. Org. Chem.*, **2009**, *74*, 932-934.
- Hashimoto, S.; Watanabe, N.; Ikegami, S. *Tetrahedron Lett.*, **1992**, *33*, 2709-2712.
- Hodgson, D. M.; Angrish, D.; Erickson, S. P.; Kloesges, J.; Lee, C. H. *Org. Lett.*, **2008**, *10*, 5553-5556.
- Hodgson, D. M.; Pierard, F. Y. T. M.; Stuppel, P. A. *Chem. Soc. Rev.*, **2001**, *30*, 50-61.
- Hoffmann, R. W. *Angew. Chem.*, **1979**, *91*, 625-634.
- Hu, W.; Xu, X.; Zhou, J.; Liu, W.-J.; Huang, H.; Hu, J.; Yang, L.; Gong, L.-Z. *J. Am. Chem. Soc.*, **2008**, *130*, 7782-7783.
- Jewett, J. C.; Rawal, V. H. *Angew. Chem., Int. Ed.*, **2007**, *46*, 6502-6504.
- Johnson, S. A.; Hunt, H. R.; Neumann, H. M. *Inorg. Chem.*, **1963**, *2*, 960-962.
- Jorgensen, K. A. *Angew. Chem., Int. Ed.*, **2000**, *39*, 3558-3588.
- Kappe, C. O. *Tetrahedron Lett.*, **1997**, *38*, 3323-3326.
- Karche, N. P.; Jachak, S. M.; Dhavale, D. D. *J. Org. Chem.*, **2001**, *66*, 6323-6332.
- Katritzky, A. R.; Dennis, N. *Chem. Rev.*, **1989**, *89*, 827-861.
- Li, A.-H.; Dai, L.-X.; Aggarwal, V. K. *Chem. Rev.*, **1997**, *97*, 2341-2372.

- Li, X.; Meng, X.; Su, H.; Wu, X.; Xu, D. *Synlett*, **2008**, 857-860.
- Lipshutz, B. H. *Chem. Rev.*, **1986**, *86*, 795-820.
- Liu, Y.; Zhang, Y.; Jee, N.; Doyle, M. P. *Org. Lett.*, **2008**, *10*, 1605-1608.
- Long, J.; Hu, J.; Shen, X.; Ji, B.; Ding, K. *J. Am. Chem. Soc.*, **2002**, *124*, 10-11.
- Lu, C.-D.; Liu, H.; Chen, Z.-Y.; Hu, W.-H.; Mi, A.-Q. *Org. Lett.*, **2005**, *7*, 83-86.
- Marmsaeter, F. P.; Murphy, G. K.; West, F. G. *J. Am. Chem. Soc.*, **2003**, *125*, 14724-14725.
- Marmsaeter, F. P.; West, F. G. *J. Am. Chem. Soc.*, **2001**, *123*, 5144-5145.
- Marmsater Fredrik, P.; Vanecko John, A.; West, F. G. *Org. Lett.*, **2004**, *6*, 1657-1660.
- Molander, G. A.; Shubert, D. C. *J. Am. Chem. Soc.*, **1987**, *109*, 6877-6878.
- Montana, A. M.; Ponzano, S.; Kociok-Koehn, G.; Font-Bardia, M.; Solans, X. *Eur. J. Org. Chem.*, **2007**, 4383-4401.
- Muthusamy, S.; Krishnamurthi, J.; Suresh, E. *Chem. Commun.*, **2007**, 861-863.
- Nazarova, L. A.; Maiorova, A. G. *Zh. Neorg. Khim.*, **1976**, *21*, 1070-1074.
- Noels, A. F.; Hubert, A. J.; Teyssie, P. *J. Organomet. Chem.*, **1979**, *166*, 79-86.
- Nozaki, H.; Takaya, H.; Moriuti, S.; Noyori, R. *Tetrahedron*, **1968**, *24*, 3655-3669.
- Nozaki, H.; Takaya, H.; Noyori, R. *Tetrahedron*, **1966**, *22*, 3393-3401.
- Oku, A.; Murai, N.; Baird, J. *J. Org. Chem.*, **1997**, *62*, 2123-2129.
- Oku, A.; Numata, M. *J. Org. Chem.*, **2000**, *65*, 1899-1906.
- Oku, A.; Ohki, S.; Yoshida, T.; Kimura, K. *Chem. Commun.*, **1996**, 1077-1078.
- Ollis, W. D.; Rey, M.; Sutherland, I. O. *J. Chem. Soc., Perkin Trans. I*, **1983**, 1009-1027.
- Padwa, A.; Hornbuckle, S. F. *Chem. Rev.*, **1991**, *91*, 263-309.

Padwa, A.; Snyder, J. P.; Curtis, E. A.; Sheehan, S. M.; Worsencroft, K. J.; Kappe, C. O. *J. Am. Chem. Soc.*, **2000**, *122*, 8155-8167.

Padwa, A.; Weingarten, M. D. *Chem. Rev.*, **1996**, *96*, 223-269.

Pangborn, A. B.; Giardello, M. A.; Grubbs, R. H.; Rosen, R. K.; Timmers, F. J. *Organometallics*, **1996**, *15*, 1518-1520.

Pellissier, H. *Tetrahedron*, **2009**, *65*, 2839-2877.

Pirrung, M. C.; Brown, W. L.; Rege, S.; Laughton, P. *J. Am. Chem. Soc.*, **1991**, *113*, 8561-8562.

Pirrung, M. C.; Werner, J. A. *J. Am. Chem. Soc.*, **1986**, *108*, 6060-6062.

Ramana, C. V.; Salian, S. R.; Gonnade, R. G. *Eur. J. Org. Chem.*, **2007**, 5483-5486.

Reymond, S.; Cossy, J. *Chem. Rev.*, **2008**, *108*, 5359-5406.

Roberts, E.; Sancon, J. P.; Sweeney, J. B. *Org. Lett.*, **2005**, *7*, 2075-2078.

Roskamp, E. J.; Johnson, C. R. *J. Am. Chem. Soc.*, **1986**, *108*, 6062-6063.

Sawada, Y.; Mori, T.; Oku, A. *J. Org. Chem.*, **2003**, *68*, 10040-10045.

Sharma, A.; Guenee, L.; Naubron, J.-V.; Lacour, J. *Angew. Chem., Int. Ed.*, **2011**, *50*, 3677-3680.

Shiina, I.; Miyao, R. *Heterocycles*, **2008**, *76*, 1313-1328.

Smith, A. B., III; Razler, T. M.; Ciavarri, J. P.; Hirose, T.; Ishikawa, T. *Org. Lett.*, **2005**, *7*, 4399-4402.

Solorio, D. M.; Jennings, M. P. *J. Org. Chem.*, **2007**, *72*, 6621-6623.

Stewart, C.; McDonald, R.; West, F. G. *Org. Lett.*, **2011**, *13*, 720-723.

Sweeney, J. B. *Chem. Soc. Rev.*, **2009**, *38*, 1027-1038.

Takao, K.-i.; Watanabe, G.; Yasui, H.; Tadano, K.-i. *Org. Lett.*, **2002**, *4*, 2941-2943.

- Tiefenbacher, K.; Mulzer, J. *Angew. Chem., Int. Ed.*, **2008**, *47*, 6199-6200.
- Tiefenbacher, K.; Mulzer, J. *Angew. Chem., Int. Ed.*, **2008**, *47*, 2548-2555.
- Unni, A. K.; Takenaka, N.; Yamamoto, H.; Rawal, V. H. *J. Am. Chem. Soc.*, **2005**, *127*, 1336-1337.
- Watanabe, Y.; Washio, T.; Shimada, N.; Anada, M.; Hashimoto, S. *Chem. Commun.*, **2009**, 7294-7296.
- Wee, A. G. H. *Curr. Org. Synth.*, **2006**, *3*, 499-555.
- West, F. G.; Eberlein, T. H.; Tester, R. W. *J. Chem. Soc., Perkin Trans.*, **1993**, 2857-2859.
- West, F. G.; Naidu, B. N.; Tester, R. W. *J. Org. Chem.*, **1994**, *59*, 6892-6894.
- Xiao, W.-L.; Gong, Y.-Q.; Wang, R.-R.; Weng, Z.-Y.; Luo, X.; Li, X.-N.; Yang, G.-Y.; He, F.; Pu, J.-X.; Yang, L.-M.; Zheng, Y.-T.; Lu, Y.; Sun, H.-D. *J. Nat. Prod.*, **2009**, *72*, 1678-1681.
- Yakura, T.; Muramatsu, W.; Uenishi, J. *Chem. Pharm. Bull.*, **2005**, *53*, 989-994.
- Yamashita, Y.; Saito, S.; Ishitani, H.; Kobayashi, S. *J. Am. Chem. Soc.*, **2003**, *125*, 3793-3798.
- Ye, T.; McKervey, M. A. *Chem. Rev.*, **1994**, *94*, 1091-1160.
- Yet, L. *Chem. Rev.*, **2000**, *100*, 2963-3007.
- Zhao, W. *Chem. Rev.*, **2010**, *110*, 1706-1745.

*Chapter 3:*

**Competition between [1,2]-Stevens and [2,3]-sigmatropic rearrangements**

---

# I. Introduction

---

## **1.1 Mechanistic background**

According to the Woodward-Hoffmann rules, [1,2]-rearrangements are symmetry-forbidden processes, whereas [2,3]-sigmatropic rearrangements are symmetry-allowed.<sup>96</sup> Nonetheless, both transformations are frequently observed when ylide intermediates are involved. Note that substrates that can undergo a [2,3]-sigmatropic rearrangement can also undergo a [1,2]-Stevens rearrangement, but the latter reaction is normally not favored. However, the [2,3]-sigmatropic rearrangement does not always prevail completely over the [1,2]-Stevens rearrangement; in fact these two reactions are competing with one another.<sup>97</sup>

### **1.1a The Woodward-Hoffmann description of the [1,2] vs. [2,3] rearrangements**

In 1981 Kenichi Fukui and Roald Hoffmann won the Nobel prize in chemistry for their contributions to orbital symmetry of pericyclic reactions. Woodward would almost certainly have shared this prize had he not died in 1979.<sup>98</sup> The Woodward-Hoffmann rule simplifies numerous parts of quantum physics and mathematical equations, but it is often condensed to an important rule which states that “In a thermal pericyclic reaction the total number of  $(4q + 2)_s$  and  $(4r)_a$  components must be odd” where a component is a bond or orbital taking part in a pericyclic reaction as a single unit and  $(4q + 2)_s$  refers to the number of aromatic suprafacial electron systems and  $(4r)_a$  refers

---

<sup>96</sup> (a) Hoffmann, R.; Woodward, R. B. *J. Am. Chem. Soc.*, **1965**, *87*, 2046-2048. (b) Woodward, R. B.; Hoffmann, R. *J. Am. Chem. Soc.*, **1965**, *87*, 395-397. (c) Hoffmann, R.; Woodward, R. B. *Acc. Chem. Res.*, **1968**, *1*, 17-22.

<sup>97</sup> Nakai, T.; Mikami, K. *Chem. Rev.*, **1986**, *86*, 885-902.

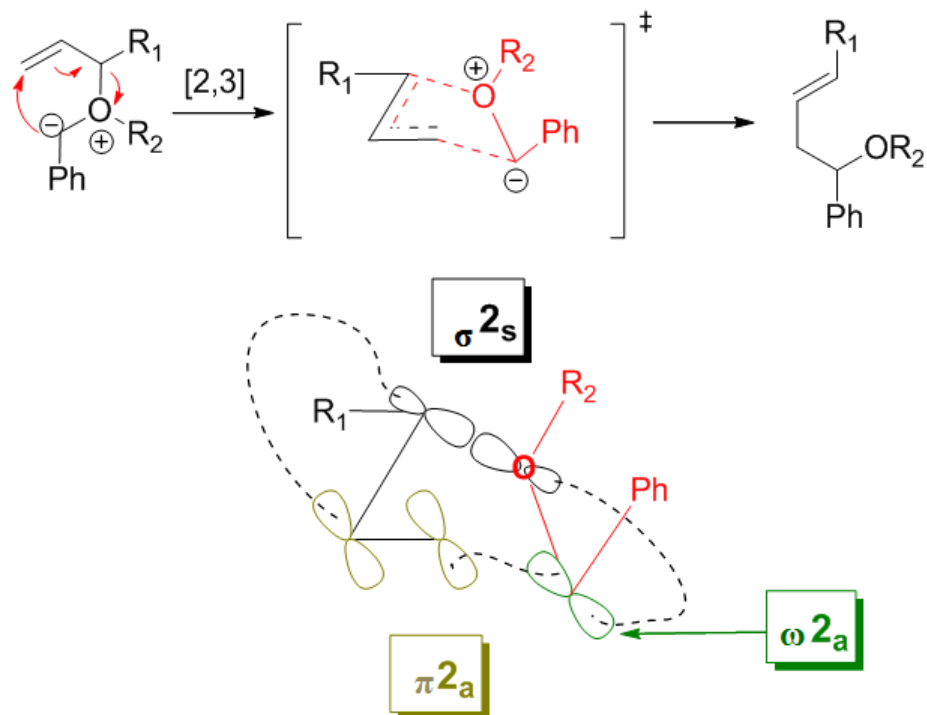
<sup>98</sup> Anslyn, E. V.; Dougherty D. A. *Modern Physical Organic Chemistry*, University Science Books, California, **2006**.

to antiaromatic antarafacial systems.<sup>98</sup> If the total number of these systems is odd then the reaction is thermally allowed, whereas if the total number is even then the reaction is thermally forbidden.<sup>98</sup>

We can understand why, according to the Woodward-Hoffman rules, the [2,3]-sigmatropic rearrangements are symmetry-allowed whereas the [1,2]-Stevens rearrangements are symmetry-forbidden processes. The [2,3]-sigmatropic rearrangements go through five-membered cyclic transition states where the bond that is to become the new  $\pi$  bond can be in a chair-like part of the five-membered ring (Scheme 49).<sup>99</sup> The symbols used for a carbanion,  $\sigma$ -bond, and  $\pi$ -bond are  $\omega 2$ ,  $\sigma 2$ , and  $\pi 2$ , respectively where number 2 refers to that component having two electrons. If the new bonds are formed to the same lobe of the orbital then it is referred to as a suprafacial interaction (s) whereas if they are formed to different lobes then the interaction is antarafacial (a). Therefore, the [2,3]-sigmatropic rearrangement is described as  $\omega 2_a + \sigma 2_s + \pi 2_a$  where there is one  $(4q + 2)_s$  and no  $(4r)_a$  components; thus the total number of  $(4q + 2)_s$  and  $(4r)_a$  is odd and hence the reaction is thermally allowed (Scheme 49).<sup>99</sup>

---

<sup>99</sup> Clayden, J., Warren, S., Greeves, N., Wothers, P. *Organic Chemistry*, Oxford University Press, New York, **2001**.



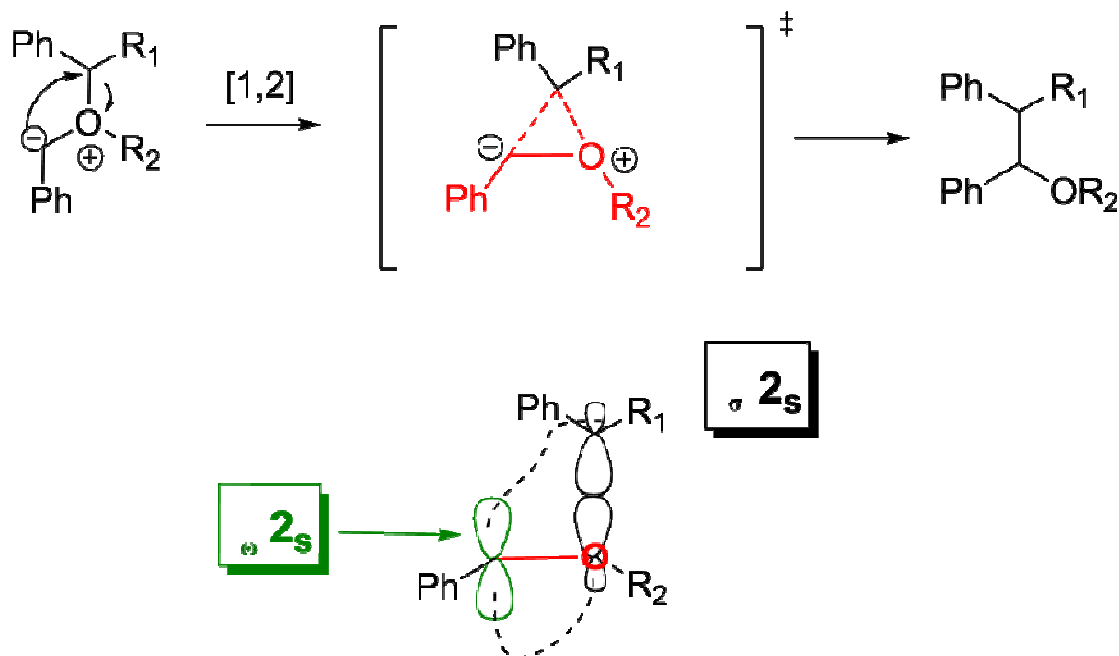
**Scheme 49.** Five-membered ring transition state of the [2,3]-sigmatropic rearrangement showing the orbital overlap as the new bond is formed.

The [1,2]-Stevens rearrangement proceeding *via* a concerted pathway would go through a three-membered cyclic transition state. According to the Woodward-Hoffman rules, the process would be described as  $\omega 2_s + \sigma 2_s$ , where there are two  $(4q + 2)_s$  and no  $(4r)_a$  components, and so the total number of  $(4q + 2)_s$  and  $(4r)_a$  is even. Hence, the reaction is thermally forbidden (Scheme 50).<sup>100</sup> However, Woodward and Hoffmann have also argued that a concerted Stevens rearrangement of an ammonium ylide is feasible in the presence of a metal.<sup>101</sup> They suggested that when the p orbital of the metal is

<sup>100</sup> (a) Anslyn, E. V.; Dougherty D. A. *Modern Physical Organic Chemistry*, University Science Books, California, **2006**. (b) Clayden, J., Warren, S., Greeves, N., Wothers, P. *Organic Chemistry*, Oxford University Press, New York, **2001**.

<sup>101</sup> Woodward, R. B.; Hoffmann, R. *Angew. Chem., Int. Ed. Engl.*, **1969**, *8*, 781-853.

involved, the metal can strongly associate with both the carbanion and the nitrogen atom when the migration is taking place, allowing the reaction to proceed.



**Scheme 50.** Three-membered ring transition state of the [1,2]-Stevens rearrangement showing the orbital overlap as the new bond is formed.

### 1.1b The HOMO-LUMO interaction

Woodward and Hoffmann developed the conservation of orbital symmetry theory that states “in-phase orbitals overlap during the course of a pericyclic reaction”.<sup>102</sup> This theory was based on the frontier orbital theory that was put forth by Kenichi Fukui in 1954 where Fukui established the importance of HOMO and LUMO orbitals.<sup>103</sup> We can also analyze the [2,3]-sigmatropic and [1,2]-Stevens rearrangements by considering the HOMO of the carbanion and the LUMO of the allylic and the benzylic site,

<sup>102</sup> Hoffmann, R.; Woodward, R. B. *Acc. Chem. Res.*, **1968**, *1*, 17-22.

<sup>103</sup> (a) Fukui, K.; Yonezawa, T.; Nagata, C.; Shingu, H. *J. Chem. Phys.*, **1954**, *22*, 1433-1442. (b) Fukui, K. *Symposium on Mol. Phys.*, **1954**, 41-42. (c) Fukui, K. *Kagaku no Ryoiki*, **1954**, *8*, 73-74.

respectively (Figure 11). The smaller the energy gap between the HOMO and the LUMO, the more readily will these rearrangements occur. Therefore, the presence of a substituent that either raises the HOMO or lowers the LUMO will promote a faster reaction.<sup>104</sup>

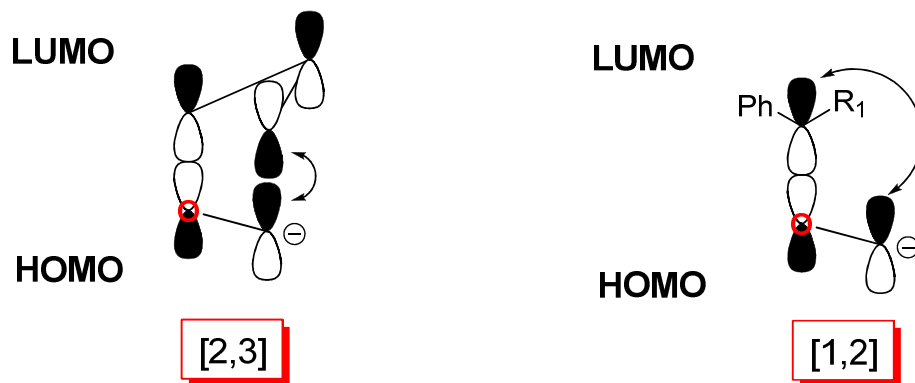


**Figure 11.** Depiction of the frontier orbitals for the [2,3] and [1,2] rearrangement processes.

### 1.1c Aromatic/antiaromatic transition state theory

Building from an earlier analysis by Evans,<sup>105</sup> Zimmerman and Dewar<sup>106</sup> developed aromatic transition state theory. According to this, reactions that follow the Woodward-Hoffmann rules have transition states which are aromatic, while reactions which violate the rules have antiaromatic transition states. Dewar argues, however, that the reactions of the latter should be feasible and should indeed occur in cases where no better alternative exists. He further states that although a concerted mechanism for the Stevens rearrangement is formally “forbidden”, according to the Woodward-Hoffmann

<sup>104</sup> (a) Nakai, T.; Mikami, K. *Chem. Rev.*, **1986**, *86*, 885-902. (b) Fukui, K. *Theory of Orientation and Stereoselection*; Springer-Verlag: Berlin, **1971**. (c) Fleming, I. *Frontier Orbitals and Organic Chemical Reactions*; Wiley: New York, **1976**.

<sup>105</sup> (a) Evans, M. G.; Warhurst, E. *Trans. Faraday Soc.*, **1938**, *34*, 614-624. (b) Evans, M. G. *Trans. Faraday Soc.*, **1939**, *35*, 824-834.

<sup>106</sup> (a) Lowry, T. H.; Richardson, K. S. *Mechanism and Theory in Organic Chemistry*, Harper & Row, New York, **1987**. (b) Dewar, M. J. S. *Spec. Publ. - Chem. Soc.*, **1967**, *21*, 177-215. (c) Dewar, M. J. S. *Angew. Chem., Int. Ed. Engl.*, **1971**, *10*, 761-776.

rules the calculated activation energy is extremely small (17 KJ mol<sup>-1</sup>).<sup>107</sup> To better understand the possibility of the [1,2]-Stevens rearrangement violating the Woodward-Hoffmann rules, we need to consider the thermodynamics of this reaction. The [1,2]-Stevens rearrangement should be an exothermic reaction because it involves a large decrease in charge separation and a corresponding large decrease in coulombic energy. Dewar argues that an antiaromatic pericyclic reaction may occur very readily if it is sufficiently exothermic.<sup>107</sup>

## **1.2 Competition between [2,3]-sigmatropic and [1,2]-Stevens rearrangements**

So far we have discussed three theories to understand pericyclic reactions. It is safe to say that no model is absolutely correct in explaining experimental observations completely. Even though the [1,2]-Stevens rearrangement is considered a “forbidden” process, this reaction often competes with the [2,3]-sigmatropic rearrangement as evidenced by numerous examples in the literature.

### **1.2a The [2,3]-sigmatropic dominates over the [1,2]-Stevens rearrangement**

Hashimoto<sup>108</sup> investigated the decomposition of  $\alpha$ -diazo- $\beta$ -keto esters **157a-c**, containing *trans*- and *cis*-crotyl and -prenyl substituents, using Rh<sub>2</sub>(S-PTTL)<sub>4</sub> as the catalyst in toluene at 0 °C. The decomposition reactions of **157a-c** were found to produce a mixture of [2,3]-sigmatropic rearrangement products **158** and [1,2]-Stevens rearrangement products **159**, with the former being favored (Table 22). It is worthy of note that the ratio of the [1,2]-Stevens rearrangement product **159a-c** becomes greater as

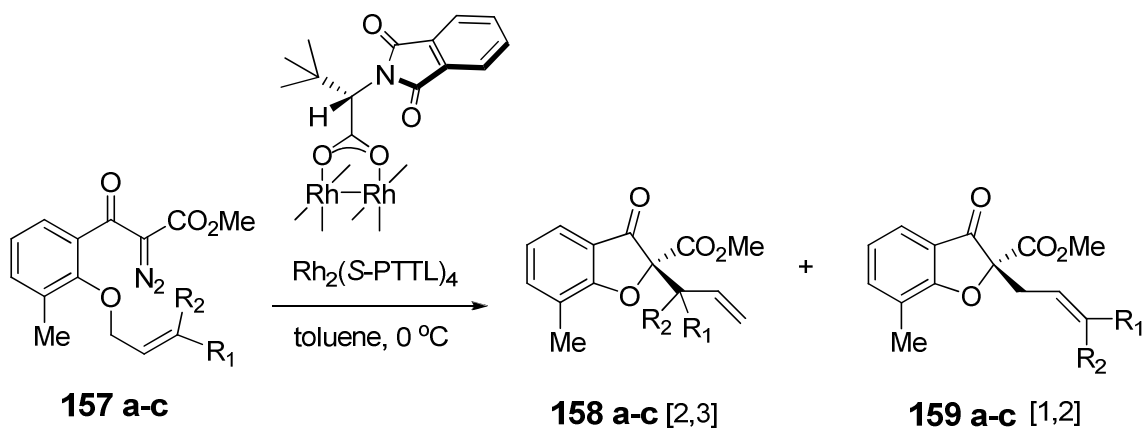
---

<sup>107</sup> Dewar, M. J. S.; Ramsden, C. A. *J. Chem. Soc., Perkin Trans. I*, **1974**, 1839-1844.

<sup>108</sup> Kitagaki, S.; Yanamoto, Y.; Tsutsui, H.; Anada, M.; Nakajima, M.; Hashimoto, S. *Tetrahedron Lett.*, **2001**, 42, 6361-6364.

the steric hindrance encountered during the [2,3]-sigmatropic rearrangement increases (prenyl > *cis*-crotyl > *trans*-crotyl).<sup>108</sup>

**Table 22.** Enantioselective cyclic allylic oxonium ylide formation and rearrangement of aromatic substrates catalyzed by Rh<sub>2</sub>(S-PTTL)<sub>4</sub>.

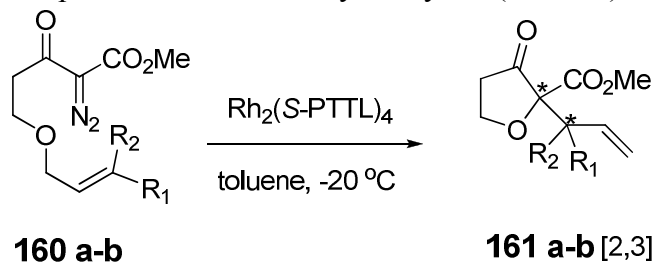


Entry	Substrate	R <sub>1</sub>	R <sub>2</sub>	Yield <sup>a</sup> (%)	Ratio <sup>b</sup> 158:159	d.r. <sup>c</sup> of 158	ee <sup>d</sup> (%) 158	ee <sup>d</sup> (%) 159
1	157a	Me	H	63	92:8	60:40	70	64
2	157b	H	Me	63	82:18	49:51	72	66
3	157c	Me	Me	37	71:29	-	59	65

<sup>a</sup> Combined yield of **158** and **159**. <sup>b</sup> Determined by HPLC (column, zolbax sil; eluent, 50:1 hexane:ethyl acetate). <sup>c</sup> Determined by 400 MHz <sup>1</sup>H NMR. <sup>d</sup> Determined after separation of **158** and **159** with AgNO<sub>3</sub>-SiO<sub>2</sub> TLC.

Interestingly, by lowering the temperature to -20°C rhodium(II) catalyzed decomposition of aliphatic substrate **160a-b** afforded the [2,3]-sigmatropic rearrangement products **161** in up to 79 % yield, but there was no evidence of the [1,2]-Stevens rearrangement products (Table 23).<sup>108</sup> One observation worth noting is the exceedingly high degree of diastereoselection of the [2,3]-sigmatropic rearrangement product **161a** (96:4) whereas the diastereomer ratios of the [2,3]-sigmatropic rearrangement product **158a-b** are poor (60:40) and (49:51), respectively.

**Table 23.** Enantioselective cyclic allylic oxonium ylide formation and rearrangement of aliphatic substrates catalyzed by  $\text{Rh}_2(\text{S-PTTL})_4$ .

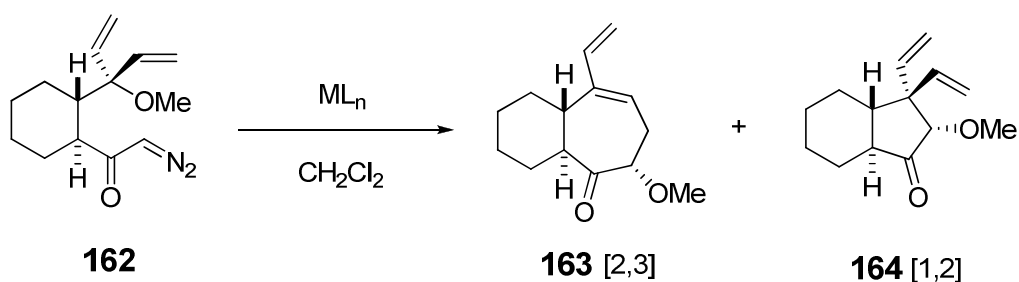


Entry	Substrate	R <sub>1</sub>	R <sub>2</sub>	Yield (%)	d.r. of <b>161</b>	ee (%) <b>161</b>
1	160a	Me	H	79	96:4	22
2	160b	Me	Me	73	-	23

Clark<sup>109</sup> and co-workers have also observed competition between [2,3]-sigmatropic and [1,2]-Stevens rearrangement processes. Rhodium and copper catalyzed reactions of diazoketone **162** furnished the [2,3]-sigmatropic rearrangement product **163** along with a small amount of the [1,2]-Stevens rearrangement product **164** (Table 24). This is yet another example where the [2,3]-sigmatropic rearrangement pathway dominates over the [1,2]-Stevens rearrangement process. Furthermore, both rearrangement products were isolated as a single diastereoisomer.

<sup>109</sup> Clark, J. S.; Walls, S. B.; Wilson, C.; East, S. P.; Drysdale, M. J. *Eur. J. Org. Chem.*, **2006**, 323-327.

**Table 24.** The [2,3]-sigmatropic rearrangement dominates over the [1,2]-Stevens rearrangement using diazoketone **162**.



Entry	Catalyst	Temp.	Yield 163 (%)	Yield 164 (%)
1	Rh <sub>2</sub> (OAc) <sub>4</sub>	0 °C	70	5
2	Cu(hfacac) <sub>2</sub>	Reflux	49	9

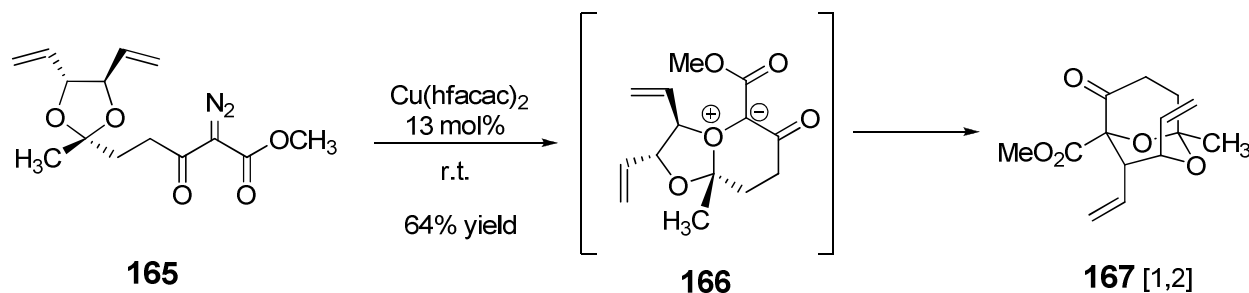
### **1.2b The [1,2]-Stevens dominates over the [2,3]-sigmatropic rearrangement**

Allylic oxonium ylides have a virtually complete preference for symmetry-allowed [2,3]-sigmatropic rearrangements over [1,2]-Stevens rearrangements. However, there are a few examples in the literature where the [2,3]-sigmatropic pathway is disfavored, allowing the [1,2]-Stevens rearrangement to compete or even dominate.

In 1997, Brogan<sup>110</sup> reported the predominant formation of the [1,2]-Stevens pathway over the [2,3]-sigmatropic one. Upon exposure to catalytic Cu(hfacac)<sub>2</sub>, diazoketone **165** afforded the [1,2]-Stevens product **167** in 64% yield (Scheme 51). The

<sup>110</sup> Brogan, J. B.; Zercher, C. K.; Bauer, C. B.; Rogers, R. D. *J. Org. Chem.*, **1997**, *62*, 3902-3909.

[2,3]-sigmatropic rearrangement product was not observed possibly due to conformational restraints of the ylide intermediate **166** that prevented the [2,3]-sigmatropic rearrangement pathway from taking place and hence the formation of the [1,2]-Stevens rearrangement product was more feasible.

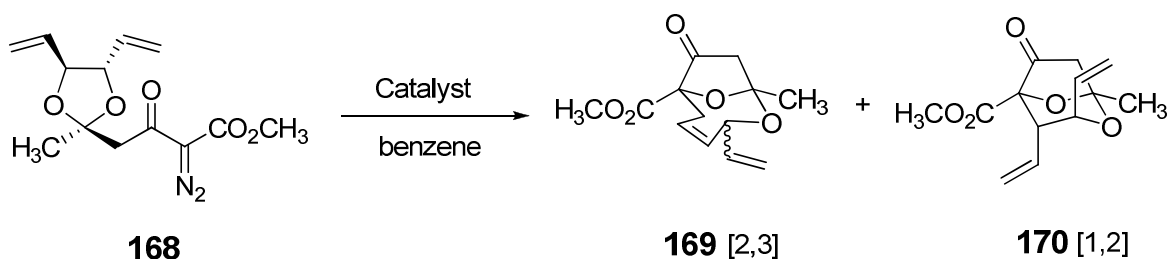


**Scheme 51.** Copper(II) catalyzed decomposition of diazoacetate **165** affords solely the [1,2]-Stevens rearrangement product.

A year later, Brogan<sup>111</sup> further reported on the rearrangements of oxonium ylides from ketals during the preparation of the Zaragozaic acid core structure. The decomposition of diazo ketone **168** afforded the [1,2]-Stevens rearrangement product **170** in 42% isolated yield while the [2,3]-sigmatropic product **169** was isolated in 20% yield, using  $\text{Cu}(\text{hfacac})_2$  as the catalyst (entry 1, Table 25). However,  $\text{Rh}_2(\text{OAc})_4$  facilitated the formation of the [1,2]-Stevens rearrangement product **170** in 64% yield while there was no evidence for the formation of the [2,3]-sigmatropic product **169** (entry 2, Table 25). The authors argued that the selectivity of the rhodium catalyst for the formation of solely the [1,2]-Stevens rearrangement product is due to the catalyst being efficient at discriminating between the two diastereotopic oxygens.<sup>111</sup> These results further illustrate the influence of catalyst on oxonium ylide generation and its rearrangement pathways.

<sup>111</sup> Brogan, J. B.; Zercher, C. K. *Tetrahedron Lett.*, **1998**, 39, 1691-1694.

**Table 25.** Catalyst influence on oxonium ylide generation and its rearrangement pathways.



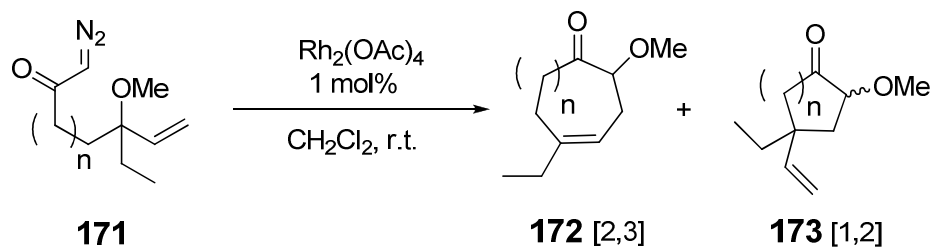
Entry	Catalyst	Temp. (°C)	Yield (%) 169	Yield (%) 170
1	Cu(hfacac) <sub>2</sub>	80	20	42
2	Rh <sub>2</sub> (OAc) <sub>4</sub>	25	--	64

Clark<sup>112</sup> reported in 2001 the cyclization reaction of diazoketone **171** from catalysis by Rh<sub>2</sub>(OAc)<sub>4</sub> to afford both the [2,3]-sigmatropic and [1,2]-Stevens rearrangement products. The conformation of the oxonium ylide intermediate, however, resulted in a different product preference. When the oxonium ylide was a six membered ring, n = 1, the [2,3]-sigmatropic rearrangement product **172** was dominant, and **172** was isolated in 49% yield (entry 1, Table 26). Whereas when the oxonium ylide was a seven

<sup>112</sup> Clark, J. S.; Bate, A. L.; Grinter, T. *Chem. Commun.*, **2001**, 459-460.

membered ring,  $n = 2$ , the [1,2]-Stevens rearrangement product **173** dominated (entry 2, Table 26).

**Table 26.** Conformational influence on oxonium ylide generation and its rearrangement pathways.



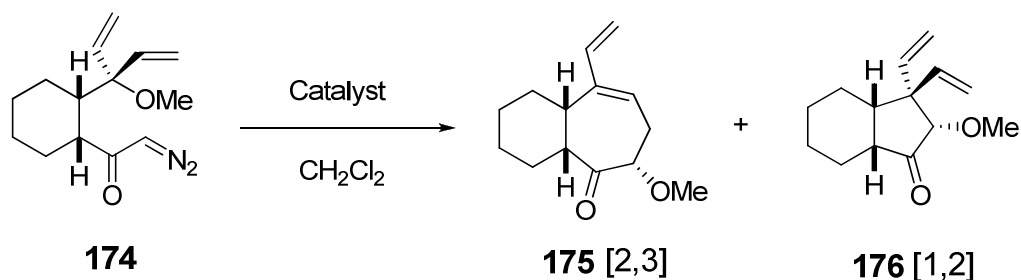
Entry	n	Yield (%) 172	Yield (%) 173	d.r. 173
1	1	49	16	1:1
2	2	8	22	2:1

As discussed previously, the work of Clark regarding the decomposition of *trans*-substituted cyclohexane diazoketone **162** afforded predominantly the [2,3]-sigmatropic rearrangement product **163** (Table 24). In that same report,<sup>113</sup> he explored the decomposition of *cis*-substituted cyclohexane diazoketone **174** that yielded the [1,2]-Stevens rearrangement product **176** as the major product. The symmetry-allowed [2,3]-

<sup>113</sup> Clark, J. S.; Walls, S. B.; Wilson, C.; East, S. P.; Drysdale, M. J. *Eur. J. Org. Chem.*, **2006**, 323-327.

sigmatropic rearrangement product **175** was minor (Table 27). The two diastereoisomeric substituted cyclohexyl diazoketones **162** and **174** resulted in different reaction outcomes. While diazoketone **162** afforded predominantly the [2,3]-sigmatropic product, diazoketone **174** yielded the [1,2]-Stevens rearrangement product as the major product. These examples further illustrate that conformation of the oxonium ylide intermediate plays a major role in determining the product outcome of the [2,3]-sigmatropic and [1,2]-Stevens rearrangements.

**Table 27.** The [1,2]-Stevens rearrangement dominates over the [2,3]-sigmatropic rearrangement using diazoketone **174**.



Entry	Catalyst	Temp.	Yield 175 (%)	Yield 176 (%)
1	Rh <sub>2</sub> (OAc) <sub>4</sub>	r. t.	20	47
2	Cu(hfacac) <sub>2</sub>	Reflux	3	14

From these results we can conclude that the [2,3]-sigmatropic pathway can be disfavored, permitting the formally symmetry-forbidden [1,2]-Stevens pathway to dominate. There are a number of primary factors that can influence regioselectivity between these two pathways. Conformational constraints, the ring size of the oxonium ylide intermediate, and the catalyst employed can play roles in determining selectivity.

These observations of selectivity are poorly understood, so there needs to be further investigations to try and understand the competition between [2,3]-sigmatropic and [1,2]-Stevens rearrangement reactions.

---

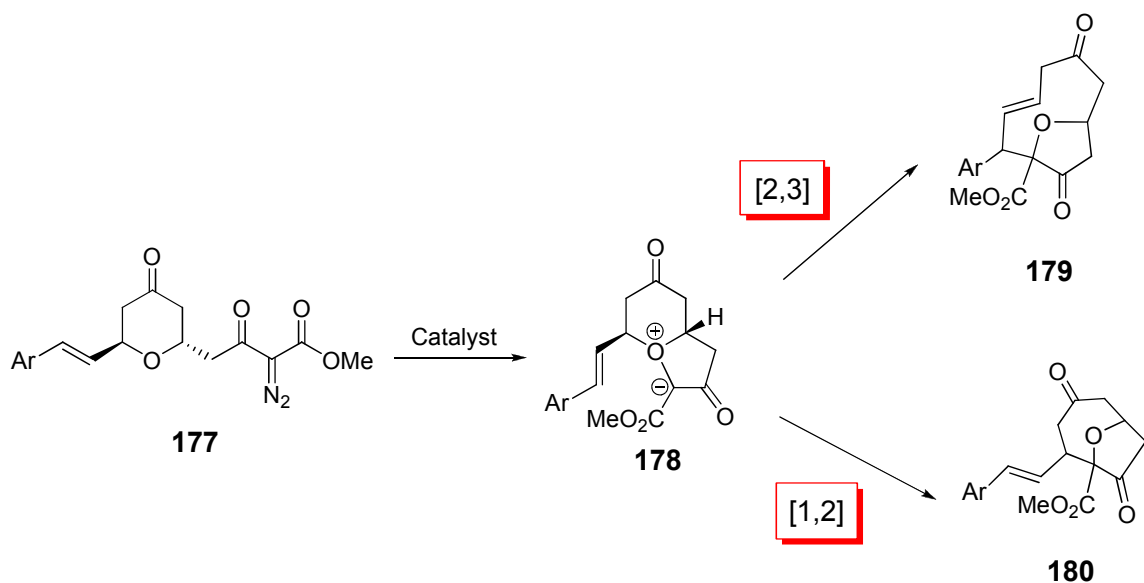
## 2. Research Discussion

---

### 2.1 Model substrate for investigating the competition between [1,2]-Stevens and [2,3]-sigmatropic rearrangements

The observation of two diastereoisomers for the [1,2]-Stevens rearrangement process as discussed in chapter 2 lead us to inquire whether two diastereoisomers for the [2,3]-sigmatropic rearrangement pathway could also be observed. Model substrate *trans*-3-styryltetrahydropyranone-5-diazoacetoacetates **177** was used to investigate the competition between the [2,3]-sigmatropic and [1,2]-Stevens rearrangement pathways. We anticipated that treatment of **177** with a transition metal catalyst would form oxonium ylide **178** and the resultant rearrangement could lead to the formation of either the [2,3]-sigmatropic product **179** or the [1,2]-Stevens rearrangement product **180**, expecting the former to dominate (Scheme 52). If both rearrangement products were observed, we would then investigate the possibility of suppressing one pathway over the other. Doing

so would provide the synthetic community with further understanding of the factors which influence these two pathways as well as how to control them.

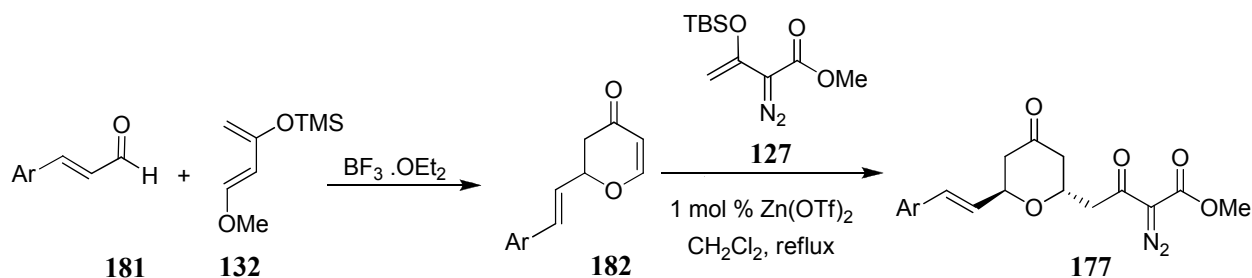


**Scheme 52.** Investigating the competition between [2,3] and [1,2] rearrangement processes.

## **2.2 Synthesis of the Mukaiyama-Michael addition products**

In order to obtain the desired **177a**, we followed our two step synthesis with the initial hetero-Diels-Alder reaction followed by the Mukaiyama-Michael addition reaction. Styryl dihydropyranone **182a** was prepared in 80% isolated yield by a  $\text{BF}_3 \cdot \text{Et}_2\text{O}$ -mediated hetero Diels-Alder reaction between cinnamaldehyde **181a** and the Danishefsky's diene **132**. The Mukaiyama-Michael reaction of **182a** with methyl 3-(*tert*-butyldimethylsilyloxy)-2-diazo-3-butenate **127**, using  $\text{Zn}(\text{OTf})_2$  (1 mol%) in refluxing dichloromethane, afforded *trans*-3-styryltetrahydropyranone-5-diazoacetoacetates **177a** in 92% isolated yield (Table 28). Product **177a** was determined to be solely the *trans* isomer by  $^1\text{H}$ NMR comparison to the previously observed *trans*-3-phenyltetrahydropyranone-5-diazoacetoacetates **134a**.

**Table 28.** Synthesis of *trans*-3-styryltetrahydropyranone-5-diazoacetates **177**.



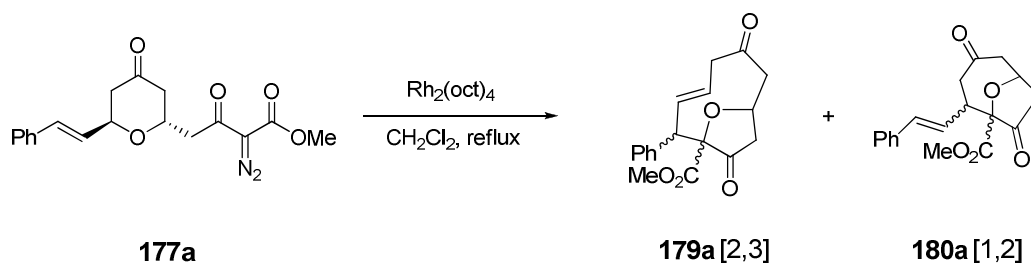
Entry	Substrate <b>181</b>	Ar	Yield (%) <b>182</b> <sup>a</sup>	Yield (%) <b>177</b> <sup>a</sup>
1	181a	C <sub>6</sub> H <sub>5</sub>	80	92
2	181b	<i>p</i> -NO <sub>2</sub> C <sub>6</sub> H <sub>4</sub>	60	88
3	181c	<i>p</i> -MeOC <sub>6</sub> H <sub>4</sub>	60	97

<sup>a</sup> Isolated yield after column chromatography.

### 2.3 Catalytic dinitrogen extrusion reactions

After obtaining *trans*-3-styryltetrahydropyranone-5-diazoacetates **177a**, we proceeded to investigate the dinitrogen extrusion reaction. Rhodium(II) catalyzed decomposition of **177a**, using 1.0 mol% of dirhodium octanoate [Rh<sub>2</sub>(oct)<sub>4</sub>] in refluxing dichloromethane, afforded a mixture of [2,3]-sigmatropic products **179a** and the [1,2]-Stevens rearrangement products **180a** (Scheme 53) in a molar ratio of 54:46, with the former slightly dominating as shown in the <sup>1</sup>H NMR reaction mixture (Figure 12). There are two sets of doublets around 6.5 ppm that correspond to the two [1,2]-Stevens rearrangement diastereoisomers and two sets of doublets around 4.3 ppm that correspond to the two [2,3]-sigmatropic rearrangement diastereoisomers. Also, four singlets between

3.5-3.7 ppm that correspond to the methyl ester functionality can be seen in the crude  $^1\text{H}$  NMR indicating that four compounds are present (Figure 12).



**Scheme 53.** Rhodium(II) catalyzed decomposition reaction of *trans*-3-styryltetrahydropyranone-5-diazoacetates **177a**.

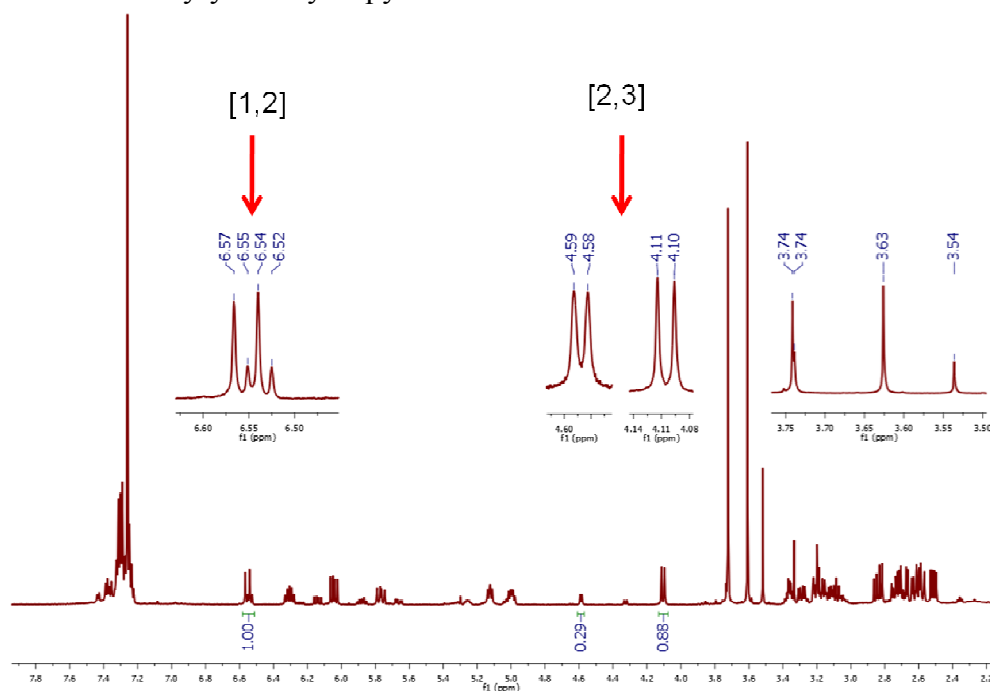
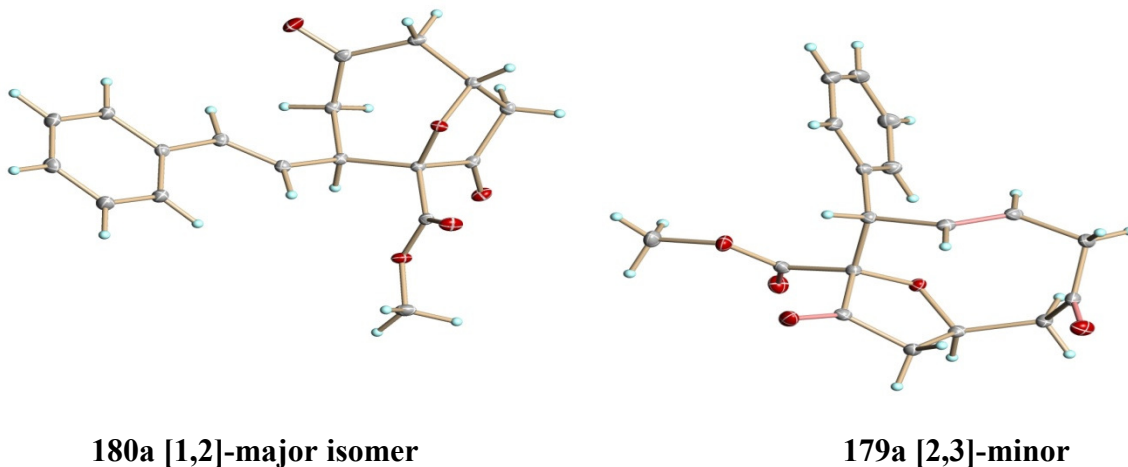


**Figure 12.**  $^1\text{H}$  NMR of rhodium(II) catalyzed decomposition reaction mixture of *trans*-3-styryltetrahydropyranone-5-diazoacetates **177a**.

After careful chromatographic and spectroscopic analysis of the reaction mixture, we isolated and identified two diastereoisomers for both rearrangement products. The major isomer of the [1,2]-Stevens rearrangement product was isolated separately, and its crystal structure was obtained (Figure 13). The minor isomer of the [1,2]-Stevens rearrangement product with the major isomer of the [2,3]-sigmatropic product were

isolated together, while the minor isomer of the [2,3]-sigmatropic product was isolated in a separate fraction and its crystal structure was also obtained (Figure 13). We expected to observe two diastereoisomers for the [1,2]-Stevens rearrangement product since this was observed previously in our investigation, however, the isolation of two diastereoisomers for the [2,3]-sigmatropic rearrangement process was intriguing.



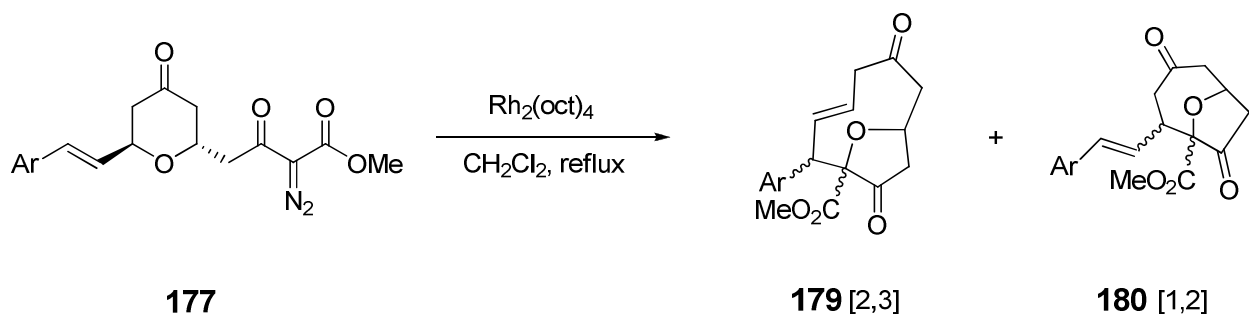
**isomer**

**Figure 13.** Crystal structure for the [1,2]-Stevens rearrangement product-major isomer and the [2,3]-sigmatropic rearrangement product-minor isomer.

We investigated the influence of substituents at the para-position of the aryl ring in **177** on the ratio of diastereomers **179** and those of **180** (Table 29). The catalytic dinitrogen extrusion of **177b**, with the strongly electron-withdrawing *p*-NO<sub>2</sub> substituent, gave almost an equal amount of the [2,3]-sigmatropic rearrangement products **179b** and the [1,2]-Stevens rearrangement products **180b** (ratio **179b:180b** almost 1:1) whereas compound **177c**, with the strongly electron-donating *p*-OMe substituent, produced a higher ratio of the [2,3]-sigmatropic rearrangement products **179c** (ratio **179c:180c** almost 2:1). This illustrates that there is a small but significant substituent effect influencing these rearrangement pathways. Nonetheless, the ratio of the diastereomers of

the [2,3]-sigmatropic rearrangement products **179** and the [1,2]-Stevens rearrangement products **180** were almost the same, within experimental error, and hence there was no substituent effect on the ratio of the diastereomers for either the [2,3]-sigmatropic or the [1,2]-Stevens rearrangement pathways.

**Table 29.**<sup>a</sup> Rh(II) catalyzed decomposition of *trans*-3-styryltetrahydropyranone-5-diazoacetates **177**.



Entry	Substrate	Ar	Ratio (179:180) <sup>b</sup>	Ratio of 179	Ratio of 180	Yield (%) 179 <sup>c</sup>	Yield (%) 180 <sup>c</sup>
1	177a	H	54:46	78:22	78:22	47	41
2	177b	NO <sub>2</sub>	52:48	76:24	76:24	44	41
3	177c	OMe	69:31	79:21	70:30	40	20

<sup>a</sup> Reactions were performed in refluxing CH<sub>2</sub>Cl<sub>2</sub> for 2 h using 1.0 mol % of Rh<sub>2</sub>(oct)<sub>4</sub>. Results reported are averages of two or more reactions ±2%. <sup>b</sup> Product ratio determined by <sup>1</sup>H NMR analysis with variance of ±2%. <sup>c</sup> NMR yield using benzaldehyde as an internal standard.

Next, we investigated the effect of ligands on dirhodium catalysts on the diastereomer ratio of both the [2,3] and [1,2] rearrangement products to investigate if the oxonium ylide intermediate was metal-associated or a free ylide. If the ratio of the two diastereomers for both the [2,3] and [1,2] rearrangement processes vary depending on the catalyst employed, then the rearrangement process must involve a metal-bound ylide. However, if the ratio of the diastereomers are independent of the catalyst being used then

the rearrangement process must involve a free ylide. Results were obtained from reactions with a wide spectrum of catalysts (Table 30), and they show a minor, but reproducible, dependence on catalyst. The [2,3]-sigmatropic product ratio, as well as that from the [1,2]-Stevens rearrangement, was invariant with common ligands on dirhodium (pfb = perfluorobutyrate, tfa = trifluoroacetate, OAc, tpa = triphenylacetate) that cover a broad range of electronic influences. This indicates that the oxonium ylide intermediate **178** is not associated to the metal that is being employed.

**Table 30.**<sup>a</sup> Catalyst screening for the decomposition of *trans*-3-styryltetrahydropyranone-5-diazoacetates **177**.

Entry	Catalyst	Ratio 179: 180 <sup>b</sup>	Ratio 179	Ratio 180	Yield <sup>c</sup> (%) 179	Yield <sup>c</sup> (%) 180
1	Rh <sub>2</sub> (oct) <sub>4</sub>	54:46	78:22	78:22	47	41
2	Rh <sub>2</sub> (OAc) <sub>4</sub>	51:49	80:20	77:23	48	46
3	Rh <sub>2</sub> (pfb) <sub>4</sub>	55:45	80:20	77:23	25	21
4	Rh <sub>2</sub> (piv) <sub>4</sub>	55:45	78:22	76:24	52	42
5	Rh <sub>2</sub> (tpa) <sub>4</sub>	53:47	73:27	75:25	49	44
6	Rh <sub>2</sub> (tfa) <sub>4</sub>	51:49	79:21	75:25	18	23

<sup>a</sup>Reactions were performed in refluxing dichloromethane for 2 h using 1.0 mol % of catalyst. Results reported are averages of two or more reactions. <sup>b</sup>Product ratio determined by <sup>1</sup>H NMR analysis with variance of ±2%. <sup>c</sup> NMR yield using benzaldehyde as an internal standard.

Our results show that the oxonium ylide intermediate **178** formed during dinitrogen extrusion from *trans*-3-styryltetrahydropyranone-5-diazoacetates **177** is a free ylide. Catalytic ylide formation and rearrangement results in a mixture of two diastereoisomers for both the [2,3]-sigmatropic and [1,2]-Stevens rearrangement processes, but with no dependence on either para substituents on the aromatic ring or on the catalyst that is employed. The formation of two diastereoisomers for the symmetry-forbidden [1,2]-Stevens process was expected as previously observed with the

rhodium(II) catalyzed decomposition of *trans*-3-phenyltetrahydropyranone-5-diazoacetoacetate **134a** (chapter 2). The identification of two diastereoisomers for the symmetry-allowed [2,3]-sigmatropic rearrangement process was intriguing. This result led us to analyze the mechanism of the [2,3]-sigmatropic rearrangement in an attempt to explain the identification of two diastereoisomers for a process that is well known to be concerted.

#### **2.4 Mechanism of the [2,3]-sigmatropic rearrangement**

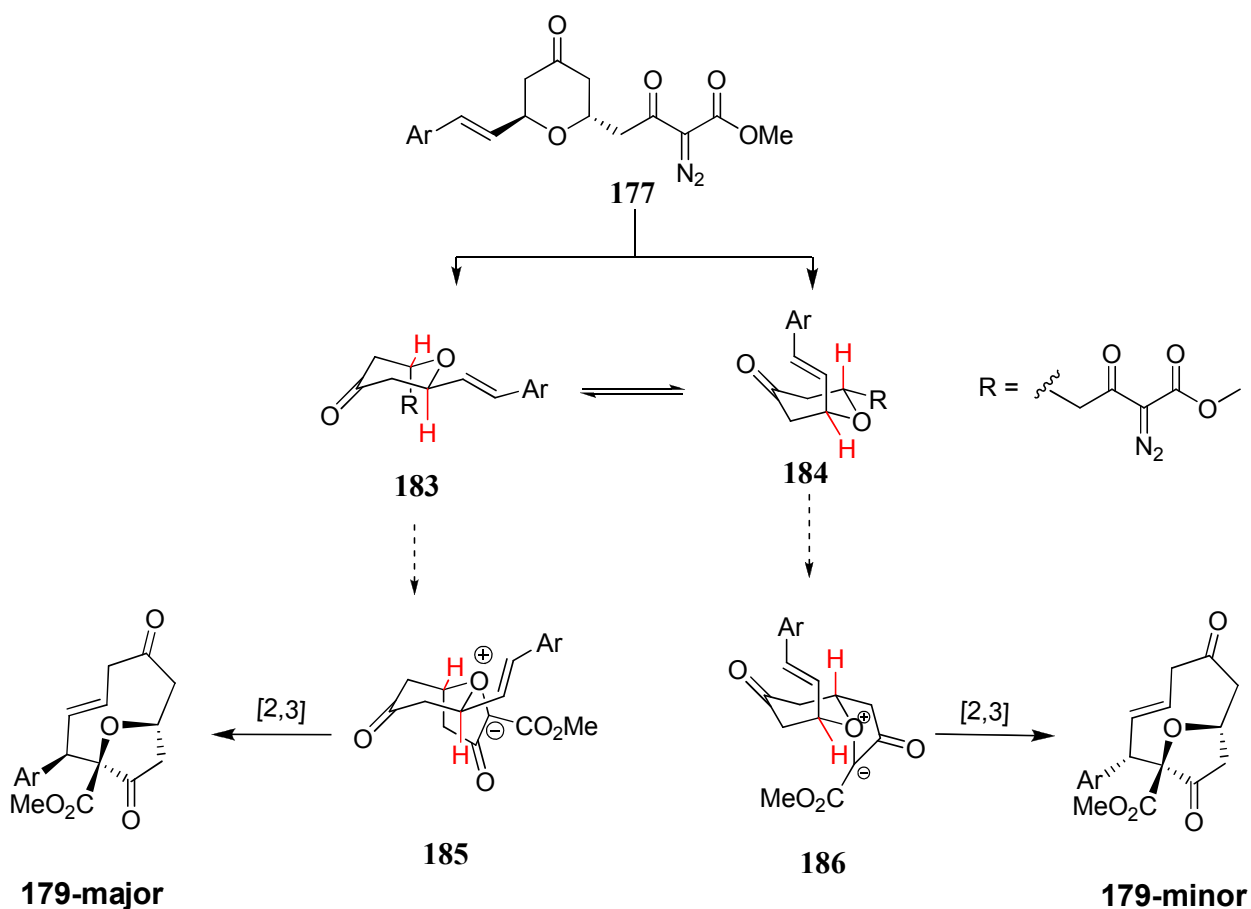
The [2,3]-sigmatropic rearrangement, unlike the controversial mechanism of the [1,2]-Stevens rearrangement, is widely accepted to proceed through a concerted mechanism and, hence, one diastereoisomer is expected to be formed as product.<sup>114</sup> As discussed previously, treating *trans*-3-styryltetrahydropyranone-5-diazoacetoacetates **177a** with rhodium(II) octanoate, two diastereoisomers for the [1,2]-Stevens rearrangement product **180a** were observed and isolated, more interestingly, however, two diastereoisomers for the [2,3]-sigmatropic rearrangement product **179a** were isolated.

This result is fascinating because the symmetry allowed [2,3]-sigmatropic process is known to proceed *via* a concerted pathway and it was interesting to observe a second diastereoisomer for this rearrangement. Reconsidering the hypothesis of conformational isomers put forward in the previous chapter, the apparent isomerization can arise from two ylide intermediates **185** and **186** formed from two conformational isomers (**183** and **184**) of the metal carbene generated from diazoacetoacetate **177** (Scheme 54). In this concerted mechanism, product stereochemistry is determined by the stereochemistry of

---

<sup>114</sup> Sweeney, J. B. *Chem. Soc. Rev.*, **2009**, 38, 1027-1038.

the two ylide intermediates, **185** and **186**, after they undergo symmetry allowed sigmatropic rearrangement to give the corresponding [2,3]-rearrangement diastereoisomers. Hence, the discovery of a minor diastereoisomer for the concerted [2,3]-sigmatropic rearrangement process further supports the idea of conformational isomers leading to the formation of diastereoisomers for both the [1,2] and [2,3] rearrangement processes. In fact, we cannot explain the formation of two diastereoisomers for the [2,3]-sigmatropic rearrangement pathway via a concerted mechanism unless we take into consideration conformational isomers.



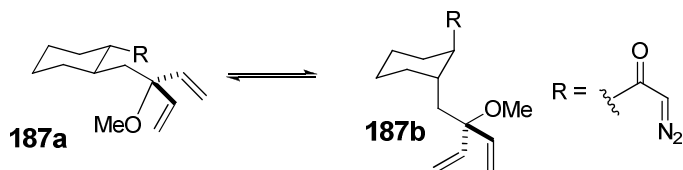
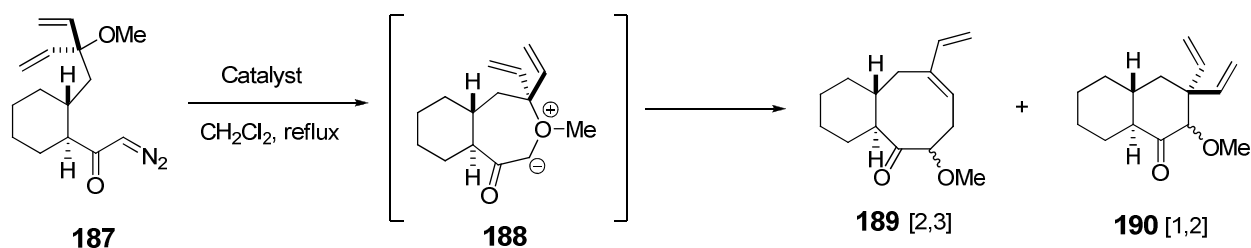
**Scheme 54.** Conformational isomers explain the formation of two diastereomers for the [2,3]-sigmatropic rearrangement process.

The formation of two diastereoisomers for the [2,3]-sigmatropic rearrangement pathway is almost unprecedented in the literature. One example reported by Clark<sup>115</sup> alludes to the fascinating results obtained for the copper catalyzed cyclisation reaction of diazoketone **187** that afforded two diastereoisomers for both the [1,2]-Stevens **190** and the [2,3]-sigmatropic **189** rearrangement pathways (Table 31). There were no attempts to explain those results or mention of any further investigation regarding the observation of a second diastereoisomer for the concerted [2,3]-sigmatropic rearrangement pathway. However, we can also apply the conformational isomer hypothesis that we used to explain the formation of the two diastereoisomers we observed in our system for the [2,3]-sigmatropic rearrangement pathway. Diazoketone **187** can exist in two chair conformational isomers (**187a** and **187b**) which upon treatment with copper(II) catalysts each diazoketone conformer generates an ylide intermediate, and each ylide intermediate will rearrange to give rise to an isomer of the [2,3]-sigmatropic rearrangement product, and hence you end up with two diastereoisomers.

**Table 31.** Cyclization reaction of diazoketone **187** leads to isomeric mixtures of both [2,3] and [1,2] rearrangement processes.

---

<sup>115</sup> Clark, J. S.; Walls, S. B.; Wilson, C.; East, S. P.; Drysdale, M. J. *Eur. J. Org. Chem.*, **2006**, 323-327.



Entry	Catalyst	Yield <sup>a</sup> (%) <b>189</b>	Yield <sup>a</sup> (%) <b>190</b>
1	Cu(acac) <sub>2</sub>	56	22
2	Cu(hfacac) <sub>2</sub>	71	20

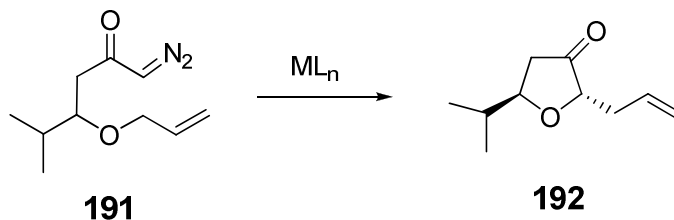
<sup>a</sup> combined yield of both diastereoisomers.

It is well accepted that the symmetry allowed [2,3]-sigmatropic rearrangement pathway proceeds *via* a concerted mechanism, but whether the oxonium ylide intermediate is metal-bound or exists as a free ylide may be substrate specific and catalyst dependant. We have argued that the oxonium ylide intermediate **178** which is generated during the rearrangement from *trans*-3-styryltetrahydropyranone-5-diazoacetates **177** is a free ylide due to a small change in the ratio diastereoisomers of the [2,3]-sigmatropic **179** as well as the [1,2]-Stevens rearrangement products **180** regardless of the catalyst employed. In contrast, Clark<sup>116</sup> reported the presence of a catalyst effect on the diastereoselective synthesis of tetrahydrofuranones *via* a [2,3]-sigmatropic rearrangement pathway. The cyclization of diazoketone **191** in a variety of solvents at reflux or room temperature using Rh<sub>2</sub>(OAc)<sub>4</sub> furnished a mixture of tetrahydrofuranones

<sup>116</sup> Clark, J. S. *Tetrahedron Lett.*, **1992**, 33, 6193-6196.

with a modest preference for the *trans*-tetrahydrofuranones **192** in yields up to 68% (entry 1, Table 32). However, using Cu(acac)<sub>2</sub> as the catalyst, excellent diastereoselection of the *trans*- tetrahydrofuranones **192** (97:3) was achieved, albeit in moderate yields (entry 2, Table 32).

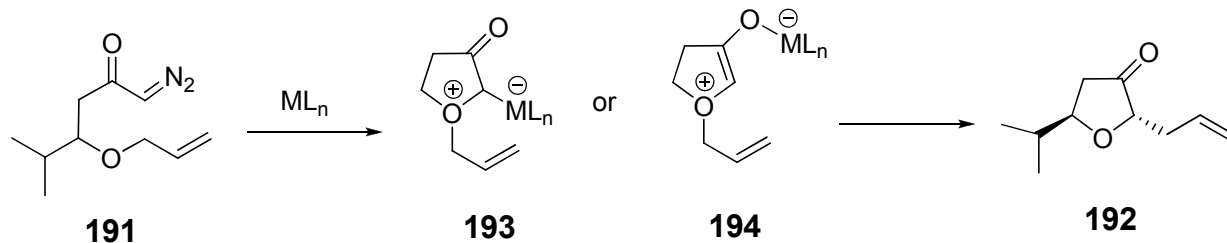
**Table 32.** Catalyst effects the diastereoselective synthesis of tetrahydrofuranones.



Entry	Catalyst	Ratio <b>192</b>	Yield (%) <b>192</b>
1 <sup>a</sup>	Rh <sub>2</sub> (OAc) <sub>4</sub>	65:35-81:19	51-68
2 <sup>b</sup>	Cu(acac) <sub>2</sub>	97:3	83-85

<sup>a</sup> The ratio and yield are given as a range for experiments done in a variety of solvents at reflux or room temperature. <sup>b</sup> Reactions done in THF or benzene at reflux.

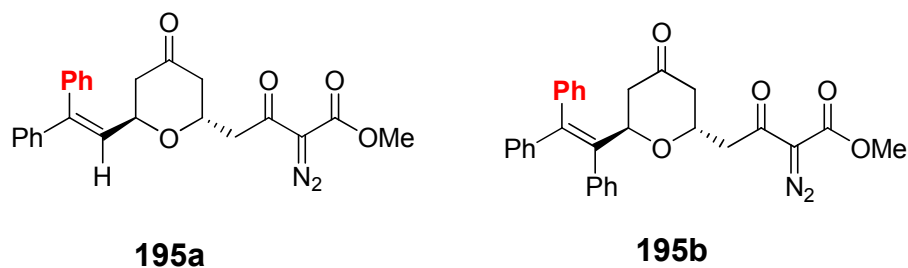
Clark<sup>116</sup> argues that the effect of the catalyst that is observed on the diastereoselection of the two isomers of tetrahydrofuranones **192** suggests that the [2,3]-sigmatropic rearrangement pathway occurs via a metal-bound ylide intermediate **193** or **194** and not *via* a metal free ylide intermediate (Scheme 55). Comparing Clark's conclusions with our own, where we argue that the [2,3]-sigmatropic pathways proceeds *via* a free ylide due to lack of catalyst effect on the ratio of the two diastereoisomers of **179**, it seems clear that the [2,3]-sigmatropic process is substrate dependant; in some cases the process occurs *via* a metal-bound ylide and in other cases it does not.



**Scheme 55.** Mechanism of the [2,3]-sigmatropic rearrangement via a metal-bound ylide.

### 2.5 Control of regioselectivity

After analyzing the decomposition of *trans*-3-styryltetrahydropyranone-5-diazoacetates **177a** and identifying the [1,2]-Stevens and [2,3]-sigmatropic rearrangement products, we decided to investigate vinyl diazoacetate tetrahydropyranones **195a** and **195b** (Scheme 56). These two substrates have an additional phenyl group on the 2-position of the vinyl diazoacetate tetrahydropyranone, shown in red, which may or may not have an effect on the decomposition reaction. The synthesis of these vinyl diazoacetate tetrahydropyranones are easily accessible by employing the methods shown previously.

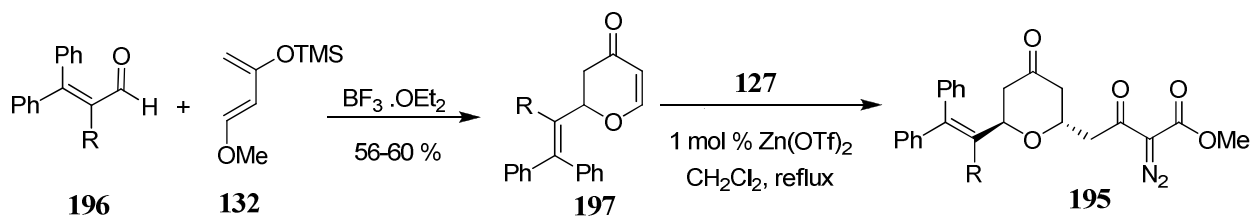


**Scheme 56.** Investigating the possibility of controlling the regioselectivity between [2,3] and [1,2] processes using diazoacetate tetrahydropyranones **195a** and **195b** as model substrate.

#### 2.5a Synthesis of vinyl diazoacetate tetrahydropyranone 195

In order to obtain vinyl diazoacetate tetrahydropyranone **195**, we followed our two step synthesis of the hetero-Diels-Alder reaction followed by the Mukaiyama-Michael addition reaction. Vinyl dihydropyranone **197** was prepared in up to 60% isolated yield by the  $\text{BF}_3 \cdot \text{Et}_2\text{O}$ -mediated hetero Diels-Alder reaction between aldehyde **196** and Danishefsky's diene **132**. Aldehyde **196a** is commercially available while aldehyde **196b** is readily available in a one step synthesis *via* palladium-catalyzed three component coupling of phenyl iodide, internal alkyne, and phenyl boronic acid.<sup>117</sup> Vinyl dihydropyranone **197** then reacted with methyl 3-(*tert*-butyldimethylsilyloxy)-2-diazo-3-butenate **127** with full conversion using  $\text{Zn}(\text{OTf})_2$  (1 mol%) in refluxing dichloromethane. After hydrolysis and purification diazoacetate **195a** and **195b** were isolated in excellent yields (Table 33) and were determined to be solely the *trans* isomers when  $\text{R} = \text{Ph}$  whereas when  $\text{R} = \text{H}$  there was a mixture of the *cis* and *trans* isomers of **195a** with the *trans* isomer dominating in a 90:10 ratio.

**Table 33.** Synthesis of vinyl diazoacetate tetrahydropyranone **195**.



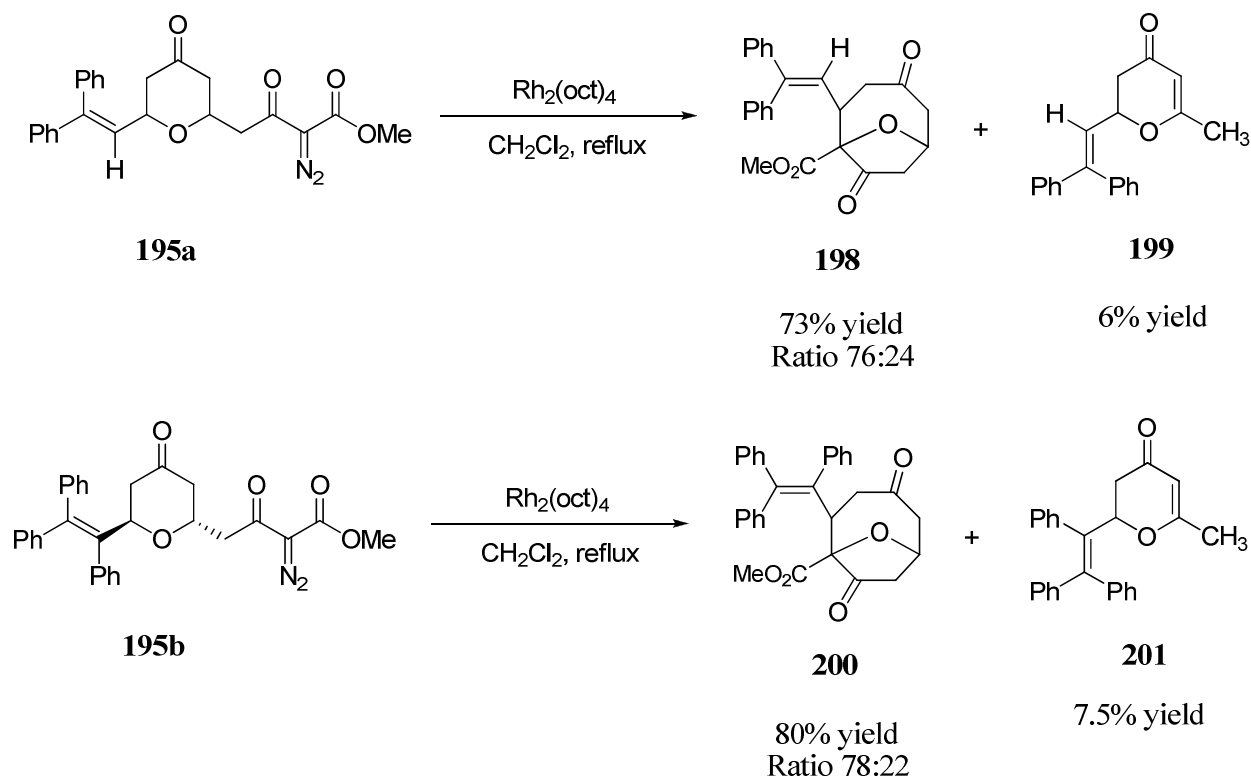
Entry	Substrate	R	Yield <sup>a</sup> (%) 197	Yield <sup>a</sup> (%) 195
1	196a	H	56	97 <sup>b</sup>
2	196b	Ph	60	98

<sup>a</sup> Isolated yield after column chromatography. <sup>b</sup> Isolated yield of both *cis* and *trans* isomers.

<sup>117</sup> Zhou, C.; Larock, R. C. *J. Org. Chem.*, **2005**, *70*, 3765-3777.

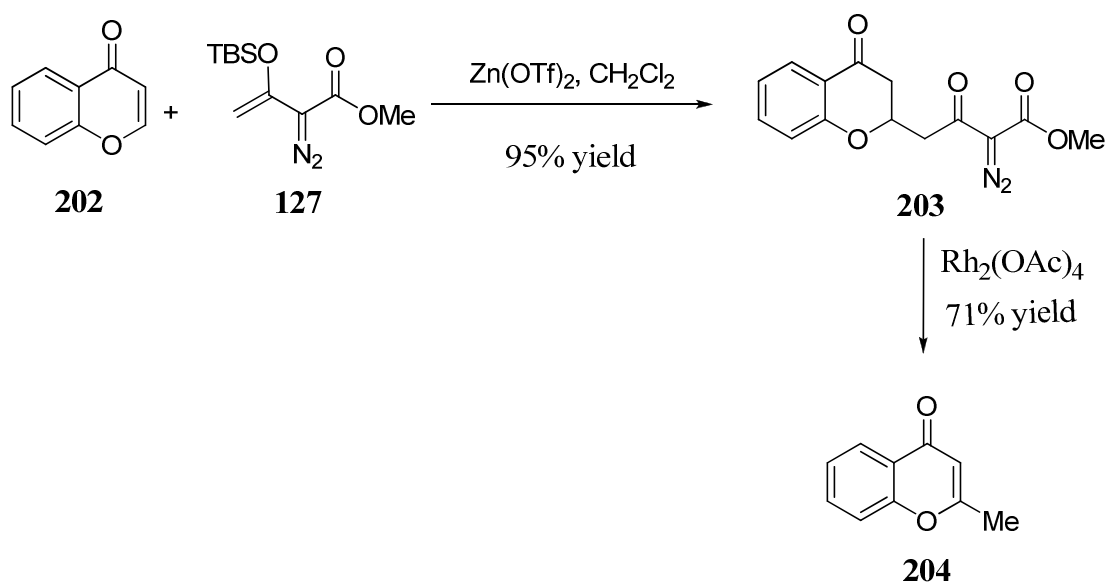
## **2.5b Nitrogen extrusion reactions of vinyl diazoacetate tetrahydropyranone 195a and 195b**

With vinyl diazoacetate tetrahydropyranone **195** in hand, we proceeded to investigate the dinitrogen extrusion reaction. Rhodium(II) catalyzed decomposition of **195a** and **195b**, using 1.0 mol% of dirhodium octanoate [Rh<sub>2</sub>(oct)<sub>4</sub>] in refluxing dichloromethane, afforded the [1,2]-Stevens rearrangement products only, **198** and **200**, in 73% and 80% yield, respectively (Scheme 57). There was no evidence of the [2,3]-sigmatropic rearrangement product in either case as seen from its absence in the <sup>1</sup>H NMR reaction mixture as well as by HPLC analysis. After chromatographic separation, we isolated the two diastereoisomers of the [1,2]-Stevens rearrangement products **198** and **200**, allowing <sup>1</sup>H and <sup>13</sup>C NMR characterization of the diastereoisomers.



**Scheme 57.** Rh(II) catalyzed decomposition of vinyl diazoacetate tetrahydropyranone **195a** and **195b**.

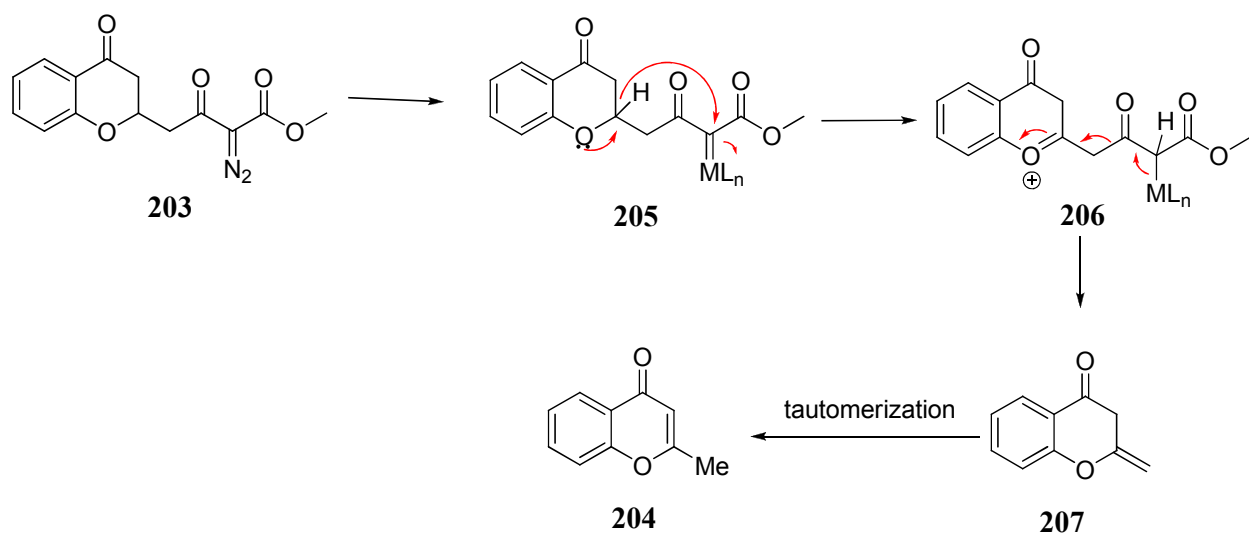
Interestingly, in addition to the [1,2]-Stevens rearrangement product we also observed the formation of byproduct methyl vinyl pyranone **199** and **201** (Scheme 57). Even though these byproducts were not formed in high yields, they are not often observed in reactions of oxonium ylides and their subsequent rearrangements.<sup>118</sup> However, during our investigation we had observed the formation of a similar product using the chromone substrate **202**. Treating diazoacetoacetate **203** with rhodium acetate furnished methyl chromone **204** in 71% yield (Scheme 58).



**Scheme 58.** Nitrogen extrusion reactions of diazoacetoacetate **203**.

We concluded from these results that in the absence of a good migrating group another pathway can take place to afford methyl chromone **204**. We hypothesized that diazoacetoacetate **203** reacts with dirhodium carboxylate to form metal carbene species **205** that undergoes a 1,4-hydride abstraction and generates intermediate **206**. This is then proceeded by loss of ketene followed by tautomerization of **207** to furnish methyl chromone **204** in 71% yield (Scheme 59).

<sup>118</sup> Doyle, M. P.; Dyatkin, A. B.; Autry, C. L. *J. Chem. Soc., Perkin Trans. 1*, **1995**, 619-621.



**Scheme 59.** Possible mechanism of the formation of methyl chromone **204**.

## 2.6 Conclusion

Rh(II) catalyzed oxonium ylide generation of *trans*-3-styryltetrahydropyranone-5-diazoacetates **177** and their subsequent rearrangements form two diastereoisomers in both the [1,2]-Stevens and [2,3]-sigmatropic processes. The crystal structure for the minor diastereoisomer of the [2,3]-sigmatropic rearrangement product, which is not reported in the literature, has been provided. The formation of a second diastereoisomer for the symmetry-allowed concerted [2,3]-sigmatropic rearrangement process is supportive of the hypothesis that the presence of two conformational isomers for *trans*-3-styryltetrahydropyranone-5-diazoacetates **177** lead to the formation of two diastereoisomers. Conformational isomers of styryl diazoacetate tetrahydropyranones (**183** and **184**) are responsible for the apparent isomerization; where each diazoacetate conformer forms a metal-free oxonium ylide, and subsequent rearrangement of each of these two oxonium ylides leads to the formation of a distinct diastereoisomeric product. This mechanistic hypothesis explains how a concerted

process, such as the [2,3]-sigmatropic rearrangement, can lead to the formation of two diastereoisomers. Furthermore, we have demonstrated that the symmetry-forbidden [1,2]-Stevens rearrangement pathway can dominate over the symmetry-allowed [2,3]-sigmatropic rearrangement pathway.

## **2.7 Experimental**

**General information.** Reagents were obtained commercially unless otherwise noted. Reactions were performed using oven-dried or flame-dried glassware under an atmosphere of nitrogen. Air and moisture sensitive liquids and solutions were transferred via syringe or stainless steel cannula. Dichloromethane (DCM) was passed through a solvent column<sup>119</sup> prior to use. Thin-layer chromatography (TLC) was performed on EM Science silica gel 60 F254 plates, and visualization of the developed plates was accomplished by ultraviolet light (254 nm) and/or by staining with iodine, butanolic ninhydrin, *p*-anisaldehyde, or phosphomolybdic acid (PMA) solution. Chromatographic purification of products was performed using air pressure to force the solvent through the column on silica gel (230 x 400 mesh). Compounds purified by chromatography on silica gel were typically applied to the absorbent bed using the indicated solvent conditions with a minimum amount of added dichloromethane as needed for solubility. Unless otherwise described, reactions were carried out at room temperature. Elevated temperatures were obtained using thermostat-controlled silicone oil baths. Low temperatures were obtained in an ice-water bath or by mixing dry-ice with organic solvents. Anhydrous zinc triflate and boron trifluoride-diethyl ether (BF<sub>3</sub>.OEt<sub>2</sub>) were purchased from Aldrich and used as received. Rhodium acetate was obtained

---

<sup>119</sup> Pangborn, A. B.; Giardello, M. A.; Grubbs, R. H.; Rosen, R. K.; Timmers, F. J. *Organometallics*, **1996**, *15*, 1518-1520.

commercially from Pressure Chemical Company, rhodium octanoate was obtained from the Padwa research group, and the rest of the rhodium catalysts were synthesized following literature procedures.<sup>120</sup> Methyl 3-(*tert*-butyldimethylsilyloxy)-2-diazo-3-butenolate was prepared by the method described by Davies.<sup>121</sup>

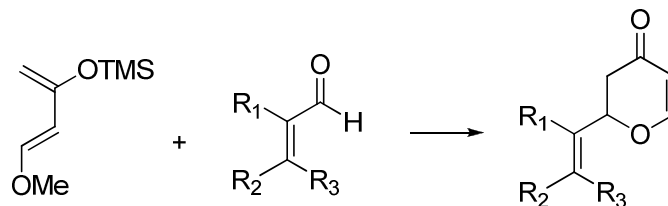
NMR spectra were obtained on Bruker AV-400, Bruker DRX-400 (<sup>1</sup>H at 400 MHz, <sup>13</sup>C at 100 MHz), Bruker DRX-500 (<sup>1</sup>H at 500 MHz, <sup>13</sup>C at 125 MHz), or Bruker AVIII-600 (<sup>1</sup>H at 600 MHz, <sup>13</sup>C at 150 MHz). Absorptions and their splitting from <sup>1</sup>H NMR spectra are recorded as follows relative to residual solvent peaks: (s = singlet, d = doublet, t = triplet, q = quartet, dd = doublet of doublets, td = triplet of doublets, dq = doublet of quartets, ddd = doublet of doublet of doublets, tdd triplet of doublet of doublets, dddd = doublet of doublet of doublet of doublets, m = multiplet, comp = composite), coupling constant (Hz), and integration. Chemical shift ( $\delta$ , ppm) for <sup>13</sup>C NMR spectra are reported relative to residual solvent peak. All spectra are recorded in CDCl<sub>3</sub> as solvent, unless otherwise described. High resolution mass spectra (HRMS) were recorded by JEOL AccuTOF-CS (ESI positive, needle voltage 1800-2400eV, flow rate 50uL/min). IR spectra were recorded on a JASCO FT-IR-4100 instrument. Melting points were determined with a MEL-TEMP digital melting point apparatus.

---

<sup>120</sup> (a) Johnson, S. A.; Hunt, H. R.; Neumann, H. M. *Inorg. Chem.*, **1963**, 2, 960-962. (b) Doyle, M. P.; Colyer, J. T. *Tetrahedron: Asymm.*, **2003**, 14, 3601-3604. (c) Cotton, F. A.; Felthouse, T. R. *Inorg. Chem.*, **1980**, 19, 323-328. (d) Hashimoto, S.; Watanabe, N.; Ikegami, S. *Tetrahedron Lett.*, **1992**, 33, 2709-2712. (e) Ohno, M.; Itoh, M.; Umeda, M.; Furuta, R.; Kondo, K.; Eguchi, S. *J. Am. Chem. Soc.*, **1996**, 118, 7075-7082.

<sup>121</sup> Davies, H. M. L.; Ahmed, G.; Churchill, M. R. *J. Am. Chem. Soc.*, **1996**, 118, 10774-10782.

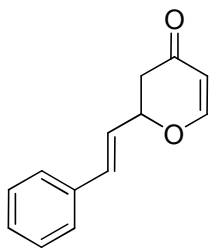
### General procedures for the hetero-Diels-Alder (HDA) reaction



A solution of cinnamaldehyde (1.0g, 7.6 mmoles) and Danishefsky's diene (1.6g, 9.1 mmoles) in dry DCM (38 mL) was cooled to (-78°C). To that was added BF<sub>3</sub>.Et<sub>2</sub>O (1.3g, 8.4 mmoles) dropwise, which produced an instant color change from colorless to yellow to dark brown. After 8 hours at -78°C, the reaction was quenched with NaHCO<sub>3</sub> (20 mL) followed by brine (20 mL), then extracted with CH<sub>2</sub>Cl<sub>2</sub> (3 × 20 mL). The combined organic layer was dried over anhydrous MgSO<sub>4</sub>, filtered, and the solvent was evaporated under reduced pressure.

#### Data Characterization for HDA products.

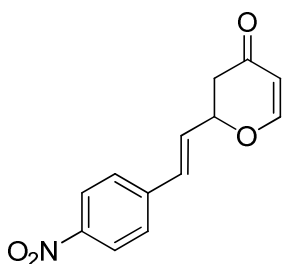
##### (*E*)-2-styryl-2*H*-pyran-4(3*H*)-one



Purified by chromatography on silica gel (gradient elution: hexane/ethyl acetate: 100% to 85% hexane; orange solid (80% yield), based on a 7.6 mmol scale of cinnamaldehyde. <sup>1</sup>H

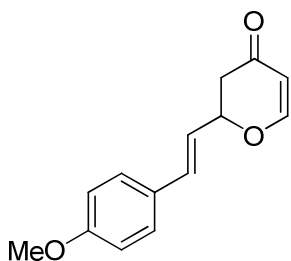
NMR (400 MHz, CDCl<sub>3</sub>)  $\delta$  7.44-7.39 (comp, 3H), 7.38-7.27 (comp, 3H), 6.72 (d,  $J$  = 16.0 Hz, 1H), 6.30 (dd,  $J$  = 16.0, 6.0 Hz, 1H), 5.47 (dd,  $J$  = 6.0, 0.8 Hz, 1H), 5.12 – 5.03 (m, 1H), 2.74 (dd,  $J$  = 16.8, 12.8 Hz, 1H), 2.62 (ddd,  $J$  = 16.8, 4.0, 0.8 Hz, 1H). <sup>13</sup>C NMR (101 MHz, CDCl<sub>3</sub>)  $\delta$  191.6, 162.8, 135.4, 133.5, 128.6, 128.4, 126.6, 124.9, 107.1, 79.5, 41.8. IR (cm<sup>-1</sup>): 1587, 1666, 1667, 3061. HRMS (ESI<sup>+</sup>): expected mass 201.0910, found 201.0915. M.p. 48-49 °C.

**(*E*)-2-(4-nitrostyryl)-2*H*-pyran-4(3*H*)-one**



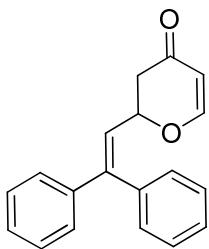
Purified by chromatography on silica gel (gradient elution: hexane/ethyl acetate: 80% to 70% hexane; yellow solid (60% yield), based on a 2.8 mmol scale of (*E*)-3-(4-nitrophenyl) acrylaldehyde. <sup>1</sup>H NMR (400 MHz, CDCl<sub>3</sub>)  $\delta$  8.26-8.18 (comp, 2H), 7.59-7.51 (comp, 2H), 7.43 (d,  $J$  = 6.0 Hz, 1H), 6.80 (dd,  $J$  = 16.0, 0.8 Hz, 1H), 6.46 (dd,  $J$  = 16.0, 6.0 Hz, 1H), 5.50 (dd,  $J$  = 6.0, 0.8 Hz, 1H), 5.17-5.11 (m, 1H), 2.74 (dd,  $J$  = 16.8, 12.4 Hz, 1H), 2.66 (ddd,  $J$  = 16.8, 4.6, 0.8 Hz, 1H). <sup>13</sup>C NMR (126 MHz, CDCl<sub>3</sub>)  $\delta$  191.1, 162.5, 147.4, 142.0, 130.9, 129.7, 127.3, 124.0, 107.5, 78.7, 41.6. IR (cm<sup>-1</sup>): 1513, 1589, 1670, 1342. HRMS (ESI<sup>+</sup>): expected mass 246.0761, found 246.0768. M.p. 97-98 °C.

**(*E*)-2-(4-methoxystyryl)-2*H*-pyran-4(3*H*)-one**



Purified by chromatography on silica gel (gradient elution: hexane/ethyl acetate: 90% to 85% hexane; orange solid (60% yield), based on a 3.1 mmol scale of (*E*)-3-(4-methoxyphenyl) acrylaldehyde.  $^1\text{H}$  NMR (400 MHz,  $\text{CDCl}_3$ )  $\delta$  7.41 (d,  $J = 6.0$  Hz, 1H), 7.37-7.33 (comp, 2H), 6.89-6.86 (comp, 2H), 6.66 (d,  $J = 16.0$  Hz, 1H), 6.17 (dd,  $J = 16.0, 6.8$  Hz, 1H), 5.46 (dd,  $J = 6.0, 1.0$  Hz, 1H), 5.08-5.02 (m, 1H), 3.82 (s, 3H), 2.74 (dd,  $J = 16.8, 13.2$  Hz, 1H), 2.61 (ddd,  $J = 16.8, 4.0, 1.0$  Hz, 1H).  $^{13}\text{C}$  NMR (126 MHz,  $\text{CDCl}_3$ )  $\delta$  192.0, 163.0, 159.9, 133.5, 128.2, 128.1, 122.7, 114.1, 107.2, 80.0, 55.3, 42.0. IR ( $\text{cm}^{-1}$ ): 1514, 1588, 1670, 2935. HRMS (ESI+): expected mass 231.1016, found 231.1024. M.p. 73-74 °C.

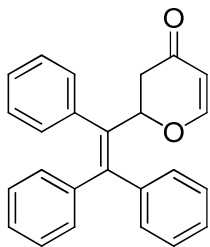
**2-(2,2-diphenylvinyl)-2H-pyran-4(3H)-one**



Purified by chromatography on silica gel (gradient elution: hexane/ethyl acetate: 100% to 90% hexane; yellow solid (56% yield), based on a 2.4 mmol scale of 3,3-diphenylacrylaldehyde.  $^1\text{H}$  NMR (400 MHz,  $\text{CDCl}_3$ )  $\delta$  7.56-7.49 (comp, 4H), 7.45-7.42 (comp, 3H), 7.41-7.38 (comp, 2H), 7.34-7.29 (comp, 2H), 6.25 (d,  $J = 10.0$  Hz, 1H), 5.35 (dd,  $J = 6.4, 1.0$  Hz, 1H), 4.87 (ddd,  $J = 14.2, 10.0, 4.0$  Hz, 1H), 2.51 (dd,  $J = 18.0, 14.2$  Hz, 1H), 2.23 (ddd,  $J = 18.0, 4.0, 1.0$  Hz, 1H).  $^{13}\text{C}$  NMR (101 MHz,  $\text{CDCl}_3$ )  $\delta$  191.8,

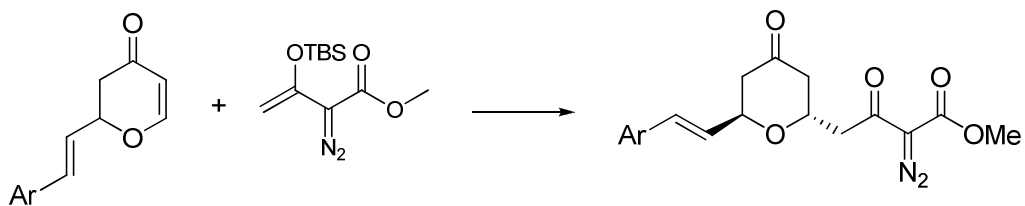
163.2, 147.7, 140.7, 138.2, 129.4, 128.5, 128.4, 128.3, 128.1, 127.7, 123.7, 107.0, 77.4, 42.2. IR (cm<sup>-1</sup>): 1585, 1648, 3051. HRMS (ESI<sup>+</sup>): expected mass 277.1223, found 277.1232. M.p. 126-127 °C.

### 2-(1,2,2-triphenylvinyl)-2H-pyran-4(3H)-one



Purified by chromatography on silica gel (gradient elution: hexane/ethyl acetate: 90% to 80% hexane; yellow solid (60% yield), based on a 1.8 mmol scale of 2,3,3-triphenylacrylaldehyde. <sup>1</sup>H NMR (400 MHz, CDCl<sub>3</sub>) δ 7.40-7.28 (comp, 4H), 7.25-7.16 (comp, 7H), 7.07-7.01 (comp, 3H), 6.96-6.93 (comp, 2H), 5.41 (dd, *J* = 15.2, 3.2 Hz, 1H), 5.27 (dd, *J* = 6.0, 1.0 Hz, 1H), 2.63 (dd, *J* = 16.8, 15.2 Hz, 1H), 2.36 (ddd, *J* = 16.8, 3.2, 1.0 Hz, 1H). <sup>13</sup>C NMR (126 MHz, CDCl<sub>3</sub>) δ 192.2, 163.0, 146.8, 141.1, 140.6, 137.3, 135.5, 131.1, 129.9, 129.0, 128.5, 127.8, 127.7, 127.5, 127.1, 126.8, 106.5, 79.6, 40.8. IR (cm<sup>-1</sup>): 1589, 1667, 3079. HRMS (ESI<sup>+</sup>): expected mass 353.1536, found 353.1532. M.p. 164-165 °C.

### General Procedure for the Mukaiyama-Michael reaction



To a flame-dried, 25-mL round bottom flask under nitrogen was added zinc triflate (8.0 mg, 0.022 mmol), followed by (*E*)-2-styryl-2H-pyran-4(3H)-one (0.44g, 2.2 mmol) that was dissolved in dry DCM (11 mL). Methyl 3-(*tert*-butyldimethylsilyloxy)-2-diazo-3-

butanoate (0.84g, 3.3 mmol) was then added via syringe all at once. The resulting orange solution was stirred in refluxing CH<sub>2</sub>Cl<sub>2</sub> for 16 hrs and then slowly cooled to room temperature. The Mukaiyama-Michael reactions were worked-up using one of two methods, either TBAF and AcOH (Method A) or 4N HCl (Method B). For the synthesis of methyl 2-diazo-3-oxo-4-[(2S\*,6S\*)-4-oxo-6-styryltetrahydro-2*H*-pyran-2-yl] butanoate, TBAF and AcOH (method A) were used for the work-up, as described below.

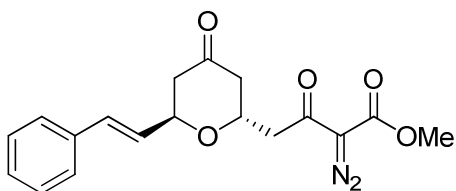
**Mukaiyama-Michael reaction work-up using TBAF and AcOH- Method A.** For diazoacetoacetate substrates where the aryl substituent is electron donating (methyl 2-diazo-3-oxo-4-((2S\*,6S\*)-4-oxo-6-styryl tetrahydro-2*H*-pyran-2-yl) butanoate and methyl-2-diazo-4-((2S\*,6S\*)-6-(4-methoxystyryl)-4-oxotetrahydro-2*H*-pyran-2-yl)-3-oxo butanoate, TBAF was used for the work up to prevent the formation of elimination byproducts that were observed when the work-up was done with 4N HCl. After the reaction was complete (16 hrs), judged by TLC analysis, the DCM was evaporated under reduced pressure and the reaction was dissolved in 25 mL of tetrahydrofuran (THF). To that solution was added AcOH (10 mL) and TBAF (1.0M THF solution, 15 mL, 2.1 mmoles). The resulting solution was stirred at 0 °C for 4 hrs. The solution was quenched with Et<sub>3</sub>N, then diluted with saturated NaHCO<sub>3</sub> (20 mL), and the aqueous layer was extracted with DCM (20 mL x 3). The combined organic extract was washed with brine (20 mL), dried over anhydrous MgSO<sub>4</sub>, and concentrated under reduced pressure after filtration.

**Mukaiyama-Michael reaction work-up using 4N HCl - Method B.** This work-up was used for Methyl 2-diazo 4-((2S\*,6S\*) 6-(4-nitro-styryl) 4-oxotetrahydro-2*H*-pyran-2-yl) 3-oxo butanoate, based on (202 mg, 1.4 mmol) of (*E*)-2-(4-nitrostyryl)-2*H*-pyran-

4(3*H*)-one. After the reaction was complete (16 hrs), judging by TLC analysis, the reaction mixture was concentrated under reduced pressure then dissolved in (15 mL) of tetrahydrofuran (THF). To that solution was added 6 mL of 4N aqueous HCl solution dropwise. After 4 hrs the reaction was quenched by slow addition of NaHCO<sub>3</sub> (10 mL) until the reaction was neutralized, measured by pH paper. The resulting solution was extracted with DCM (3 × 15 mL), and the combined organic layer was dried over anhydrous MgSO<sub>4</sub> and filtered. The solvent was evaporated under reduced pressure.

#### Data Characterization for Mukaiyama-Michael products

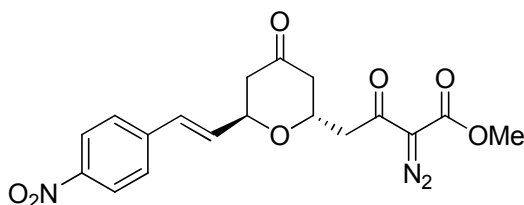
**Methyl 2-diazo-3-oxo-4-((2*R*\*,6*R*\*)-4-oxo-6-styryltetrahydro-2*H*-pyran-2-yl)butanoate**



Purified by chromatography on silica gel (gradient elution: hexane/ethyl acetate: 90% to 70% hexane; orange solid (85% yield), based on a 2.2 mmol scale of (*E*)-2-styryl-2*H*-pyran-4(3*H*)-one, using TBAF and AcOH (method A) for work-up. <sup>1</sup>H NMR (400 MHz, CDCl<sub>3</sub>) δ 7.43-7.39 (comp, 2H), 7.36-7.32 (comp, 2H), 7.30-7.26 (m, 1H), 6.61 (dd, *J* = 16.0, 1.6 Hz, 1H), 6.27 (dd, *J* = 16.0, 5.0 Hz, 1H), 4.99 – 4.95 (m, 1H), 4.76 – 4.70 (m, 1H), 3.84 (s, 3H), 3.41 (dd, *J* = 16.0, 8.0 Hz, 1H), 3.00 (dd, *J* = 16.0, 5.0 Hz, 1H), 2.78 (ddd, *J* = 14.6, 6.0, 1.0 Hz, 1H), 2.68 (ddd, *J* = 14.6, 4.6, 1.4 Hz, 1H), 2.58 (ddd, *J* = 14.6,

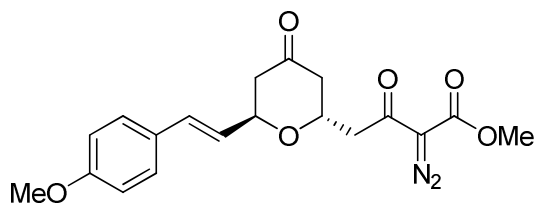
4.0, 1.4 Hz, 1H), 2.43 (ddd,  $J = 14.6, 9.0, 1.0$  Hz, 1H).  $^{13}\text{C}$  NMR (101 MHz,  $\text{CDCl}_3$ )  $\delta$  205.9, 188.9, 161.5, 136.0, 133.3, 128.6, 128.1, 127.7, 126.6, 73.1, 68.0, 52.3, 46.8, 45.1, 45.0, missing diazo carbon. IR ( $\text{cm}^{-1}$ ): 1711, 1649, 2132 ( $\text{C}=\text{N}_2$ ), 2952. HRMS (ESI+): expected mass 343.1288, found 343.1285. M.p. 77-78 °C.

**Methyl 2-diazo-4-((2*R*\*,6*R*\*)-6-(4-nitrostyryl)-4-oxotetrahydro-2*H*-pyran-2-yl)-3-oxo butanoate**



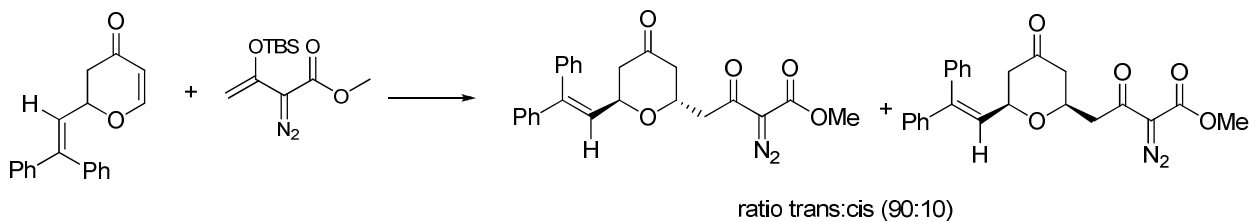
Purified by chromatography on silica gel (gradient elution: hexane/ethyl acetate: 90% to 60% hexane; yellow solid (88% yield), based on a 1.0 mmol scale of (*E*)-2-(4-nitrostyryl)-2*H*-pyran-4(3*H*)-one, using 4*N* HCl (method B) for work-up.  $^1\text{H}$  NMR (400 MHz,  $\text{CDCl}_3$ )  $\delta$  8.19-8.17 (comp, 2H), 7.54-7.52 (comp, 2H), 6.69 (dd,  $J = 16.0, 1.6$  Hz, 1H), 6.41 (dd,  $J = 16.0, 4.4$  Hz, 1H), 5.00-4.96 (m, 1H), 4.71 (dq,  $J = 13.0, 4.4$  Hz, 1H), 3.83 (s, 3H), 3.43 (dd,  $J = 16.0, 8.0$  Hz, 1H), 2.95 (dd,  $J = 16.0, 4.4$  Hz, 1H), 2.78 (ddd,  $J = 14.8, 6.0, 0.6$  Hz, 1H), 2.64 (ddd,  $J = 14.8, 4.8, 1.2$  Hz, 1H), 2.55 (ddd,  $J = 14.8, 4.0, 1.2$  Hz, 1H), 2.44 (ddd,  $J = 14.8, 8.8, 0.6$  Hz, 1H).  $^{13}\text{C}$  NMR (101 MHz,  $\text{CDCl}_3$ )  $\delta$  205.4, 188.9, 161.5, 147.2, 142.5, 132.7, 130.9, 127.2, 124.0, 72.8, 68.3, 52.3, 46.7, 44.9, 44.8, missing diazo carbon. IR ( $\text{cm}^{-1}$ ): 1651, 1710, 2141 ( $\text{C}=\text{N}_2$ ), 2954. HRMS (ESI+): expected mass 388.1139, found 388.1143. M.p. 131-132 °C.

**Methyl-2-diazo-4-((2*R*\*,6*R*\*)-6-(4-methoxystyryl)-4-oxotetrahydro-2*H*-pyran-2-yl)-3-oxo butanoate**



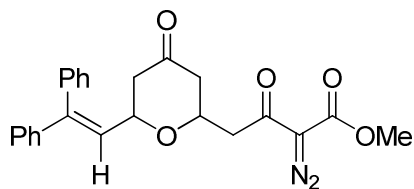
Purified by chromatography on silica gel (gradient elution: hexane/ethyl acetate: 90% to 70% hexane; yellow oil (98% yield), based on a 1.0 mmol scale of (*E*)-2-(4-methoxystyryl)-2*H*-pyran-4(3*H*)-one, using TBAF and AcOH (method A) for work-up. <sup>1</sup>H NMR (400 MHz, CDCl<sub>3</sub>) δ 7.32-7.30 (comp, 2H), 6.84-6.82 (comp, 2H), 6.50 (dd, *J* = 16.0, 1.5 Hz, 1H), 6.09 (dd, *J* = 16.0, 5.0 Hz, 1H), 4.92-4.88 (m, 1H), 4.73-4.62 (m, 1H), 3.79 (s, 3H), 3.78 (s, 3H), 3.35 (dd, *J* = 16.0, 8.0 Hz, 1H), 2.95 (dd, *J* = 16.0, 5.0 Hz, 1H), 2.72 (ddd, *J* = 14.4, 6.0, 0.6 Hz, 1H), 2.63 (ddd, *J* = 14.4, 4.4, 1.0 Hz, 1H), 2.53 (ddd, *J* = 14.4, 3.8, 1.0 Hz, 1H), 2.38 (ddd, *J* = 14.4, 9.0, 0.6 Hz, 1H). <sup>13</sup>C NMR (101 MHz, CDCl<sub>3</sub>) δ 206.1, 188.9, 161.5, 159.5, 132.8, 128.7, 127.8, 125.3, 113.9, 73.2, 67.8, 55.2, 52.2, 46.7, 45.1, 45.0, missing diazo carbon. IR (cm<sup>-1</sup>): 1651, 1714, 2138 (C=N<sub>2</sub>), 2972. HRMS (ESI<sup>+</sup>): expected mass 373.1394, found 373.1401.

### Synthesis of Methyl 2-diazo-4-(6-(2,2-diphenylvinyl)-4-oxotetrahydro-2*H*-pyran-2-yl)-3-oxobutanoate



To a flame-dried, 25-mL round bottom flask under nitrogen was added zinc triflate (4.2 mg, 0.012 mmol), followed by 2-(2,2-diphenylvinyl)-2*H*-pyran-4(3*H*)-one (0.32g, 1.2 mmol) that was dissolved in dry DCM (6.0 mL). Methyl 3-(*tert*-butyldimethylsilyloxy)-2-diazo-3-butenolate (0.45 g, 1.8 mmol) was then added via syringe all at once. The resulting orange solution was stirred and heated using an oil bath to 40°C for 16 hrs and then slowly cooled to room temperature. After the reaction was complete, judged by TLC analysis, the DCM was evaporated under reduced pressure, and the reaction was dissolved in 10 mL of tetrahydrofuran (THF). To that solution was added AcOH (6.0 mL) and TBAF (1.0M THF solution, 8.0 mL, 2.1 mmoles). The resulting solution was stirred at 0 °C for 4 hrs. The solution was quenched with Et<sub>3</sub>N, then diluted with saturated NaHCO<sub>3</sub> (10 mL), and the aqueous layer was extracted with DCM (10 mL x 3). The combined organic extract was washed with brine (10 mL), dried over anhydrous MgSO<sub>4</sub> and concentrated under reduced pressure after filtration.

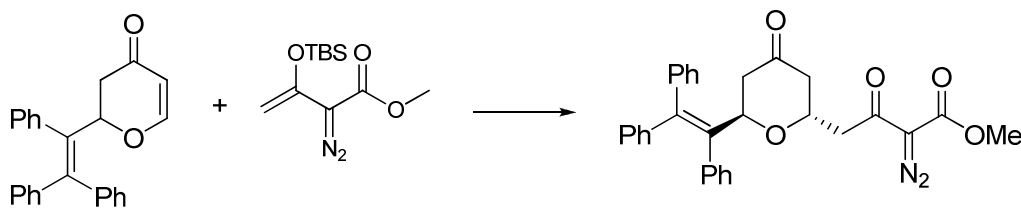
**Methyl 2-diazo-4-(6-(2,2-diphenylvinyl)-4-oxotetrahydro-2*H*-pyran-2-yl)-3-oxobutanoate**



Purified by chromatography on silica gel (gradient elution: hexane/ethyl acetate: 95% to 85% hexane; yellow oil (97% yield) (d.r. 90:10), based on a 1.2 mmol scale of 2-(2,2-diphenylvinyl)-2*H*-pyran-4(3*H*)-one, using TBAF and AcOH (method A) for work-up. <sup>1</sup>H NMR (400 MHz, CDCl<sub>3</sub>) δ 7.42-7.36 (comp, 6H), 7.30-7.24 (comp, 14H), 6.13 (d, *J* = 9.2 Hz, 1H), 6.04 (d, *J* = 8.8 Hz, 1H), 4.82 (comp, 2H), 4.72 (dt, *J* = 9.2, 5.4 Hz, 2H), 3.86 (s, 3H), 3.82 (s, 3H), 3.49 (dd, *J* = 16.4, 7.6 Hz, 1H), 3.26 (dd, *J* = 16.0, 7.6 Hz, 1H),

3.00 (dd,  $J = 16.4, 5.4$  Hz, 2H), 2.69-2.62 (comp, 4H), 2.50-2.39 (comp, 4H).  $^{13}\text{C}$  NMR (101 MHz,  $\text{CDCl}_3$ )  $\delta$  206.3 and 205.6, 188.8 and 188.7, 161.5 and 161.4, 146.8 and 146.0, 141.4 and 141.3, 138.6 and 138.6, 129.7 (2C), 128.3 and 128.1, 128.1 and 128.1, 127.9 (2C), 127.7 (2C), 126.7 and 125.4, 74.7 and 70.7, 72.0 and 68.3, 52.2 (2C), 47.4 and 46.7, 46.9 and 46.7, 45.9 and 45.0, missing diazo carbon. IR ( $\text{cm}^{-1}$ ): 1649, 1713, 2134 ( $\text{C}=\text{N}_2$ ), 2930. HRMS (ESI<sup>+</sup>): expected mass 419.1601, found 419.1610.

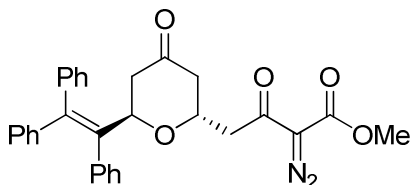
**Synthesis of Methyl-2-diazo-3-oxo-4-((2*R*\*,6*R*\*)-4-oxo-6-(1,2,2-triphenylvinyl)tetrahydro-2*H*-pyran-2-yl)butanoate**



To a flame-dried, 25-mL round bottom flask under nitrogen was added zinc triflate (3.1 mg, 0.011 mmol), followed by 2-(1,2,2-triphenylvinyl)-2*H*-pyran-4(3*H*)-one (0.30 g, 1.0 mmol) that was dissolved in dry DCM (6.0 mL). Methyl 3-(*tert*-butyldimethylsilyloxy)-2-diazo-3-butenoate (0.35g, 1.4 mmol) was then added via syringe all at once. The resulting orange solution was stirred and heated using an oil bath to 40°C for 16 hrs and then slowly cooled to room temperature. After the reaction was complete, judged by TLC analysis, the DCM was evaporated under reduced pressure and the reaction was dissolved in 10 mL of tetrahydrofuran (THF). To that solution was added AcOH (6.0 mL) and TBAF (1.0 M THF solution, 8.0 mL, 2.1 mmol). The resulting solution was stirred at 0 °C for 4 hrs. The solution was quenched with  $\text{Et}_3\text{N}$ , then diluted with saturated  $\text{NaHCO}_3$  (10 mL), and the aqueous layer was extracted with DCM (10mL x 3). The combined

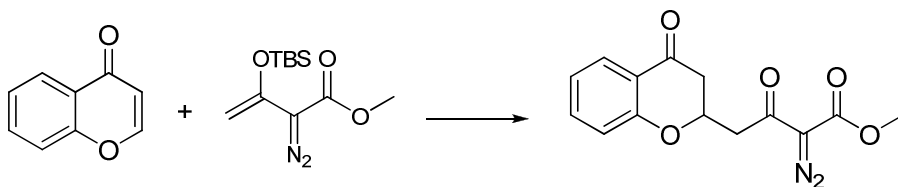
organic extracts were washed with brine (10 mL), dried over anhydrous MgSO<sub>4</sub> and concentrated under reduced pressure after filtration.

**Methyl-2-diazo-3-oxo-4-((2*R*\*,6*R*\*)-4-oxo-6-(1,2,2-triphenylvinyl)tetrahydro-2*H*-pyran-2-yl)butanoate**



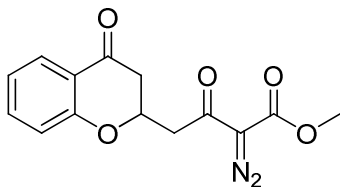
Purified by chromatography on silica gel (gradient elution: hexane/ethyl acetate: 95% to 80% hexane; yellow oil (98% yield), based on a 1.0 mmol scale of 2-(1,2,2-triphenylvinyl)-2*H*-pyran-4(3*H*)-one, using TBAF and AcOH (method A) for work-up. <sup>1</sup>H NMR (400 MHz, CDCl<sub>3</sub>) δ 7.38-7.34 (comp, 2H), 7.30-7.23 (comp, 5H), 7.21-7.14 (comp, 3H), 7.03-6.96 (comp, 3H), 6.92-6.89 (comp, 2H), 4.97 (dd, *J* = 11.8, 3.2 Hz, 1H), 4.75 (p, *J* = 6.4 Hz, 1H), 3.82 (s, 3H), 3.02 (dd, *J* = 16.4, 6.4 Hz, 1H), 2.79 (dd, *J* = 16.4, 6.4 Hz, 1H), 2.59 – 2.44 (comp, 2H), 2.33 (ddd, *J* = 15.2, 3.2, 1.2 Hz, 1H), 2.21 (ddd, *J* = 15.6, 5.2, 1.2 Hz, 1H). <sup>13</sup>C NMR (101 MHz, CDCl<sub>3</sub>) δ 207.2, 188.7, 161.2, 144.3, 141.5, 141.2, 137.8, 137.8, 131.3, 130.0, 129.1, 128.3, 127.7, 127.4, 127.2, 126.9, 126.4, 71.6, 69.3, 52.3, 45.2, 45.1, 43.3, missing diazo carbon. IR (cm<sup>-1</sup>): 1650, 1715, 2135 (C=N<sub>2</sub>), 3019. HRMS (ESI<sup>+</sup>): expected mass 495.1914, found 495.1921.

**Synthesis of Methyl 2-diazo-3-oxo-4-(4-oxochroman-2-yl)butanoate**



To a flame-dried, 25-mL round bottom flask under nitrogen was added zinc triflate (5.0 mg, 0.014 mmol), followed by 4*H*-chromen-4-one (0.20 g, 1.4 mmol) that was dissolved in dry DCM (4.0 mL). Methyl 3-(*tert*-butyldimethylsilyloxy)-2-diazo-3-butenate (0.53 g, 2.1 mmol) was then added via syringe all at once. The resulting orange solution was stirred and heated using an oil bath to 40°C for 16 hrs and then slowly cooled to room temperature. After the reaction was complete, judging by TLC analysis, the reaction mixture was concentrated under reduced pressure then the residue was dissolved in (10 mL) of tetrahydrofuran (THF). To that solution was added 4.0 mL of 4*N* aqueous HCl solution dropwise. After 4 hrs the reaction was quenched by slow addition of NaHCO<sub>3</sub> (10 mL) until the reaction was neutralized, measured by pH paper. The resulting solution was extracted with DCM (3 × 15 mL), and the combined organic layer was dried over anhydrous MgSO<sub>4</sub> and filtered. The solvent was evaporated under reduced pressure.

#### Methyl 2-diazo-3-oxo-4-(4-oxochroman-2-yl)butanoate



Purified by chromatography on silica gel (gradient elution: hexane/ethyl acetate: 90% to 80% hexane; yellow solid (95% yield), based on a 1.4 mmol scale of 4*H*-chromen-4-one, using 4*N* HCl (method B) for work-up. <sup>1</sup>H NMR (400 MHz, CDCl<sub>3</sub>) δ 7.85 (dd, *J* = 8.0, 1.6 Hz, 1H), 7.44 (ddd, *J* = 8.4, 7.2, 1.6 Hz, 1H), 7.01-6.97 (m, 1H), 6.93 (d, *J* = 8.0 Hz, 1H), 5.06 – 4.99 (m, 1H), 3.83 (s, 3H), 3.57 (dd, *J* = 16.8, 7.2 Hz, 1H), 3.16 (dd, *J* = 16.8, 5.2 Hz, 1H), 2.78-2.76 (comp, 2H). <sup>13</sup>C NMR (101 MHz, CDCl<sub>3</sub>) δ 191.5, 188.2, 161.5, 161.1, 136.0, 126.9, 121.4, 120.8, 117.9, 73.5, 52.3, 44.7, 42.5, missing diazo carbon. IR

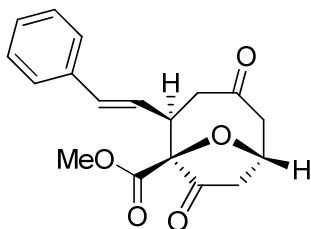
( $\text{cm}^{-1}$ ): 1658, 1683, 2133 ( $\text{C}=\text{N}_2$ ), 2930. HRMS (ESI+): expected mass 289.0819, found 289.0825. M.p. 73-74 °C.

### General Procedure for catalytic dinitrogen extrusion

The catalyst  $\text{Rh}_2(\text{oct})_4$  (9.7 mg, 0.012 mmoles) was transferred to a flame-dried two-neck flask and then dissolved in anhydrous  $\text{CH}_2\text{Cl}_2$  (6.0 mL). Methyl 2-diazo 3-oxo-4-((2*S*\*,6*S*\*)-4-oxo-6-styryltetrahydro-2*H*-pyran-2-yl)butanoate (0.42g, 1.2 mmoles) was dissolved in anhydrous  $\text{CH}_2\text{Cl}_2$  (3.0 mL) and added dropwise to the reaction mixture via a syringe pump over two hrs. Once the addition was complete, the reaction mixture was left to stir in refluxing  $\text{CH}_2\text{Cl}_2$  for an additional two hrs. After the reaction reached completion, judging by TLC analysis, the reaction mixture was cooled to room temperature and the solvent was evaporated under reduced pressure. The catalyst  $\text{Rh}_2(\text{oct})_4$  was used for the decomposition reactions of all styryl and vinyl diazoacetoacetate substrates described in this chapter.

### Data Characterization for Dinitrogen Extrusion Products

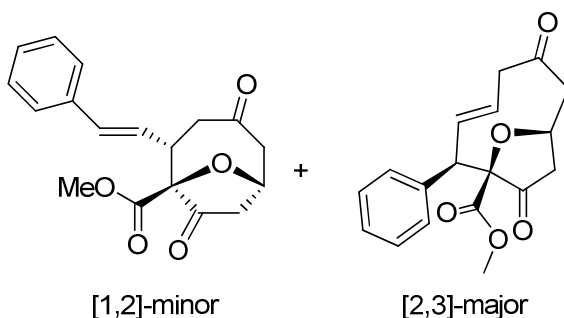
**(1*S*\*,2*R*\*,6*R*\*)-Methyl 4,8-dioxo-2-styryl-9-oxabicyclo[4.2.1]nonane-1-carboxylate-major isomer**



Isolated *via* preparative thin-layer chromatography (gradient elution: hexane/ethyl acetate: 50% to 50% hexane, white solid.  $^1\text{H}$  NMR (400 MHz,  $\text{CDCl}_3$ )  $\delta$  7.35-7.24

(comp, 5H), 6.57 (d,  $J = 16.0$  Hz, 1H), 6.06 (dd,  $J = 16.0, 9.4$  Hz, 1H), 5.16-5.12 (m, 1H), 3.74 (s, 3H), 3.40-3.35 (m, 1H), 3.30 (dd,  $J = 16.0, 6.8$  Hz, 1H), 3.11 (dd,  $J = 18.8, 10.0$  Hz, 1H), 2.78-2.69 (comp, 2H), 2.64-2.58 (comp, 2H).  $^{13}\text{C}$  NMR (126 MHz,  $\text{CDCl}_3$ )  $\delta$  207.8, 205.8, 165.7, 136.2, 134.4, 128.5, 128.0, 126.5, 124.7, 89.3, 69.7, 53.2, 51.8, 46.3, 44.3, 41.9. IR ( $\text{cm}^{-1}$ ): 1699, 1732, 1760. HRMS (ESI<sup>+</sup>): expected mass 315.1227, found 315.1235. M.p. 120-121 °C.

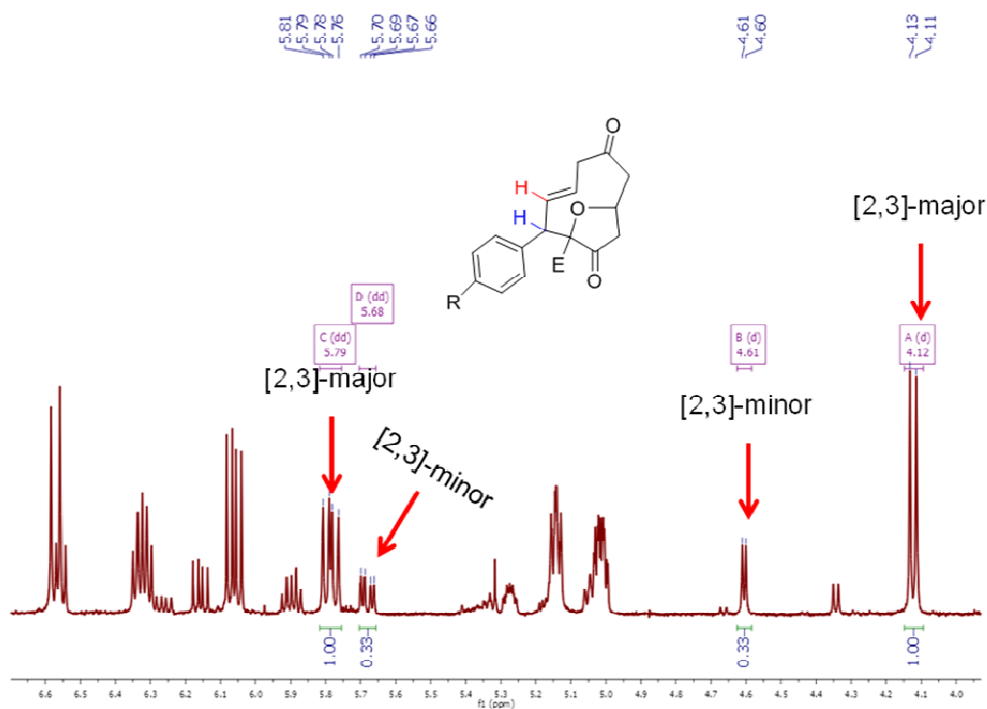
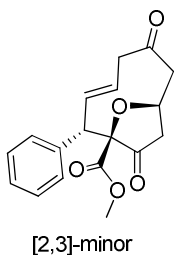
**(1*S*\*,2*S*\*,6*R*\*) methyl 4,8-dioxo-2-styryl-9-oxabicyclo [4.2.1] nonane-1-carboxylate and (1*S*\*,2*R*\*,8*S*\*) methyl 6,10-dioxo-2-phenyl-11-oxabicyclo[6.2.1]undec-3-ene-1-carboxylate**



Isolated *via* preparative thin-layer chromatography (gradient elution: hexane/ethyl acetate: 50% to 50% hexane).  $^1\text{H}$  NMR (400 MHz,  $\text{CDCl}_3$ )-minor isomer of the [1,2]-Stevens  $\delta$  7.36-7.22 (m, 5H), 6.53 (d,  $J = 16.0$  Hz, 1H), 6.13 (dd,  $J = 16.0, 9.3$  Hz, 1H), 5.03-4.96 (m, 1H), 3.71 (s, 3H), 3.28-3.10 (m, 3H), 2.87-2.79 (m, 1H), 2.63-2.55 (m, 3H).  $^1\text{H}$  NMR (400 MHz,  $\text{CDCl}_3$ )-major isomer of the [2,3]-sigmatropic  $\delta$  7.36-7.22 (m, 5H), 6.29 (dt,  $J = 16.0, 8.0$  Hz, 1H), 5.76 (dd,  $J = 16.0, 11.0$  Hz, 1H), 5.03-4.96 (m, 1H), 4.10 (d,  $J = 11.0$  Hz, 1H), 3.60 (s, 3H), 3.28-3.10 (m, 3H), 2.83 (dd,  $J = 19.7, 9.5$  Hz, 1H), 2.64 (dd,  $J = 19.7, 6.0$  Hz, 1H), 2.50 (dd,  $J = 13.0, 6.6$  Hz, 1H).  $^{13}\text{C}$  NMR (101 MHz,  $\text{CDCl}_3$ ) -minor isomer of the [1,2]-Stevens  $\delta$  208.2, 205.3, 166.5, 136.5, 134.2, 128.5, 127.8, 126.5, 124.1, 86.7, 70.0, 53.0, 51.8, 46.7, 44.7, 43.7.  $^{13}\text{C}$  NMR (101 MHz,

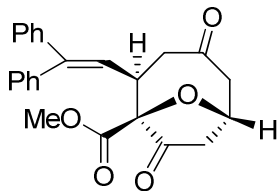
CDCl<sub>3</sub>)-major isomer of the [2,3]-sigmatropic  $\delta$  207.4, 204.6, 167.4, 133.6, 132.3, 129.2, 128.5, 128.0, 127.7, 87.3, 75.3, 56.3, 52.71, 49.0, 46.3, 40.0.

<sup>1</sup>H NMR spectra of reaction mixture supporting the existence of the (1*S*\*,2*S*\*,8*S*\*)-methyl 6,10-dioxo-2-phenyl-11-oxabicyclo[6.2.1]undec-3-ene-1-carboxylate-[2,3]-minor isomer



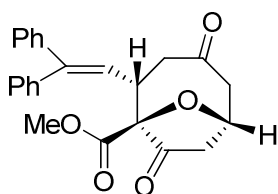
<sup>1</sup>H NMR (600 MHz, CDCl<sub>3</sub>)  $\delta$  5.79 (dd,  $J = 16.0, 11.0$  Hz, 1H), 5.68 (dd,  $J = 16.0, 6.0$  Hz, 1H), 4.61 (d,  $J = 6.0$  Hz, 1H), 4.12 (d,  $J = 11.0$  Hz, 1H).

(1*S*\*,2*R*\*,6*R*\*)-Methyl-2-(2,2-diphenylvinyl)-4,8-dioxo-9-oxabicyclo[4.2.1]nonane-1-carboxylate- major isomer



Purified by chromatography on silica gel (gradient elution: hexane/ethyl acetate: 90% to 70% hexane; white solid (50% yield), isolated from 0.53 mmol scale of methyl 2-diazo-4-(6-(2,2-diphenylvinyl)-4-oxotetrahydro-2*H*-pyran-2-yl)-3-oxobutanoate. Since this compound is the major isomer, the stereochemistry was assigned by analogy to the crystal structure of methyl (1*S*\*,2*R*\*,6*R*\*)-4,8-dioxo-2-styryl-9-oxabicyclo[4.2.1]nonane-1-carboxylate (**189**-major isomer). <sup>1</sup>H NMR (400 MHz, CDCl<sub>3</sub>) δ 7.55-7.48 (comp, 3H), 7.38-7.36 (comp, 4H), 7.29-7.26 (comp, 3H), 6.00 (d, *J* = 11.6 Hz, 1H), 5.10-5.05 (m, 1H), 3.52 (s, 3H), 3.19 (dt, *J* = 11.6, 6.0 Hz, 1H), 3.07 (dd, *J* = 17.4, 7.4 Hz, 1H), 2.84 (dd, *J* = 20.4, 10.8 Hz, 1H), 2.33-2.24 (comp, 4H). <sup>13</sup>C NMR (101 MHz, CDCl<sub>3</sub>) δ 207.7, 205.5, 165.9, 146.1, 141.7, 138.9, 129.2, 128.5, 128.1, 127.8, 127.7, 127.6, 123.0, 88.8, 69.6, 53.2, 51.8, 46.8, 42.2, 40.8. IR (cm<sup>-1</sup>): 1706, 1733, 1771, 2920. HRMS (ESI+): expected mass 391.1540, found 391.1529. M.p. 187-188 °C.

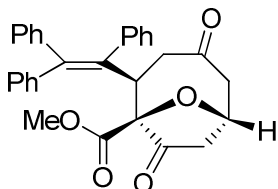
**(1*S*\*,2*S*\*,6*R*\*)-Methyl-2-(2,2-diphenylvinyl)-4,8-dioxo-9-oxabicyclo[4.2.1]nonane-1-carboxylate- minor isomer**



Purified by chromatography on silica gel (gradient elution: hexane/ethyl acetate: 90% to 70% hexane; white solid (23% yield), isolated from 0.53 mmol scale of methyl 2-diazo-4-[6-(2,2-diphenylvinyl)-4-oxotetrahydro-2*H*-pyran-2-yl]-3-oxobutanoate. <sup>1</sup>H NMR (400 MHz, CDCl<sub>3</sub>) δ 7.55-7.44 (comp, 3H), 7.43-7.34 (comp, 5H), 7.26-7.23 (comp, 2H), 6.16

(d,  $J = 11.6$  Hz, 1H), 4.87 (t,  $J = 9.2$  Hz, 1H), 3.46 (s, 3H), 3.14 (td,  $J = 11.6, 4.8$  Hz, 1H), 3.00-2.88 (comp, 2H), 2.52 (dd,  $J = 14.8, 4.8$  Hz, 1H), 2.35-2.28 (comp, 3H).  $^{13}\text{C}$  NMR (101 MHz,  $\text{CDCl}_3$ )  $\delta$  208.2, 205.1, 166.0, 145.0, 141.8, 138.9, 129.3, 128.5, 128.2, 127.7, 127.6, 127.6, 122.9, 86.3, 69.6, 52.9, 51.7, 47.5, 43.7, 41.9. IR ( $\text{cm}^{-1}$ ): 1706, 1733, 1771, 2920. HRMS (ESI+): expected mass 391.1540, found 391.1536. M.p. 136-137 °C.

**(1*S*\*,2*R*\*,6*R*\*)-Methyl-4,8-dioxo-2-(1,2,2-triphenylvinyl)-9-oxabicyclo[4.2.1]nonane-1-carboxylate- major isomer**

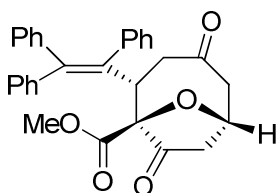


Purified by chromatography on silica gel (gradient elution: hexane/ethyl acetate: 90% to 70% hexane; white solid (66% yield), isolated from 0.43 mmol scale of Methyl-2-diazo-3-oxo-4-((2*R*\*,6*R*\*)-4-oxo-6-(1,2,2-triphenylvinyl)tetrahydro-2*H*-pyran-2-yl)butanoate.

Since this compound is the major isomer, the stereochemistry was assigned by analogy to the crystal structure of (1*S*\*,2*R*\*,6*R*\*)-Methyl 4,8-dioxo-2-styryl-9-oxabicyclo[4.2.1]nonane-1-carboxylate (**189**-major isomer).  $^1\text{H}$  NMR (400 MHz,  $\text{CDCl}_3$ )  $\delta$  7.48-7.35 (comp, 5H), 7.20-7.16 (comp, 5H), 7.01-6.96 (comp, 3H), 6.88-6.86 (comp, 2H), 5.00-4.96 (m, 1H), 4.10 (dd,  $J = 9.6, 7.0$  Hz, 1H),

3.70 (s, 3H), 3.15 (t,  $J = 11.0$  Hz, 1H), 3.04 (dd,  $J = 13.0, 6.2$  Hz, 1H), 2.78 (dd,  $J = 17.6, 8.8$  Hz, 1H), 2.50 (dd,  $J = 11.0, 7.0$  Hz, 1H), 2.29 (dd,  $J = 17.6, 13.0$  Hz, 2H).  $^{13}\text{C}$  NMR (101 MHz,  $\text{CDCl}_3$ )  $\delta$  207.1, 206.9, 166.5, 145.4, 142.7, 141.8, 138.5, 137.3, 131.9, 130.3, 129.1, 128.6, 127.4, 127.4, 127.4, 127.0, 126.1, 88.8, 69.9, 53.1, 52.3, 46.2, 43.2, 39.9. IR ( $\text{cm}^{-1}$ ): 1706, 1732, 1771, 2850. HRMS (ESI<sup>+</sup>): expected mass 467.1853, found 467.1865. M.p. 218-219 °C.

**(1*S*\*,2*S*\*,6*R*\*)-Methyl-4,8-dioxo-2-(1,2,2-triphenylvinyl)-9-oxabicyclo[4.2.1]nonane-1-carboxylate- minor isomer**

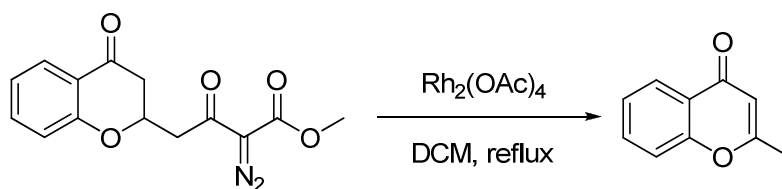


Purified by chromatography on silica gel (gradient elution: hexane/ethyl acetate: 90% to 70% hexane; white solid (17% yield), isolated from 0.43 mmol scale of Methyl-2-diazo-3-oxo-4-((2*R*\*,6*R*\*)-4-oxo-6-(1,2,2-triphenylvinyl)tetrahydro-2*H*-pyran-2-yl)butanoate.

$^1\text{H}$  NMR (400 MHz,  $\text{CDCl}_3$ )  $\delta$  7.42-7.39 (comp, 2H), 7.32-7.26 (comp, 5H), 7.20-7.14 (comp, 3H), 7.02-6.94 (comp, 5H), 4.80-4.76 (m, 1H), 4.10 (dd,  $J = 13.2, 2.8$  Hz, 1H), 3.85 (s, 3H), 3.11 (dd,  $J = 17.2, 5.2$  Hz, 1H), 2.93 (dd,  $J = 19.2, 9.6$  Hz, 1H), 2.85 (dd,  $J = 16.0, 2.8$  Hz, 1H), 2.69 (dd,  $J = 16.0, 13.2$  Hz, 1H), 2.59 (dd,  $J = 17.2, 2.0$  Hz, 1H), 2.39 (dd,  $J = 19.2, 2.0$  Hz, 1H).  $^{13}\text{C}$  NMR (101 MHz,  $\text{CDCl}_3$ )  $\delta$  206.8, 204.6, 165.8, 145.3,

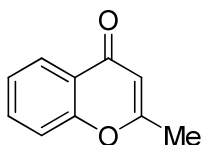
142.1, 141.7, 137.6, 137.3, 131.7, 129.7, 128.7, 128.7, 127.4, 127.3, 127.2, 126.9, 126.1, 86.6, 69.1, 52.9, 51.0, 47.5 (2C), 42.71. IR (cm<sup>-1</sup>): 1700, 1719, 1742, 1773, 2850. HRMS (ESI<sup>+</sup>): expected mass 467.1853, found 467.1863. M.p. 210-211 °C.

**Dinitrogen extrusion reaction of Methyl 2-diazo-3-oxo-4-(4-oxochroman-2-yl)butanoate**



The catalyst Rh<sub>2</sub>(OAc)<sub>4</sub> (5.6 mg, 0.013 mmoles) was transferred to a flame-dried two-neck flask and then dissolved in anhydrous CH<sub>2</sub>Cl<sub>2</sub> (7.0 mL). Methyl 2-diazo-3-oxo-4-(4-oxochroman-2-yl)butanoate (0.36g, 1.3 mmoles) was dissolved in anhydrous CH<sub>2</sub>Cl<sub>2</sub> (7.0 mL) and then was added dropwise to the reaction mixture via a syringe pump over two hrs. Once the addition was complete, the reaction mixture was left to stir in refluxing CH<sub>2</sub>Cl<sub>2</sub> for an additional two hrs. After the reaction reached completion, judging by TLC analysis, it was cooled to room temperature, and the solvent was evaporated under reduced pressure.

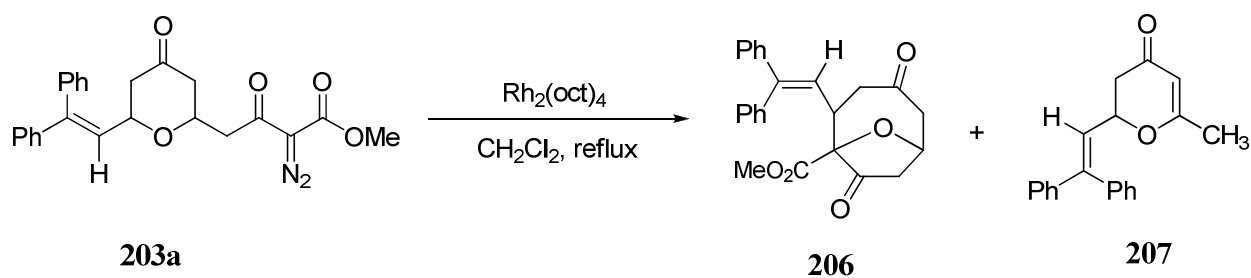
**2-Methyl-4H-chromen-4-one**



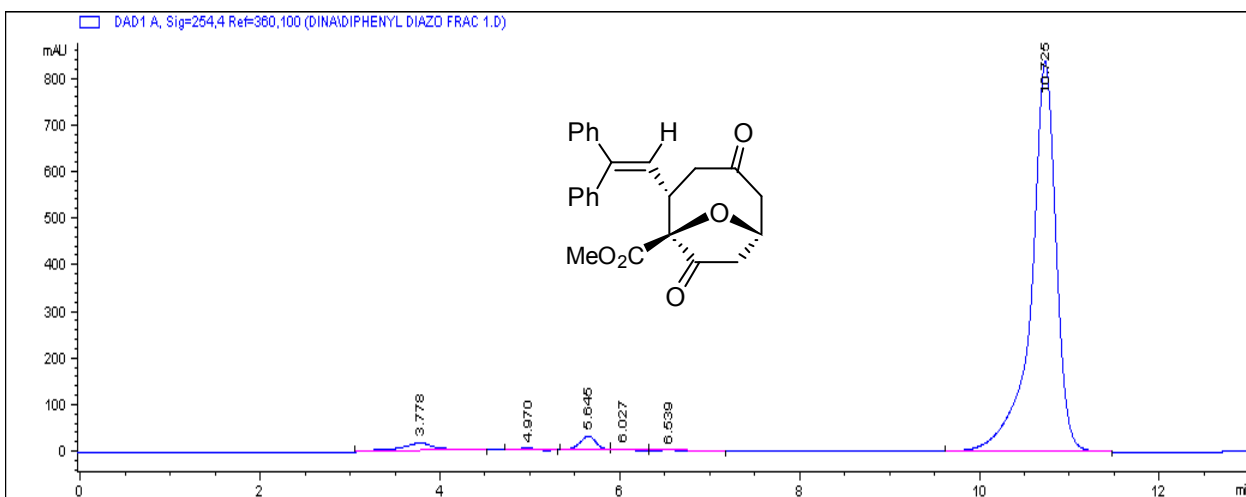
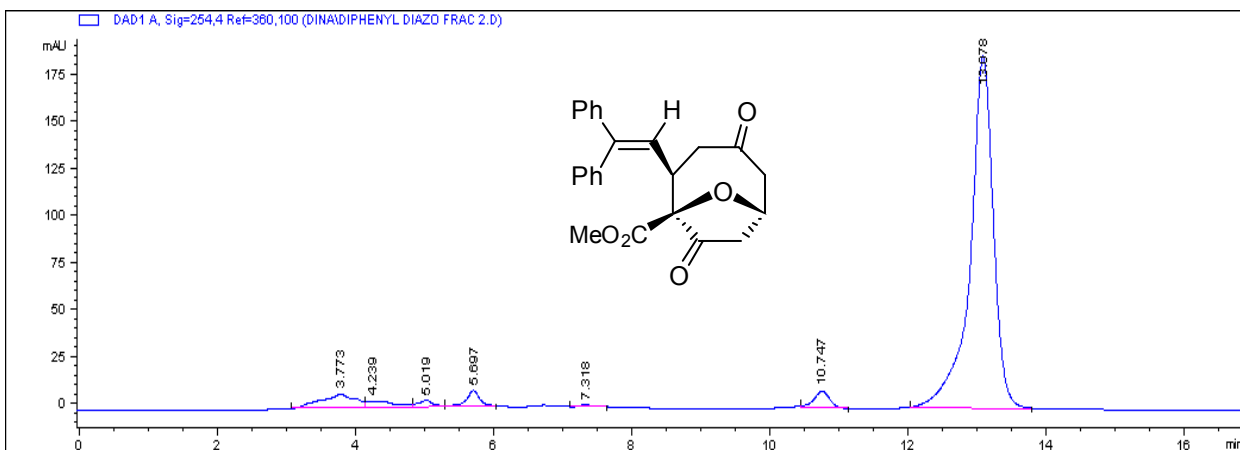
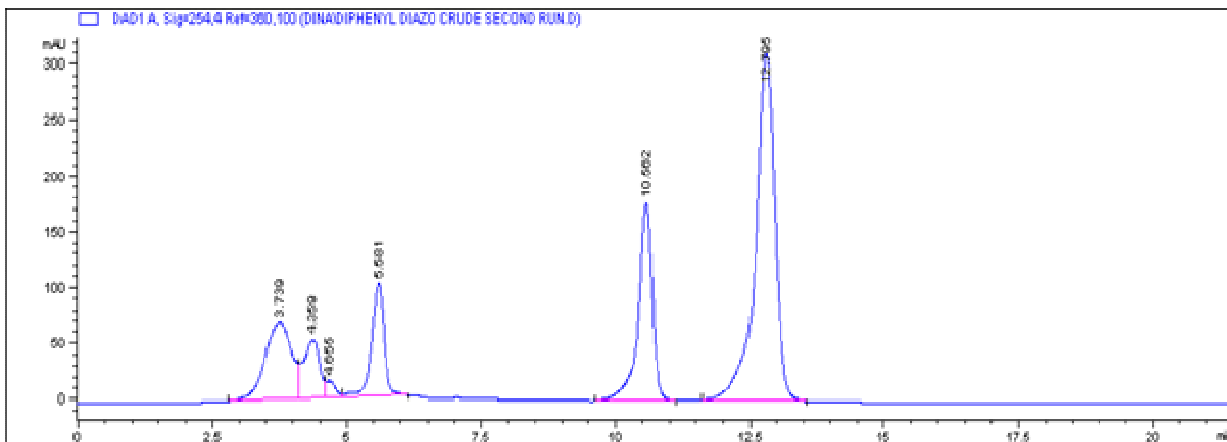
Purified by chromatography on silica gel (gradient elution: hexane/ethyl acetate: 100% to 60% hexane; white solid (71% yield), isolated from a 1.3 mmol scale of Methyl 2-diazo-3-oxo-4-(4-oxochroman-2-yl)butanoate. <sup>1</sup>H NMR (400 MHz, CDCl<sub>3</sub>) δ 8.16 (dd, *J* = 8.0,

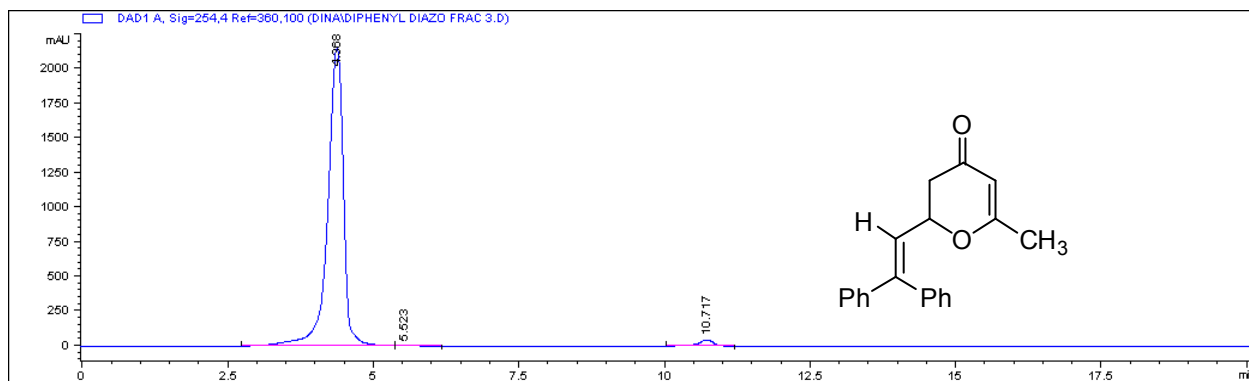
1.6 Hz, 1H), 7.62 (dtd,  $J = 8.4, 1.6, 1.2$  Hz, 1H), 7.40 – 7.33 (comp, 2H), 6.15 (s, 1H), 2.37 (s, 3H).  $^{13}\text{C}$  NMR (101 MHz,  $\text{CDCl}_3$ )  $\delta$  178.2, 166.1, 156.4, 133.4, 125.6, 124.9, 123.5, 117.7, 110.5, 20.6. IR ( $\text{cm}^{-1}$ ): 1572, 1627, 2919, 3057. HRMS (ESI+): expected mass 161.0597, found 161.0606. M.p. 67-68 °C.

**HPLC Analysis:** Rh(II) decomposition reaction of diazoacetoacetate 203a.

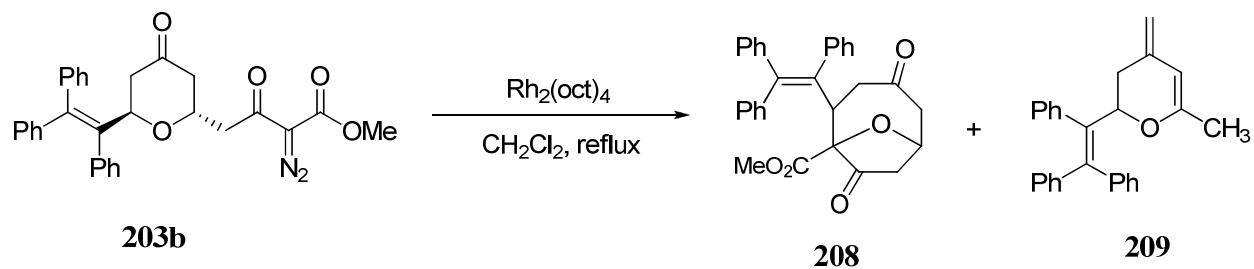


**HPLC of reaction mixture:** conditions: Silica column, 1ml/min, Hexane:iPrOH 70:30

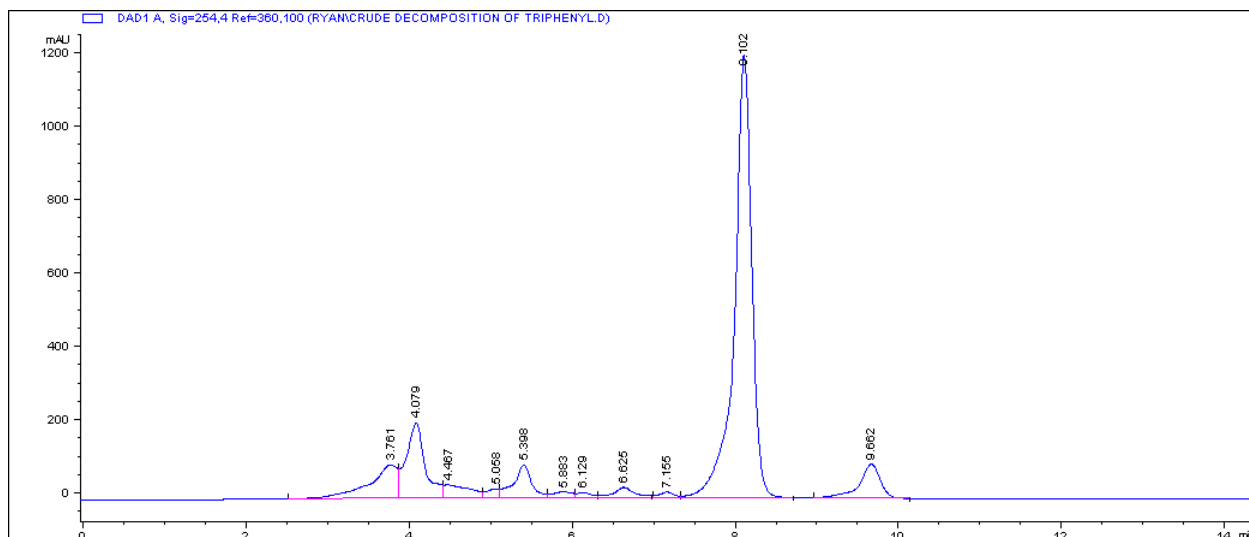




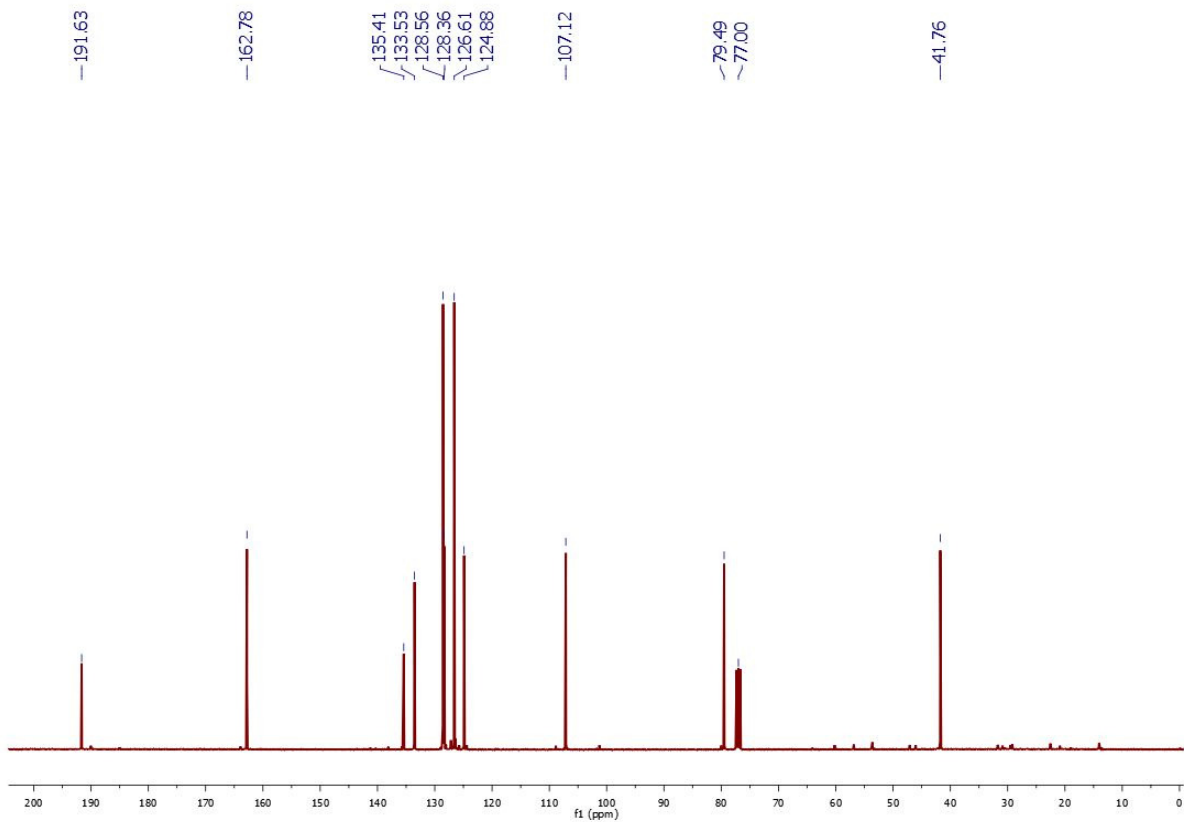
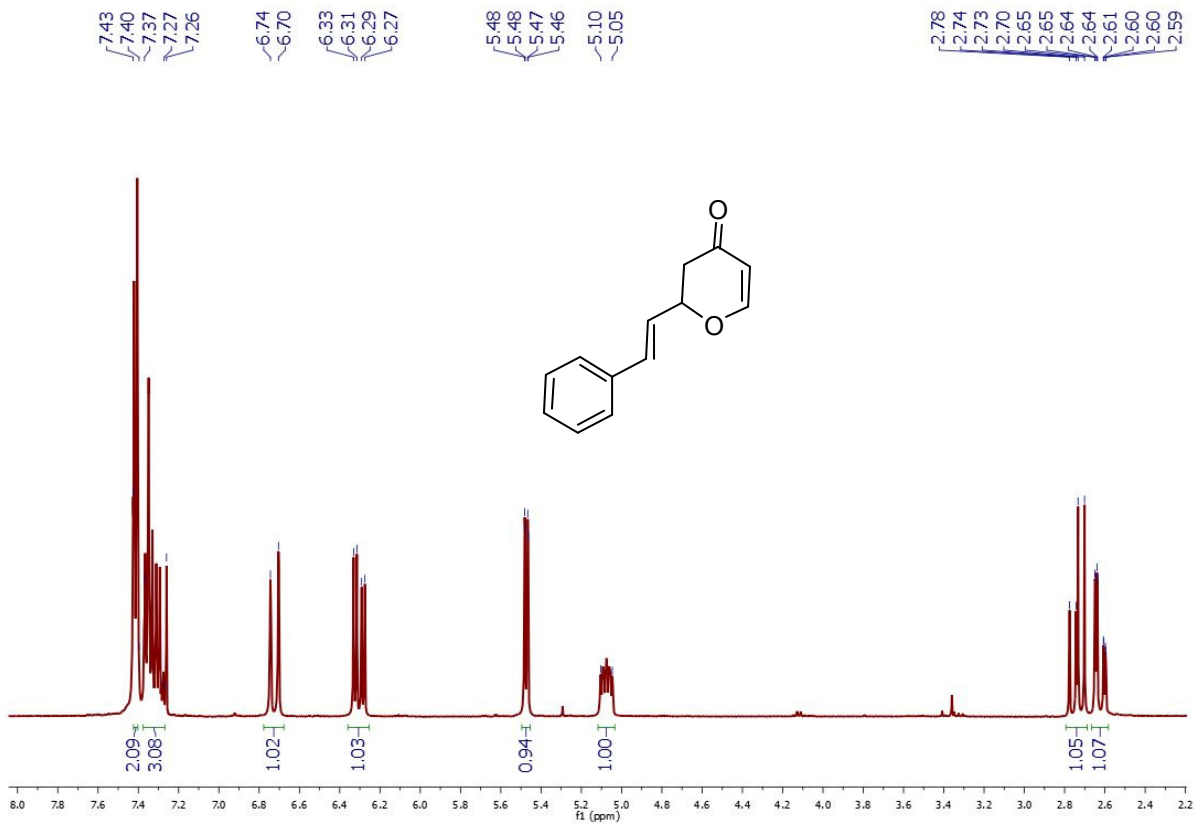
**HPLC Analysis:** Rh(II) decomposition reaction of diazoacetate 203b.

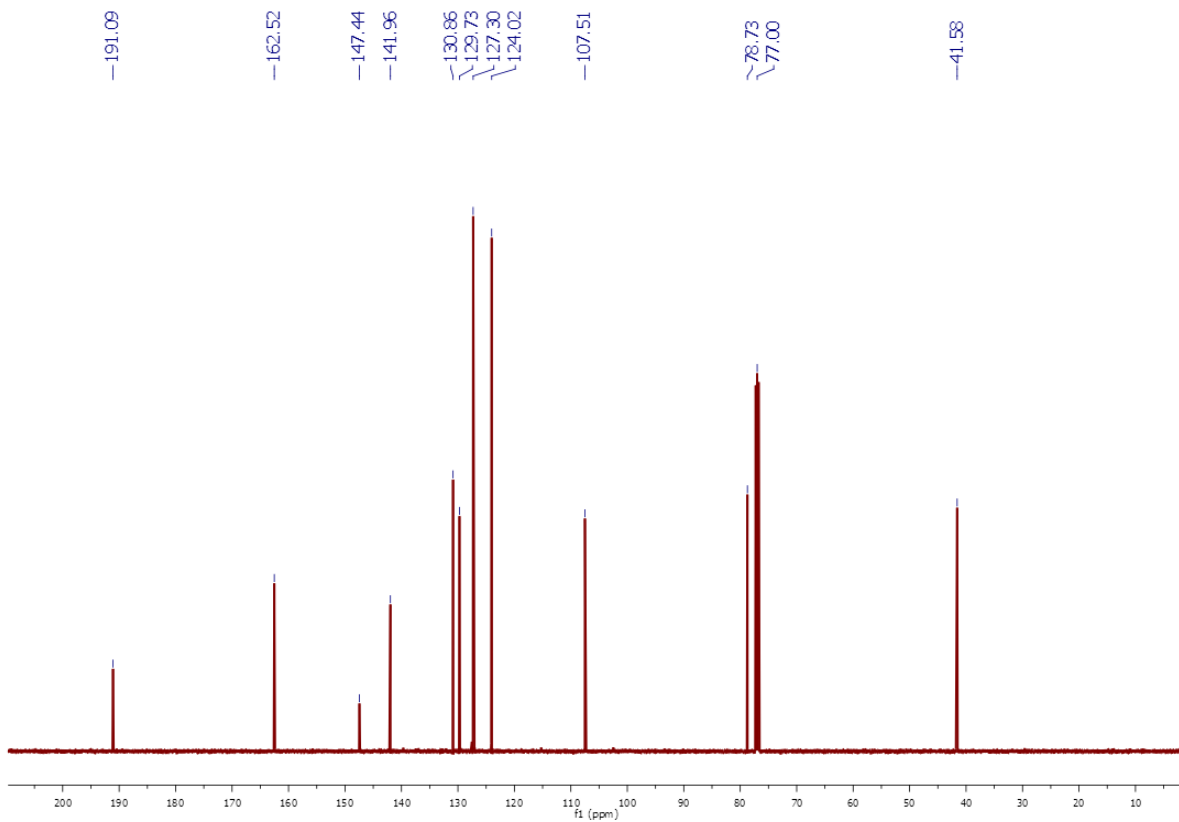
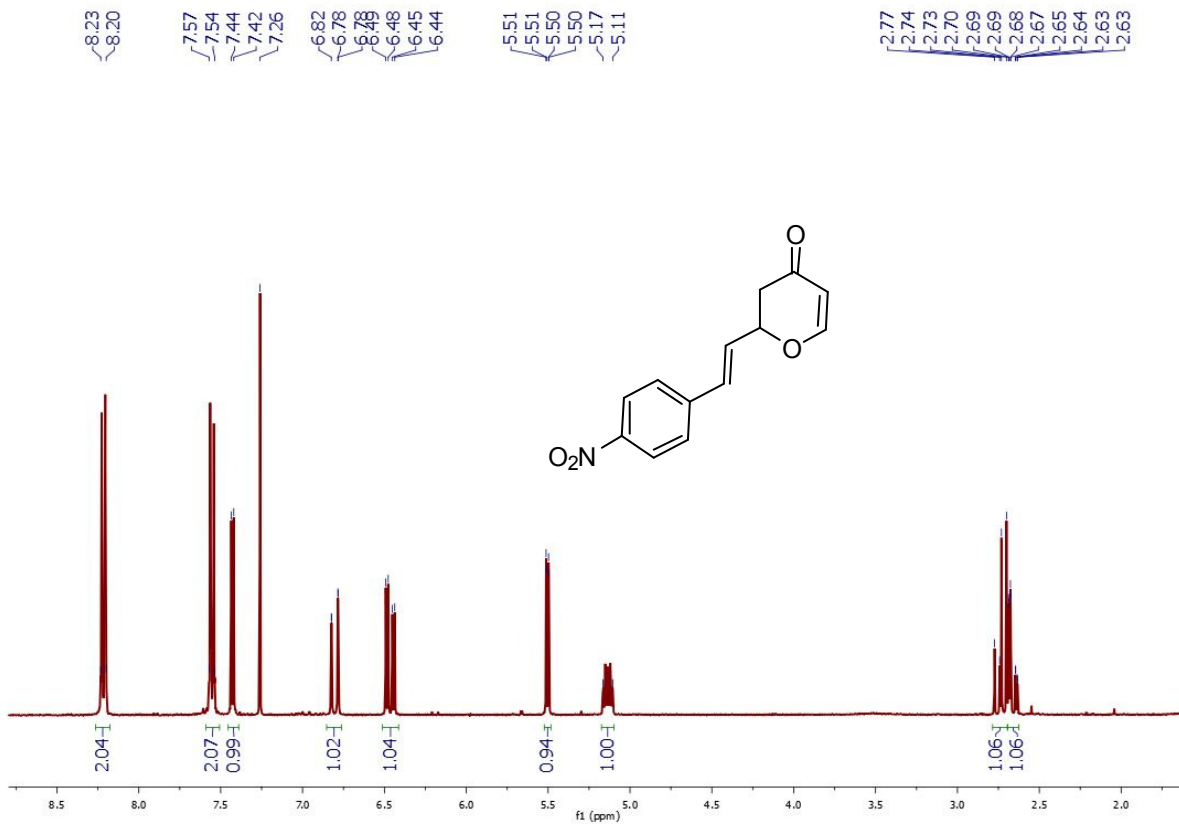


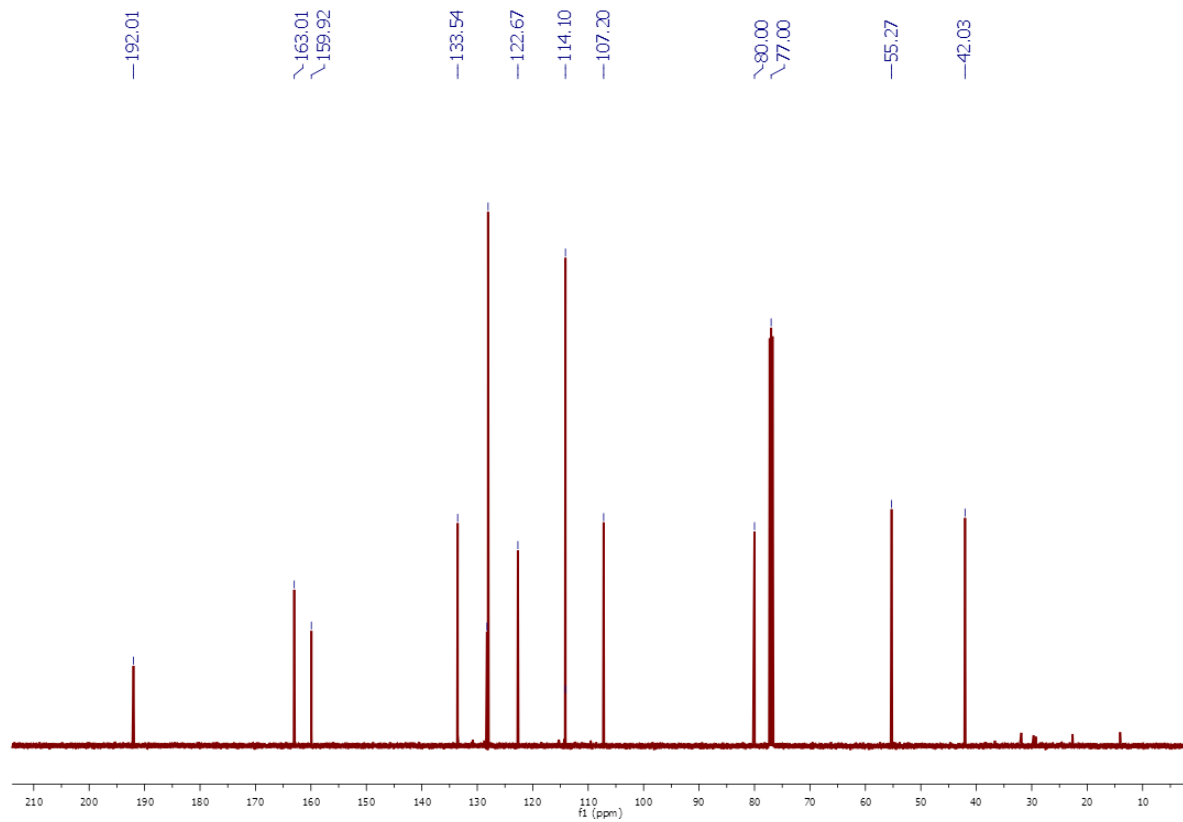
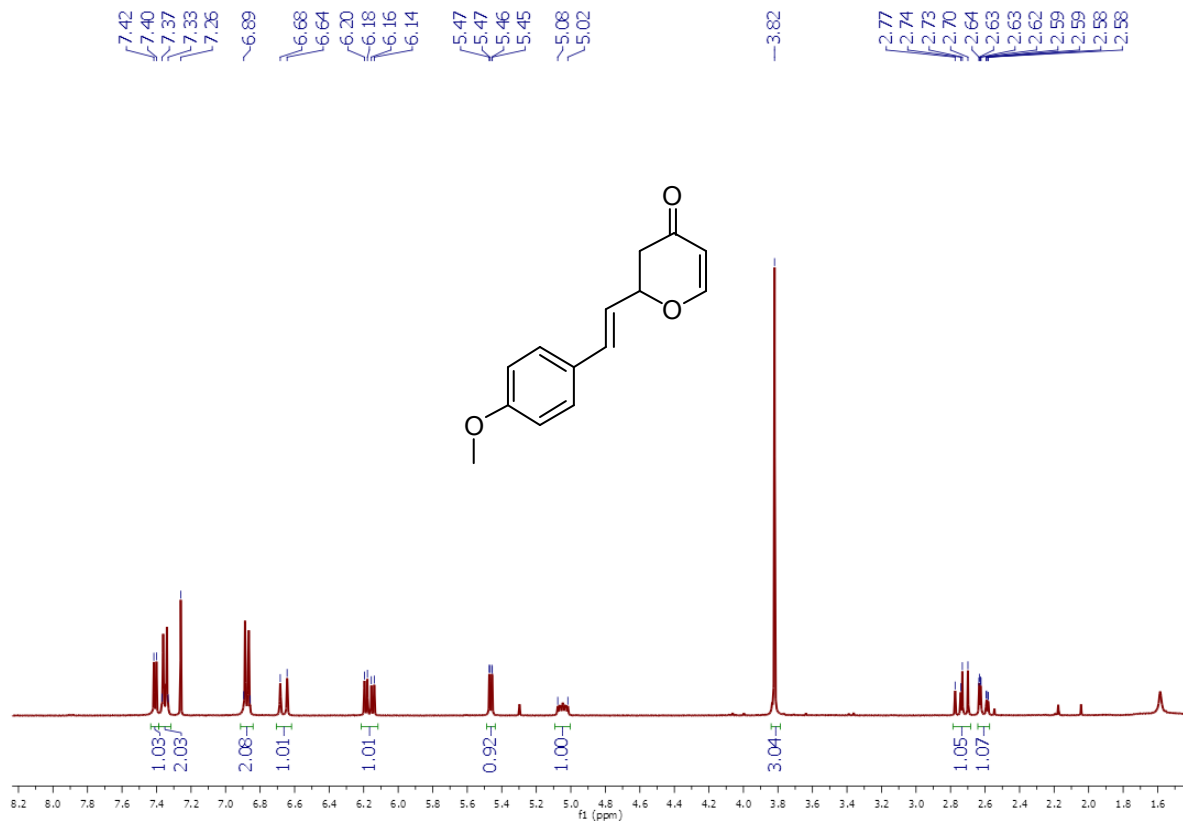
**HPLC of reaction mixture:** conditions: Silica column, 1ml/min, Hexane:iPrOH 70:30

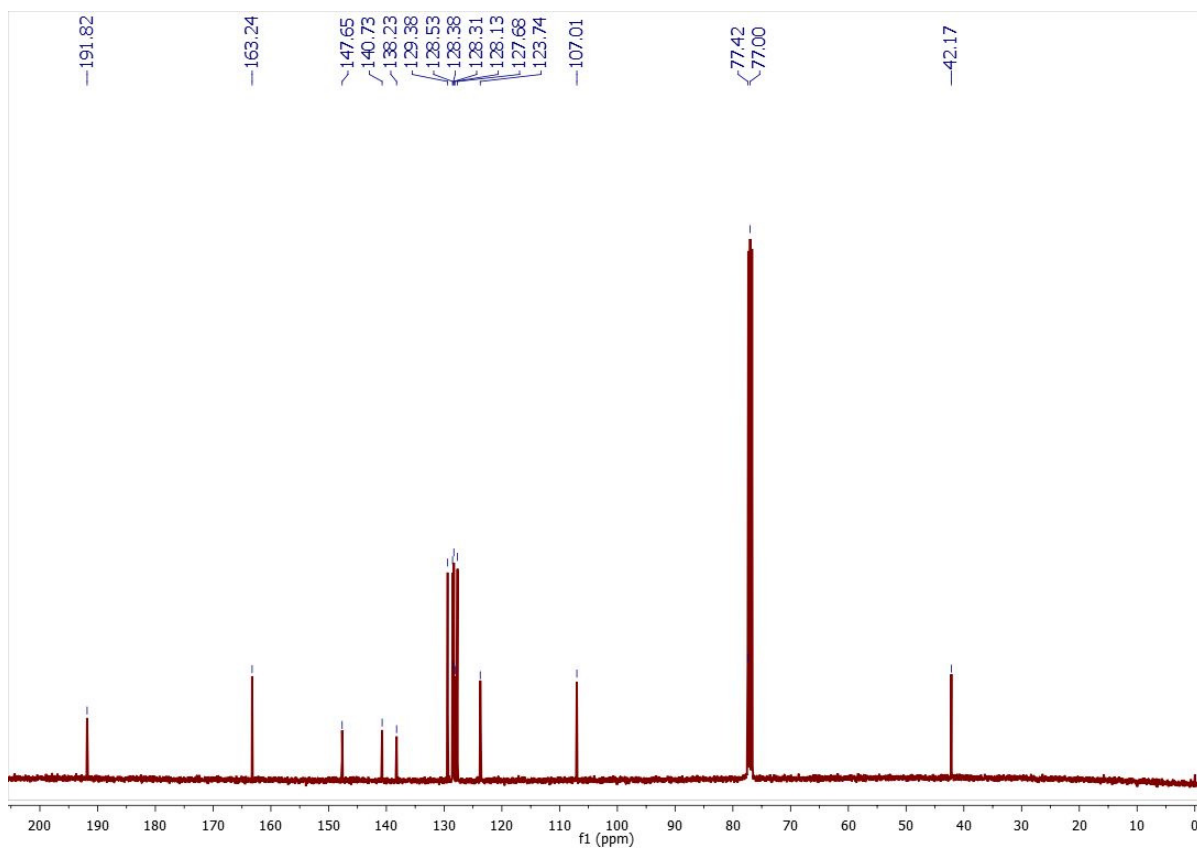
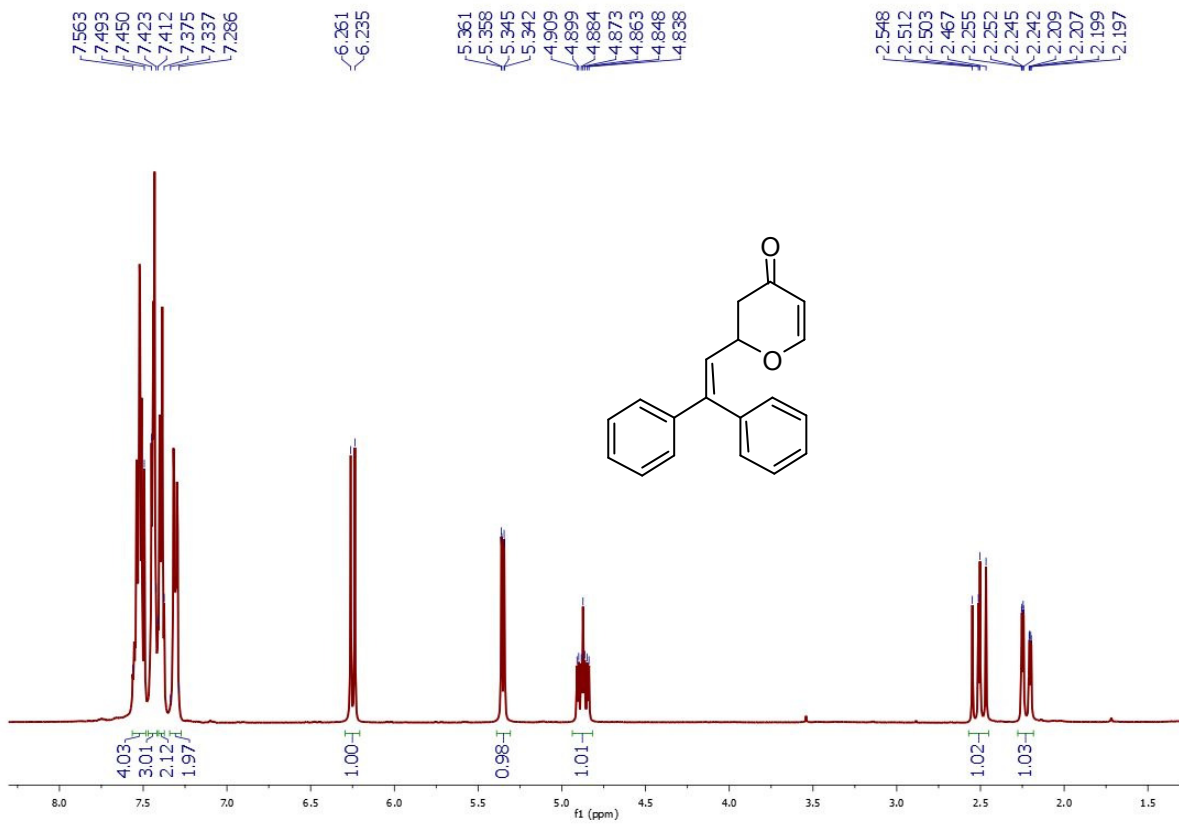


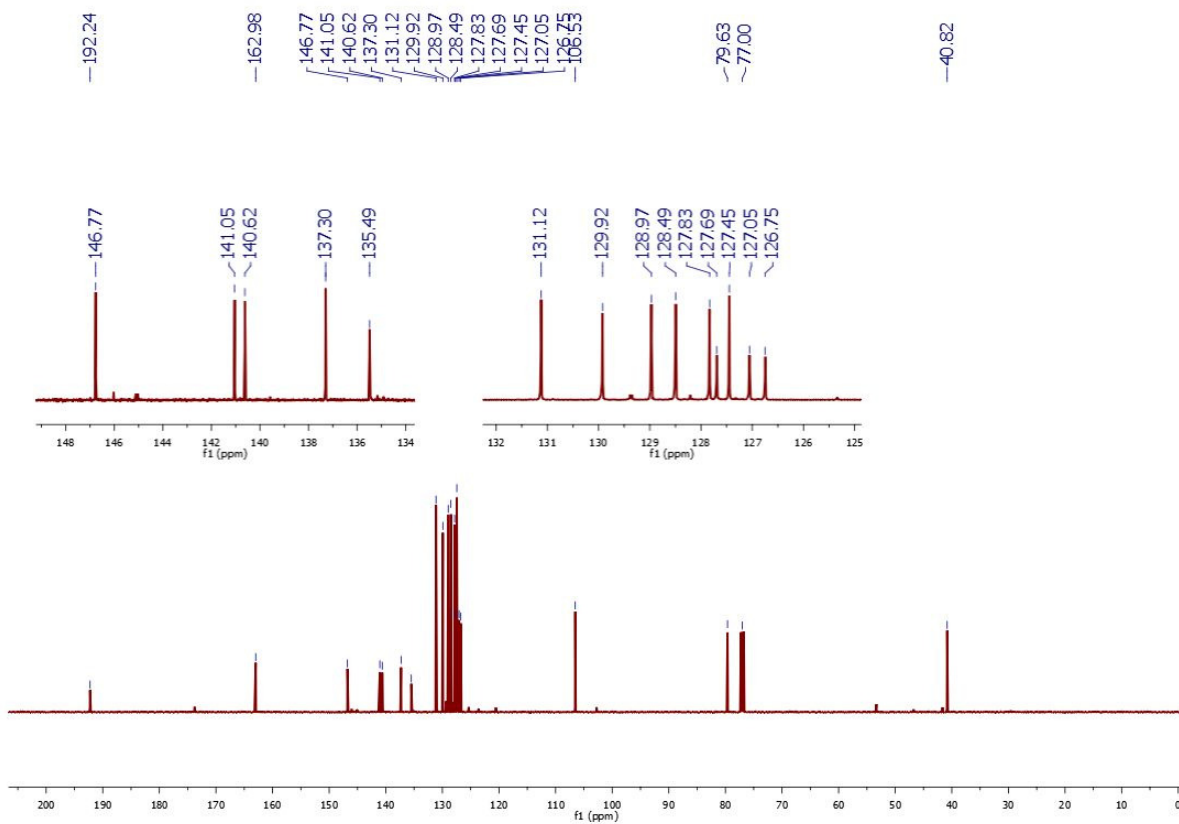
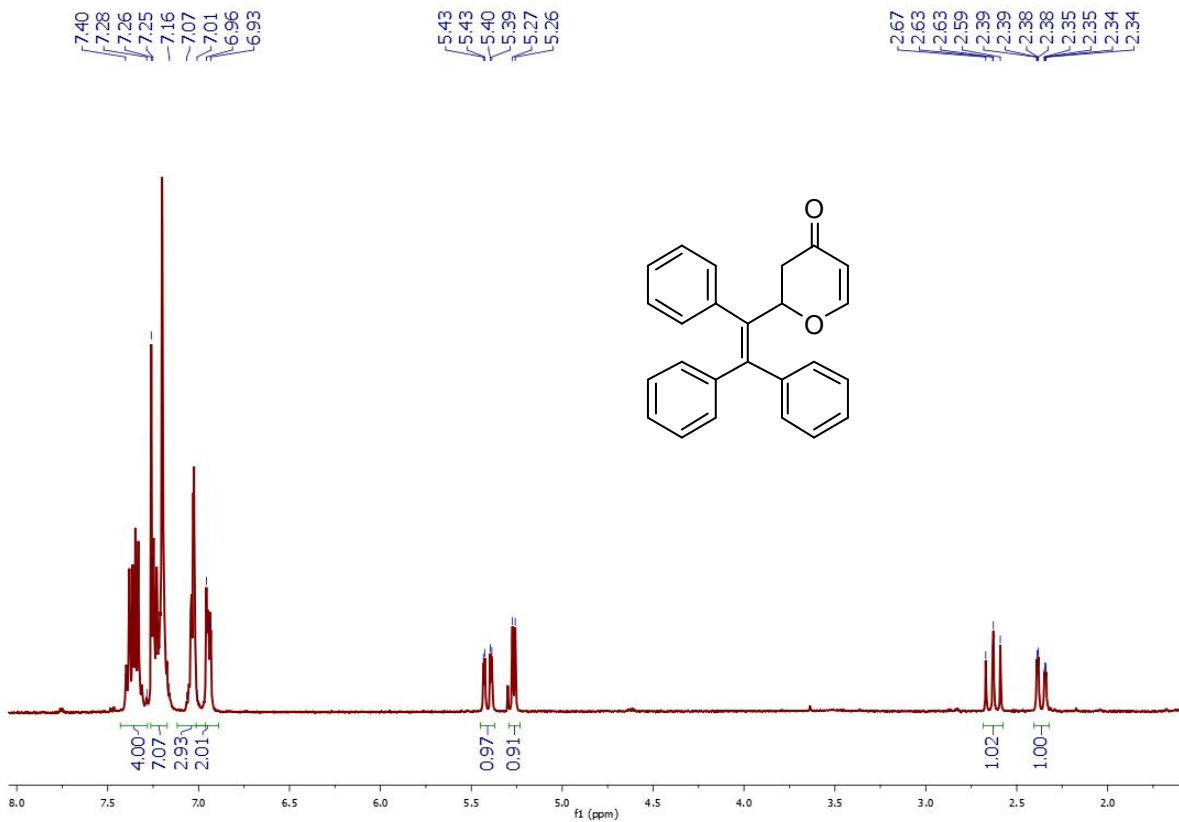


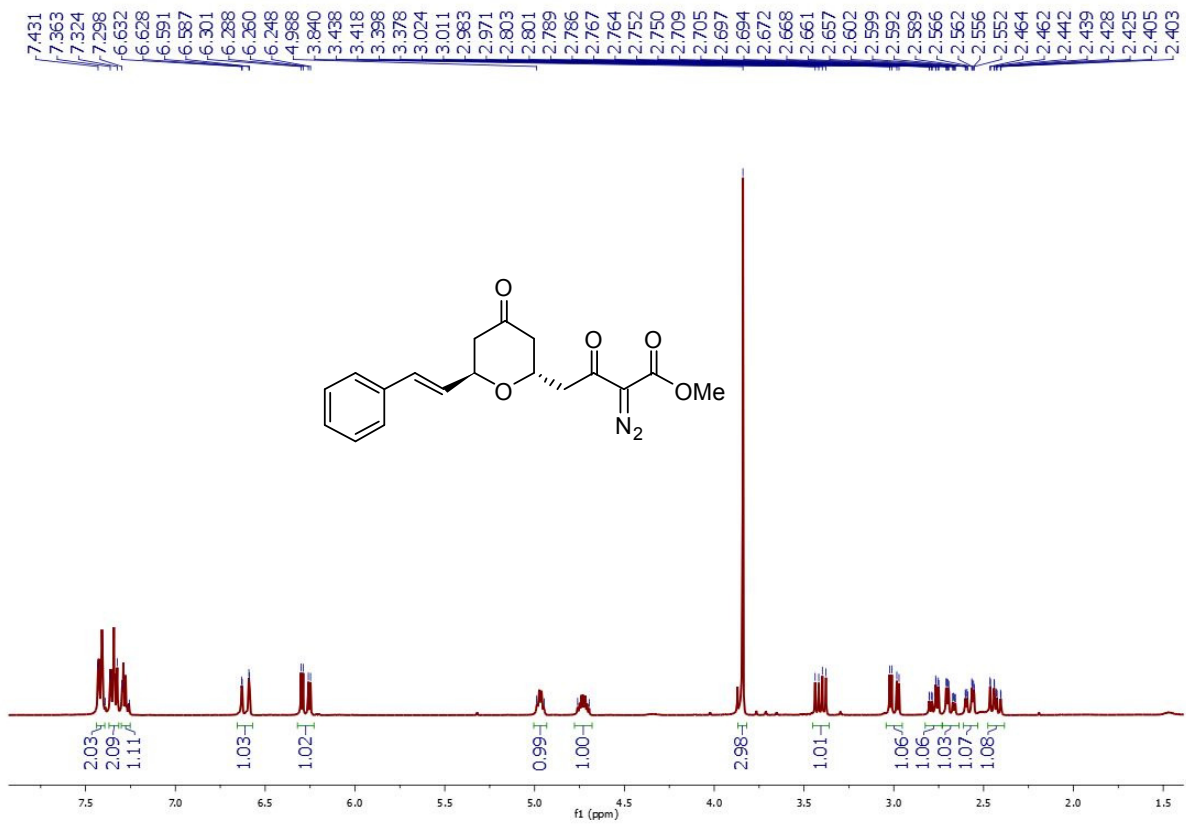




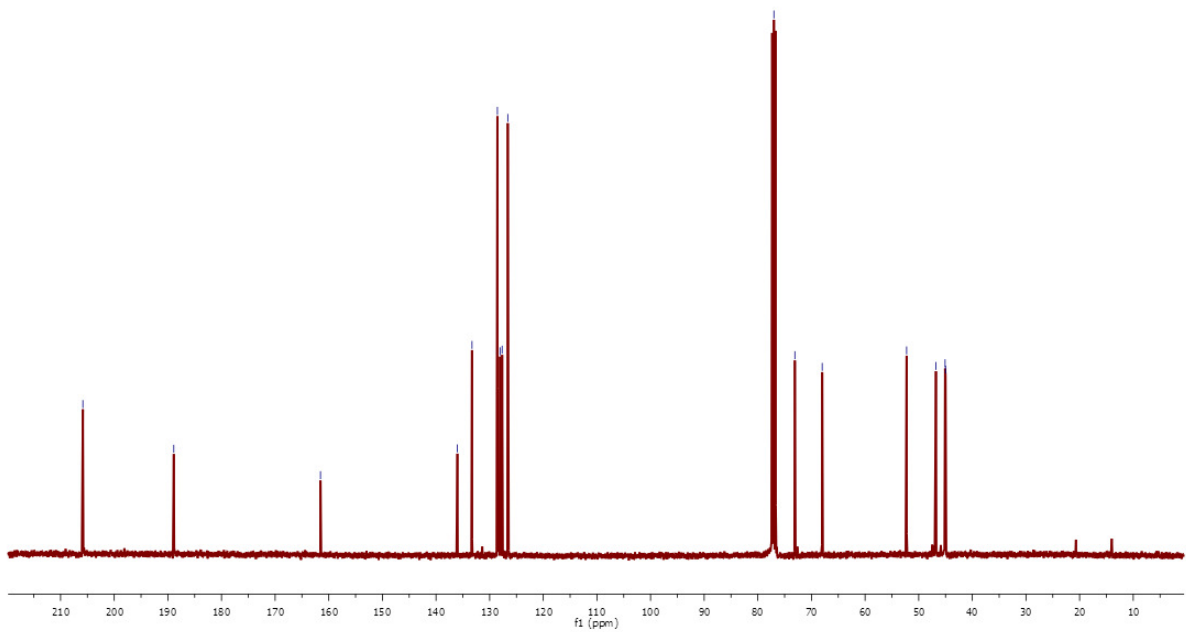


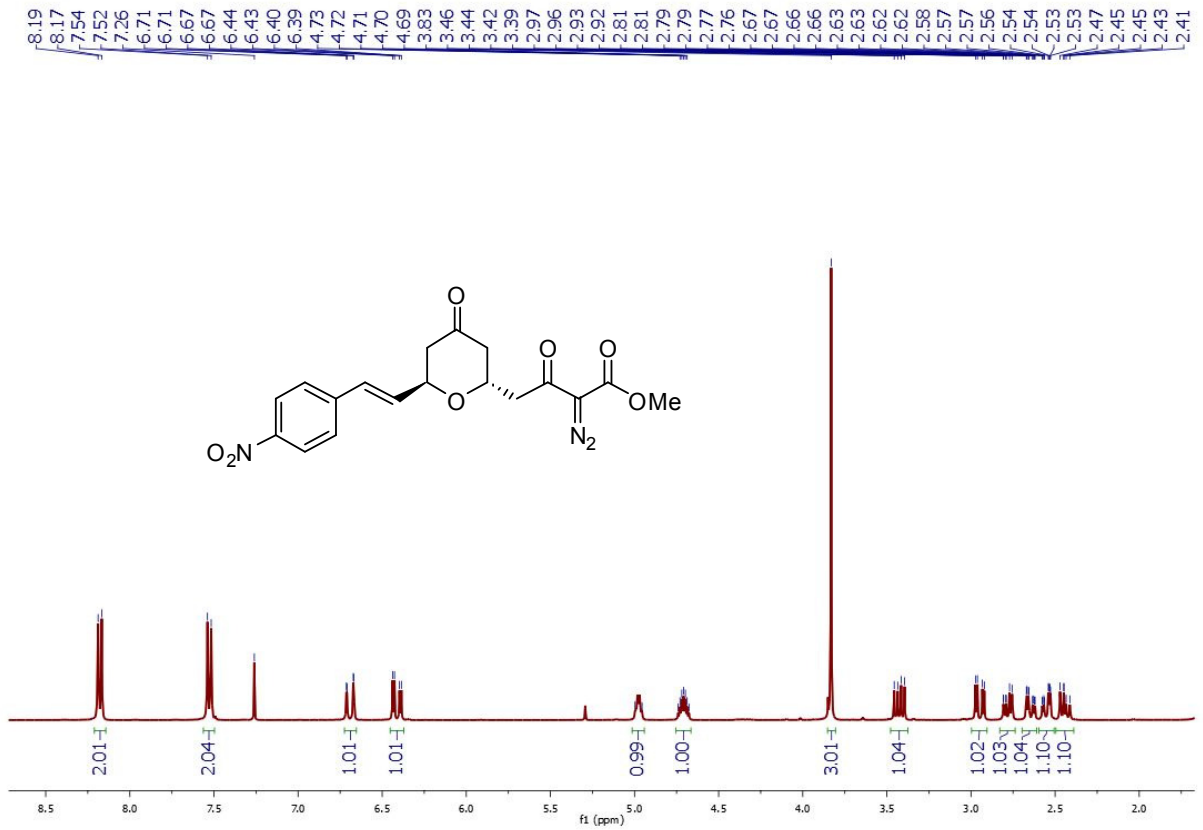




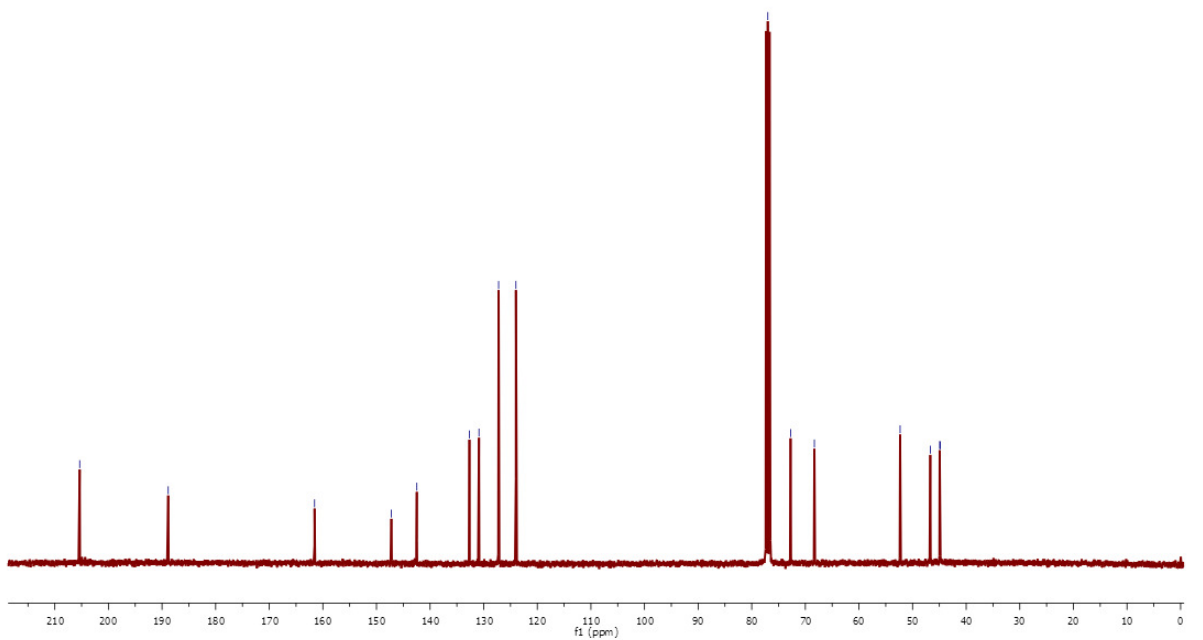


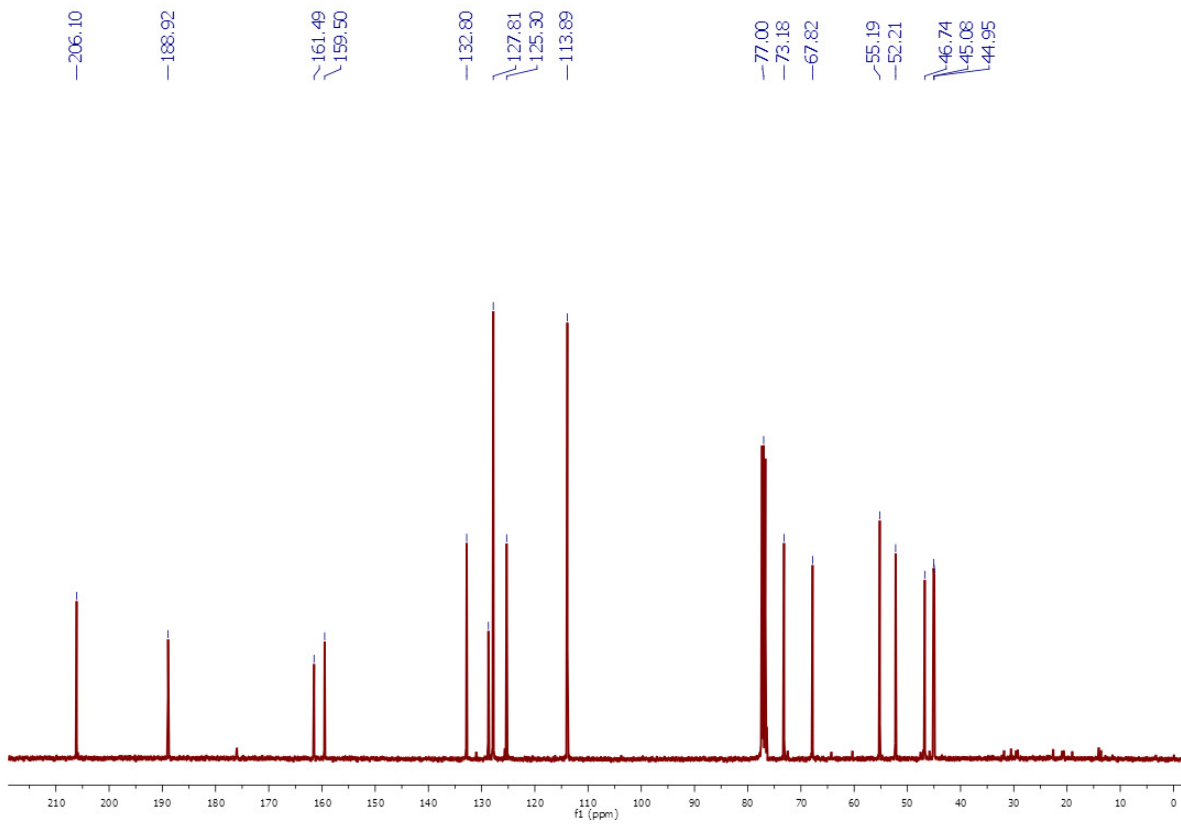
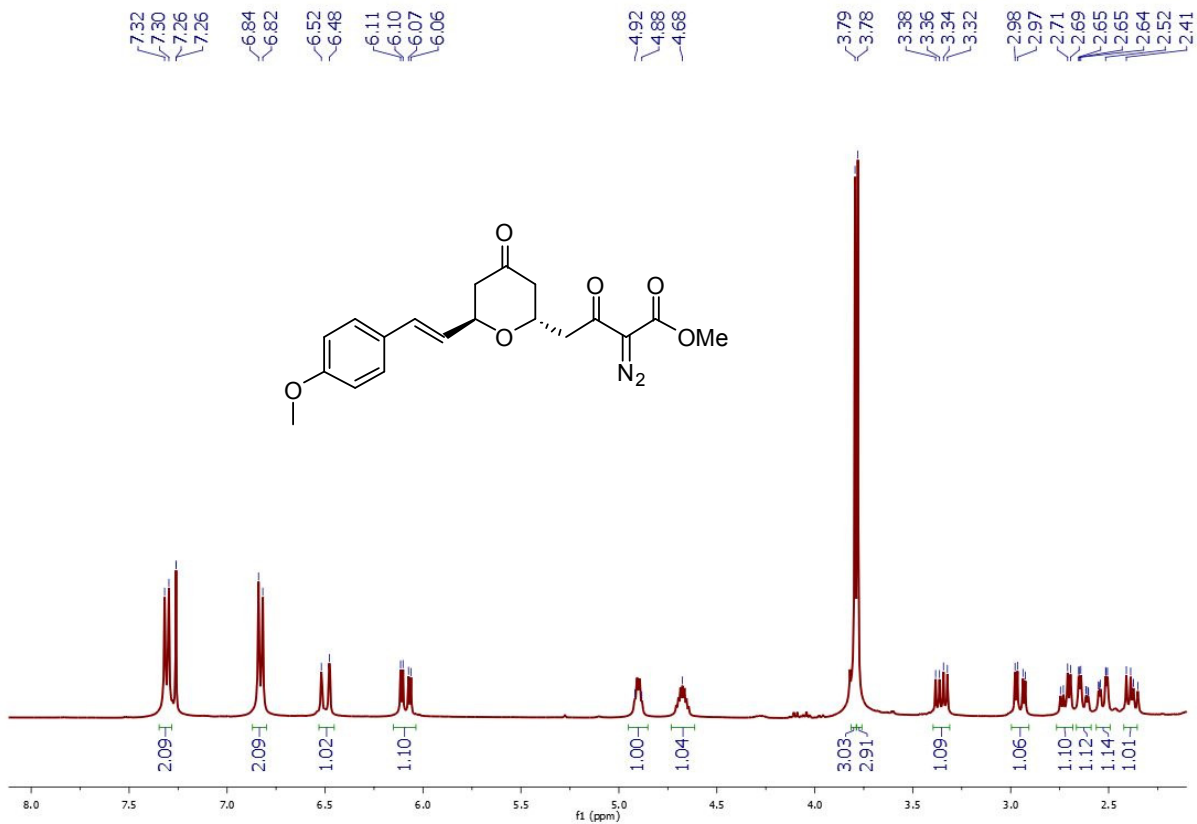
Chemical shifts (ppm): -205.85, -188.89, -161.54, 136.01, 133.29, 128.55, 128.06, 127.67, 126.62, 77.00, 73.09, 67.99, 52.25, 46.79, 45.08, 45.00.

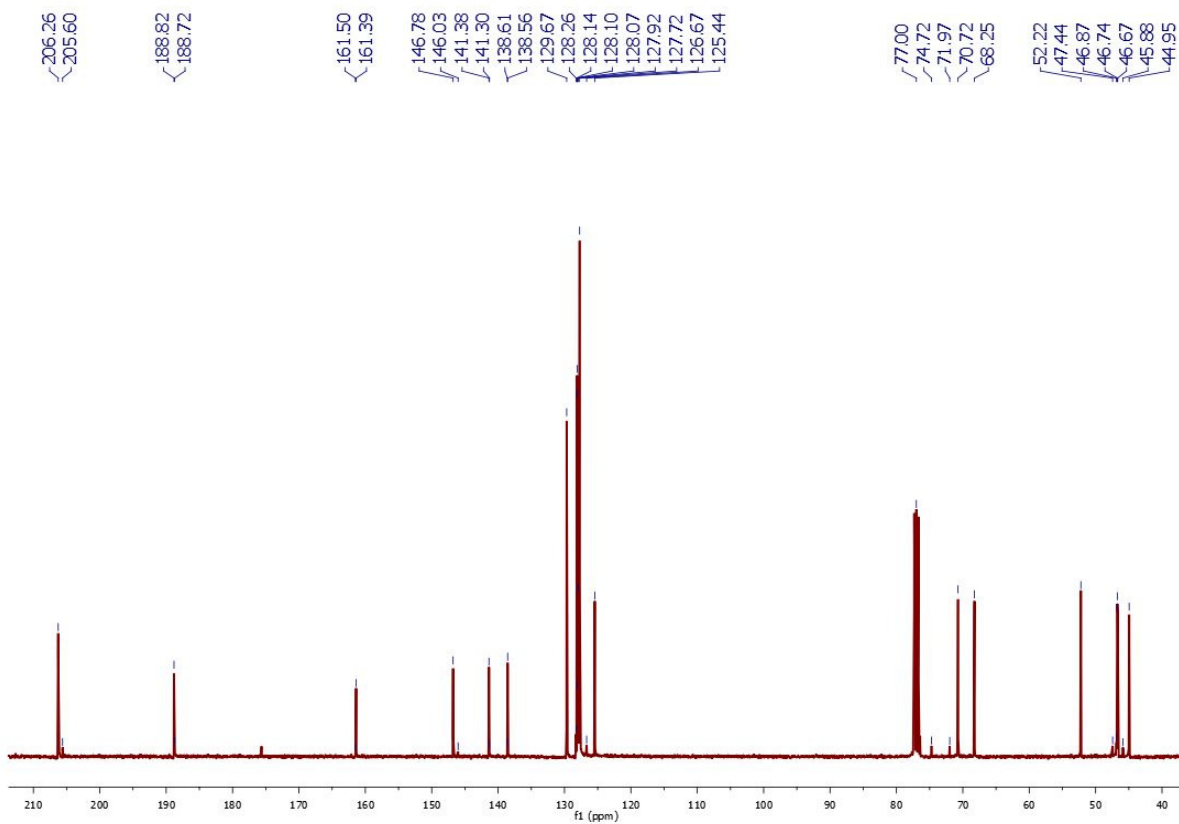
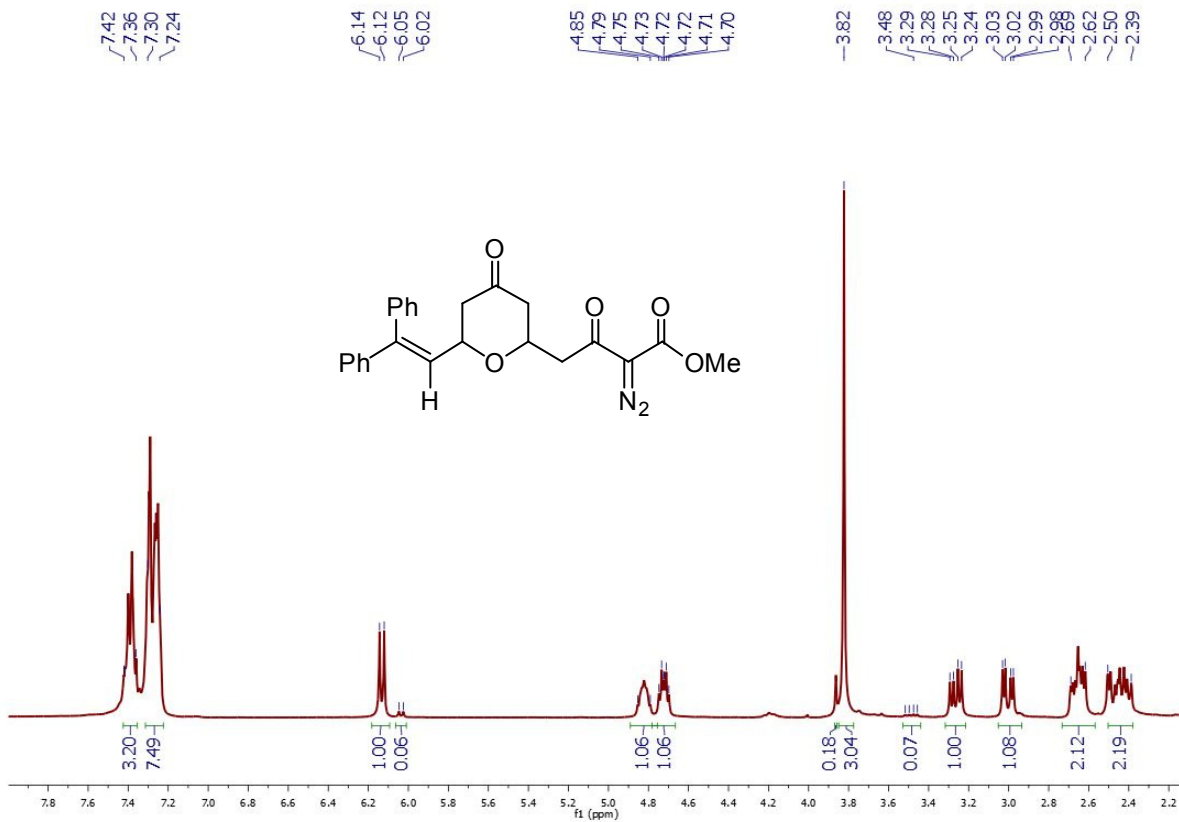


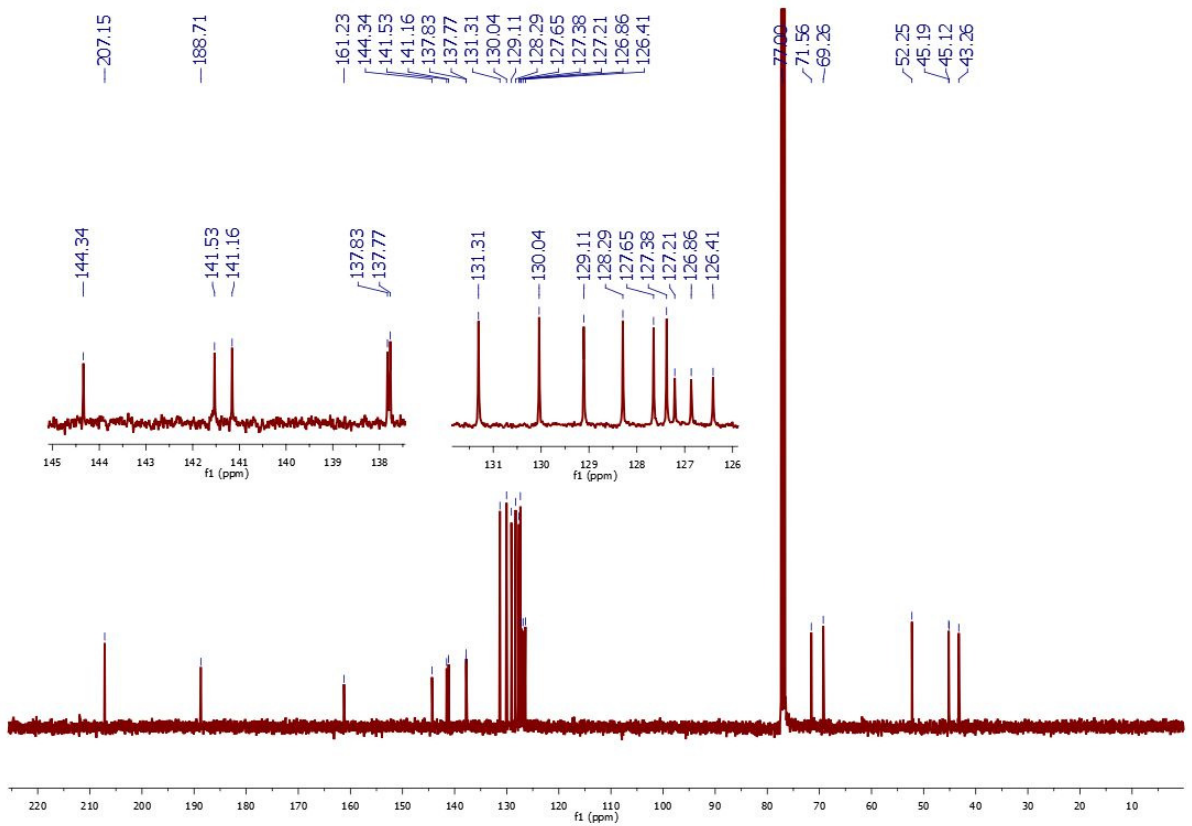
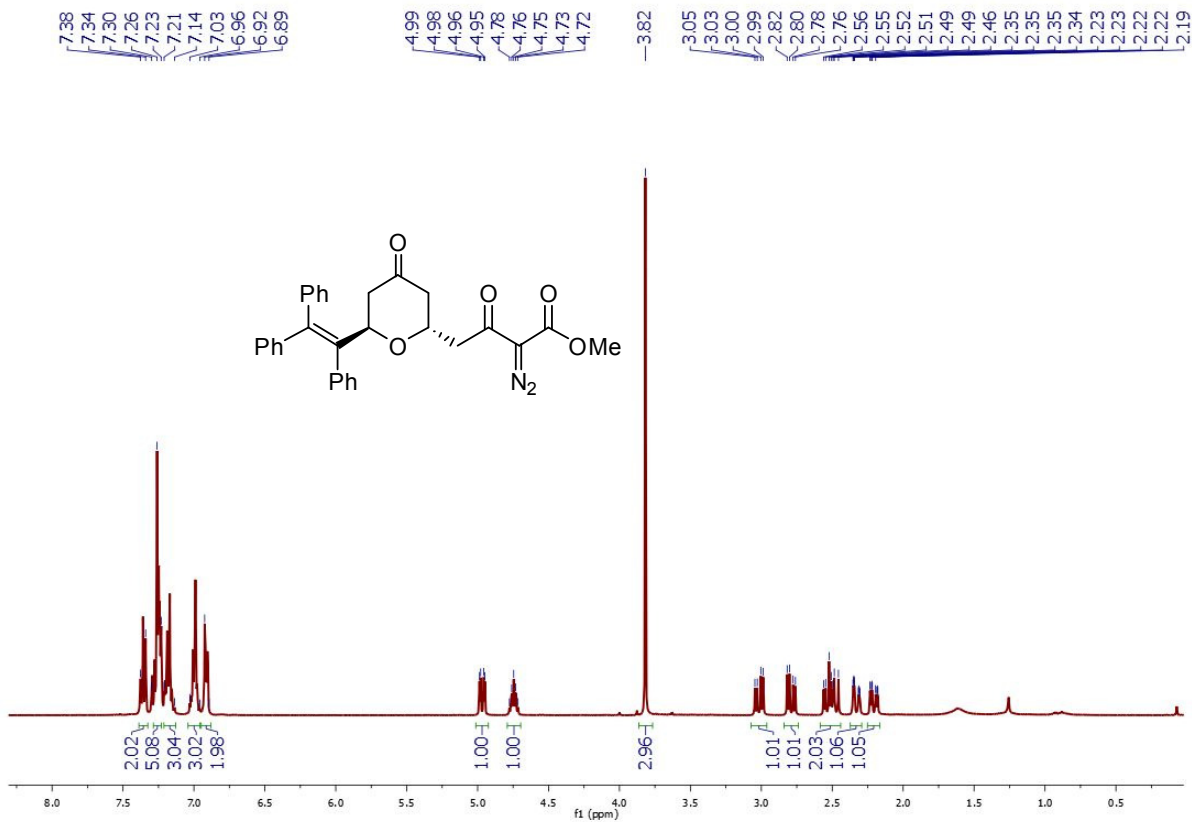


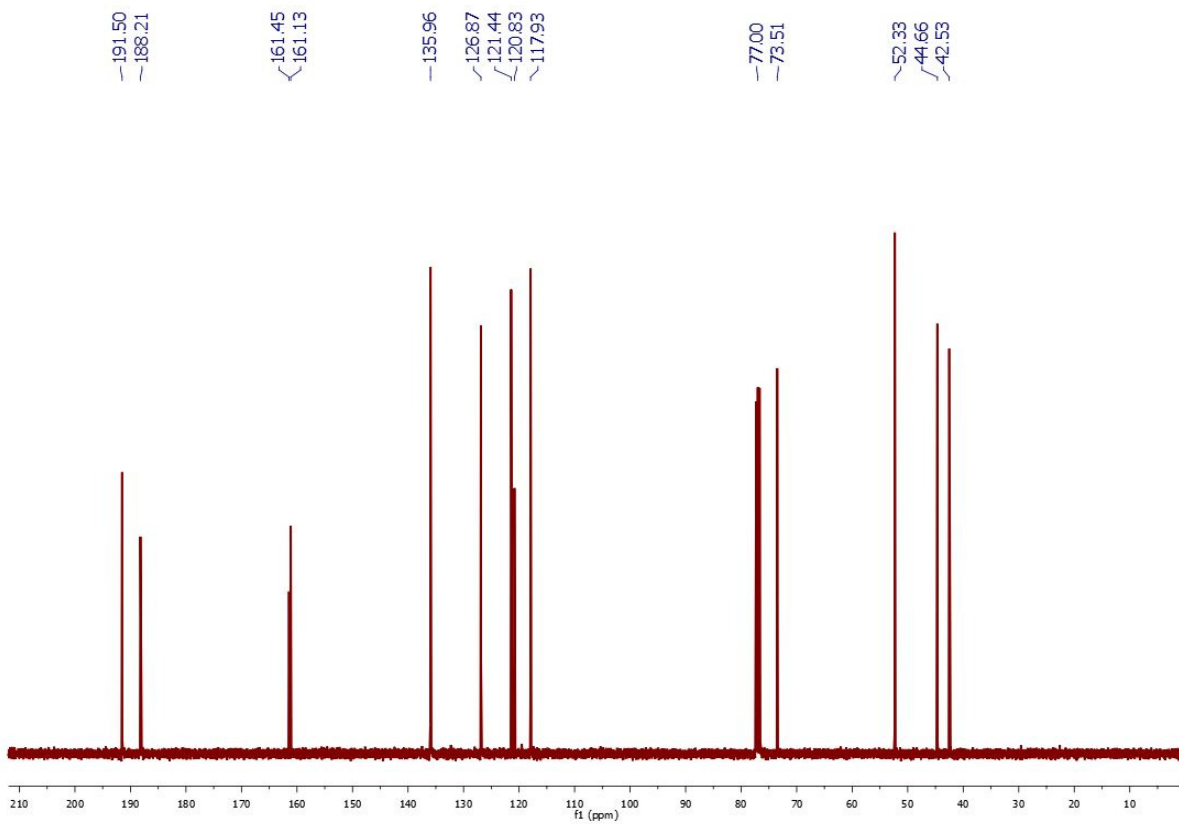
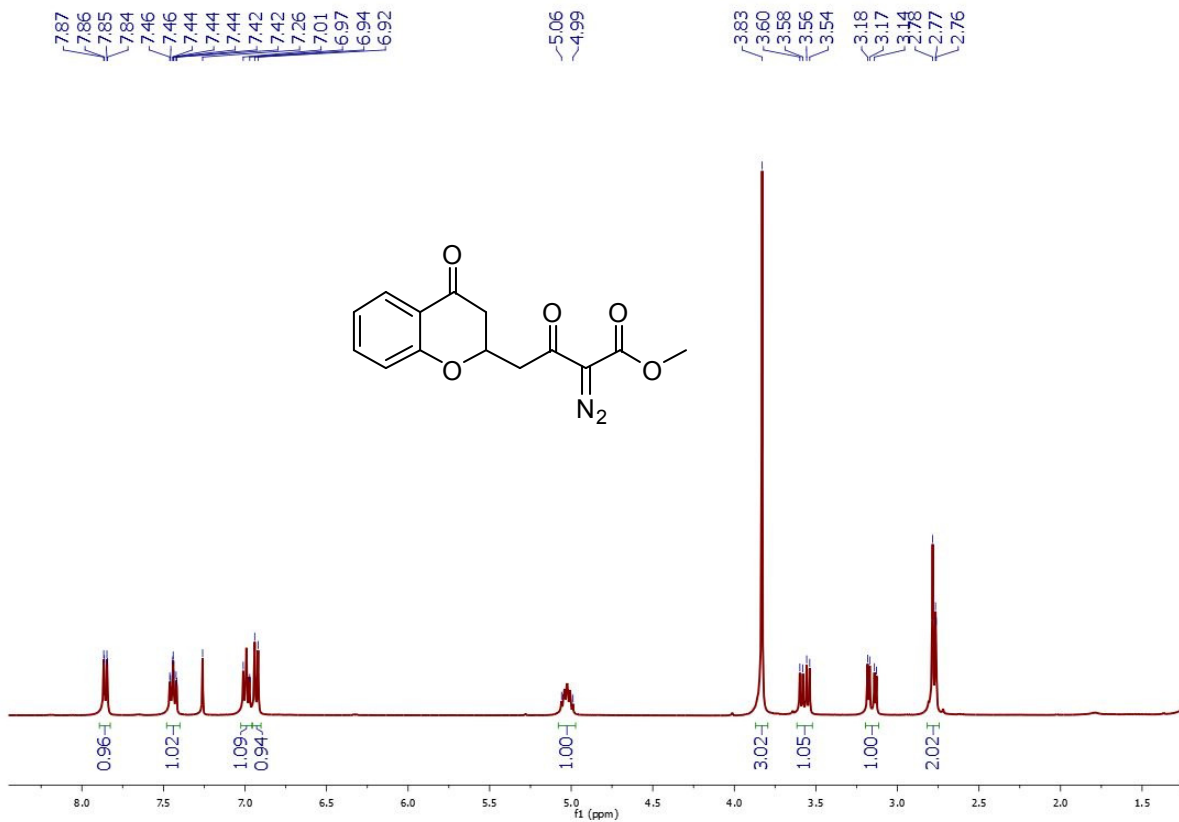
-205.36  
 -188.85  
 -161.54  
 -147.22  
 -142.47  
 -132.66  
 -130.88  
 -127.22  
 -123.99  
 -77.00  
 -72.76  
 -68.32  
 -52.32  
 -46.69  
 -44.94  
 -44.83



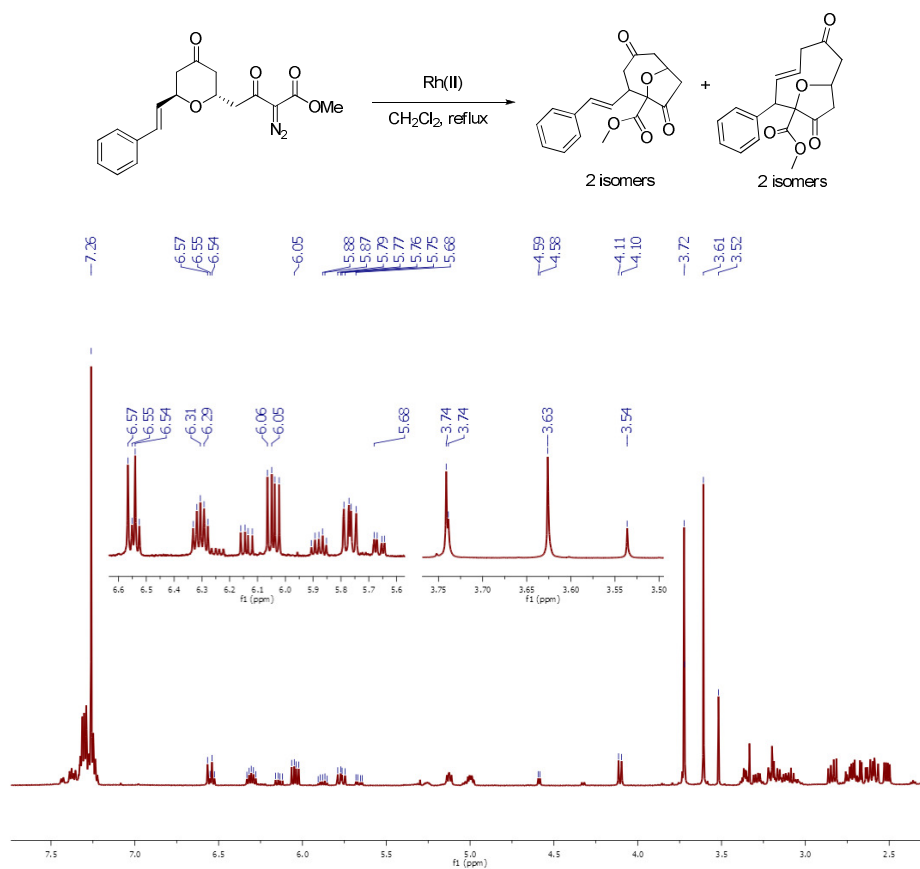


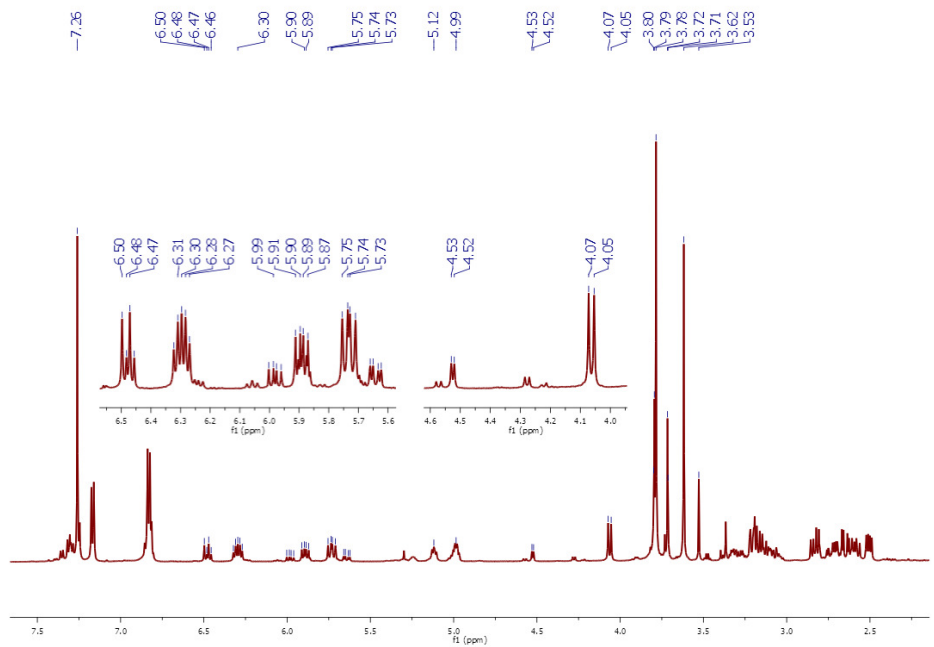
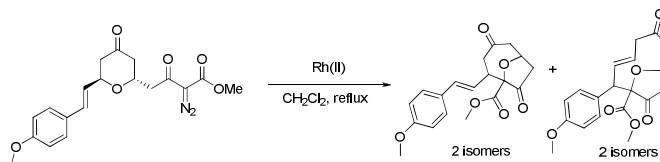
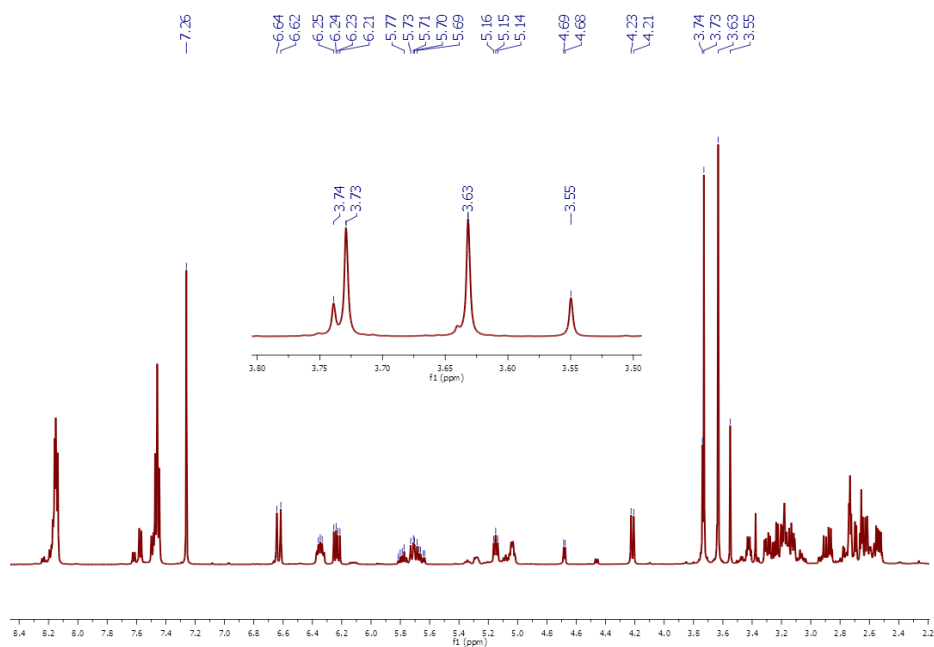
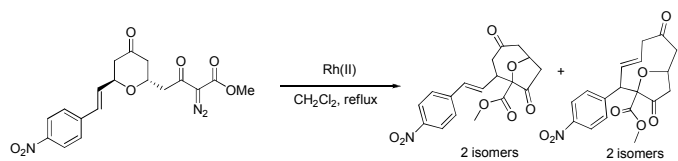


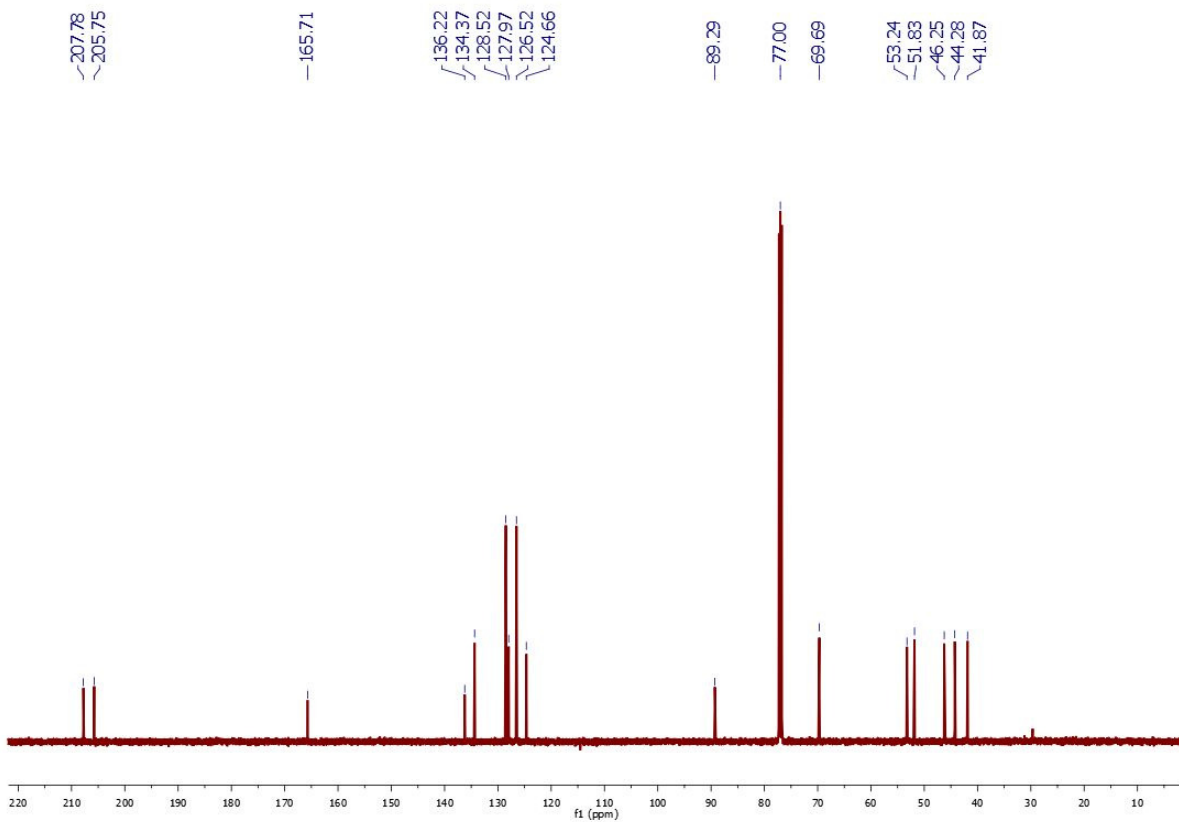
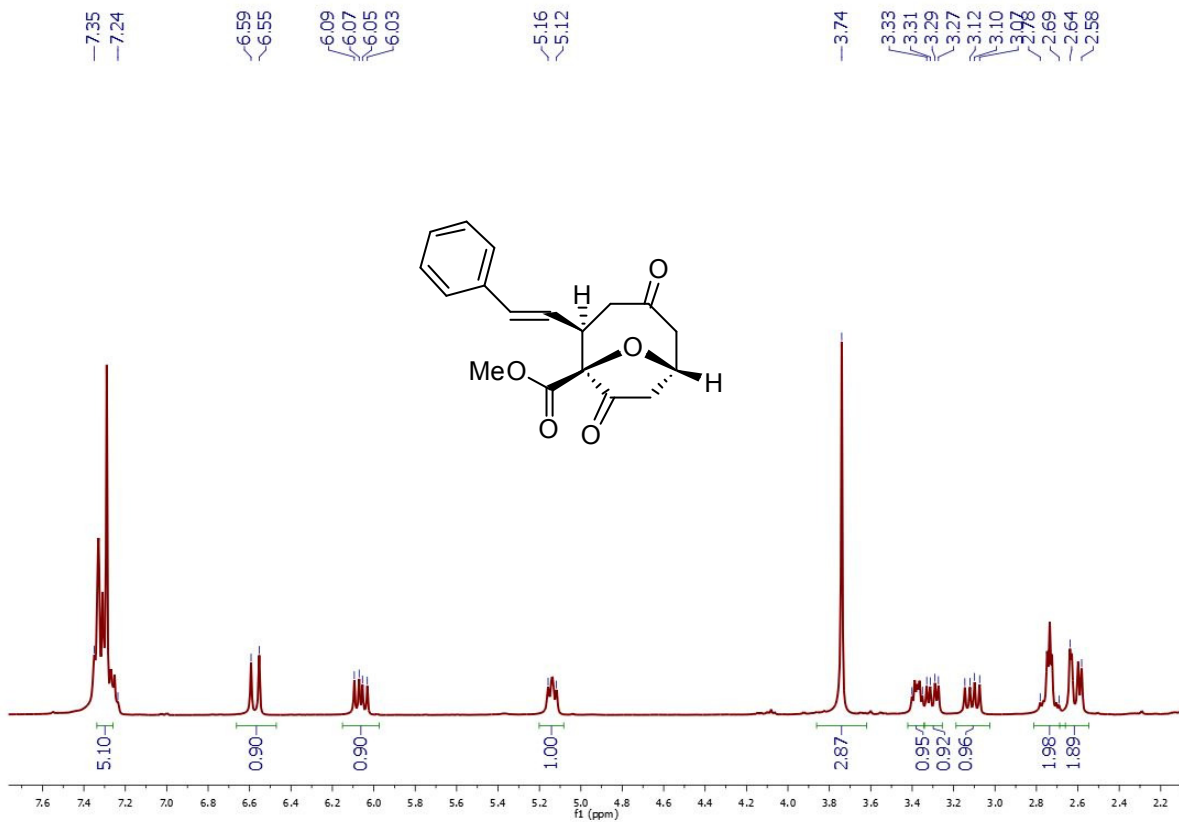


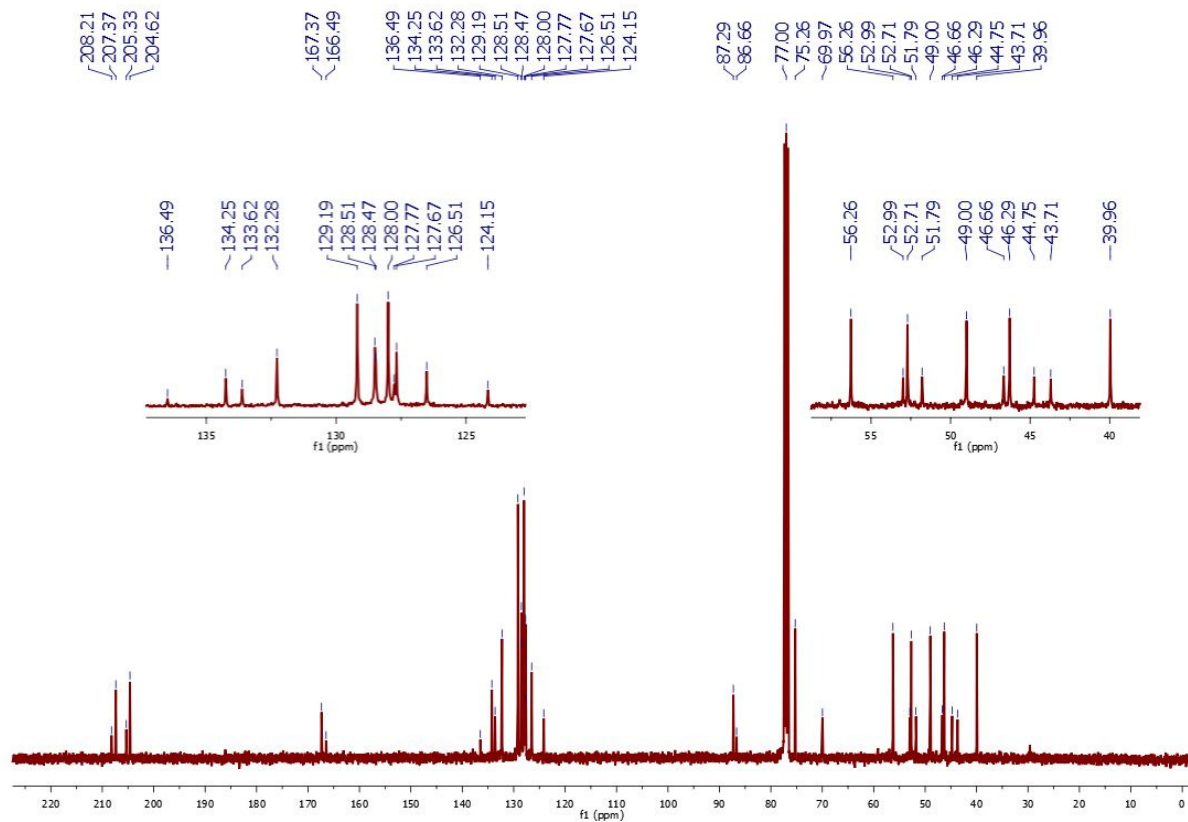
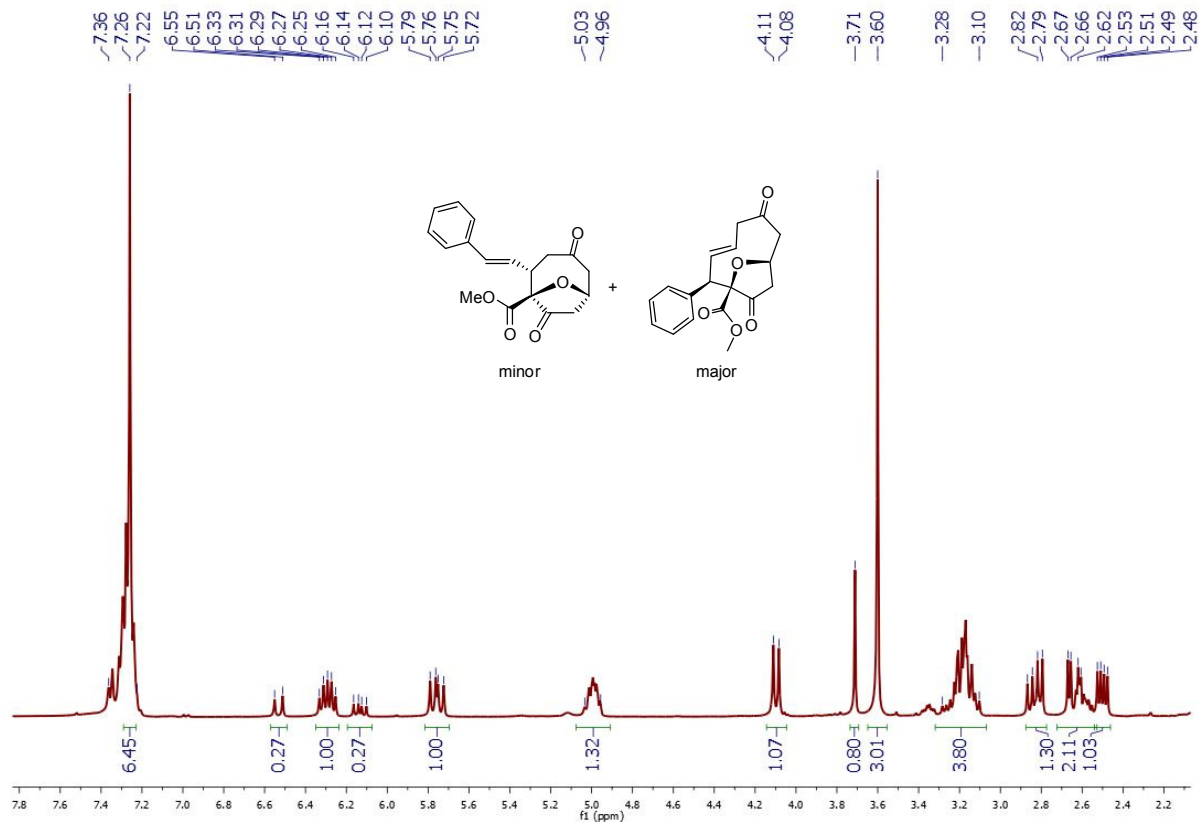


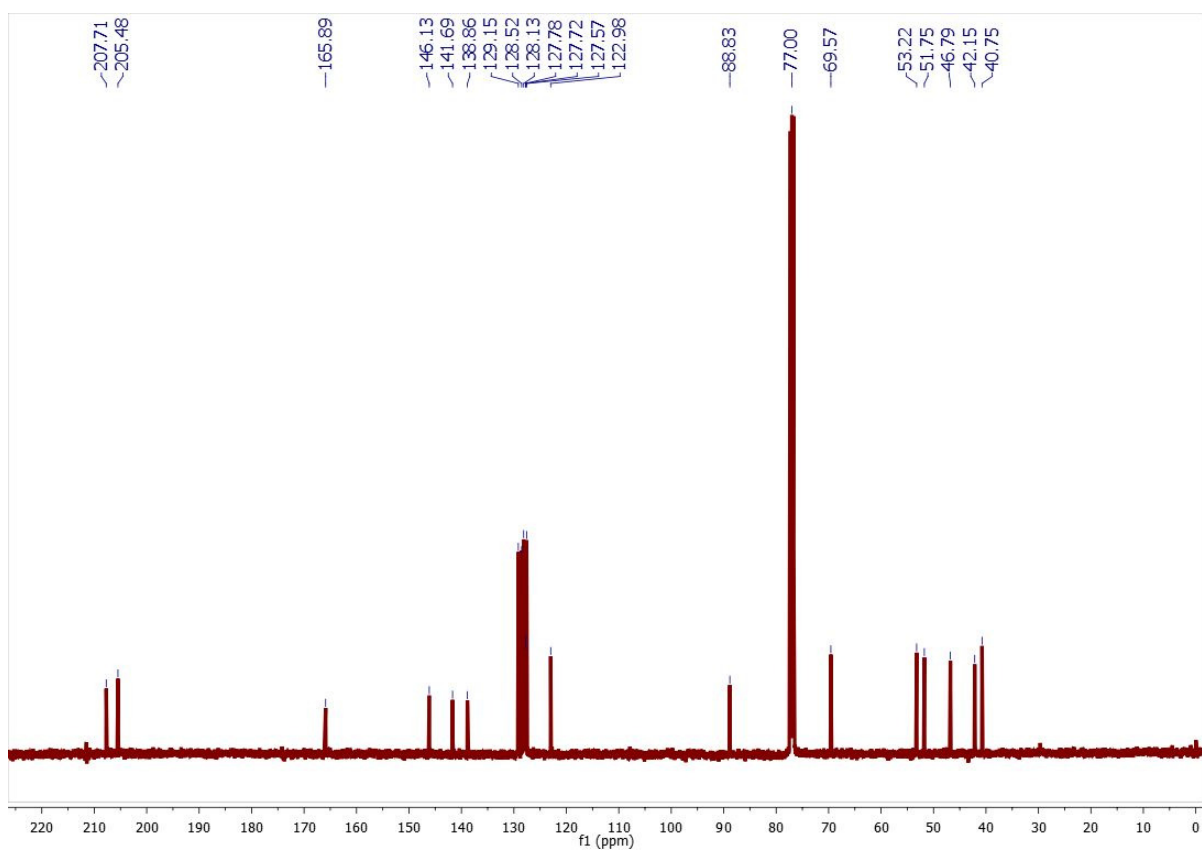
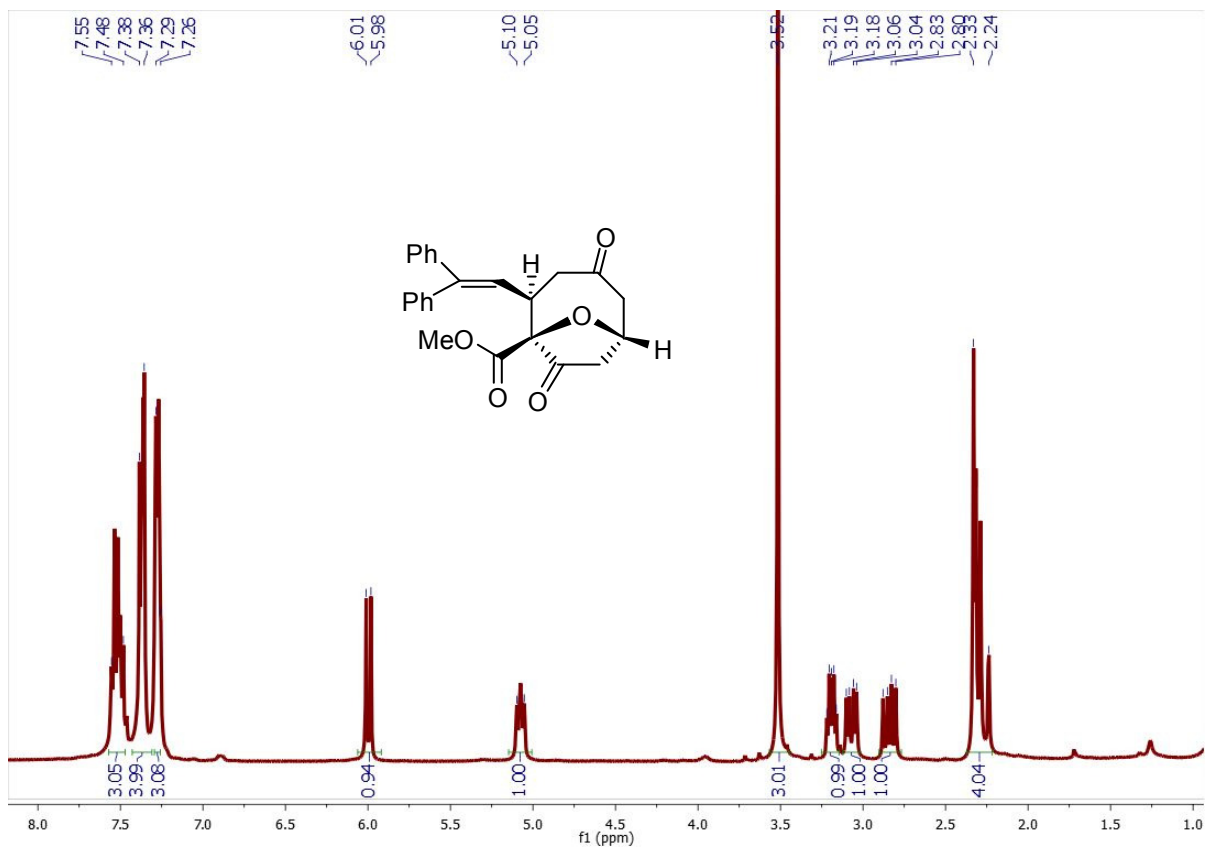
# $^1\text{H}$ NMR for reaction mixture of styryl diazoacetate decomposition reactions

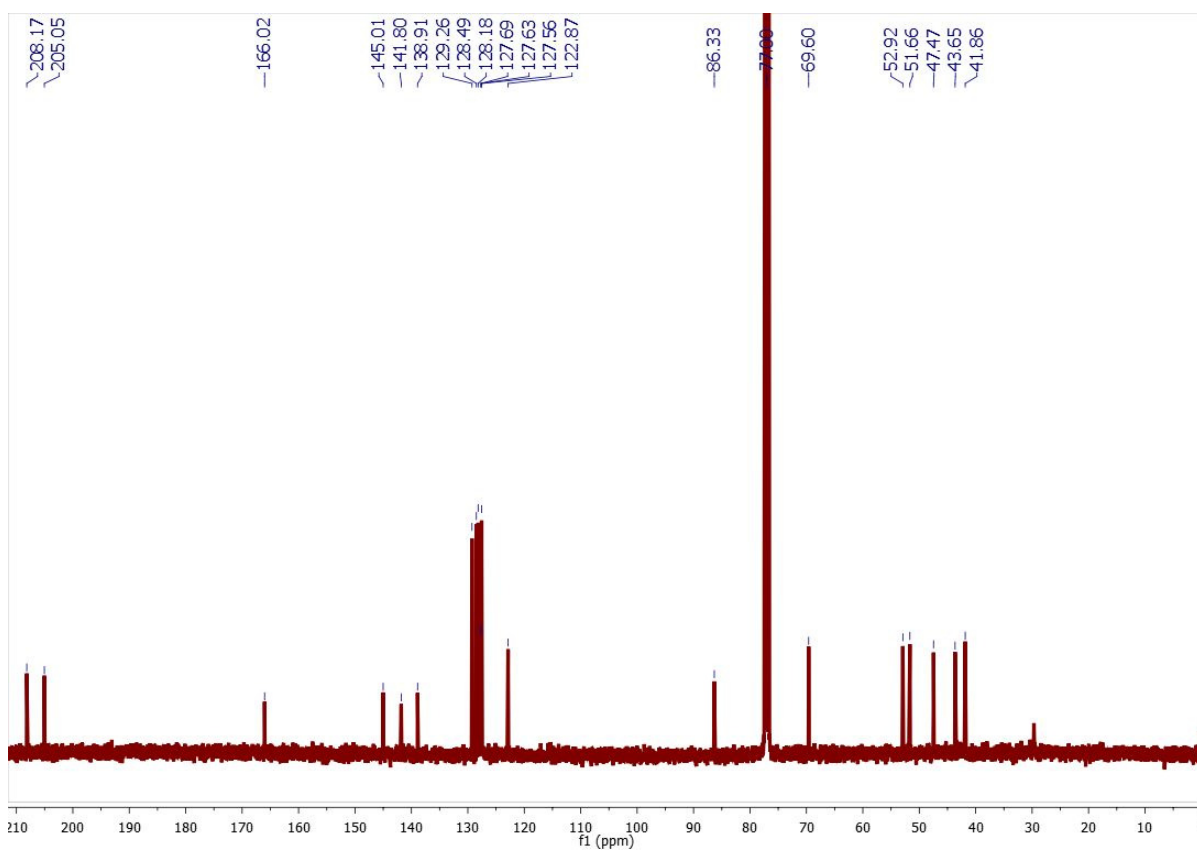
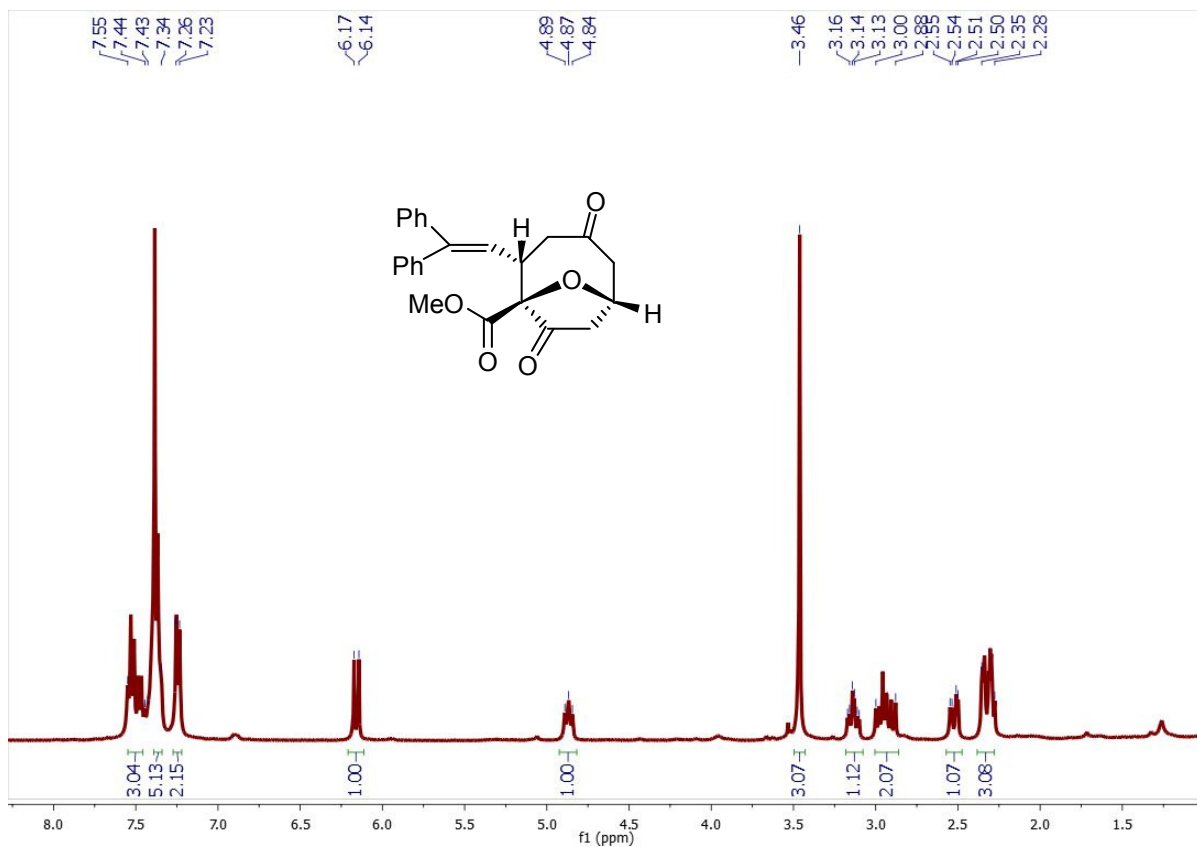


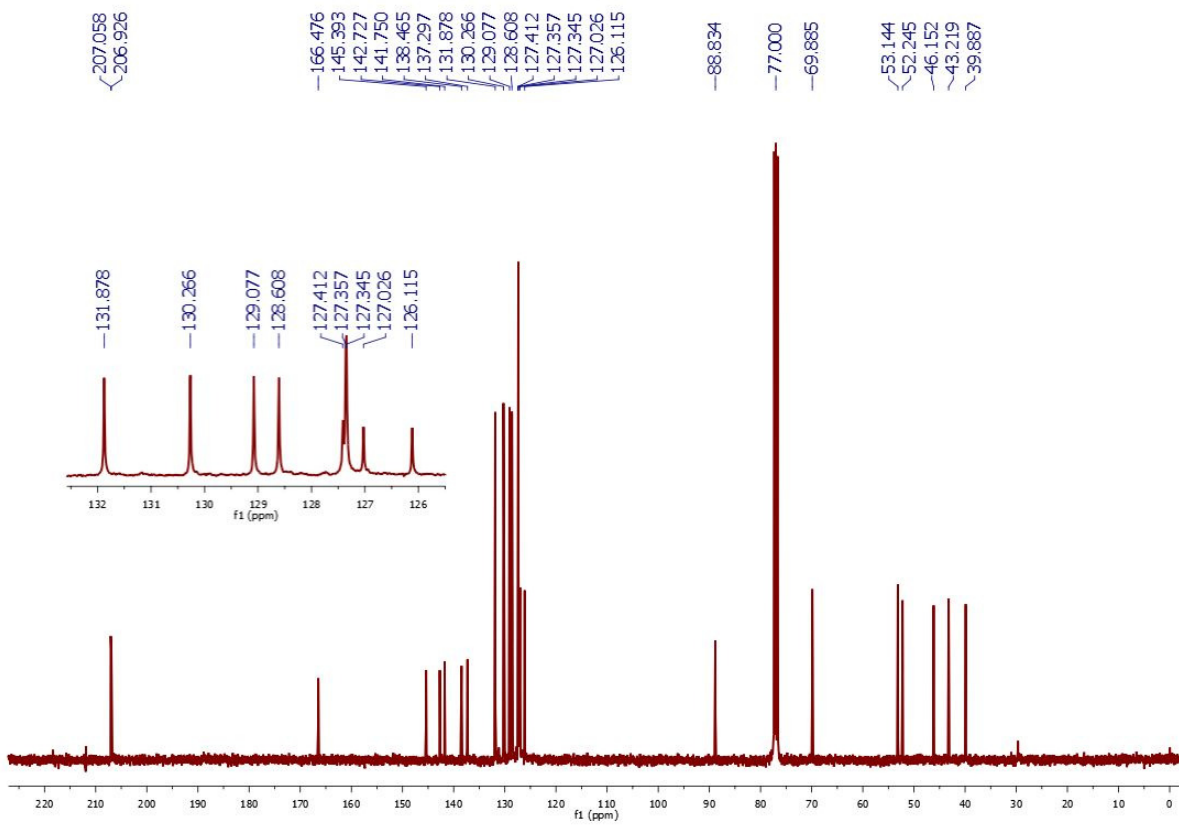
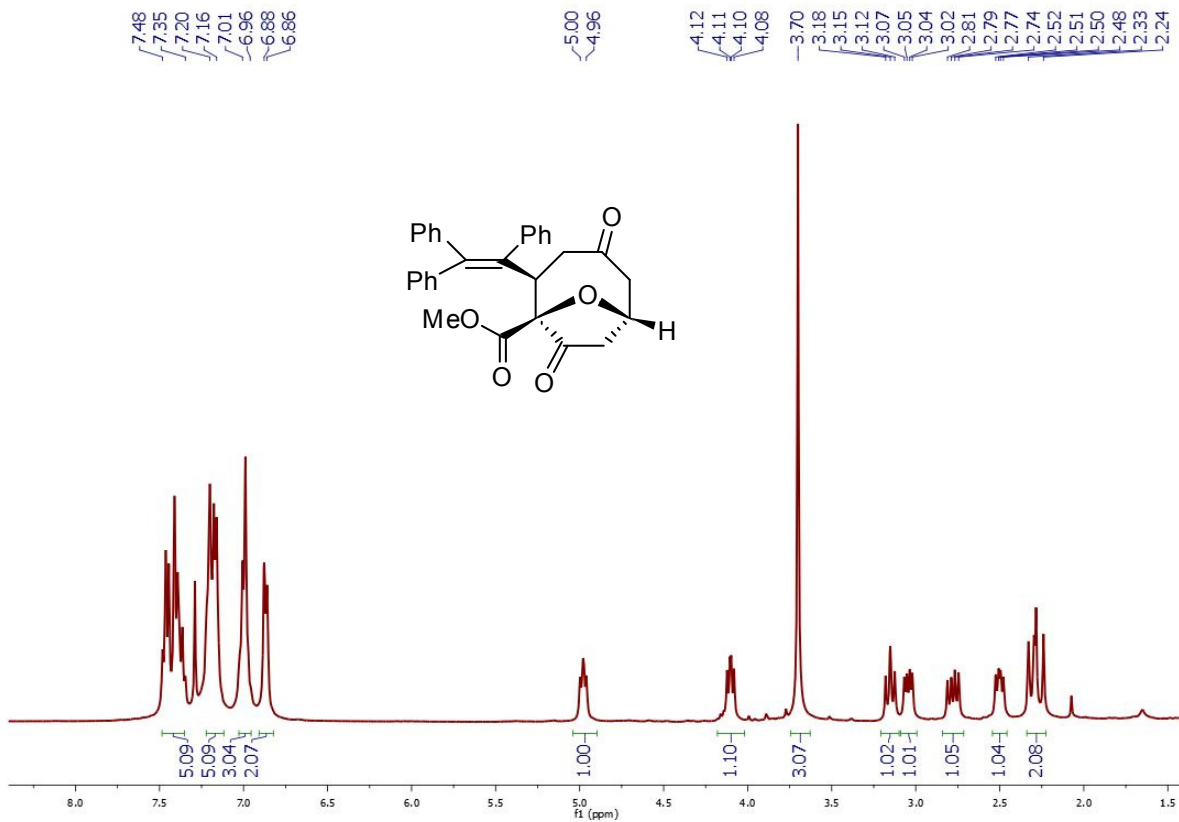


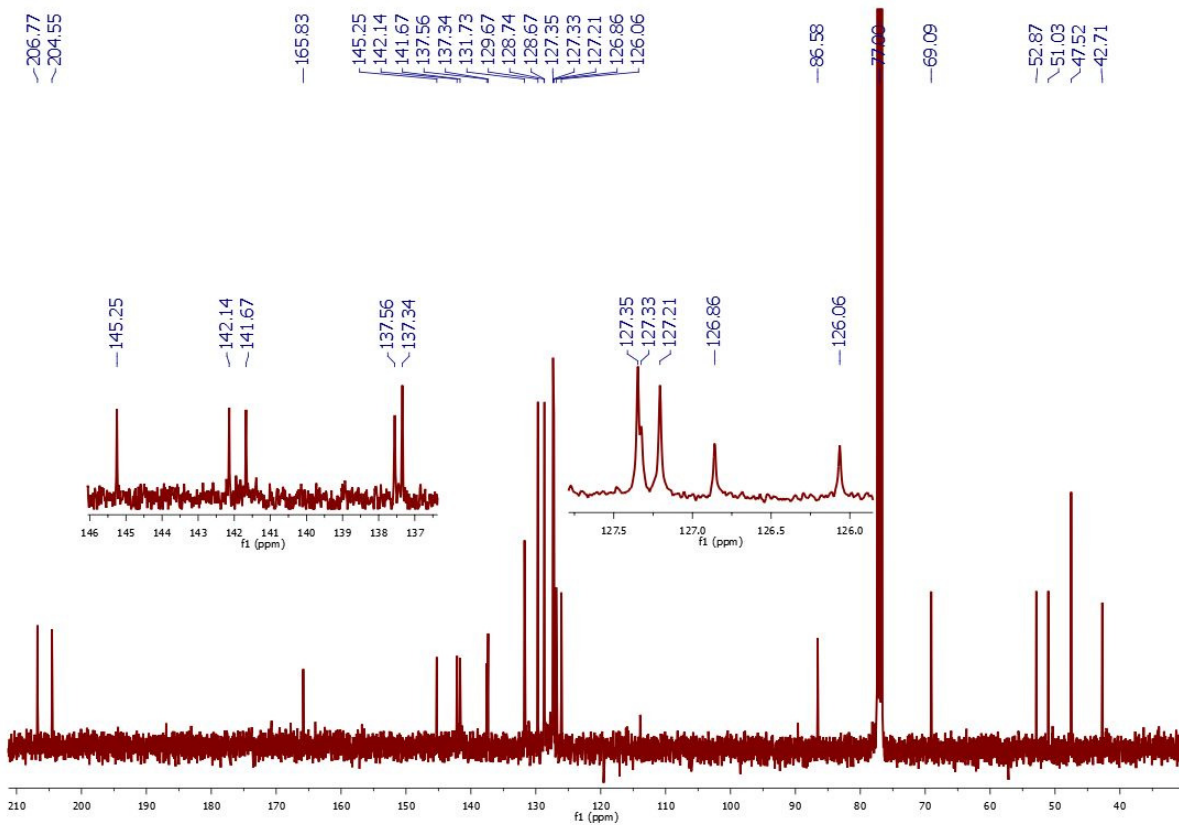
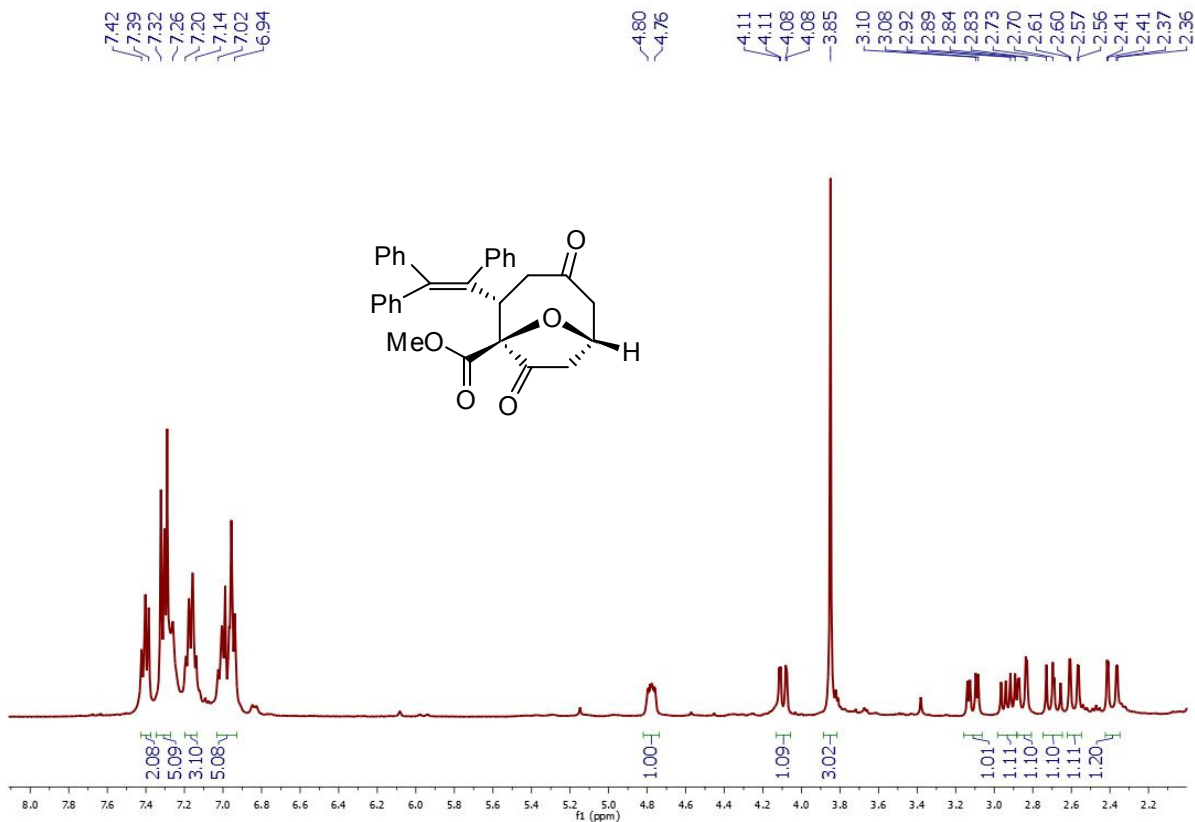


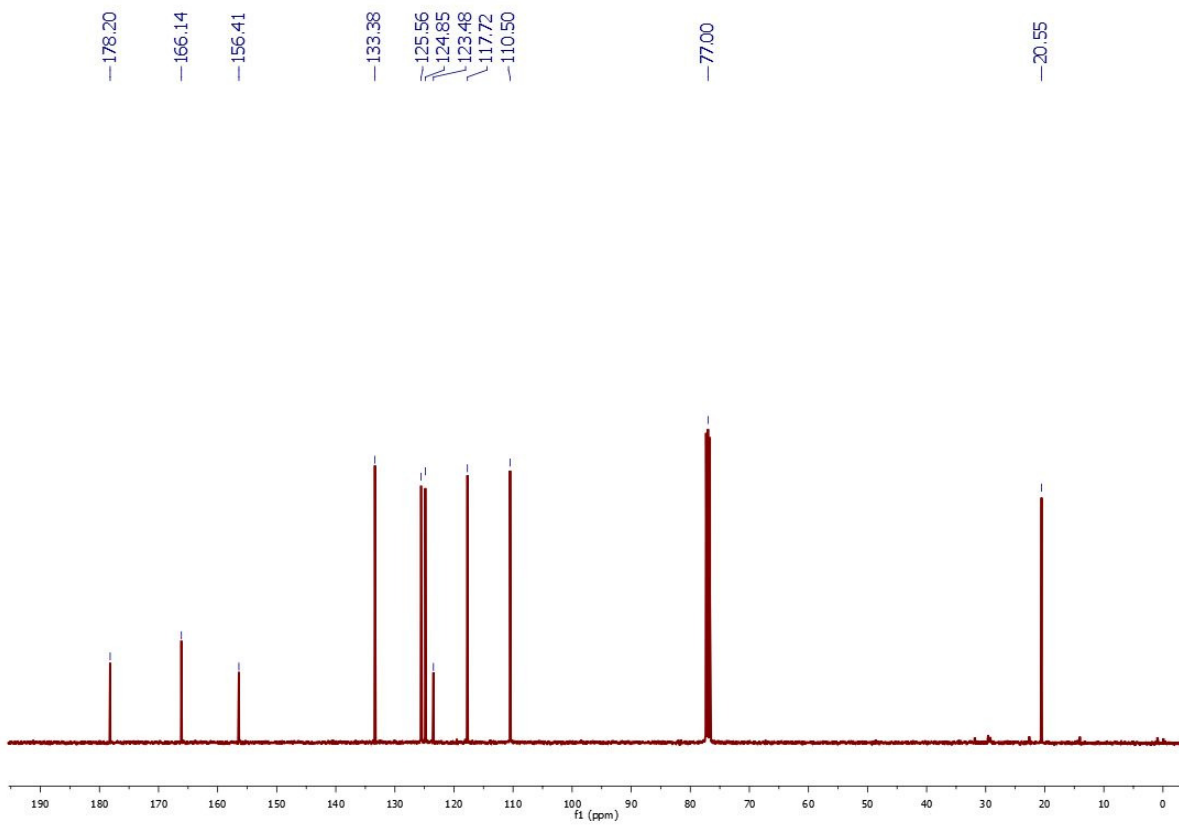
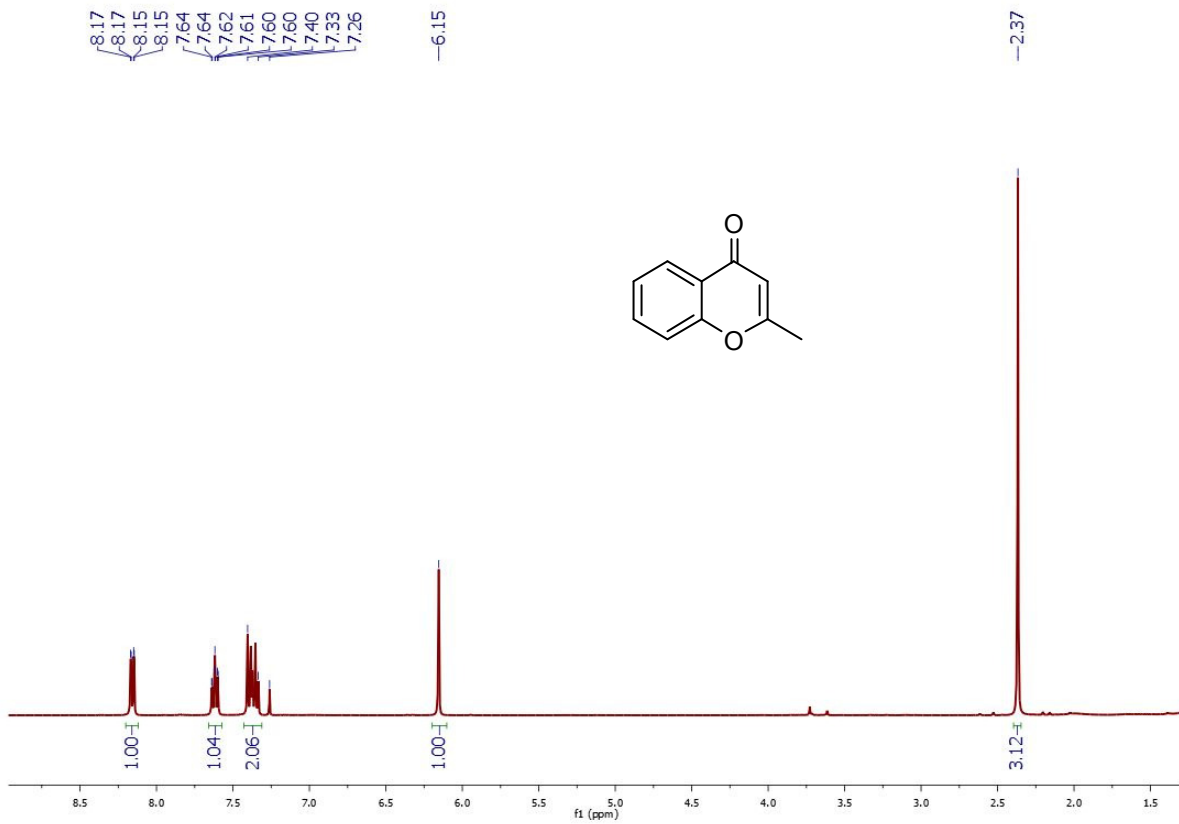












## 2.6 (c) Crystal Structure Data

Crystal No. & ID : **238**-[1,2] Major Product  
Compound name : styryl[1,2] major product  
Chemical formula : C<sub>18</sub>H<sub>18</sub>O<sub>5</sub>  
Final R<sub>1</sub> [I>2σ(I)] : **3.70 %**

---

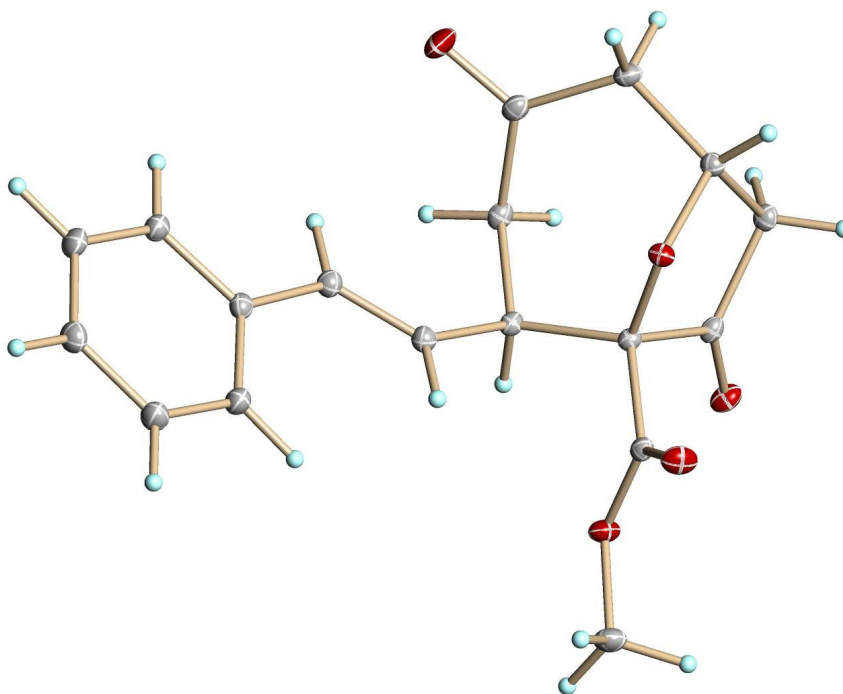


**Figure 1.** A view of UM#1975 showing the anisotropic atomic displacement ellipsoids for the non-hydrogen atoms at the 30% probability level. Hydrogen atoms are displayed with an arbitrarily small radius.

Crystals were obtained by dissolving 10 mg of white solid **238**-[1,2]-major isomer with minimum amount of ethyl ether:DCM (10:1). A colorless prism of C<sub>18</sub>H<sub>18</sub>O<sub>5</sub>, approximate dimensions 0.27x0.40x0.44 mm<sup>3</sup>, was used for the X-ray crystallographic analysis. The X-ray intensity data were measured at 150(2) °K on a three-circle diffractometer system equipped with Bruker Smart Apex II CCD area detector using a graphite monochromator and a MoK  $\alpha$  fine-focus sealed tube ( $\lambda$ = 0.71073 Å) . The detector was placed at a distance of 5.000 cm from the crystal.

A total of 1518 frames were collected with a scan width of -0.5° an exposure time of

10 sec/frame using Apex2 (Bruker, 2005). The total data collection time was 6.7 hours. The frames were integrated with Apex2 software package using a narrow-frame integration algorithm. The integration of the data using a Monoclinic unit cell yielded a total of 21226 reflections to a maximum  $\theta$  angle of  $30.00^\circ$ , of which 4364 were independent (completeness = 100.0%,  $R_{\text{int}} = 2.17\%$ ,  $R_{\text{sig}} = 1.61\%$ ) and 3892 were greater than  $2\sigma(I)$ . The final cell dimensions of  $a = 13.8355(15) \text{ \AA}$ ,  $b = 10.4469(11) \text{ \AA}$ ,  $c = 10.3765(11) \text{ \AA}$ ,  $\alpha = 90^\circ$ ,  $\beta = 95.847(2)^\circ$ ,  $\lambda = 90^\circ$ ,  $V = 1492.0(3) \text{ \AA}^3$ , are based upon the refinement of the XYZ-centroids of 11430 reflections with  $2.3 < \theta < 32.4^\circ$  using Apex2 software. Analysis of the data showed 0 % decay during data collection. Data were corrected for absorption effects with the Semi-empirical from equivalents method using SADABS (Sheldrick, 1996). The minimum and maximum transmission coefficients were 0.898 and 0.973.

The structure was solved and refined using the SHELXS-97 (Sheldrick, 1990) and SHELXL-97 (Sheldrick, 1997) software in the space group  $P2_1/c$  with  $Z = 4$  for the formula unit  $C_{18}H_{18}O_5$ . The final anisotropic full-matrix least-squares refinement on  $F^2$  with 280 variables converged at  $R_1 = 3.70\%$  for the observed data and  $wR_2 = 7.54\%$  for all data. The goodness-of-fit was 1.001. The largest peak on the final difference map was  $0.424 \text{ e}/\text{\AA}^3$  and the largest hole was  $-0.191 \text{ e}/\text{\AA}^3$ . On the basis of the final model, the calculated density was  $1.399 \text{ g/cm}^3$  and  $F(000)$ , 664 e.

**Comments:**

- H-atoms: all refined
- Residual density: in the middle of the bonds

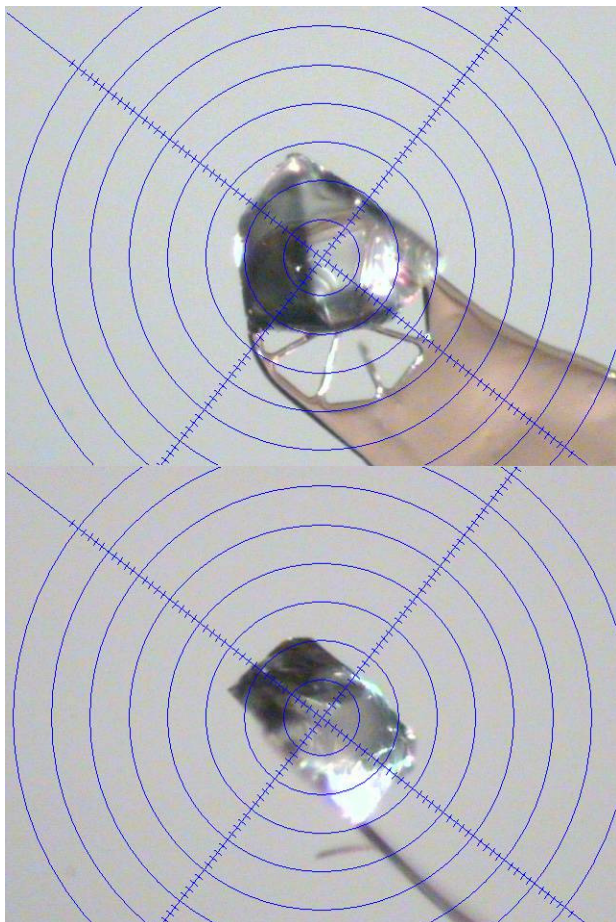


**Table 1.** Crystal data and structure refinement for UM#1975.

X-ray lab book No.	1975	
Crystal ID	Doyle/Jaber styryl-[1,2] Major Product 150K	
Empirical formula	$C_{18}H_{18}O_5$	
Formula weight	314.32	
Temperature	150(2) K	
Wavelength	0.71073 Å	
Crystal size	0.44×0.40×0.27 mm <sup>3</sup>	
Crystal habit	colorless prism	
Crystal system	Monoclinic	
Space group	$P2_1/c$	
Unit cell dimensions	$a = 13.8355(15)$ Å	$\alpha = 90^\circ$
	$b = 10.4469(11)$ Å	$\beta = 95.847(2)^\circ$
	$c = 10.3765(11)$ Å	$\gamma = 90^\circ$
Volume	1492.0(3) Å <sup>3</sup>	
Z	4	
Density, $\rho_{\text{calc}}$	1.399 g/cm <sup>3</sup>	
Absorption coefficient, $\mu$	0.102 mm <sup>-1</sup>	
F(000)	664 e	
Diffractometer	Bruker Smart Apex II CCD area detector	
Radiation source	fine-focus sealed tube, MoK $\alpha$	
Detector distance	5.000 cm	
Data collection method	$\omega$ and $\varphi$ scans	



C15	0.57558(7)	0.86082(10)	0.78952(9)	0.01774(18)
O15	0.56332(6)	0.94013(7)	0.70542(7)	0.02427(16)
C16	0.64779(7)	0.87193(9)	0.91301(9)	0.01562(17)
C17	0.63715(7)	0.99952(9)	0.98182(9)	0.01768(18)
O17	0.60443(6)	1.01227(8)	1.08394(7)	0.02853(18)
O18	0.67028(6)	1.09443(7)	0.91315(7)	0.02395(16)
C19	0.66514(9)	1.22066(11)	0.96847(12)	0.0282(2)
H1	0.9424(11)	1.0108(14)	1.1700(14)	0.035(4)
H2	1.0666(11)	1.0380(15)	1.3377(14)	0.036(4)
H3	1.1872(11)	0.8818(14)	1.3852(14)	0.036(4)
H4	1.1865(11)	0.6944(14)	1.2543(14)	0.035(4)
H5	1.0638(10)	0.6673(14)	1.0843(13)	0.029(3)
H7	0.9247(10)	0.7361(14)	0.9479(13)	0.031(4)
H8	0.8171(10)	0.9411(14)	1.0402(14)	0.032(4)
H9	0.7591(9)	0.9238(12)	0.8108(12)	0.019(3)
H10A	0.8263(10)	0.7269(13)	0.7649(13)	0.025(3)
H10B	0.7152(9)	0.7309(13)	0.7161(13)	0.025(3)
H12A	0.6623(10)	0.5215(14)	0.9852(14)	0.032(4)
H12B	0.6235(10)	0.5018(14)	0.8435(14)	0.031(4)
H13	0.5262(8)	0.6331(11)	0.9700(11)	0.015(3)
H14A	0.5390(10)	0.6828(13)	0.7173(13)	0.027(3)
H14B	0.4597(10)	0.7439(13)	0.7976(13)	0.029(4)
H19A	0.5969(12)	1.2486(15)	0.9623(15)	0.043(4)
H19B	0.7029(11)	1.2741(15)	0.9172(15)	0.039(4)
H19C	0.6911(11)	1.2199(15)	1.0603(15)	0.041(4)

\*  $U_{eq}$  is defined as one third of the trace of the orthogonalized  $U_{ij}$  tensor.

**Table 3.** Anisotropic atomic displacement parameters\* ( $\text{\AA}^2$ ) for UM#1975.

Atom	$U_{11}$	$U_{22}$	$U_{33}$	$U_{23}$	$U_{13}$	$U_{12}$
C1	0.0214(5)	0.0228(5)	0.0297(5)	-0.0017(4)	-0.0003(4)	0.0026(4)
C2	0.0254(5)	0.0262(5)	0.0299(5)	-0.0060(4)	-0.0005(4)	-0.0002(4)
C3	0.0227(5)	0.0310(6)	0.0263(5)	-0.0002(4)	-0.0037(4)	-0.0009(4)
C4	0.0211(5)	0.0275(5)	0.0309(5)	0.0013(4)	-0.0022(4)	0.0045(4)
C5	0.0202(5)	0.0227(5)	0.0258(5)	-0.0015(4)	0.0014(4)	0.0023(4)
C6	0.0169(4)	0.0218(5)	0.0202(4)	0.0018(4)	0.0023(3)	-0.0003(3)
C7	0.0204(5)	0.0231(5)	0.0207(4)	-0.0009(4)	0.0011(4)	0.0011(4)
C8	0.0192(4)	0.0216(5)	0.0183(4)	-0.0011(4)	0.0016(3)	0.0001(4)
C9	0.0175(4)	0.0188(4)	0.0155(4)	0.0012(3)	0.0024(3)	0.0022(3)
C10	0.0203(4)	0.0236(5)	0.0159(4)	-0.0026(4)	0.0027(3)	0.0042(4)
C11	0.0242(5)	0.0207(5)	0.0215(5)	-0.0047(4)	0.0004(4)	0.0043(4)
O11	0.0314(5)	0.0283(4)	0.0675(7)	0.0075(4)	0.0092(4)	0.0131(4)
C12	0.0253(5)	0.0173(4)	0.0223(5)	-0.0003(4)	0.0003(4)	0.0022(4)
C13	0.0194(4)	0.0179(4)	0.0169(4)	-0.0010(3)	0.0002(3)	-0.0008(3)
O13	0.0219(3)	0.0171(3)	0.0133(3)	0.0006(2)	0.0006(2)	-0.0014(3)
C14	0.0188(4)	0.0230(5)	0.0172(4)	-0.0013(4)	-0.0020(3)	0.0010(4)
C15	0.0177(4)	0.0215(4)	0.0139(4)	-0.0019(3)	0.0012(3)	0.0051(3)
O15	0.0305(4)	0.0250(4)	0.0167(3)	0.0023(3)	-0.0008(3)	0.0079(3)
C16	0.0178(4)	0.0161(4)	0.0129(4)	0.0006(3)	0.0012(3)	0.0018(3)
C17	0.0170(4)	0.0181(4)	0.0174(4)	-0.0012(3)	-0.0009(3)	0.0019(3)

O17	0.0407(5)	0.0247(4)	0.0217(4)	-0.0047(3)	0.0105(3)	0.0006(3)
O18	0.0312(4)	0.0161(3)	0.0255(4)	-0.0004(3)	0.0074(3)	0.0012(3)
C19	0.0344(6)	0.0178(5)	0.0320(6)	-0.0037(4)	0.0021(5)	0.0007(4)

\* The anisotropic atomic displacement factor exponent takes the form:  $-2\pi^2 [ h^2 a^{*2} U_{11} + \dots + 2hka^*b^*U_{12} ]$

**Table 5.** Bond lengths (Å) and angles (°) for UM#1975.

C1-C2	1.3867(15)	C1-C6	1.3977(15)	C1-H1	0.987(15)
C2-C3	1.3849(16)	C2-H2	0.959(15)	C3-C4	1.3867(16)
C3-H3	0.977(15)	C4-C5	1.3893(15)	C4-H4	0.983(15)
C5-C6	1.3996(14)	C5-H5	0.952(14)	C6-C7	1.4760(14)
C7-C8	1.3289(14)	C7-H7	0.979(14)	C8-C9	1.5089(14)
C8-H8	0.953(14)	C9-C10	1.5440(14)	C9-C16	1.5555(13)
C9-H9	0.976(13)	C10-C11	1.5185(15)	C10-H10A	0.976(13)
C10-H10B	0.986(13)	C11-O11	1.2115(13)	C11-C12	1.5142(15)
C12-C13	1.5170(14)	C12-H12A	0.950(15)	C12-H12B	0.966(14)
C13-O13	1.4589(12)	C13-C14	1.5281(14)	C13-H13	0.978(12)
O13-C16	1.4153(11)	C14-C15	1.5077(14)	C14-H14A	0.964(14)
C14-H14B	0.967(14)	C15-O15	1.2028(12)	C15-C16	1.5468(13)
C16-C17	1.5264(13)	C17-O17	1.2014(12)	C17-O18	1.3294(12)
O18-C19	1.4428(13)	C19-H19A	0.984(16)	C19-H19B	0.961(16)
C19-H19C	0.983(16)				
C2-C1-C6	120.76(10)	C2-C1-H1	118.6(9)	C6-C1-H1	120.6(9)
C3-C2-C1	120.46(11)	C3-C2-H2	119.8(9)	C1-C2-H2	119.7(9)
C2-C3-C4	119.58(10)	C2-C3-H3	119.8(9)	C4-C3-H3	120.6(9)
C3-C4-C5	120.14(10)	C3-C4-H4	120.4(9)	C5-C4-H4	119.4(9)
C4-C5-C6	120.86(10)	C4-C5-H5	119.2(8)	C6-C5-H5	119.9(8)
C1-C6-C5	118.16(9)	C1-C6-C7	123.12(9)	C5-C6-C7	118.72(9)
C8-C7-C6	125.45(10)	C8-C7-H7	119.6(8)	C6-C7-H7	114.9(8)
C7-C8-C9	126.38(9)	C7-C8-H8	118.8(9)	C9-C8-H8	114.6(9)
C8-C9-C10	114.32(8)	C8-C9-C16	111.82(8)	C10-C9-C16	112.17(8)
C8-C9-H9	107.3(7)	C10-C9-H9	106.2(7)	C16-C9-H9	104.2(7)
C11-C10-C9	117.24(8)	C11-C10-H10A	107.4(8)	C9-C10-H10A	108.2(8)
C11-C10-H10B	108.3(8)	C9-C10-H10B	109.0(8)	H10A-C10-H10B	106.1(11)
O11-C11-C12	117.83(10)	O11-C11-C10	120.84(10)	C12-C11-C10	121.24(9)
C11-C12-C13	118.37(9)	C11-C12-H12A	106.1(9)	C13-C12-H12A	109.2(9)
C11-C12-H12B	106.8(8)	C13-C12-H12B	110.0(8)	H12A-C12-H12B	105.7(12)
O13-C13-C12	109.47(8)	O13-C13-C14	105.65(8)	C12-C13-C14	116.91(8)
O13-C13-H13	105.8(7)	C12-C13-H13	106.8(7)	C14-C13-H13	111.7(7)
C16-O13-C13	109.46(7)	C15-C14-C13	105.02(8)	C15-C14-H14A	110.0(8)
C13-C14-H14A	113.3(8)	C15-C14-H14B	107.8(8)	C13-C14-H14B	110.9(8)
H14A-C14-H14B	109.7(11)	O15-C15-C14	127.80(9)	O15-C15-C16	125.51(9)
C14-C15-C16	106.64(8)	O13-C16-C17	107.43(7)	O13-C16-C15	104.97(7)
C17-C16-C15	111.59(8)	O13-C16-C9	113.46(7)	C17-C16-C9	111.78(8)
C15-C16-C9	107.47(7)	O17-C17-O18	124.86(9)	O17-C17-C16	124.91(9)
O18-C17-C16	110.22(8)	C17-O18-C19	115.77(8)	O18-C19-H19A	109.3(9)
O18-C19-H19B	105.1(9)	H19A-C19-H19B	111.3(13)	O18-C19-H19C	110.5(9)
H19A-C19-H19C	108.6(13)	H19B-C19-H19C	112.0(13)		
C6-C1-C2-C3	0.11(18)	C1-C2-C3-C4	0.83(18)	C2-C3-C4-C5	-0.24(18)
C3-C4-C5-C6	-1.29(17)	C2-C1-C6-C5	-1.59(16)	C2-C1-C6-C7	177.73(10)
C4-C5-C6-C1	2.18(16)	C4-C5-C6-C7	-177.17(10)	C1-C6-C7-C8	-11.94(17)
C5-C6-C7-C8	167.38(11)	C6-C7-C8-C9	174.92(10)	C7-C8-C9-C10	15.17(15)
C7-C8-C9-C16	144.00(10)	C8-C9-C10-C11	65.06(11)	C16-C9-C10-C11	-63.59(11)
C9-C10-C11-O11	-115.23(12)	C9-C10-C11-C12	68.22(12)	O11-C11-C12-C13	
161.37(10)	C10-C11-C12-C13	-21.98(14)	C11-C12-C13-O13	-48.28(12)	C11-C12-C13-C14
71.74(12)	C12-C13-O13-C16	97.61(9)	C14-C13-O13-C16	-29.09(10)	O13-C13-C14-C15

16.92(10)	C12-C13-C14-C15	-105.11(10)	C13-C14-C15-O15	177.05(10)	C13-C14-C15-
C16	-0.46(10)	C13-O13-C16-C17	147.29(7)	C13-O13-C16-C15	28.39(9)
C13-O13-C16-C9	-88.65(9)	O15-C15-C16-O13	165.79(9)	C14-C15-C16-O13	-16.62(9)
O15-C15-C16-C17	49.74(13)	C14-C15-C16-C17	-132.68(8)	O15-C15-C16-C9	-73.14(12)
C14-C15-C16-C9	104.44(9)	C8-C9-C16-O13	-68.23(10)	C10-C9-C16-O13	61.73(10)
C8-C9-C16-C17	53.43(10)	C10-C9-C16-C17	-176.61(8)	C8-C9-C16-C15	176.20(8)
C10-C9-C16-C15	-53.84(10)	O13-C16-C17-O17	-4.71(13)	C15-C16-C17-O17	
109.83(11)	C9-C16-C17-O17	-129.78(10)	O13-C16-C17-O18	174.62(8)	C15-C16-C17-O18
-70.84(10)	C9-C16-C17-O18	49.55(10)	O17-C17-O18-C19	-0.13(15)	C16-C17-O18-C19
-179.46(9)					

---

### **Crystal Structure Data**

Crystal No. & ID : **237**-styryl-[2,3]-minor product  
 Compound name : styryl-[2,3]-minor product  
 Chemical formula : C<sub>18</sub>H<sub>18</sub>O<sub>5</sub>  
 Final R<sub>1</sub> [I>2σ(I)] : **3.78 %**

---

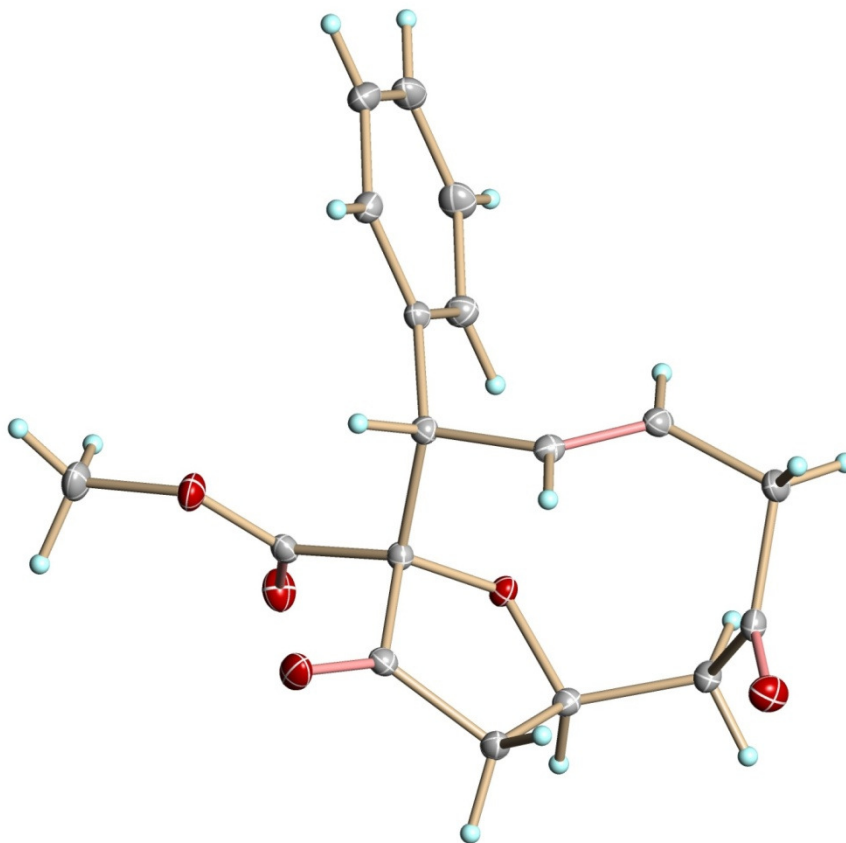


**Figure 1.** A view of UM#1993 showing the anisotropic atomic displacement ellipsoids for the non-hydrogen atoms the 30% probability level. Hydrogen atoms are displayed with an arbitrarily small radius.

Crystals were obtained by dissolving 10 mg of white solid **237**-[2,3]-minor isomer with minimum amount of ethyl ether:DCM (10:1). A colorless prism of  $C_{18}H_{18}O_5$ , approximate dimensions  $0.20 \times 0.32 \times 0.35 \text{ mm}^3$ , was used for the X-ray crystallographic analysis. The X-ray intensity data were measured at  $150(2) \text{ }^\circ\text{K}$  on a three-circle diffractometer system equipped with Bruker Smart Apex II CCD area detector using a graphite monochromator and a  $\text{MoK}\alpha$  fine-focus sealed tube ( $\theta = 0.71073 \text{ \AA}$ ). The detector was placed at a distance of 5.000 cm from the crystal.

A total of 3030 frames were collected with a scan width of  $-0.30^\circ$  an exposure time of 15 sec/frame using Apex2 (Bruker, 2005). The total data collection time was 17.7 hours. The frames were integrated with Apex2 software package using a narrow-frame

integration algorithm. The integration of the data using a Monoclinic unit cell yielded a total of 24755 reflections to a maximum  $\theta$  angle of  $30.00^\circ$ , of which 4363 were independent (completeness = 99.9%,  $R_{\text{int}} = 1.86\%$ ,  $R_{\text{sig}} = 1.19\%$ ) and 4007 were greater than  $2\sigma(I)$ . The final cell dimensions of  $a = 6.4080(5) \text{ \AA}$ ,  $b = 32.530(3) \text{ \AA}$ ,  $c = 7.8956(6) \text{ \AA}$ ,  $\alpha = 90^\circ$ ,  $\beta = 113.8418(12)^\circ$ ,  $\lambda = 90^\circ$ ,  $V = 1505.4(2) \text{ \AA}^3$ , are based upon the refinement of the XYZ-centroids of 15412 reflections with  $2.5 < \theta < 31.1^\circ$  using Apex2 software. Analysis of the data showed 0 % decay during data collection. Data were corrected for absorption effects with the Semi-empirical from equivalents method using SADABS (Sheldrick, 1996). The minimum and maximum transmission coefficients were 0.916 and 0.980.

The structure was solved and refined using the SHELXS-97 (Sheldrick, 1990) and SHELXL-97 (Sheldrick, 1997) software in the space group  $P2_1/n$  with  $Z = 4$  for the formula unit  $C_{18}H_{18}O_5$ . The final anisotropic full-matrix least-squares refinement on  $F^2$  with 268 variables converged at  $R_1 = 3.78 \%$  for the observed data and  $wR_2 = 7.44 \%$  for all data. The goodness-of-fit was 1.000. The largest peak on the final difference map was  $0.425 \text{ \AA}^{-3}$  and the largest hole was  $-0.197 \text{ \AA}^{-3}$ . On the basis of the final model, the calculated density was  $1.387 \text{ g/cm}^3$  and  $F(000)$ , 664  $\bar{e}$ .

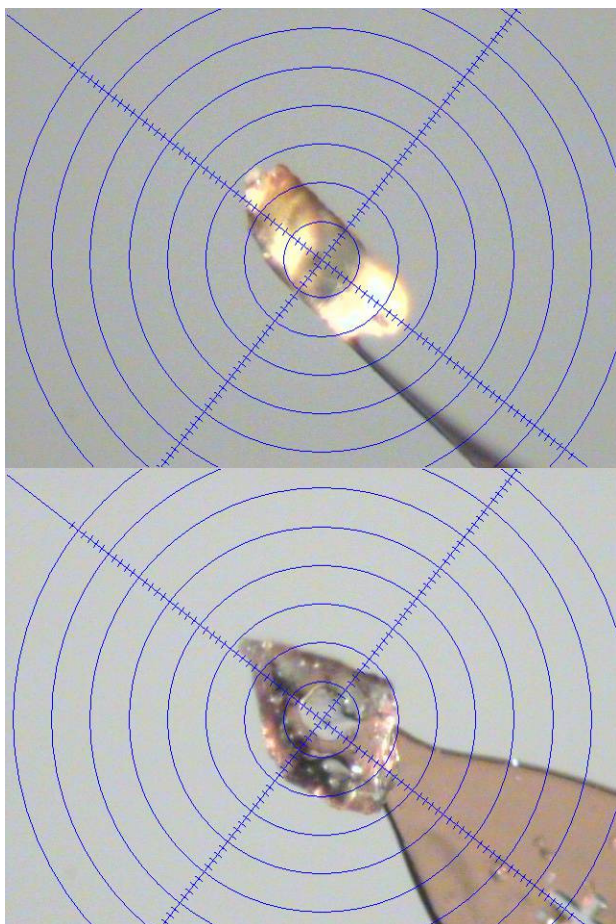


**Table 1.** Crystal data and structure refinement for UM#1993.

X-ray lab book No.	1993	
Crystal ID	Doyle/Jaber styryl-[2,3]-minor product - prisms 150K	
Empirical formula	$C_{18}H_{18}O_5$	
Formula weight	314.32	
Temperature	150(2) K	
Wavelength	0.71073 Å	
Crystal size	0.35×0.32×0.20 mm <sup>3</sup>	
Crystal habit	colorless prism	
Crystal system	Monoclinic	
Space group	P2 <sub>1</sub> /n	
Unit cell dimensions	$a = 6.4080(5)$ Å	$\alpha = 90^\circ$
	$b = 32.530(3)$ Å	$\beta = 113.8418(12)^\circ$
	$c = 7.8956(6)$ Å	$\gamma = 90^\circ$
Volume	1505.4(2) Å <sup>3</sup>	
Z	4	
Density, $\rho_{\text{calc}}$	1.387 g/cm <sup>3</sup>	
Absorption coefficient, $\mu$	0.101 mm <sup>-1</sup>	
F(000)	664 e <sup>-</sup>	
Diffractometer	Bruker Smart Apex II CCD area detector	
Radiation source	fine-focus sealed tube, MoK $\alpha$	
Detector distance	5.000 cm	
Data collection method	$\omega$ and $\phi$ scans	
Total frames	3030	

Frame size	512 pixels
Frame width	-0.30°
Exposure per frame	15 sec
Total measurement time	17.7 hours
θ range for data collection	2.50 to 30.00°
Index ranges	-9 ≤ h ≤ 9, -44 ≤ k ≤ 45, -11 ≤ l ≤ 11
Reflections collected	24755
Independent reflections	4363
Observed reflection, I > 2σ(I)	4007
Coverage of independent reflections	99.9 %
Variation in check reflections	0 %
Absorption correction	Semi-empirical from equivalents SADABS (Sheldrick, 1996)
Max. and min. transmission	0.980 and 0.916
Structure solution technique	direct
Structure solution program	SHELXS-97 (Sheldrick, 1990)
Refinement technique	Full-matrix least-squares on F <sup>2</sup>
Refinement program	SHELXL-97 (Sheldrick, 1997)
Function minimized	Σw(F <sub>o</sub> <sup>2</sup> - F <sub>c</sub> <sup>2</sup> ) <sup>2</sup>
Data / restraints / parameters	4363 / 0 / 268
Goodness-of-fit on F <sup>2</sup>	1.000
Δ/σ <sub>max</sub>	0.000
Final R indices:	
R <sub>1</sub> , I > 2σ(I)	0.0378
wR <sub>2</sub> , all data	0.0744
R <sub>int</sub>	0.0186
R <sub>sig</sub>	0.0119
Weighting scheme	w = 1/[σ <sup>2</sup> (F <sub>o</sub> <sup>2</sup> ) + (0.01P) <sup>2</sup> + 1.001P], P = [max(F <sub>o</sub> <sup>2</sup> , 0) + 2F <sub>o</sub> <sup>2</sup> ]/3
Largest diff. peak and hole	0.425                      and                      -0.197 e/Å <sup>3</sup>

$$R_1 = \Sigma||F_o| - |F_c|| / \Sigma|F_o|, \quad wR_2 = [\Sigma w(F_o^2 - F_c^2)^2 / \Sigma w(F_o^2)^2]^{1/2}$$

**Table 2.** Atomic coordinates and equivalent\* isotropic atomic displacement parameters (Å<sup>2</sup>) for UM#1993.

Atom	x/a	y/b	z/c	U <sub>eq</sub>
C1	0.95413(18)	0.19039(3)	0.11266(15)	0.0226(2)
C2	0.9643(2)	0.23159(3)	0.06813(16)	0.0279(2)
C3	1.1683(2)	0.24891(4)	0.08173(16)	0.0290(2)
C4	1.3628(2)	0.22478(4)	0.13989(16)	0.0275(2)
C5	1.35468(18)	0.18361(3)	0.18472(14)	0.0220(2)
C6	1.14969(17)	0.16591(3)	0.17052(13)	0.01751(18)
C7	1.15061(16)	0.12039(3)	0.21219(13)	0.01637(17)
C8	1.07402(17)	0.09322(3)	0.04235(14)	0.01812(18)
C9	0.91109(18)	0.10294(3)	-0.12080(14)	0.01978(19)
C10	0.78307(19)	0.06983(3)	-0.25793(14)	0.0228(2)
C11	0.68420(17)	0.04100(3)	-0.15808(13)	0.01944(18)
O11	0.72066(15)	0.00427(2)	-0.15027(12)	0.02797(17)
C12	0.54134(17)	0.05929(3)	-0.06222(14)	0.01891(18)
C13	0.65763(16)	0.06689(3)	0.14885(14)	0.01768(18)
O13	0.75886(11)	0.10798(2)	0.18641(10)	0.01745(14)
C14	0.84268(18)	0.03678(3)	0.26469(14)	0.01962(19)
C15	1.04337(17)	0.06303(3)	0.38109(13)	0.01799(18)

O15	1.21686(14)	0.05186(2)	0.50497(11)	0.02662(17)
C16	0.99057(16)	0.10790(3)	0.31076(13)	0.01592(17)
C17	1.02132(17)	0.13641(3)	0.47396(13)	0.01853(18)
O17	0.86760(14)	0.14971(3)	0.50718(11)	0.02783(17)
O18	1.24270(13)	0.14347(2)	0.57415(10)	0.02503(16)
C19	1.2942(2)	0.16958(4)	0.73473(16)	0.0292(2)

\*  $U_{eq}$  is defined as one third of the trace of the orthogonalized  $U_{ij}$  tensor.

\*\* Occupation factor for H19A - H19C = 0.802(17) and H19D - H19F = 0.198(17)

**Table 2a.** Hydrogen atom coordinates and isotropic atomic displacement parameters ( $\text{\AA}^2$ ) for UM#1993.

Atom	$x/a$	$y/b$	$z/c$	$U_{iso}$
H1	0.812(2)	0.1789(4)	0.1026(19)	0.031(4)
H2	0.828(3)	0.2477(5)	0.026(2)	0.037(4)
H3	1.173(3)	0.2768(5)	0.051(2)	0.036(4)
H4	1.505(3)	0.2363(5)	0.150(2)	0.035(4)
H5	1.490(2)	0.1671(4)	0.226(2)	0.030(4)
H7	1.305(2)	0.1133(4)	0.2989(17)	0.017(3)
H8	1.125(2)	0.0653(4)	0.0652(17)	0.020(3)
H9	0.855(2)	0.1305(4)	-0.1461(18)	0.026(3)
H10A	0.882(2)	0.0538(4)	-0.302(2)	0.031(3)
H10B	0.659(2)	0.0820(4)	-0.363(2)	0.031(3)
H12A	0.421(2)	0.0396(4)	-0.0796(18)	0.022(2)
H12B	0.477(2)	0.0853(4)	-0.1205(18)	0.022(2)
H13	0.536(2)	0.0674(4)	0.1936(17)	0.019(3)
H14A	0.795(2)	0.0189(4)	0.3428(19)	0.030(3)
H14B	0.896(2)	0.0185(4)	0.191(2)	0.030(3)
H19A	1.2052	0.1950	0.6975	0.032(3)
H19B	1.4573	0.1762	0.7883	0.032(3)
H19C	1.2551	0.1552	0.8269	0.032(3)
H19D	1.4065	0.1559	0.8443	0.032(3)
H19E	1.1544	0.1747	0.7535	0.032(3)
H19F	1.3566	0.1958	0.7149	0.032(3)

**Table 3.** Anisotropic atomic displacement parameters\* ( $\text{\AA}^2$ ) for UM#1993.

Atom	$U_{11}$	$U_{22}$	$U_{33}$	$U_{23}$	$U_{13}$	$U_{12}$
C1	0.0228(5)	0.0202(5)	0.0242(5)	0.0019(4)	0.0089(4)	0.0004(4)
C2	0.0334(6)	0.0205(5)	0.0277(5)	0.0038(4)	0.0102(5)	0.0043(4)
C3	0.0418(7)	0.0189(5)	0.0240(5)	0.0013(4)	0.0109(5)	-0.0054(4)
C4	0.0313(6)	0.0259(5)	0.0249(5)	-0.0025(4)	0.0109(5)	-0.0110(4)
C5	0.0217(5)	0.0229(5)	0.0205(5)	-0.0025(4)	0.0076(4)	-0.0042(4)
C6	0.0205(4)	0.0172(4)	0.0145(4)	-0.0010(3)	0.0066(3)	-0.0017(3)
C7	0.0153(4)	0.0170(4)	0.0164(4)	0.0001(3)	0.0060(3)	0.0001(3)
C8	0.0196(4)	0.0168(4)	0.0205(4)	-0.0016(3)	0.0106(4)	-0.0008(3)
C9	0.0231(5)	0.0192(5)	0.0189(4)	-0.0010(4)	0.0105(4)	-0.0022(4)
C10	0.0272(5)	0.0247(5)	0.0168(4)	-0.0026(4)	0.0091(4)	-0.0043(4)
C11	0.0186(4)	0.0211(5)	0.0158(4)	-0.0025(4)	0.0040(3)	-0.0017(4)

O11	0.0347(4)	0.0203(4)	0.0315(4)	-0.0016(3)	0.0160(4)	0.0018(3)
C12	0.0167(4)	0.0196(4)	0.0184(4)	-0.0016(4)	0.0049(4)	-0.0003(3)
C13	0.0166(4)	0.0179(4)	0.0189(4)	-0.0012(3)	0.0075(4)	-0.0018(3)
O13	0.0145(3)	0.0166(3)	0.0187(3)	-0.0008(3)	0.0041(3)	0.0001(2)
C14	0.0211(4)	0.0168(4)	0.0189(4)	0.0013(4)	0.0060(4)	-0.0017(3)
C15	0.0204(4)	0.0178(4)	0.0165(4)	0.0010(3)	0.0082(4)	0.0003(3)
O15	0.0250(4)	0.0235(4)	0.0235(4)	0.0047(3)	0.0016(3)	0.0015(3)
C16	0.0158(4)	0.0160(4)	0.0149(4)	-0.0002(3)	0.0050(3)	0.0003(3)
C17	0.0232(5)	0.0164(4)	0.0151(4)	0.0015(3)	0.0067(4)	-0.0001(3)
O17	0.0278(4)	0.0334(4)	0.0228(4)	-0.0053(3)	0.0108(3)	0.0045(3)
O18	0.0238(4)	0.0288(4)	0.0194(3)	-0.0072(3)	0.0057(3)	-0.0045(3)
C19	0.0362(6)	0.0253(5)	0.0210(5)	-0.0074(4)	0.0062(4)	-0.0065(4)

\* The anisotropic atomic displacement factor exponent takes the form:  $-2\pi^2 [ h^2a^{*2}U_{11} + \dots + 2hka^*b^*U_{12} ]$

**Table 4.** Bond lengths (Å), valence and torsion angles (°) for UM#1993.

C1-C2	1.3938(15)	C1-C6	1.3965(14)	C1-H1	0.960(14)
C2-C3	1.3870(17)	C2-H2	0.954(15)	C3-C4	1.3852(18)
C3-H3	0.942(15)	C4-C5	1.3917(15)	C4-H4	0.956(15)
C5-C6	1.3966(14)	C5-H5	0.958(14)	C6-C7	1.5163(13)
C7-C8	1.5128(13)	C7-C16	1.5709(13)	C7-H7	0.977(12)
C8-C9	1.3275(14)	C8-H8	0.956(13)	C9-C10	1.5124(14)
C9-H9	0.954(14)	C10-C11	1.5185(14)	C10-H10A	0.985(15)
C10-H10B	0.972(15)	C11-O11	1.2144(13)	C11-C12	1.5248(14)
C12-C13	1.5459(14)	C12-H12A	0.967(13)	C12-H12B	0.973(13)
C13-O13	1.4627(12)	C13-C14	1.5250(14)	C13-H13	0.979(13)
O13-C16	1.4107(11)	C14-C15	1.5074(14)	C14-H14A	0.985(14)
C14-H14B	0.985(14)	C15-O15	1.2023(12)	C15-C16	1.5497(13)
C16-C17	1.5343(13)	C17-O17	1.1980(13)	C17-O18	1.3356(12)
O18-C19	1.4489(13)				
C2-C1-C6	120.23(10)	C2-C1-H1	119.5(9)	C6-C1-H1	120.3(9)
C3-C2-C1	120.65(11)	C3-C2-H2	120.1(9)	C1-C2-H2	119.3(9)
C4-C3-C2	119.29(11)	C4-C3-H3	120.8(9)	C2-C3-H3	120.0(9)
C3-C4-C5	120.55(11)	C3-C4-H4	120.2(9)	C5-C4-H4	119.2(9)
C4-C5-C6	120.47(10)	C4-C5-H5	120.3(9)	C6-C5-H5	119.3(9)
C1-C6-C5	118.80(9)	C1-C6-C7	123.51(9)	C5-C6-C7	117.65(9)
C8-C7-C6	114.02(8)	C8-C7-C16	104.19(7)	C6-C7-C16	114.46(8)
C8-C7-H7	110.9(7)	C6-C7-H7	107.3(7)	C16-C7-H7	105.7(7)
C9-C8-C7	124.54(9)	C9-C8-H8	118.9(8)	C7-C8-H8	115.1(8)
C8-C9-C10	120.75(10)	C8-C9-H9	120.5(8)	C10-C9-H9	118.0(8)
C9-C10-C11	106.71(8)	C9-C10-H10A	112.8(8)	C11-C10-H10A	108.5(8)
C9-C10-H10B	109.9(9)	C11-C10-H10B	109.1(8)	H10A-C10-H10B	109.7(12)
O11-C11-C10	121.46(10)	O11-C11-C12	120.03(9)	C10-C11-C12	118.49(9)
C11-C12-C13	118.23(8)	C11-C12-H12A	105.9(8)	C13-C12-H12A	105.6(8)
C11-C12-H12B	109.3(8)	C13-C12-H12B	107.3(8)	H12A-C12-H12B	110.4(11)
O13-C13-C14	106.97(8)	O13-C13-C12	110.23(8)	C14-C13-C12	117.58(8)
O13-C13-H13	105.3(7)	C14-C13-H13	109.6(7)	C12-C13-H13	106.5(7)
C16-O13-C13	113.28(7)	C15-C14-C13	105.47(8)	C15-C14-H14A	111.1(8)
C13-C14-H14A	113.1(8)	C15-C14-H14B	106.9(8)	C13-C14-H14B	113.7(8)
H14A-C14-H14B	106.6(11)	O15-C15-C14	127.25(9)	O15-C15-C16	124.91(9)
C14-C15-C16	107.83(8)	O13-C16-C17	108.97(8)	O13-C16-C15	105.49(7)
C17-C16-C15	109.45(8)	O13-C16-C7	111.65(7)	C17-C16-C7	111.82(8)
C15-C16-C7	109.24(7)	O17-C17-O18	125.36(9)	O17-C17-C16	124.36(9)
O18-C17-C16	110.27(8)	C17-O18-C19	115.53(9)		
C6-C1-C2-C3	-0.44(17)	C1-C2-C3-C4	0.14(18)	C2-C3-C4-C5	-0.14(17)

C3-C4-C5-C6	0.44(16)	C2-C1-C6-C5	0.73(15)	C2-C1-C6-C7	-
176.82(10)	C4-C5-C6-C1	-0.73(15)	C4-C5-C6-C7	176.96(9)	C1-C6-C7-C8
81.84(12)	C5-C6-C7-C8	-95.73(10)	C1-C6-C7-C16	-37.99(13)	C5-C6-C7-
C16	144.44(9)	C6-C7-C8-C9	-36.28(13)	C16-C7-C8-C9	
89.18(11)	C7-C8-C9-C10	-156.38(9)	C8-C9-C10-C11	55.31(13)	C9-C10-C11-
O11	-125.71(11)	C9-C10-C11-C12	52.74(12)	O11-C11-C12-C13	
79.96(12)	C10-C11-C12-C13	-98.52(11)	C11-C12-C13-O13	89.13(10)	C11-C12-C13-
C14	-33.78(13)	C14-C13-O13-C16	1.27(10)	C12-C13-O13-C16	-
127.65(8)	O13-C13-C14-C15	5.10(10)	C12-C13-C14-C15	129.65(9)	C13-C14-C15-
O15	172.01(10)	C13-C14-C15-C16	-9.13(10)	C13-O13-C16-C17	-
124.34(8)	C13-O13-C16-C15	-6.90(10)	C13-O13-C16-C7	111.65(8)	O15-C15-C16-
O13	-171.17(9)	C14-C15-C16-O13	9.94(10)	O15-C15-C16-C17	-
54.06(13)	C14-C15-C16-C17	127.05(8)	O15-C15-C16-C7	68.68(12)	C14-C15-C16-
C7	-110.21(9)	C8-C7-C16-O13	-49.99(10)	C6-C7-C16-O13	
75.19(10)	C8-C7-C16-C17	-172.39(8)	C6-C7-C16-C17	-47.21(11)	C8-C7-C16-
C15	66.30(9)	C6-C7-C16-C15	-168.52(8)	O13-C16-C17-O17	
13.52(13)	C15-C16-C17-O17	-101.37(11)	C7-C16-C17-O17	137.44(10)	O13-C16-
C17-O18	-167.61(8)	C15-C16-C17-O18	77.50(10)	C7-C16-C17-O18	-
43.69(11)	O17-C17-O18-C19	-0.18(15)	C16-C17-O18-C19	-179.04(8)	

### **3.8 References**

Brogan, J. B.; Zercher, C. K. *Tetrahedron Lett.*, **1998**, *39*, 1691-1694.

Brogan, J. B.; Zercher, C. K.; Bauer, C. B.; Rogers, R. D. *J. Org. Chem.*, **1997**, *62*, 3902-3909.

Clark, J. S. *Tetrahedron Lett.*, **1992**, *33*, 6193-6196.

Clark, J. S.; Bate, A. L.; Grinter, T. *Chem. Commun.*, **2001**, 459-460.

Clark, J. S.; Walls, S. B.; Wilson, C.; East, S. P.; Drysdale, M. J. *Eur. J. Org. Chem.*, **2006**, 323-327.

Cotton, F. A.; Felthouse, T. R. *Inorg. Chem.*, **1980**, *19*, 323-328.

Davies, H. M. L.; Ahmed, G.; Churchill, M. R. *J. Am. Chem. Soc.*, **1996**, *118*, 10774-10782.

- Dewar, M. J. S. *Spec. Publ. - Chem. Soc.*, **1967**, *21*, 177-215.
- Dewar, M. J. S. *Angew. Chem., Int. Ed. Engl.*, **1971**, *10*, 761-776.
- Dewar, M. J. S.; Ramsden, C. A. *J. Chem. Soc., Perkin Trans. 1*, **1974**, 1839-1844.
- Doyle, M. P.; Colyer, J. T. *Tetrahedron: Asymm.*, **2003**, *14*, 3601-3604.
- Doyle, M. P.; Dyatkin, A. B.; Autry, C. L. *J. Chem. Soc., Perkin Trans. 1*, **1995**, 619-621.
- Evans, M. G. *Trans. Faraday Soc.*, **1939**, *35*, 824-834.
- Evans, M. G.; Warhurst, E. *Trans. Faraday Soc.*, **1938**, *34*, 614-624.
- Fukui, K. *Symposium on Mol. Phys.*, **1954**, 41-42.
- Fukui, K. *Kagaku no Ryoiki*, **1954**, *8*, 73-74.
- Fukui, K.; Yonezawa, T.; Nagata, C.; Shingu, H. *J. Chem. Phys.*, **1954**, *22*, 1433-1442.
- Hashimoto, S.; Watanabe, N.; Ikegami, S. *Tetrahedron Lett.*, **1992**, *33*, 2709-2712.
- Hoffmann, R.; Woodward, R. B. *J. Am. Chem. Soc.*, **1965**, *87*, 2046-2048.
- Hoffmann, R.; Woodward, R. B. *Acc. Chem. Res.*, **1968**, *1*, 17-22.
- Johnson, S. A.; Hunt, H. R.; Neumann, H. M. *Inorg. Chem.*, **1963**, *2*, 960-962.
- Kitagaki, S.; Yanamoto, Y.; Tsutsui, H.; Anada, M.; Nakajima, M.; Hashimoto, S. *Tetrahedron Lett.*, **2001**, *42*, 6361-6364.
- Nakai, T.; Mikami, K. *Chem. Rev.*, **1986**, *86*, 885-902.
- Ohno, M.; Itoh, M.; Umeda, M.; Furuta, R.; Kondo, K.; Eguchi, S. *J. Am. Chem. Soc.*, **1996**, *118*, 7075-7082.

Pangborn, A. B.; Giardello, M. A.; Grubbs, R. H.; Rosen, R. K.; Timmers, F. J. *Organometallics*, **1996**, *15*, 1518-1520.

Sweeney, J. B. *Chem. Soc. Rev.*, **2009**, *38*, 1027-1038.

Woodward, R. B.; Hoffmann, R. *J. Am. Chem. Soc.*, **1965**, *87*, 395-397.

Woodward, R. B.; Hoffmann, R. *Angew. Chem., Int. Ed. Engl.*, **1969**, *8*, 781-853.

Zhou, C.; Larock, R. C. *J. Org. Chem.*, **2005**, *70*, 3765-3777.

## Works Cited

- Ahmed, A. F.; Su, J.-H.; Kuo, Y.-H.; Sheu, J.-H. *J. Nat. Prod.*, **2004**, *67*, 2079-2082.
- Anada, M.; Washio, T.; Shimada, N.; Kitagaki, S.; Nakajima, M.; Shiro, M.; Hashimoto, S. *Angew. Chem., Int. Ed.*, **2004**, *43*, 2665-2668.
- Anada, M.; Washio, T.; Watanabe, Y.; Takeda, K.; Hashimoto, S. *Eur. J. Org. Chem.*, **2010**, 6850-6854.
- Anciaux, A. J.; Hubert, A. J.; Noels, A. F.; Petiniot, N.; Teyssie, P. *J. Org. Chem.*, **1980**, *45*, 695-702.
- Ando, W.; Hagiwara, T.; Migita, T. *Tetrahedron Lett.*, **1974**, 1425-1428.
- Ando, W.; Kondo, S.; Nakayama, K.; Ichibori, K.; Kohoda, H.; Yamato, H.; Imai, I.; Nakaido, S.; Migita, T. *J. Am. Chem. Soc.*, **1972**, *94*, 3870-3876.
- Ando, W.; Yagihara, T.; Kondo, S.; Nakayama, K.; Yamato, H.; Nakaido, S.; Migita, T. *J. Org. Chem.*, **1971**, *36*, 1732-1736.
- Ando, W.; Yagihara, T.; Tozune, S.; Nakaido, S.; Migita, T. *Tetrahedron Lett.*, **1969**, 1979-1982.
- Bols, M.; Skrydstrup, T. *Chem. Rev.*, **1995**, *95*, 1253-1277.
- Cai, P.; McPhail, A. T.; Krainer, E.; Katz, B.; Pearce, C.; Boros, C.; Caceres, B.; Smith, D.; Houck, D. R. *Tetrahedron Lett.*, **1999**, *40*, 1479-1482.
- Cane, D. E.; Thomas, P. J. *J. Am. Chem. Soc.*, **1984**, *106*, 5295-303.
- Chavez, D. E.; Jacobsen, E. N. *Org. Synth.*, **2005**, *82*, 34-42.
- Chen, Z.; Chen, Z.; Jiang, Y.; Hu, W. *Tetrahedron*, **2005**, *61*, 1579-1586.
- Clark, J. S.; Baxter, C. A.; Castro, J. L. *Synthesis*, **2005**, 3398-3404.
- Clark, J. S.; Baxter, C. A.; Dossetter, A. G.; Poigny, S.; Castro, J. L.; Whittingham, W. G. *J. Org. Chem.*, **2008**, *73*, 1040-1055.
- Clark, J. S.; Fessard, T. C.; Whitlock, G. A. *Tetrahedron*, **2005**, *62*, 73-78.
- Clark, J. S.; Fessard, T. C.; Wilson, C. *Org. Lett.*, **2004**, *6*, 1773-1776.
- Clark, J. S.; Hayes, S. T.; Wilson, C.; Gobbi, L. *Angew. Chem., Int. Ed.*, **2007**, *46*, 437-440.

Clark, J. S.; Walls, S. B.; Wilson, C.; East, S. P.; Drysdale, M. J. *Eur. J. Org. Chem.*, **2006**, 323-327.

Clark, J. S.; Whitlock, G.; Jiang, S.; Onyia, N. *Chem. Commun.*, **2003**, 2578-2579.

Clemens, R. J.; Hyatt, J. A. *J. Org. Chem.*, **1985**, *50*, 2431-2435.

Cope, A. C.; McKervey, M. A.; Weinshenker, N. M. *J. Org. Chem.*, **1969**, *34*, 2229-2231.

Cotton, F. A.; Felthouse, T. R. *Inorg. Chem.*, **1980**, *19*, 323-328.

Danheiser, R. L.; Miller, R. F.; Brisbois, R. G.; Park, S. Z. *J. Org. Chem.*, **1990**, *55*, 1959-1964.

Danishefsky, S.; Kerwin, J. F., Jr.; Kobayashi, S. *J. Am. Chem. Soc.*, **1982**, *104*, 358-360.

Danishefsky, S.; Larson, E.; Askin, D.; Kato, N. *J. Am. Chem. Soc.*, **1985**, *107*, 1246-1255.

Davies, H. M. L.; Ahmed, G.; Churchill, M. R. *J. Am. Chem. Soc.*, **1996**, *118*, 10774-10782.

Davies, H. M. L.; Du Bois, J.; Yu, J.-Q. *Chem. Soc. Rev.*, **2011**, *40*, 1855-1856.

Davies, H. M. L.; Manning, J. R. *Nature*, **2008**, *451*, 417-424.

Desimoni, G.; Faita, G.; Jorgensen, K. A. *Chem. Rev.*, **2006**, *106*, 3561-3651.

Diekmann, J. *J. Org. Chem.*, **1965**, *30*, 2272-2275.

Dossetter, A. G.; Jamison, T. F.; Jacobsen, E. N. *Angew. Chem., Int. Ed.*, **1999**, *38*, 2398-2400.

Doyle, M. P. *Acc. Chem. Res.*, **1986**, *19*, 348-356.

Doyle, M. P. *Chem. Rev.*, **1986**, *86*, 919-940.

Doyle, M. P.; Bagheri, V.; Harn, N. K. *Tetrahedron Lett.*, **1988**, *29*, 5119-5122.

Doyle, M. P.; Bagheri, V.; Pearson, M. M.; Edwards, J. D. *Tetrahedron Lett.*, **1989**, *30*, 7001-7004.

Doyle, M. P.; Duffy, R.; Ratnikov, M.; Zhou, L. *Chem. Rev.*, **2010**, *110*, 704-724.

Doyle, M. P.; Ene, D. G.; Forbes, D. C.; Tedrow, J. S. *Tetrahedron Lett.*, **1997**, *38*, 4367-4370.

Doyle, M. P.; Forbes, D. C. *Chem. Rev.*, **1998**, *98*, 911-935.

Doyle, M. P.; Griffin, J. H.; Chinn, M. S.; Van Leusen, D. *J. Org. Chem.*, **1984**, *49*, 1917-

1925.

Doyle, M. P.; Kundu, K.; Russell, A. E. *Org. Lett.*, **2005**, *7*, 5171-5174.

Doyle, M. P.; Phillips, I. M.; Hu, W. *J. Am. Chem. Soc.*, **2001**, *123*, 5366-5367.

Doyle, M. P.; Pieters, R. J.; Taunton, J.; Pho, H. Q.; Padwa, A.; Hertzog, D. L.; Precedo, L. J. *Org. Chem.*, **1991**, *56*, 820-829.

Doyle, M. P.; Tamblyn, W. H.; Bagheri, V. *J. Org. Chem.*, **1981**, *46*, 5094-5102.

Doyle, M. P.; Taunton, J.; Pho, H. Q. *Tetrahedron Lett.*, **1989**, *30*, 5397-5400.

Doyle, M. P.; Valenzuela, M.; Huang, P. *PNAS*, **2004**, *101*, 5391-5395.

Doyle, M. P.; Westrum, L. J.; Wolthuis, W. N. E.; See, M. M.; Boone, W. P.; Bagheri, V.; Pearson, M. M. *J. Am. Chem. Soc.*, **1993**, *115*, 958-964.

Doyle, M. P.; Winchester, W. R.; Protopopova, M. N.; Kazala, A. P.; Westrum, L. J. *Org. Synth.*, **1996**, *73*, 13-24.

Du, H.; Zhang, X.; Wang, Z.; Bao, H.; You, T.; Ding, K. *Eur. J. Org. Chem.*, **2008**, 2248-2254.

Eberlein, T. H.; West, F. G.; Tester, R. W. *J. Org. Chem.*, **1992**, *57*, 3479-3482.

Fananas, F. J.; Fernandez, A.; Cevic, D.; Rodriguez, F. *J. Org. Chem.*, **2009**, *74*, 932-934.

Fleming, I.; Henning, R.; Plaut, H. *J. Chem. Soc., Chem. Commun.*, **1984**, 29-31.

Grochowski, E.; Jurczak, J. *Synthesis*, **1976**, 682-684.

Hashimoto, S.; Watanabe, N.; Ikegami, S. *Tetrahedron Lett.*, **1992**, *33*, 2709-2712.

Hinman, A.; Du Bois, J. *J. Am. Chem. Soc.*, **2003**, *125*, 11510-11511.

Hodgson, D. M.; Angrish, D.; Erickson, S. P.; Kloesges, J.; Lee, C. H. *Org. Lett.*, **2008**, *10*, 5553-5556.

Hodgson, D. M.; Pierard, F. Y. T. M.; Stuppel, P. A. *Chem. Soc. Rev.*, **2001**, *30*, 50-61.

Hoffmann, R. W. *Angew. Chem.*, **1979**, *91*, 625-634.

Hu, W.; Xu, X.; Zhou, J.; Liu, W.-J.; Huang, H.; Hu, J.; Yang, L.; Gong, L.-Z. *J. Am. Chem. Soc.*, **2008**, *130*, 7782-7783.

Jewett, J. C.; Rawal, V. H. *Angew. Chem., Int. Ed.*, **2007**, *46*, 6502-6504.

John, J. P.; Novikov, A. V. *Organic Lett.*, **2007**, *9*, 61-63.

Johnson, S. A.; Hunt, H. R.; Neumann, H. M. *Inorg. Chem.*, **1963**, *2*, 960-962.

Jorgensen, K. A. *Angew. Chem., Int. Ed.*, **2000**, *39*, 3558-3588.

Kablean, S. N.; Marsden, S. P.; Craig, A. M. *Tetrahedron Lett.*, **1998**, *39*, 5109-5112.

Kappe, C. O. *Tetrahedron Lett.*, **1997**, *38*, 3323-3326.

Karche, N. P.; Jachak, S. M.; Dhavale, D. D. *J. Org. Chem.*, **2001**, *66*, 6323-6332.

Katritzky, A. R.; Dennis, N. *Chem. Rev.*, **1989**, *89*, 827-861.

Lee, E.; Choi, I.; Song, S. Y. *J. Chem. Soc., Chem. Commun.*, **1995**, 321-322.

Li, A.-H.; Dai, L.-X.; Aggarwal, V. K. *Chem. Rev.*, **1997**, *97*, 2341-2372.

Li, X.; Meng, X.; Su, H.; Wu, X.; Xu, D. *Synlett*, **2008**, 857-860.

Lipshutz, B. H. *Chem. Rev.*, **1986**, *86*, 795-820.

Liu, Y.; Zhang, Y.; Jee, N.; Doyle, M. P. *Org. Lett.*, **2008**, *10*, 1605-1608.

Long, J.; Hu, J.; Shen, X.; Ji, B.; Ding, K. *J. Am. Chem. Soc.*, **2002**, *124*, 10-11.

Lu, C.-D.; Liu, H.; Chen, Z.-Y.; Hu, W.-H.; Mi, A.-Q. *Org. Lett.*, **2005**, *7*, 83-86.

Marmsaeter, F. P.; Murphy, G. K.; West, F. G. *J. Am. Chem. Soc.*, **2003**, *125*, 14724-14725.

Marmsaeter, F. P.; West, F. G. *J. Am. Chem. Soc.*, **2001**, *123*, 5144-5145.

Marmsater Fredrik, P.; Vanecko John, A.; West, F. G. *Org. Lett.*, **2004**, *6*, 1657-1660.

Molander, G. A.; Shubert, D. C. *J. Am. Chem. Soc.*, **1987**, *109*, 6877-6878.

Montana, A. M.; Ponzano, S.; Kociok-Koehn, G.; Font-Bardia, M.; Solans, X. *Eur. J. Org. Chem.*, **2007**, 4383-4401.

Morikawa, K.; Park, J.; Andersson, P. G.; Hashiyama, T.; Sharpless, K. B. *J. Am. Chem. Soc.*, **1993**, *115*, 8463-8464.

Muthusamy, S.; Krishnamurthi, J.; Suresh, E. *Chem. Commun.*, **2007**, 861-863.

- Nakamura, E.; Yoshikai, N.; Yamanaka, M. *J. Am. Chem. Soc.*, **2002**, *124*, 7181-7192.
- Nazarova, L. A.; Maiorova, A. G. *Zh. Neorg. Khim.*, **1976**, *21*, 1070-1074.
- Noels, A. F.; Hubert, A. J.; Teyssie, P. *J. Organomet. Chem.*, **1979**, *166*, 79-86.
- Nozaki, H.; Takaya, H.; Moriuti, S.; Noyori, R. *Tetrahedron*, **1968**, *24*, 3655-3669.
- Nozaki, H.; Takaya, H.; Noyori, R. *Tetrahedron*, **1966**, *22*, 3393-3401.
- Oku, A.; Murai, N.; Baird, J. *J. Org. Chem.*, **1997**, *62*, 2123-2129.
- Oku, A.; Numata, M. *J. Org. Chem.*, **2000**, *65*, 1899-1906.
- Oku, A.; Ohki, S.; Yoshida, T.; Kimura, K. *Chem. Commun.*, **1996**, 1077-1078.
- Ollis, W. D.; Rey, M.; Sutherland, I. O. *J. Chem. Soc., Perkin Trans. I*, **1983**, 1009-1027.
- Padwa, A.; Austin, D. J. *Angew. Chem. Int. Ed. Engl.*, **1994**, *33*, 1797-1815.
- Padwa, A.; Austin, D. J.; Hornbuckle, S. F.; Semones, M. A.; Doyle, M. P.; Protopopova, M. N. *J. Am. Chem. Soc.*, **1992**, *114*, 1874-1876.
- Padwa, A.; Hornbuckle, S. F. *Chem. Rev.*, **1991**, *91*, 263-309.
- Padwa, A.; Snyder, J. P.; Curtis, E. A.; Sheehan, S. M.; Worsencroft, K. J.; Kappe, C. O. *J. Am. Chem. Soc.*, **2000**, *122*, 8155-8167.
- Padwa, A.; Weingarten, M. D. *Chem. Rev.*, **1996**, *96*, 223-269.
- Pangborn, A. B.; Giardello, M. A.; Grubbs, R. H.; Rosen, R. K.; Timmers, F. J. *Organometallics*, **1996**, *15*, 1518-1520.
- Pellissier, H. *Tetrahedron*, **2009**, *65*, 2839-2877.
- Pirrung, M. C.; Brown, W. L.; Rege, S.; Laughton, P. *J. Am. Chem. Soc.*, **1991**, *113*, 8561-8562.
- Pirrung, M. C.; Werner, J. A. *J. Am. Chem. Soc.*, **1986**, *108*, 6060-6062.
- Ramana, C. V.; Salian, S. R.; Gonnade, R. G. *Eur. J. Org. Chem.*, **2007**, 5483-5486.
- Reymond, S.; Cossy, J. *Chem. Rev.*, **2008**, *108*, 5359-5406.
- Roberts, E.; Sancon, J. P.; Sweeney, J. B. *Org. Lett.*, **2005**, *7*, 2075-2078.

- Roskamp, E. J.; Johnson, C. R. *J. Am. Chem. Soc.*, **1986**, *108*, 6062-6063.
- Sawada, Y.; Mori, T.; Oku, A. *J. Org. Chem.*, **2003**, *68*, 10040-10045.
- Sharma, A.; Guenee, L.; Naubron, J.-V.; Lacour, J. *Angew. Chem., Int. Ed.*, **2011**, *50*, 3677-3680.
- Shi, W.; Zhang, B.; Zhang, J.; Liu, B.; Zhang, S.; Wang, J. *Org. Lett.*, **2005**, *7*, 3103-3106.
- Shiina, I.; Miyao, R. *Heterocycles*, **2008**, *76*, 1313-1328.
- Smith, A. B., III; Razler, T. M.; Ciavarrri, J. P.; Hirose, T.; Ishikawa, T. *Org. Lett.*, **2005**, *7*, 4399-4402.
- Solorio, D. M.; Jennings, M. P. *J. Org. Chem.*, **2007**, *72*, 6621-6623.
- Stewart, C.; McDonald, R.; West, F. G. *Org. Lett.*, **2011**, *13*, 720-723.
- Stork, G.; Nakatani, K. *Tetrahedron Lett.*, **1988**, *29*, 2283-2286.
- Sweeney, J. B. *Chem. Soc. Rev.*, **2009**, *38*, 1027-1038.
- Taber, D. F. In *Comprehensive organic synthesis : selectivity, strategy, and efficiency in modern organic chemistry*; Trost, B. M.; Fleming, I. Eds.; Pergamon Press: New York, 1991.
- Taber, D. F.; Petty, E. H. *J. Org. Chem.*, **1982**, *47*, 4808-4809.
- Taber, D. F.; Petty, E. H.; Raman, K. *J. Am. Chem. Soc.*, **1985**, *107*, 196-199.
- Taber, D. F.; Ruckle, R. E., Jr. *J. Am. Chem. Soc.*, **1986**, *108*, 7686-7693.
- Takao, K.-i.; Watanabe, G.; Yasui, H.; Tadano, K.-i. *Org. Lett.*, **2002**, *4*, 2941-2943.
- Tiefenbacher, K.; Mulzer, J. *Angew. Chem., Int. Ed.*, **2008**, *47*, 2548-2555.
- Tiefenbacher, K.; Mulzer, J. *Angew. Chem., Int. Ed.*, **2008**, *47*, 6199-6200.
- Tietze, L. F.; Schuenke, C. *Eur. J. Org. Chem.*, **1998**, 2089-2099.
- Unni, A. K.; Takenaka, N.; Yamamoto, H.; Rawal, V. H. *J. Am. Chem. Soc.*, **2005**, *127*, 1336-1337.
- Wang, J.; Stefane, B.; Jaber, D.; Smith, J. A. I.; Vickery, C.; Diop, M.; Sintim, H. O. *Angew. Chem., Int. Ed.*, **2010**, *49*, 3964-3968.
- Watanabe, Y.; Washio, T.; Shimada, N.; Anada, M.; Hashimoto, S. *Chem. Commun.*, **2009**,

7294-7296.

Weber, B.; Seebach, D. *Angew. Chem. Int. Ed.*, **1992**, *31*, 84-86.

Weber, B.; Seebach, D. *Tetrahedron*, **1994**, *50*, 6117-6128.

Wee, A. G. H. *Curr. Org. Synth.*, **2006**, *3*, 499-555.

Wee, A. G. H.; Liu, B.; Zhang, L. *J. Org. Chem.*, **1992**, *57*, 4404-4414.

West, F. G.; Eberlein, T. H.; Tester, R. W. *J. Chem. Soc., Perkin Trans.*, **1993**, 2857-2859.

West, F. G.; Naidu, B. N.; Tester, R. W. *J. Org. Chem.*, **1994**, *59*, 6892-6894.

Wolckenhauer, S. A.; Devlin, A. S.; Du Bois, J. *Organic Lett.*, **2007**, *9*, 4363-4366.

Xiao, W.-L.; Gong, Y.-Q.; Wang, R.-R.; Weng, Z.-Y.; Luo, X.; Li, X.-N.; Yang, G.-Y.; He, F.; Pu, J.-X.; Yang, L.-M.; Zheng, Y.-T.; Lu, Y.; Sun, H.-D. *J. Nat. Prod.*, **2009**, *72*, 1678-1681.

Yakura, T.; Muramatsu, W.; Uenishi, J. *Chem. Pharm. Bull.*, **2005**, *53*, 989-994.

Yamashita, Y.; Saito, S.; Ishitani, H.; Kobayashi, S. *J. Am. Chem. Soc.*, **2003**, *125*, 3793-3798.

Ye, T.; McKervey, M. A. *Chem. Rev.*, **1994**, *94*, 1091-1160.

Yet, L. *Chem. Rev.*, **2000**, *100*, 2963-3007.

Yoon, U. C.; Jin, Y. X.; Oh, S. W.; Park, C. H.; Park, J. H.; Campana, C. F.; Cai, X.; Duesler, E. N.; Mariano, P. S. *J. Am. Chem. Soc.*, **2003**, *125*, 10664-10671.

Zhao, W. *Chem. Rev.*, **2010**, *110*, 1706-1745.